Higher Degree by Research/

Habilitation à Diriger des Recherches-HDR

Presented by

Faouzi BADER

Doctor in Telecommunication from
Universidad Politécnica de Madrid-UPM, SPAIN
Associate Professor/ Enseignant Chercheur, CentraleSupélec, Rennes-FRANCE

Signal Processing for Future Multicarrier Systems

A dissertation submitted in partial fulfillment
of the Higher Degree by Research (HDR)
at University of Rennes 1, Rennes- Brittany, FRANCE

September 2016

The Jury Members

Prof. Luc Vandendorpe	Université Catholique de Louvain, Belgium	(Examinateur)
Prof. Eric Pottier	Université de Rennes 1, France	(Membre invité)
Prof. Bernard Uguen	Université de Rennes 1, France	(Examinateur)
Prof. Jacques Palicot	CentraleSupélec, France	(Examinateur)
Prof. Michel Terré	Conservatoire National des Arts et Métier, France	(Rapporteur)
Prof. Ana Pérez Neira	Universitat Politècnica de Catalunya, Spain	(Rapportrice)
Prof. Linda Doyle	Trinity College of Dublin, Ireland	(Rapportrice)

Notice: To introduce the reader, in France, HDR (habilitation à diriger les recherches) is a degree (diploma) which accredits to supervise alone PhD students and allows to run for positions of full professor in universities.
"Habilitation" [1](from Latin habilis "fit, proper, skillful") is the highest academic qualification a scholar can achieve by his or her own pursuit in many countries in Europe, Central Asia, Egypt and the Caucasus. Earned usually after obtaining a research doctorate, such as a PhD, "habilitation" requires that the candidate write a professorial thesis (also "habilitation" thesis or inaugural dissertation) based on independent scholarship, reviewed by and defended before an academic committee in a process similar to that of the doctoral dissertation. However, the level of scholarship has to be considerably higher than that required for a research doctoral (PhD) thesis in terms of quality and quantity, and must be accomplished independently, in contrast with a PhD dissertation typically directed or guided by a faculty supervisor. In the sciences, publication of numerous (frequently ten or more) research articles is required during the "habilitation" period of about four to ten years. In the humanities, a major book publication may be a prerequisite for defense. The teaching ability of the "habilitation" candidate may also be evaluated [2].

Whereas a PhD is sufficient qualification for a full university faculty position in many other countries, where in use, only the HDR qualifies the holder to independently supervise doctoral candidates.
This clarification on academic credentials is very specific to France (and above cited countries or regions). To the best of my knowledge, there is no equivalence in the US higher education system or any other Anglo Saxon countries. If you have a PhD and you are hired as an assistant professor, you will supervise doctoral students if your university issues doctoral degrees. There is no separate degree or accreditation legally required for doing so.

[1] Wikipedia definition citation
[2] end of the definition

Acknowledgements

I would like to express my deep acknowledgment to my advisor Prof. Santiago Zazo Bello from Universidad Politécnica de Madrid (UPM)-Spain for having instilled in me the love of the scientific research, to Prof. Miguel Ángel Lagunas Hernandez, professor at Universitat Politècnica de Catalunya (UPC)- Barcelona, and director of the Centre Tecnològic de Telecomunicacions de Catalunya (CTTC)- Barcelona, Spain, for always trusting me and giving me the opportunity to work in an environment of excellence such as the CTTC for more than ten years, and to Prof. Jacques Palicot from CentraleSupélec, campus of Rennes (France), for his long and fruitful technical discussions and advices, and for learning me everyday to not be afraid to shake and undermine a lot of principles taken for granted in the scientific community. I would like also to thank a lot the SCEE research team of CentraleSupélec for having adopted me in a so short time, for their professionalism, humanism, and for the so nice working environment they are creating at every day.

I would like also to confess my deep gratitude to all my PhD students, postdocs, researchers, I had, or I have, the privilege to advise and/or to collaborate with them. Without all these brilliant persons and their hard motivation, I would never be able to write one word of this document. Thank you guys for making me enjoying with you the exiting world of research.

There is not enough words in this world to express my gratefulness to my lovely family, for their continuous support, patience, and love, "Habbkoum Mucho !".

Faouzi Bader

Contents

List of Figures

List of Acronyms

AF Amplify and Forward

ASER Average Symbol Error Rate

AWGN additive white Gaussian noise

BER Bit Error Rate

B3G Beyond 3rd Generation

B5G Beyond 5th Generation

CBS Cognitive Base Station

CCDF Complementary Cumulative Distribution Function

CDF Cumulative Distribution Function

CMA Constant Modulus Algorithm

C-MTC Critical Machine Type Communications

CNA Constant Norm Algorithm

CP Cyclic Prefix

CR Cognitive Radio

CSI Channel State Information

CLT Central Limit Theorem

D2D Device-To-Device

EC European Community

ES Exhaustive Search

EVM Error Vector Magnitude

FBMC Filter Bank Multiple Carriers

FCC Federal Communications Commission

FFT Fast Fourier Transform

F-OFDM Filtered Orthogonal Frequency Division Multiplexing

GA Genetic Algorithm

GFDM Generalized Frequency Division Multiplexing

5G 5th Generation

3GPP The 3rd Generation Partnership Project

HPA High Power Amplifier

ICI Inter-Carrier Interference

ICT Information and Communication Technologies

IEEE Institute of Electrical and Electronics Engineers

IMT International Mobile Telecommunications

IoT Internet of Things

IOTA Isotropic Orthogonal Transform Algorithm

LTE long Term Evolution

LPWA Low Power Wide Area

MAC Multiple Access Control layer

MC-CDMA Multi-Carrier Code Division Multiple Access

MGF Moment Generating Function

MIMO Multiple Input Multiple Output

MMA Multi-Modulus Algorithm

MMSE Minimum Mean Square Error

MRC Maximal Ratio Combining

MT-CDMA Multi-Tone Code Division Multiple Access

MTR Modified Tone Reservation

MUD Multi-User Detection

OFDMA Orthogonal Frequency Division Multiple Access

OOB Out-Of-Band

OQAM Offset Quadrature Amplitude Modulation

PA Power Allocation

PAP Phase Adaptation Procedure

PAPR Peak to Average Power Ratio

PDF Probability Distribution Function

PHY Physical layer

PI Power Interference algorithm

PMR Professional Mobile Radio

PN Primary Network

PPDR Public Protection Disaster Relief

PSACE Pilot Aided Channel Estimation

PSD Power Spectrum Density

PU Primary User

QCQP Quadratic Constrained Quadratic Program

QoS Quality of Service

RA Resource Allocation

RB Resource block

RF Radio Frequency

RRA radio Resource Allocation

RRM radio resource Management

SC Selection Combining

SC-FDMA Single carrier Frequency Division Multiple Access

SN Secondary Network

SNR Signal to Noise Ratio

SOCP Second Order Cone Program

SS Spread Spectrum

SS-MC-MA Spread Spectrum Multi-Carrier Multiple-Access

STREP Specific Targeted Research Projects

SU Secondary User

TAS Transmit Antenna Selection

TEQ Time-domain EQualizer

TR Tone Reservation

TTI Transmission Time Interval

UFMC Universal-Filtered Multi-Carrier

UTRA UMTS Terrestrial Radio Access

WAN Wide Area Network

WLAN Wireless Local Area Network

Chapter 1

Extended Curriculum Vitae

Brief and preliminary information

Status:

Name: BADER
Surname: Faouzi
Actual position: Associate Professor/EC
Actual institution: CentraleSupélec, Campus of Rennes-France.
Address: Avenue de la Boulaie CS 47601. F-35576. Cesson-Sévigné Cedex
E-mails: faouzi.bader@supelec.fr/carlos.bader@centralesupelec.fr.
Contacts: +33 (0) 299844536, fax: +33 (0)299844599,
Home page: http://www.faouzibader.com

Academia:

- 1998-2002: PhD degree in Signal Processing and Telecommunication (with "cum laude" honor) at ETSIT –Universidad Politécnica de Madrid (UPM), Madrid, Spain.

  Dissertation titled: "*New Signal Processing Techniques Applied to MC-CDMA System in the Reverse Link*" (document in Spanish). 6th November 2002.
  Adviser: Prof. Santiago Zazo, Universidad Politécnica de Madrid-UPM, Madrid-Spain.
  Examination committee:
  Prof. José Manuel Paez Borrallo, Universidad Politécnica de Madrid (UPM), (President), Prof. Francisco Javier Casajús Quirós, Universidad Politécnica de Madrid (UPM), Prof. Luis Castedo Ribas, Universidad A Coruña, A Coruña (UDC), Prof. Miguel Ángel Lagunas Hernandez, Universitat Politècnica de Catalunya (UPC), Barcelona, Prof. Javier Rodriguez Fonollosa, Universitat Politècnica de Catalunya (UPC), Barcelona.

- 1991-1996: Electronic Engineering Degree, with honor at Institute of Electronics, Faculty of Engineering Sciences of University Mentouri of Constantine (UMC), Constantine-Algeria.

Professional experience:

- Since June 2013- present: Associate Professor/ Enseignant Chercheur at Signal, Communication & Embedded Electronics (SCEE) research group of CentraleSupelec, Campus of Rennes-France.
- From February 2012-May 2012: Visiting researcher at Department of Electronics and Communications Engineering, of Tampere University of Technology-TUT at Tampere, Finland.
- From 2006- June 2013: Senior Research Associate at Catalonia's Telecommunications and Technology Centre-CTTC (http://www.cttc.es), Barcelona-Spain.

- From 2002-2005: Research Associate and Coordinator of Access Technologies research area at Telecommunications Technological Center of Catolonia-CTTC, Barcelona, Spain.
- From 2000- 2001: Development Engineer at Massana Technologies SL. company (Ireland). In 2002 the company has been bought by Ageere System (USA), and in 2007 merged with LSI Corporation http://www.lsi.com/ (USA).
- From 1997-2002: Research member of the "Systems and Signal Processing" research group (GAPS) of department of Systems and Radio Communications (SSR) at the High School of Engineers of Telecommunications (ETSIT) of Universidad Politécnica de Madrid (UPM), Spain.

Scientific and Professional Society Membership

- Project reviewer at the «French National Research Agency» (ANR)-France, since 2014.
- Project reviewer at the "Fonds de la Recherche Scientifique" of Belgium (FNRS), since 2013.
- Chair of the working group "WG1" on High Capacity PHY for future radio access of the European Commission Radio Access and Spectrum (RAS) Cluster (2012-2014).
- Project reviewer at Natural Sciences and Engineering Research Council of Canada (NSERC)-Canada, since 2014.
- IEEE Standards Association Member
- IEEE Senior Member since 2007.
- Member of IEEE Communication Society (ComSoc IEEE).
- Member of Cognitive Communications (CogCom) of WorldWide Universities Network Initiative (WUN-CogCOM), since 2009.

Main research activities:

- Advanced Multi-carrier Waveforms for future communication Systems (5G),
- Cooperative, relay and multi-(two-way) scenarios,
- Professional Mobile Radio PMR/PPDR for public safety and beyond,
- Cross layer System design,
- Cognitive Radio and Spectrum sharing,
- Radio Resource Management.

Publications:

- In journals: 23 including 3 editorials, see all the list in Subsection 2.1.1, page 30.
- Book chapters: 15, see the details in Subsection 2.1.3, page 33.
- In international Conferences: 100 with peer review process see detailed list of conference papers in Subsection 2.1.4, page 34.
- In National Conferences: 5 with peer review process.
- Edited books: 3, see all the edited books in Subsection 2.1.2, page 32.
- Standardization: 9, all the details are in Subsection 2.1.5, page 42.

Advised young researchers

- Postdocs: 2.
- PhD Students under supervision: 3.
- Supervised PhDs: 4.
- Masters (MS2): 6.

International collaborations with academia and research centers

Below you have the list of my collaborations to the date. I mean by collaboration any action with joint technical output(s) representing a joint project collaboration(s), publication(s), or research mobility. My main research relationships are among others with:

Asia: Dr. Sumit Darak from Indraprastha Institute of Information Technology Delhi -IIID (India).
Australia: Prof. Eryk Dutkiewicz and Prof. Michael Heimlich from Macquarie University of Sydney-MQ, Dr. Beeshanga Abewardana Jayawickrama from University of technology Sidney-UTS, prof. Kandeepan Sithamparanathan from Royal Melbourne Institute of Technology-RMIT.
Europe: Prof. Maurice Bellanger, Prof. Didier Le Ruyet, Prof. Daniel Roviras, Dr. Yahia Medjahdi from Conservatoire National des Arts et Métiers (CNAM), Dr. Dominique Noguet, Dr. Vincent Berg, Dr. J. B. Dore from CEA-Leti-Grenoble, Prof. Hakima Chaouchi from Université Paris-Sud (France), Université Catholique de Louvain-(UCL) (Belgium), Prof. Nikos Passas from University of Athens, Prof. Panagiotis Demestichas and Dr. Lefteris Kofidis from University of Piraeus (Greece), Dr. Oliver Holland, Dr. Vassilis Friderikos from King's College of London, Prof. Klaus Moessner from University of Surrey (UK), Prof. Martin O'Droma, and Dr. Ivan Ganchev from University of Limerik, Prof. Luiz DaSilva, and Dr. Arman Farhang from Trinity College of Dublin, Dr. Hamed Ahmadi from University College of Dublin (Ireland), Prof. Markku Renfors from Tampere University of Technology and Prof. T. Ristaniemi from University of Jyväskylä, Dmitry Petrov from Magister (Finland), Dr. Jonathan Rodriguez and Shahid Mumtaz from Instituto de Telecomunicações-IT Lisbon and Aveiro (Portugal), Prof. Santiago Zazo Bello from Universidad Politécnica de Madrid, Prof. Luis Muñoz, Dr. Ramon Agüero from Universidad de Cantabria, Dr. Ivan A. Perez-Alvarez from Universidad de Las Palmas de Gran Canaria, Prof. A. Perez Neira, Dr. Christian Ibars, Dr. Stephan Pfletschinger from CTTC, Prof. Oriol Sallent from Universitat Politècnica de Catalunya-UPC (Spain), Dr. Simon Plass from German Aerospace Center-DLR, Prof. Thomas Kaiser from Duisburg-Essen University, Prof. Eduard Jorswieck from Dresden University of Technology, RWTH Aachen University (Germany), Prof. S. Ben-Slimane from Royal Institute of Technology-KTH (Sweden), Prof. Hanna Bogucka and Dr. Adrian Kliks from Poznan University of Technology-PUT (Poland), Ringset Vidar from SINTEF research centre (Norway), Prof. M. Gabriella Di Benedetto, Dr. Luca De Nardis from University of Rome La Sapienza, Dr. Gianmarco Baldini from European Research Center, Andrea Giorgetti from University of Bologna (Italy), Dr. Andrea Fabio Cattoni from Aalborg University (Denmark).
Middle East: Dr. Youssef Nasser from American University of Beirut-AUB, Prof. Oussama Baazi from Lebanese University of Beirut (Lebanon), Prof. Mohammad Banat from Jordan University of Science and Technology-JUST (Jordan), Prof. Mohamed-Slim Alouini from King Abdullah University of Science and Technology-KAUST (Saudi Arabia), Dr. Nizar Zorba from Qatar University (Qatar).
North America: Prof. B. Farhang-Boroujeny from University of Utah (USA), Prof. Sofiene Affés from Institut National de la Recherche Scientifique-INRS of Quebec, Prof. Mohamed Ibnkahla from Queen's University, Dr. Kareem Emile Baddour from Communications Research Centre-CRC (Canada).

Involved research projects

- EU Funded projects: 10 projects (7 STREPs, 1 COST Action, and 2 CELTICs).
- National projects: 7 projects, from which 3 funded by the Spanish Ministry of Industry, Tourism and Commerce (MITYC), and 4 from the French National Research Agency (ANR).
- Industrial projects: 3 projects.
- Grants: 1 PHC (ULYSSES with Ireland).

More details on my involvement in projects can be found in Subsection 1.5, page 22.

Awards & Recognitions

2012: Assumed the role of General Coordinator and Manager of FP7 STREP Project titled: Enhanced Multicarrier Techniques for Professional Ad-hoc and Cell Based Communications [ICT-EMPhAtiC], with contract code: ICT-318362.
- 2010: BEST CONFERENCE PAPER AWARD of the Sixth International Conference on Wireless and Mobile Communications (ICWMC'2010) on the paper "Pilot Pattern Adaptation and Channel Estimation in MIMO WiMAX-like FBMC System" Sept 2010.
- 2007: Member of "Bridge Technologies" team, finalist at the 7th Competition of Business Ideas, organized by the Spanish Ministry of Innovation, Universities and Enterprise of the local Government of Catalonia (CIDEM). 2007 edition.
- 2007: Nominated IEEE Senior Member.

- 2003: Certificate of Appreciation for contributions to The IEE European Personal Mobile Communications Conference (IEE EPMCC), Glasgow, UK. April 2003.
- 2002: PhD degree titled: "New Signal Processing Techniques Applied on the MC-CDMA System in the Reverse Link" (In Spanish) obtained with Honours (CUM LAUDE) from the High School of Engineers of Telecommunications (ETSIT) at Universidad Politécnica de Madrid (UPM), Madrid-Spain. November 2002.
- 2000: Certificate of Appreciation for contributions to The IEEE Boston Fall Vehicular Technologies Conference. Boston -USA. September 2000.
- 1999: BEST CONFERENCE PAPER AWARD -Arthec House Publishers Award on the paper “Optimum Pilot Pattern for Multi-carrier CDMA Systems”, presented at WPMC’99/IEEE VTC-Fall’99.

1.1 About my PhD thesis

At early of the nineteenths, several research works focusing on the combination of the OFDM and the CDMA have been developed and proposed as the MC-CDMA by N. Yee et al, in [2], the MC-DS-CDMA by K. Fazel in [3], and the MT-CDMA by L. Vandendorpe in [4]. In all these schemes, the users share the same time-frequency dimension, and can be separated in the code domain.

The general focus of my dissertation (1998-2002) is on wireless communication systems, more precisely on the development of new signal processing techniques for multi-carrier code division multiple access (MC-CDMA) system for the uplink communication mode. My dissertation is about 231 pages and six chapters including the further research lines. Main technical contributions are presented in chapter 3 on: "*Channel Estimation*", Chapter 4 on: "*Synchronization in MC-CDMA in Uplink communication mode*", and Chapter 5 on: *"Multi-User Detection in Uplink Mode"*. In Chapter 3, a hexagonal pilot pattern design has been designed and developed to be compatible with the MC-CDMA systems for the uplink communications mode. At that time no such pilot pattern scheme was either contemplated nor developed for MC-CDMA. Only conventional patterns as; diagonal, rectangular or square were available in the scientific literature. The performances of proposed scheme have been analysed and published in (see in Subsection 2.1.4 and Subsection 2.1.3) [C1, C2, C3],and [CB1, CB2].

The second main technical contribution (Chapter 4) is related with the uplink acquisition of synchronization parameters in MC-CDMA. The uplink communication case of the MC-CDMA sygnal is a critical communication mode that may degrade severely the system performance and the data demodulation, where the signal detection is much more difficult to treat in an asynchronous (as uplink) mode than the synchronous one. When the base station intends to detect the signal of a specific user, the first step for the demodulation process at the receiver is the frame synchronization. Note that each MC-CDMA mobile system has its own spreading code, which is shared with the base station. When a mobile station transmits only the spreading code with no data, the base station can know the time domain of the spreading signal. The good detection process is related in big part with the periodic cross-correlation characteristics of the used spreading code during the transmission process. According with the observation in [5, 6], the repetition of the spread code in frequency domain has bad cross-correlation characteristics in the time domain. One solution is the use of a concatenate distribution of the later. This mode can improve significantly the cross-correlation characteristics between the spreading used sequences in the time domain.
To design proposed scheme, we consider K (K is the total number of active users) orthogonal Gold sequences, the first user concatenate the codes from 1 to P code (P is an integer factor that can be equal or lower that the maximum active users depending on the total available carriers, and indicating the number of the code words used in one OFDM-symbol) in a specific order. The second assigned user code is and L (L correspond to the length of one orthogonal code spread sequence) shifts displacement of the first generated code, and the rest of users adopt the same technique up to last active user. At the end, all the symbols in the same frequency band are spread by different orthogonal Gold codes, such that the different frequency bands may be spread by the same Gold code.
The combination of the T. M. Schmild and D. Cox frequency offsets correction algorithm in [7], [8] and the use of spreading sequences and the reservation of PSACE positions allowed a design of a combined scheme to get the essential acquisition parameters which are: the detection of the user's time arrivals frames, the correction of the time-frequency offsets misalignment, and a rough estimation of the CSI of every transmitting user in the uplink mode. Note that The use of the proposed spreading code allows the exploitation of the correlation properties in time domain by permitting a good detection of the starting time of the user's signal at the base station. The support of the offset correction sequence in the initial channel estimation jointly with the inserted pilots is very benefit permitting a higher channel estimation accuracy. More details on achieved performances with proposed acquisition scheme in terms of bit error rate (BER), initial channel estimation minimum mean square error (MSE), and MSE values of the offset correction, are available in (see in Subsection 2.1.4) [C4] and [CB4] publications.

Two multi-user detection (MUD) schemes have been developed in Chapter 5, proposed have been adapted to the transmission block developed by Z. Wang and B. Giannakis in [9] to the MC-CDMA scheme for the uplink communications mode.In addition, their combination with preliminary studies undertaken by S. Verdu allowed to encompass different detection schemes (synchronous, quasi-synchronous, and asynchronous) under a unique mathematical formulation [10], and the development of different MUD (decorrelators, and MMSE detector) all adapted to the uplink communication mode. The developed detection models allowed us to address the MC-CDMA wireless communications for uplink mode with a higher grade of delay than those usually used in small cells environments

where only quasi-synchronous detections are possible. More details on proposed decorrelators for MC-CDMA combined with SIC and PIC cancellation schemes and achieved performances can be found at (see in Subsection 2.1.4 and Subsection 2.1.3) [C4, C5, C6] and in [CB3, CB3] references.

Here are the main publications[1] directly related with my PhD thesis:

- Linked with Chapter 3 on: "Pilot pattern design", [C2, C3] and [CB2].
- Linked with Chapter 4 on: "Uplink acquisition of synchronization parameters in MC-CDMA", [C4, C7].
- Linked with Chapter 5 on: "Multi-User detection in reverse mode", [C2, C3, C5, C8], [CB3], and [J1].

1.2 Teaching activities

1.2.1 @ CentraleSupélec, France

My teaching activities formally started at my coming to CentraleSupélec in 2013 (June). Below are listed the main courses:

- Since 2014: Teaching fellow, lecture on: "Random Processes and Probabilities" for undergraduate students (first year), 18 hours. Period: first semester.
- Since 2014: Teaching Assistant-ship, tutorials/integrated[2] courses on: "Random Processes and Probabilities", for undergraduate students (first year), 4 classes of 1h:30min each. Period: first semester.
- Since 2013: Teaching Assistant-ship, tutorials/integrated courses on: “Statistical Representation and Analysis of Signals", for undergraduate students (second year), 4 classes of 1h:30min. Period: first semester.
- Since 2013: Teaching Assistant-ship, tutorials/integrated courses on: “Signals and Systems I“, for undergraduate students (second year), 4 classes of 1h:30min each. Period: first semester.
- Since 2013: Teaching Assistant-ship[3], laboratory work related with course "Statistical Representation and Analysis of Signals", for undergraduate students (second year), 8 sessions of 5h:30min each. Period: first semester.

1.2.2 @ University of Jyväskylä-JUY, Finland

Bellow are the lectures I gave during two years (2014 and 2015) at JUY.

- Lecture on: “Potential Multi-carrier Techniques and Waveforms for Future 5G Communication Networks“ (40 hours), at faculty of information and technology of University of Jyväskylä, Finland. Period: August 2015. The number of students registered in this course is: 26 students.
- Lecture on: “Beyond OFDM Radio Interfaces Facilitating Spectrum Coexistence and Secondary Access”, (40 hours), at faculty of information and technology of University of Jyväskylä, Finland. Period: August 2014. The number of students registered in this course is: 20 students.

1.2.3 Tutorials

- *Candidate Multi-carrier Waveforms for Future 5G Communication Systems*, by F. Bader (CentralSupélec-France) and Dmitry Petrov (Magister Solutions Ltd., Jyväskylä, Finland), at the 8th International Congress on Ultra Modern Telecommunications & Control Systems (ICUMT’2016). Lisbon-Portugal. October 2016.
- *Beyond OFDM Radio Interfaces Facilitating Spectrum Coexistence and Secondary Access: New Unsuspected Applications*, by F. Bader (Supélec-France) and A. Kliks (Poznan University of Technology-Poland). Five hours tutorial taught for postgraduate class of 40 students at King’s College of London (KCL). July 2013. London-UK.

[1] indexes: [JX], [CBX], [CX], and [OX] refer to published: journal, chapter book, conference, and other publication respectively. The "X" is referring to the publication number

[2] the equivalent of "Travaux Dirigés-TD" in French Universities.

[3] the equivalent of "Travaux de Laboratoire-TL" in French Universities.

- *OFDM vs. FBMC System Performances in Non-Relay and Relay Cognitive Radio Scenarios*, by F. Bader and Musbah Shaat. (4) hours tutorial taught for postgraduate class at CTTC, 2012.
- *Technologies Evolution and Regulation in Communication Systems*, (at Telefónica I+D). Postgraduate class of 14 students, Telefónica (Spain). Years 2007 and 2008.
- Technology Bases for Spectrum Management Evolution, by F. Bader, four (4) hours tutorial taught at Mosharaka International Conference on Signal, Image and Speech Processing (M-SISP2007), Amman, Jordan. June 2007.
- *WiMAX a New Broadband Access Solution*, three (3) hours tutorial taught for postgraduate class of 16 students at the 1st IEEE Mobile Computing and Wireless Conference (IEEE MCWC'2006). 16th September 2006, Amman-Jordan.
- *Enabling Technologies and Key Issues for QoS Enabled Reconfigurable Mobile/Wireless Networks*, by F. Bader, M. Navarro, S. Pfletschinger, C. Pinart. Three (3) hours tutorial taught for postgraduate class of 24 students at the 1st IST-ANWIRE Summer School on Wireless Internet: Network Architectures, Quality of Service and Applications, 21-25 July 2003, IT-Lisbon, Portugal.

1.2.4 Organization of schools

- Network of Excellence in Wireless Communications-(Newcom#) **Spring School** on "Flexible Multi-carrier Waveforms for Future Communications Wireless Networks", at Supélec, campus of Rennes- France, 21-23 May 2014.
- **Spring School** Tutorials days on "Advances on Signal Waveforms, Decision Making and Implementation in CR Radio", supported by the COST Action IC 0902 "Cognitive Radio and Networking for Cooperative Coexistence of Heterogeneous Wireless Networks". Location: CTTC, Castelldefels-Barcelona-Spain. 11-13 February 2013.
- European Network of Excellence "Advanced Coexistence Technologies for Radio Optimization in Licensed and Unlicensed Spectrum"-ACROPOLIS **Winter School** 2013. Location: CTTC, Castelldefels-Barcelona-Spain. 14-15 February 2013.

1.3 Research Activities

1.3.1 Short Terms Scientific Cooperation

2014

- Laura Beatriz Melián Gutiérrez, PhD student from Universidad de Las Palmas de Gran Canaria - ULPGC (Spain). Supervisor: Dr. Iván A. Pérez Álvarez IDeTIC-ULPGC-Spain, and Dr. Santiago Zazo Bello, UPM- Madrid, Spain. Research collaboration topic on: "HF Spectrum Activity Prediction Model Based on Learning Techniques for Cognitive Radio Applications." Period: September-December 2014 at SUPELEC, Rennes-France.

2013

- Sener Dikmese PhD student of Tampere University of Technology (TUT), Tampere-Finland. Supervisor: Prof. Markku Renfors (TUT). Research cooperative topic: "Spectrum Sensing and Spectrum Allocation for 802.11g based WLAN & Filter Bank Multi-carrier based cognitive radios using compressed sensing technique". Period: November-December 2013 at SUPELEC, Rennes-France.

2012

- Prof. Eryk Dutkiewicz from Macquarie University of Sydney-MQUS (Australia). Research collaboration topic on: "Dynamic Spectrum Access in Cognitive Radio Networks. Period: July to September 2012 at CTTC, Barcelona-Spain.

- Jing Lv PhD student of Dresden University of Technology (TUD), Dresden-Germany. Supervisor: Prof. Eduard Jorswieck (TUD). Research collaboration topic on: "Advanced Coexistence Technologies for Radio Resource Usage Optimization". Period: September-October 2012 at CTTC, Barcelona-Spain.

- Dr Yahia Medjahdi from Conservatoire National des Arts et Métiers (CNAM), Paris-France. Research collaboration topic on: Interference Modeling of Asynchronous FBMC Based System for primary Narrow-band Coexistence. Period: October 2012 at CTTC, Barcelona-Spain.

- Sener Dikmese PhD student of Tampere University of Technology (TUT), Tampere-Finland. Supervisor: Prof. Markku Renfors (TUT). Research collaboration topic on: "Spectrum Sensing and Spectrum Allocation for IEEE 802.11g based WLAN & FBMC based Cognitive radios". Period. November-December 2012 at CTTC, Barcelona-Spain.

- Jin Lai PhD student from Macquarie University of Sydney-MQUS (Australia). Supervisor: Prof. Eryk Dutkiewicz (MQUS). Research collaboration topic on: "Radio Resource Management in Broadband Wireless Networks: Maximizing Resource Utilization in LTE and CR Networks". Period: November-December 2012 at CTTC, Barcelona-Spain.

- Dr. Djamel Slimani from University Ferhat Abbas (UFA) of Sétif in Algeria. Research cooperative topic: "IMT advanced Multi-carrier Communication Systems for Cellular Networks". Period: December 2012, at CTTC Barcelona-Spain.

2011

- Dr. Mohammad M. Banat from Jordan University of Science and Technology (JUST), Amman-Jordan. Research collaboration topic on: "Three Dimensional Pilot Aided Channel Estimation for Filter Bank Multi-carrier MIMO Systems with Spatial Channel Correlation". Period: January –July 2011, at CTTC, Barcelona-Spain.

- Dr. Adrian Kliks from Poznan University of Technology-PUT (Poznan-Poland). Research collaboration topic on: Advanced AMC techniques for throughput enhancement and interference mitigation in cognitive systems. Period: August-September 2011 at CTTC, Barcelona-Spain.

1.3.2 Postdocs

- Vincent SAVAUX (CentraleSupélec), on research topic: "Blind detection strategies for OQAM-OFDM Systems". Under the French National Research Agency project PROFIL: ANR-13-INFR-0007-03. Period: 2013-2015. Related publications: [J24, J23, J20, J18], and [C104, C101, C99, C94, C92, C91, C87].

- Malek NAOUS (CentraleSupélec), on research topic: "FBMC Equalization- HW Implementation". Under the French National Research Agency project PROFIL: ANR-13-INFR-0007-03. Period: 2014-June 2016. Related publications: [C104, C92], and [O1].

1.3.3 PhD Supervisions

1.3.3.1 In progress

- Hussein CHOUR, PhD. title: "Cognitive Radio in Device-to-Device (D2D) Future Communication Systems", Joint doctoral supervision with the Lebanese University in Beirut (Lebanon), and CentraleSupélec (France).
  Advisors: Prof. Yves Louët and Dr. Faouzi Bader (France), and Prof. Oussama Bazzi with Dr. Youssef Nasser (Lebanon).
  Period: Oct. 2016 end 2019.

- Antonio Cristo SUAREZ RODRIGUEZ, PhD. titled: "Device-to-Device Communication in 5G Cellular Networks". Joint doctoral supervision with Macquarie University of Sydney (Australia) and CentraleSupélec (France).
  Advisors: Prof. Jacques Palicot and Dr. Faouzi Bader (France), and Prof. Eryk Dutkiewicz and Prof. Michael Heimlich (Australia).
  Period: April 2016- end 2019.

- Quentin BODINIER, PhD. titled (provisional): "GFDM Multi-User Detection Scheme in Asynchronous Coordinated Multi-point Scenario". Advisors: Prof. Jacques Palicot (30%), and Dr. Faouzi Bader (70%).
Period: Oct. 2014-end Oct. 2017. Related papers to the date: [C96, C97, C100, C103, C105, C106] (page 34).

1.3.3.2 Finished

- Marwa CHAFII, PhD. title: "Study of a New Multi-Carrier Waveform with Reduced PAPR" (original in French), at SCEE Research group, SUPELEC-Rennes-France.
Advisors: 50% Prof. Jacques Palicot (Supélec, France), 30% Prof. Rémi Gribonval (INRIA-Rennes, France), and 20% Dr. Faouzi Bader (Supélec, France).
Period: Sept. 2013- end Oct. 2016.

  Related publications (see Section 2.1), were I'm directly involved journal(s): [J25] (page 30); and conferences: [C102, C98] (page 34). Other publications in this thesis are: in journals: [11], in conferences: [12, C98, 13, 14, 15, 16, 17].

  Examination Committee:
  - Prof. Laurent Jacques, University Catholic of Louvain, Belgium.
  - Prof. Michel Terré, CNAM, Paris-France.
  - Prof. Cyrille Siclet, Université Gronole Alpes-UGA, Grenoble, France.
  - Prof. Geneviève Baudoin, ESSIEE, Noisy le Grand, France.
  - Dr. Matthieu Gautier, University Rennes 1-UR1, Rennes, France.

  Short description: OFDM is a multi-carrier modulation system widely used in wireline and wireless applications such as DVB-T/T2,Wifi, and 4G, due to its resilience against frequency selective channels compared with the single carrier modulation systems. However, the OFDM signal suffers from large amplitude variations. The fluctuations of the OFDM envelope generate non-linear distortions when we introduce the signal into a non-linear device like the power amplifier. Reducing the variations of the signal improves the power amplifier efficiency, reduces the energy consumption and decreases CO2 emissions. The peak-to-average power ratio (PAPR) has been introduced as a random variable that measures the power variations of the signal. There exist several multi-carrier modulation systems based on different modulation basis and shaping filters. We first prove in this work that the PAPR depends on this modulation structure. Moreover, the behavior of the PAPR regarding to the modulation waveforms is analyzed and the PAPR reduction problem is formulated as an optimization problem. Furthermore, a necessary condition for designing waveforms with better PAPR than OFDM is developed. This necessary condition is particularly satisfied by wavelet basis. Finally, a new adaptive wavelet packet waveform is proposed, allowing significant gain in terms of PAPR, while keeping the advantages of multi-carrier modulations.

  Keywords: PAPR, OFDM, wavelet modulation, adaptive modulation.

- Lamarana DIALLO, PhD. title: "Contributions to Techniques for Crest Factor Reduction in OFDM Signals" (original in French), at SCEE Research group of Supélec-Rennes. Advisors: Prof. Jacques Palicot (70%), and Dr. Faouzi Bader (30%) both from Supélec-Rennes. Period: Nov 2012- March 2016.
Related publications (see Section 2.1): Journal(s): [J22] (page 30); Conferences: [C89, C93, C95, C98, C102] (page 34).

  Examination Committee:
  - Prof. Marie Laure Boucheret, INP-ENSEEIHT-Toulouse-France. - Prof. Geneviene Baudouin, ESSIEE, Noisy le Grand, France.
  - Prof. Daniel Roviras, CNAM, Paris-France.
  - Dr. Mohamad Mroué, Université Libanaise, Beirut, Lebanon

  Short description: The Orthogonal Frequency Division Multiplexing (OFDM) is the most commonly used multi-carriers modulation scheme in the telecommunication systems. It is used in most communication standards such as DVB-T2, Wireless Local Area Networks (WLAN), WiMAX and the LTE (Long Term Evolution)

standard. The success of the OFDM comes from its robustness in presence of multi-paths and frequency selective fading channels, and the simplicity of the implementation of its transmitter and receiver. One of the main drawbacks of the OFDM modulation scheme is its high Peak-To-Average Power variation (PAPR) which can induce poor power efficiency at the transmitter amplifier. The digital base band pre-distortion for the linearization of the power amplifier (PA) and the PAPR mitigation are the most commonly used solutions in order to deal with efficiency and the linearisation at the high power amplifier. This thesis is focused on this last solution, and particularly on the addition of signal based techniques to mitigate the PA effects. Developed solutions in this thesis are about improving the Tone Reservation method which is the most popular adding signal based technique for PAPR mitigation, and also the classical clipping method which is nowadays the most simple method (in terms of computational complexity).

Keywords: OFDM, PAPR, high power amplifier, tone reservation, clipping;

- Musbah SHAAT, PhD. title: "Resource Management in Multi-carrier Based Cognitive Radio Systems", at theory of signal and communications department, Polytechnic University of Catalonia-UPC, Spain.
  Advisors: Dr. Faouzi Bader (70%), and Prof. Miguel Angel Lagunas (30%) from Polytechnic University of Catalonia-UPC, Barcelona, Spain.
  Duration: March 2008-2012 (4 years)

  Examination Committee:
  - Prof. Ana Isabel Perez Neira, Universitat Polit'ecnica de Catalunya (UPC), Barcelona-Spain
  - Prof. Didier Le Ruyet, Conservatoire National des Arts et Métiers (CNAM), Paris-France
  - Prof. Santiago Zazo Bello, Universidad Politécnica de Madrid (UPM), Madrid-Spain
  - Prof. Mohamed-Slim Alouini King Abdullah University of Science and Technology (KAUST), Thuwal-Saudi Arabia
  - Dr. Jocelyn Fiorina, Supélec, Paris-France

  Related publications (see Section 2.1): Journal(s): [J11, J10, J9, J5] (page 30); Chapters in books: [CB14, CB11] (page 33); Conferences: [C44, C48, C51, C52, C56, C57, C58, C59, C65, C67, C68, C69, C70, C71, C76] (page 34).

  Short description: In this dissertation, the resource management problem in multi-carrier based CR systems is considered. The dissertation focuses on three main issues: 1) design of efficient resource allocation algorithms to allocate subcarriers and powers between SUs such that no harmful interference is introduced to PUs, 2) compare the spectral efficiency of using different multi-carrier schemes in the CR physical layer, specifically, orthogonal frequency division multiplexing (OFDM) and filter bank multi-carrier (FBMC) schemes, 3) investigate the impact of the different constraints values on the overall performance of the CR system. Three different scenarios are considered in this dissertation, namely downlink transmission, uplink transmission, and relayed transmission. For every scenario, the optimal solution is examined and efficient sub-optimal algorithms are proposed to reduce the computational burden of obtaining the optimal solution. The suboptimal algorithms are developed by separate the subcarrier and power allocation into two steps in downlink and uplink scenarios. In the relayed scenario, dual decomposition technique is used to obtain an asymptotically optimal solution, and a joint heuristic algorithm is proposed to find the suboptimal solution. Numerical simulations show that the proposed suboptimal algorithms achieve a near optimal performance and perform better than the existing algorithms designed for cognitive and non-cognitive systems. Eventually, the ability of FBMC to overcome the OFDM drawbacks and achieve more spectral efficiency is verified which recommends the consideration of FBMC in the future CR systems.

  Keywords: Power allocation, relay, multi-relays, cognitive radio, multi-carrier.

- Ismael GUTIERREZ GONZALEZ, PhD. title on: "Adaptive Communications for Next Generation Broadband Wireless Access Systems".
  Advisors: Faouzi Bader (70%)-CTTC, and Dr. Joan Luis Pijoan (30%) from Ramon Llull University-URL, Barcelona-Spain.
  Duration: 2005-2009 (4 years)

Examination Committee:
- Prof. Santiago Zazo Bello, Universidad Politécnica de Madrid (UPM), Madrid-Spain
- Dr. Alain Mourad, Samsung research center, London UK.
- Dr. Jaume Anguera, Universitat Ramon Llull (URL), Barcelona-Spain.
- Dr. Joan Ramon Regue, Universitat Ramon Llull (URL), Barcelona-Spain.

Related publications (see Section 2.1): Journal(s): [J4] (page 30); Chapters in books: [CB13, CB12, CB10, CB8, CB7] (page 33); Conferences: [C60, C55, C53, C50, C47, C43, C42, C41, C40, C39, C36, C34, C32, C31, C28, C27] (page 34).

Short description: In this Ph.D. thesis, different adaptive techniques for B3G multi-carrier wireless systems are developed and proposed focusing on the SS-MC-MA and the OFDM(A) (IEEE 802.16a/e/m standards) communication schemes. The research lines emphasize into the adaptation of the transmission having (Partial) knowledge of the Channel State Information for both; single antenna and multiple antenna links. For single antenna links, the implementation of a joint resource allocation and scheduling strategies by including adaptive modulation and coding is investigated. A low complexity resource allocation and scheduling algorithm is proposed with the objective to cope with real- and/or non-real- time requirements and constraints. A special attention is also devoted in reducing the required signaling both in the downlink and the uplink. Moreover, for multiple antenna links, the performance of a proposed adaptive transmit antenna selection scheme jointly with space-time block coding selection is investigated and compared with conventional structures. In this research line, mainly two optimizations criteria are proposed for spatial link adaptation, one based on the minimum error rate for fixed throughput, and the second focused on the maximization of the rate for fixed error rate. Finally, some indications are given on how to include the spatial adaptation into the investigated and proposed resource allocation and scheduling process developed for single antenna transmission.

Keywords: RRM, adaptive modulation, WiMAX, multi-carrier, spatial link adaptation.

1.3.4 Masters (M2)

- Quentin Bodinier from Supélec. Master degree topic on: "Contributions to PHY and MAC layers for GFDM in the Context of Cognitive Radio", in collaboration with Trinity College in Dublin (Ireland). Supervisors: Dr. Christophe Moy and Faouzi Bader (Supélec), Dr. Hamed Ahmadi and Prof. Luiz DaSilva (Trinity College Dublin, Ireland). Period: March 2013-Aug 2014.

- Ahmad-Sharoa, from Electrical Engineering (EE) department of King Abdullah University of Science and Technology-KAUST (Saudi Arabia). Supervisor: Prof. Mohamed Slim-Alouini (KAUST). Master degree topic on: "Resource Allocation in Two-way Relaying and the Adaptive Relaying in Cognitive Radio". Period: May-August 2012, at CTTC Barcelona-Spain.

- Zahed F. Kilani, from Electrical Engineering (EE) department of King Abdullah University of Science and Technology-KAUST (Saudi Arabia). Co-Supervision with: Prof. Mohamed Slim-Alouini (KAUST). Master degree topic on: "Incremental Power Allocation to Maximize per Energy Capacity in Macro-Femtocell environment". Period: May-August 2012, at CTTC Barcelona-Spain.

- Hamza Souri, from Electrical Engineering (EE) department of King Abdullah University of Science and Technology-KAUST (Saudi Arabia). Co-Supervision with: Prof. Mohamed Slim-Alouini (KAUST). Master degree topic on: "Optimal Power Allocation Algorithm for Adaptive Relay Networks in Cognitive Systems". Period: May-July 2011, at CTTC Barcelona-Spain.

- Jaime Peña, from Electrical Engineering (EE) department of King Abdullah University of Science and Technology-KAUST (Saudi Arabia). Co-Supervision with: Prof. Mohamed Slim-Alouini (KAUST). Master degree topic on: "Energy Efficiency Resource Allocation in (Two-tier) Cellular Network". Period: May-July 2011, at CTTC Barcelona-Spain.

- Mahmoud Roumieh from Lebanese University–(UL) of Doctoral School of Science and Technology, Beirut-Lebanon. Co-Supervision with: Dr. Oussama Baazzi. Master degree topic on: "Spectral Sensing for Filter

Bank Multicarrier System and OFDM in Cognitive Radio". Period: January-July 2010, at CTTC Barcelona-Spain.

1.4 PhD Examination and Committee Member

- Juwendo Denis, PhD title: "Resource allocation Frameworks for Multi-Carrier-based Cognitive Radio Networks with full and Statistical CSI", in English. Conservatoire National des Arts et Métiers- CNAM, Paris-France. June 2016.
  Advisor(s): Prof. Didier le Ruyet (CNAM, Paris-France) and Mylène Pischella (CNAM, Paris-France).
  Role: committee member.

- Valentin Rakovic, PhD title: "Spatial Diversity Aspects un Medium Access Control for Cognitive Radio Access", Ss Cyril and Methodius University of Skopje, Faculty of Electrical Engineering and Information technologies, Institute of Telecommunications. May 2016.
  Advisor(s): Prof. Liljana Gavrilovska (University in Skopje), and Prof. Petri Mähönen (RWTH Aachen University, Germany).
  Role: examiner.

- Candidate: Marwa CHAMI. PhD title: "Resource Allocation in Cognitive Radio Systems." in English. Conservatoire National des Arts et Métiers- CNAM, Paris-France. April 2016.
  Advisor(s): Prof. Didier le Ruyet (CNAM, Paris-France) and Mylène Pischella (CNAM, Paris-France).
  Role: committee member.

- Candidate: Laura Beatriz Melián Gutiérrez. PhD title: "Cognitive Radio in HF Communications: Selective Transmission and Broadband Acquisition", in English. Universidad Las Palmas de Gran Canarias, Spain. April 2016.
  Advisor(s): Dr. Ivan Alejandro Pérez Alvarez (Universidad De las Palmas de Gran Canaria, Spain) and Prof. Santiago Zazo (Universidad Politécnica de Madrid-Spain).
  Role: examiner.

- Candidate: Beeshanga Abewardana Jayawickrama. PhD title: "On the Usage of Geolocation Aware Spectrum Measurements in Spectrum Sharing", in English. Macquarie University of Sydney, Australia. October 2015.
  Advisor(s): Prof. Eryk Dutkiewicz (Macquarie University of Sydney, Australia), Dr. Markus Dominik Mueck (Intel Mobile Communications, Germany), and Dr. Ian Oppermann (CSIRO, Australia).
  Role: examiner.

- Candidate: Alberto Padilla Diaz, PhD title: "Synthesis and Design of Dissipative Filters with Improved performances ", In English. Universitat Politècnica de Catalunya-UPC, Barcelona-Spain. End September 2015.
  Advisor(s): Prof. Jordi Mateu Mateu (Universitat Politècnica de Catalunya-UPC, Spain).
  Role: examiner & committee member.

- Candidate: Arman Farhang, PhD title: "Multiuser Communications For Next generation Wireless Networks", in English. Trinity College of Dublin, University of Dublin- Ireland. July 2015.
  Advisor(s): Prof. L. Doyle (Trinity College of Dublin, Ireland) and Dr. N. Marchetti (Trinity College of Dublin, Ireland).
  Role: examiner & committee member.

- Candidate: M.G.S. Sriyananda, PhD title: "Analysis and Performance of FBMC Techniques with Application to Relay Networks", in English. University of Jyväskylä, Finland. July 2014.
  Advisor(s): Prof. R. M. A. P. Rajatheva (University of Oulu Finland), and Prof. T. Hämäläinen and Prof. T. Ristaniemi (both from University of Jyväskylä, Finland).
  Role: examiner.

- Candidate: Lai Jin, PhD title: "Optimizing Channel Sensing and Allocation In Opportunistic Spectrum Access Networks" in English. Macquarie University of Sydney, Australia. July 2013.
  Advisor(s): Prof. Eryk Dutkiewicz (Macquarie University of Sydney, Australia).
  Role: examiner.

- Candidate: Yu Yiwei, PhD title: "Resource Allocation for Next Generation Wireless Networks Subject to Inter Cell Interference" in English. Macquarie University of Sydney, Australia. April 2013.
  Advisor(s): Prof. Eryk Dutkiewicz (Macquarie University of Sydney, Australia).
  Role: examiner.

- Candidate: Ziad Khalaf, PhD title: "Contributions à l'étude de détection des bandes libres dans le contexte de la radio intelligente" in French. Supélec, Rennes-France, February 2013.
  Advisor(s): Dr. Jacques Palicot and Dr. M. Amor Nafkha (both, Supélec, Rennes-France).
  Role: committee member.

- Candidate: Yahia Medjahdi, PhD title: ''Interference Modeling and Performance Analysis of Asynchronous OFDM and FBMC Wireless Communication Systems" in English. Conservatoire National des Arts et Métiers-CNAM, Paris-France. May 2012.
  Advisor(s): Dr. Michel Terré, Dr. Didier Le Ruyet, Dr. Daniel Roviras, all from CNAM (Paris-France).
  Role: committee member.

1.5 R&D Projects participation

1.5.1 Project(s) starting soon

- Project titled: Enhanced PHY for Cellular Low power communication IoT-EPHYL. Project type: French National Research Agency (ANR).
  Duration: Oct 2016- end 2019.
  Role: Main coordinator and researcher at CentraleSupélec.
  Main focus: EPHYL proposes to evaluate and experiment improvements to the new cellular networks that have been emerging in the context of the internet of things (IoT). The project will be based on the extremely active standardization in the field of Cellular IoT that will be closely followed by the industrial partner of the consortium. Then, the research entities will evaluate and propose improvements to these emerging standards considering the physical layer and the radio resource management levels. Coverage aspects, data link quality and energy consumption will be used for comparison as performance criteria. Some of the most promising technologies will be implemented on a prototype and tested within mutual research facility of the French FIT-CorteXlab. The impact of the project will principally be found in innovations where patents,contributions to standardization are to be expected.

1.5.2 Ongoing R&D projects

- Project title : Waveforms MOdels for Machine Type CommuNication inteGrating 5G Networks-WONG5. Project type: French National Research Agency (ANR) with grant agreement code: ANR -15-CE25-0005-03.
  Duration: Jan 2016- end 2019.
  Role : Researcher CentraleSupelec.
  Main focus: project will focus on waveforms (WF) well adapted to the context of Critical Machine Type Communications (C-MTC). For C-MTC, important data rates are necessary together with robust and reliable communications with low latency. Constrains related to consumption and asynchronism are also to be taken into account. Targeted application are Intelligent Transport Systems and Industry 4.0 with autonomous machines (robots, drones, ..). The WF under study are multi-carrier 5G WF (FBMC-OQAM, FMT, GFDM, MC-FTN). MTCWF5 objectives are to study and determine the best WF for C-MTC. Several criteria will be studied on commons C-MTC scenarios. Aspects like adaptation to asynchronism, spectral efficiency, latency, energy efficiency, MIMO techniques and coexistence between C-MTC and other 5G services will be studied.

- Project title: Advanced Waveforms, MAC Design and Dynamic Radio Resource Allocation for D2D in 5G Wireless Networks-ACCENT5. Project type The French National Research Agency (ANR) with grant agreement code: ANR- 14-CE28-0026-02. Duration: 4 years, Dec. 2014 end 2018. Role: Main coordinator and researcher at CentraleSupélec.
  Main focus: Main focus: The project proposes innovative technological approaches for a smooth integration of D2D communication in future (5G) wireless networks. The proposed solutions allow increased data

throughput and dynamic resource allocation in D2D communications in a relaxed and completely omitted synchronization manner in order to satisfy the emerging new data service needs in cohabitation with the existing cellular communications in the same frequency bands. The project will study advanced waveforms to provide additional enhancements to FBMC and OFDM based physical layer performance for D2D. It will define a new MAC layer to include the possibility of D2D communications and considering the characteristics of the waveform defined for D2D transmissions. It will study D2D-related green aspects for 5G systems, including interference reduction and HPA efficiency optimization. Active participation to standardization bodies (i.e., 3GPP) and publications will guarantee a strong dissemination.

- Project title: Broadband Professional Mobile Radio Based on Filter Band Multi-carrier modulation-PROFIL. Project type: The French National Research Agency (ANR-13-INFR-0007-03), France. Duration: 3 years. Starting date: January 2014. Role: Main coordinator and researcher at CentraleSupelec.
  Main focus: aims at contributing to PMR (Professional Mobile Radio) networks evolutions. These networks, which transmit low data bit rate services for public safety and mission critical applications (usually voice), are asked to meet new requirements for larger bit rate transmission (video). Nevertheless these future PMR Broadband services are required (at first) to share channel bandwidths with current (narrow band) PMR services and to access free spaces between these PMR narrow bands. As a consequence a deep study has to be done in order to keep quality of service (especially of currently deployed PMR services) and to meet new requirements.

1.5.3 Completed R&D projects

- PHC (Hubert Curien Partnerships) ULYSSES, French-Irish research mobility program titled: Generalized Frequency Division Multiplexing (GFDM) for the Next Generation Wireless Systems. Partners: IETR-Institut d'Electronique et de Telcommunications de Rennes (SCEE) France, and CTVR Trinity College University of Dublin, Ireland. Code Project: 34151SA. Duration: year 2015.

- FP7 Call 8 EC funded project titled: Network of Excellence in Wireless Communications NEWCOM#, with contract code: FP7-ICT-318306. Project duration: Nov. 2012 to Oct. 2015. Role: SUPELEC researcher.

- FP7 Call 8 EC funded project titled: Enhanced Multi-carrier Techniques for Professional Ad-hoc and Cell Based Communications-EMPhAtiC, with contract code: ICT-318362. Project duration: 2012-2015. Role: General project coordinator and manager. I left the project by end of November 2013.
  Main focus: is to develop, evaluate and demonstrate the capability of enhanced multi-carrier techniques to make better use of the existing radio frequency bands in providing broadband data services in coexistence with narrow band legacy services. The project will address the Professional Mobile Radio (PMR) application, and in particular the evolution of the Public Protection & Disaster Relief (PPDR) service currently using TETRA or other legacy systems for voice and low-speed data services. The core idea is to develop a multi-mode radio platform, based on variable filter-bank processing, which is able to perform modulation/detection functions simultaneously for different signal formats with adjustable centre frequencies, bandwidths and subchannel spacings. SC-FDMA waveforms are included in the study in order to relax the transmitter power amplifier requirements of mobile terminals. Enhanced OFDM solutions are also considered as alternatives aiming at minimal modifications to the 3GPP LTE standard, which serves as the reference system in the studies. In addition to physical layer functionality, the project also develops MIMO and MAC-layer techniques, as well as relay networking solutions which are compatible and maximize the benefits of the waveform level solutions.

- FP7- EC funded Project: Advanced coexistence Technologies for Radio Optimization in Licensed and unlicensed Spectrum-ACROPILIS-NoE (ICT project with code: ICT-2009.1.1) with duration: 2009-2013. Role: project coordinator and main researcher at the CTTC.
  Main focus: The purpose of ACROPOLIS is to link experts from around Europe working on coexistence technologies such as spectrum sharing and cognitive radio, to obtain a rounded complement of European research and to investigate and bolster relevant research areas that are under-represented in the current European research repertoire. Such coexistence technologies within ACROPOLIS are aimed towards the optimization of radio spectrum usage. The main emphasis is to reduce fragmentation in European research in this field, and to translate cognitive communications and other coexistence paradigms into economic benefits.

- Project tiled: Self-Organised FemtoCells for Broadband Services-SOFOCLES. National project funded by Spanish Ministry of Industry, Tourism and Commerce-MITYC, duration: 2011-2013. Main role: main researcher at the CTTC.
  Main focus: project aims to research and develop evolved femtocell technologies that accelerate the cost-effective provision of ubiquitous broadband services by convergence between fixed and wireless broadband. The approach adopted is pragmatic. On the one hand, this project aims at solving the main open issues and concerns related with the expected mid-term massive deployment of femtocells. In this context, non-cooperative femtocells will be considered and issues related with interference management and coexistence with cellular macro system and with other femtocells, admission control, handoff, self-organization for low operational costs, QoS provided by the backhaul, low power consumption, low cost, business model, etc., will be addressed and performance results will be analyzed through system level simulations. On the other hand, it expands the market opportunities for femtocells and facilitates the entrance of new services, by proposing new deployment scenarios like cooperative, networked femtocells, to provide service to big areas like malls, airports, etc., where unprecedented spectrum efficiency will be achieved by means of a novel joint access and wireless backhaul network design. Particular attention will be paid to self-organization of femtocells, supported by machine learning schemes, which is expected to significantly decrease the operational costs and facilitate the scalability of the operator's management of the femto network

- FP7 EC Project titled: Beyond Next Generation Mobile Broadband-BunGee, STREP. (ICT project, EU public funding, duration: 2010-2012). Role: researcher.
  Main focus: BuNGee's goal is to dramatically improve the overall infrastructure capacity density of the mobile network by an order of magnitude (10x) to an ambitious goal of 1Gbps/Km2 anywhere in the cell – thereby removing the barrier to beyond next-generation networks deployment. To achieve this objective, the project will target the following breakthroughs:

  1. unprecedented joint design of access and backhaul over licensed and license exempt spectrum,
  2. unconventional below-rooftop backbone solutions exploiting natural radio isolation,
  3. beyond next-generation networked and distributed MIMO & interference techniques,
  4. protocol suite facilitating autonomous ultra-high capacity deployment.

  To evaluate the effectiveness of these approaches, a high capacity radio cell prototype will be built targeting over 1Gbps/Km2. It shall serve as proof-of-concept in real life scenarios and demonstrate the superiority of BuNGee's architecture for mobile networks.

- EC funded project from FP7 frame work titled: Physical Layer for Dynamic Spectrum Access and Cognitive Radio-ICT-PHYDYAS STREP. Project duration: 2008-2010.
  Main focus: a Physical layer best suited to the new concepts of dynamic access spectrum management and cognitive radio is needed for future efficient wireless and mobile radio networks. The requirements of high data rates and flexible spectrum allocation are met by multicarrier techniques which can approach the theoretical capacity limits in communications. The scheme used so far, Orthogonal Frequency Division Multiplexing (OFDM), is a block processing technique, which lacks flexibility and has poor spectral resolution. In contrast, a filter bank-based multi-carrier (FBMC) technique offers high spectrum resolution and can provide independent sub-channels, while maintaining or enhancing the high data rate capability. In the project, a short term objective is to develop and demonstrate algorithms for single and multiantenna terminals, scalability and adaptability, and multiple access. In the longer term, the impact on cognitive radio will be investigated. FBMC has the potential to fulfill the requirements of the new concepts, but a major research effort is necessary for full exploitation and optimization in all aspects of the radio context. The physical layer is the basis on which the networks are built and, with the numerous scenarios and environments, a complex and coherent set of techniques and algorithms has to be worked out. Therefore, the effort is carried out at the European level, in order to benefit from the vast amount of knowledge and experience available and make the time scale compatible with the on-going or planned standardization actions.

- European COST Action IC0902: Cognitive Radio and Networking for Cooperative Coexistence of Heterogeneous Wireless Networks (EU public funding, duration: 2009-2013). Role: project coordinator at CTTC, Management committee member (MCM) representing Spain, and working group WG1 leader of the COST Action.

Main focus: The main objective of the COST Action IC0902 is to integrate the cognitive concept across all layers of communication systems, resulting in the definition of a European platform for cognitive radio and networks. The Action proposes coordinated research in the field of cognitive radio and networks. The cognitive concept applies to coexistence between heterogeneous wireless networks that share the electromagnetic spectrum for maximum efficiency in resource management. Several efforts are currently in place in European research centers and consortia to introduce cognitive mechanisms at different layers of the communications protocol stack. This Action goes beyond the above trend by integrating the cognitive concept across all layers of system architecture, in view of joint optimization of link adaptation based on spectrum sensing, resource allocation, and selection between multiple networks, including underlay technologies. The cross-layer approach will provide a new perspective in the design of cognitive systems, based on a global optimization process that integrates existing cognitive radio projects, thanks to the merge of a wide-range of expertise, from hardware to applications, provided by over 30 academic and industrial partners.

- Project titled: Mobility Concepts for IMT-Advances- MOBILIA. Project type: EUREKA /CELTIC project funded by Spanish Ministry of Industry, Tourism and Commerce-MITYC. Duration: 2008-2010.
  Role: project coordinator at CTTC, main researcher, and work package leader.
  Main focus: MOBILIA project targets ITU IMT-advanced requirements for future wireless systems, i.e. peak data rates of 100 Mbps for mobile applications and 1 Gbps for low mobility. The IMT-advanced vision of future network as being formed of inter-working access systems will also be considered. A derived target is to obtain an increased aggregate throughput/ user satisfaction vs. existing systems.

- Project titled: WiMAX Base for General Audio & Visual Applications-(Wi4GOAL). Industrial funded project. Duration: 2007-2008. Project coordinator and main researcher at CTTC.

- Project tiled: Cooperative and Cross layer Techniques for Wireless Sensor Networks-(PERSEO). National project funded by Spanish Ministry of Industry, Tourism and Commerce-MITYC, duration: 2007-2009.
  Role: researcher at the CTTC.
  Main focus: The PERSEO aims to contribute to technical innovation by exploiting the potential of cooperative transmission and cross-layer techniques for wireless sensor networks. The main objectives of the project are:

  1. Definition of a network stack architecture able to accommodate a rich variety of sensor devices and applications.
  2. Analysis of possible Cross-Layer techniques that can be used in order to enhance the efficiency of wireless sensor networks.
  3. In-depth study of the potential benefits that can be obtained from using these techniques in different environments.
  4. Study of energy saving techniques based on cooperative diversity.
  5. Study of virtual MIMO (multiple input – multiple output) channels using individual SISO antennas of the sensor devices.
  6. Development of advanced, decentralized, self-organized MAC protocols that guarantee certain QoS for different scenarios.
  7. A demonstrator with standard wireless sensor devices will be implemented to assess the proposed algorithms in a real scenario.

- Project titled: Wireless System Providing High Quality of Service- (WISQUAS). Project type: EUREKA/CELTIC/ National project funded by Spanish Ministry of Industry, Tourism and Commerce-MITYC.
  Role: project coordinator at CTTC, and main researcher.
  Duration: 2005-2007.
  Main focus: The WISQUAS project aims at enabling multimedia services in future wireless networks. On the one hand, wireless bandwidth is a scarce resource. On the other hand, users want terminals to be light and consume minimal power. Within these constraints, a wide variety of multimedia services are desired. Thereto, current wireless systems need to be upgraded to offer:

  – Higher data rates, More flexibility, and Quality of Service (QoS) provisions

These goals can only be achieved by focusing the research on new solutions at the physical layer and at the same time meet the QoS requisites of higher layers. To fulfil the above needs, innovative research needs to be performed and demonstrated on the following topics:

– System specification and innovative design flow to allow cross-layer optimization,

Advanced physical-layer air interfaces, featuring flexibility, scalability, adaptivity, high capacity and bandwidth efficiency, Advanced protocols and architectures for QoS at higher layers, and System integration and validation.
WISQUAS aims at playing a key role in providing the enabling technologies for the future wireless multimedia communications, by conceiving excellent fast physical layers, and appropriate higher layers that can bring the

- Project title: Intelligent radio Resource Management for High-Speed Ad-hoc Networks Through the Development of Technique of Fuzzy Logic, Signal processing and Media Access Control Protocols- (GIRAFA). Project type: Public funding, from Spanish Minister of Science and Technologies-CYCIT. Project code: TIC 2002-04594-C02-02.
  Duration: 2002-2005.
  Main role: project coordinator at CTTC.
  Main focus: This project deals with the interference problem in WLAN networks in a novel way, i.e. the intelligent radio resource management. Intelligent management involves: on one hand, (i) not only using traditional signal processing techniques or classical medium access protocols, but also the deployment of fuzzy logic techniques. On the other hand, (ii) the development of adaptive/reconfigurable algorithms depending on the scenario, which may adapt the requirements on Quality of Service (QoS) without losing the communication and finally (iii) the joint resource optimization between physical and link layers.

- EC funded project FP5 titled: Academic Network for Wireless Internet Research in Europe (IST-ANWIRE). Project type: NoE.
  Duration: 2002-2004.
  Role: Researcher at CTTC.
  Main focus: ANWIRE is a thematic network established by academic and research institutions from various countries of the EU acting in two main overlapping research tracks: Wireless Internet and Reconfigurability. ANWIRE aims at organizing and coordinating parallel actions in key research areas of Wireless Internet and Reconfigurability, in order to encompass research activities towards the design of a fully integrated system; and at promoting and disseminating Wireless Internet and Reconfigurability solutions, in order to make them available to the research and industrial community. -

- FP4 European Project: MC-CDMA Transmission Techniques for Integrated Broadband Cellular Systems- (IST-MATRICE). Project type: STREP. Public funding, duration: 2001-2003 (I left the project by end of 2002).
  Role: researcher at Polytechnic University of Madrid-UPM, Spain.
  Main focus: aims at defining a methodology for the performance evaluation of a Beyond 3G radio interfaces based on MC-CDMA.

- Project title: Analysis of Transmission and Radio Propagation Conditions for UTRA, Industrial contract with Alcatel, Spain.
  Duration: 1999-2000.
  Role: researcher at Universidad Politécnica de Madrid-UPM, Madrid-Spain.

1.6 Services

1.6.1 Chairing Events

- **General Track Chair** of "Cognitive Radio and Spectrum Management," at the IEEE Vehicular Technology Conference [VTC'2017-Spring], Sydney, Australia. June 2017.

- **General Co-Chair** of Workshop on, Cognitive Radio and Innovative Spectrum Sharing Paradigms for Future Networks [CRAFT2016], at 27th Annual IEEE International Symposium on Personal, Indoor and Mobile radio Communications [PIMRC'2016]. Valencia, Spain. September 2016.

- **TPC Co-Chair** of the fourth International Workshop on Next Generation Green Wireless Networks [Next-GWING'2016], Dublin, Ireland. September 2016.
- **General Co-Chair** of Twelfth International Symposium on Wireless Communications Systems [ISWCS'2015] conference, Brussels, Belgium. 26-29 August 2015.
- **General Chair** of Eleventh International Symposium on Wireless Communications Systems [ISWCS'2014] conference, Barcelona, Spain. 26-29 August 2014.
- **General co-Chair** of the Workshop on "Advanced Multi-carrier Waveforms and Mechanisms for Future Ad-Hoc and Cell-Based Systems", jointly organized with the 10th International Symposium on Wireless Communication Systems Conference, [IEEE ISWCS'2013], Ilmenau, Germany, August, 2013.
- **Special Sessions co-Chair** at 20th International Conference on Telecommunications [IEEE ICT 2013] 6-8 May 2013 Casablanca Morocco.
- **General Co-Chair** of the 2nd International Workshop of the COST Action IC0902 on: "Cognitive Radio and Networking for Cooperative Coexistence of Heterogeneous Wireless Networks". Castelldefels-Barcelona, Spain. 5-7 October 2011.
- **Session Chair** of "Innovations in Cognitive Technologies" session at the Cognitive Radio and Innovative Spectrum Sharing Paradigms for Future Networks (CRAFT'2016), Valencia, Spain. September 2016.
- **Session Chair**: R9 on; "Spectrum Sensing for Cognitive Radio", at the 9th International Symposium on Wireless Communication Systems [IEEE ISWCS'2012], Paris, France, 28-31 August 2012.
- **Special Session Chair**: on "Advances on Cognitive Radio and Learning Mechanisms", at the 9th International Symposium on Wireless Communication Systems [IEEE ISWCS'2012] , Paris, France, 28-31 August 2012.
- **Session Chair**: on "Cognitive Radio Systems" Session -CRSM9, at the IEEE 22nd International Symposium on Personal, Indoor and Mobile Radio Communications [IEEE PIMRC'2011]. Toronto, Canada. September 2011.
- **Special Session Chair** on: Technical Enablers and Platforms for Cognitive Radio Session, at the 19th European Signal Processing Conference [EUSIPCO'2011] in Barcelona, Spain. September 2011.
- **Special Session Chair** on: Wireless Communications Track 3 Session, at the 17th IEEE International Conference on Telecommunications [IEEE ICT'2010]. Doha-Qatar. April 2010.
- **Special Session Chair** on: Cognitive Radio Network I Session, at the IEEE Wireless Communications and Networking Conference [IEEE WCNC'2010], Sydney, Australia. April 2010.
- **Session Chair** on: MAC-LTE, at the IEEE Wireless Communications and Networking Conference [IEEE WCNC'09], Budapest, Hungary. April 2009.
- **TCP General Chair**, at 1st IEEE International Workshop on Broadband Wireless Network Communications Performance [BWNCP'09], Phoenix, Arizona, USA. December 2009.
- **Session Chair**: 2D: OFDM II session, at the IEEE Vehicular Technology Conference [IEEE VTC-Spring'09], Barcelona, Spain. April 2009.
- **Sponsorships Chair** at IEEE Create-Net Conference on Testbeds and Research Infrastructures for the Development of Networks and Communities, (TridentCom'2006), Barcelona. Spain

1.6.2 Organization of Special Sessions

- Special session on: "Using Cognitive Radio to Achieve Green Radio Networks", at the IEEE International Workshop on Cognitive Cellular Systems [CCS'2014]. Rhine River, Germany | September 2-4, 2014.
- Special session on: "Advances on Cognitive Radio and Learning Mechanisms", at the 9th International Symposium on Wireless Communication Systems [ISWCS'2012], Paris, France, 28-31 August 2012.
- Special session on: "Cognition in Green Next Generation Networks", at the Eighth International Symposium on Wireless Communication Systems [ISWCS'2011]. Aachen, Germany, 6th - 9th November, 2011.
- Special session on: Technical Enablers and Platforms for Cognitive Radio, at the 19th European Signal Processing Conference [EUSIPCO'2011] in Barcelona, Spain. September 2011.
- Special session on: "Mobility Concepts and IMT-advanced-MOBILIA" at the 6th International Mobile Multimedia Communications Conference |MobiMedia]. Aveiro, Portugal. September 2010.
- Special session on: "Filter Bank Multi-Carrier PHY versus OFDM for Unsynchronized Cognitive Radio Networks" at the 5th International Conference on Cognitive Radio Oriented Wireless Networks and Communications [CrownCom'2010], Canne, France. June 2010.
- Special session on: "Mobility Concepts and IMT-advanced-MOBILIA" at the 2nd International Conference on Mobile Lightweight Wireless Systems (MOBILIGHT'2010). Barcelona, Spain. May 2010.

1.6.3 Editor

- Editorial Board Member of Transactions on Emerging Telecommunications Technologies (ETT) Wiley&Sons Journal (since 2013).
- Lead guest editor of special issue on: "*Future Evolution of Public Safety Communications in the 5G Era*," in Transactions on Emerging Telecommunications Technologies - ETT Wiley Journal (formerly known as European Transactions on Telecommunications Journal), December 2015.
- Guest editor of special issue on: "*Advances in Flexible Multi-carrier Waveforms for Future Wireless Communications*", in EURASIP Journal on Advances on Signal Processing (ASP), November 2013.
- Lead guest editor of special issue on: "*Cognitive Radio in Emerging Communications Systems - Small Cells, Machine-to-Machine Communications, TV White Spaces, and Green Radios*", in Wiley Journal Transactions on Emerging Telecommunications Technologies - ETT (formerly known as European Transactions on Telecommunications Journal), December 2012. Published Nov 2013 at: http://onlinelibrary.wiley.com/doi/10.1002/ett.v24.7-8/issuetoc
- Guest editor of Special issue on: "*Filter Banks for Next Generation Multi-carrier Wireless Communications*" in EURASIP Journal on Advances on Signal Processing (JASP), May 2009.
- Lead Guest editor of Special issue on: "*Simulators and Experimental Testbeds Design and Development for Wireless Networks*", in EURASIP Journal on Wireless Communications and Networking (JWCN), June 2009.

1.6.4 Panels and Invited keynotes

- Invited talk on: **"Candidate Multi-carrier Waveforms for Future 5G Communication System-Why Do we Look for Beyond OFDM Systems?"**, at Centre de Developement des Technologies Avancées - CDTA, Algiers- Algeria, April 2016.
- Invited Keynotes on: **" Current PMR Status, Migration, and Flexible Waveform for an Evolution to Broadband LTE-like Scheme for Public Safety Communications"**, at the IoE^2 Lab University College Dublin (UCD), Dublin-Ireland, 16 Oct 2015.
- Invited keynotes on: **"Why Looking for Beyond OFDM in 5G Wireless Network Systems?"**, at CTVR Lab, Trinity College, University of Dublin, July 2015.

- Keynote on **"Why Looking for Beyond OFDM in 5G Wireless Network Systems ?"**, at The 8th International Wireless Internet Conference-Symposium on Wireless and Vehicular Communications- WICON'2014. November 13–14, 2014. Lisbon, Portugal.
- Invited Panelist on: **"Transition from Static Frequency Management to a Dynamic Frequency Management (DFM) in the Military Context"**, at the Cognitive Radio Workshop of the "Military Communications and Information Systems Conference" (MCC'2013), Saint Malo-France. 7th-9th October 2013.
- Invited talk on: **"Tecnología y Regulación en Sistemas de Comunicación"** (in Spanish), at the 10th Anniversary of Barcelona Digital Global Congress, 20th-22nd of May 2008. Barcelona, Spain.
- Invited talk on: **"Key notes on: New Opportunities for Spectrum Sharing and Cognitive Radio"**, at Joint public workshop on Cognitive Radio and Spectrum Sharing Strategies for Wireless Broadband, COST 095 -TERRA at Thessaloniki, Greece. 17th-19th April 2013.
- Chair and Panel organizer on:**"Cognitive Radio Networks: Operators Perspective,"** at 2nd International Workshop of the COST Action IC 0902 on: "Cognitive Radio and Networking for Cooperative Coexistence of Heterogeneous Wireless Networks". Castelldefels-Barcelona, Spain. 5th-7th October 2011.
- Invited Panelist on: **"Practical Scenarios and Opportunities for Future Cognitive Radio Systems"**, in Workshop on "Cognitive Radio and Networking: Challenges and Solutions Ahead" at IEEE PIMRC-WS-CRN, Toronto, Canada 2011.

1.6.5 Technical Program Committee (TPC) Member

- **2016**: at, IEEE WCNC, CROWNCOM, IEEE ISWCS, IEEE VTC-Spring, IEEE PIMRC, IEEE GLOBECOM.
- **2015**: at,IEEE ICC, IEEE VTC'fall, IEEE VTC-Spring, IEEE PIMRC, IEEE ICUWB.
- **2014**: at,IEEE ICC, IEEE ITS, IEEE CSS, IEEE WCNC, IEEE GLOBECOM, IEEE MELECON ICT, ICUWB, EUCNC, IEEE VTC-Fall.
- **2013**: at,IEEE WCNC, IEEE ICC, IEEE ICUWB, FuNMS, IEEE VTC-Spring, IEEE ICCIT, IEEE ISWCS, IEEE ICT, IEEE VTC-Fall, IEEE PIMRC, IEEE GlobalSIP.
- **2012**: at,IEEE ISCIT, IEEE PIMRC, CIP, IEEE ISWCS, IEEE WCNC, IEEE IWCRN, IEEE CAMAD.
- **2011**: at,IEEE PIMRC, EUSIPCO, ACC, MOBIMEDIA, ICWMC, MONAMI, MOBILITY, IEEE ICC.
- **2010**: at,MONAMI'2010.
- **2009**: at,IEEE BWNCP, MWNS, IEEE VTC-Spring.
- **2008**: at,IEEE WiMob, MIC-CSC.
- **2007**: at,M-SISP, IEEE VTC-Spring, IEEE ICSPC.
- **2006**: at,IEEE MWC.

Chapter 2

Scientific Production

2.1 Publications

In this chapter you have all my scientific production to the date in terms of journals, magazines, papers in national or international conferences, in workshops, and in standardization working groups. The hereafter indexes: [JX], [CBX], [CX], and [OX] refer to: journal, chapter book, conference, and other publication respectively. The "X" is referring to the publication number. The list does not include technical reports or deliverable related with the R&D projects listed in Subsection 1.5, page 22. The publications are sorted from the most recent to less recent paper.

2.1.1 In Journals

In this Subsection are listed my publications in different transactions and magazines.

[J26] - Faouzi Bader, Laurent Martinod, Gianmarco Baldini, Fred Frantz, Sithamparanathan Kandeepan, and Oriol Sallent, "Future Evolution of Public Safety Communications in the 5G Era", (editorial) at the Transactions on Emerging Telecommunications Technologies-ETT Journal, doi: 10.1002/ett.3101. year 2016.

[J25] - Marwa Chafii, Jacques Palicot, Rémi Gribonval, and Faouzi Bader, "A Necessary Condition for Waveforms with Better PAPR than OFDM", IEEE Transactions on Communications, vol. 64, issue: 8, pp. 3395-3405, doi 10.1109/TCOMM.2016.2584068, August 2016.

[J24] - Vincent Savaux, Faouzi Bader, and Jacques Palicot, "OFDM/OQAM Blind Equalization Using CNA Approach", IEEE Transactions on Signal Processing, vol. 64, issue 9, pp.2324-2333, doi: 10.1109/TSP.2016.2519000, May 2016.

[J23] - Vincent Savaux, Faouzi Bader, and Jacques Palicot, "Correcting CNA Phase Mismatch Phenomena in Frequency Blind Equalization for OFDM Systems", Elsevier Signal Processing Journal, vol. 127, pp. 227–238, doi: 10.1016/j.sigpro.2016.02.024, October 2016.

[J22] - Lamarana Mamadou Diallo, Jacques Palicot, and Faouzi Bader, "A Step Forward on Adaptive Iterative Clipping Approach for PAPR Reduction in OFDM System," IARIA International Journal on Advances in Telecommunications, vol 9, no 1&2, 2016.

[J21] Laura Melian-Gutierrez, Navikkumar Modi, Christophe Moy, Faouzi Bader, Ivan Pérez-Alvarez, and Santiago Zazo "Hybrid UCB-HMM: A Machine Learning Strategy for Cognitive Radio in HF Band", IEEE Transactions on Cognitive Communications and Networking, vol. 1, issue: 3, pp. 347-358, doi: 10.1109/TCCN.2016.2527021, September 2015.

[J20] - Vincent Savaux, Faouzi Bader and Yves Louët, "A Joint MMSE Channel and Noise Variance Estimation for OFDM/OQAM Modulation", IEEE Transactions on Communications, vol. 63, issue:11, pp. 4254-4266, doi 10.1109/TCOMM.2015.2476798. November 2015.

[J19] -Mohammed El-Absi, Musbah Shaat, Faouzi Bader, and Thomas. Kaiser, "Interference Alignment with Frequency-Clustering for Efficient Resource Allocation in Cognitive Radio Networks". IEEE Transactions on Wireless Communications, vol. 14, issue: 12, pp. 7070-7082, doi: 10.1109/TWC.2015.2464371. December 2015.

[J18] - Vinsant Savaux, and Faouzi Bader, "Mean Square Error Analysis and LMMSE Application for Preamble-Based Channel Estimation in OFDM/OQAM Systems", IET Communications Journal, vol. 9, issue: 14, pp. 1763-1773, doi: 10.1049/iet-com.2014.1181, September 2015.

[J17] - Sener Dikmese, Sudharsan Srinivasan, Musbah Shaat, Faouzi Bader, and Markku Renfors, "Spectrum Sensing and Resource Allocation for Multicarrier Cognitive Radio Systems under Interference and Power Constraints". EURASIP Journal on Advances on Signal Processing, doi: 10.1186/1687-6180-2014-68. May 2014.

[J16] - Hamza Soury, Faouzi Bader, Musbah Shaat, and Mohamed-Slim Alouini, "Joint Subcarrier Pairing and Resource Allocation for Cognitive Networks with Adaptive Relaying", EURASIP Journal on Wireless Communications and Networking. Doi: 10.1186/1687-1499-2013-259. November 2013.

[J15] Faouzi Bader, Panagiotis Demestricas, Luiz DaSilva, and Hiroshi Harada, "Cognitive Radio in Emerging Communications Systems - Small Cells, Machine-to-Machine Communications, TV White Spaces, and Green Radios" (editorial), at Transactions on Emerging Telecommunications Technologies - (ETT), Wiley&Sons Journal, doi: 10.1002/ett.2732, October 2013.

[J14] - Ahmad Alsharoa, Faouzi Bader, and Mohamed-Slim Alouini, "Relay Selection and Resource Allocation for Two Way DF-AF Cognitive Radio Network". IEEE Wireless Communications Letters (WCL), vol. 2, issue: 4, pp. 427-430, doi: 10.1109/WCL.2013.13.130211. August 2013.

[J13] - Jaime Peña Leon, Faouzi Bader, and Mohamed Slim Alouini, "Analysis of Handoff Strategies in Macro-Femto Cells Environment Based on Per-Energy Capacity". IET Communications Journal, vol. 6, issue 14, pp. 2218-2227, doi: 10.1049/iet-com.2011.0810. year 2012.

[J12] - V. Stavroulaki, A. Bantouna, Y. Kritikou, K. Tsagkaris, P. Demestichas, P. Blasco, Faouzi Bader, M. Dohler, D. Denkovski, V. Atanasovski, L. Gavrilovska, and K. Moessner, "Learning and Knowledge Management Toolbox for Cognitive Radio Network Applications, at special issue on: Applications of Cognitive Radio Networks", IEEE Vehicular Technology Magazine, vol. 7, issue 2, pp. 91-99, doi: 10.1109/MVT.2012.2190196. June 2012.

[J11] - Musbah Shaat and Faouzi Bader, "Asymptotically Optimal Resource Allocation in OFDM-Based Cognitive Networks with Multiple Relays", IEEE Transactions on Wireless Communications, vol.11, issue 3, doi 10.1109/TWC.2012.011012.110880. March 2012.

[J10] - Musbah Shaat and Faouzi Bader, "Efficient Resource Allocation Algorithm for Uplink in Multicarrier Based CR Networks with Fairness Consideration", IET Communications Journal, vol. 5, issue 16. pp. 2328-2338, doi: 10.1049/iet-com.2010.1062. November 2011.

[J9] - Faouzi Bader, Musbah Shaat, "Pilot Pattern Design for PUSC MIMO WiMAX-like Filter Banks Multi-carrier System", at IARIA International Journal On Advances in Telecommunications 2011, vol 4, no. 1 and 2. January to June 2011.

[J8] - Nizar Zorba and Faouzi Bader, "Spatial Diversity Scheme to Efficiently Cancel ISI and ICI in OFDM-OQAM Systems", EURASIP Journal of Computer Systems, Networks, and Communications, vol. 2010, doi:10.1155/2010/57624. October 2010.

[J7] -Markku Renfors, Pierre Siohan,Behrouz Farhang-Boroujeny, Faouzi Bader, "Filter Bank for Next Generation Multi-carrier Wireless System", EURASIP Journal on Advances on Signal Processing (ASP)-(editorial). Vol. 2010, doi: 10.1155/2010/314193. May 2010.

[J6] - Faouzi Bader, Guillame Chelius, Christian Ibars, Mohamed Ibnkahla, Nikos Passas,and Arnd-Ragnar Rhiemeier, "Simulators and Experimental Testbeds Design and Development for Wireless Networks", EURASIP Journal on Wireless Communications and Networking, Vol. 2010, Article ID 603970, doi:10.1155/2010/603970 (editorial). May 2010.

[J5] - M. Shaat, Faouzi Bader, "Computationally Efficient Power Allocation Algorithm in Multi-carrier Based Cognitive Radio Networks: OFDM and FBMC Systems", EURASIP Journal on Advanced Signal Processing (ASP). Vol. 2010, Article ID 528378, 13 pages, doi:10.1155/2010/528378. March 2010.

[J4] - I. Gutiérrez, Faouzi Bader, R. Aquilué, and J. L. Pijoan, "Contiguous Frequency-Time Resource Allocation and Scheduling for Wireless OFDMA Systems with QoS Support", EURASIP Journal on Wireless Communications and Networking, Vol. 2009, Article ID 134579, doi:10.1155/2009/134579, June 2009.

[J3] - M. S. O' Droma, I. Ganchez, M. Siebert, Faouzi Bader, H. Chaouchi, I. Armuelles, I. Demeure, F. McEvoy, "A 4G ANWIRE Generic System and Service Integration Architecture". Mobile Computing and Communications Review -MC2R. Vol 10, nº1, pp. 13-30. January 2006.

[J2] - Nikos Passas, Sarantis Paskalis, Alexandros Kaloxylos, Faouzi Bader, Renato Narcisi, Evangelos Tsontsis, and Adil S. Jahan, "Enabling Techologies of Always Best Connected Concept". Wiley&Sons, Wireless Communications & Mobile Computing Journal. No 5, Issue 2, pp. 175-191, doi: 10.1002/wcm.207. August 2004.

[J1] - S. Zazo, Faouzi Bader, J. M. Páez Borrallo, "Spread Spectrum OFDM Modem for HF Voice Band Link over Fading Channels". The European Transaction on Telecommunications-ETT. Vol. 11, issue 6, doi: 10.1002/ett.4460110610. pp. 593–598, November/December 2000.

2.1.2 Books Edited

I was involved from 2012 to 2014 in the edition of three books. The focus of the below referred book [**B1**], was on the exhibition of part of my research works on "Scheduling and Resource Allocation," and those of my close collaborations with the chapters' co-authors of this book. The book [**B2**] and book [**B3**], are the result of several years of close collaboration with different partners of the European COST Action IC0902 research project in the field of cognitive radio and cooperative networks, and spectrum access (see details in subsection 1.5.3).

[**B1**] Book title: Advances on Processing for Multiple Carrier Schemes: OFDM & OFDMA. Editors: F. Bader and N. Zorba (CTTC, Barcelona-Spain).
Editorial: Series: Computer Science, Technology and Applications. Nova Science Publishers, ©2012. ISBN: 978-1-61470-634-2.
Content Level: Research.
Table of contents:
Introduction to Wireless Multi-Carrier Schemes, Peak-to-Average Power Ratio Issues for Pulse-Shaped Multi-carrier Modulations, Synchronization in OFDM Based Systems, Channel Estimation, Channel Coding and Equalization, Adaptive Modulation and Predistortion Techniques Over Nonlinear Fading Channels, Scheduling and Resource Allocation, MIMO-OFDM Applications for Satellite Communications, Medium Access Control Layer, Performance Evaluation of Mobile WiMAX System, 3GPP-Lte Cellular System.

[**B2**] Book title: Cognitive Communication and Cooperative HetNet Coexistence-Selected Advances on Spectrum Sensing, Learning, and Security Approaches (book I). Editors: Maria Gabriella Di Benedetto (Sapienza University of Rome-Italy) and Faouzi Bader (Supélec-France).
Editorial: Signals and Communication Technology Series of Springer International Publishing (SIP), Copyright ©2014. Book doi: 10.1007/978-3-319-01402-9, ISBN 978-3-319-01402-9. January 2014 (with peer reviewed process per chapter).
Content Level: Research.
Number of Pages: 365.
Table of contents:
Recent Advances on Wide-band Spectrum Sensing for Cognitive Radio.- Complexity of Spectrum Activity and its effect on Opportunistic Access.- Analysis and Optimization of Energy Detection for Non-Flat Spectral Characteristics.- Spectrum Sensing Algorithms for Cognitive White-Space Systems.- New Blind Free Bands Detectors Exploiting Cyclic Autocorrelation Function Sparsity.- Intersystem Coexistence and Cooperation Through Cognitive Control Channels.- Cooperative Spectrum Sensing with Censoring of Cognitive Radios in Rayleigh Fading Under Majority Logic Fusion.- Medium Access Control in Cognitive Impulse Radio UWB networks.- Integration of Heterogeneous Spectrum Sensing Devices Towards Accurate REM Construction.- Cellular Coverage Optimization: A Radio Environment Map for Minimization of Drive Tests.- Use of Learning, Game Theory and Optimization as Biomimetic Approaches for Self-Organization in Macro-Femtocell Coexistence - Detection of Primary user Emulation (PUE) Attacks Based on Cooperative Localization.- Cognition as a tool for Green Next generation Networks.- Testbeds

and Implementation Issues.

[B3] Book title: Cognitive Communication and Cooperative HetNet Coexistence-Recent Advances and Visions for the Future (book II). Editors: Maria Gabriella Di Benedetto, Andrea Fabio Cattoni, Jocelyn Fiorina, Faouzi Bader, Luca De Nardis.
Editorial: Signals and Communication Technology Series of Springer International Publishing (SIP), Copyright ©2014. (with peer reviewed process per chapter). ISBN 978-3-319-01718-1.
Content Level: Research.
Number of Pages: 450.
Table of contents:
New Types of Air Interface based on Filter Banks for Spectrum Sharing and Coexistence.- Cognitive Interference Alignment for Spectral Coexistence.- Cooperative Spectrum Sensing.- Medium Access Control Protocols in Cognitive Radio Networks.- Dynamic Channel Selection for Cognitive Femtocells.- Towards Cognitive Internet: an Evolutionary Vision.- Automatic best wireless network selection based on Key Performance Indicators.- Localization in Cognitive Radio Networks.- Challenges Towards a Cloud-RAN Realization.- A Regulatory Perspective on Cognitive Radio and Spectrum Sharing.-Simulation of Cognitive Radio Networks in OMNeT++.- Designing a CR Test bed - Practical Issues.- Low-cost testbed development and its applications in cognitive radio prototyping.

[B4] Book title: Orthogonal Waveforms and Filter Banks for Future Communication Systems. Editors: Markku Renfors, Xavier Mestre, Eleftherios Kofidis, and Faouzi Bader.
Editorial: ELSEVIER INC (with peer reviewed process per chapter).
Expected publication: June 2017.
Content Level: Research.
Number of Pages: 450.
Table of contents:
Part 1: Application drivers
New Waveforms for New Services in 5G, TVWS as an Emerging Application of Cognitive Radio, Broadband PMR/PPDR, Optical Communications.
Part 2: FBMC basics
Multirate Signal Processing and Filter Banks, Filter Banks for Software Defined Radio, Orthogonal Communication Waveforms, FBMC Design and Implementation.
Part 3: FBMC Signal Processing
FBMC Over Frequency Selective Channels, FBMC Synchronization Techniques, FBMC Channel Estimation Techniques, FBMC Channel Equalization Techniques.
Part 4: Multiantenna and multiuser techniques
MIMOFBMC Precoding and Beamforming, MIMOFBMC Receivers, SpaceTime Coding for FBMC, Distributed and Cooperative FBMC Systems, FBMC Multiple Access.
Part 5: Implementation
High Power Amplifier Effects and Peak to Average Power Ratio Mitigation, FBMC Implementation of a TVWS System, The EMPhAtiC Demonstrator of an FBMCbased PMR System: Design, Implementation and Results.

2.1.3 Book Chapters

[CB14] - Musbah Shaat and Faouzi Bader, Channel Assignment and Power Allocation Algorithms in Multi-carrier Based Cognitive Radio Environment. Book: Cognitive Communications: Distributed Artificial Intelligence (DAI), Regulatory Policy & Economics, Implementation. Eds. David Grace and Honggang Zhang. ©Wiley. ISBN: 978-11-199-5150-6.

[CB13] - Ismael Gutierrez, Faouzi Bader, Chapter on: Space-Time Adaptation and MIMO Standardization Status. Book: Advanced Transmission Techniques in WiMAX, edited by: Roberto C. Hincapie, Javier E. Sierra, and Roberto Hincapie, ©INTECH Publisher January 2012, ISBN 978-953-307-965-3.

[CB12] - Ismael Gutierrez, Faouzi Bader, Chapter: Scheduling and Resource Allocation . Book title: Advances on Processing for Multiple Carrier Schemes: OFDM & OFDMA, edited by: Faouzi Bader and Nizar Zorba, NOVA Publisher 2011, ISBN: 978-1-61470-634-2.

[CB11] - M. Shaat, F. Bader, Power Allocation with Interference Constraint in Multi-carrier Based Cognitive Radio Systems. Book Title: Multi-Carrier Systems and Solutions. Chapter 4: Adaptive Transmission .Eds. Plass, S.; Dammann, A.; Kaiser, S.; Fazel, K. Springer ©2009. ISBN: 978-90-481-2529-6 (HB). Netherlands.

[CB10] - I. Gutierrez, F. Bader, A. Mourad, J. L. Pijoan, Transmit Antenna and Space-Time Code Selection for Downlink MIMO System. Book title: Multi-Carrier Systems and Solutions. Chapter 2: Multiple-Input and Multiple-Output (MIMO).Eds. Plass, S. Dammann, A. Kaiser, S. Fazel, K. Springer ©2009. ISBN: 978-90-481-2529-6 (HB). Netherlands.

[CB9] - N. Zorba, S. Pfletschinger, F. Bader, Increasing the Performance of OFDM-OQAM Communication Systems through Smart Antennas Processing. Editors: Fabrizio Granelli, Charalabos Skianis, Periklis Chatzimisios, Yang Xiao, Simone Redana. Book title: Mobile Lightweight Wireless Systems, pp.315-324. Springer ©2009 ISBN-13 978-3-642-03818-1.

[CB8] - I. Gutierrez, F. Bader, J. Pijoan, Cross-Layer Design for Resource Allocation under QoS Requirements for Multiuser SS-MC-MA Systems, Editors: Thomas Magedanz, Markus Muek, et al. Book title: Middleware Technologies for Enabling Next Generation Network Services and Applications. Chapter: NGN Networking and Security, pp123-136. ISBN-13 978-3-930736-12-6. Edition Multicon Verlag,©copyright 2008.

[CB7] - I. Gutierrez, F. Bader, J. L. Pijoan, Radio Resource Allocation in MC-CDMA Under QoS Requirements. Book title: Multi-Carrier Spread Spectrum 2007. Chapter 5: Adaptive Transmission, pp. 207-216. Ed.: S. Plass, A. Dammann, S. Kaiser and K. Fazel, Springer ©2007. ISBN: 978-1-4020-6128-8. Netherlands.

[CB6] - S. Pfletchinger, F. Bader, OFDMA with Subcarrier Sharing. Book title: Multi-Carrier Spread Spectrum.Chapter 5: MIMO and Adaptivity, pp. 319-326. Ed. Springer ©copyright 2006, ISBN: 10 1-4020-4435-6(HB). Netherlands.

[CB5] - F. Bader, Pilot Time-Frequency Location Adjustment in OFDM Systems Based on Channel Variability Parameters. Chapter 4: Channel Estimation, pp. 257-264. Book tile: Multi-Carrier Spread Spectrum. Ed. Springer ©copyright 2006, ISBN:101-4020-4435-6(HB) [8]. Netherlands.

[CB4] - F. Bader, S. Zazo, Synchronism Loss Effect on the Signal Detection at the Base Station Using an OFDM-CDMA Systems. Book: Multi-Carrier Spread Spectrum. Editor(s): Khaled Fazel and Stephan Kaiser. Chaper 05: Multiplexing, Detection & Interference Cancellation .pp. 421-428. Ed. Kluwer Academic Publisher- KAP ©2004. ISBN-1-4020-1837-1.

[CB3] - F. Bader, S. Zazo, P. Borrallo, Decorrelation MUD for MC-CDMA in an Uplink Transmission Mode. Book: Multi-Carrier Spread Spectrum & Related Topics. Editor(s): Khaled Fazel and Stefan Kaiser. Ed Kluwer Academic Publishers -KAP © 2002. ISBN-0-7923-7653-6.

[CB2] - F. Bader, S. Zazo, P. Borrallo, MUD Improvement by Using Hexagonal Pilot Distributions for Multi-channel Acquisition and Tracking in MC- CDMA. Book: Multi-Carrier Spread Spectrum & Related Topics. Editor(s): Khaled Fazel and Stefan Kaiser. Ed. Kluwer Academic Publishers -KAP ©2000. ISBN-0-7923-7740-0.

[CB1] - S. Zazo, F. Bader, P. Borrallo, On the Improvement of HF Multi-Carrier Modem Behaviour by Using Spread Spectrum. Book: Multi-Carrier Spread Spectrum & Related Topics. Editor(s): Khaled Fazel and Stefan Kaiser. Ed. Kluwer Academic Publishers -KAP ©2000. ISBN-0-7923-7740-0.

2.1.4 In Conferences

Following are listed all my publications in national and international conference with peer review process.

[C106] - Conor Sexton, Quentin Bodinier, Arman Farhang, Nicola Marchetti, Faouzi Bader, and Luiz DaSilva, "Coexistence of OFDM and FBMC for Underlay D2D Communication in 5G Networks", in Proc. of the IEEE Global Communications Conference (Globecom'2016). Washington DC, USA, December 2016.

[C105] -Quentin Bodinier, Faouzi Bader, and Jacques Palicot, "Coexistence in 5G: Analysis of Cross-Interference between OFDM/OQAM and Legacy Users", in Proc. of the IEEE Global Communications Conference (Globecom'2016). Washington DC, USA, December 2016.

[C104] - Vincent Savaux, Faouzi Bader, and Malek Naoues, "Blind Equalization using Constant Modulus Algorithm Adapted to OFDM/OQAM Modulation", at the IEEE International Symposium on Wireless Communication Systems (ISWCS'2016), Poznan, Poland, Sept 2016.

[C103] - Quentin Bodinier, Faouzi Bader, and Jacques Palicot, "Coexistence of Filter Banks and CP-OFDM: What are the Real Gains?", (invited paper) in Proc. of the IEEE International Symposium on Wireless Communication Systems (ISWCS'2016), Poznan, Poland, Sept 2016.

[C102] - Mamadou Lamarana Diallo, Marwa Chafii, Jacques Palicot, and Faouzi Bader,"Modified Tone Reservation for PAPR Reduction in OFDM Systems", in Proc. of th European Signal Processing Conference (EUSIPCO'2016), Budapest, Hungary. September 2016.

[C101] - Vincent Savaux, Yves Louet, and Faouzi Bader, "Low-Complexity Approximations for LMMSE Channel Estimation in OFDM/OQAM", in Proc. of the International Conference on Telecommunications (ICT'2016), Thessaloniki-Greece. May 2016.

[C100] - Quentin Bodinier, Faouzi Bader, and Jacques Palicot, "Modeling Interference Between OFDM/OQAM and CP-OFDM: Limitations of the PSD-Based Model", in Proc. of the International Conference on Telecommunications (ICT'2016), Thessaloniki-Greece. May 2016.

[C99] - Vincent Savaux, Faouzi Bader, and Jacques Palicot, "CMA-Based Blind Equalization and Phase Recovery in OFDM/OQAM Systems", in Proc. of the International Conference on Telecommunications (ICT'2016), Thessaloniki-Greece. May 2016.

[C98] - Marwa Chafii, M. Lamarana Diallo, Jacques Palicot, Faouzi Bader, Rémi Gribonval, "Adaptive Tone Reservation for Better BER Performance in Frequency Selective Fading Channel", in Proc. of the IEEE 83rd Vehicular Technology Conference (VTC'2016-Spring), 15–18 May 2016. Nanjing, China.

[C97] - Quentin Bodinier, Arman Farhang, Faouzi Bader, Hamed Ahmadi, Jacques Palicot, and Luiz A. DaSilva, "5G Waveforms for Overlay D2D Communications: Effects of Time-Frequency Misalignment", in Proc. of the IEEE International Communications Conference (IEEE ICC '2016). Kuala Lumpur, Malaysia. May 2016.

[C96] - Marius Caus, Ana I. Perez-Neira, Adrian Kliks, Quentin Bodinier, Faouzi Bader, "Capacity Analysis of WCC-FBMC/OQAM Systems", in Proc. of the IEEE International Conference on Acoustics, Speech and Signal Processing (IEEE ICASSP '2016) Shanghai, China. March 2016.

[C95] - Diallo Mamadou Lamarana, Palicot Jacques and Faouzi Bader, "Carrier Parity distribution influence on PAPR mitigation Using Tones Reservation Method", in Proc. of the IEEE International Congress on Ultra Modern Telecommunications and Control Systems (IEEE ICUMT'2015), Brno, Cezch Republic, October 2015.

[C94] - V. Savaux, Y. Louët, F. Bader, "Estimation de Canal MMSE pour la Modulation OFDM/OQAM", (in French) Seminar (GRETSI'15), Lyon-France. September 2015.

[C93] - Lamarana Mamadou Diallo, Jacques Palicot, Faouzi Bader, "Diminution du Facteur de Crête d'un Signal Multiporteuse par Décomposition Selon Deux Signaux, Symétrique et Antisymétrique", (in French) Seminar (GRETSI'15), Lyon-France. September 2015.

[C92] - Vincent Savaux, Malek Naoues, Faouzi Bader and Jacques Palicot, "Ultra-Fast Blind Equalization for OFDM: Principle and Steps Towards Implementation", in Proc. of the 12th International Symposium on Wireless Communication Systems (ISWCS'2015). Brussels, Belgium. August 2015.

[C91] - Vincent Savaux and Faouzi Bader, "Sub-Optimal Initialization for Blind Equalization with Fast Convergence in OFDM/OQAM Modulation", at European Conference on Networks and Communications, (EuCNC'2015) Paris, France, June 29/July 2, 2015.

[C90] - Laura Melian-Gutierrez, Navikkumar Modi, Christophe Moy, Ivan Pérez-Alvarez, Faouzi Bader, and Santiago Zazo, "Upper Confidence Bound Learning Approach for Real HF Measurements", in Proc. of the IEEE International Conference on Communications (IEEE ICC 2015) - International Workshop on Advances in Software Defined and Context Aware Cognitive Networks 2015, London, UK, June 2015.

[C89] - Lamarana Mamadou Diallo, Jacques Palicot, Faouzi Bader, "Achieving a Desired Deterministic Upper Bounded PAPR Value Using a Fast Adaptive Clipping Algorithm", The Eleventh Advanced International Conference on Telecommunications. (AICT'2015) Brussels, Belgium. June 21 - 26, 2015.

[C88] - Laura Melian-Gutierrez, Navikkumar Modi, Christophe Moy, Ivan Pérez-Alvarez, Faouzi Bader, and Santiago Zazo, "DSA With Reinforcement Learning in the HF band", The 1st URSI Atlantic Radio Science Conference (URSI AT-RASC), Gran Canaria, Spain. May 2015.

[C87] - Vincent Savaux and Faouzi Bader, "Pilot Adaptation for Broadband LTE-Like FBMC System in PMR Band", in Proc. of the IEEE Vehicular Technology Conference (IEEE VTC'2015 Spring), Glasgow, Scotland. May 2015.

[C86] - Mohammed El-Absi, Musbah Shaat, Faouzi Bader, and Thomas Kaiser, "Spectral Efficiency Comparison of OFDM/FBMC for Interference Alignment Based Power Loading in MIMO Cognitive Radio Systems". In Proc. of the 11th International Symposium on Wireless Communication Systems (ISWCS'2014). Barcelona, Spain. August 2014.

[C85] - Mohammed El-Absi , Musbah Shaat, Faouzi Bader, and Thomas Kaiser, "Interference Alignment with Frequency-Clustering for Efficient Resource Allocation in Cognitive Radio Networks", at the Proc. of the IEEE Global Communications Conference (Globecom'2014), Austin, TX USA. 8-12 December 2014.

[C84] - Ahmed Jendeya, Musbah Shaat, Ammar Abu Hdrouss, and Faouzi Bader, "Joint Allocation in Multi-carrier Based Cognitive Networks with Two-Way Relaying", at the Proc. of the IEEE Workshop on Cognitive Cellular Systems (IEEE CCS'2014). Rhine River, Germany, September 2-4, 2014.

[C83] - Yahia Medjahdi, Didier le Ruyet, Faouzi Bader, and Laurent Martinod, "Integrating LTE Broadband System in PMR Band: OFDM vs. FBMC Coexistence Capabilities and Performances", in the Proc. of the 11th International Symposium on Wireless Communication Systems (ISWCS'2014). Barcelona, Spain. August 2014.

[C82] - Mohammed El-Absi, Musbah Shaat, Faouzi Bader, and Thomas Kaiser, "Interference Alignment Based Resource Management in MIMO Cognitive Radio Systems", at the 20th European Wireless (EW) Conference, Barcelona-Spain. May 2014.

[C81] - Alexandra Oborina, Christian Ibars, Lorenza Giupponi, Faouzi Bader, "Link Performance Model for System Level Simulations of Filter Bank Multicarrier-Based Systems in PMR Networks", at workshop on Advanced Multicarrier Waveforms and Mechanisms for Future Ad-Hoc and Cell-Based Systems at the Tenth International Symposim on Wireless Communication Systems (IEEE ISWCS'2013), Ilmenau, Germany. August 2013.

[C80] - Faouzi Bader, Musbah Shaat, and Yahia Medjahdi, "New Opportunities for Spectrum Coexistence Using Advanced Multicarrier Scheme", at workshop on Cognitive Radio at Military Communications and Information Systems Conference MCC'2013 (Invited paper). Saint Malo, France, October 2013.

[C79] - Mohamad Kalil, Mohammad M. Banat, and Faouzi Bader, "Three Dimensional Pilot Aided Channel Estimation for Filter Bank Multicarrier MIMO Systems with Spatial Channel Correlation", at the 8th Jordanian International Electrical and Electronic Engineering Conference (JIEEEC'2013), April 2013. Aman, Jordan.

[C78] - Adrian Kliks, Faouzi Bader, "Bit and Power loading for FBMC systems: an analysis with Mercury-filling Approach, Submitted to the SS on: Cognitive Radio for Energy Efficient Next Generation Networks", in Proc. of the 20th IEEE International Conference on Telecommunications (IEEE ICT 2013) May 6-8, 2013 in Casablanca, Morocco.

[C77] - Markku Renfors, Faouzi Bader, Leonardo Baltar, Didier Le Ruyet, Daniel Roviras, Philippe Mege, Martin Haardt, "On the Use of Filter Bank Based Multicarrier Modulation for Professional Mobile Radio", at the IEEE Vehicular Technology Conference (VTC-Spring'2013), 2-5 June 2013. Dresden, Germany.

[C76] - M. Shaat and F. Bader, "Comparison of OFDM and FBMC Performance in Multi-Relay Cognitive Radio Network", in Proc. of the Ninth IEEE International Symposium in Wireless Communication Systems (ISWCS'2012), on 29 August 2012, at Paris, France.

[C75] - A. Kliks and F. Bader, "Application of the mercury-filling principle in FBMC/GMC systems", in Proc. of the ICT-ACROPOLIS Workshop, on 28 June, in Brussels. 2012.

[C74] - Hamza Soury, F. Bader, M. Shaat, and M. Slim Alouini, "Near Optimal Power Allocation Algorithm for OFDM-Based Cognitive Using Adaptive Relaying Strategy", in Proc. of the 7th International Conference on Cognitive Radio Oriented Wireless Networks (CrownCom'2012), June 18–20, 2012 Stockholm, Sweden.

[C73] - Jaime Peña Leon, F. Bader, M. Slim Alouini, "Energy Scope of Handoff Strategies in Macro-Femtocell Environments", in Proc. of the IEEE International Conference on Communications (IEEE ICC'2012). Ottawa, Canada. June 2012.

[C72] - Jaime Peña Leon, F. Bader, M. Slim Alouini, "Per-energy Capacity and Handoff Strategies in Macro-Femto Cells Environment", in Proc. of the IEEE Wireless Communications and Networking Conference, (IEEE WCNC'2012),(Future Green Communications Workshop). Paris, France. April 2012.

[C71] - M. Shaat and F. Bader, "Joint Resource Optimization in Decode and Forward Multi-Relay Cognitive Network With Direct Link", in Proc. of the IEEE Wireless Communications and Networking Conference (IEEE WCNC'2012). Paris, France. April 2012.

[C70] - M. Shaat and F. Bader, "Asymptotically Optimal Subcarrier Matching and Power Allocation for Cognitive Relays With Power and Interference Constraints", in Proc. of the IEEE Wireless Communications and Networking Conference (IEEE WCNC'2012). Paris, France. April 2012.

[C69] - M. Shaat and F. Bader, "Joint Subcarrier Pairing and Power Allocation for DF-Relayed OFDM Cognitive Systems", in Proc. of the IEEE Global Communications Conference (IEEE GLOBECOM'2011), Houston, Texas, USA. December 2011.

[C68] - M. Shaat and F. Bader, "Optimal and Suboptimal Resource Allocation For Two-Hop OFDM-Based Multi-Relay Cognitive Networks", in Proc. of the 22nd IEEE International Symposium on Personal, Indoor and Mobile Radio Communications (IEEE PIMRC'2011). Toronto, Canada, 11-14 September, 2011.

[C67] - M. Shaat and F. Bader, "Optimal Resource Allocation in Multi-Relay Cognitive Networks Using Dual Decomposition", in the 22nd Annual IEEE International Symposium on Personal, Indoor and Mobile Radio Communications (IEEE PIMRC'2011). Toronto, Canada, 11-14 September, 2011.

[C66] - F. Bader and M. Banat, "Radio Resource Unit Allocation and Rate Adaptation in Filter Banks Multicarrier System", the seventh International Conference on Wireless and Mobile Communications and Mobile Communications (ICWMC'2011) conference in Luxembourg, 19-24 June 2011.

[C65] - M. Shaat, F. Bader," Optimal Power Allocation Algorithm for OFDM-Based Decode-and-Forward Dual-Hop Cognitive Systems", in Proc. of the IEEE 73rd Vehicular Technology Conference (IEEE VTC'2011-Spring) 15-18 May 2011, Budapest, Hungary.

[C64] - Adrian Kliks, Ivan Stupia, Vincenzo Lottici, Filippo Giannetti, F. Bader, "Generalized Multi-Carrier: an Efficient Platform for Cognitive Wireless Applications", in Proc. of the 8th International Workshop on Multicarrier Systems & Solutions (MC-SS'2011), Herrsching, Germany. May 2011.

[C63] - D. Pubill, M. Miozzo, L. Giupponi, F. Bader, "Hybrid Simulator for Heterogeneous Networks– WiMax Module"s, (in Spanish) in Proc. of the 20th Telecom I+D Conference (Telecom I+D'2010), Valladolid, Spain. September 2010.

[C62] - J. Bastos, V. Monteiro, J. Rodriguez, R. Aguero, D. Gomez, Y. Fernández, M. Peña, F. Bader, C. Verikoukis, J. Herrero, B. Cendón, M. Raspopoulos, S. Stavrou, M. Cabañas, J. Sainz and M. R. Santos, "Mobility Concepts for IMT-Advanced", in ICST 6th International Mobile Multimedia Communications Conference (MOBIMEDIA'2010), Lisbon, Portugal. September 2010.

[C61] - M. Miozzo, F. Bader, "Accurate Modelling of OFDMA Transmission Technique using IEEE 802.16m Recommendations for WiMAX Network Simulator Design", in Proc. 2nd International ICST Conference on Mobile Networks and Management (MONAMI'2010), Santander, Spain. September 2010.

[C60] - I. Gutierrez, F. Bader, "Linear Dispersion Codes Selection Using WiMAX over Uncorrelated MIMO Rayleigh Channel", in Proc. of ICST 6th International Mobile Multimedia Communications Conference (MOBIMEDIA'2010), Lisbon, Portugal. September 2010.

[C59] -M. Shaat, F. Bader, "Efficient Uplink Subcarrier and Power Allocation Algorithm in Cognitive Radio Networks", in Proc. of the IEEE Seventh International Symposium on Wireless Communication Systems (IEEE ISWCS'2010). York, United Kingdom, 19th-22nd September, 2010

[C58] - F. Bader, M. Shaat," Pilot Pattern Adaptation and Channel Estimation in MIMO WIMAX-Like FBMC System", in Proc. of Sixth International Conference on Wireless and Mobile Communications (ICWMC'2010). September 20-25, 2010 - Valencia, Spain. BEST CONFERENCE PAPER AWARD.

[C57] - M. Shaat, F. Bader, "Fair and Efficient Resource Allocation Algorithm for Uplink Multicarrier Based Cognitive Networks", in Proc. of the 21st IEEE Personal, Indoor and Mobile Radio Communications Symposium (IEEE PIMRC 2010). Istambul, Turkey. September 2010.

[C56] - M. Shaat, F. Bader, "An Uplink Resource Allocation Algorithm for OFDM and FBMC Based Cognitive Radio Systems" , in Proc. of the 5th International Conference on Cognitive Radio Oriented Wireless Networks and Communications (IEEE CrownCom'2010). Canne, France. June 2010.

[C55] - I. Gutierrez, F. Bader, "Spectral Efficiency using Combinations of Transmit Antenna Selection with Linear Dispersion Code Selection", in Proc. of the ICST 2nd International Conference on Mobile Lightweight Wireless Systems (MOBILIGHT'2010). Barcelona, Spain. May 2010.

[C54] - Ismahene Ikhlef, Abdellatif Said, Faouzi Soltani and Faouzi Bader, "Performance of MC-DS-CDMA System in Rayleigh Fading Channel with Non-Coherent Combining Schemes and MAI Interference", in Proc. of the ICST 2nd International Conference on Mobile Lightweight Wireless Systems (MOBILIGHT'2010). Barcelona, Spain. May 2010.

[C53] - I. Gutierrez, F. Bader, A. Mourad, "Spectral Efficiency Under Transmit Antenna and STC Selection with Throughput Maximization Using WiMAX", in Proc. of the IEEE 17th International Conference on Telecommunications (IEEE ICT'2010), Doha-Qatar. April 2010.

[C52] - M. Shaat and F. Bader, "A Two-Step Resource Allocation Algorithm in Multicarrier Based Cognitive Radio Systems", in Proc. of the IEEE Wireless Communications and Networking Conference (IEEE WCNC'2010). Sydney, Australia. April 2010.

[C51] - M. Shaat and F. Bader, "Downlink Resource Allocation Algorithm in OFDM/FBMC Cognitive Radio Networks". The third Mosharaka International Conference on Communications, Signals and Coding (MIC-CSC2009). Amman, Jordan. November 2009.

[C50] - I. Gutiérrez, F. Bader, J.L. Pijoan, "Combining resource Allocation and Packet Scheduling with New Proirization Function in SISO WiMAX System". The third Mosharaka International Conference on Communications, Signals and Coding (MIC-CSC2009). Amman, Jordan. November 2009.

[C49] - G. Ruiz, D. Pubill, F. Bader, J. A. Ortega, "Video Streaming in Uplink mode Using WiMAX System – Experimental Results", in Proc. of The 20th IEEE Personal, Indoor and Mobile Radio Communications Symposium 2009 (IEEE PIMRC'09). Tokyo, Japan. 13th-16th September 2009.

[C48] - M. Shaat, F. Bader, "Low Complexity Power Loading Scheme in Cognitive Radio Networks: FBMC Capability", in Proc. of The 20th IEEE Personal, Indoor and Mobile Radio Communications Symposium 2009 (IEEE PIMRC'09). Tokyo, Japan. 13th-16th September 2009.

[C47] - I. Gutierrez, F. Bader, A. Mourad, "Joint Transmit Antenna and Space-Time Coding Selection for WiMAX MIMO System", in Proc. of The 20th IEEE Personal, Indoor and Mobile Radio Communications Symposium 2009 (IEEE PIMRC'09). Tokyo, Japan. 13th-16th September 2009.

[C46] - N. Zorba, S. Pfletschinger, F. Bader, "Increasing the Performance of OFDM-OQAM Communication Systems through Smart Antennas Processing", in Proc. of the 1st ICST International Conference on Mobile Lightweight Wireless Systems (Mobilight'09). Athens, Greece. May 2009.

[C45] - F. Bader, M. Shaat, "Power Loading Scheme in Cognitive Radio Networks: FBMC Capability", in Proc. of the 10th IEEE International Workshop on Signal Processing Advances in Wireless Communications (IEE SPAWC 2009) jointly with the PHYDYAS (Physical Layer For Dynamic Spectrum Access And Cognitive Radio) workshop, 21-24 June 2009, Perugia (Italy).

[C44] - M. Shaat, F. Bader, "Power Allocation and Throughput Comparison in OFDM and FBMC Based Cognitive Radio", the 22nd Meeting of the Wireless World Research Forum (WWRF'2009), Paris, France. May 2009.

[C43] - I. Gutierrez, F. Bader, J. L.Pijoan, "Mixed TUSC and Band AMC Permutation Zone in OFDMA Systems with Limited Feedback", in the proc. of the 69th IEEE Vehicular Technology Conference (IEEE VTC-Spring '09). Barcelona, Spain. April 2009.

[C42] - I. Gutierrez, F. Bader, J. L. Pijoan, "New Prioritization function for User Scheduling in OFDMA Systems", IEEE Radio Wireless Symposium (IEEE RWS'2009), San Diego, California, USA. Jan 2009.

[C41] - I. Gutierrez, F.Bader, J.Pijoan, "Cross-Layer Design for Resource Allocation under QoS Requirements for Multiuser SS-MC-MA Systems", 4th International Week on Management of Networks and Services Manweek 2008, Samos Island, Greece. September 2008.

[C40] - I. Gutierrez, F. Bader, J. L.Pijoan, "Prioritization Function for Packet Data Scheduling in WiMAX Systems", The Fourth International Wireless Internet Conference (WiCON 2008), Maui, Hawai, USA. Nov 2008.

[C39] - I. Gutierrez, F. Bader, J. L.Pijoan, "Subchannel Power Allocation and Rate Adaptation for a MC-CDMA Satisfying Mixed QoS Requirements", Mosharaka International Conference on Communications, Signals and Coding (MIC-CSC'2008), Amman, Jordan. 17th-19th October 2008.

[C38] - F. Bader, "Tecnología y Regulación en Sistemas de Comunicación", 10th Anniversary of Barcelona Digital Global Congress, 20-22 of May 2008. Barcelona, Spain.

[C37] - F. Bader, The Technology Basis for Spectrum Management Evolution, 3 hours Tutorial taught at the Musharaka Multi-Conference on Communications, Signals and Control (MM-CSC-2007). 7-9 June, Amman-Jordan, 2007.

[C36] - I. Gutierrez, F. Bader, J. L. Pijoan, S. Ben Slimane, "Adaptive Resource Management for a MC-CDMA System with Mixed QoS Classes Using a Cross Layer Strategy". The IEEE 65th Vehicular Technology Conference (IEEE VTC-Spring 2007). 22nd-25th April, Dublin-Ireland 2007.

[C35] - F. Bader, N. Labed, I. Gutierrez, "Intercell Interference Investigation in a MC-CDMA System with Iterative Demaping". In the proceedings of the Semi Annual 64th IEEE Vehicular Technology Conference (IEEE VTC'2006 Spring). 25th-28th of September. Montréal, Québec-Canada 2006.

[C34] - N. Labed, F. Bader, I. Gutierrez, "Supported Active Users in a MC-CDMA System Under Intercell Interference". The Proc. of the 1st IEEE Mobile Computing and Wireless Conference (MCWC'2006). 16th-20th September, Amman-Jordan, 2006.

[C33] - F. Bader, "WiMAX a New Broadband Access Solution". 3 hours Tutorial taught at the 1st IEEE Mobile Computing and Wireless Conference (MCWC'2006). 16 September, Amman-Jordan, 2006.

[C32] - I. Gutierrez, F. Bader, J. Pijoan, "Adaptive Bit Loading with Multi-User Diversity in MC-CDMA". In proceedings of the 12th European Wireless Conference (EWC'2006), 2-5 April, Athens-Greece 2006.

[C31] - I. Gutierrez, J. Pijoan, F. Bader, R. Aquilué, "New Channel Interpolation Method for OFDM Systems by Nearest Pilot Padding", in Proc. of the 12th European Wireless Conference (EWC'2006), 2-5 April, Athens-Greece, 2006.

[C30] - F. Bader, "Pilot Time-Frequency Location Adjustment in OFDM Systems Based on the Channel Variability Parameters". The 5th International Workshop on Multi-Carrier Spread Spectrum (MC-SS'2005), 14-16 September, Oberpfaffenhofen, Munich-Germany, 2005.

[C29] - S. Pfletschinger, F. Bader, "Adaptive Assignment of Subcarriers and Spreading Codes for Throughput Maximization in a Multi-User MC-SS System". The 5th International Workshop on Multi-Carrier Spread Spectrum (MC-SS'2005),14-16 September, Oberpfaffenhofen, Munich-Germany, 2005.

[C28] - I. Gutierrez, F. Bader, J. Pijoan, M. Deumal, "Performance of a New Adaptive Grouping and Modulation Procedure For Multiuser Group Orthogonal MC-CDMA". In the proceedings of the 4th IASTED International Conference on Communications Systems and Networks (CSN 2005). September 12-14, Benidorm-Spain, 2005.

[C27] - I. Gutierrez, F. Bader, J. Pijoan, M. Deumal, "Agrupación de Usuarios con Modulación Adaptativa en Sistemas GO-MC-CDMA" (original title in Spanish). El XX Simposio Nacional de la Unión Científica Internacional de Radio U.R.S.I.2005). Sept. 2005, Gandía-Spain, 2005.

[C26] - F. Bader, R. Gonzalez, "Analysis of the Design of the Optimum Pilot Pattern Using Different Bi-dimensional Interpolation Filters". The Proc. of the 16th IEEE International Symposium on Personal Indoor Mobile Radio Communications (IEEE PIMRC'2005). Sept 11-14, International Congress Center ICC) Berlin-Germany, 2005.

[C25] - F. Bader, R. Gonzalez, "Seeking the Time-Frequency Location of Pilot Symbol based on The Channel Variability Parameters". The Proc. of the 7th IFIP International Conference on Mobile and Wireless Communication Networks MWCN 2005), Marrakech, Morocco, 19-21-September 2005.

[C24] - Hakima Chaouchi, F. Bader, Josep Mangues, Nino Kubinidze, Ivan Ganchev, Mairtin O'Droma, Ivan Armuelles, "On the Mobility Support in Multi-Access Wireless Networks". The 1st International Workshop on Convergence of Heterogeneous Wireless Networks. Budapest, Hungary In Conjunction with (WICON 2005), July 10, 2005.

[C23] - R. Gonzalez, F. Bader, "Time-Frequency Spacing Desing for PACE on OFDM System", in Proc. of the IST Mobile & Communication Summit 2005 (IST 2005). 19-23 of June 2005, Dresden-Germany.

[C22] - R. Gonzalez, F. Bader, M. A. Lagunas, "Analysis of the Behaviour of Different 2D Inetrpolation Techniques Using an Adaptive Pilot Symbol Aided OFDM Wireless Systems". The Proc. of the IEEE Symposium on Trends in Communications (IEEE SympoTIC'04). Bratislava, Slovakia.24th-26th October 2004.

[C20] - Ivan Armuelles, Tomas Robles, F. Bader, C. Pinart, H Chaouchi, M. O'Droma, I. Ganchev, M. Siebert, "Modelos de Integración de Sistemas para el Desarrollo de Redes de Comunicaciones Móviles de 4ta Generación" (in Spanish). The XIV Jornadas Telecom. I+D. Madrid, Spain. 18th-20th November 2004.

[C19] - F. Bader, "Multiple Access Technologies For Future Wireless Communication Systems". 2 hours Tutorial taught at the 9a Setmana de la Ciència. 8 October, Barcelona, Spain, 2004.

[C18] - R. Gonzalez, F. Bader, M. A. Lagunas, Adaptive Distribution of Pilot Symbols Aided Channel Estimation in an OFDM System. The 1st International Workshop on End-to End Reconfigurable Mobile Systems and Networks Beyond 3G (E2R'04). Barcelona, Spain. 5th September 2004.

[C17] - Hakima Chaouchi, Guy Pujolle, Ivan Armuelles, Matthias Siebert, Faouzi Bader, Ivan Ganchev, Mairtin O' Droma, Nikos Passas, "Policy Based Networking in the Integration Effort of 4G Networks and Services". The Proc. of the IEEE Vehicular Technology Conference (IEEE VTC'2004 Spring). Milan, Italy, 17th-19th May 2004.

[C16] - N. Alonistioti, N. Passas, A. Kaloxylos, H. Chaouchi, M. Sibert, M. O'Droma, I. Ganchev, F. Bader, "Buisness Model and Generci Architecture for Integrated Systems and Services- The ANWIRE Approach". Wireless World Research Forum meeting (WWRF8 Bis). Beijing, China. 26th-27th February 2004.

[C15] - I. Armuelles Voinov, C. Bader, T. Robles Valladares, "System Integration Towards a 4G Mobile Communications Architecture" (Original title in Spanish). The XIII Jornadas Telecom. I+D. Madrid, Spain. 18th-20th November 2003.

[C14] - F. Bader, C. Pinart, C. Christophi, I. Ganchev, E. Tsiakkouri, C. Bohoris, V. Friderikos, L. Correia, "User-Centric Analysis of Perceived QoS in 4G IP Mobile/Wireless Networks". The Proc. of the 14th IEEE International Symposium on Personal, Indoor and Mobile Radio Communications (IEEE PIMRC'2003). Beijing, China. 7-10 of September, 2003.

[C13] - F. Bader, M. Navarro, S. Pfletschinger, C. Pinart, Enabling Technologies and Key Issues for QoS Enabled Reconfigurable Mobile/Wireless Networks. 3 hours Tutorial taught at the 1st ANWIRE Summer School on Wireless Internet: Network Architectures, Quality of Service, Services and Applications, 21-25 July, Lisbon, Portugal, 2003.

[C12] - M. O'Droma, I. Ganchev, G. Morabito, R. Narcisi, N. Passas, S. Paskalis, V. Friderikos, A. S. Jahan, E. Tsontsis, C. F. Bader, J. Rotrou, H. Chaouchi, "Always Best Connected" Enabled 4G Wireless World". The Proc. of the IST Mobile and Wireless Communications Summit 2003. Aveiro, Portugal, June 15th-18th 2003.

[C11] - F. Bader, C. Pinart, "Physical Layer Strategies and Issues for ABC Vision", First ANWIRE International Workshop on Wireless, Mobile & Always Best Connected. Glasgow (Scotland, UK). 22th April 2003.

[C10] - F. Bader, S. Zazo, "MC-CDMA System Evaluation Using the MMSE Decorrelator and PIC in the Reverse Link Over an Asynchronous Channel Environment". The Proc. of the IEE 5th European Personal Mobile Communications Conference (IEE EPMCC 2003). Glasgow (Scotland, UK). April 22th-24th 2003.

[C9] - I. Raos, S. Zazo, F. Bader, "Prolate Sheroidal Functions: A General Framework for MC-CDMA Wave Forms Without Time Redundancy". The Proc. of the 13th IEEE International Symposium on Personal Indoor and Mobile Radio Communications (IEEE PIMRC'2002), Lisboa, Portugal. September 2002.

[C8] - F. Bader, S. Zazo, I. Raos," Improvement on the Multi-User Detection Decorrelator of a MC-CDMA Used in the Reverse Link". The 13th IEEE International Symposium on Personal Indoor and Mobile Radio Communications (IEEE PIMRC'2002). Lisboa, Portugal. September 2002.

[C7] - F. Bader, S. Zazo, J. M. Páez Borrallo, "Pre-Rake and Multi-User Detection Techniques in UTRA-TDD System". The IEEE Vehicular Technology Conference (IEEE VTC2000-spring). Tokyo-Japan, May 2000.

[C6] - S. Zazo, F. Bader. J. M. Páez Borrallo, "A Multiple Access s/ Self Interference Canceller Receiver for DS-CDMA Multi-User Detection Over Channels". The IEEE Vehicular Technology Conference (IEEE VTC Fall-2000), Boston-Massachusetts-USA. September 2000.

[C5] - F. Bader, S. Zazo, J. M. Páez Borrallo, "Decorrelation MUD for MC-CDMA in an Uplink Transmission Mode", The Third International Workshop in Multi-Carrier Spread Spectrum (MCSS'2001). Oberfafenhoffen -Munich- Germany. September 2001.

[C4] - F. Bader, S. Zazo, J. M. Páez Borrallo, "Uplink Acquisition of Synchronization Parameters in MC-CDMA Systems". The IEEE Vehicular Technology Conference (IEEE VTC Fall-2000) , Boston-Massachusetts, USA, September 2000.

[C3] - F. Bader, S. Zazo, J. M. Páez Borrallo, "Optimum Pilot Pattern for the Uplink Multi-carrier CDMA System". The First International Symposium on Wireless Personal Multimedia Conference (WPMC'99), Amsterdam-Netherlands, September 1999. BEST CONFERENCE PAPER AWARD.

[C2] - F. Bader, S. Zazo, J. M. Páez Borrallo, "MUD Improvement by Using Hexagonal Pilot Distributions for Multi-channel Acquisition and Tracking in MC- CDMA". The Second International Workshop in Multi-Carrier Spread Spectrum (MCSS'99), Oberfafenhoffen -Munich-Germany, Sept 1999.

[C1] - F. Bader, S. Zazo, J. M. Páez Borrallo, "On the Improvement of HF Multi-Carrier Modem Behaviour by Using Spread Spectrum". The Second International Workshop in Multi-Carrier Spread Spectrum (MCSS'99), Oberfafenhoffen -Munich- Germany. September 99.

2.1.5 Others

[O1] - Jean-Baptiste Doré, Malek Naous, Vincent Savaux, F. Bader, Laurent Martinod, and Olivier Rousset, "New Multicarrier Waveforms for Broadband Professional Mobile Radio: Make it Real!", testbed demonstration, at the 11th EAI International Conference on Cognitive Radio Oriented Wireless Networks (Crowncom'2016). May 30–June 1, 2016. Grenoble, France.

[O2] - Adrian Kliks, Hanna Bogucka, Faouzi Bader, Musbah Shaat, Oliver Holland, "FBMC and GMC capabilities for TV White Space and Cognitive Radio", IEEE 1900.7 Working Group Meeting, Osaka, Japan, 26-29 March 2012.

[O3] - Paweł Kryszkiewicz, Hanna Bogucka, Adrian Kliks, Oliver Holland, Faouzi Bader, "Spectrum Shaping Algorithms for Cognitive Radio", IEEE 1900.7 Working Group Meeting, Osaka, Japan, 26-29 March 2012.

[O4] - Adrian Kliks, Hanna Bogucka, Faouzi Bader, Musbah Shaat, Oliver Holland, "Signal Adaptation and Dynamic Spectrum Masks Used for Cognitive Radio", IEEE 1900.7 Working Group Meeting, Osaka, Japan, 26-29 March 2012.

[O5] - Hanna Bogucka, Adrian Kliks, Oliver Holland, Faouzi Bader, "Femto-Cell Use-Case", IEEE 1900.7 Working Group Meeting, Osaka, Japan, 26-29 March 2012.

[O6] - A. Kliks and F. Bader, "Application of the Mercury-Filling Principle in FBMC/GMC Systems", at the EC funded project ICT-ACROPOLIS NoE Workshop, on 28th June, in Brussels, Belgium. 2012

[O7] - M. Shaat and F. Bader, "Subcarrier Selection and Power Loading for Multicarrier Based Cognitive Networks Under Interference and Fairness Constraints", at the EC-funded COST Action IC0902/WG1-Cognitive Radio and Networking for Cooperative Coexistence of Heterogeneous Wireless Networks, Sept. 2011.

[O8] - F. Bader, C. Pinart, "Physical Layer Strategies and Issues for ABC Vision". The first ICT-ANWIRE International Workshop on Wireless, Mobile & Always Best Connected. Glasgow (Scotland), UK. 22th April 2003

[O9] - F. Bader, "Tecnología y Regulación en Sistemas de Comunicación", (in Spanish). The 10th Anniversary of Barcelona Digital Global Congress, 20th-22nd of May 2008. Barcelona, Spain (invited talk).

[O10] - M. A. Lagunas, F. Bader, "Open Spectrum Technology and Regulation". Amena (Orange, Spain) Mobile Operator pavilion, at the 3rd GSM World Congress, 13-16 February 2006. Barcelona, Spain.

Chapter 3

Research Synthesis

In this Chapter are described my main and different research lines. Despite my involvement in different types of research projects (2002-2016), my undertaken researches during all these years essentially focused on multi-carrier communication systems and can be categorized into three major research fields/lines. The first field is centered on "Resource allocation in cognitive radio" (details of this research field are in Subsection 3.1) that involves essentially two scenarios: i) that without any relay communication in page 44, and ii) that with relays in page 83. The second research field encompass different aspects of the coexistence between communication systems using different types of physical layers with distinct multi-carrier waveforms (see the details in Subsection 3.2). In this field the coexistence issues are considered for two main communication contexts which are: i) the professional mobile radio system (PMR) in page 104, and ii) the Device-to-Device (D2D) communication environment in page 125. The third presented field of my researches includes aspects of signal processing for OFDM and beyond OFDM schemes in page 152. In the hereafter, starts the description of the above mentioned research lines.
Note: All the cited references in this Chapter with the following indication: [JX], [CBX], [CX], or/and [OX], and with "X" the number of this publication, is referring to my publications listed in the Chapter 2, pp. 30-42.

3.1 Resource allocation in cognitive radio

My research activities in this field started during my involvement in the EC funded project ICT-PHYDYAS (2007-2009) (see more details on this project in Subsection 1.5.3, page 24) being at the CTTC research center. The target of this project was to design suited concepts for dynamic access spectrum management and cognitive radio (CR) context. The originality of this project was that it brings new challenges at the PHY layer by proposing new signal processing advances using the filter bank-based multi-carrier (FBMC) scheme that offers high spectrum resolution than the OFDM, and can provide independent sub-channels, while maintaining or enhancing the high data rate capability. The use of the FBMC (also named OFDM/OQAM) modulation at that time and in such context was considered by the EC as one the most interesting ICT funded projects. My research line on resource allocation (RA) in the CR context, can be divided in two parts. One dedicated to the non relaying context, and the second part by considering the relaying scenario.
The obtained CTTC's fellowship by Mr. Musbah Shaat for a PhD career, allowed me to supervise him and to carry through research the main technical challenges raised in the project PHYDYAS. My researches in this field were not only conducted in PHYDYAS project but also in the COST Action IC0902 project on "Cognitive Radio and Networking for Cooperative Coexistence of Heterogeneous Wireless Networks" (see page 24 for more details), and the EC network of excellence (NoE) project ACROPOLIS on "Advanced Coexistence Technologies for Radio Optimization in Licensed and Unlicensed Spectrum" (see more details on this project in Subsection 1.5.3, page 23).

3.1.1 Resource allocation in CR without relaying communications

Cognitive Radio (CR) was first introduced by Mitola in [18] as a radio that can change its parameters based on interaction with the environment in which it operates. According to Federal Communications Commission (FCC) [19], temporal and geographical variation in the utilization of the assigned spectrum range from 15% to 85% which means that assigning frequency bands to specific users or service providers exclusively does not guarantee that the bands are being used efficiently all the time. The CR technology aims to increase the spectrum utilization by allowing a group of unlicensed users [referred to as secondary users (SU's)] to use the licensed frequency channels

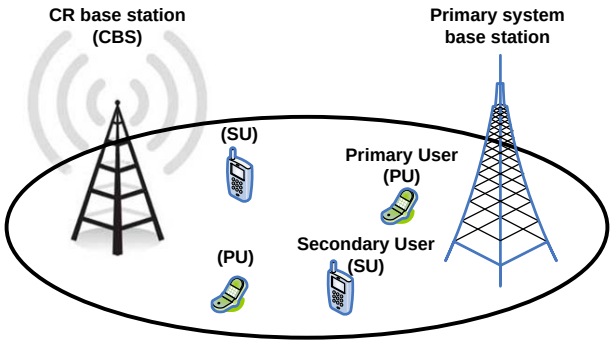

Figure 3.1: Cognitive Radio Network

(spectrum holes) without causing a harmful interference to the licensed users [referred to as primary users (PU's)] and thus implement efficient reuse of the licensed channels.
Multi-carrier communication systems have been considered as an appropriate candidate for CR systems due to its flexibility in allocating different resources among different users as well as its ability to fill the spectrum holes left by the PU's [20]. The mutual interference depends on the transmitted power as well as the spectral distance between PU and SU [21]. Orthogonal frequency division multiplexing (OFDM) based CR system suffers from high interference to the PU's due to large side lobes of its filter frequency response. The insertion of the cyclic prefix (CP) in each OFDM symbol decreases the system capacity. The filter bank multi-carrier system (FBMC) does not require any CP extension and can overcome the spectral leakage problem by minimizing the side lobes of each subcarrier and therefore lead to high efficiency (in terms of spectrum and interference). The hereafter description focus on the downlink communication mode considering the single and multiple active PU bands.

3.1.1.1 Case 1: Single Active PU Band

The first analyzed algorithm for RA in CR is that presented by G. Bansal et, al,. in [22], where an optimal and two suboptimal power loading schemes using the Lagrange formulation to maximize the downlink capacity of the CR system have been proposed while keeping the interference induced to only one PU below a pre-specified threshold without the consideration of the total power constraint. P. Wang et al. in [23] proposed an iterative partitioned single user water-filling algorithm. The algorithm aims to maximize the capacity of the CR system under the total power constraint with the consideration of the per subcarrier power constraint caused by the PU's interference limit. The mutual interference between the SU and PU was not considered. In [24], an algorithm called RC algorithm was presented for multi-user resource allocation in OFDM based CR systems. This algorithm uses a greedy approach for subcarrier and power allocations by successively assign bits, one at time, based on minimum SU power and minimum interference to PU considerations. The algorithm has a high computational complexity and a limited performance with comparison to the optimal solution.
From the above observed lacks a two step resource allocation algorithm in multi-carrier based CR system was developed from our researches and presented in paper [C52] (see presented work in first paper depicted at the end of this Subsection).

As shown in Fig. 3.1, the CR system coexist with the PU's radio in the same geographical location. The cognitive base station (CBS) transmits to its SU's and causes interference to the PU's. Moreover, the PU's base station interferes with the SU's. The CR system's frequency spectrum is divided into N subcarriers each having a Δf bandwidth. The side by side frequency distribution of the PU and SU's will be assumed (see Fig. 3.2). The frequency band B has been occupied by the PU (active PU band) while the other band represent the CR band (non-active PU band). It's assumed that the CR system can use the non-active PU bands provided that the total interference introduced to the PU band does not exceed I_{th}, where $I_{th} = T_{th}B$ denotes the maximum interference power that can be tolerated by the PU and T_{th} is the interference temperature limit for the PU.

Assume that Φ_i is the power spectrum density (PSD) of the i^{th} subcarrier. The expression of the PSD depends on the used multi-carrier technique. If an OFDM based CR is assumed, the PSD of the i^{th} subcarrier can be written

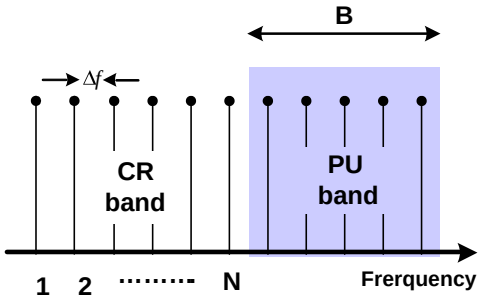

Figure 3.2: Frequency distribution of the primary and cognitive bands

as [21]

$$\Phi_i(f) = P_i T_s \left(\frac{\sin \pi f T_s}{\pi f T_s} \right)^2 \tag{3.1}$$

where P_i is the total transmit power emitted by the i^{th} subcarrier and T_s is the symbol duration. If FBMC based CR system is assumed, the PSD of the i^{th} subcarrier can be written as

$$\Phi_i(f) = P_i |H_i(f)|^2 \tag{3.2}$$

where $|H_i(f)|$ is the frequency response of the prototype filter with coefficients $h[n]$ with $n = 0, \cdots, W-1$, where $W = KN$ and K is the length of each polyphase components (overlapping factor). Assuming that the prototype coefficients have even symmetry around the $\left(\frac{KN}{2}\right)^{th}$ coefficient, and the first coefficient is zero [25], we get

$$|H_i(f)| = h[W/2] + 2 \sum_{n=1}^{\frac{W}{2}-1} h[(W/2) - n] \cos\left(2\pi n \left(f - {}^{i}/_{N}\right)\right) \tag{3.3}$$

The interference introduced by the i^{th} subcarrier to PU band, $I_i(d_i, P_i)$, is the integration of the PSD of the i^{th} subcarrier across the PU band, B , and can be expressed as [21]

$$I_i(d_i, P_i) = \int_{di-B_l/2}^{di+B_l/2} |g_i|^2 \Phi_i(f)\, df = P_i \Omega_i \tag{3.4}$$

where d_i is the spectral distance between the i^{th} subcarrier and the PU band. Ω_i denotes the interference factor of the i^{th} subcarrier.

The interference power introduced by the PU signal into the band of the i^{th} subcarrier is [21]

$$J_i(d_i, P_{PU}) = \int_{di-\Delta f/2}^{di+\Delta f/2} |y_i|^2 \psi_l\left(e^{j\omega}\right) d\omega \tag{3.5}$$

where $\psi\left(e^{j\omega}\right)$ is the power spectrum density of the PU signal and y_i is the channel gain between the i^{th} subcarrier and PU signal.

It will be assumed that all the instantaneous fading gains are perfectly known at the CBS and there is no inter-carrier interference (ICI). Let $v_{i,m}$ to be a subcarrier allocation indicator, i.e. $v_{i,m} = 1$ if and only if the subcarrier is allocated to m^{th} user. It is assumed that each subcarrier can be used for transmission to at most one user at any given time. Our objective is to maximize the total capacity of the CR system subject to the instantaneous interference introduced to the PU's and total transmit power constraint. Therefore, the optimization problem can

Algorithm 1 Subcarriers to User Allocation

Initialization:
Set $\upsilon_{i,m} = 0 \; \forall i, m$
Subcarrier Allocation:
for $i = 1$ to N **do**
$m^* = \arg\max_m \{h_{i,m}\}$; $\upsilon_{i,m^*} = 1$
end for

be formulated as follows

$$\begin{aligned} &P1: \max_{P_i} \sum_{m=1}^{M} \sum_{i=1}^{N} \upsilon_{i,m} \log_2 \left(1 + \tfrac{P_{i,m}|h_{i,m}|^2}{\sigma_i^2}\right) \\ &\textit{Subject to} \\ &\upsilon_{i,m} \in \{0,1\}, \; \forall i, m \\ &\sum_{m=1}^{M} \upsilon_{i,m} \leq 1, \; \forall i \\ &\sum_{m=1}^{M} \sum_{i=1}^{N} \upsilon_{i,m} P_{i,m} \leq P_T \\ &P_i \geq 0, \; \forall i \in \{1, 2, \cdots, N\} \\ &\sum_{m=1}^{M} \sum_{i=1}^{N} \upsilon_{i,m} P_i \Omega_i \leq I_{th} \end{aligned} \tag{3.6}$$

where $h_{i,m}$ is the i^{th} subcarrier fading gain from the CBS to the m^{th} SU. $P_{i,m}$ is the transmit power across the i^{th} subcarrier. $\sigma_i^2 = \sigma_{AWGN}^2 + J_i$ where σ_{AWGN}^2 is the mean variance of the additive white Gaussian noise (AWGN) and J_i is the interference introduced by the PU band into the i^{th} subcarrier and can be evaluated using (3.17). N denotes the total number of subcarriers, while I_{th} denotes the interference threshold prescribed by the PU. P_T is the total power budget and M is the number of SU's.

Subcarrier to User Assignment (First Step)

The optimization problem $P1$ is a combinatorial optimization problem and its complexity grows exponentially with the input size. In order to reduce the computational complexity, the problem is solved in two steps where in the first step, the subcarriers are assigned to the users and then the power is allocated for these subcarriers in the second step. Once the subcarriers are allocated to the users, the multiuser system can be viewed virtually as a single user multi-carrier system. Generalizing the proof given in [26] to consider the CR system, it can be easily shown that the maximum data rate in downlink can be obtained if the subcarriers are assigned to the user who has the best channel gain for that subcarrier as described in Algorithm 1.

Proposed Algorithm for Power Allocation (Second Step)

By applying the Algorithm 1, the values of the channel indicators $\upsilon_{i,m}$ are determined where $\upsilon_{i,m} = 1$ if and only if the subcarrier is allocated to m^{th} user, and hence for notation simplicity, single user notation can be used. The different channel gains can be determined form the subcarrier allocation step as follows

$$h_i = \sum_{m=1}^{M} \sum_{i=1}^{N} \upsilon_{i,m} h_{i,m} \tag{3.7}$$

and hence problem $P1$ can be reformulated as follows

$$\begin{aligned} &P2: \quad \max_{P_i} \sum_{i=1}^{N} \log_2 \left(1 + \tfrac{P_i|h_i|^2}{\sigma_i^2}\right) \\ &\textit{Subject to} \\ &\sum_{i=1}^{N} P_i \Omega_i \leq I_{th} \\ &\sum_{i=1}^{N} P_i \leq P_T; \quad P_i \geq 0 \end{aligned} \tag{3.8}$$

The problem $P2$ is a convex optimization problem. The Lagrangian can be written as

$$\begin{aligned} G = &- \sum_{i=1}^{N} \log_2 \left(1 + \tfrac{P_i^* |h_i|^2}{\sigma_i^2}\right) + \alpha \left(\sum_{i=1}^{N} P_i^* \Omega_i - I_{th}\right) \\ &+ \beta \left(\sum_{i=1}^{N} P_i^* - P_T\right) - \sum_{i=1}^{N} P_i^* \mu_i \end{aligned} \tag{3.9}$$

where α, $\mu_i, i \in \{1, 2, \ldots, N\}$, and β are the Lagrange multipliers. The Karush-Kuhn-Tucker (KKT) conditions can be written as follows

$$\begin{aligned} & P_i^* \geq 0; \quad \alpha \geq 0; \quad \beta \geq 0; \quad \mu_i \geq 0; \quad \mu_i P_i^* = 0 \\ & \alpha \left(\sum_{i=1}^{N} P_i^* \Omega_i - I_{th}\right) = 0 \\ & \beta \left(\sum_{i=1}^{N} P_i^* - P_T\right) = 0 \\ & \tfrac{\partial G}{\partial P_i^*} = \tfrac{-1}{\frac{\sigma^2}{|h_i|^2} + P_i^*} + \alpha \Omega_i + \beta - \mu_i = 0 \end{aligned} \tag{3.10}$$

and also the solution should satisfy the total power and interference constraints. Rearranging the last condition in (3.10) we get

$$P_i^* = \frac{1}{\alpha \Omega_i + \beta - \mu_i} - \frac{\sigma^2}{|h_i|^2} \tag{3.11}$$

Since $P_i^* \geq 0$, we get $\frac{\sigma^2}{|h_i|^2} \leq \frac{1}{\alpha \Omega_i + \beta - \mu_i}$. If $\frac{\sigma^2}{|h_i|^2} < \frac{1}{\alpha \Omega_i + \beta}$, then $\mu_i = 0$ and hence $P_i^* = \frac{1}{\alpha \Omega_i + \beta} - \frac{\sigma^2}{|h_i|^2}$. Moreover, if $\frac{\sigma^2}{|h_i|^2} > \frac{1}{\alpha \Omega_i + \beta}$, from (3.11) we get $\frac{1}{\alpha \Omega_i + \beta - \mu_i} \geq \frac{\sigma^2}{|h_i|^2} > \frac{1}{\alpha \Omega_i + \beta}$ and since $\mu_i P_i^* = 0$ and $\mu_i \geq 0$, we get that $P_i^* = 0$.

Therefore, the optimal solution can be written as follows

$$P_i^* = \left[\frac{1}{\alpha \Omega_i + \beta} - \frac{\sigma^2}{|h_i|^2}\right]^+ \tag{3.12}$$

where $[x]^+ = \max(0, x)$. Solving for the more than one Lagrangian multiplier is computational complex. These multipliers can be found numerically using ellipsoid or interior point method with a polynomial time complexity $\mathcal{O}\left(N^3\right)$ [27]. The high computational complexity makes the optimal solution unsuitable for practical application and hence a low complexity algorithm will be proposed.

If the interference constraints are ignored in $P2$, the solution of the problem will follow the well known water-filling interpretation. On the other side, if the total power constraint is ignored, the Lagrangian of the problem can be written as

$$\begin{aligned} \mathrm{G}' = &- \sum_{i \in N_l} \log_2 \left(1 + \tfrac{P_i' |h_i|^2}{\sigma_i^2}\right) \\ &+ \alpha' \left(\sum_{i \in N_l} P_i' \Omega_i - I_{th}\right) \end{aligned} \tag{3.13}$$

where α' is the Lagrange multiplier. Equating $\frac{\partial \mathrm{G}'}{\partial P_i'}$ to zero, we get

$$P_i' = \left[\frac{1}{\alpha' \Omega_i} - \frac{\sigma^2}{|h_i|^2}\right]^+ \tag{3.14}$$

The value of α' can be calculated by substituting (3.14) into $\sum_{i \in N} P_i' \Omega_i = I_{th}$ to get

$$\alpha' = \frac{|N|}{I_{th} + \sum_{i \in N} \frac{\Omega_i \sigma_i^2}{|h_i|^2}} \tag{3.15}$$

It is obvious that if the summation of the allocated power under only the interference constraints is lower than or equal the available total power budget, i.e. $\sum_{i=1}^{N} P_i' \leq P_T$, then (3.14)-(3.15) will be the optimal solution for the

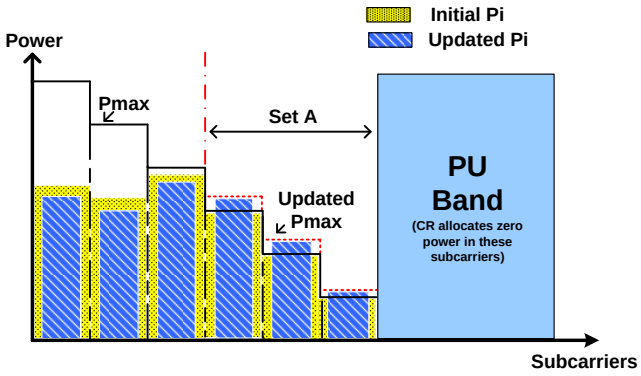

Figure 3.3: An Example of the SU's allocated power using PI-Algorithm

optimization problem $P2$. In most of the cases, the total power budget is quite lower than this summation and hence the **P**ower **I**nterference (PI) constrained algorithm, referred to as *PI-Algorithm*, is proposed to allocate the power under both the total power and interference constraints.
In order to solve the optimization problem $P2$, we can start by assuming that the maximum power that can be allocated for a given subcarrier P_i^{Max} is determined according to the interference constraints only by using (3.14)-(3.15) for every subcarriers $i \in N$. By such an assumption, we can guarantee that the interference introduced to the PU band will be under the pre-specified threshold. Once the maximum power P_i^{Max} is determined, the total power constraint is tested. If the total power constraint is satisfied, then the solution has been found and equal to the maximum power that can be allocated to each subcarrier, i.e. $P_i^* = P_i^{Max}$. Otherwise, the available power budget should be distributed among the subcarriers giving that the power allocated to each subcarrier is lower than or equal to the maximum power P_i^{Max}. This can be done optimally by applying successive conventional water-fillings on the subcarriers. Given the initial water-filling solution, the channels that violate the maximum power P_i^{Max} are determined and upper bounded with P_i^{Max}. The total power budget is reduced by subtracting the power assigned so far. At the next step, the algorithm proceeds to successive water-filling over the subcarriers that not violated the maximum power P_i^{Max} in the last step. This procedures is repeated until the allocated power $P_i^{W.F}$ doesn't violate the maximum power P_i^{Max} in any of the subcarriers in the new iteration. Once the power allocated to each subcarriers is determined, the total interference induced to the PU is evaluated. According to the left interference, the maximum power that can be allocated to each subcarrier is relaxed and the successive water-fillings are performed again to get the final solution. The final power allocation vector P_i^* is satisfying approximately the interference constraint with equality as well as guaranteeing that the total power used is equal to P_T. A graphical description of this algorithm can be found in Fig. 3.3 while the algorithm steps are described in Algorithm 2.

The computational complexity of Step 1 in the proposed Algorithm (Algorithm 2) is $\mathcal{O}(N \log N)$. Steps 2 and 4 of the algorithm execute the successive water-fillings which has a complexity of $\mathcal{O}(N \log N + \eta N)$ where $\eta \leq N$ is the number of the iterations. Step 3 has a complexity of $\mathcal{O}(1)$. Hence, The overall complexity of the algorithm is lower than $\mathcal{O}(N \log N + \eta N) + \mathcal{O}(1)$. The value of η is estimated via simulation with an average value $\eta = 2.953$ and never exceeds five, i.e. $\eta \in [0, 5]$. Comparing to the computational complexity of the optimal solution , $\mathcal{O}\left(N^3\right)$, the proposed algorithm has much lower computational complexity specially when the number of the subcarriers N increased.
The achievable capacities versus the interference constraint of the OFDM based CR system using the optimal, two-step and RC algorithm are plotted in Fig. 3.4 with $P_T = 1$ and $P_T = 2$ watts. It can be noted that the capacity achieved using two-step algorithm is very close to that achieved using the optimal algorithm with a good reduction in the computational complexity. Moreover, the proposed algorithm outperform the RC algorithm. As the allowed interference increase, the total throughput increase.

It can be noticed that the throughput increased as the total power increased. When the total power exceeds a certain value, the throughput become constant regardless of the increase in total power. This is because with such a given interference constraint, the system reach to the maximum total power that can be used to keep the interference to the primary user below the prescribed threshold.
The filter bank multi-carrier system (FBMC) can overcome the spectral leakage problem by minimizing the sidelobes

Algorithm 2 Power Allocation Algorithm

- Let $\mathcal{N} = \{1, 2, \cdots, N\}$ to be the set of all the CR available subcarriers and P_i^* to be the solution of the optimization problem.
- **Step 1**
  1. Find the power allocation vector P_i' according to interference constraint only using equations (3.14)-(3.15) and make it to be the maximum power that can be allocated to each subcarrier $P_i^{Max} = P_i'$.
  2. If $\sum_{i=1}^{N} P_i^{Max} \leq P_T$, then the solution is found and hence $P_i^* = P_i^{Max}$, else continue.
- **Step 2** Find the power allocation vector $P_i^{W.F}$ using the iterative water-filling under the constraints of total power, P_T, and the maximum power that can be allocated to each subcarrier, P_i^{Max}.
- **Step 3** Find the set of subcarriers $\mathcal{A} \subset \mathcal{N}$ (See Fig. 3.3) in which $P_i^{W.F} = P_i^{Max}$ and evaluate the left available interference $I_{Left} = I_{th} - \sum_{i \in \mathcal{N}} P_i^{W.F} \Omega_i$.
- **Step 4** Update P_i^{Max} by applying equations (3.14)-(3.15) on the subcarriers in the set $\mathcal{A}$ ***only*** under the interference constraint $I'_{th} = I_{Left} + \sum_{i \in \mathcal{A}} P_i^{W.F} \Omega_i$ and execute the iterative water-filling again under the P_T and updated P_i^{Max} constraints.

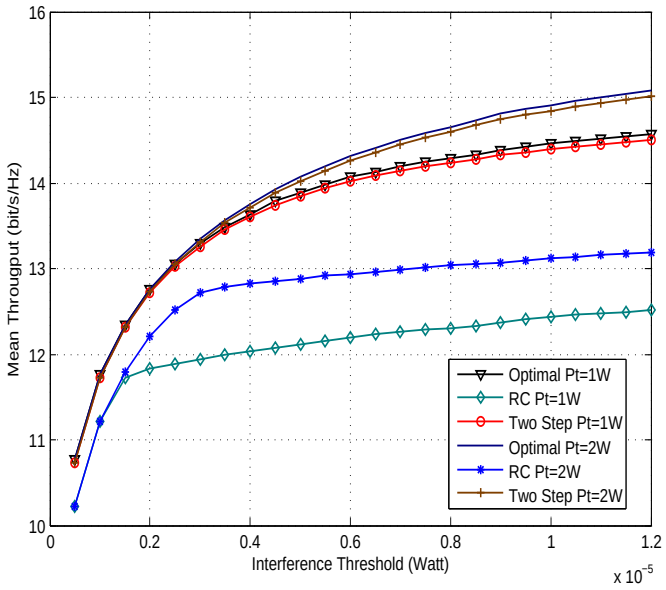

Figure 3.4: Mean throughput vs. interference constraints for OFDM based CR.

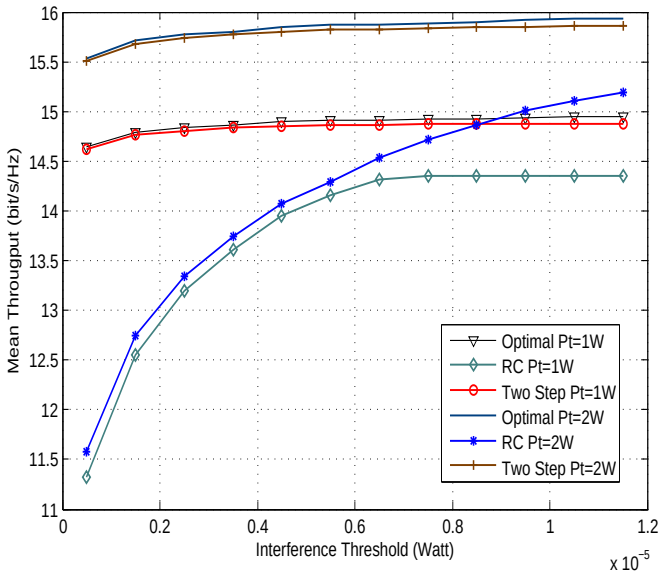

Figure 3.5: Mean throughput vs. interference constraints for FBMC based CR.

of each subcarrier. Fig. 3.5 plot the average throughput for FBMC based CR system using different algorithms versus different interference constraint with $P_T = 1$ and $P_T = 2$ watts and different total power constraints with $I_{th} = 5\mu$ and $I_{th} = 10\mu$ watts.

The proposed two-step algorithm approaches the optimal solution and outperform the RC algorithm. Comparing with the OFDM based CR system in Fig. 3.4, the throughput of FBMC system is higher than that of OFDM because the side lobes in FBMC PSD is smaller than that in OFDM and also the inserted CP in OFDM based CR systems reduces the total throughput of the system. It can be noticed also that the interference condition introduce a small restriction on the overall average throughput in FBMC based CR systems which is not the case in OFDM based CR systems. These results are contributing to recommend the using of the FBMC as a candidate for a physical layer in the future communication environments with heterogeneous systems.

As a general conclusion, we can say that proposed two-step algorithm solves the problem efficiently and achieves approximately the same optimal capacity with a good reduction in the computational complexity. The proposed algorithm outperformed the RC algorithm that uses a greedy approach for the subcarrier and power allocation. Simulation results prove that the FBMC based CR systems have more capacity than OFDM based ones.

3.1.1.2 Case 2: Two Active PU Bands

In this case, two interference constraints belonging to two active PU bands, i.e. $L = 2$, are assumed as depicted in Fig. 3.6. Each active PU band is assumed to have six subcarriers ($|N_1| = |N_2| = 16$). The achieved capacity using *optimal*, *PI* defined in [J5] (PI algorithm is detailed in page 9 of first journal paper depicted at the end Subsection 3.1), and *Zhang* algorithm is defined in [28], for different interference constraints where $I^1_{th} = I^2_{th}$ is plotted in Fig. 3.7. It can be noted that the proposed *PI-algorithm* approaches the optimal solution and outperforms *Zhang* algorithm.

The effect of assuming that every subcarrier belongs to the closest PU band and introducing interference to it only on the net interference introduced to the active PU bands is studied in Fig. 8 and Fig. 9 in [J5][1] for PU_1 and PU_2 respectively.

It can be observed that the net interference induced using the *PI-algorithm* approximately satisfies the pre-

[1]See page 10 in EURASIP journal paper depicted at the end Subsection 3.1

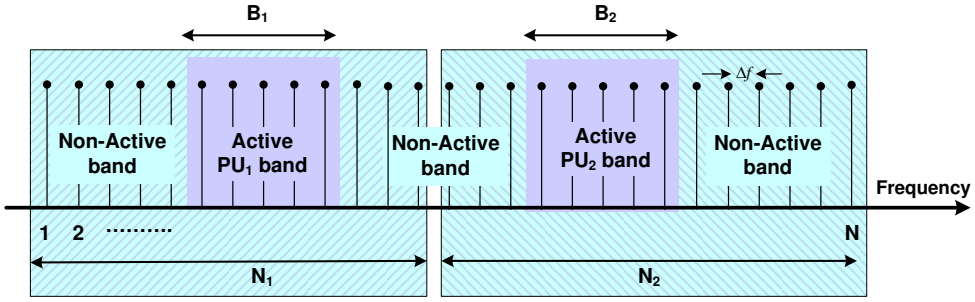

Figure 3.6: Frequency distribution with two active PU bands.

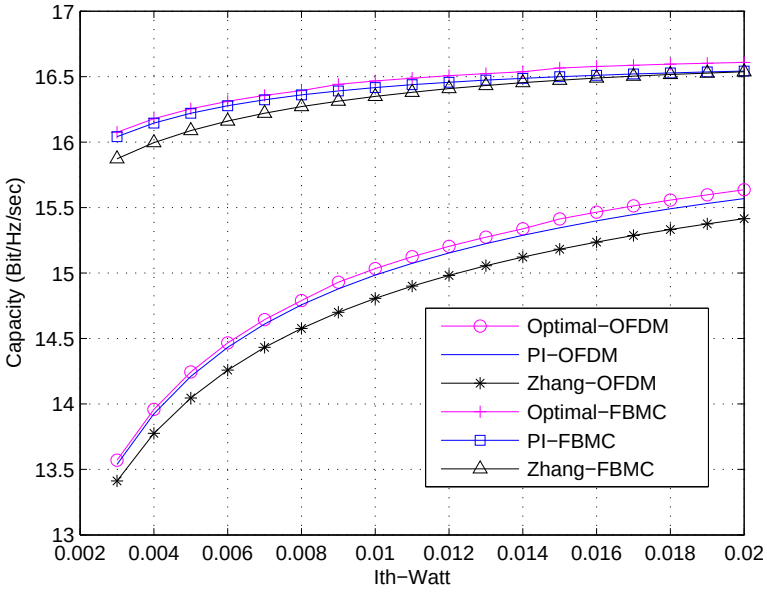

Figure 3.7: Achieved capacity vs. allowed interference threshold for OFDM and FBMC based CR systems - Two active PU bands.

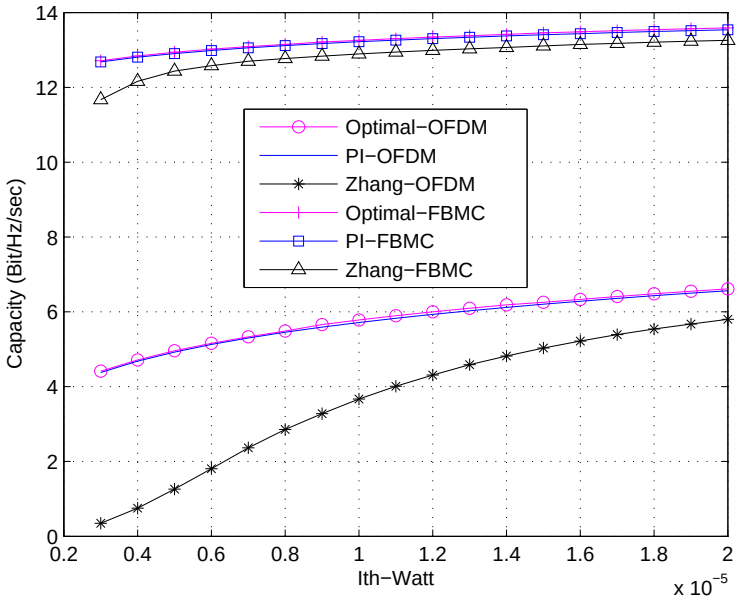

Figure 3.8: Achieved CR vs allowed interference threshold (low) for OFDM and FBMC based CR systems - Two active bands.

specified interference constraints which makes the assumption reasonable. Unlike the OFDM based CR system, the interference induced by the FBMC based system does not reach the pre-specified thresholds. This is because the FBMC based CR system reaches the maximum interference that can be introduced to the PU using the given power budget. Moreover, the interference induced by the proposed algorithm is less than that using *Zhang* algorithm. Returning to Fig.3.7, one can notice that the interference constraints above $I_{th}^{l} = 10$ mWatt start to have no effect on the achieved capacity of the FBMC system. This indicates also that the FBMC system reaches the maximum interference for the given power budget. The small difference between the net interference values above $I_{th}^{l} = 10$ mWatt is due to the averaging over different channel realizations.

The achieved capacity of the different algorithms is plotted in Fig. 3.8 with lower values of the interference constraints. It can be noticed that *Zhang* algorithm has a limited performance with low interference constraints because the algorithm turns off the subcarriers that have a noise level which is higher than the initial water-filling level (see the cap-limited water-filling algorithm [29] adapted for multi-active PU bands in page 8 of EURASIP journal paper depicted at the end of this Subsection 3.1) and never uses these subcarriers again even if the new water-filling level exceeds its noise level. Moreover, the algorithm deactivates some subcarriers, i.e. transmit zero power, in order to ensure that the interference introduced to PU bands is below the pre-specified thresholds. The lower the interference constraints, the higher the number of deactivated subcarriers is, which justifies the limited performance of this algorithm in case of low interference constraints.

To show the efficiency of transmitting over the active PU bands as well as the non-active bands, Fig. 11 and Fig. 12 in [J5][2] show the achieved capacity using the PI algorithm with and without allowing the SUs to transmit over the PU active bands. The capacity of the CR system transmitting on both the active and non-active bands is higher than that of the system in which the transmission takes place on the non-active bands only. Since the cognitive transmission in the active PU band introduces more interference to the PUs than the other subcarriers, low power levels can be used in these bands with low interference constraints. This justifies why the difference between the two systems decreases when the interference constraints decrease.

For all the presented results, the capacity of FBMC based CR system is higher than that of the one based on OFDM because the side lobes in FBMC's PSD are smaller than those in OFDM, which introduces less interference to the PUs. Moreover, the inserted CP in OFDM based CR systems reduces the total capacity of the system. It can be noticed also that the interference condition introduces a small restriction on the capacity of FBMC based CR systems which is not the case in OFDM based CR systems.

In what follows, an efficient resource allocation algorithm in uplink OFDM-based CR systems is proposed. The

[2]See page 11 in EURASIP journal paper depicted at the end of this Subsection 3.1

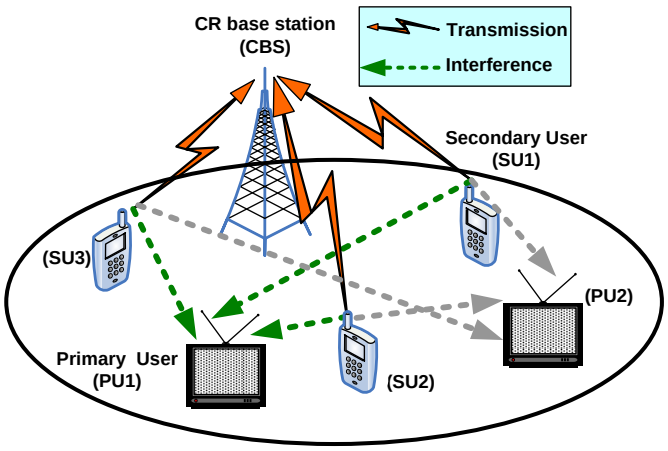

Figure 3.9: Uplink Cognitive Radio Network.

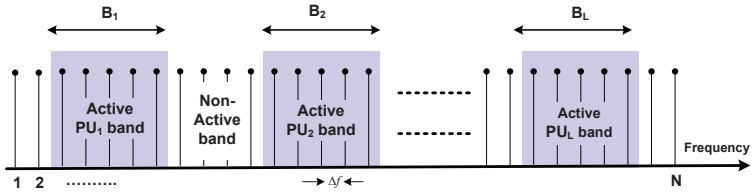

Figure 3.10: Frequency distribution of active and non-active primary bands.

scenario in which the SUs are transmitting on the unused PU bands and causing interference to the active ones is considered. This scenario has been investigated within the project COST Action IC0902, and the network of excellence (NoE) ICT project ACROPOLIS.

The main objective of this research is to maximize the capacity while respecting the per-user power constraints and guaranteeing that no excessive interference is induced to the PUs. The research work carried out in [J10][3] summarizes the main contribution which are the following points:

- As the resource allocation algorithm is a mixed-integer optimization problem, we proposed an efficient algorithm that reduces the computational complexity by separating the subcarrier and power allocation processes into two different steps. The proposed algorithm is shown to have a near-optimal performance and outperforms the algorithms presented in [30, 31, 32, 33]. Additionally, the performance of the algorithm used in non-cognitive multi-carrier systems is discussed.

- Different from the algorithms developed in [30, 31, 32, 33], the fairness among users is considered within the subcarrier allocation by reducing the probability of having users whose instantaneous rate is below the minimum required value.

- The efficiency of the proposed algorithm is investigated for OFDM and FBMC based systems to show the capability of using FBMC in the cognitive networks.

In the carried researches for the **uplink transmission mode**, the PUs and SUs are co-existing in the same geographical location as described in Fig.3.9, and it is assumed that SUs are opportunistically accessing the unused PU bands and transmitting to their cognitive base station (CBS) without causing harmful interference to PUs. As shown in Fig.3.10, the frequency bands B_1, B_2,$\cdots$,B_L represent the L active PU bands while the non-active bands represent the bands that can be used by CR system (CR band). The CR band is divided into N subcarriers each having a Δf bandwidth. There is no synchronization between the primary and secondary systems. The interference induced to the l^{th} PU band should not exceed the predefined interference temperature limit I_{th}^{l}.

The objective is to maximize the total CR data rate while limiting the interference introduced to the PUs. Fairness among users is considered within the subcarrier allocation by reducing the probability of having users

[3]See IET Communication journal paper depicted at the end of this Subsection 3.1

whose instantaneous rate is below a given value. The proposed resource allocation is divided into two phases. The assignment of subcarriers to users is performed first and then the power is allocated to the different subcarriers. The scheme for subcarrier to user assignment proposed in [34] for non-cognitive systems is adopted in order to be suitable for cognitive ones. Subcarriers are allocated based on the channel quality, amount of interference imposed to PUs, instantaneous rate achieved by every user and the increment in the total data rate. For the power allocation phase, an efficient power allocation algorithm is proposed to distribute the powers among the subcarriers under the per-user total power and interference constraints. The system model used in [22] is considered where the PUs and SUs are co-existing in the same geographical location. The interference introduced by the transmission of the i^{th} subcarrier of the CR system to the l^{th} PU band, $I_i^l\left(d_i^l, P_i\right)$, is the integration of the power spectrum density (PSD) of the i^{th} subcarrier across the l^{th} PU band, B_l. If an ideal Nyquist pulse is assumed, the mutual interference can be expressed as [21]

$$I_i^l\left(d_i^l, P_i\right) = P_i \Omega_i^l\,;\;\; \Omega_i^l = \int\limits_{d_i^l - B_l/2}^{d_i^l + B_l/2} \left|g_i^l\right|^2 T_s \left(\frac{\sin \pi f T_s}{\pi f T_s}\right)^2 df \tag{3.16}$$

where d_i^l is the spectral distance between the i^{th} subcarrier and the l^{th} PU band. g_i^l denotes the channel gain (can include path loss and shadowing part) between the i^{th} subcarrier and the l^{th} PU band while P_i is the total transmit power emitted by the i^{th} subcarrier. $T_s = 1/\Delta f$ is the symbol duration and Ω_i^l denotes the interference factor of the i^{th} subcarrier to the l^{th} PU band. By the same way, the interference power introduced by the l^{th} PU signal into the band of the i^{th} subcarrier is [21]

$$J_i^l = \int\limits_{d_i^l - \Delta f/2}^{d_i^l + \Delta f/2} \left|y_i^l\right|^2 \psi_l\left(e^{j\omega}\right)\, d\omega \tag{3.17}$$

where $\psi_l\left(e^{j\omega}\right)$ is the power spectrum density of the l^{th} PU signal and y_i^l is the channel gain between the i^{th} subcarrier and l^{th} PU signal. Several parameters should be considered to built a reliable CR system such that the appearance of the PU during CR transmission which can be taken into account by applying a risk-return model like in [30], the effect of spectrum sensing error like false alarm and misdetection probability as in [35], and the channel estimation errors in the transmission and interfering links as in [36]. Dealing with such a general model is out of the range of the target of developed research work.

The transmission rate for the i^{th} subcarrier, R_i can be evaluated as

$$R_i\left(P_{i,m}, h_{i,m}\right) = \Delta f \log_2\left(1 + \frac{P_{i,m}\left|h_{i,m}\right|^2}{\sigma_i^2}\right) \tag{3.18}$$

where $P_{i,m}$ is the transmission power and $h_{i,m}$ is the i^{th} subcarrier fading gain from the m^{th} SU to the CBS. Additionally, $\sigma_i^2 = \sigma_{AWGN}^2 + \sum\limits_{l=1}^{L} J_i^l$ where σ_{AWGN}^2 is the variance of the additive white Gaussian noise (AWGN) and J_i^l is the interference introduced by the l^{th} PU band into the i^{th} subcarrier which is evaluated using (3.17) and can be modeled as AWGN as described in [22]. Throughout this analysis, all the instantaneous fading gains are assumed to be perfectly known at the CBS. The channel gains between SUs and the CBS can be obtained practically by classical channel estimation techniques while the channel gains between SUs and PUs can be obtained by estimating the received signal power from each primary terminal when it transmits, under the assumptions of pre-knowledge on the primary transmit power levels and the channel reciprocity [37, 38]. Based on the channel gains, the CBS assigns the subcarriers and powers to each SU through a reliable low-rate signaling channel. Let $a_{i,m}$ be the subcarrier allocation indicator, i.e. $a_{i,m} = 1$ if and only if the i^{th} subcarrier is allocated to the m^{th} user. It is assumed that each subcarrier can be used for transmission to at most one user at any given time. Fairness among SUs is guaranteed by assuming that every SU has a minimum instantaneous rate R_{min}. Our objective is to maximize the total data rate of the CR system subject to the constraints on the interference introduced to the PUs, the per-user transmit power constraints and the per-user minimum rate constraints. Therefore, the optimization problem can be formulated as follows

$$
\begin{aligned}
P1: \quad & \max_{P_{i,m}, a_{i,m}} \sum_{m=1}^{M} \sum_{i=1}^{N} a_{i,m} R_i \left(P_{i,m}, h_{i,m}\right) \\
s.t. \quad & \sum_{m=1}^{M} \sum_{i=1}^{N} a_{i,m} P_{i,m} \Omega_{i,m}^{l} \leq I_{th}^{l} \quad \forall l \in \{1, \cdots, L\} \\
& \sum_{i=1}^{N} a_{i,m} P_{i,m} \leq \overline{P_m}, \qquad \forall m \\
& P_{i,m} \geq 0, \qquad \forall i, m \\
& a_{i,m} \in \{0, 1\}, \qquad \forall i, m \\
& \sum_{m=1}^{M} a_{i,m} \leq 1, \qquad \forall i \\
& \sum_{i=1}^{N} a_{i,m} R_i \left(P_{i,m}, h_{i,m}\right) \geq R_{min}, \qquad \forall m
\end{aligned}
\tag{3.19}
$$

where N denotes the total number of subcarriers while M denotes the number of SUs. L is the number of active PU bands and I_{th}^{l} is the interference threshold prescribed by the l^{th} PU. $\overline{P_m}$ is the m^{th} SU total power budget. Without loss of generality, the minimum instantaneous rate R_{min} is assumed constant for all the users. The solution can be easily extended to consider different minimum instantaneous rates for the different SUs. The CBS will perform the subcarrier and power allocation and then diffuse the result to the different SUs.

The optimization problem $P1$ is a mixed optimization problem in which achieving the optimal solution needs high computational complexity. Additionally, the minimum rate constraints increase the complexity of the problem. In order to solve the problem, we propose an algorithm to perform the resource allocation in two phases. In the first phase, a heuristic sub-optimal algorithm is used to allocate the subcarriers to the different users. Afterward, the optimal power allocation is evaluated in the second phase. The optimal power allocation algorithm requires high computational complexity and hence a low complexity power algorithm is proposed to perform the power allocation phase. Depending on the values of I_{th}^{l}, $\overline{P_m}$ and the channel gains, the CR system may not be able to satisfy the minimum rate R_{min} for all the users. Therefore, the last constraint in the optimization problem $P1$ is relaxed by trying to reduce the probability of having users whose rates are below the minimum rate [34]. The outage probability can be defined as

$$
P_{outage} = Pr\{M_{low} \geq 1\} \tag{3.20}
$$

where M_{low} is the number of SUs whose instantaneous rate are below R_{min}.

First the optimal downlink subcarriers to users allocation scheme in multi-carrier systems is achieved by allocating each subcarrier to the user with the maximum SNR [15–18 dB]. This scheme of subcarrier allocation is not efficient in uplink case because of the per-user power constraints. Moreover, the interference introduced to the primary system by each SU should be considered in the CR context, which makes the schemes used in classical multi-carrier systems not efficient. An heuristic subcarrier and power allocation algorithm is presented. Proposed algorithm was first evaluated for one PU band with a single interference constraint and fairness considerations, and then generalized for the multiple PU case in Section 3 and Section 4 respectively of depicted IET journal paper at the end of this Subsection.

For performance comparison, the following algorithms are considered:

1. **Optimal**: the subcarriers are allocated by exhaustive enumeration while the power is allocated using (3.12). The optimal capacity is found without considering the minimum rate requirements.
2. **Wang**: the method proposed in[39] is used. The interference constraint is converted into per-subcarrier power constraints.
3. **Fadel**: the method proposed in [32] is used. The per SU maximum power constraint is generated by converting the interference constraint into per-subcarrier power.
4. **Classical+Pr**: the subcarriers are allocated according to the scheme used in non-cognitive OFDM systems [40], while the power is allocated using (3.12).

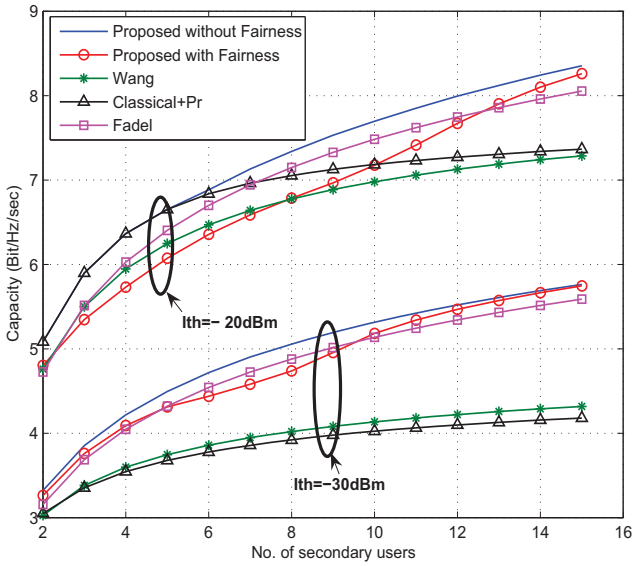

Figure 3.11: Achieved capacity vs No. of SUs when $N = 128$ subcarriers, $\overline{P_m} = 1m$Watt, $B^1 = B^2 = 10$ MHz, and $R_{min} = 20$ Mbits/sec.

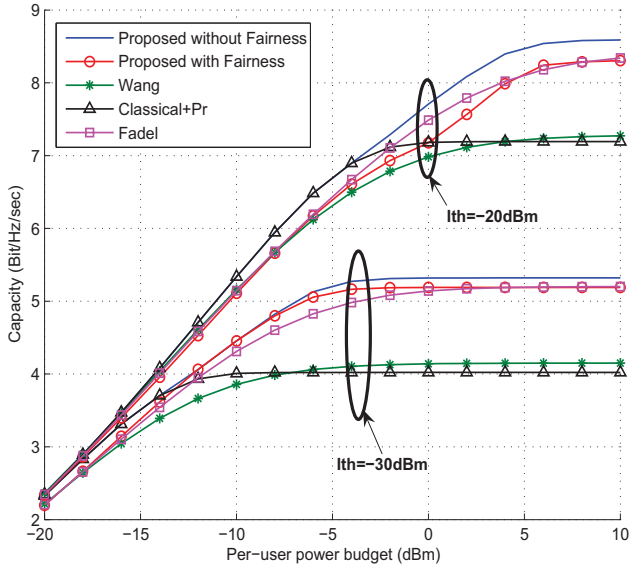

Figure 3.12: Achieved capacity vs per-user power $\overline{P_m}$ when $N = 128$ subcarriers, $M = 8$ SUs, $B^1 = B^2 = 10$ MHz, and $R_{min} = 20$ Mbits/sec.

Hereafter, you have an overview of main obtained results by the proposed algorithm for the uplink mode with Fairness considerations in a CR scenario. Fig.3.11 shows the average capacity against the number of SUs when the interference thresholds are 220 and 230 dBm. The capacity increases with the number of users because of the multiuser diversity. The lower the number of SUs, the smaller the difference between the proposed and Classical+ Pr algorithm. This is because the number of subcarriers that will be allocated to each user will increase, which reduces the amount of power that will be allocated to each subcarrier and consequently the amount of interference imposed to the primary system. This makes the CR system to act relatively as a non-cognitive system. The gap between the different algorithms decreases with the interference thresholds as the CR system becomes closer to the classical (non-cognitive) system.

Fig.3.12 shows the average capacity against per-user power constraint, $\overline{P_m}$, when the interference thresholds are 220

and 230 dBm. The proposed algorithm outperforms the reference algorithms and the capacity of the CR system increases as the per-user power budget increases up to certain total power value. After this value, the capacity remains constant regardless of the increase of the per-user power because the system reaches the maximum power that can be used with the given interference threshold. Remark that when the available SUs power is too low and unable to cause the pre-defined interference constraint, the CR system acts as a non-cognitive one where the proposed algorithm performs very close to the Classical+ Pr algorithm. More extended results can be found at the IET communication journal depicted at end of this Subsection 3.1.1.1.

To resume, all the publications (See Subsection 2.1.1, pp. 30-42) related with this research orientation are: Journals: [J5, J10, J17], Conferences: [C45, C48, C51, C52, C65, C67, C69, C70, C76, C86], Chapter book: [CB14], and the PhD thesis of Mr. Musbah Shaat (2008-2012).
Efforts have been made to disseminate obtained results on FBMC vs. OFDM resource allocation capabilities in CR scenario over the DysPAN-IEEE 1900.7 White Space Radio Working Group. See publications from [O2] to [O6] in Subsection 2.1.5, page 42.

Following are the corresponding depicted papers:

1. [J5] - M. Shaat, Faouzi Bader, "Computationally Efficient Power Allocation Algorithm in Multi-carrier Based Cognitive Radio Networks: OFDM and FBMC Systems", EURASIP Journal on Advanced Signal Processing (ASP). Vol. 2010, Article ID 528378, 13 pages, doi:10.1155/2010/528378. March 2010.

2. [J10] - Musbah Shaat and Faouzi Bader, "Efficient Resource Allocation Algorithm for Uplink in Multicarrier Based CR Networks with Fairness Consideration", IET Communications Journal, vol. 5, issue 16. pp. 2328-2338, doi:10.1049/iet-com.2010.1062. November 2011.

Hindawi Publishing Corporation
EURASIP Journal on Advances in Signal Processing
Volume 2010, Article ID 528378, 13 pages
doi:10.1155/2010/528378

Research Article

Computationally Efficient Power Allocation Algorithm in Multicarrier-Based Cognitive Radio Networks: OFDM and FBMC Systems

Musbah Shaat and Faouzi Bader

Centre Tecnològic de Telecomunicacions de Catalunya (CTTC), Parc Mediterrani de la Tecnología (PMT), Avenida Carl Friedrich Gauss 7, Castelldefels, 08860 Barcelona, Spain

Correspondence should be addressed to Musbah Shaat, musbah.shaat@cttc.es

Received 4 June 2009; Revised 19 October 2009; Accepted 23 December 2009

Academic Editor: Behrouz Farhang-Boroujeny

Cognitive Radio (CR) systems have been proposed to increase the spectrum utilization by opportunistically access the unused spectrum. Multicarrier communication systems are promising candidates for CR systems. Due to its high spectral efficiency, filter bank multicarrier (FBMC) can be considered as an alternative to conventional orthogonal frequency division multiplexing (OFDM) for transmission over the CR networks. This paper addresses the problem of resource allocation in multicarrier-based CR networks. The objective is to maximize the downlink capacity of the network under both total power and interference introduced to the primary users (PUs) constraints. The optimal solution has high computational complexity which makes it unsuitable for practical applications and hence a low complexity suboptimal solution is proposed. The proposed algorithm utilizes the spectrum holes in PUs bands as well as active PU bands. The performance of the proposed algorithm is investigated for OFDM and FBMC based CR systems. Simulation results illustrate that the proposed resource allocation algorithm with low computational complexity achieves near optimal performance and proves the efficiency of using FBMC in CR context.

1. Introduction

Federal Communications Commission (FCC) has reported that many licensed frequency bands are severely under-utilized in both time and spatial domain [1]. Assigning frequency bands to specific users or service providers exclusively does not guarantee that the bands are being used efficiently all the time. Cognitive radio (CR) [2–4], which is an intelligent wireless communication system capable of learning from its radio environment and dynamically adjusting its transmission characteristics accordingly, is considered to be one of the possible solutions to solve the spectrum efficiency problem. By CR, a group of unlicensed users (referred to as secondary users (SUs)) can use the licensed frequency channels (spectrum holes) without causing a harmful interference to the licensed users (referred to as primary users (PUs)) and thus implement efficient reuse of the licensed channels.

Multicarrier communication systems have been suggested as a candidate for CR systems due to its flexibility to allocate resources between the different SUs. As the SU and PU bands may exist side by side and their access technologies may be different, the mutual interference between the two systems is considered as a limiting factor affects the performance of both networks. In [5], the mutual interference between PU and SU was studied. The mutual interference depends on the transmitted power as well as the spectral distance between PU and SU. Orthogonal frequency division multiplexing- (OFDM-) based CR system suffers from high interference to the PUs due to large sidelobes of its filter frequency response. The insertion of the cyclic prefix (CP) in each OFDM symbol decreases the system capacity. The leakage among the frequency subbands has a serious impact on the performance of FFT-based spectrum sensing, and in order to combat the leakage problem of OFDM, a very tight and hard synchronization

implementation has to be imposed among the network nodes [6].

The filter bank multicarrier system (FBMC) does not require any CP extension and can overcome the spectral leakage problem by minimizing the sidelobes of each subcarrier and therefore lead to high efficiency (in terms of spectrum and interference) [6, 7]. Moreover, efficient use of filter banks for spectrum sensing when compared with the FFT-based preiodogram and the Thomson's multitaper (MT) spectrum sensing methods have been recently discussed in [6, 8].

The problem of resource allocation for conventional (noncognitive) multiuser multicarrier systems has been widely studied [9–12]. The maximum aggregated data rate in downlink can be obtained by assigning each subcarrier to the user with the highest signal-to-noise ratio (SNR) and then the optimal power allocation that maximizes the channel capacity is waterfilling on the subcarriers with a given total power constraint [9]. In cognitive radio systems, two types of users (SU and PU) and the mutual interference between them should be considered. The use of the power allocation based on conventional waterfilling algorithm is not always efficient. An additional constraint should be introduced due to the interference caused by the sidelobes in different subcarriers. The transmit power of each subcarrier should be adjusted according to the channel status and the location of the subcarrier with respect to the PU spectrum.

Wang et al. in [13] proposed an iterative partitioned single user waterfilling algorithm. The algorithm aims to maximize the capacity of the CR system under the total power constraint with the consideration of the per subcarrier power constraint caused by the PUs interference limit. The per subcarrier power constraint is evaluated based on the pathloss factor between the CR transmitter and the PU protection area. The mutual interference between the SU and PU was not considered. In [14, 15], the authors proposed an optimal and two suboptimal power loading schemes using the Lagrange formulation. These loading schemes maximize the downlink transmission capacity of the CR system while keeping the interference induced to only one PU below a prespecified interference threshold without the consideration of the total power constraint. In [16], an algorithm called *RC algorithm* was presented for multiuser resource allocation in OFDM-based CR systems. This algorithm uses a greedy approach for subcarrier and power allocations by successively assigning bits, one at a time, based on minimum SU power and minimum interference to PUs. The algorithm has a high computational complexity and a limited performance in comparison with the optimal solution. In [17], a low complexity suboptimal solution is proposed. The algorithm initially assumes that the maximum power that can be allocated to each subcarrier is equal to the power found by the conventional waterfilling and then modifies these values by applying a power reduction algorithm in order to satisfy the interference constraints. Experimental results like [18] emphasize the need of low interference constraints where this algorithm has a limited performance. Moreover, the nontransmission of the data over the subcarriers below the waterfilling level or the deactivated subcarriers due to the power reduction algorithm decreases the overall capacity of the CR system. In [19], we give some preliminary research results for resource allocation in OFDM-based CR systems. This preliminary work considers a simple model with one PU. The performance of the algorithm was not compared with neither the optimal nor the existed suboptimal algorithms.

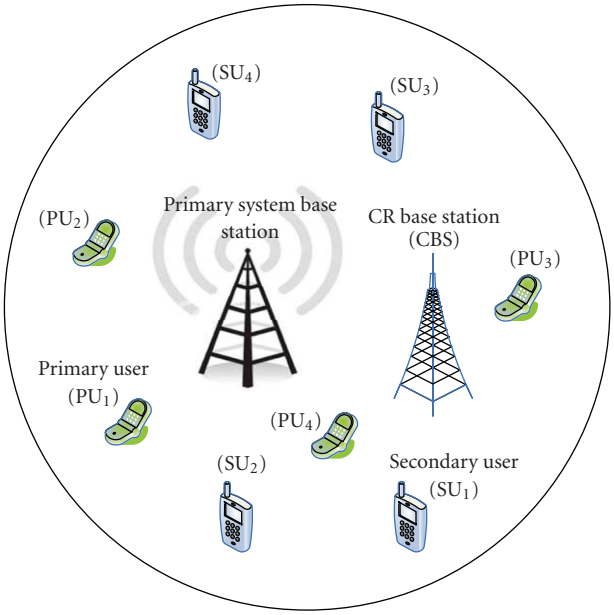

Figure 1: Cognitive Radio Network.

In this paper, considering more realistic scenario with several primary user interference constraints, a computationally efficient resource allocation algorithm in multicarrier-based CR systems is proposed. The proposed algorithm maximizes the downlink capacity of the CR system under both total power and interference induced to the PUs constraints. The CR system can use the nonactive and active PU bands as long as the total power and the different interference constraints are satisfied. The simulation results demonstrate that the proposed solution is very close to the optimal solution with a good reduction in the computational complexity. Moreover, the proposed algorithm outperforms the previously presented algorithms in the literature. The efficiency of using FBMC in CR systems is investigated and compared to OFDM-based CR systems. The rest of this paper is organized as follows. Section 2 gives the system model while Section 3 formulates the problem. The proposed algorithm is presented in Section 4. Selected numerical results are presented in Section 5. Finally, Section 6 concludes the paper.

2. System Model

In this paper, the downlink scenario will be considered. As shown in Figure 1, the CR system coexists with the PUs radio in the same geographical location. The cognitive base station (CBS) transmits to its SUs and causes interference to the PUs. Moreover, the PUs base station interferes with the SUs. The CR system's frequency spectrum is divided into N

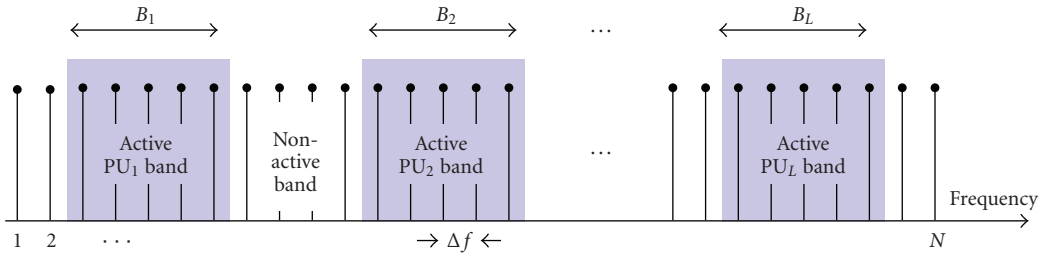

Figure 2: Frequency distribution of the active and nonactive primary bands.

subcarriers each having a Δf bandwidth. The side by side frequency distribution of the PUs and SUs will be assumed (see Figure 2). The frequency bands B_1,B_2,...,B_L have been occupied by the PUs (active PU bands) while the other bands represent the nonactive PU bands. Its assumed that the CR system can use the nonactive and active PU bands provided that the total interference introduced to the l^{th} PU band does not exceed I_{th}^l where $I_{th}^l = T_{th}^l B_l$ denotes that the maximum interference power that can be tolerated by the PU_l and T_{th}^l is the interference temperature limit for PU_l.

The interference introduced by the i^{th} subcarrier to l^{th} PU, $I_i^l(d_i, P_i)$, is the integration of the power spectrum density (PSD), Φ_i, of the i^{th} subcarrier across the l^{th} PU band, B_l, and can be expressed as [5]

$$I_i^l(d_i, P_i) = \int_{di-B_l/2}^{di+B_l/2} \left| g_i^l \right|^2 \Phi_i(f) df = P_i \Omega_i^l, \tag{1}$$

where P_i is the total transmit power emitted by the i^{th} subcarrier and d_i is the spectral distance between the i^{th} subcarrier and the l^{th} PU band. g_i^l denotes the channel gain between the i^{th} subcarrier and the l^{th} PU. Ω_i^l denotes the interference factor of the i^{th} subcarrier.

The interference power introduced by the l^{th} PU signal into the band of the i^{th} subcarrier is [5]

$$J_i^l(d_i, P_{PU_l}) = \int_{di-\Delta f/2}^{di+\Delta f/2} \left| y_i^l \right|^2 \psi_l\left(e^{j\omega}\right) d\omega, \tag{2}$$

where $\psi_l(e^{j\omega})$ is the power spectrum density of the PU_l signal and y_i^l is the channel gain between the i^{th} subcarrier and l^{th} PU signal. The PSD expression, Φ_i, depends on the used multicarrier technique. The OFDM and FBMC PSDs are described in the following subsections.

2.1. OFDM System and Its PSD. The OFDM symbol is formed by taking the inverse discrete Fourier transform (IDFT) to a set of complex input symbols $\{X_k\}$ and adding a cyclic prefix. This can be written mathematically as

$$x(n) = \sum_k \sum_{w \in Z} X_{k,w} g_T(n - wT) e^{j2\pi(n-wT-C)k/N}, \tag{3}$$

where $\{k\}$ is the set of data subcarrier indices and is a subset of the set $\{0, 1, \ldots, N-1\}$, N is the IDFT size, C is the length of the cyclic prefix in number of samples, and $T = C + N$ is the length of the OFDM symbol in number of samples. g_T denotes the pulse shape, while w denotes the w^{th} OFDM symbol.

Following the derivation of the PSD for general baseband signal given in [20], it can be shown that the OFDM PSD is

$$\Phi_{\text{OFDM}}(f) = \frac{\sigma_x^2}{T} \sum_k \left| G_T\left(f - \frac{k}{N}\right) \right|^2, \tag{4}$$

where $G_T(f)$ is the Fourier transform of $g_T(n)$, and σ_x^2 is the variance of the zero mean (symmetrical constellation) and uncorrelated input symbols. The assumption of the uncorrelated input symbols can be justified because of coding and interleaving in practical symbols [21].

$g_T(n)$ can be chosen as

$$g_T(n) = \begin{cases} 1, & n = 0, 1, \ldots, T-1, \\ 0, & \text{otherwise}, \end{cases} \tag{5}$$

and hence its Fourier transform is

$$\left| G_T(f) \right|^2 = T + 2 \sum_{r=1}^{T-1} (T - r) \cos(2\pi f r). \tag{6}$$

2.2. FBMC System and Its PSD. Each subcarrier in FBMC system is modulated with a staggered QAM (offset QAM) [22]. The basic idea is to transmit real-valued symbols instead of transmitting complex-valued ones. Due to this time staggering of the in-phase and quadrature components of the symbols, orthogonality is achieved between adjacent subcarriers. The modulator and the demodulator are implemented using the synthesis and analysis filter banks. The filters in the synthesis and analysis filter bank are obtained by frequency shifts of a single prototype filter. Figure 3 depicts the structure of the synthesis and analysis filter bank at the transmitter and receiver in FBMC-based multicarrier systems.

The FBMC, also called OQAM/OFDM, signal can be written mathematically as [23]

$$x(n) = \sum_k \sum_{w \in Z} a_{k,w} h(n - w\tau_o) e^{j2\pi(k/N)n} e^{j\phi_{k,w}}, \tag{7}$$

where $\{k\}$ is the set of subcarrier indices, h is the pulse shape, $\phi_{k,w}$ is an additional phase term, and τ_o is FBMC symbol duration. $a_{k,w}$ are the real symbols obtained from the complex QAM symbols having a zero mean and variance

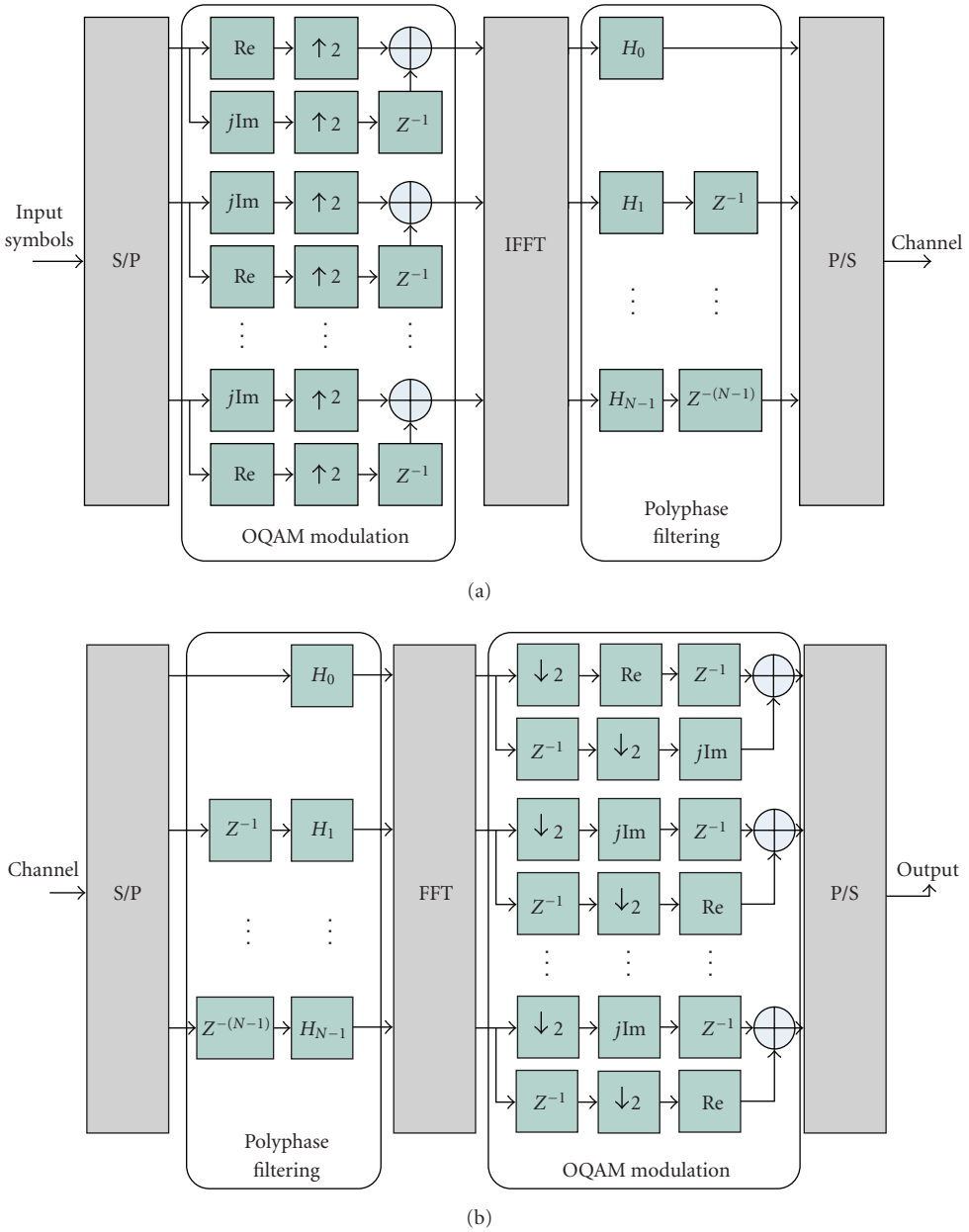

Figure 3: FBMC system's transmitter and receiver.

σ_x^2. Hence, the FBMC symbols have a zero mean and finite variance $\sigma_r^2 = \sigma_x^2/2$. The PSD of the FBMC can be expressed by [23]

$$\Phi_{\text{FBMC}} = \frac{\sigma_r^2}{\tau_\circ} \sum_k \left| H\left(f - \frac{k}{N}\right) \right|^2, \tag{8}$$

where $H(f)$ is the frequency response of the prototype filter with coefficients $h[n]$ with $n = 0, \ldots, W-1$, where $W = KN$ and K is the length of each polyphase components (overlapping factor) while N is the number of the subcarriers. Assuming that the prototype coefficients have even symmetry around the $(KN/2)^{th}$ coefficient, and the first coefficient is zero [21], we get

$$|H(f)| = h\left[\frac{W}{2}\right] + 2 \sum_{r=1}^{W/2-1} h\left[\left(\frac{W}{2}\right) - r\right] \cos(2\pi f r). \tag{9}$$

To make a parallel between OFDM and FBMC, we place ourselves in the situation where both systems transmit the same quantity of information. This is the case if they have the same number of subcarriers N together with duration of τ_o samples for FBMC real data and $T = 2\tau_o$ for the complex QAM ones [21, 23].

From the relations above we can notice that the PSDs of OFDM and FBMC are the summation of the spectra of

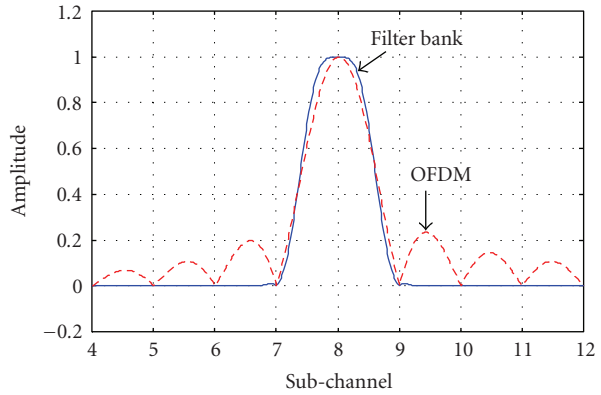

Figure 4: Single subcarrier PSDs of the OFDM and FBMC systems.

the individual subcarriers. Using the PHYDYAS prototype filter [24], Figure 4 plots a single subcarrier power spectral densities of the OFDM and FBMC systems. It can be noted that the FBMC system has very small side lobes in comparison with that of the OFDM system. Note that in order to solve the large sidelobes problem in OFDM system, many methods have already been employed, such as the insertion of guard subcarriers [25] or cancelation subcarriers [26], windowing (in time domain) [27, 28], and filtering before transmitting [29]. It is known that the guard subcarriers decrease the spectral efficiency, while windowing reduces the delay spread tolerance and filtering is more complex and introduces distortion in the desired signals [30].

3. Problem Formulation

The transmission rate of the i^{th} subcarrier, R_i, with the transmit power P_i can be evaluated using the Shannon capacity formula and is given by

$$R_i(P_i, h_i) = \Delta f \log_2\left(1 + \frac{P_i|h_i|^2}{\sigma_i^2}\right), \tag{10}$$

where h_i is the subcarrier fading gain from the CBS to the user. $\sigma_i^2 = \sigma_{\text{AWGN}}^2 + \sum_{l=1}^{L} J_i^l$ where σ_{AWGN}^2 is the mean variance of the additive white Gaussian noise (AWGN) and J_i^l is the interference introduced by the l^{th} PUs band into the i^{th} subcarrier. The interference from PUs to the i^{th} subcarrier is assumed to be the superposition of large number of independent components, that is, $\sum_{l=1}^{L} J_i^l$. Hence, we can model the interference as AWGN. This assumption may not be valid for low number of PU bands but can be considered as a good approximation for large number of PU bands. The same model can be found in [6, 15, 17]. Remark that the nature of the PUs interference on SUs band is the same on both OFDM and FBMC systems. The difference is only in the SUs interference to the PU bands, which is in that case FBMC has significantly lower interference, because of its significantly smaller sidelobes as compared to those of OFDM.

Assuming that each subcarrier band is narrow, subcarriers can be approximated as channel with flat fading gains [31, 32]. It will be assumed that the channel changes slowly so that the channel gains will be constant during transmission. The total achievable rate for OFDM and FBMC systems is evaluated by summing the transmission rate across the different subcarriers [7, 33]. All the instantaneous fading gains are assumed perfectly known at the CR system and there is no intercarrier interference (ICI). Let $v_{i,m}$ to be a subcarrier allocation indicator, that is, $v_{i,m} = 1$ if and only if the subcarrier is allocated to the m^{th} user. It is assumed that each subcarrier can be used for transmission to at most one user at any given time. Our objective is to maximize the total capacity of the CR system subject to the instantaneous interference introduced to the PUs and total transmit power constraints. Therefore, the optimization problem can be formulated as follows:

$$P1: \max_{P_{i,m}} \sum_{m=1}^{M} \sum_{i=1}^{N} v_{i,m} R_{i,m}(P_{i,m}, h_{i,m}) \tag{11}$$

subject to

$$v_{i,m} \in \{0, 1\}, \quad \forall i, m, \tag{12}$$

$$\sum_{m=1}^{M} v_{i,m} \leq 1, \quad \forall i, \tag{13}$$

$$\sum_{m=1}^{M} \sum_{i=1}^{N} v_{i,m} P_{i,m} \leq P_T, \tag{14}$$

$$P_{i,m} \geq 0, \quad \forall i \in \{1, 2, \ldots, N\}, \tag{15}$$

$$\sum_{m=1}^{M} \sum_{i=1}^{N} v_{i,m} P_{i,m} \Omega_i^l \leq I_{th}^l, \quad \forall l \in \{1, 2, \ldots, L\}, \tag{16}$$

where N denotes the total number of subcarriers, M is the number of users, I_{th}^l denotes the interference threshold prescribed by the l^{th} PU, and P_T is the total SUs power budget. L is the number of the active PU bands. Inequality (13) ensures that any given subcarrier can be allocated to at most one user.

The optimization problem $P1$ is a combinatorial optimization problem and its complexity grows exponentially with the input size. In order to reduce the computational complexity, the problem is solved in two steps by many of the suboptimal algorithms [9–12]. In the first step, the subcarriers are assigned to the users and then the power is allocated for these subcarriers in the second step. Once the subcarriers are allocated to the users, the multiuser system can be viewed virtually as a single user multicarrier system. As proved in [9], the maximum data rate in downlink can be obtained if the subcarriers are assigned to the user who has the best channel gain for that subcarrier as described in Algorithm 1.

By applying Algorithm 1, the values of the channel indicators $v_{i,m}$ are determined and hence for notation simplicity, single user notation can be used. The different channel gains

can be determined from the subcarrier allocation step as follows:

$$h_i = \sum_{m=1}^{M} v_{i,m} h_{i,m}. \tag{17}$$

Therefore, problem $P1$ in (11) can be reformulated as follows:

$$P2: \max_{P_i} \sum_{i=1}^{N} \log_2\left(1 + \frac{P_i |h_i|^2}{\sigma_i^2}\right) \tag{18}$$

subject to

$$\sum_{i=1}^{N} P_i \Omega_i^l \le I_{th}^l \quad \forall l \in \{1, 2, \ldots, L\}, \tag{19}$$

$$\sum_{i=1}^{N} P_i \le P_T, \tag{20}$$

$$P_i \ge 0 \quad \forall i \in \{1, 2, \ldots, N\}. \tag{21}$$

The problem $P2$ is a convex optimization problem. The Lagrangian can be written as [17]

$$\begin{aligned} G = &-\sum_{i=1}^{N} \log_2\left(1 + \frac{P_i^* |h_i|^2}{\sigma_i^2}\right) + \sum_{l=1}^{L} \alpha_l \left(\sum_{i=1}^{N} P_i^* \Omega_i^l - I_{th}^l\right) \\ &+ \beta\left(\sum_{i=1}^{N} P_i^* - P_T\right) - \sum_{i=1}^{N} P_i^* \mu_i, \end{aligned} \tag{22}$$

where $\alpha_l, l \in \{1, 2, \ldots, L\}$, $\mu_i, i \in \{1, 2, \ldots, N\}$, and β are the Lagrange multipliers. The Karush-Kuhn-Tucker (KKT) conditions can be written as follows:

$$\begin{aligned} P_i^* &\ge 0, \quad \forall i \in \{1, 2, \ldots, N\}, \\ \alpha_l &\ge 0, \quad \forall l \in \{1, 2, \ldots, L\}, \\ \beta &\ge 0, \\ \mu_i &\ge 0, \quad \forall i \in \{1, 2, \ldots, N\}, \\ \alpha_l &\left(\sum_{i=1}^{N} P_i^* \Omega_i^l - I_{th}^l\right) = 0, \quad \forall l \in \{1, 2, \ldots, L\}, \\ \beta &\left(\sum_{i=1}^{N} P_i^* - P_T\right) = 0, \\ \mu_i P_i^* &= 0, \quad \forall i \in \{1, 2, \ldots, N\}, \\ \frac{\partial G}{\partial P_i^*} &= \frac{-1}{\sigma_i^2/|h_i|^2 + P_i^*} + \sum_{l=1}^{L} \alpha_l \Omega_i^l + \beta - \mu_i = 0, \end{aligned} \tag{23}$$

and also the solution should satisfy the total power and interference constraints given by (20) and (19). Rearranging the last condition in (23) we get

$$P_i^* = \frac{1}{\sum_{l=1}^{L} \alpha_l \Omega_i^l + \beta - \mu_i} - \frac{\sigma_i^2}{|h_i|^2}. \tag{24}$$

Initialization:
Set $v_{i,m} = 0 \quad \forall i, m$
Subcarrier Allocation:
for $i = 1$ to N **do**
$m^* = \underset{m}{\operatorname{argmax}}\{h_{i,m}\}$; $v_{i,m^*} = 1$
end for

Algorithm 1: Subcarriers to user allocation.

Since $P_i^* \ge 0$, we get

$$\frac{\sigma_i^2}{|h_i|^2} \le \frac{1}{\sum_{l=1}^{L} \alpha_l \Omega_i^l + \beta - \mu_i}. \tag{25}$$

If $\sigma_i^2/|h_i|^2 < 1/(\sum_{l=1}^{L} \alpha_l \Omega_i + \beta)$, then $\mu_i = 0$ and hence

$$P_i^* = \frac{1}{\sum_{l=1}^{L} \alpha_l \Omega_i^l + \beta} - \frac{\sigma_i^2}{|h_i|^2}. \tag{26}$$

Moreover, if $\sigma_i^2/|h_i|^2 > 1/(\sum_{l=1}^{L} \alpha_l \Omega_i^l + \beta)$, from (24) we get

$$\frac{1}{\sum_{l=1}^{L} \alpha_l \Omega_i^l + \beta - \mu_i} \ge \frac{\sigma_i^2}{|h_i|^2} \ge \frac{1}{\sum_{l=1}^{L} \alpha_l \Omega_i^l + \beta}, \tag{27}$$

and since $\mu_i P_i^* = 0$ and $\mu_i \ge 0$, we get that $P_i^* = 0$.

Therefore, the optimal solution can be written as follows:

$$P_i^* = \begin{cases} \dfrac{1}{\sum_{l=1}^{L} \alpha_l \Omega_i^l + \beta} - \dfrac{\sigma_i^2}{|h_i|^2} & \text{if } \dfrac{\sigma_i^2}{|h_i|^2} < \dfrac{1}{\sum_{l=1}^{L} \alpha_l \Omega_i^l + \beta}, \\ 0 & \text{if } \dfrac{\sigma_i^2}{|h_i|^2} \ge \dfrac{1}{\sum_{l=1}^{L} \alpha_l \Omega_i^l + \beta}, \end{cases} \tag{28}$$

or more simply, (28) can be written as the follows:

$$P_i^* = \left[\frac{1}{\sum_{l=1}^{L} \alpha_l \Omega_i^l + \beta} - \frac{\sigma_i^2}{|h_i|^2}\right]^+, \tag{29}$$

where $[x]^+ = \max(0, x)$. Solving for $L + 1$ Lagrangian multipliers is computational complex. These multipliers can be found numerically using ellipsoid or interior point method with a complexity $\mathcal{O}(N^3)$ [17, 34]. In what follows we will propose a low complexity algorithm that achieves near optimal performance.

4. Proposed Algorithm

The optimal solution for the optimization problem has a high computational complexity which makes it unsuitable for the practical applications. A low complexity algorithm is proposed in [17]. The subcarriers nulling and deactivating throughout this algorithm degrade the system capacity and causing the algorithm to have a limited performance in low interference constraints. To overcome the drawbacks of this algorithm, a low complexity power allocation algorithm will be presented.

As described in [5, 17], most of the interference introduced to the PU bands is induced by the cognitive transmission in the subcarriers where the PU is active as well as the subcarriers that are directly adjacent to the PU bands. Considering this fact, it can be assumed that each subcarrier is belonging to the closest PU band and only introducing interference to it, then the optimization problem $P2$ can be reformulated as follows:

$$P3: \max_{P_i'} \sum_{i=1}^{N} \log_2\left(1 + \frac{P_i'|h_i|^2}{\sigma_i^2}\right) \tag{30}$$

subject to

$$\begin{aligned} \sum_{i\in N_l} P_i'\Omega_i^l &\le I_{th}^l \quad \forall l \in \{1,2,\ldots,L\}, \\ \sum_{i=1}^{N} P_i' &\le P_T, \\ P_i' &\ge 0 \quad \forall i \in \{1,2,\ldots,N\}, \end{aligned} \tag{31}$$

where N_l denotes the set of the subcarriers belong to the l^{th} PU band. Using the same derivation leading to (29), we get

$$P_i' = \left[\frac{1}{\alpha_l'\Omega_i^l + \beta'} - \frac{\sigma_i^2}{|h_i|^2}\right]^+, \tag{32}$$

where α_l' and β' are the non-negative dual variables corresponding to the interference and power constraints respectively. The solution of the problem still has high computational complexity which encourages us to find a faster and efficient power allocation algorithm.

If the interference constraints are ignored in $P3$, the solution of the problem will follow the well-known waterfilling interpretation [35]

$$P_i^{'(P_T)} = \left[\lambda - \frac{\sigma_i^2}{|h_i|^2}\right]^+, \tag{33}$$

where λ is the waterfilling level. On the other side, if the total power constraint is ignored, the Lagrangian of the problem can be written as [15]

$$\begin{aligned} \mathrm{G}^{(\mathrm{Int})} = &-\sum_{i\in N_l} \log_2\left(1 + \frac{P_i^{'(\mathrm{Int})}|h_i|^2}{\sigma_i^2}\right) \\ &+ \alpha_l^{'(\mathrm{Int})}\left(\sum_{i\in N_l} P_i^{'(\mathrm{Int})}\Omega_i^l - I_{th}^l\right), \end{aligned} \tag{34}$$

where α_l' is the Lagrange multiplier. Equating $\partial \mathrm{G}^{(\mathrm{Int})}/\partial P_i^{'(\mathrm{Int})}$ to zero, we get

$$P_i^{'(\mathrm{Int})} = \left[\frac{1}{\alpha_l^{'(\mathrm{Int})}\Omega_i^l} - \frac{\sigma_i^2}{|h_i|^2}\right]^+, \tag{35}$$

where the value of α_l' can be calculated by substituting (35) into $\sum_{i\in N_l} P_i^{'(\mathrm{Int})}\Omega_i = I_{th}^l$ to get

$$\alpha_l^{'(\mathrm{Int})} = \frac{|N_l|}{I_{th}^l + \sum_{i\in N_l}\left(\Omega_i^l\sigma_i^2/|h_i|^2\right)}. \tag{36}$$

It is obvious that if the summation of the allocated power under only the interference constraints is lower than or equal the available total power budget, that is, $\sum_{i=1}^{N} P_i^{'(\mathrm{Int})} \le P_T$, for all $i \in \{1,2,\ldots,N\}$, then (35)-(36) will be the optimal solution for the optimization problem $P3$. In most of the cases, the total power budget is quite lower than this summation, and hence the Power Interference (PI) constrained algorithm, referred to as *PI-Algorithm*, is proposed to allocate the power under both total power and interference constraints.

In order to solve the optimization problem $P3$, we can start by assuming that the maximum power that can be allocated for a given subcarrier P_i^{Max} is determined according to the interference constraints only by using (35)-(36) for every set of subcarriers N_l, for all $l \in \{1,2,\ldots,L\}$. By such an assumption, we can guarantee that the interference introduced to PU bands will be under the prespecified thresholds. Once the maximum power P_i^{Max} is determined, the total power constraint is tested. If the total power constraint is satisfied, then the solution has been found and is equal to the maximum power that can be allocated to each subcarrier, that is, $P_i' = P_i^{\mathrm{Max}}$. Otherwise, the available power budget should be distributed among the subcarriers giving that the power allocated to each subcarrier is lower than or equal to the maximum power that can be allocated to each subcarrier P_i^{Max}, and hence the following problem should be solved:

$$P4: \max_{P_i^{W.F}} \sum_{i=1}^{N} \log_2\left(1 + \frac{P_i^{W.F}|h_i|^2}{\sigma_i^2}\right) \tag{37}$$

subject to

$$\begin{aligned} \sum_{i=1}^{N} P_i^{W.F} &\le P_T, \\ 0 \le P_i^{W.F} &\le P_i^{\mathrm{Max}}. \end{aligned} \tag{38}$$

The problem $P4$ is called "*cap-limited*" waterfilling [36]. The problem can be solved efficiently using the concept of the conventional waterfilling. Given the initial waterfilling solution, the channels that violate the maximum power P_i^{Max} are determined and upper bounded with P_i^{Max}. The total power budget is reduced by subtracting the power assigned so far. At the next step, the algorithm proceeds to successive waterfilling over the subcarriers that did not violate the maximum power P_i^{Max} in the last step. This procedure is repeated until the allocated power $P_i^{W.F}$ does not violate the maximum power P_i^{Max} in any of the subcarriers in the new iteration. The "*cap-limited*" waterfilling algorithm implementation is described in Algorithm 2.

The solution $P_i^{W.F}$ of the problem $P4$ is satisfying the total power constraint of the problem $P3$ with equality which is not the case for the different interference constraints I_{th}^l. Since it is assumed that $P_i^{W.F} \le P_i^{\mathrm{Max}}$, some of the powers allocated to subcarriers will not reach the maximum allowable values. This will make the interference introduced to the PU bands below the thresholds I_{th}^l. In order to take advantage of all the allowable interference, the values of the

(1) **Initialize** $\mathcal{F} = \mathcal{M} = \mathcal{N} = \{1, 2, \ldots, N\}$, $\overline{P_i} = P_i^{\text{Max}}$, and $S = P_T$.
(2) Sort $\left\{ T_i = \dfrac{\sigma_i^2}{|h_i|^2}, i \in \mathcal{N} \right\}$ in decreasing order with J being the sorted index. Find the waterfilling λ as follows:
  (a) $T_{\text{sum}} = \sum_{i \in \mathcal{N}} T_i$, $\lambda = (T_{\text{sum}} + S)/|\mathcal{N}|$, $n = 1$.
  (b) **While** $T_{J(n)} > \lambda$ **do**
    $T_{\text{sum}} = T_{\text{sum}} - T_{J(n)}$, $\mathcal{N} = \mathcal{N} \setminus \{J(n)\}$, $\lambda = (T_{\text{sum}} + S)/|\mathcal{N}|$, $n = n + 1$
  end while
  (c) Set $P_i^{W.F} = [\lambda - T_i]^+, \forall i \in \mathcal{F}$
(3) **repeat**
  if $P_i^{W.F} \geq \overline{P_i}$
  Let $P_i^{W.F} = \overline{P_i}$, $S = S - P_i^{W.F}$, $\mathcal{M} = \mathcal{M} \setminus \{i\}$, $\mathcal{N} = \mathcal{M}$, and go to step 2;
  end if
until $P_i^{W.F} \leq \overline{P_i}, \forall i \in \mathcal{F}$

Algorithm 2: Cap-limited waterfilling.

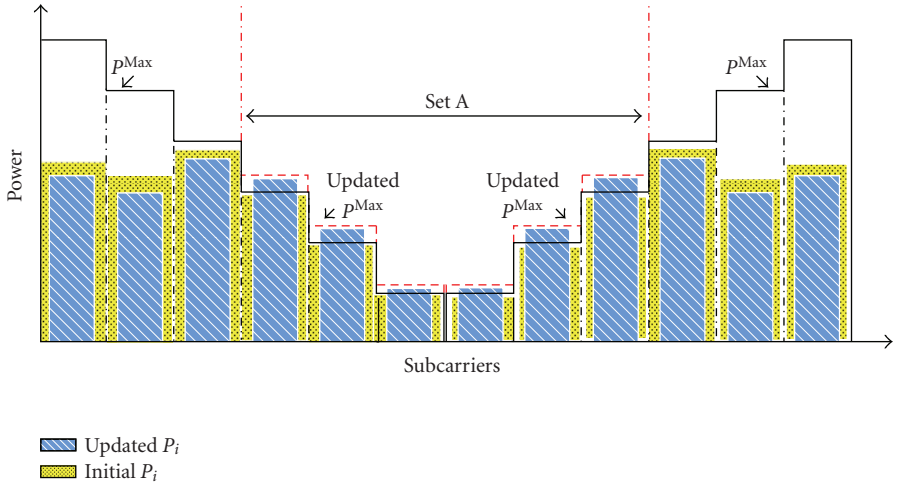

Figure 5: An Example of the SUs allocated power using PI-Algorithm.

maximum power that can be allocated to each subcarrier P_i^{Max} should be updated depending on the left interference. The left interference can be determined as follows:

$$I_{\text{Left}}^l = I_{th}^l - \sum_{i \in N_l} P_i^{W.F} \Omega_i^l. \tag{39}$$

Assuming that $A_l \subset N_l$ is the set of the subcarriers that reach its maximum, that is, $P_i^{W.F} = P_i^{\text{Max}}$, for all $i \in A_l$, then, P_i^{Max}, for all $i \in A_l$ can be updated by applying (35)-(36) on the subcarriers in the set A_l with the following interference constraints:

$$I_{th}^{'l} = I_{\text{Left}}^l + \sum_{i \in A_l} P_i^{W.F} \Omega_i^l. \tag{40}$$

After determining the updated values of P_i^{Max}, the "*cap-limited*" waterfilling is performed again to find the final solution $P_i' = P_i^{W.F}$. Now, the solution P_i' is satisfying approximately the interference constraints with equality as well as guaranteing that the total power used is equal to P_T. A graphical description of the *PI-Algorithm* is given in Figure 5 while the implementation procedures are described in Algorithm 3.

The computational complexity of Step 2 in the proposed PI-Algorithm (Algorithm 3) is $\sum_{l=1}^{L} \mathcal{O}(|N_l| \log |N_l|) \leq \mathcal{O}(N \log N)$. Steps 4 and 6 of the algorithm execute the "*cap-limited*" waterfilling which has a complexity of $\mathcal{O}(N \log N + \eta N)$, where $\eta \leq N$ is the number of the iterations. Step 5 has a complexity of $\sum_{l=1}^{L} \mathcal{O}(|A_l| \log |A_l|) + \mathcal{O}(L) \leq \mathcal{O}(N \log N) + \mathcal{O}(L)$. Therefore, The overall complexity of the algorithm is lower than $\mathcal{O}(N \log N + \eta N) + \mathcal{O}(L)$. The value of η is estimated via simulation to be lower than five, that is, $\eta \in [0, 5]$. Comparing to the computational complexity of the optimal solution, $\mathcal{O}(N^3)$, the proposed algorithm has much lower computational complexity specially when the number of the subcarriers N increased.

5. Simulation Results

The simulations are performed under the scenario given in Figure 1. A multicarrier system of $M = 3$ cognitive users and $N = 32$ subcarriers is assumed. The values

(1) **Initialize** $\mathcal{N} = \{1, 2, \cdots, N\}$, $\mathcal{N}_l = N_l$, $I^l_{\text{Left}} = 0$, $S = P_T$ and $\mathcal{A}_l = \emptyset$.

(2) $\forall l \in \{1, 2, \cdots, L\}$, sort $\left\{H_i = \dfrac{\sigma_i^2}{|h_i|^2}\Omega_i^l, i \in \mathcal{N}_l\right\}$ in decreasing order with k being the sorted index.

Find the P_i^{Max} as follows:

(a) $H_{\text{sum}} = \sum_{i\in\mathcal{N}_l} H_i$, $\alpha_l^{'(\text{Int})} = |\mathcal{N}_l|/(I^l_{th} + H_{\text{sum}})$, $n = 1$.

(b) **while** $\alpha_l^{'(\text{Int})} > H^{-1}_{k(n)}$ **do**

$H_{\text{sum}} = H_{\text{sum}} - H_{k(n)}$, $\mathcal{N}_l = \mathcal{N}_l \setminus \{k(n)\}$, $\alpha_l^{'(\text{Int})} = |\mathcal{N}_l|/(I^l_{th} + H_{\text{sum}})$, $n = n + 1$

end while

(c) Set $P_i^{\text{Max}} = \left[\dfrac{1}{\alpha_l^{'(\text{Int})}\Omega_i^l} - \dfrac{\sigma_i^2}{|h_i|^2}\right]^+$

(3) **if** $\sum_{i\in\mathcal{N}} P_i^{\text{Max}} \le P_T$

Let $P_i' = P_i^{\text{Max}}$ and stop the algorithm.

end if

(4) Execute the "*cap-limited*" waterfilling (Algorithm 2) and find the set $\mathcal{A}_l \subset N_l$ where $P_i^{W.F} = P_i^{\text{Max}}$.

(5) Evaluate $I^l_{\text{Left}} = I^l_{th} - \sum_{i\in N_l} P_i^{W.F}\Omega_i^l$ and set $\mathcal{N}_l = \mathcal{A}_l$, $I^l_{th} = I^l_{\text{Left}} + \sum_{i\in\mathcal{A}_l} P_i^{W.F}\Omega_i^l$ and apply again only step 2 to update P_i^{Max}.

(6) Execute the "*cap-limited*" waterfilling (Algorithm 2) and set $P_i' = P_i^{W.F}$.

Algorithm 3: PI-Algorithm.

of Δf and P_T are assumed to be 0.3125 MHz and 1 watt, respectively. AWGN of variance 10^{-6} is assumed. Without loss of generality, the interference induced by PUs to the SUs band is assumed to be negligible. The channel gains h and g are outcomes of independent, identically distributed (i.i.d) Rayleigh distributed random variables (rv's) with mean equal to "1" and assumed to be perfectly known at the (CBS). OFDM and FBMC-based cognitive radio systems are evaluated. The OFDM system is assumed to have a 6.67% of its symbol time as cyclic prefix (CP). For FBMC system, the prototype coefficients are assumed to be equal to PHYDYAS coefficients with overlapping factor $K = 4$ and are defined by [24, 37]

$$h[n] = 1 - 1.94392\cos\left(\frac{2\pi n}{128}\right) + \sqrt{2}\cos\left(\frac{4\pi n}{128}\right) - 0.470294\cos\left(\frac{6\pi n}{128}\right), \quad 0 \le n \le 127, \tag{41}$$

The optimal solution is implemented using the interior point method. We refer to the method proposed in [17] by Zhang algorithm. All the results have been averaged over 1000 iterations.

Two interference constraints belonging to two active PU bands, that is, $L = 2$, is assumed as given in Figure 6. Each active PU band is assumed to have six subcarriers where $|N_1| = |N_2| = 16$. The achieved capacity using optimal, PI and Zhang algorithms for different interference constraints where $I^1_{th} = I^2_{th}$ is plotted in Figure 7. It can be noted that the proposed PI-algorithm approaches the optimal solution and outperforms Zhang algorithm. The effect of assuming that every subcarrier is belonging to the closest PU band and introducing interference to it only on the net interference introduced to the active PU bands is studied in Figures 8 and 9 for PU_1 and PU_2, respectively. It can be observed that the net interference induced using the PI-algorithm is approximately satisfying the prespecified interference constraints which makes the assumption reasonable. Unlike the OFDM-based CR system, the interference induced by the FBMC-based system does not reach the pre-specified thresholds. This is because the FBMC-based CR system reaches to the maximum interference that can be introduced to the PU using the given power budget. Moreover, the interference induced by the proposed algorithm is less than that using Zhang algorithm. Returning to Figure 7, one can notice that the interference constraints after $I^l_{th} = 10m$ Watt start to have no effect on the achieved capacity of the FBMC system. This indicates also that the FBMC system reaches the maximum interference for the given power budget. The small difference between the net interference values after $I^l_{th} = 10m$ Watt is due to averaging over different channel realizations. The achieved capacity of the different algorithms is plotted in Figure 10 with lower values of the interference constraints. It can be noticed that Zhang algorithm has a limited performance with low interference constraints because the algorithm turns off the subcarriers that have a noise level more than the initial waterfilling level and never uses these subcarriers again even if the new waterfilling level exceeds its noise level. Moreover, the algorithm deactivates some subcarriers, that is, transmit zero power, in order to ensure that the interference introduced to PU bands is below the prespecified thresholds. The lower the interference constraints, the more the deactivated subcarriers which justifies the limited performance of this algorithm in low interference constraints.

To show the efficiency of transmitting over the active PU bands as well as the nonactive bands, Figures 11 and 12 plot the achieved capacity using the PI algorithm with and without allowing the SUs to transmit over the PU active bands. The capacity of the CR system transmitting on both the active and nonactive bands is more than that one transmitting only on the nonactive band. Since the cognitive transmission in the active PU band introduces

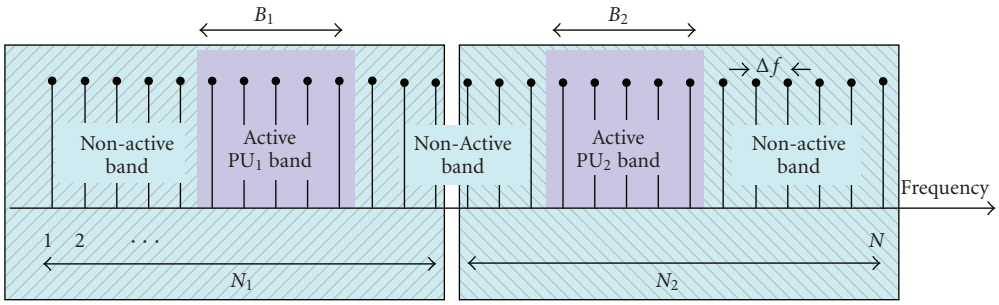

Figure 6: Frequency distribution with two active PU bands.

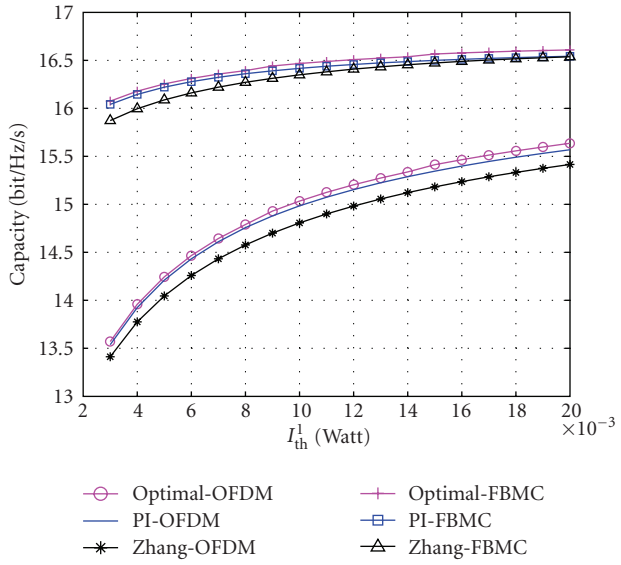

Figure 7: Achieved capacity versus allowed interference threshold for OFDM- and FBMC-based CR systems—two active PU bands.

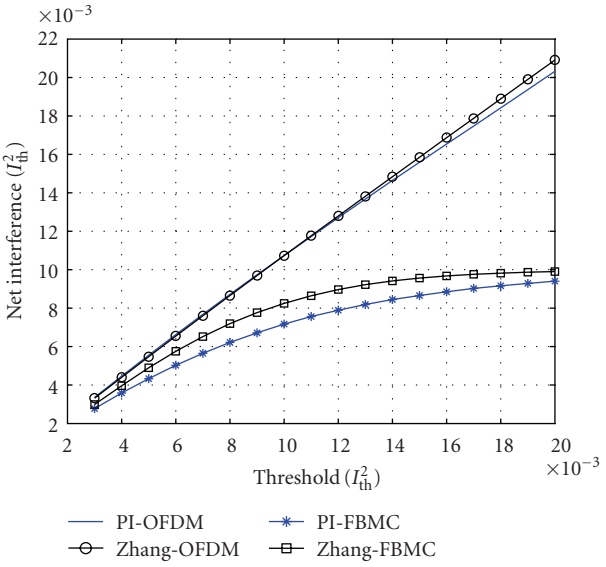

Figure 9: Total interference introduced to the PU_2 versus interference threshold.

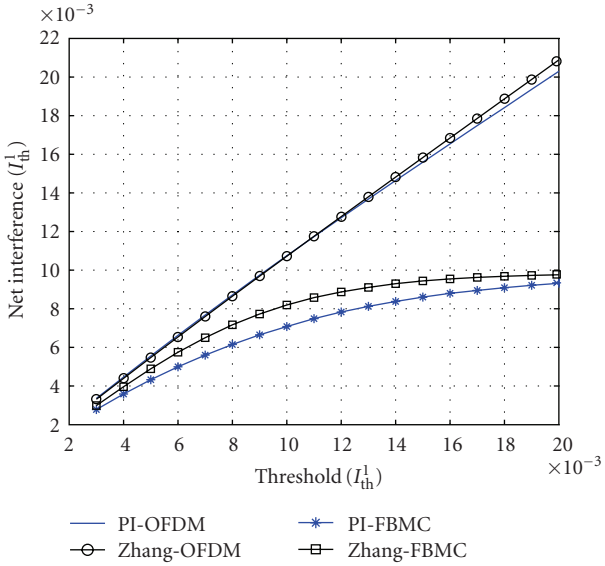

Figure 8: Total interference introduced to the PU_1 versus interference threshold.

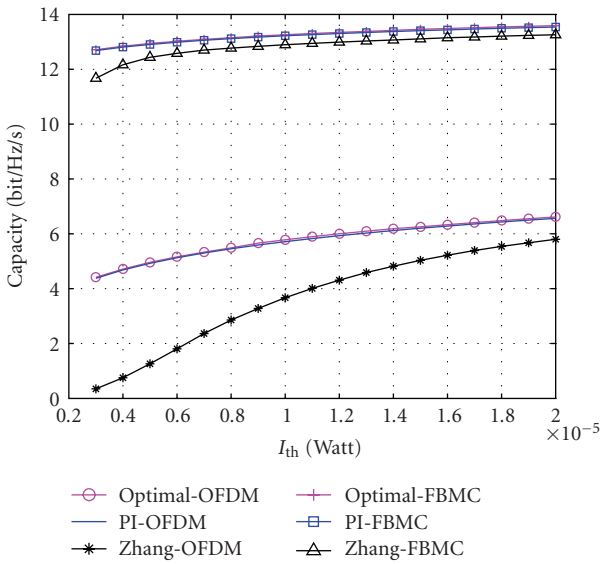

Figure 10: Achieved CR versus allowed interference threshold (low) for OFDM- and FBMC-based CR systems—two active bands.

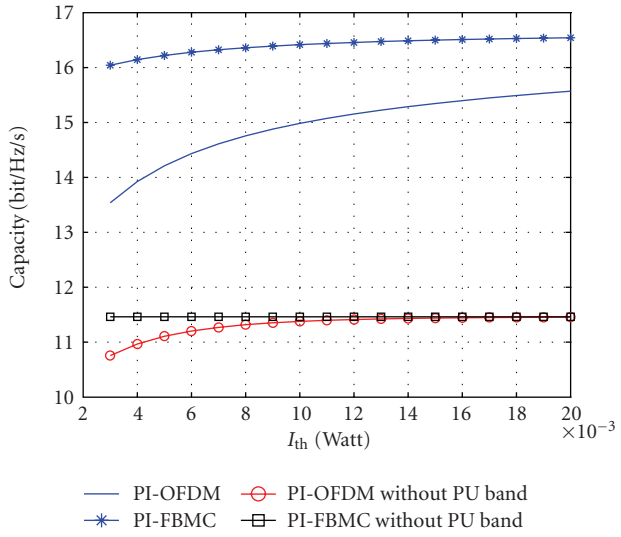

Figure 11: Achieved capacity versus allowed interference threshold with and without transmitting over active bands—two active PU bands.

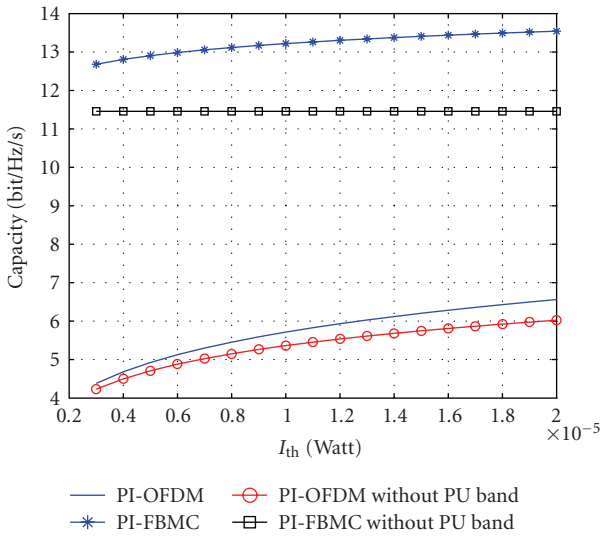

Figure 12: Achieved capacity versus allowed interference threshold (low) with and without transmitting over active bands—two active PU bands.

more interference to the PUs than the other subcarriers, low power levels can be used in these bands with low interferences constraints. This justifies why the difference between the two systems decreases when the interference constraints decrease.

RC algorithm can be used if there is only one active PU band, that is, $L = 1$. The RC algorithm allocates the subcarriers and bits considering the relative importance between the power needed to transmit and the interference induced to the PU band. In order to compare the proposed PI-algorithm with RC algorithm, One active PU band with "12" subcarriers will be assumed as given in Figure 13. For

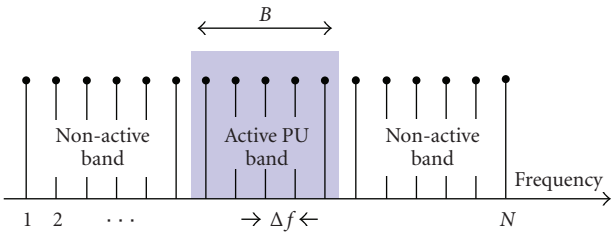

Figure 13: Frequency distribution with one active PU band.

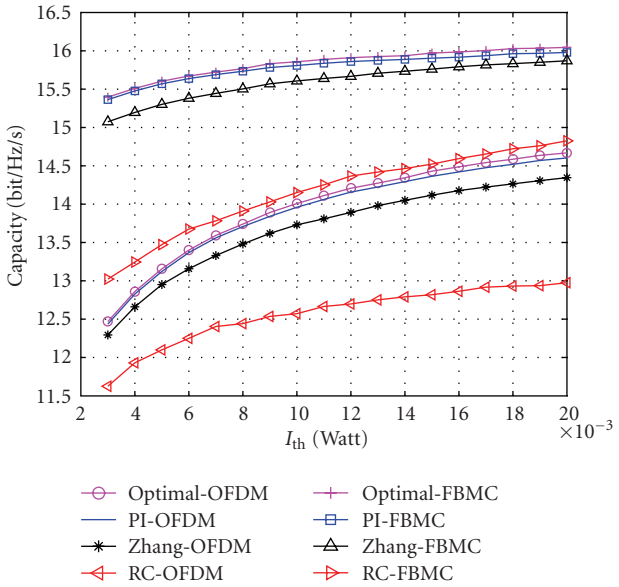

Figure 14: Achieved capacity versus allowed interference threshold for OFDM- and FBMC-based CR systems—one active PU band.

fair comparison, the same bit mapping used in [16] is considered as follows:

$$b_i = \left\lfloor \log_2\left(1 + \frac{P_i' |h_i|^2}{\sigma_i^2}\right) \right\rfloor, \tag{42}$$

where b_i denotes the maximum number of bits in the symbol transmitted in the i^{th} subcarrier and $\lfloor \cdot \rfloor$ denotes the floor function. Figures 14 and 15 show that the proposed algorithm performs better than the RC and Zhang algorithms. In low interference constraints, RC algorithm performs better than Zhang algorithm because of the limited performance of Zhang algorithm with low interference constraints.

For all the so far presented results, the capacity of FBMC-based CR system is higher than that of OFDM-based one because the sidelobes in FBMC's PSD is smaller than that in OFDM which introduces less interference to the PUs. Moreover, the inserted CP in OFDM-based CR systems reduces the total capacity of the system. It can be noticed also that the interference condition introduces a small restriction on the capacity of FBMC-based CR systems which is not the case in OFDM-based CR systems. The significant increase in the capacity of FBMC-based CR systems over the OFDM-based ones recommends the FBMC as a candidate for the CR network applications.

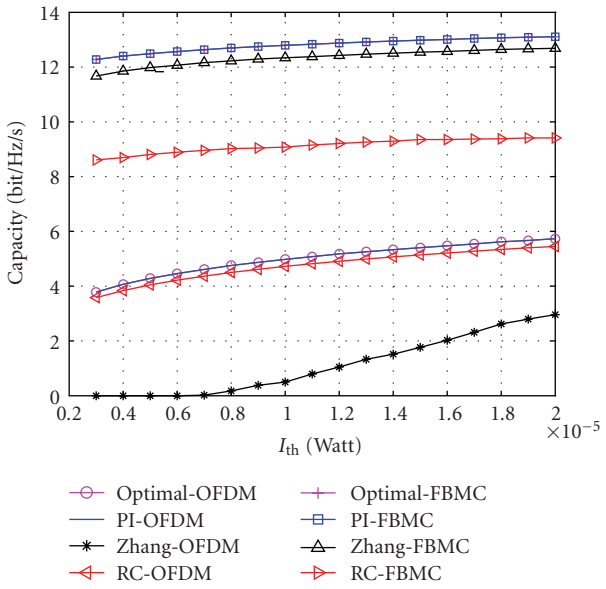

FIGURE 15: Achieved capacity versus allowed interference threshold (low) for OFDM- and FBMC-based CR systems—one active PU band.

6. Conclusion

In this paper, a low complexity suboptimal resource allocation algorithm for multicarrier-based CR networks is presented. Our objective was to maximize the total downlink capacity of the CR network while respecting the available power budget and guaranteeing that no excessive interference is caused to the PUs. With a significant reduction in the computational complexity from $\mathcal{O}(N^3)$ to $\mathcal{O}(N \log N + \eta N) + \mathcal{O}(L), \eta \in [0, 5]$, It is shown that the proposed PI-algorithm achieves a near optimal performance and outperforms the suboptimal algorithms proposed so far. It is found that the net total interference introduced to the PUs band is relatively not affected by assuming that each subcarrier is belonging to the closest PU band and only introducing interference to it. Its demonstrated also that capacity of the CR system uses the nonactive as well as the active bands is more than that only uses the nonactive bands. Simulation results prove that the FBMC-based CR systems have more capacity than OFDM-based ones. FBMC offers more spectral efficiency and introduces small interference to the PUs. The obtained results contribute in recommending the use of FBMC physical layer in the future cognitive radio systems. Developing a resource allocation algorithm that considers the fairness among different users as well as their quality of service (QoS) will be the guideline of our future research work towards better radio resource management.

Acknowledgment

This work was partially supported by the European ICT-2008-211887 project PHYDYAS.

References

[1] Federal Communication Commission, "Spectrum Policy Task Force," Report of ET Docket 02-135, November 2002.

[2] J. Mitola III, "Cognitive radio for flexible mobile multimedia communications," in *Proceedings of IEEE International Workshop on Mobile Multimedia Communications (MoMuC '99)*, pp. 3–10, San Diego, Calif, USA, November 1999.

[3] T. A. Weiss and F. K. Jondral, "Spectrum pooling: an innovative strategy for the enhancement of spectrum efficiency," *IEEE Communications Magazine*, vol. 42, no. 3, pp. S8–S14, 2004.

[4] S. Haykin, "Cognitive radio: brain-empowered wireless communications," *IEEE Journal on Selected Areas in Communications*, vol. 23, no. 2, pp. 201–220, 2005.

[5] T. Weiss, J. Hillenbrand, A. Krohn, and F. K. Jondral, "Mutual interference in OFDM-based spectrum pooling systems," in *Proceedings of the 59th IEEE Vehicular Technology Conference (VTC '04)*, vol. 59, Milan, Italy, May 2004.

[6] B. Farhang-Boroujeny and R. Kempter, "Multicarrier communication techniques for spectrum sensing and communication in cognitive radios," *IEEE Communications Magazine*, vol. 46, no. 4, pp. 80–85, 2008.

[7] H. Zhang, D. L. Ruyet, and M. Terre, "On spectral efficiency analysis between OFDM/OQAM and OFDM based CR networks," in *Proceedings of the IEEE Vehicular Technology Conference (VTC '09)*, Barcelona, Spain, 2009.

[8] B. Farhang-Boroujeny, "Filter bank spectrum sensing for cognitive radios," *IEEE Transactions on Signal Processing*, vol. 56, no. 5, pp. 1801–1811, 2008.

[9] J. Jang and K. B. Lee, "Transmit power adaptation for multiuser OFDM systems," *IEEE Journal on Selected Areas in Communications*, vol. 21, no. 2, pp. 171–178, 2003.

[10] D. Kivanc, G. Li, and H. Liu, "Computationally efficient bandwidth allocation and power control for OFDMA," *IEEE Transactions on Wireless Communications*, vol. 2, no. 6, pp. 1150–1158, 2003.

[11] Z. Shen, J. G. Andrews, and B. L. Evans, "Optimal power allocation in multiuser OFDM systems," in *Proceedings of IEEE Global Telecommunications Conference (GLOBECOM '03)*, vol. 1, pp. 337–341, San Francisco, Calif, USA, December 2003.

[12] C. Y. Wong, R. S. Cheng, K. B. Letaief, and R. D. Murch, "Multiuser OFDM with adaptive subcarrier, bit, and power allocation," *IEEE Journal on Selected Areas in Communications*, vol. 17, no. 10, pp. 1747–1758, 1999.

[13] P. Wang, M. Zhao, L. Xiao, S. Zhou, and J. Wang, "Power allocation in OFDM-Based cognitive radio systems," in *Proceedings of IEEE Global Telecommunications Conference (GLOBECOM '07)*, pp. 4061–4065, 2007.

[14] G. Bansal, M. J. Hossain, and V. K. Bhargava, "Adaptive power loading for OFDM-based cognitive radio systems," in *Proceedings of IEEE International Conference on Communications (ICC '07)*, pp. 5137–5142, Glasgow, UK, 2007.

[15] G. Bansal, M. J. Hossain, and V. K. Bhargava, "Optimal and suboptimal power allocation schemes for OFDM-based cognitive radio systems," *IEEE Transactions on Wireless Communications*, vol. 7, no. 11, pp. 4710–4718, 2008.

[16] T. Qin and C. Leung, "Fair adaptive resource allocation for multiuser OFDM cognitive radio systems," in *Proceedings of the 2nd International Conference on Communications and Networking in China (ChinaCom '07)*, August 2007.

[17] Y. Zhang, *Resource allocation for OFDM-based cognitive radio systems*, Ph.D. dissertation, University of British Columbia, Vancouver, Canada, December 2008.

[18] G. Stuber, S. Almalfouh, and D. Sale, "Interference analysis of TV-band whitespace," *Proceedings of the IEEE*, vol. 97, no. 4, pp. 741–754, 2009.

[19] M. Shaat and F. Bader, "Power allocation with interference constraint in multicarrier based cognitive radio systems," in *Proceedings of the 7th International Workshop on Multi-Carrier Systems and Solutions (MCSS '09)*, Herrsching, Germany, May 2009.

[20] J. G. Proakis and M. Salehi, *Communication Systems Engineering*, Prentice-Hall, Upper Saddle River, NJ, USA, 2nd edition, 2002.

[21] L. G. Baltar, D. S. Waldhauser, and J. Nossek, "Out-of-band radiation in multicarrier systems: a comparison," in *Proceedings of the International Workshop on Multi-Carrier Systems & Solutions (MC-SS '07)*, pp. 107–116, Springer, May 2007.

[22] B. Hirosaki, "An orthogonally multiplexed QAM system using the discrete fourier transform," *IEEE Transactions on Communications Technology*, vol. 29, no. 7, pp. 982–989, 1981.

[23] A. Skrzypczak, P. Siohan, and J.-P. Javaudin, "Power spectral density and cubic metric for the OFDM/OQAM modulation," in *Proceedings of the 6th IEEE International Symposium on Signal Processing and Information Technology (ISSPIT '06)*, Vancouver, Canada, August 2006.

[24] "PHYDYAS-Physical layer for dynamic spectrum access and cognitive radio," http://www.ict-phydyas.org/.

[25] A. Jayalath and C. Tellambura, "Reducing the out-of-band radiation of OFDM using an extended guard interval," in *Proceedings of the 53rd Vehicular Technology Conference (VTC '01)*, vol. 2, pp. 829–833, Rhodes, Greece, May 2001.

[26] S. Brandes, I. Cosovic, and M. Schnell, "Reduction of out-of-band radiation in OFDM systems by insertion of cancellation carriers," *IEEE Communications Letters*, vol. 10, no. 6, pp. 420–422, 2006.

[27] Y.-P. Lin and S.-M. Phoong, "Window designs for DFT-based multicarrier systems," *IEEE Transactions on Signal Processing*, vol. 53, no. 3, pp. 1015–1024, 2005.

[28] H. A. Mahmoud and H. Arslan, "Sidelobe suppression in OFDM-based spectrum sharing systems using adaptive symbol transition," *IEEE Communications Letters*, vol. 12, no. 2, pp. 133–134, 2008.

[29] A. Vahlin and N. Holte, "Optimal finite duration pulses for OFDM," *IEEE Transactions on Communications*, vol. 44, no. 1, pp. 10–14, 1996.

[30] R. Xu and M. Chen, "Spectral leakage suppression of DFT-based OFDM via adjacent subcarriers correlative coding," in *Proccedings of IEEE Global Telecommunications Conference (GLOBECOM '08)*, pp. 3029–3033, December 2008.

[31] A. Amini, R. Kempter, L. Lin, and B. Farhang-Boroujeny, "Filter bank multitone: a candidate for physical layer of cognitive radio," in *Proceedings of the Software Defined Radio Technical Conference and Product Exhibition (SDR '05)*, Orange County, Calif, USA, November 2005.

[32] A. Amini, R. Kempter, and B. Farhang-Boroujeny, "A comparison of alternative filterbank multicarrier methods in cognitive radios," in *Proceedings of the Software Defined Radio Technical Conference and Product Exhibition (SDR '06)*, Orlando, Fla, USA, November 2006.

[33] H. Zhang, D. Le Ruyet, and M. Terre, "Spectral efficiency comparison between OFDM/OQAM- and OFDM-based CR networks," *Wireless Communications and Mobile Computing*, vol. 9, no. 11, pp. 1487–1501, 2009.

[34] S. Boyd and L. Vandenberghe, *Convex Optimization*, Cambridge University Press, Cambridge, UK, 2004.

[35] A. Leke and J. Cioffi, "A maximum rate loading algorithm for discrete multitone modulation systems," in *Proceedings of the IEEE Global Telecommunications Conference (GLOBECOM '97)*, vol. 3, pp. 1514–1518, 1997.

[36] N. Papandreou and T. Antonakopoulos, "Bit and power allocation in constrained multicarrier systems: the single-user case," *EURASIP Journal on Advances in Signal Processing*, vol. 2008, Article ID 643081, 14 pages, 2008.

[37] M. Bellanger, "Filter banks and OFDM-OQAM for high throughput wireless LAN," in *Proceedings of the 3rd International Symposium on Communications, Control, and Signal Processing (ISCCSP '08)*, pp. 758–761, St Julians, Malta, March 2008.

www.ietdl.org

Published in IET Communications
Received on 2nd December 2010
Revised on 23rd June 2011
doi: 10.1049/iet-com.2010.1062

ISSN 1751-8628

Efficient resource allocation algorithm for uplink in multicarrier-based cognitive radio networks with fairness consideration

M. Shaat F. Bader

Centre Tecnològic de Telecomunicacions de Catalunya (CTTC), Parc Mediterrani de la Tecnología, Av. Canal Olimpia s/n. 08860, Castelldefels-Barcelona, Spain
E-mail: musbah.shaat@cttc.es

Abstract: An efficient fairness-aware uplink resource allocation algorithm in orthogonal frequency-division multiplexing-based cognitive radio systems is presented. The proposed resource allocation algorithm is divided into two steps. The subcarriers to user assignment is first performed, and then the power is allocated to the different subcarriers. The objective is to maximise the total data rate while guaranteeing that the interference introduced to the primary system is under the prescribed interference temperature limit. The fairness among users is considered within the subcarrier allocation by reducing the probability of having users whose instantaneous rates are below a given minimum rate. Many factors will be considered during the resource allocation process like the channel quality, potential interference caused to the primary bands, instantaneous rate achieved by every user and the increment in the total data rate. Simulation results confirm the efficiency of the proposed algorithm.

1 Introduction

The available spectrum is divided into several frequency bands that are allocated traditionally to a specific user or service provider exclusively in order to be protected from any interference. Since most of the current frequency bands have been already allocated [1], it will be very hard to find vacant bands for the emerging wireless systems or services. Moreover, recent measurements by the Federal Communications Commission show that the spectrum utilisation in the 0–6 GHz band varies from 15 to 85% depending on time, frequency and geographical location [2, 3]. These observations motivate the development of cognitive radio (CR) communications [4, 5] whereby the secondary users (SUs), also called unlicensed users, are allowed to access the radio spectrum originally allocated to the primary users (PUs), also called licensed user. In this way, CR will greatly improve the spectrum utilisation without major changes to the existing primary systems. By using one of the spectrum sensing techniques [6, 7], SUs need to periodically monitor the radio spectrum in order to detect in time and frequency the PUs transmission. The interference introduced to the PUs because of CR transmission should be below a predefined value called the interference temperature limit [3, 5]. In order to maximise the CR system throughput without causing harmful interference to the PUs, the available radio resources (powers, rates and bandwidth) should be distributed carefully and efficiently. To that end, the problem of resource allocation in CR networks has been widely studied recently. For a single channel (carrier) CR systems, the optimal resource allocation schemes in uplink and downlink have been presented for both single and multiuser environments (see e.g. [8–12]).

By virtue of its flexibility in the allocation of different resources among different users as well as its ability to fill the spectrum holes left by PUs, multicarrier communication systems have been considered as an appropriate candidate for CR systems [13, 14]. Uncounted research work has been done to find optimal/efficient resource allocation techniques in conventional (non-cognitive) multicarrier systems. For non-cognitive downlink scenario (see e.g. [15–18] and references therein), the maximum throughput can be achieved by allocating each subcarrier to the user with the maximum signal-to-noise ratio (SNR) and then allocate the power according to waterfilling solution. Many algorithms to solve resource allocation problem in uplink non-cognitive systems have been proposed (see e.g. [19–22] and references therein). In [21], the authors proposed a greedy subcarrier allocation algorithm based on marginal rate function and iterative waterfilling power allocation algorithm. This algorithm is developed in [22] to consider fairness among the different users. The algorithms used in non-cognitive multicarrier systems are not efficient in CR ones because of the existence of the interference temperature constraints. Although the downlink multicarrier-based CR system has been addressed well recently (see e.g. [14, 23–27]), there is a few existed research on subcarrier and power allocation in uplink multicarrier-based CR systems [28–30].

In [28], the author proposed an algorithm for jointly allocating channels and powers among different users under individual user's power constraints. The problem is relaxed to obtain a convex version and then the solution is quantised

to yield a binary channel allocation. Afterwards, the solution is modified to consider the constraints on the in-band interference to the licensed system. Wang *et al.* proposed in [29] an algorithm to allocate resources in uplink orthogonal frequency-division multiplexing access (OFDMA)-based CR systems under per subcarrier power constraints (in-band interference constraints). Subcarriers are allocated initially to the users with the best channel quality and then adjusted according to different user's waterfilling levels. The algorithm has high computational complexity and limited performance. In [30], the authors proposed a resource allocation algorithm in which subcarrier assignment and power allocation are carried out sequentially under mutual interference and per user power constraints. The proposed scheme requires pre-knowledge about the number of subcarriers that should be allocated to each user as well as the capacity that can be achieved by each subcarrier. The power allocation was performed using gradient projection algorithm. Instantaneous fairness among users was not taken into consideration in the algorithms proposed in [28–30].

In this paper, we propose an efficient resource allocation algorithm in uplink OFDM-based CR systems. The objective is to maximise the total CR data rate while limiting the interference introduced to the PUs. Fairness among users is considered within the subcarrier allocation by reducing the probability of having users whose instantaneous rate is below a given value. The proposed resource allocation is divided into two phases. The assignment of subcarriers to users is performed first and then the power is allocated to the different subcarriers. The scheme for subcarrier to user assignment proposed in [22] for non-cognitive systems is adopted in order to be suitable for cognitive ones. Subcarriers are allocated based on the channel quality, amount of interference imposed to PUs, instantaneous rate achieved by every user and the increment in the total data rate. For the power allocation phase, an efficient power allocation algorithm is proposed to distribute the powers among the subcarriers under the per-user total power and interference constraints.

The rest of this paper is organised as follows: Section 2 introduces the system model and formulates the problem. The proposed algorithm is presented for single PU in Section 3 and then generalised for multiple PUs in Section 4. The computational complexity of the algorithm is discussed and selected numerical results are presented in Section 5. Finally, Section 6 concludes the paper.

2 System model and problem formulation

There are several models that can be used to model and formulate the multicarrier-based CR systems depending on the spectrum access technique. Using underlay spectrum access, CR system can use both active and non-active PU bands. In this access technique, CR system should have a maximum transmitting power limit in order to avoid inducing interference to the PU operating in the same frequency as given in [8–10, 23, 29]. In overlay spectrum access-based CR systems, CR system can transmit only on non-active PU bands. Although there is no in-band interference to PUs, the CR transmission will cause interference to the PU bands located adjacent to the CR band because of side-lobes of its filter frequency response [14, 25–27, 30]. Fig. 1. describes underlay and overlay access schemes for multicarrier-based CR system.

In this paper, the system model used in [14] is considered where the PUs and SUs are co-existing in the same

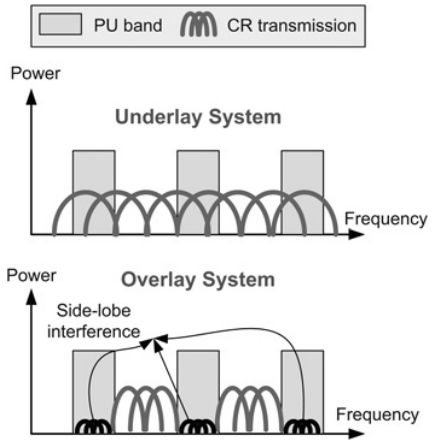

Fig. 1 *Underlay and overlay spectrum access techniques*

geographical location as described in Fig. 2. For the CR system, uplink transmission will be assumed in which SUs are opportunistically accessing the unused PU bands to transmit to their cognitive base station (CBS) without causing harmful interference to PUs. As shown in Fig. 3, the frequency bands $B_1, B_2, \ldots, B_L$ represent the L active PU bands, whereas the non-active bands represent the bands that can be used by CR system (CR band). The CR band is divided into N subcarriers each having a Δf bandwidth. There is no synchronisation between the primary and CR systems. The interference induced to the lth PU band should not exceed the predefined interference temperature limit I_{th}^l.

The interference introduced by the transmission of the ith subcarrier of the CR system to the lth PU band, $I_i^l(d_i^l, P_i)$, is the integration of the power spectrum density (PSD) of the ith subcarrier across the lth PU band, B_l. If an ideal Nyquist pulse is assumed, the mutual interference can be expressed as [31]

$$I_i^l(d_i^l, P_i) = P_i \Omega_i^l;\ \Omega_i^l = \int_{d_i^l - B_l/2}^{d_i^l + B_l/2} |g_i^l|^2 T_s \left(\frac{\sin \pi f T_s}{\pi f T_s}\right)^2 \mathrm{d}f \quad (1)$$

where d_i^l is the spectral distance between the ith subcarrier and the lth PU band. g_i^l denotes the channel gain (can include path loss and shadowing part) between the ith subcarrier and the lth PU band whereas P_i is the total transmit power emitted by the ith subcarrier. $T_s = 1/\Delta f$ is the symbol duration and

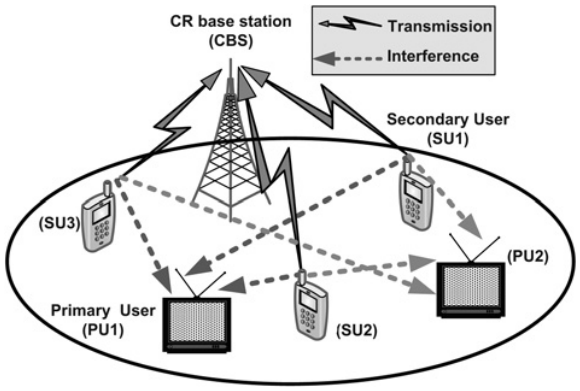

Fig. 2 *Uplink CR network*

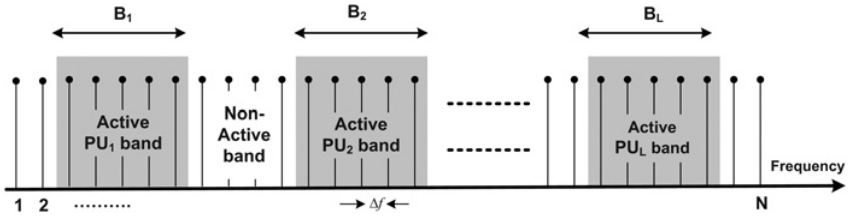

Fig. 3 *Frequency distribution of the active and non-active primary bands*

Ω_i^l denotes the interference factor of the ith subcarrier to the lth PU band. By the same way, the interference power introduced by the lth PU signal into the band of the ith subcarrier is [31]

$$J_i^l = \int_{d_i^l - \Delta f/2}^{d_i^l + \Delta f/2} |y_i^l|^2 \psi_l(e^{j\omega})\, d\omega \tag{2}$$

where $\psi_l(e^{j\omega})$ is the power spectrum density of the lth PU signal and y_i^l is the channel gain between the ith subcarrier and lth PU signal. Several parameters should be considered to built a reliable CR system such as the appearance of the PU during CR transmission, which can be taken into account by applying a risk-return model like in [26], the effect of spectrum sensing error like false alarm and misdetection probability as in [32], and the channel estimation errors in the transmission and interfering links as in [33]. Dealing with such a general model is out of the range of this paper.

The transmission rate for the ith subcarrier, R_i can be evaluated as

$$R_i(P_{i,m}, h_{i,m}) = \Delta f \log_2\left(1 + \frac{P_{i,m}|h_{i,m}|^2}{\sigma_i^2}\right) \tag{3}$$

where $P_{i,m}$ is the transmission power and $h_{i,m}$ is the ith subcarrier fading gain from the mth SU to the CBS. Additionally, $\sigma_i^2 = \sigma_{\text{AWGN}}^2 + \Sigma_{l=1}^{L} J_i^l$ where σ_{AWGN}^2 is the variance of the additive white Gaussian noise (AWGN) and J_i^l is the interference introduced by the lth PU band into the ith subcarrier which is evaluated using (2) and can be modelled as AWGN as described in [14]. Throughout this paper, all the instantaneous fading gains are assumed to be perfectly known at the CBS. The channel gains between SUs and the CBS can be obtained practically by classical channel estimation techniques whereas the channel gains between SUs and PUs can be obtained by estimating the received signal power from each primary terminal when it transmits, under the assumptions of pre-knowledge on the primary transmit power levels and the channel reciprocity [12, 34]. Based on the channel gains, the CBS assigns the subcarriers and powers to each SU through a reliable low-rate signalling channel. Let $a_{i,m}$ be the subcarrier allocation indicator, that is, $a_{i,m} = 1$ if and only if the ith subcarrier is allocated to the mth user. It is assumed that each subcarrier can be used for transmission to at most one user at any given time. Fairness among SUs is guaranteed by assuming that every SU has a minimum instantaneous rate $R_{\min}$. Our objective is to maximise the total data rate of the CR system subject to the constraints on the interference introduced to the PUs, the per-user transmit power constraints and the per-user minimum rate constraints. Therefore the optimisation problem can be formulated as follows

$$\begin{aligned}
P1: \quad & \max_{P_{i,m}, a_{i,m}} \sum_{m=1}^{M}\sum_{i=1}^{N} a_{i,m} R_i(P_{i,m}, h_{i,m}) \\
\text{s.t.} \quad & \sum_{m=1}^{M}\sum_{i=1}^{N} a_{i,m} P_{i,m} \Omega_{i,m}^l \le I_{\text{th}}^l, \quad \forall l \in \{1, \ldots, L\} \\
& \sum_{i=1}^{N} a_{i,m} P_{i,m} \le \overline{P_m}, \quad \forall m \\
& P_{i,m} \ge 0, \quad \forall i, m \\
& a_{i,m} \in \{0, 1\}, \quad \forall i, m \\
& \sum_{m=1}^{M} a_{i,m} \le 1, \quad \forall i \\
& \sum_{i=1}^{N} a_{i,m} R_i(P_{i,m}, h_{i,m}) \ge R_{\min}, \quad \forall m
\end{aligned} \tag{4}$$

where N denotes the total number of subcarriers whereas M denotes the number of SUs. L is the number of active PU bands and I_{th}^l is the interference threshold prescribed by the lth PU. $\overline{P_m}$ is the mth SU total power budget. Without loss of generality, the minimum instantaneous rate $R_{\min}$ is assumed constant for all the users. The solution can be easily extended to consider different minimum instantaneous rates for the different SUs. The CBS will perform the subcarrier and power allocation and then diffuse the result to the different SUs.

The optimisation problem $P1$ is a mixed optimisation problem in which achieving the optimal solution needs high computational complexity. Additionally, the minimum rate constraints increase the complexity of the problem. In order to solve the problem, we propose an algorithm to perform the resource allocation in two phases. In the first phase, a heuristic sub-optimal algorithm is used to allocate the subcarriers to the different users. Afterwards, the optimal power allocation is evaluated in the second phase. The optimal power allocation algorithm requires high computational complexity and hence a low complexity power algorithm is proposed to perform the power allocation phase. Depending on the values of I_{th}^l, $\overline{P_m}$ and the channel gains, the CR system may not be able to satisfy the minimum rate $R_{\min}$ for all the users. Therefore the last constraint in the optimisation problem $P1$ is relaxed by trying to reduce the probability of having users whose rates are below the minimum rate [22]. The outage probability can be defined as

$$P_{\text{outage}} = \Pr\{M_{\text{low}} \ge 1\} \tag{5}$$

where M_{low} is the number of SUs whose instantaneous rate are below $R_{\min}$.

The proposed algorithm will be discussed in the next section. For the sake of description clarity, the single PU case will be discussed first and then the solution will be generalised for multiple PUs case.

doi: 10.1049/iet-com.2010.1062

3 Proposed algorithm (single PU case)

The optimal downlink subcarriers to users allocation scheme in multicarrier systems is achieved by allocating each subcarrier to the user with the maximum SNR [15–18]. This scheme of subcarrier allocation is not efficient in uplink case because of the per-user power constraints. Moreover, the interference introduced to the primary system by each SU should be considered in the CR context, which makes the schemes used in classical multicarrier systems not efficient. In this section, a heuristic subcarrier and power allocation algorithm is presented. To better describe the proposed algorithm, only one PU band, that is, single interference constraint, will be considered in this section. The solution will be generalised in the next section to consider multiple interference constraints. We will refer to the single interference constraint by I_{th}^{l*}, and hence the first constraint in the optimisation problem $P1$ can be rewritten as follows

$$\sum_{m=1}^{M}\sum_{i=1}^{N} a_{i,m}P_{i,m}\Omega_{i,m}^{l*} \le I_{\text{th}}^{l*} \tag{6}$$

where $\Omega_{i,m}^{l*}$ denotes the interference factor of the ith subcarrier to the PU band (l^*) when the ith subcarrier is allocated to mth SU. In the sequel, the proposed subcarrier to user assignment scheme with low outage probability is introduced and then an efficient power allocation algorithm is presented.

3.1 Proposed subcarrier allocation algorithm with fairness consideration

To achieve an efficient subcarrier allocation, the proposed algorithm should assign the subcarriers to the different SUs considering not only their channel quality and per-user power constraints but also the interference that will be induced to the PU band. Moreover, the probability of having users with instantaneous rates below the minimum rate should be reduced.

The scheme assumes that the interference introduced to the primary system, that is, I_{th}^{l*}, is divided uniformly among the different subcarriers [14]. Accordingly, the maximum amount of interference, I_{Uniform}^{l*}, that can be introduced by any subcarrier is

$$I_{\text{Uniform}}^{l*} = \frac{I_{\text{th}}^{l*}}{N} \tag{7}$$

By using (1), the maximum power, $P_{i,m}^{\text{Uni}}$, that can be allocated to the ith subcarrier when it is allocated to the mth SU is

$$P_{i,m}^{\text{Uni}} = \frac{I_{\text{Uniform}}^{l*}}{\Omega_{i,m}^{l*}} \tag{8}$$

Let us define the following sets:

- $\mathcal{C}$: the set of unassigned subcarriers.
- $\mathcal{U}$: the set that contains the indices of the users whose rates are below $R_{\min}$.
- $\mathcal{A}_m$: the set that includes the subcarriers already allocated to the mth user with powers equal to the maximum power $P_{i,m}^{\text{Uni}}$.
- $\mathcal{B}_m$: the set that includes the subcarriers already allocated to the mth user with powers equal to the average power. The average power means here that the remaining power for the mth user after allocating the powers to the subcarriers in $\mathcal{A}_m$ is divided equally among the subcarriers in the set B_m, i.e.

$$P_m^{\text{avg}} = \frac{\overline{P_m} - \Sigma_{x\in\mathcal{A}_m} P_{x,m}^{\text{Uni}}}{|\mathcal{B}_m|}$$

where $|\mathcal{B}_m|$ means the cardinality of the set $\mathcal{B}_m$.

According to the previous definition, the instantaneous rate of the mth user, $R(m, \mathcal{A}_m, \mathcal{B}_m)$, is the summation of the rates of the subcarriers in the sets $\mathcal{A}_m$ and $\mathcal{B}_m$ and is given by

$$R(m, \mathcal{A}_m, \mathcal{B}_m) = \sum_{i\in\mathcal{A}_m} R_i(P_m^{\text{Uni}}, h_{i,m}) + \sum_{i\in\mathcal{B}_m} R_i(P_m^{\text{avg}}, h_{i,m}) \tag{9}$$

where $R_i(P_{i,m}, h_{i,m})$ is evaluated using (3). Note that the allocated powers according to either the maximum or average power are only used to simplify the calculation of the increment in the data rate. The optimal power allocation will be derived later based on the subcarrier allocation information.

The algorithm begins by allocating the subcarriers that are located next to the PU band, that is, subcarriers that have more interference to the PU, and moving towards the distant ones. The subcarriers are allocated sequentially to the users until all the subcarriers are assigned. In order to reduce the probability of having users whose rates are below the minimum, the allocation of the subcarriers will be confined within the users in the set $\mathcal{U}$. Initially the set $\mathcal{U}$ is assumed to contain all SUs. Throughout the allocation of the different subcarriers, if the rate of the mth user become more than the minimum required rate $R_{\min}$, the user will be removed from the set $\mathcal{U}$. If the minimum rate constraints are satisfied for all the users, that is, $\mathcal{U}$ is empty, the subcarrier can be allocated to any one of the SUs. If the optimisation problem is assumed to be solved without any minimum rate constraints, the set $\mathcal{U}$ will assumed always empty and accordingly the subcarrier can be allocated to any one of the SUs. Remark that the subcarriers with high interference gains will have a low transmitting power even that they have a good channel quality. Therefore the limitation that will be introduced to any subcarrier assignment due the interference constraints should be considered and the subcarriers should be classified according to their interference gains. To allocate a given subcarrier, the algorithm initially assigns the subcarrier to the set $\mathcal{B}_m$ and evaluates the new average power, P_{Test}. If the average power exceeds the maximum power, that is, $P_{\text{Test}} \ge P_{i,m}^{\text{Uni}}$, then the subcarrier should be moved to the set $\mathcal{A}_m$. Afterwards, the increments of the individual data rates because of the allocation of a particular subcarrier to different SUs are evaluated and the subcarrier is allocated to the SU with maximum data rate increment. The scheme is repeated until the allocation of all subcarriers. Note that the final set of allocated subcarriers to mth SU is $\mathcal{N}_m = \mathcal{A}_m \cup \mathcal{B}_m$. By assuming initially that $\mathcal{U} = \{1, \ldots, M\}$, and both sets $\mathcal{A}_m$ and $\mathcal{B}_m$ are empty sets, the assigning procedures of a particular subcarrier $i^* \in \mathcal{C}$ are as follows

1. $\forall m \in \mathcal{U}$.

   Evaluate $P_{\text{Test}} = \dfrac{\overline{P_m} - \Sigma_{r\in\mathcal{A}_m} P_{r,m}^{\text{Uni}}}{|\mathcal{B}_m| + 1}$

   if $P_{\text{Test}} \ge P_{i^*,m}^{\text{Uni}}$

   let $\mathcal{A}_m^* = \mathcal{A}_m \cup \{i^*\}$ and $\mathcal{B}_m^* = \mathcal{B}_m$

else let $\mathcal{B}_m^* = \mathcal{B}_m \cup \{i^*\}$ and $\mathcal{A}_m^* = \mathcal{A}_m$.

2. Compute the amount of increment Δ_m in the data rate when the subcarrier $\{i^*\}$ is assigned to mth SU, that is

$$\Delta_m = R_m^{\text{new}} - R_m^{\text{old}} = R(m, \mathcal{A}_m^*, \mathcal{B}_m^*) - R(m, \mathcal{A}_m, \mathcal{B}_m)$$

where $R(m, \mathcal{A}_m^*, \mathcal{B}_m^*)$ and $R(m, \mathcal{A}_m, \mathcal{B}_m)$ are evaluated using (9).
3. Find m^* satisfying $m^* = \arg\max_m(\Delta_m)$, set $a_{i^*,m^*} = 1$, and update the sets $\mathcal{A}_{m^*} = \mathcal{A}_{m^*}^*$ and $\mathcal{B}_{m^*} = \mathcal{B}_{m^*}^*$.
4. If $R(m^*, \mathcal{A}_{m^*}, \mathcal{B}_{m^*}) \geq R_{\min}$, remove m^* from the set $\mathcal{U}$. If $\mathcal{U}$ is empty, let $\mathcal{U} = \{1, \ldots, M\}$.
5. Remove the subcarrier i^* from the set $\mathcal{C}$ and repeat the above procedures until the set $\mathcal{C}$ is empty.

3.2 Proposed power allocation algorithm

By the subcarrier to users assignment phase, the subcarriers are allocated to the different users with the consideration of the minimum rates constraints. Therefore the values of the subcarrier indicators, that is, $a_{i,m}$, are already known from the previous phase. The multiuser system can be viewed virtually as a single user multicarrier system and the power allocation problem can be formulated as follows

$$\begin{aligned} P2: \quad & \max_{P_{i,m}} \sum_{i=1}^{N} R_i(P_{i,m}, h_{i,m}) \\ \text{s.t.} \quad & \sum_{i=1}^{N} P_{i,m}\Omega_{i,m}^{l*} \leq I_{\text{th}}^{l*} \\ & \sum_{i \in \mathcal{N}_m} P_{i,m} \leq \overline{P_m}, \quad \forall m \\ & P_{i,m} \geq 0, \quad \forall i \end{aligned} \tag{10}$$

where m in $P_{i,m}$, $h_{i,m}$ and $\Omega_{i,m}^{l*}$ refers to the user who's already got the subcarrier i, that is, $a_{i,m} = 1$. $\mathcal{N}_m$ denotes the set of subcarriers allocated to the mth SU. Remark that having too much power comparing to the interference constraint will lead to an interference-only optimisation problem while having high interference constraint in relative with the total power will lead to a non-cognitive, that is, classical, resource allocation problem.

The problem $P2$ is a convex optimisation problem. Solving for the optimal solution (see the Appendix for the derivation), we can obtain

$$P_{i,m}^* = \left[\frac{1}{\alpha^{l*}\Omega_{i,m}^{l*} + \beta_m} - \frac{\sigma_i^2}{|h_{i,m}|^2}\right]^+ \tag{11}$$

where α^{l*} and β_m are the non-negative Lagrange multipliers and $[x]^+ = \max(0, x)$. Solving for $(M+1)$ Lagrangian multipliers is computational complex. The optimal solution can be found numerically using ellipsoid or interior point method with a complexity $\mathcal{O}(N^3)$ [35]. The high computational complexity makes the optimal solution unsuitable for practical application and hence a low complexity algorithm is proposed.

On the one side, ignoring the interference constraint in problem $P2$ will let the optimal solution to be the distribution of the per-user power budget $\overline{P_m}$ among the set of subcarriers $\mathcal{N}_m$ according to the well-known waterfilling interpretation [36]. On the other side, if the per-user power constraints are ignored, the analysis given in [14] can be followed where the Lagrangian of the problem can be written as

$$\begin{aligned} G^{(\text{Int})}(l^*) = & -\sum_{i=1}^{N} R_i(P_{i,m}^{(\text{Int})}, h_{i,m}) \\ & + \gamma_{l*}^{(\text{Int})}\left(\sum_{i=1}^{N} P_{i,m}^{(\text{Int})}\Omega_{i,m}^{l*} - I_{\text{th}}^{l*}\right) \end{aligned} \tag{12}$$

where $\gamma_{l*}^{(\text{Int})}$ is the Lagrange multiplier. (Int) stands for optimisation under the interference constraint only. Equating

$$\frac{\partial G^{(\text{Int})}(l^*)}{\partial P_{i,m}^{(\text{Int})}}$$

to zero, we obtain

$$P_{i,m}^{(\text{Int})}(l^*) = \left[\frac{1}{\gamma_{l*}^{(\text{Int})}\Omega_{i,m}^{l*}} - \frac{\sigma_i^2}{|h_{i,m}|^2}\right]^+ \tag{13}$$

Hence, substituting (13) into $\Sigma_{i=1}^{N} P_{i,m}^{(\text{Int})}\Omega_{i,m}^{l*} = I_{\text{th}}^{l*}$ we obtain

$$\gamma_{l*}^{(\text{Int})} = \frac{|N|}{I_{\text{th}}^{l*} + \Sigma_{i=1}^{N}(\Omega_{i,m}^{l*}\sigma_i^2/|h_{i,m}|^2)} \tag{14}$$

One can note that if the solution found by (13) and (14) satisfies the different per-user power constraints, that is, $\Sigma_{i \in \mathcal{N}_m} P_{i,m}^{(\text{Int})}(l^*) \leq \overline{P_m}$, $\forall_m$, then (13) and (14) will be the optimal solution for the optimisation problem $P2$ where the case of interference-only optimisation problem occurred. In most of the cases, this relation does not hold which motivates developing an efficient algorithm considering both the interference and per-user power constraints.

In our work in [27], downlink power allocation problem is solved considering one total power constraint. The algorithm presented in [27] is extended here to consider the uplink scenario with several per-user power constraints. We can start by assuming that the maximum power $P_{i,m}^{\text{Max}}$ that can be allocated to each subcarrier is determined according to the interference constraint only using (13) and (14), that is, $P_{i,m}^{\text{Max}} = P_{i,m}^{(\text{Int})}(l^*)$. Afterwards, the per-user power constraints are tested to check whether $\Sigma_{i \in \mathcal{N}_m} P_{i,m}^{(\text{Int})}(l^*) \leq \overline{P_m}$, $\forall m$ holds or not. If the relation is satisfied, then the solution is found where $P_{i,m}^* = P_{i,m}^{\text{Max}}$. Otherwise, the available power $\overline{P_m}$ for each SU should be distributed among the subcarriers in $\mathcal{N}_m$ given that the power allocated to each subcarrier is lower than or equal to $P_{i,m}^{\text{Max}}$. For every SU, the following problem should be solved

$$\begin{aligned} P3: \quad & \max_{P_{i,m}^{\text{W.F}}} \sum_{i \in \mathcal{N}_m} R_i(P_{i,m}^{\text{W.F}}, h_{i,m}) \\ \text{s.t.} \quad & \sum_{i \in \mathcal{N}_m} P_{i,m}^{\text{W.F}} \leq \overline{P_m} \\ & 0 \leq P_{i,m}^{\text{W.F}} \leq P_{i,m}^{\text{Max}} \end{aligned} \tag{15}$$

The problem $P3$ is called 'cap-limited' waterfilling [37, 38]

doi: 10.1049/iet-com.2010.1062

where $P_{i,m}^{\mathrm{W.F}}$ is cap-limited waterfilling allocated power. The problem is solved efficiently using the concept of the conventional waterfilling and can be explained as follows: given the initial waterfilling solution, the channels that violate the maximum power $P_{i,m}^{\mathrm{Max}}$ are determined and upper bounded with $P_{i,m}^{\mathrm{Max}}$. The total power budget of the user is reduced by subtracting the power assigned so far. At the next step, the algorithm proceeds to successive waterfilling over the subcarriers that did not violate the maximum power $P_{i,m}^{\mathrm{Max}}$ in the last step. This procedures is repeated until the allocated power $P_{i,m}^{\mathrm{W.F}}$ does not violate the maximum power $P_{i,m}^{\mathrm{Max}}$ in any of the subcarriers in the new iteration. Low computational complexity implementation of the 'cap-limited' waterfilling can be found in [38]. Since it is assumed that $P_{i,m}^{\mathrm{W.F}} \leq P_{i,m}^{\mathrm{Max}}$, some of the powers allocated to subcarriers will not reach the maximum allowable values which will make the interference introduced to the primary system below the threshold I_{th}^{l*}. In order to take the advantage of the allowable interference, some power can be taken from one subcarrier and given to another hoping to increase the total system capacity. Therefore the values of the maximum power that can be allocated to each subcarrier $P_{i,m}^{\mathrm{Max}}$ should be updated depending on the remaining interference. The residual interference can be determined as follows

$$I_{\mathrm{Residual}}^{l*} = I_{\mathrm{th}}^{l*} - \sum_{i=1}^{N} P_{i,m}^{\mathrm{W.F}} \Omega_{i,m}^{l*} \tag{16}$$

Assuming that $\mathcal{S}_m \subset \mathcal{N}_m$ is the set of the subcarriers that reach its maximum, that is, $P_{i,m}^{\mathrm{W.F}} = P_{i,m}^{\mathrm{Max}}, \forall i \in \mathcal{S}_m$, then $P_{i,m}^{\mathrm{Max}}, \forall i \in \mathcal{S}_m$ can be updated by applying (13) and (14) on the subcarriers in the set $\mathcal{S} = \{S_1 \cup S_2 \cdots \cup S_m\}$ with the following interference constraint

$$I_{\mathrm{updated}}^{l*} = I_{\mathrm{Residual}}^{l*} + \sum_{i \in \mathcal{S}} P_{i,m}^{\mathrm{W.F}} \Omega_{i,m}^{l*} \tag{17}$$

After determining the updated values of $P_{i,m}^{\mathrm{Max}}$, the 'cap-limited' waterfilling is performed again for every SU to find the final solution $P_{i,m}^{*} = P_{i,m}^{\mathrm{W.F}}$. A graphical description of the proposed power allocation algorithm is given in Fig. 4.

4 Generalisation of the proposed algorithm (multiple PU case)

In this section, the algorithm presented in the previous section to solve the optimisation problem $P1$ considering only one interference constraint will be generalised to consider L interference constraints, that is, multiple PU bands.

For the subcarrier allocation phase, considering the same assumption in which every subcarrier is able to introduce the same amount of interference to the the different PU bands, the value of the maximum power that can be allocated to each subcarrier, that is, $P_{i,m}^{\mathrm{Uni}}$, is determined by choosing the minimum among the different maximum powers evaluated according to the different interference constraints. Therefore (8) can be generalised as follows

$$P_{i,m}^{\mathrm{Uni}} = \min\left\{\frac{I_{\mathrm{Uniform}}^{1}}{\Omega_{i,m}^{1}}, \frac{I_{\mathrm{Uniform}}^{2}}{\Omega_{i,m}^{2}}, \ldots, \frac{I_{\mathrm{Uniform}}^{L}}{\Omega_{i,m}^{L}}\right\} \tag{18}$$

Once the maximum power $P_{i,m}^{\mathrm{Uni}}$ is determined, the same subcarrier assigning procedures presented previously can be used for the multiple PU bands case.

In the power allocation phase, if multiple interference constraints are considered in the optimisation problem $P2$,

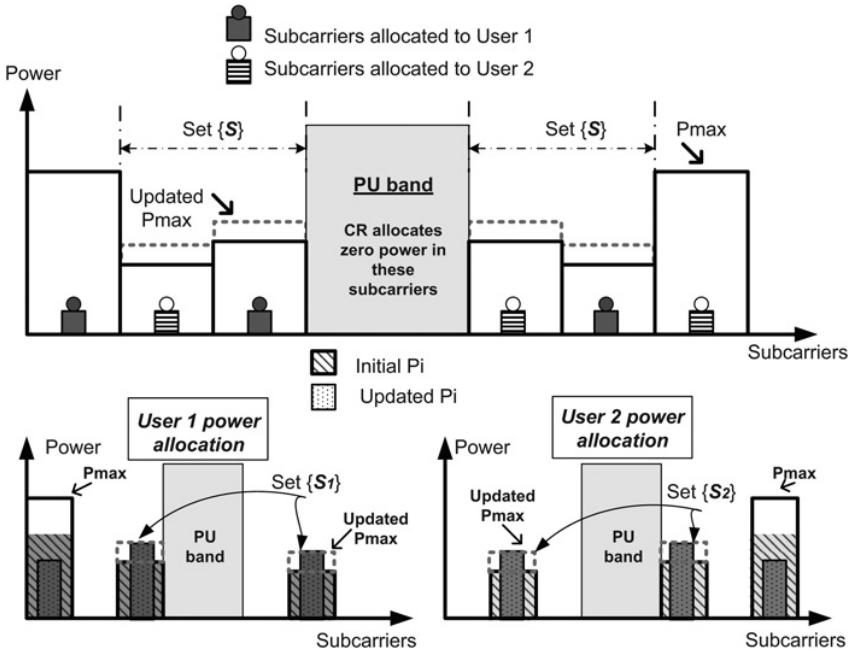

Fig. 4 *Example of the SUs allocated power using the proposed power allocation algorithm*

the solution given in (11) can be generalised as follows

$$P_{i,m}^{*} = \left[\frac{1}{\sum_{l=1}^{L}\alpha^{l}\Omega_{i,m}^{l} + \beta_{m}} - \frac{\sigma_{i}^{2}}{|h_{i,m}|^{2}}\right]^{+} \tag{19}$$

where α^{l} and β_{m} are the non-negative Lagrange multipliers. Therefore the problem become more computationally complex where $(M+L)$ Lagrangian multipliers should be determined. To find a suboptimal solution for the multiple PUs case, the values of the allocated power $P_{i,m}^{(\mathrm{Int})}(l)$ under every interference constraint I_{th}^{l} are determined using (13) and (14). Then, the maximum power $P_{i,m}^{\mathrm{Max}}$ that can be allocated to each subcarrier is determined according to the following formula

$$P_{i,m}^{\mathrm{Max}} = \min\{P_{i,m}^{(\mathrm{Int})}(1), P_{i,m}^{(\mathrm{Int})}(s), \ldots, P_{i,m}^{(\mathrm{Int})}(L)\} \tag{20}$$

Afterwards, the per-user power constraints are tested and the 'cap-limited' waterfilling is applied for every user m. Using (16) and (17), the updated values of the interference thresholds can be found and then (13) and (14) are applied to find the values of $P_{i,m}^{(\mathrm{Int})}(l)\ \forall i \in \mathcal{S}$. Accordingly, the new values of $P_{i,m}^{\mathrm{Max}}$ can be determined using (20). The 'cap-limited' waterfilling is performed again for every SU considering the updated maximum values to find the final solution. The implementation procedures of the power allocation algorithm with multiple interference constraints are described in Fig. 5. Step 1 in Fig. 5 initialises the variables values whereas Step 2 finds the optimal power allocation under the interference only constraint for every PU where the powers are evaluated using a waterfilling-like solution. Afterwards, the maximum power that can be allocated to every subcarrier is determined in Step 3. Step 4 checks whether the user power constraints are violated or not. If they are violated, the 'cap-limited' waterfilling is performed in Step 5 to distribute the user power among the subcarriers that were allocated to this user in the subcarriers allocation phase, that is, $\mathcal{N}_{m}$. The subcarriers which reached the maximum allowable power are determined for every user and the maximum power that can be allocated to these subcarriers are updated in Step 6. The last step performs the 'cap-limited' waterfilling over the subcarriers under the updated maximum power constraints to find the final power allocation vector.

5 Complexity analysis and simulations

The exhaustive enumeration scheme needs to iterate M^{N} times to exhaust all the cases, and its complexity of $\mathcal{O}(N^{3}M^{N})$ is very hard to afford. The algorithm proposed in [28] has a complexity of $\mathcal{O}(NM)$ with the assumption of sorted channel gains matrices. Therefore including the sorting complexity of the different matrices as well as the iterative nature of the algorithm, the complexity will be more than $\mathcal{O}(N\log N) + \mathcal{O}(NM)$. Moreover, the algorithm proposed by Wang *et al.* in [29] has a complexity larger than $\mathcal{O}(N^{2}M)$ and lower than $\mathcal{O}(N^{3}M)$. Note that the algorithms presented in [28, 29] are not considering fairness among users and are dealing with interference temperature constraint as several per-subcarrier maximum power constraints.

Recall that our proposed algorithm to solve problem $P1$ is divided into two phases: the subcarriers to users allocation phase and the power allocation phase. Each subcarrier in the first phase requires no more than M function evaluations to be assigned to one user depending on the size of the set $\mathcal{U}$. Hence, the computational complexity of the proposed subcarrier to user allocation algorithm is lower than or equal $\mathcal{O}(NM)$. In the power allocation algorithm, Step 2 in

Algorithm 1

1) **Initialise** $\mathcal{N} = \{1, 2, \cdots, N\}$, $I_{Left}^{l} = 0$ and $\mathcal{S} = \emptyset$.

2) $\forall l \in \{1, \cdots, L\}$, Sort $\left\{H_i = \frac{\sigma_i^2}{|h_{i,m}|^2}\Omega_{i,m}^{l}, i \in \mathcal{N}\right\}$ in decreasing order with k being the sorted index. Find the P_{i}^{Max} as follows:

   a) $H_{sum} = \sum_{i\in\mathcal{N}_l} H_i$, $\gamma_{l}^{(Int)} = |\mathcal{N}| / (I_{th}^{l} + H_{sum})$, $n = 1$.

   b) **while** $\gamma_{l}^{(Int)} > H_{k(n)}^{-1}$ **do**

      $H_{sum} = H_{sum} - H_{k(n)}$, $\mathcal{N} = \mathcal{N} \backslash \{k(n)\}$, $\gamma_{l}^{(Int)} = |\mathcal{N}| / (I_{th}^{l} + H_{sum})$, $n = n + 1$

      end while

   c) Set $P_{i,m}^{(Int)}(l) = \left[\frac{1}{\gamma_{l}^{(Int)}\Omega_{i,m}^{l}} - \frac{\sigma_i^2}{|h_{i,m}|^2}\right]^{+}$

3) Evaluate $P_{i,m}^{Max} = \min\{P_{i,m}^{(Int)}(1), P_{i,m}^{(Int)}(2), \cdots, P_{i,m}^{(Int)}(L)\}$

4) **if** $\sum_{i\in\mathcal{N}_m} P_{i,m}^{Max} \leq \overline{P_m}; \forall m$

   Let $P_{i,m}^{*} = P_{i,m}^{Max}$ and stop the algorithm.

   end if

5) $\forall m$, Perform the *"cap-limited"* waterfilling on the set of subcarriers $\mathcal{N}_m$ under the per-user constraint $\overline{P_m}$ and the maximum power that can be allocated to each subcarrier $P_{i,m}^{Max}$ and find the set $\mathcal{S}_m \subset \mathcal{N}_m$ where $P_{i,m}{}^{W.F} = P_{i,m}^{Max}$.

6) Let $\mathcal{S} = \{S_1 \cup S_2 \cdots \cup S_m\}$, evaluate $I_{Residual}^{l} = I_{th}^{l} - \sum_{i=1}^{N} P_{i,m}^{W.F}\Omega_{i,m}^{l}$, set $\mathcal{N} = \mathcal{S}$, $I_{updated}^{l} = I_{Residual}^{l} + \sum_{i\in\mathcal{S}} P_{i,m}^{W.F}\Omega_{i,m}^{l}$ and apply again only steps $(2-3)$ to update $P_{i,m}^{Max}$.

7) $\forall m$, Perform the *"cap-limited"* waterfilling on the set of subcarriers $\mathcal{N}_m$ under the per-user constraint $\overline{P_m}$ and the maximum power that can be allocated to each subcarrier $P_{i,m}^{Max}$ and set $P_{i,m}^{*} = P_{i,m}^{W.F}$.

Fig. 5 *Power allocation algorithm*

doi: 10.1049/iet-com.2010.1062

Fig. 5 has a computational complexity of $\mathcal{O}(N \log N)$ whereas Steps 5 and 7 of the algorithm execute the 'cap-limited' waterfilling for every SU with a complexity of $\Sigma_{m=1}^{M} \mathcal{O}(\mathcal{N}_m) \leq \mathcal{O}(N) \leq \mathcal{O}(N \log N)$ [38]. Step 6 has a complexity of $\mathcal{O}(|\mathcal{S}| \log |\mathcal{S}|) \leq \mathcal{O}(N \log N)$. Hence, the complexity of the power allocation algorithm is lower than $\mathcal{O}(N \log N)$. Thus, the overall asymptotic complexity of the proposed uplink resource allocation algorithm is lower than $\mathcal{O}(N \log N) + \mathcal{O}(NM)$. Table 1 summarises the complexity of the different algorithms.

The simulations are performed under the scenario given in Fig. 2. The values of T_s, Δ_f and σ_i^2 are assumed to be 4 μs, 0.3125 MHz and 10^{-6}, respectively. For simplicity, the channel gains h and g are outcomes of independent Rayleigh distributed random variables with mean equal to 1. Two interference constraints belonging to two active PU bands, that is, $L = 2$, are assumed with $B^1 = B^2$ and $I_{\text{th}}^1 = I_{\text{th}}^2$ (see Fig. 3). Perfect synchronisation is assumed between SUs. All the results have been averaged over 1000 iterations. For the purpose of performance comparison, the following algorithms are considered:

1. *Optimal*: The subcarriers are allocated by exhaustive enumeration whereas the power is allocated using (11). The optimal capacity is found without considering the minimum rate requirements.
2. *Wang*: The method proposed in [29] is used. The interference constraint is converted into per-subcarrier power constraints using (18).
3. *Fadel*: The method proposed in [28] is used. The per SU maximum power constraint is generated by converting the interference constraint into per-subcarrier power constraints using (18).
4. *Classical + Pr*: The subcarriers are allocated according to the scheme used in non-cognitive OFDM systems [21], whereas the power is allocated using (11).

Fig. 6 plots the average capacity of a CR system with $M = 3$ SUs against the interference thresholds when the number of subcarriers is $N = 8$, the per-user power budget $\overline{P_m} = 1m$ W and $B^1 = B^2 = 1.25$ MHz. The proposed algorithm without fairness achieves a good performance in comparison with optimal and outperforms the other algorithms. When the minimum user's rate constraint of 4 Mbits/s is applied, that is, $R_{\min} = 16$ bits per OFDM symbol, the proposed algorithm with fairness still performs well where the outage probability of having users below $R_{\min}$ is reduced as described in Fig. 7. For the rest of the results, the CR system is assumed to have $M = 10$ SUs and $N = 128$ subcarriers. The per-user power budget is set to be $\overline{P_m} = 1m$ W. The active PU bands bandwidths are assumed to be $B^1 = B^2 = 10$ MHz. The minimum rate for each user is set to be 20 Mbits/s, that is, $R_{\min} = 80$ bits per OFDM symbol. To that end, the optimal solution will not be simulated

Table 1 Complexity comparison

Algorithm	Complexity
Optimal	$\mathcal{O}(N^3 M^N)$
Wang [29]	$\in [\mathcal{O}(N^2 M), \mathcal{O}(N^3 M)]$
Fadel [28]	$\mathcal{O}(N \log N) + \mathcal{O}(NM)$
Proposed	$\mathcal{O}(N \log N) + \mathcal{O}(NM)$
Classical + Pr	$\mathcal{O}(N \log N) + \mathcal{O}(NM)$

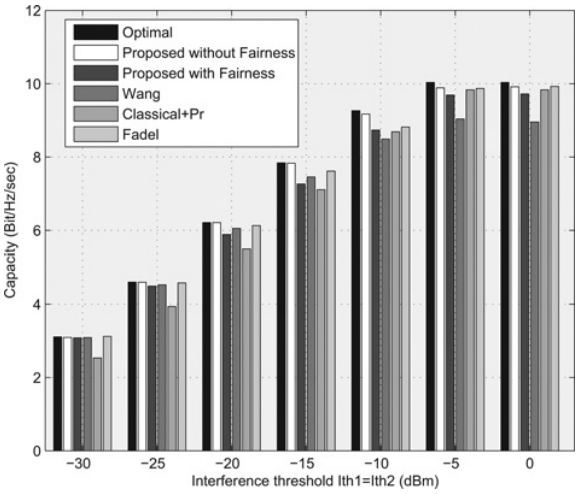

Fig. 6 *Three SUs achieved capacity against interference threshold when $N = 8$ subcarriers, $P_m = 1\,mW$, $B^1 = B^2 = 1.25$ MHz and $R_{min} = 4$ Mbits/s*

because of its extremely high computational complexity when the numbers of subcarriers and users are increased.

Fig. 8 plots the average capacity against the interference thresholds with $I_{\text{th}}^1 = I_{\text{th}}^2$. It can be observed that as the interference thresholds increase, the average sum rate increases since each SU is allowed to have more flexibility in allocating more power on its subcarriers. Remark that the algorithms *Wang*, *Fadel* and *Classical + Pr* are not considering any fairness among users. The performance of the proposed algorithm without considering the fairness among the users outperforms the reference algorithms. Moreover, it is worth noting that the performance of the proposed algorithm without fairness is considered as an upper bound for the case when fairness is taken into account. From this fact, numerical results reveal that the proposed algorithm with fairness consideration achieves a very good performance. Fig. 9 plots the outage probability of the different algorithms. The outage probability of the proposed

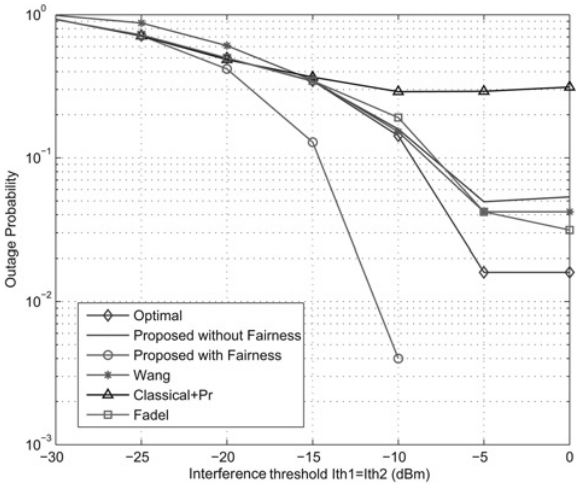

Fig. 7 *Outage probability against allowed interference thresholds when $N = 8$ subcarriers, $P_m = 1\,mW$, $B^1 = B^2 = 1.25$ MHz and $R_{min} = 4$ Mbits/s*

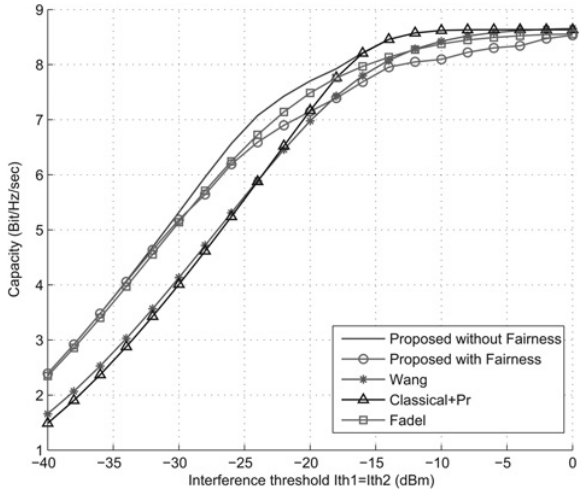

Fig. 8 *Achieved capacity against allowed interference thresholds when $N = 128$ subcarriers, $M = 8$ SUs, $P_m = 1\,mW$, $B^1 = B^2 = 10$ MHz and $R_{min} = 20$ Mbits/s*

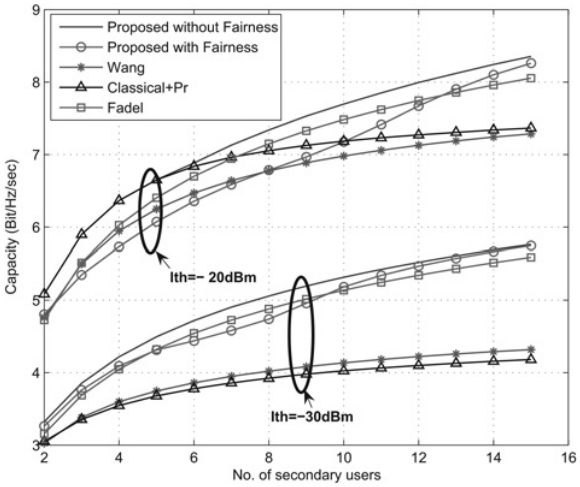

Fig. 10 *Achieved capacity against no. of SUs when $N = 128$ subcarriers, $P_m = 1\,mW$, $B^1 = B^2 = 10$ MHz and $R_{min} = 20$ Mbits/s*

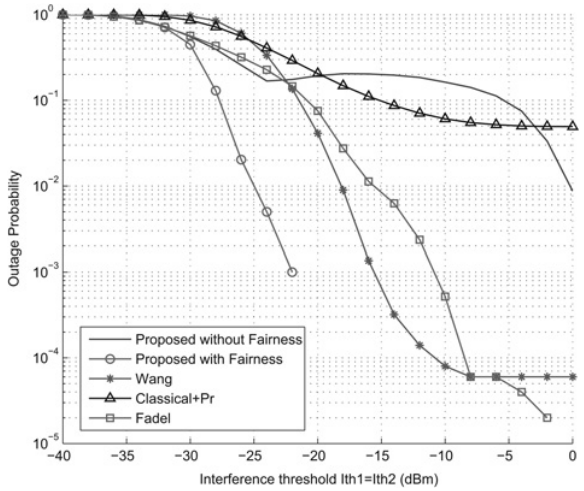

Fig. 9 *Outage probability against allowed interference thresholds when $N = 128$ subcarriers, $M = 8$ SUs, $P_m = 1\,mW$, $B^1 = B^2 = 10$ MHz and $R_{min} = 20$ Mbits/s*

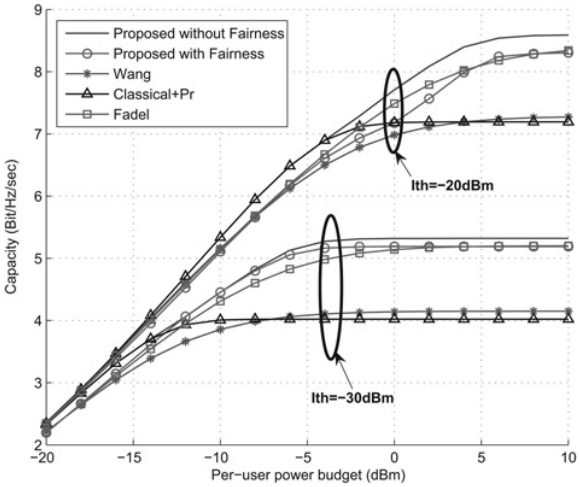

Fig. 11 *Achieved capacity against per-user power $P_m = 1\,mW$ when $N = 128$ subcarriers, $M = 8$ SUs, $B^1 = B^2 = 10$ MHz and $R_{min} = 20$ Mbits/s*

algorithm with fairness is much lower than that of the reference algorithms. Moreover, the outage probability decreases with the increase of the interference constraints because the different algorithms become more able to fulfill the minimum instantaneous rate for the different users.

Fig. 10 shows the average capacity against the number of SUs when the interference thresholds are -20 and -30 dBm. The capacity increases with the number of users because of the multiuser diversity. The lower the number of SUs, the smaller the difference between the proposed and *Classical + Pr* algorithm. This is because the number of subcarriers that will be allocated to each user will increase, which reduces the amount of power that will be allocated to each subcarrier and consequently the amount of interference imposed to the primary system. This makes the CR system to act relatively as a non-cognitive system. The gap between the different algorithms decreases with the interference thresholds as the CR system becomes closer to the classical (non-cognitive) system. Fig. 11 shows the average capacity against per-user power constraint, $\overline{P_m}$, when the interference thresholds are -20 and -30d Bm. The proposed algorithm outperforms the reference algorithms and the capacity of the CR system increases as the per-user power budget increases up to certain total power value. After this value, the capacity remains constant regardless of the increase of the per-user power because the system reaches the maximum power that can be used with the given interference threshold. Remark that when the available SUs power is too low and unable to cause the pre-defined interference constraint, the CR system acts as a non-cognitive one where the proposed algorithm performs very close to the *Classical + Pr* algorithm. Fig. 12 plots an example of the instantaneous data rate for a given user over time for the proposed algorithm with and without fairness consideration when $I_{\text{th}}^1 = I_{\text{th}}^2 = -20$ dBm. It can be noted that the proposed algorithm with fairness keeps the instantaneous rate above $R_{\min} = 80$ bits/symbol.

doi: 10.1049/iet-com.2010.1062

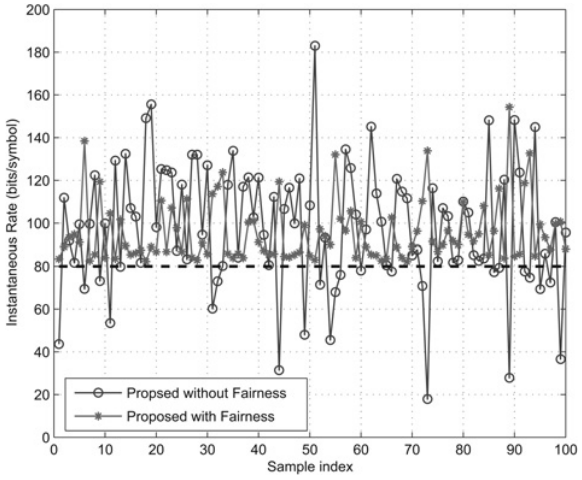

Fig. 12 *Instantaneous rates over time when $N = 128$ subcarriers, $M = 8$ SUs, $P_m = 1\,mW$, $B^1 = B^2 = 10$ MHz, $I^1_{th} = I^2_{th} = -20$ dBm and $R_{min} = 20$ Mbits/s (80 bits per OFDM symbol)*

6 Conclusion

In this paper, we propose an efficient resource allocation algorithm for uplink in multicarrier-based CR networks with fairness consideration. The allocation process is separated into two phases. In the first phase, the subcarriers are allocated to the users according to their channel quality as well as the interference that they may introduce to the primary system. In the second phase, the per-user power budget is distributed among the subcarriers so that the total system capacity is maximised without causing excessive interference to the primary system. The fairness among users is considered within the subcarrier allocation by reducing the probability of having users whose instantaneous rates are below a given minimum rate. Without applying the fairness constraints, the proposed algorithm can achieve lower computational complexity along with better performance relative to the reference algorithms in which the fairness among users are not considered. The proposed algorithm achieves superior outage performance when the fairness among users is considered. Developing a distributed resource allocation algorithm will be the guideline of our future research.

7 Acknowledgment

This work was partially supported by the European ICT-2009.1.1 project ACROPOLIS, COST Action IC0902 and National project Sofocles with code TEC 2010-21100. Part of this work was presented in the 5th International Conference on Cognitive Radio Oriented Wireless Networks and Communications (CrownCom 2010).

8 References

1 National Telecommunications and Information Administration (NTIA): 'FCC frequency allocation chart'. Available at www.ntia.doc.gov/osmhome/allochrt.pdf, 2003
2 Federal Communication Commission: 'Spectrum policy task force'. Report of ET Docket 02-135, November 2002
3 Akyildiz, I., Won-Yeol, L., Vuran, M., Mohanty, S.: 'NeXt generation/dynamic spectrum access/cognitive radio wireless networks: a survey', *Comput. Netw.*, 2006, **50**, (13), pp. 2127–2159
4 Mitola, J.: 'Cognitive radio for flexible mobile multimedia communications'. IEEE Int. Workshop on Mobile Multimedia Communications, MoMuC'99, November 1999, pp. 3–10
5 Haykin, S.: 'Cognitive radio: brain-empowered wireless communications', *IEEE J. Sel. Areas Commun.*, 2005, **23**, (2), pp. 201–220
6 Yucek, T., Arslan, H.: 'A survey of spectrum sensing algorithms for cognitive radio applications', *IEEE Commun. Surv. Tutor.*, 2009, **11**, (1), pp. 116–130 (first quarter 2009)
7 Zeng, Y., Liang, Y.-C., Hoang, A.T., Zhang, R.: 'A review on spectrum sensing for cognitive radio: Challenges and solutions', *EURASIP J. Adv. Signal Process.*, 2010, **2010**, 15pp, article id 381465
8 Musavian, L., Aissa, S.: 'Capacity and power allocation for spectrum-sharing communications in fading channels', *IEEE Trans. Wirel. Commun.*, 2009, **8**, (1), pp. 148–156
9 Kang, X., Liang, Y.-C., Nallanathan, A., Garg, H., Zhang, R.: 'Optimal power allocation for fading channels in cognitive radio networks: ergodic capacity and outage capacity', *IEEE Trans. Wirel. Commun.*, 2009, **8**, (2), pp. 940–950
10 Zhang, R.: 'On peak versus average interference power constraints for protecting primary users in cognitive radio networks', *IEEE Trans. Wirel. Commun.*, 2009, **8**, (4), pp. 2112–2120
11 Zhang, R., Liang, Y.-C.: 'Exploiting multi-antennas for opportunistic spectrum sharing in cognitive radio networks', *IEEE J. Sel. Topics Signal Process.*, 2008, **2**, (1), pp. 88–102
12 Zhang, R., Cui, S., Liang, Y.-C.: 'On ergodic sum capacity of fading cognitive multiple-access and broadcast channels', *IEEE Trans. Inform. Theory*, 2009, **55**, (11), pp. 5161–5178
13 Weiss, T., Jondral, F.K.: 'Spectrum pooling: an innovative strategy for the enhancement of spectrum efficiency', *IEEE Commun. Mag.*, 2004, **42**, pp. S8–S14
14 Bansal, G., Hossain, M.J., Bhargava, V.K.: 'Optimal and suboptimal power allocation schemes for OFDM-based cognitive radio systems', *IEEE Trans. Wirel. Commun.*, 2008, **7**, (11), pp. 4710–4718
15 Jang, J., Lee, K.: 'Transmit power adaptation for multiuser OFDM systems', *IEEE J. Sel. Areas Commun.*, 2003, **21**, (2), pp. 171–178
16 Kivanc, D., Li, G., Liu, H.: 'Computationally efficient bandwidth allocation and power control for OFDMA', *IEEE Trans. Wirel. Commun.*, 2003, **2**, (6), pp. 1150–1158
17 Shen, Z., Andrews, J., Evans, B.: 'Optimal power allocation in multiuser OFDM systems'. IEEE Global Telecommunications Conf., (GLOBECOM'03), 2003, vol. 1
18 Wong, C., Cheng, R., Lataief, K., Murch, R.: 'Multiuser OFDM with adaptive subcarrier, bit, and power allocation', *IEEE J. Sel. Areas Commun.*, 1999, **17**, (10), pp. 1747–1758
19 Yu, W., Rhee, W., Boyd, S., Cioffi, J.: 'Iterative water-filling for gaussian vector multiple-access channels', *IEEE Trans. Inf. Theory*, 2004, **50**, (1), pp. 145–152
20 Munz, G., Pfletschinger, S., Speidel, J.: 'An efficient waterfilling algorithm for multiple access OFDM'. IEEE Global Telecommunications Conf., (GLOBECOM'02), November 2002, vol. 1, pp. 681–685
21 Kim, K., Han, Y., Kim, S.-L.: 'Joint subcarrier and power allocation in uplink OFDMA systems', *IEEE Commun. Lett.*, 2005, **9**, (6), pp. 526–528
22 Gao, L., Cui, S.: 'Efficient subcarrier, power, and rate allocation with fairness consideration for OFDMA uplink', *IEEE Trans. Wirel. Commun.*, 2008, **7**, (5), pp. 1507–1511
23 Wang, P., Zhao, M., Xiao, L., Zhou, S., Wang, J.: 'Power allocation in OFDM-Based cognitive radio systems'. IEEE Global Telecommunications Conf., (GLOBECOM'07), 2007, pp. 4061–4065
24 Bansal, G., Hossain, M.J., Bhargava, V.K.: 'Adaptive power loading for OFDM-Based cognitive radio systems'. IEEE Int. Conf. on Communication, (ICC'07), 2007, pp. 5137–5142
25 Zhang, Y., Leung, C.: 'Resource allocation in an OFDM-based cognitive radio system', *IEEE Trans. Commun.*, 2009, **57**, (7), pp. 1928–1931
26 Hasan, Z., Bansal, G., Hossain, E., Bhargava, V.: 'Energy-efficient power allocation in OFDM-based cognitive radio systems: a risk-return model', *IEEE Trans. Wirel. Commun.*, 2009, **8**, (12), pp. 6078–6088
27 Shaat, M., Bader, F.: 'Computationally efficient power allocation algorithm in multicarrier-based cognitive radio networks: OFDM and FBMC systems', *EURASIP J. Adv. Signal Process.*, 2010, **2010**, 13pp, article id 528378
28 Digham, F.: 'Joint power and channel allocation for cognitive radios'. IEEE Wireless Communications and Networking Conf., WCNC'08, April 2008, pp. 882–887
29 Wang, W., Wang, W., Lu, Q., Peng, T.: 'An uplink resource allocation scheme for OFDMA-based cognitive radio networks', *Int. J. Commun. Syst.*, 2009, **22**, (5), pp. 603–623
30 Zhang, H., Ruyet, D.L., Roviras, D., Medjahdi, Y., Sun, H.: 'Spectral efficiency comparison of OFDM/FBMC for uplink cognitive radio networks', *EURASIP J. Adv. Signal Process.*, 2010, **2010**, 14pp, article id 621808

31 Weiss, T., Hillenbrand, J.: 'Mutual interference in OFDM-based spectrum pooling systems'. Vehicular Technology Conf., (VTC'04-Spring), May 2004, vol. 4

32 Almalfouh, S.M., Stuber, G.L.: 'Interference-aware power allocation in cognitive radio networks with imperfect spectrum sensing'. IEEE Int. Conf. on Communications (ICC), May 2010, pp. 1–6

33 Tao Qin, C.M., Leung, C., Shen, Z.: 'Resource allocation in a cognitive radio system with imperfect channel state estimation', *J. Electr. Comput. Eng.*, 2010, **2010**, 5pp, article id 419430

34 Zhang, R.: 'Optimal power control over fading cognitive radio channel by exploiting primary user CSI'. IEEE Global Telecommunications Conf., (IEEE GLOBECOM'08), Dec. 2008, pp. 1–5

35 Boyd, S., Vandenberghe, L.: 'Convex optimization' (Cambridge University Press, Cambridge, UK, 2004)

36 Leke, A., Cioffi, J.: 'A maximum rate loading algorithm for discrete multitone modulation systems'. IEEE Global Telecommunications Conf., (GLOBECOM'97), 1997, vol. 3, pp. 1514–1518

37 Papandreou, N., Antonakopoulos, T.: 'Bit and power allocation in constrained multicarrier systems: the single-user case', *EURASIP J. Adv. Signal Process.*, 2008, **2008**, 4pp, article id 643081

38 Zhao, C., Kwak, K.: 'Power/bit loading in OFDM-based cognitive networks with comprehensive interference considerations: the single-SU case', *IEEE Trans. Veh. Technol.*, 2010, **59**, (4), pp. 1910–1922

9 Appendix

9.1 Derivation of the optimal power allocation given by (11) and (19)

We want to find the optimal solution for the following optimisation problem

$$\max_{P_{i,m}} \sum_{i=1}^{N} \log_2\left(1+\frac{P_{i,m}|h_{i,m}|^2}{\sigma_i^2}\right) \tag{21}$$

$$\text{s.t.} \quad \sum_{i=1}^{N} P_{i,m}\Omega_{i,m}^{l} \le I_{\text{th}}^{l}, \quad \forall l \in \{1, \ldots, L\} \tag{22}$$

$$\sum_{i\in\mathcal{N}_m} P_{i,m} \le \overline{P_m}, \quad \forall m \tag{23}$$

$$P_{i,m} \ge 0, \quad \forall i \tag{24}$$

The problem above is a convex optimisation problem. Introducing the lagrange multipliers α^l, μ_i and β_m for the inequality constraints in (22), (23) and (24), respectively, the Lagrangian can be written as

$$G = -\sum_{i=1}^{N} R_i(P_{i,m}, h_{i,m}) + \sum_{l=1}^{L}\alpha^l\left(\sum_{i=1}^{N} P_{i,m}\Omega_{i,m}^{l} - I_{\text{th}}^{l}\right) + \sum_{m=1}^{M}\beta_m\left(\sum_{i\in\mathcal{N}_m} P_{i,m} - \overline{P_m}\right) - \sum_{i=1}^{N} P_{i,m}\mu_i \tag{25}$$

The Karush–Kuhn–Tucker conditions can be written as follows

$$\alpha^l \ge 0, \quad \forall l \in \{1, 2, \ldots, L\}; \quad \beta_m \ge 0, \quad \forall m \in \{1, 2, \ldots, M\}$$
$$\mu_i \ge 0 \quad \forall i \in \{1, 2, \ldots, N\}; \quad P_{i,m}^{*} \ge 0$$
$$\alpha^l\left(\sum_{i=1}^{N} P_{i,m}^{*}\Omega_{i,m}^{l} - I_{\text{th}}^{l}\right) = 0$$
$$\beta_m\left(\sum_{i\in\mathcal{N}_m} P_{i,m}^{*} - \overline{P_m}\right) = 0, \quad \forall m \in \{1, 2, \ldots, M\}$$
$$\mu_i P_i^{*} = 0, \quad \forall i \in \{1, 2, \ldots, N\}$$
$$\sum_{i=1}^{N} P_{i,m}\Omega_{i,m}^{l} - I_{\text{th}}^{l} \le 0$$
$$\sum_{i\in\mathcal{N}_m} P_{i,m} - \overline{P_m} \le 0, \quad \forall m \in \{1, 2, \ldots, M\}$$
$$\frac{\partial G}{\partial P_{i,m}^{*}} = \frac{-1}{(\sigma_i^2/|h_{i,m}|^2) + P_{i,m}^{*}} + \sum_{l=1}^{L}\alpha^l\Omega_{i,m}^{l} + \beta_m - \mu_i = 0 \tag{26}$$

Rearranging the last condition in (26) we obtain

$$P_{i,m}^{*} = \frac{1}{\sum_{l=1}^{L}\alpha^l\Omega_{i,m}^{l} + \beta_m - \mu_i} - \frac{\sigma_i^2}{|h_{i,m}|^2} \tag{27}$$

Since $P_{i,m}^{*} \ge 0$, we obtain

$$\frac{\sigma_i^2}{|h_{i,m}|^2} \le \frac{1}{\sum_{l=1}^{L}\alpha^l\Omega_{i,m}^{l} + \beta_m - \mu_i} \tag{28}$$

If

$$\frac{\sigma_i^2}{|h_{i,m}|^2} < \frac{1}{\sum_{l=1}^{L}\alpha^l\Omega_{i,m}^{l} + \beta_m}$$

then $\mu_i = 0$ and hence

$$P_{i,m}^{*} = \frac{1}{\sum_{l=1}^{L}\alpha^l\Omega_{i,m}^{l} + \beta_m} - \frac{\sigma_i^2}{|h_{i,m}|^2} \tag{29}$$

Moreover, if

$$\frac{\sigma_i^2}{|h_{i,m}|^2} > \frac{1}{\sum_{l=1}^{L}\alpha^l\Omega_{i,m}^{l} + \beta_m}$$

from (27) we obtain

$$\frac{1}{\sum_{l=1}^{L}\alpha^l\Omega_{i,m}^{l} + \beta_m - \mu_i} \ge \frac{\sigma_i^2}{|h_{i,m}|^2} > \frac{1}{\sum_{l=1}^{L}\alpha^l\Omega_{i,m}^{l} + \beta_m} \tag{30}$$

and since $\mu_i P_{i,m}^{*} = 0$ $\mu_i \ge 0$, we obtain that $P_{i,m}^{*} = 0$.

Therefore the optimal solution can be written as follows

$$P_{i,m}^{*} = \left[\frac{1}{\sum_{l=1}^{L}\alpha^l\Omega_{i,m}^{l} + \beta_m} - \frac{\sigma_i^2}{|h_{i,m}|^2}\right]^{+} \tag{31}$$

where $[x]^{+} = \max(0, x)$. If only one PU is assumed with interference constraint I_{th}^{l*}, (31) is reduced to

$$P_{i,m}^{*} = \left[\frac{1}{\alpha^{l*}\Omega_{i,m}^{l*} + \beta_m} - \frac{\sigma_i^2}{|h_{i,m}|^2}\right]^{+} \tag{32}$$

doi: 10.1049/iet-com.2010.1062

3.1.2 Resource allocation in CR using relay communication

As a continuation to the above research and cited works in CR environment, the relying mode was introduced to analyze the behavior and achieved performance of the previously developed algorithms.

Combining cognitive radio (CR) with cooperative communications can further improve the spectrum utilization and enhance the network performance. Different relays in the network can collaborate in the spectrum sensing and assist the network transmission [41]. An overview of the cooperative communication in cognitive scenario has been presented in [42, 43]. The relay assisted transmission can be categorized into two basic strategies; amplify and forward (AF) and decode and forward (DF). In the AF strategy, the relay amplifies the received signal and then forwards it to the destination. On the other hand, in DF scheme, the relay decodes the received massage before the retransmission. In multi-carrier based relay networks, in addition to the power and subcarrier allocation required in non-cooperative networks, proper relay selection and subcarrier coupling in the different hops are required to improve the system performance.
As it's well known, the communications in CR environment should not disturb the operation of the primary system or negatively altering its performance and hence, the different resources should be distributed adequately so that the interference introduced to the primary system is not harmful (see Fig.3.13).

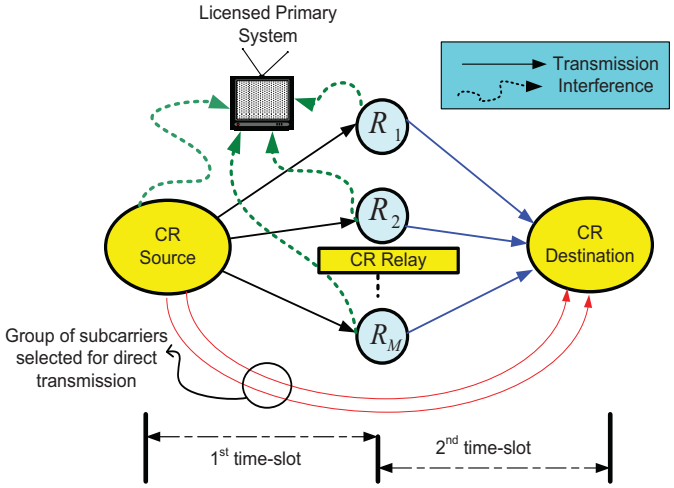

Figure 3.13: Relayed cognitive radio network.

My main analyzed work is that of Jia et al. that proposed in [44] a centralized heuristic algorithm to select the most profitable pair of nodes and to allocate the different channels based on the availability of the spectrum. However, the interference to the primary system was not considered. In [45], a power allocation algorithm in a single relay DF orthogonal frequency division multiplexing (OFDM) based CR system has been proposed. Under the assumption of prior perfect subcarrier matching in the two hops, the authors treated the optimization problem in the source and the relay individually. The algorithm performance degrades significantly if the relay has to forward the receiving message on the same subcarrier, i.e. there is no subcarrier pairing. Same can be found in the researches developed in [46] to deal with the bit loading problem in relay.
Liying et al. presented in [47] a joint relay selection and power allocation algorithm where the cognitive relay system is prevented from inducing severe interference to the primary system by limiting its maximum transmission power. In [48], the authors proposed an algorithm to select the best transmit way between the network nodes. The algorithm can select direct, dual or diversity transmission based on the available spectrum as well as the maximum allowable transmission powers. The systems in [47] and [48] are considering single carrier channels. The resource allocation with the consideration of the interference constraint in OFDM based multi-relay CR has not been investigated in the previously cited works.

Thus, the resource allocation problem in a dual-hop multi-relay DF multi-carrier based CR system has been considered in my conducted researches. The different system resources, i.e. powers, subcarriers and relays, are optimized jointly in order to maximize the system capacity. The resource allocation process is performed under the per-node power constraint as well as the interference to the primary system constraint. These research works have been realized in Musbah Shaat PhD. thesis, and under the framework of the EC funded projects the COST Action IC0902, the network of excellence (NoE) ICT project ACROPOLIS, and the Spanish national project SOFOCLES (more details in Subsection 1.5.3, page 24). An extension to the conducted works with M. Shaat is that developed in close collaboration with KAUST institution on relay resource allocation in two-way DF-AF in CR networks in [J14] (listed in Subsection 2.1.1), and that of optimal power allocation algorithm for adaptive relay networks in cognitive systems (see details in Subsection 1.3.4) in [C74] and [J16]. My main contributions can be summarized to the following:

- The resource allocation problem has been formulated as a mixed-integer programming problem. Thanks to the fulfillment of the time sharing condition, the dual decomposition technique is used to find jointly the optimal subcarrier pairs, selected relays and allocated powers. The group of subcarriers used for the direct transmission (without relaying) is determined as well. Related works can be found in: [CB14], and in [C52, C65, C67, C69, C70].
- Due to the high computational complexity of the optimal algorithm, an heuristic suboptimal algorithm has been also proposed. The suboptimal algorithm allocates jointly the different resources taking into consideration the channel qualities, interference to the primary system, individual power budgets and the limitation introduced from applying the DF relaying strategy. Related papers with this research part are: [C56, C67, C68, C71, C74].
- The performance of the OFDM and FBMC based CR systems have been compared. Moreover, the impact of the different constraints values on the system performance is investigated. Extended details on this work can be found in the second paper depicted the end of this Subsection 3.1.2, and at [C45, C48, C51, C76].
- A new formulation on relay selection in two-way relaying CR system that selects between the AF and DF protocols based on the higher sum rate (SR) achieved by the secondary network (SN) without affecting the QoS of the primary network has been also developed in [J14], and [C84] (see Subsections 2.1.1 and 2.1.4 respectively).

In the simulations, the following algorithms are considered for performance comparison purpose:

- **Optimal** with direct: apply the solution based on the dual decomposition technique presented in Section III of [J11], the first paper depicted at the end of Subsection 3.1.2.
- **Optimal without direct**: apply the solution based on the dual decomposition technique when the relayed transmission is allowed only while the direct link is always blocked, i.e. the direct/relayed transmission indicator α_j [4] is assumed to be $\alpha_j = 1$, $\forall j$.
- **Suboptimal**: apply the proposed suboptimal algorithm described in Algorithm 1, Section IV of [J11], the first paper depicted at the end of Subsection 3.1.2.
- **SNR**: the subcarriers are paired and assigned to the relays based on their SNR. The powers are evaluated [5] with the known values of α_j , $t_{j,k}$ ($t_{j,k} \in \{0,1\}$ is the subcarrier pairing indicator, i.e. $t_{j,k} = 1$ if the j^{th} subcarrier in the source is paired with the k^{th} in the destination, and zero otherwise) and $\pi_{j,k}^{m}$ (is the relay assignment indicator which equals to one when the pair (j,k) [6] is assigned to the m^{th} relay and zero otherwise).
- **Random**: the subcarriers are paired and assigned to the relays randomly. The powers are evaluated by solving equation (6) in Section III of [C76] with the known values of α_j, $t_{j,k}$ $\pi_{j,k}^{m}$.

[4] $_j \forall \{0,1\}$ is the subcarrier transmission mode indicator which has a value of one when the subcarrier is used for relayed transmission while equals zero if the subcarrier is used for the direct transmission.

[5] by solving equation (6) in Section III in [C76] the second depicted paper at the end of this Subsection 3.1.2.

[6] The j^{th} subcarrier in the source should be paired with only one subcarrier k in the destination which may not be the same as j to form the (j,k) pair that should be assigned to only one relay m.

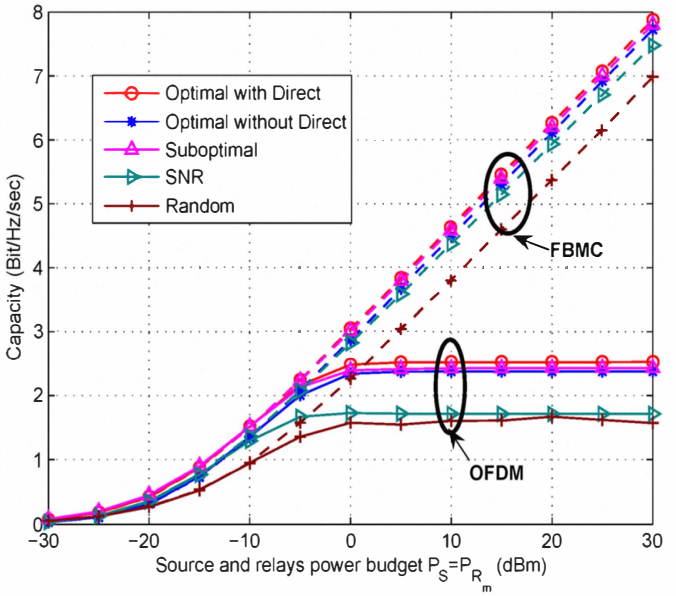

Figure 3.14: Achieved capacity vs available power budget with $P_S = P_R$, when I_{th} = -30 dBm. OFDM based system is plotted by the solid lines while the dashed ones represent the FBMC based systems.

As main results, to compare the performance of OFDM and FBMC based system in cooperative relay networks, Fig. 3.15 and Fig. 3.14 plot the achieved capacity of the algorithms against different interference thresholds and different power constraints, respectively. In Fig. 3.14 , two different performance regions can be identified as follows

1. When Ith 30 dBm: the capacity of the FBMC based CR systems is more that that of the OFDM based ones. This is because of the small side lobes of the FBMC systems as well as because of loss of the spectrum efficiency in OFDM due to the use of the CP. Therefore, the interference constraint generally has small effect on the performance of the FBMC based systems which is not the case in OFDM ones.

2. When Ith $>$ 30 dBm: both of the system has almost the same performance when operating with high interference thresholds or low power budgets. This is can be justified by noting that the systems in this region operate in non-cognitive-like environment.

Similarly, in Fig. 3.14, the region when $P_S = P_{Rm} \leq 5$ dBm represents the non-cognitive like environment; where the available power budget is not able to introduce high interference. When the power constraints increase more than this value, FBMC system has significantly improves the CR capacity since FBMC based systems can use more transmission power which increase the total system capacity.

The transmission process in the two-way relaying technique takes place in two time slots. In the first slot, the terminals transmit their signals simultaneously to the relay. Subsequently, in the second slot, the relay broadcasts its signal to the terminals. The works in [49, 50, 51] brought some solutions providing a useful framework to solve the relay selection and the optimum power allocation in cooperative way and two-way relaying CR (see the system model depicted in Fig. 3.16).

The main research contributions and achievements in the two-way relay context can be summarized as follow:

1. Formulate a new relay selection scheme in two-way relaying CR system which selects between the AF and DF protocols depending on the higher Sum Rate (SR) achieved by a Secondary Network (SN) without affecting the Quality of Service (QoS) of a Primary Network (PN). For that reason, additional interference constraints are considered in the optimization problem for both time slots.

2. Derivation of the optimal terminals power and relay power that maximize the cognitive SR of the system

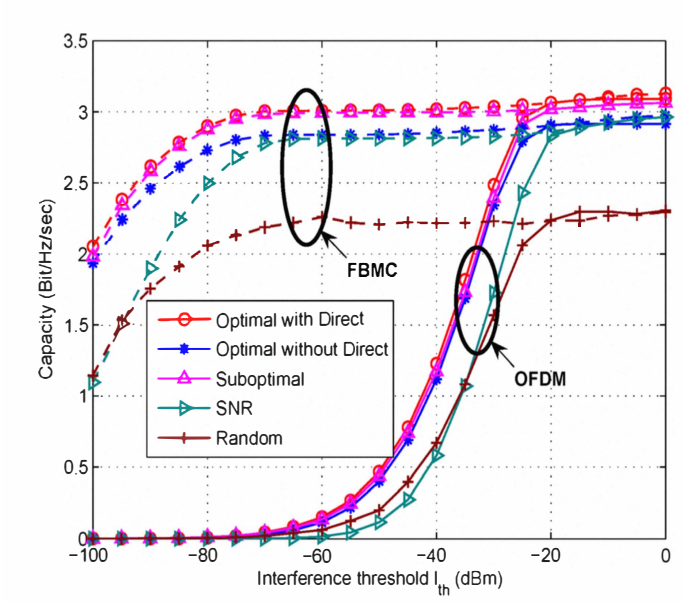

Figure 3.15: Achieved capacity vs the interference threshold with $P_s = P_R = 0$ dBm. OFDM based system is plotted by the solid lines while the dashed ones represent the FBMC based systems.

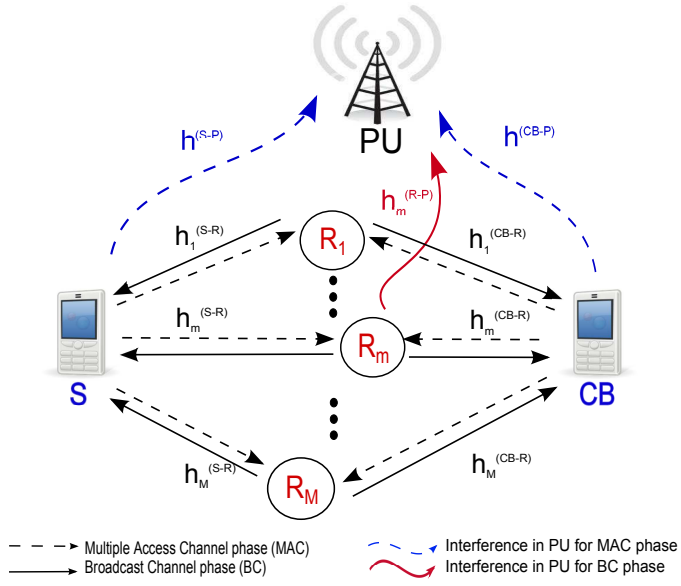

Figure 3.16: System model of the cooperative two way relaying cognitive radio system.

3. Using dual decomposition and sub-gradient methods for both AF and DF protocols in order to solve the SR maximization problem and select the best relay with the best protocol

4. Design a practical low complexity suboptimal approach based on Genetic Algorithm (GA) to solve the formulated optimization problem [52], and compare it with the optimal and Exhaustive Search (ES) solutions. Some of the details are given in a comparison technical report available online [53].

Developed algorithms related with the above numbered achievements are depicted in [J14], the last paper depicted at the end of this Subsection 3.1.2.

To resume, all the publications (See Subsection 2.1.1, pp. 30-41) related with this research orientation are: Journals: [J11, J14, J16], Conferences: [C56, C67, C68, C71, C74, C84], the PhD thesis of Mr. Musbah Shaat (2008-2012), and the following masters:

- Ahmad-Sharoa, from Electrical Engineering (EE) department of King Abdullah University of Science and Technology-KAUST (Saudi Arabia). Supervisor: Prof. Mohamed Slim-Alouini (KAUST). Master degree topic on: "Resource Allocation in Two-way Relaying and the Adaptive Relaying in Cognitive Radio". Period: May-August 2012, at CTTC Barcelona-Spain.

- Hamza Souri, from Electrical Engineering (EE) department of King Abdullah University of Science and Technology-KAUST (Saudi Arabia). Co-Supervision with: Prof. Mohamed Slim-Alouini (KAUST). Master degree topic on: "Optimal Power Allocation Algorithm for Adaptive Relay Networks in Cognitive Systems". Period: May-July 2011, at CTTC Barcelona-Spain.

Following are the corresponding depicted papers:

1. [J11]- Musbah Shaat and Faouzi Bader, "Asymptotically Optimal Resource Allocation in OFDM-Based Cognitive Networks with Multiple Relays", IEEE Transactions on Wireless Communications, vol.11, issue 3, doi 10.1109/TWC.2012.011012.110880. March 2012.

2. [C76]- M. Shaat and F. Bader, "Comparison of OFDM and FBMC Performance in Multi-Relay Cognitive Radio Network", in Proc. of the Ninth IEEE International Symposium in Wireless Communication Systems (ISWCS'2012), on 29 August 2012, at Paris, France.

3. [J14] - Ahmad Alsharoa, Faouzi Bader, and Mohamed-Slim Alouini, "Relay Selection and Resource Allocation for Two Way DF-AF Cognitive Radio Network". IEEE Wireless Communications Letters (WCL), vol. 2, issue: 4, pp. 427-430, doi: 10.1109/WCL.2013.13.130211. August 2013.

Asymptotically Optimal Resource Allocation in OFDM-Based Cognitive Networks with Multiple Relays

Musbah Shaat, *Student Member, IEEE,* and Faouzi Bader, *Senior Member, IEEE*

***Abstract*—In this letter, the problem of resources allocation in decode-and-forward (DF) relayed OFDM based cognitive system is considered. The dual decomposition technique is adopted to obtain an asymptotically optimal subcarrier pairing, relay selection, and power allocation. The resources are optimized under the individual power constraints in source and relays so that the sum rate is maximized while the interference induced to the primary system is kept below a pre-specified interference temperature limit. Moreover, a sub-optimal scheme is presented to avoid the high computational complexity of the optimal scheme. The sub-optimal algorithm allocates jointly the different resources taking into account the channel qualities, the DF-relaying strategy, the interference induced to the primary system ,and the individual power budgets. The performance of the different schemes and the impact of the constraints values are discussed through the numerical simulation results.**

***Index Terms*—Cooperative cognitive radio system, decode-and-forward, joint resource allocation, OFDM, resource management, throughput.**

I. Introduction

COGNITIVE radio (CR) has been proposed to solve the spectrum under-utilization problem by allowing a group of secondary users (SU) to access the unused radio spectrum originally allocated to the primary user (PU). The CR performance and the spectrum utilization can be further improved by using the cooperative communications in which several relays are used to assist the source to destination transmission. An overview of cooperative communications in cognitive scenario can be found in [1].

A lot of work has been already done on the resources allocation in non-cognitive relay systems (see e.g. [2], [3] and references therein). In [2] and [3], the dual approach has been used to allocate the different system resources where [2] deals with multiple amplify-and-forward (AF) relays system while Hsu et al. considered decode-and-forward (DF) single relay system in [3]. In cognitive systems, the different resources (i.e. power and frequency) should be distributed such that the interference induced to the primary system is minimized. Liying et al. presented in [4] a joint relay selection and power allocation algorithm where the cognitive relay system is prevented from inducing severe interference to the primary system by limiting its maximum transmission power. In [5], the authors proposed an algorithm to select the best transmit way between the network nodes. The algorithm can select direct, dual or diversity transmission based on the available spectrum as well as the maximum allowable transmission powers. The systems in [4] and [5] are considering single carrier channels.

In this letter, a dual-hop multiple relays DF-orthogonal frequency division multiplexing (OFDM) based cognitive system is considered. The different system resources, i.e. powers, subcarriers and relay selection, are optimized jointly in order to maximize the total system capacity. The resource allocation process is performed under the per node power constraint as well as the interference to the primary system constraint. To the best of our knowledge, the resource allocation with the consideration of the interference constraint in OFDM based multi-relay CR has not been investigated before. The main contributions of the paper are as follows: 1) The resource allocation problem is formulated as a mixed integer programming problem taking into account that the different relays are applying DF-protocol. Thanks to the fulfillment of the time sharing condition described in [6], the dual decomposition technique is used to find jointly the asymptotically optimal subcarrier pairs, selected relays and allocated powers; 2) Due to the high computational complexity of the optimal algorithm, a sub-optimal algorithm is proposed. The sub-optimal algorithm allocates jointly the different resources taking into consideration the channel qualities, interference to the primary system, individual power budgets and the limitations introduced from applying the DF relaying strategy. The sub-optimal algorithm performs close to optimal with less computational complexity.

The rest of this letter is organized as follows. Section II gives the system model while the problem is formulated and the optimal algorithm is presented in Section III. The sub-optimal scheme is presented in Section IV. Section V demonstrates selected numerical results and concludes the paper.

II. System Model

In this letter, an OFDM-based cooperative CR system is considered. As shown in Fig. 1, the CR system coexists with the primary system in the same geographical location. Due to the existence of an obstacle or a large distance, there is no direct link between the source and the destination so that the source tries to communicate with destination through M relays. The CR system's frequency spectrum is divided into N subcarriers each having a Δf bandwidth. It is assumed that the CR system can use the inactive PU bands provided that the total interference introduced to the PU band, I_{th}, does not exceed the maximum interference power that can be tolerated by PU. The relays are assumed to operate in half-duplex mode with DF-protocol, thus receiving and transmitting in two different time slots. In the first time slot, the source transmits

Manuscript received May 10, 2011; revised October 13, 2011; accepted November 27, 2011. The associate editor coordinating the review of this letter and approving it for publication was J. R. Luo.

This work was partially supported by the European (ICT-2009.1.1) project (ACROPOLIS-NoE), COST Action IC0902, and the Spanish Research Council under SOFOCLES grant (TEC2010-21100).

The authors are with the Centre Tecnologic de Telecomunicacions de Catalunya (CTTC), Barcelona, Spain (e-mail: {musbah.shaat, faouzi.bader}@cttc.es).

Digital Object Identifier 10.1109/TWC.2012.011012.110880

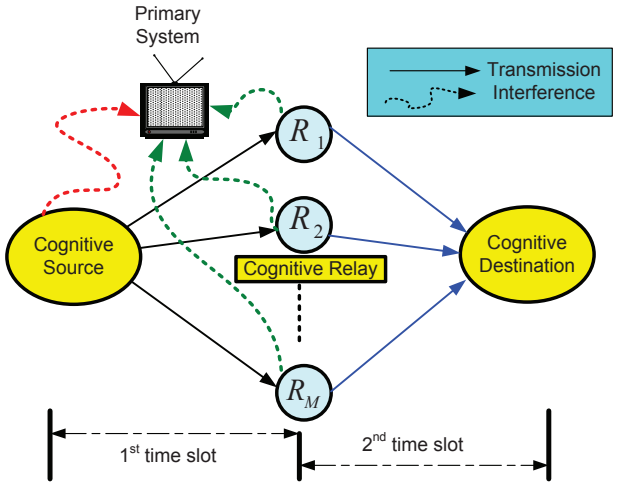

Fig. 1. Cooperative relay cognitive radio network.

to the different relays while in the second time slot the relays decode the message, re-encode it and then forward it to the destination. The j^{th} subcarrier in the source should be paired with only one subcarrier k in the destination which may not be the same as j to form the (j,k) pair that should be assigned to only one relay m. The maximum total transmission powers that can be used in the source and the different relays are P_S and P_{R_m} respectively.

In OFDM systems, the mutual interference introduced by the i^{th} subcarrier to PU, $I_i\left(d_i,P_i\right)$, can be expressed as [7]

$$I_i\left(d_i,P_i\right)=\int_{d_i-B/2}^{d_i+B/2} G_iP_iT_s\left(\frac{\sin\pi fT_s}{\pi fT_s}\right)^2 df \triangleq P_i\Omega_i \quad (1)$$

where d_i is the spectral distance between the i^{th} subcarrier and the PU band. G_i denotes the square of the channel gain between the i^{th} subcarrier and the PU band. P_i is the total transmit power emitted by the i^{th} subcarrier and T_s is the symbol duration. Ω_i denotes the interference factor of the i^{th} subcarrier to the PU band. Similarly, the interference power introduced by PU signal with power spectrum density $\Upsilon\left(e^{j\omega}\right)$ into the band of the i^{th} subcarrier is [7]

$$J_i=\int_{d_i-\Delta f/2}^{d_i+\Delta f/2} Y_i\Upsilon\left(e^{j\omega}\right)\,d\omega \quad (2)$$

where Y_i is the square of the channel gain between the i^{th} subcarrier and the PU signal.

III. Problem Formulation and Optimal Solution

The transmission rate of the j^{th} subcarrier in the source coupled with the k^{th} subcarrier in the destination and assigned to the m^{th} relay, $Rate_{(j,k,m)}$, can be evaluated as follows

$$Rate_{(j,k,m)}=\frac{1}{2}\min\left\{\begin{array}{l}\log_2\left(1+\frac{P^j_{SR_m}H^j_{SR_m}}{\sigma^2_{j,m}}\right)\\ \log_2\left(1+\frac{P^k_{R_mD}H^k_{R_mD}}{\sigma^2_{k,m}}\right)\end{array}\right. \quad (3)$$

where $P^j_{SR_m}(P^k_{R_mD})$ is the power transmitted over the $j^{th}(k^{th})$ subcarrier in the Source to $R_m(R_m$ to Destination) link. R_m means the m^{th} relay. Moreover, $H^j_{SR_m}(H^k_{R_mD})$ is the square of the $j^{th}(k^{th})$ subcarrier fading gain over Source to $R_m(R_m$ to Destination) link. $\sigma^2_{j,m(k,m)}=\sigma^2_{AWGN_{j,m(k,m)}}+J_{j(k)}$ where $\sigma^2_{AWGN_{j,m(k,m)}}$ is the variance of the additive white Gaussian noise (AWGN) on the Source to $R_m(R_m$ to Destination) link and $J_{j(k)}$ is the interference introduced by the PU signal into the $j^{th}(k^{th})$ subcarrier which is evaluated using (2) and can be modeled as AWGN by applying the law of large number as described in [8] or by assuming that the primary and cognitive systems are using an independent and random Gaussian codewords [9].

Our objective is to maximize the CR system throughput by optimizing the subcarrier pairing, relays assignment, and distributing the available power budgets among the assigned subcarrier pairs so that the instantaneous interference introduced to the primary system is kept below the maximum limit. Therefore, the optimization problem can be formulated as follows

$$\begin{array}{l}\max\limits_{\substack{\pi_{(j,k,m)},t_{j,k}\\ P^j_{SR_m}\geq 0,P^k_{R_mD}\geq 0}} \sum\limits_{m=1}^{M}\sum\limits_{j=1}^{N}\sum\limits_{k=1}^{N}\pi_{(j,k,m)}t_{j,k}Rate_{m(j,k)}\\ s.t.\\ \text{- (C1: Source power constraint):}\\ \sum\limits_{m=1}^{M}\sum\limits_{j=1}^{N}P^j_{SR_m}\leq P_S\\ \text{- (C2: Relays individual power constraints):}\\ \sum\limits_{k=1}^{N}P^k_{R_mD}\leq P_{R_m},\quad \forall m\\ \text{- (C3: Interference at the first time slot):}\\ \sum\limits_{m=1}^{M}\sum\limits_{j=1}^{N}P^j_{SR_m}\Omega_j\leq I_{th}\\ \text{- (C4: Interference at the second time slot):}\\ \sum\limits_{m=1}^{M}\sum\limits_{k=1}^{N}P^k_{R_mD}\Omega_{k,m}\leq I_{th}\\ \text{- (C5: Subcarrier pairing constraint):}\\ \sum\limits_{k=1}^{N}t_{j,k}\leq 1,\quad \forall j;\quad \sum\limits_{j=1}^{N}t_{j,k}\leq 1,\quad \forall k\\ \text{- (C6: Relay Assignment constraint):}\\ \sum\limits_{m=1}^{M}\pi_{(j,k,m)}=1,\quad \forall j,k\end{array} \quad (4)$$

where N denotes the total number of subcarriers while I_{th} is the interference threshold prescribed by PU. P_S and P_{R_m} are the available power budget in the source and the m^{th} relay respectively. Ω_j and $\Omega_{k,m}$ are the $j^{th}(k^{th})$ subcarrier interference factor to the PU band from the source and the m^{th} relay respectively. Note that the interference factor in the first time slot depends only on the source subcarrier index regardless of the assigned relay like the downlink case in non-cooperative multicarrier based CR system [10]. In contrast, the interference factor in the second time slot depends on the destination subcarrier index as well as the assigned relay like the uplink case in non-cooperative multicarrier based CR system [11]. The subcarrier pairing constraint ensures that each subcarrier in the source is paired with only one subcarrier in the destination; where $t_{j,k}\in\{0,1\}$ is the subcarrier pairing indicator, i.e. $t_{j,k}=1$ if the j^{th} subcarrier in the source is paired with the k^{th} in the destination, and

zero otherwise. Additionally, $\pi_{(j,k,m)}$ is the relay assignment indicator which equals to one when the pair (j,k) is assigned to the m^{th} relay and zero otherwise. The source performs the resources allocation where all the instantaneous fading gains are assumed to be perfectly known. The assumption of perfect knowledge of all the channels is a typical assumption for researchers in this area [8], [12], [13]. The result of the ideal case can serve as an upper-bound for the work include another assumption or relaxation. The work in [14], [15] discusses the capacity loss due to the imperfect estimation and the resource allocation under the imperfect channel estimation respectively. Remark that the channel gains between the CR system nodes can be obtained practically by the classical channel estimation techniques while the channel gains between the CR system and PU can be obtained by estimating the received signal power from the primary terminal when it transmits, under the assumptions of pre-knowledge on the primary transmit power levels and the channel reciprocity [16].

To make the mathematical analysis more clear and without loss of generality, the noise variance is assumed to be constant for all the subcarriers and users, i.e. $\sigma^2_{j,m} = \sigma^2_{k,m} = \sigma^2$. From (3), the maximum capacity over the (j,k) subcarrier pair which allocated to the m^{th} relay can be achieved when $P^j_{SR_m} H^j_{SR_m} = P^k_{R_m D} H^k_{R_m D}$. Therefore, the power allocated at R_m can be expressed as function of the power at the source as $P^k_{R_m D} = \frac{P^j_{SR_m} H^j_{SR_m}}{H^k_{R_m D}}$. Hence, the optimization problem in (4) can be re-written as follows

$$\begin{aligned}
&\max_{\substack{\pi_{(j,k,m)}, t_{j,k} \\ P^j_{SR_m} \geq 0}} \quad \sum_{m=1}^{M}\sum_{j=1}^{N}\sum_{k=1}^{N} \left\{ \tfrac{1}{2}\pi_{(j,k,m)} t_{j,k} \right. \\
&\qquad\qquad \left. \cdot \log\left(1 + \tfrac{P^j_{SR_m} H^j_{SR_m}}{\sigma^2}\right)\right\} \\
&s.t. \qquad \text{(C1)}, \text{(C3)}, \text{(C5)}, \text{(C6)} \\
&\sum_{j=1}^{N}\sum_{k=1}^{N} \pi_{(j,k,m)} t_{j,k} \tfrac{P^j_{SR} H^j_{SR}}{H^k_{RD}} \leq P_{R_m}; \quad \forall m \\
&\sum_{m=1}^{M}\sum_{j=1}^{N}\sum_{k=1}^{N} \pi_{(j,k,m)} t_{j,k} \tfrac{P^j_{SR} H^j_{SR}}{H^k_{RD}} \Omega_{k,m} \leq I_{th}
\end{aligned} \tag{5}$$

Finding the optimization variables $P^j_{SR_m}$, $t_{j,k}$ and $\pi_{(j,k,m)}$ in (5) is a mixed binary integer programming problem. There are $(M^N \times N!)$ subcarrier matching and relay assignment possibilities and hence, the complexity is prohibitive for large number of subcarriers. The problem in (5) is satisfying the time sharing condition described in [6]. Therefore, the duality gap of the problem is negligible as the number of subcarrier is sufficiently large, i.e. $N > 8$, regardless of the convexity of the problem. The solution obtained by the dual method is asymptotically optimal [6].

The dual problem associated with the primal problem (5) can be written as

$$\min_{\beta \geq 0; \gamma_m \geq 0; \lambda \geq 0; \mu \geq 0} g(\beta, \gamma_m, \lambda, \mu) \tag{6}$$

where β and γ_m are the dual variables associated with the power constraint at the source and the different relays respectively. Moreover, the dual variables λ and μ are related to the interference constraints at the first and second time slots respectively. The dual function $g(\beta, \gamma_m, \lambda, \mu)$ is defined as follows

$$\begin{aligned}
&g(\beta, \gamma_m, \lambda, \mu) \triangleq \max_{P^j_{SR_m} > 0, t_{j,k}, \pi_{(j,k,m)}} \mathcal{L} \\
&s.t. \qquad \text{(C5)}, \text{(C6)}
\end{aligned} \tag{7}$$

where the Lagrangian $\mathcal{L}$ is given in (8) at the top of the next page.

The dual function in (7) can be rewritten as follows

$$\begin{aligned}
g(\beta, \gamma_m, \lambda, \mu) = &\max_{\substack{\pi_{(j,k,m)}, t_{j,k} \\ P^j_{SR_m} \geq 0}} \left[\sum_{m=1}^{M}\sum_{j=1}^{N}\sum_{k=1}^{N} \pi_{(j,k,m)} t_{j,k} \right. \\
&\left. \cdot D\left(P^j_{SR_m}, k\right) + \beta P_S + \sum_{m=1}^{M} \gamma_m P_{R_m} + I_{th}(\lambda + \mu) \right] \\
s.t. \qquad &\text{(C5)}, \text{(C6)}
\end{aligned} \tag{9}$$

where

$$\begin{aligned}
D\left(P^j_{SR_m}, k\right) = &\tfrac{1}{2}\log\left(1 + \tfrac{P^j_{SR_m} H^j_{SR_m}}{\sigma^2}\right) - \beta P^j_{SR_m} \\
&- \gamma_m \tfrac{P^j_{SR_m} H^j_{SR_m}}{H^k_{R_m D}} - \lambda P^j_{SR_m} \Omega_j - \mu \tfrac{P^j_{SR_m} H^j_{SR_m}}{H^k_{R_m D}} \Omega_{k,m}
\end{aligned} \tag{10}$$

Hence, to get the solution, we can commence by assuming any initial values for the different dual variables and also assuming that (j,k) is a valid subcarrier pair; that is already matched and allocated to the m^{th} relay. Hence, (9) is decomposed into $N^2 M$ independent power allocation sub-problems. The optimal power allocation can be determined by solving the following subproblem for every (j,k,m) pair

$$\begin{aligned}
&\max_{P^j_{SR_m}} \quad D\left(P^j_{SR_m}, k\right) \\
&s.t. \qquad P^j_{SR_m} \geq 0
\end{aligned} \tag{11}$$

Solving (11) for the optimal power, we can find

$$P^{*j}_{SR_m} = \left[\frac{1}{\beta + \gamma_m \frac{H^j_{SR_m}}{H^k_{R_m D}} + \lambda \Omega_j + \mu \frac{H^j_{SR_m}}{H^k_{R_m D}} \Omega_{k,m}} - \frac{\sigma^2}{H^j_{SR_m}} \right]^+ \tag{12}$$

where $[x]^+ = \max(0, x)$.

The optimal power allocation found by (12) can be substituted in (9) to eliminate the power variable. Accordingly, the following problem should be solved for every (j,k) pair

$$\begin{aligned}
\max_{\pi_{(j,k,m)}} &\left[\sum_{m=1}^{M}\sum_{j=1}^{N}\sum_{k=1}^{N} \pi_{(j,k,m)} t_{j,k}\, D\left(P^{*j}_{SR_m}, k\right) + \beta P_S \right. \\
&\left. + \sum_{m=1}^{M} \gamma_m P_{R_m} + I_{th}(\lambda + \mu) \right] \\
s.t. \qquad &\text{(C6)}
\end{aligned} \tag{13}$$

Therefore, the optimal relay assignment strategy is achieved by allocating the (j,k) pair to the relay which maximizes the function $D\left(P^{*j}_{SR_m}, k\right)$, i.e. $\pi^*_{(j,k,m)} = 1$ if $m = \arg\max_m D\left(P^{*j}_{SR_m}, k\right)$ and zero otherwise. By performing this allocation, the best relay is determined for every possible subcarrier pair .

$$\mathcal{L} = \sum_{m=1}^{M}\sum_{j=1}^{N}\sum_{k=1}^{N} \tfrac{1}{2}\pi_{(j,k,m)} t_{j,k} \log\left(1+\tfrac{P^j_{SR_m} H^j_{SR_m}}{\sigma^2}\right) + \beta\left(P_S - \sum_{m=1}^{M}\sum_{j=1}^{N} P^j_{SR_m}\right) + \lambda\left(I_{th} - \sum_{m=1}^{M}\sum_{j=1}^{N} P^j_{SR_m}\Omega_j\right) + \sum_{m=1}^{M}\gamma_m\left(P_{R_m} - \sum_{j=1}^{N}\sum_{k=1}^{N}\pi_{(j,k,m)} t_{j,k}\tfrac{P^j_{SR_m} H^j_{SR_m}}{H^k_{R_m D}}\right) + \mu\left(I_{th} - \sum_{m=1}^{M}\sum_{j=1}^{N}\sum_{k=1}^{N}\pi_{(j,k,m)} t_{j,k}\tfrac{P^j_{SR_m} H^j_{SR_m}}{H^k_{R_m D}}\Omega_{k,m}\right) \quad (8)$$

Once the power and relay allocation are determined for every subcarrier pair, the following dual function is obtained

$$\max_{t_{j,k}} \left[\sum_{j=1}^{N}\sum_{k=1}^{N} t_{j,k} D\left(P^{*j}_{SR}, k\right) + \beta P_S + \sum_{m=1}^{M}\gamma_m P_{R_m} + I_{th}\left(\lambda+\mu\right)\right] \quad s.t. \quad (C5) \quad (14)$$

The problem in (14) is a linear assignment problem that can be solved efficiently by using the Hungarian method with a complexity of $O\left(N^3\right)$ [17].

The subgradient method can be used to solve the dual problem with guaranteed convergence. After finding the optimal solution, i.e. P^{*j}_{SR}, $\pi^*_{(j,k,m)}$ and $t^*_{j,k}$, of the dual function at a given dual points β, γ_m, λ and μ, the dual variables at the $(i+1)^{th}$ iteration are updated as

$$\begin{aligned}
\beta^{(i+1)} &= \beta^{(i)} - \delta^{(i)}\left(P_S - \sum_{m=1}^{M}\sum_{j=1}^{N} P^{*j}_{SR_m}\right)\\
\gamma^{(i+1)}_m &= \gamma^{(i)}_m - \delta^{(i)}\left(P_{R_m} - \sum_{k=1}^{N}\sum_{j=1}^{N} t^*_{j,k}\tfrac{P^{*j}_{SR_m} H^j_{SR_m}}{H^k_{R_m D}}\right); \forall m\\
\lambda^{(i+1)} &= \lambda^{(i)} - \delta^{(i)}\left(I_{th} - \sum_{m=1}^{M}\sum_{j=1}^{N} P^{*j}_{S_m R}\Omega_j\right)\\
\mu^{(i+1)} &= \mu^{(i)} - \delta^{(i)} \cdot \left(I_{th} - \sum_{m=1}^{M}\sum_{k=1}^{N}\sum_{j=1}^{N}\pi_{(j,k,m)} t^*_{j,k}\tfrac{P^{*j}_{SR_m} H^j_{SR_m}}{H^k_{R_m D}}\Omega_{k,m}\right)
\end{aligned} \quad (15)$$

where $\delta^{(i)}$ is the step size that can be updated according to the nonsummable diminishing step size policy [18]. With the updated values of the dual variables, the optimal power allocation and subcarrier matching are evaluated again. The iterations are repeated until convergence.

IV. Sub-optimal Algorithm

In order to solve the problem efficiently, we propose in this section a sub-optimal algorithm by which the different system resources are allocated jointly with lower computational complexity than that of the optimal solution. The sub-optimal algorithm takes into consideration the interference introduced to the primary system, the different channel qualities, the available power budgets and the limitation introduced by using DF-protocol.

We commence the description of the sub-optimal scheme by defining the sets $\mathcal{A}$ and $\mathcal{B}$ to include all the non-assigned subcarriers in the source and the destination sides respectively. Moreover, define the set $\mathcal{M}$ to contain all the relays in the network. In the source side, assume that the available source power is distributed uniformly over the subcarriers, i.e. $P^{uni}_j = \frac{P_S}{N}$, and also assume that the interference introduced to the primary system by every subcarrier is equal; and hence from (1), the maximum allowable power that can be allocated to the j^{th} subcarrier is $P^{max}_j = \frac{I_{th}}{N\Omega_j}$. Therefore, the allocated power to the j^{th} subcarrier in the source side is $P^j_{SR_m} = \min(P^{uni}_j, P^{max}_j)$. The assigning procedures of a particular subcarrier $j \in \mathcal{A}$ are as follows

1) For every relay $m \in \mathcal{M}$, evaluate the rate $R^{Source}_{j,m} = \frac{1}{2}\log_2\left(1+\frac{P^j_{SR_m} H^j_{SR_m}}{\sigma^2}\right)$ achieved by allocating the subcarrier j to the m^{th} relay.
2) For every relay $m \in \mathcal{M}$ and subcarrier $k \in \mathcal{B}$, compute the required power to achieve a rate in the relay to destination link equal to that in the source to relay link, i.e. $P^{\text{rate}}_{j,k,m} = \frac{(2^{(2*R^{Source}_{j,m})}-1)\sigma^2}{H^k_{R_m D}}$.
3) For every relay $m \in \mathcal{M}$ and subcarrier $k \in \mathcal{B}$, evaluate $P^{uni}_{k,m} = \frac{P_{R_m}}{|\mathcal{B}|}$ and $P^{max}_{k,m} = \frac{I_{th}}{N\Omega_{k,m}}$ where $|\mathcal{B}|$ means the cardinality of the set $\mathcal{B}$. Afterwards, set $Power_{j,k,m} = \min(P^{\text{rate}}_{j,k,m}, P^{uni}_{k,m}, P^{max}_{k,m})$.
4) Find k^* and m^* satisfying $(k^*, m^*) = \arg\max_{k,m}(Power_{j,k,m} H^k_{R_m D})$. Set $t_{j,k^*} = 1$, $\pi_{m^*(j,k^*)} = 1$ and $P^k_{R_m D} = Power_{j,k^*,m^*}$ and update the $m^{*^{th}}$ relay power budget as $P_{R^*_m} = P_{R^*_m} - Power_{j,k^*,m^*}$.
5) Remove the subcarriers j and k^* from the sets $\mathcal{A}$ and $\mathcal{B}$ respectively and repeat the procedures until the set $\mathcal{A}$ is empty.

The first step in the proposed algorithm determines the achieved capacity by allocating a given subcarrier j in the source side to a specific relay. From (3), the rate achieved on the relay to destination link should be equal to that in the source to relay link in order to maximize the capacity. Therefore, the amount of power required to achieve this equality is evaluated in the second step. The limitation of the power and interference constraints are considered by the third step. The subcarrier pairing and relay selection indicators as well as the remaining relays power are updated in the last step.

For the optimal solution derived in the previous section, $(M+3)$ dual variables are updated in every iteration. Using these values, MN^2 function evaluations are performed to find the power allocation. Afterwards, M function evaluations are performed for every possible subcarrier pair where there are N^2 different subcarrier pairs. By including the computational complexity of the Hungarian method, the optimal solution derived in the previous section has a complexity of $\mathcal{O}\left(T(MN^2)+N^3\right)$ where T is the number of iterations required to converge which is usually high [6]. In the proposed scheme, every subcarrier in the source side requires no more than $(M+MN)$ function evaluations to be paired and assigned to the relay. Therefore, the complexity of the proposed algorithm is $\mathcal{O}(MN^2)$.

V. Simulation Results and Conclusions

The simulations are performed under the scenario given in Fig.1. An OFDM system of $N = 64$ subcarriers is assumed with $M = 5$ relays. The values of T_s, Δf, and σ^2 are assumed to be 4μ seconds, 0.3125 MHz and 10^{-6} respectively. The channel gains are outcomes of independent Rayleigh distributed random variables with mean equal to 1. All the results have been averaged over 1000 iterations. In the simulations, *Optimal* and *Sub-optimal* algorithms apply the dual decomposition technique presented in Sec. III and the proposed method presented in Sec. IV respectively. Additionally, *SNR* algorithm refers to the method by which the subcarriers and users are selected according to the signal to noise ratio values; while in *Random*, the subcarriers are matched and assigned randomly. For both *SNR* and *Random*, the powers are evaluated by solving (5) with the known $t_{j,k}$ and $\pi_{(j,k,m)}$.

Fig. 2 depicts the achieved capacity of the optimal and sub-optimal schemes vs. the interference constraint. The solid lines plots the case when $P_S = P_{R_m} = 0$ dBm while the dashed ones when $P_S = P_{R_m} = 20$ dBm. The achieved capacity is compared with that when only one of the interference or power constraint is applied. The interference (power) only performance forms an upper bound for that with both constraints. To that end, the performance of the optimal solution under both constraints has three different regions. Considering the case of $P_S = P_{R_m} = 0$ dBm, the three region could be explained as follows: **1)** if $I_{th} \leq -35$ dBm, the performance is equal to that of the interference only case. The limited effect of the power constraints comes from the small value of the allowed interference since only a small quantity of the available power can induce the maximum allowed interference. **2)** if $I_{th} \geq -20$ dBm, the performance is equal to that of the power only case. The system in this region performs like a non-cognitive one since the available power budgets cannot induce the maximum allowed interference threshold. **3)** if $-35 < I_{th} \leq -20$ dBm, in this region both power and interference constraints are affecting the optimization problem. Optimal solution performs close to the upper bound formed by the interference and power only curves. The same observations can be applied on the case of $P_S = P_{R_m} = 20$ dBm but with different ranges of the regions.

To more clarify the different regions, Fig. 3 plots the *optimal* achieved capacity for different interference and power constraints. By fixing one of the constraints, one can see that the achieved capacity increases with the other up to certain point. After this point, the change of the constraint value does not affect the achieved capacity. This is can be justified -as described above- by working in the non-cognitive regions or in the regions in which the interference limit can be reached by only a small part of the available power budgets.

Fig. 4 shows the achieved capacity of the different algorithms vs. the interference threshold. One can notes that the CR system capacity increases with the interference threshold as the CR system become able to use more power on the different subcarriers. Additionally, the throughput increases -as expected- with the increase of the available power budgets. However, the increment in the throughput by changing the

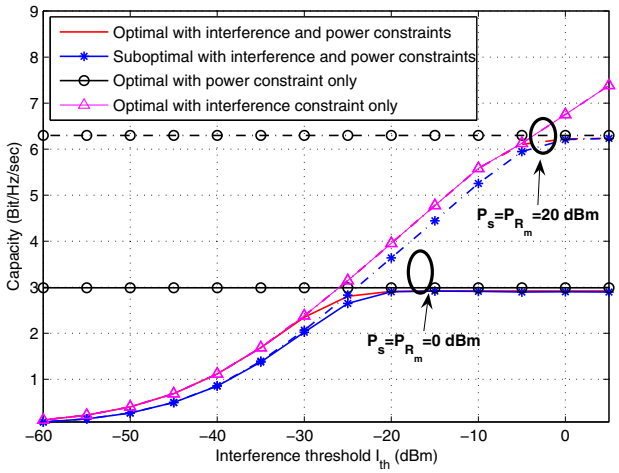

Fig. 2. Achieved capacity vs allowed interference threshold. The solid lines when $P_S = P_R = 0$ dBm while the dashed ones when $P_S = P_R = 20$ dBm.

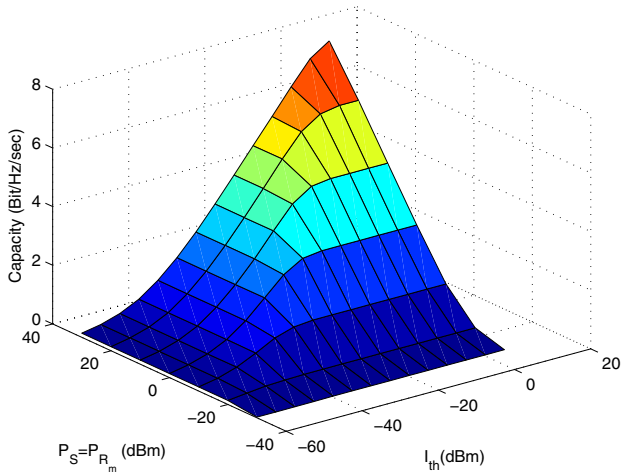

Fig. 3. Achieved capacity vs allowed interference thresholds and power budget constraints.

available power from 0 dBm to 20 dBm is very small in the low interference region since both systems use approximately the same amount of power to induce the maximum allowed interference to the PU. In the low interference thresholds region, the SNR-based matching criteria applied in the non-cognitive system has limited performance in comparison with *optimal* because it does not take the interference to the primary system into account. Furthermore, the gap between the *optimal* algorithm and the *SNR* algorithm is decreased with the interference threshold as the system behaves closer to the non-cognitive one. The same interpretation can be applied on Fig. 5 in which the achieved capacities are plotted vs. the available power budgets in the source and the relays. In this figure, the non-cognitive behavior lies on the low power region where the available power budgets are not able to induce the pre-specified interference threshold.

Its worth mentioning that the performance loss of the *sub-optimal* algorithm relative to the *optimal* one is caused by different factors. In the *sub-optimal* algorithm, the available power budgets in the source and the destination are dis-

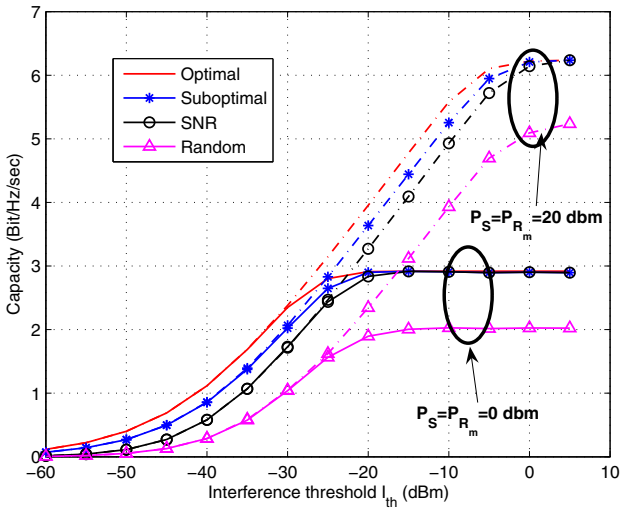

Fig. 4. Achieved capacity vs allowed interference threshold. The solid lines when $P_S = P_R = 0$ dBm while the dashed ones when $P_S = P_R = 20$ dBm.

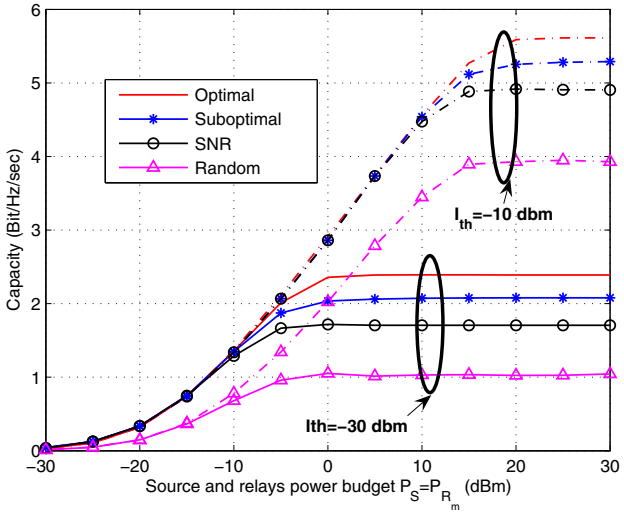

Fig. 5. Achieved capacity vs available power budget with $P_S = P_R$. The solid lines when $I_{th} = -30$ dBm while the dashed ones when $I_{th} = -10$ dBm.

tributed equally between the subcarrier which is not always optimal depending on whether the system is operating on high or low SNR. Moreover, the step ladder power allocation in which every subcarrier is assumed to induce the same amount of interference to the PU is shown to create some performance degradation as presented in [8]. Additionally, the *sub-optimal* algorithm performs the subcarrier pairing and the power allocation in sequential way starting by the first subcarrier up to the last one. When a given subcarrier in the source side is paired with another one in destination side, the latter cannot be used anymore for the next steps. Hence, the order of the subcarrier assignment process may slightly degrades the performance of the *sub-optimal* scheme. Despite of the performance loss generated by these factors, the *sub-optimal* algorithm with low computational complexity has a near optimal performance and outperforms *SNR* and *random* algorithms.

Summarizing, we have considered the resource allocation problem in multiple relay DF-OFDM based CR system. To maximize the achieved capacity while maintain the interference introduced to the primary system below a pre-specified threshold, the subcarrier pairing, relay assignment and power allocation are performed jointly using the dual decomposition technique. Due to the high computational complexity of the optimal scheme, a sub-optimal algorithm is presented. The sub-optimal algorithm allocates the different resources jointly and achieve a near optimal performance with much less complexity. Moreover, the proposed scheme outperforms the SNR and Random based methods. We are currently working on extension of the proposed scheme by considering more interference constraints as well as channel estimation errors in the cognitive and primary links.

REFERENCES

[1] J. Jia, J. Zhang, and Q. Zhang, "Cooperative relay for cognitive radio networks," in *Proc. 2009 IEEE INFOCOM*, pp. 2304–2312.

[2] W. Dang, M. Tao, H. Mu, and J. Huang, "Subcarrier-pair based resource allocation for cooperative multi-relay OFDM systems," *IEEE Trans. Wireless Commun.*, vol. 9, no. 5, pp. 1640–1649, May 2010.

[3] C.-N. Hsu, H.-J. Su, and P.-H. Lin, "Joint subcarrier pairing and power allocation for OFDM transmission with decode-and-forward relaying," *IEEE Trans. Signal Process.*, vol. 59, no. 1, pp. 399–414, Jan. 2011.

[4] L. Li, X. Zhou, H. Xu, G. Li, D. Wang, and A. Soong, "Simplified relay selection and power allocation in cooperative cognitive radio systems," *IEEE Trans. Wireless Commun.*, vol. 10, no. 1, pp. 33–36, Jan. 2011.

[5] G. Zhao, C. Yang, G. Li, D. Li, and A. Soong, "Power and channel allocation for cooperative relay in cognitive radio networks," *IEEE J. Sel. Topics Signal Process.*, vol. 5, no. 1, pp. 151–159, Feb. 2011.

[6] W. Yu and R. Lui, "Dual methods for nonconvex spectrum optimization of multicarrier systems," *IEEE Trans. Commun.*, vol. 54, no. 7, pp. 1310–1322, July 2006.

[7] T. Weiss and J. Hillenbrand, "Mutual interference in OFDM-based spectrum pooling systems," in *2004 IEEE Vehicular Technology Conference – Spring*, vol. 4.

[8] G. Bansal, M. J. Hossain, and V. K. Bhargava, "Optimal and suboptimal power allocation schemes for OFDM-based cognitive radio systems," *IEEE Trans. Wireless Commun.*, vol. 7, no. 11, pp. 4710–4718, Nov. 2008.

[9] T. M. Cover and J. A. Thomas, *Elements of Information Theory*, 2nd edition. John Wiley and Sons, 2006.

[10] M. Shaat and F. Bader, "Computationally efficient power allocation algorithm in multicarrier-based cognitive radio networks: OFDM and FBMC systems," *EURASIP J. Advances in Signal Process.*, vol. 2010, article ID 528378, 13 pages.

[11] ——, "Fair and efficient resource allocation algorithm for uplink multicarrier based cognitive networks," in *Proc. 2010 IEEE International Symposium on Personal Indoor and Mobile Radio Communications*, pp. 1212–1217.

[12] C.-X. Wang, H.-H. Chen, X. Hong, and M. Guizani, "Cognitive radio network management," *IEEE Veh. Technol. Mag.*, vol. 3, no. 1, pp. 28–35, Mar. 2008.

[13] P. Gong, P. Xue, D. Park, and D. K. Kim, "Optimum power allocation in a nonorthogonal amplify-and-forward relay-assisted network," *IEEE Trans. Veh. Technol.*, vol. 60, no. 3, pp. 890–900, Mar. 2011.

[14] H. Suraweera, P. Smith, M. Shafi, and M. Faulkner, "Channel capacity limits of cognitive radio with imperfect channel knowledge," in *Proc. 2009 IEEE Global Telecommunications Conference*, pp. 1–6.

[15] C. M. Tao Qin, C. Leung, and Z. Shen, "Resource allocation in a cognitive radio system with imperfect channel state estimation," *J. Electrical and Computer Engineering*, vol. 2010, article ID 419430, 5 pages.

[16] R. Zhang, S. Cui, and Y.-C. Liang, "On ergodic sum capacity of fading cognitive multiple-access and broadcast channels," *IEEE Trans. Inf. Theory*, vol. 55, no. 11, pp. 5161–5178, Nov. 2009.

[17] H. W. Kuhn, "The Hungarian method for the assignment problem," in *50 Years of Integer Programming 1958-2008*. Springer Berlin Heidelberg, 2010, pp. 29–47.

[18] S. Boyd and A. Mutapcic, "Subgradient methods," notes for EE364, Standford University, Winter. 2006-07.

Comparison of OFDM and FBMC Performance in Multi-Relay Cognitive Radio Network

Musbah Shaat and Faouzi Bader
Centre Tecnològic de Telecomunicacions de Catalunya (CTTC), Castelldefels-Barcelona, Spain
Email:{musbah.shaat,faouzi.bader}@cttc.es

***Abstract*— A multicarrier based cognitive radio (CR) network is considered in this paper. The goal is to maximize the total sum rate of the CR system while ensuring that no excessive interference is induced to the primary system.The optimal scheme adopts the dual decomposition technique and in order to reduce the computational complexity of the optimal scheme, a greedy suboptimal algorithm is proposed. Selected numerical results is discussed to reveal the near-optimal performance of the suboptimal scheme and the superiority of the proposed algorithm over the random and the signal-to-noise ratio (SNR) based schemes. This paper highlights the advantages of using filter bank multicarrier (FBMC) instead of OFDM in the physical layer of the future CR systems.**

I. Introduction

The dynamic spectrum access (DSA) scheme has been proposed to replace the current inadequate spectrum licensing scheme and make a balance between the spectrum scarcity and the spectrum underutilization. Cognitive radio (CR) has been received a significant attention as the enabling technology for DSA by provide the wireless system with the required capability to adapt its parameters intelligently according to the surrounding environment and users requirements to achieve a highly reliable communication.

Orthogonal frequency division multiplexing (OFDM) is the most common multicarrier technique that is considered by several communication standards including IEEE 802.22 TV based cognitive system that develops an unlicensed wireless regional area network (WRAN) to exploit the unused TV bands. In spite of this, there are several factors that limit the achieved capacity in OFDM systems. The large frequency domain sidelobes of the OFDM signal produces high mutual interference to the adjacent licensed system due to the lack of the synchronization. Moreover, OFDM utilize the transmission of the cyclic prefix (CP) to compact the effect of the multiple path propagation which reduces the overall spectral efficiency. To overcome the limitations of the OFDM, the light is shed recently on the filter bank multicarrier (FBMC) system which was developed before the OFDM. FBMC systems have received limited attention in comparison with OFDM due to the simple concept and low complexity of OFDM. In FBMC systems, the sidelobes of each subcarrier frequency response is reduced by using signals with high spectral containment. Additionally, FBMC doesn't require any CP extension and offers more robustness to the time and frequency offset that OFDM.

The operation of the CR networks should not negatively affect the performance of the primary system. Therefore, careful design of the resource allocation algorithm is required to deal with the interference control and to guarantee efficient share of the radio spectrum. Jia et al. proposed in [1] a centralized heuristic algorithm to select the most profitable pair of nodes and to allocate the different channels based on the availability of the spectrum. The interference to the primary system was not considered. In [2], the protection of the primary system from the secondary systems transmission is achieved by limiting the maximum power that can be transmitted by every relay in the CR network. In [3], the authors proposed an algorithm to select the best transmit way between the network nodes based on the spectrum availability and maximum power levels that limit the transmission. Three different transmission forms between the network nodes are considered : direct, dual or diversity transmission.

This paper tackles the resource allocation problem in OFDM and FBMC based CR systems with multiple relays. The target is to jointly optimize the different radio resources in order to achieve the maximum CR sum rate under the per-relay power and per-time slot interference constraints and compare the performance of using OFDM and FBMC physical layers. The optimal solution is derived by using the dual decomposition technique with the limit of having sufficient number of subcarriers. To decrease the computational complexity of the optimal scheme, an efficient suboptimal algorithm is proposed. The suboptimal algorithm has a near-optimal performance with a significant reduction in the computational complexity.

II. System Model

In this paper, an multicarrier based cooperative CR system is considered. The source can transmit to the destination through the direct link. If the direct link is blocked due to the existence of an obstacle in some frequencies or if the direct channel has a poor quality, the source will communicate with the destination through M relays. The CR frequency spectrum is accommodates N subcarriers each of them has a Δf bandwidth. The CR can use the vacant primary bands under the condition of not inducing interference to the primary bands higher than the maximum interference limit, I_{th}. Each of the source subcarriers can either be used for relayed or direct transmission. The relays are assumed to operate in half-duplex mode with decode-and-forward (DF)-protocol. The j^{th} subcarrier in the source which is selected for relayed transmission should be paired with only one subcarrier k in the destination which may not be the same as j to form the (j,k) pair that should be assigned to only one relay m. The

978-1-4673-0762-8/12/$31.00 ©2012 IEEE

maximum total transmission powers that can be used in the source and the different relays are P_S and P_{R_m} respectively.

The mutual interference introduced by the i^{th} subcarrier to the PU band, $I_i^l(d_i, P_i)$, can be expressed as [4]

$$I_i(d_i, P_i) = \int_{di-B/2}^{di+B/2} |g_i|^2 P_i \Phi_i(f)\, df \triangleq P_i\, \Omega_i \tag{1}$$

where Φ_i is the power spectrum density (PSD) of the i^{th} subcarrier and P_i is the total transmit power emitted by the i^{th} subcarrier. Additionally, d_i is the spectral distance between the i^{th} subcarrier and the PU band. The channel gain between the i^{th} subcarrier and the PU is denoted by g_i. Ω_i refers to the interference factor of the i^{th} subcarrier to the PU band.

The expression of Φ_i depends on the used transmission technique. In OFDM system with rectangular pulse of length $T_s = N+C$ where N is the number of subcarriers (IDFT size) and C is the length of the CP, Φ_i can be written as follows

$$\Phi_i = T_s + 2\sum_{r=1}^{T_s-1} (T_s - r)\cos(2\pi f r) \tag{2}$$

In FBMC systems, if the prototype filter with coefficients $h[n]$ with $n = 0, \cdots, W-1$ is used, where $W = KN$ and K is the length of each polyphase components (overlapping factor) and under the assumption of that the prototype coefficients have even symmetry around the $\left(\frac{KN}{2}\right)^{th}$ coefficient, and the first coefficient is zero, the FBMC PSD can be expressed as $\Phi_i(f) = |H_i(f)|^2$ where $|H_i(f)|$ is the frequency response of the prototype filter and can be written as $|H_i(f)| = h[W/2] + 2\sum_{r=1}^{\frac{W}{2}-1} h[(W/2) - r]\cos(2\pi f r)$ [5].

III. Problem Formulation and Optimal Solution

The relayed transmission rate of the j^{th} subcarrier in the source coupled with the k^{th} subcarrier in the destination and assigned to the m^{th} relay, $R_{Relayed}(j,k,m)$, can be evaluated as follows

$$R_{Relayed}(j,k,m) = \frac{1}{2}\min\left\{\begin{array}{c} \log_2\left(1 + \frac{P_S^j \overline{H_{SR_m}^j}}{\sigma_{j,m}^2}\right) \\ \log_2\left(1 + \frac{P_{R_m D}^k \overline{H_{R_m D}^k}}{\sigma_{k,m}^2}\right) \end{array}\right. \tag{3}$$

where P_S^j is the power transmitted over the j^{th} subcarrier while in $P_{R_m D}^k$ is the power transmitted over the k^{th} in the R_m to Destination link. R_m means the m^{th} relay. Moreover, $\overline{H_{SR_m}^j}(\overline{H_{R_m D}^k})$ is the square of the $j^{th}(k^{th})$ subcarrier fading gain over Source to $R_m(R_m$ to destination) link. $\sigma_{j,m(k,m)}^2 = \sigma_{AWGN_{j,m(k,m)}}^2 + J_{j(k)}$, where $\sigma_{AWGN_{j,m(k,m)}}^2$ is the variance of the additive white Gaussian noise (AWGN) on the source to $R_m(R_m$ to destination) link, and $J_{j(k)}$ is the interference introduced by the PU signal into the $j^{th}(k^{th})$ subcarrier which can be modeled as AWGN as described in [6]. If the source transmits to the destination over the direct link, the transmission rate of the j^{th} subcarrier is given by

$$R_{Direct}(j) = \frac{1}{2}\log_2\left(1 + \frac{P_S^j \overline{H_{SD}^j}}{\sigma_{j,D}^2}\right) \tag{4}$$

where $\overline{H_{SD}^j}$ is the square of the j^{th} subcarrier fading gain over source to destination link. $\sigma_{j,D}^2$ is the the direct link noise variance. The factor $\frac{1}{2}$ in (3) and (4) accounts for the two time slots in each transmission frame. To make the mathematical analysis more clear and without loss of generality, the following variables substitutions are considered: $H_{SR_m}^j = \frac{\overline{H_{SR_m}^j}}{\sigma_{j,m}^2}$, $H_{R_m D}^k = \frac{\overline{H_{R_m D}^k}}{\sigma_{k,m}^2}$, and $H_{SD}^j = \frac{\overline{H_{SD}^j}}{\sigma_{j,D}^2}$. Our objective is to maximize the CR system throughput by determining the subcarriers best transmission way (direct/relayed) and optimize the subcarrier pairing and relays assignment for the subcarriers used for relayed transmission. The instantaneous interference introduced to the primary system by the CR network nodes should be below the maximum limit. Therefore, the optimization problem can be formulated as follows

$$\begin{aligned} &\max_{P_S^j \geq 0, P_{R_m D}^k \geq 0, \alpha_j, \pi_{j,k}^m, t_{j,k}} \quad \mathcal{R} \\ &s.t. \\ &\text{- (C1: Source power constraint):} \\ &\sum_{j=1}^{N} P_S^j \leq P_S \\ &\text{- (C2: Relays individual power constraints):} \\ &\sum_{k=1}^{N} P_{R_m D}^k \leq P_{R_m}, \quad \forall m \\ &\text{- (C3: Interference at the first time slot):} \\ &\sum_{j=1}^{N} P_S^j \Omega_j \leq I_{th} \\ &\text{- (C4: Interference at the second time slot):} \\ &\sum_{m=1}^{M}\sum_{k=1}^{N} P_{R_m D}^k \Omega_{k,m} \leq I_{th} \\ &\text{- (C5: Relayed/Direct transmission constraint):} \\ &\alpha_j \in \{0,1\}, \quad \forall j \\ &\text{- (C6: Subcarrier pairing constraint):} \\ &\sum_{k=1}^{N} \alpha_j t_{j,k} \leq 1, \forall j; \quad \sum_{j=1}^{N} \alpha_j t_{j,k} \leq 1, \quad \forall k \\ &\text{- (C7: Relay Assignment constraint):} \\ &\sum_{m=1}^{M} \alpha_j \pi_{j,k}^m = 1, \quad \forall j,k \end{aligned} \tag{5}$$

with $\mathcal{R} \triangleq [\sum_{m=1}^{M}\sum_{j=1}^{N}\sum_{k=1}^{N} \frac{1}{2}\alpha_j \pi_{m(j,k)} t_{j,k} R_{Relayed}(j,k,m) + \sum_{j=1}^{N} \frac{1}{2}(1-\alpha_j) R_{Direct}(j)]$; where N denotes the total number of subcarriers while I_{th} is the interference threshold prescribed by PU. P_S and P_{R_m} are the available power budgets in the source and the m^{th} relay respectively. Ω_j and $\Omega_{k,m}$ are the $j^{th}(k^{th})$ subcarrier interference factor to the PU band from the source and the m^{th} relay respectively. $\alpha_j \in \{0,1\}$ is the subcarrier transmission mode indicator which has a value of one when the subcarrier is used for relayed transmission while equals zero if the subcarrier is used for the direct transmission. The subcarrier pairing constraint ensures that each relayed transmission subcarrier in the source is paired with only one subcarrier in the destination where $t_{j,k} \in \{0,1\}$ is the subcarrier pairing indicator, i.e. $t_{j,k} = 1$ if the j^{th} subcarrier in the source is paired with the k^{th} in the destination, and zero otherwise. Additionally, $\pi_{j,k}^m$ is the relay assignment indicator which has a binary value. $\pi_{j,k}^m = 1$ when the subcarriers pair (j,k) is assigned to relay m while $\pi_{j,k}^m = 0$ otherwise.

Assume that the subcarrier j is used for the relayed transmission, i.e. $\alpha_j = 1$, and paired with the k^{th} subcarrier in the destination side. From (3), the maximum capacity over the (j,k) subcarrier pair which is allocated to the m^{th} relay

can be achieved when $P_S^j H_{SR_m}^j = P_{R_m D}^k H_{R_m D}^k$. Therefore, the power allocated at R_m can be expressed as function of the power at the source as $P_{R_m D}^k = \frac{P_S^j H_{SR_m}^j}{H_{R_m D}^k}$. Hence, the optimization problem in (5) can be re-written as follows

$$\begin{aligned} & \max_{P_S^j \geq 0, \alpha_j, \pi_{j,k}^m, t_{j,k}} \quad \widehat{\mathcal{R}} \\ & s.t. \quad \text{(C1), (C3), (C5), (C6), (C7)} \\ & \text{- } \hat{\text{C}}2: \quad \sum_{j=1}^{N} \sum_{k=1}^{N} \alpha_j \pi_{j,k}^m t_{j,k} \frac{P_S^j H_{SR}^j}{H_{RD}^k} \leq P_{R_m}; \quad \forall m \\ & \text{- } \hat{\text{C}}4: \quad \sum_{m=1}^{M} \sum_{j=1}^{N} \sum_{k=1}^{N} \alpha_j \pi_{j,k}^m t_{j,k} \frac{P_S^j H_{SR}^j}{H_{RD}^k} \Omega_{k,m} \leq I_{th} \end{aligned} \tag{6}$$

where $\widehat{\mathcal{R}} \triangleq \left[\sum_{m=1}^{M} \sum_{j=1}^{N} \sum_{k=1}^{N} \frac{1}{2} \alpha_j \pi_{j,k}^m t_{j,k} \log_2 \left(1 + P_S^j H_{SR_m}^j\right) + \sum_{j=1}^{N} \frac{1}{2} \left(1 - \alpha_j\right) \log_2 \left(1 + P_S^j H_{SD}^j\right) \right]$. Finding the optimization variables P_S^j, α_j, $t_{j,k}$ and $\pi_{j,k}^m$ in (6) is a mixed binary integer programming problem where the complexity is prohibitive for large number of subcarriers. The time sharing condition is satisfied by (6) in the limit of having large number of subcarriers, i.e. $N > 8$, as described in [7]. Accordingly, although that the problem in (6) is not convex, zero-duality gap solution can be obtained by applying the dual decomposition technique.

The dual problem associated with the primal problem (6) can be written as

$$\min_{\beta \geq 0; \gamma_m \geq 0; \lambda \geq 0; \mu \geq 0} g\left(\beta, \gamma_m, \lambda, \mu\right) \tag{7}$$

where β and γ_m are the dual variables associated with the power constraints at the source and at the different relays respectively. Moreover, the dual variables λ and μ are related to the interference constraints at the first and second time slots respectively. The dual function $g\left(\beta, \gamma_m, \lambda, \mu\right)$ is defined as follows

$$\begin{aligned} g\left(\beta, \gamma_m, \lambda, \mu\right) \triangleq & \max_{P_S^j > 0, \alpha_j, t_{j,k}, \pi_{j,k}^m} \quad \mathcal{L} \\ & s.t. \quad \text{(C5), (C6), (C7)} \end{aligned} \tag{8}$$

where the Lagrangian $\mathcal{L}$ is given in (9) at the top of the next page.The dual function in (8) can be rewritten as follows

$$\begin{aligned} g\left(\beta, \gamma_m, \lambda, \mu\right) = \max [& \sum_{m=1}^{M} \sum_{j=1}^{N} \sum_{k=1}^{N} \alpha_j \pi_{j,k}^m t_{j,k} \mathcal{D}_{relay}(P_S^j, k, m) \\ & + \sum_{j=1}^{N} \left(1 - \alpha_j\right) \mathcal{D}_{direct}(j) + \beta P_S + \sum_{m=1}^{M} \gamma_m P_{R_m} + I_{th} \left(\lambda + \mu\right)] \\ s.t. \quad & \text{(C5), (C6), (C7)} \end{aligned} \tag{10}$$

where $\mathcal{D}_{relay}(P_S^j, k, m) = \frac{1}{2} \log_2 \left(1 + P_S^j H_{SR_m}^j\right) - \beta P_S^j - \lambda P_S^j \Omega_j - \gamma_m \frac{P_S^j H_{SR_m}^j}{H_{R_m D}^k} - \mu \frac{P_S^j H_{SR_m}^j}{H_{R_m D}^k} \Omega_{k,m}$ and $\mathcal{D}_{direct}(j) = \frac{1}{2} \log_2 \left(1 + P_S^j H_{SD}^j\right) - \beta P_S^j - \lambda P_S^j \Omega_j$.

Therefore, We can commence by initializing the different dual variables and assume that the value of the variable α_j is already known. Accordingly, (10) is decomposed into $N(NM+1)$ independent power allocation subproblems. Depending on the value of the variable α_j, we have the following two cases:

A. Case 1: If $\alpha_j = 1$, (j,k) will be assumed as a valid subcarrier pair and is already matched and allocated to the m^{th} relay. Hence, by solving the following subproblem for every $m\,(j,k)$ pair, the optimal power allocation can be evaluated

$$\max_{P_S^j} \quad \mathcal{D}_{relay}(P_S^j, k, m) \qquad s.t. \qquad P_S^j \geq 0 \tag{11}$$

Solving (11) for the optimal power we can get

$$P_S^{*j} = \left[\frac{1}{\beta + \gamma_m \frac{H_{SR_m}^j}{H_{R_m D}^k} + \lambda \Omega_j + \mu \frac{H_{SR_m}^j}{H_{R_m D}^k} \Omega_{k,m}} - \frac{1}{H_{SR_m}^j} \right]^+ \tag{12}$$

where $[x]^+ = \max(0, x)$. As the value of the variable α_j is assumed to be one in this case, the optimal power allocation found by (12) can be substituted in the first part of (10) to eliminate the power variable and hence the following problem should be solved for every (j,k) pair

$$\begin{aligned} g\left(\beta, \gamma_m, \lambda, \mu\right) = \max_{\pi_{j,k}^m} [& \sum_{m=1}^{M} \sum_{j=1}^{N} \sum_{k=1}^{N} \pi_{j,k}^m t_{j,k} \mathcal{D}_{relay}(P_S^{*j}, k, m) \\ & + \beta P_S + \sum_{m=1}^{M} \gamma_m P_{R_m} + I_{th} \left(\lambda + \mu\right)] \quad s.t. \quad \text{(C7)} \end{aligned} \tag{13}$$

Therefore, the optimal relay assignment strategy is achieved by allocating the (j,k) pair to the relay which maximizes the function $\mathcal{D}_{relay}(P_S^{*j}, k, m)$, i.e. $\pi_{j,k}^{m^*} = 1$ if $m = \arg\max_m \mathcal{D}_{relay}(P_S^{*j}, k, m)$ and zero otherwise. By performing this allocation, the best relay is assigned for every possible subcarrier pair .

B. Case 2: If $\alpha_j = 0$, the following subproblem should be solved for every subcarrier j

$$\max_{P_S^j} \quad \mathcal{D}_{direct}(j) \qquad s.t. \qquad P_S^j \geq 0 \tag{14}$$

Solving (14) for the optimal power we can find

$$P_S^{*j} = \left[\frac{1}{\beta + \lambda \Omega_j} - \frac{\sigma^2}{H_{SD}^j} \right]^+ \tag{15}$$

Using the previous analysis, and for given dual variables values, we can find the optimal power levels and relay assignment of the pair (j,k) when the subcarrier is used for relayed transmission, and we can evaluate the optimal power allocation when it is used for direct transmission. The last remaining step is to determine the optimal subcarrier pairs and to decide whether the j^{th} subcarrier should be used for direct transmission or for relayed one. Therefore, the following problem should be solved

$$\begin{aligned} g\left(\beta, \gamma_m, \lambda, \mu\right) = \max_{\alpha_j, t_{j,k}} & \left[\sum_{j=1}^{N} \sum_{k=1}^{N} \alpha_j t_{j,k} \mathcal{D}_{relay}\left(P_S^{*j}, k, m^*\right) + \right. \\ & \left. \sum_{j=1}^{N} \left(1 - \alpha_j\right) \mathcal{D}_{direct}\left(j\right) + \beta P_S + \sum_{m=1}^{M} \gamma_m P_{R_m} + I_{th} \left(\lambda + \mu\right) \right] \\ s.t. \quad & \text{(C5), (C6)} \end{aligned} \tag{16}$$

where m^* in $\mathcal{D}_{relay}\left(P_S^{*j}, k, m^*\right)$ denotes the best relay selected for the (j,k) pair as described previously. The maximum value between $\mathcal{D}_{direct}\left(j\right)$ and $\mathcal{D}_{relay}\left(P_S^{*j}, k, m^*\right)$ decides whether the subcarrier j should be used for direct

$$\mathcal{L} = \sum_{m=1}^{M}\sum_{j=1}^{N}\sum_{k=1}^{N} \tfrac{1}{2}\alpha_j \pi_{m(j,k)} t_{j,k} \log_2\left(1 + P_S^j H_{SR_m}^j\right) + \sum_{j=1}^{N}(1-\alpha_j)\log_2\left(1 + P_S^j H_{SD}^j\right) + \beta(P_S - \sum_{m=1}^{M}\sum_{j=1}^{N} P_S^j) + \lambda(I_{th} - \sum_{m=1}^{M}\sum_{j=1}^{N} P_S^j \Omega_j) + \sum_{m=1}^{M}\gamma_m(P_{R_m} - \sum_{j=1}^{N}\sum_{k=1}^{N}\alpha_j \pi_{m,(j,k)} t_{j,k} \frac{P_S^j H_{SR_m}^j}{H_{R_m D}^k}) + \mu(I_{th} - \sum_{m=1}^{M}\sum_{j=1}^{N}\sum_{k=1}^{N}\alpha_j \pi_{m,(j,k)} t_{j,k} \frac{P_S^j H_{SR_m}^j}{H_{R_m D}^k}\Omega_{k,m}) \tag{9}$$

transmission or for relayed transmission based on to the assignment (j, k, m^*). Therefore, (16) can rewritten as follows

$$g(\beta, \gamma_m, \lambda, \mu) \triangleq \max_{t_{j,k}} \left[\sum_{j=1}^{N}\sum_{k=1}^{N} t_{j,k}\mathcal{D}_{max}(P_S^{*j}, k, m^*) + \beta P_S + \sum_{m=1}^{M}\gamma_m P_{R_m} + I_{th}(\lambda + \mu)\right] \quad s.t. \quad \text{(C6)} \tag{17}$$

where

$$\mathcal{D}_{max}(P_S^{*j}, k, m^*) = \max\{\mathcal{D}_{relay}\left(P_S^j, k, m^*\right), \mathcal{D}_{direct}(j)\} \tag{18}$$

The problem in (17) is a linear assignment problem that can be solved efficiently by the Hungarian method with a complexity of $O\left(N^3\right)$ [8]. Note that the set of subcarriers used for direct transmission can be determined from the optimal solution $t_{j,k}^*$ when the profit value associated with the optimal pair (j, k) with $t_{j,k}^* = 1$ is $\mathcal{D}_{max}(P_S^{*j}, k, m^*) = \mathcal{D}_{direct}(j)$.

With a guaranteed convergence, the subgradient method can be used to solve the dual problem [9].

IV. Suboptimal Algorithm

Using the dual decomposition technique, $(M + 3)$ dual variables are updated in every iteration. Using these values, $N(M + 1)$ function evaluations are performed to find the power allocation. Then, M function evaluations are performed for every possible subcarrier pair considering that there are $N!$ subcarrier matching possibilities. By including the computational complexity of the Hungarian method and the N functions evaluations required to classify the subcarrier into the direct or relayed transmission, the optimal solution derived in the previous section has a complexity of $\mathcal{O}\left(T(MN) + M(N!) + 2N + N^3\right)$ where T is the number of iterations required to converge which is usually high [7]. To reduce the computational complexity, a suboptimal algorithm is proposed in this section to jointly optimize the different system resources.

The suboptimal algorithm commences by defining the sets $\mathcal{A}$ and $\mathcal{B}$; where $\mathcal{A}$ contains all the un-assigned subcarriers in the source side while $\mathcal{B}$ contains the un-assigned ones in the destination side. Additionally, define $\mathcal{M}$ to be the set that includes the different relays in the network. The source power P_S is assumed to be uniformly distributed among the subcarriers in the source side, i.e. $P_j^{uni} = \frac{P_S}{N}$. Additionally, every subcarrier in the source side is assumed to induce the same amount of interference to the primary system, i.e. the interference is uniformly distributed among the subcarriers and by using (1), the maximum power that can be used by the j^{th} subcarrier is $P_j^{max} = \frac{I_{th}}{N\Omega_j}$. From these assumption, the power for every subcarrier in the source side is evaluated by $P_S^j = \min(P_j^{uni}, P_j^{max})$. Based on this, the assigning steps of a particular subcarrier $j \in \mathcal{A}$ are detailed in Algorithm 1.

Algorithm 1 Sub-optimal Algorithm

1) For every relay $m \in \mathcal{M}$, evaluate the rate $R_{j,m}^{Source} = \frac{1}{2}\log_2\left(1 + P_S^j H_{SR_m}^j\right)$ achieved by allocating the subcarrier j to the m^{th} relay.
2) For every relay $m \in \mathcal{M}$ and subcarrier $k \in \mathcal{B}$, compute the required power to achieve a rate in the relay to destination link equal to that in the source to relay link, i.e. $P_{j,k,m}^{\text{rate}} = \frac{\left(2^{\left(2R_{j,m}^{Source}\right)} - 1\right)}{H_{R_m D}^k}$. Then, evaluate $P_{k,m}^{uni} = \frac{P_{R_m}}{|\mathcal{B}|}$ and $P_{k,m}^{max} = \frac{I_{th}}{N\Omega_{k,m}}$ where $|\mathcal{B}|$ means the cardinality of the set $\mathcal{B}$. Afterwards, set $Power_{j,k,m} = \min\left(P_{j,k,m}^{\text{rate}}, P_{k,m}^{uni}, P_{k,m}^{max}\right)$.
3) Find k^* and m^* satisfying $(k^*, m^*) = \arg\max_{k,m}\left(Power_{j,k,m} H_{R_m D}^k\right)$. If $P_S^j H_{SD}^j > Power_{j,k^*,m^*} H_{R_{m^*} D}^k$, the direct link is selected. Otherwise, set $t_{j,k^*} = 1$, $\pi_{(j,k^*)}^{m^*}$ and $P_{R_m D}^k = Power_{j,k^*,m^*}$ and update the $m^{*^{th}}$ relay power budget as $P_{R_m^*} = P_{R_m^*} - Power_{j,k^*,m^*}$.
4) Remove the subcarriers j and k^* (in case of relayed transmission) from the sets $\mathcal{A}$ and $\mathcal{B}$ respectively and repeat the procedures until the set $\mathcal{A}$ is empty.

In the proposed scheme, every subcarrier in the source side requires no more than $(M + MN)$ function evaluations to be paired and assigned to the relay or selected for the direct transmission. Therefore, the complexity of the proposed algorithm is $\mathcal{O}(MN^2)$.

V. Simulation Results

The simulations are performed under the assumption of having a multicarrier system of $N = 64$ subcarriers with $M = 5$ relays. The values of T_s, Δf, and σ^2 are assumed to be 4μ seconds, 0.3125 MHz and 10^{-6} respectively. The channel gains are outcomes of independent Rayleigh distributed random variables with mean equal to 1. All the results have been averaged over 1000 iterations. In the simulations, *optimal with direct* and *suboptimal* algorithms apply the dual decomposition technique presented in Sec. III and the proposed method presented in Sec. IV respectively. We will refer to the case when the direct/relayed transmission indicator α_j is assumed to be $\alpha_j = 1$, $\forall j$ by *optimal without direct*. Additionally, in *SNR*, the subcarriers and users are selected according to their *SNR* values while in *random*, the subcarriers are matched and assigned randomly. For both *SNR* and *random*, the powers are evaluated by solving (6) with the known $\alpha_j, t_{j,k}$ and $\pi_{j,k}^m$.

Fig. 1 shows the achieved capacity of the different algorithms vs. the interference threshold using OFDM and FBMC

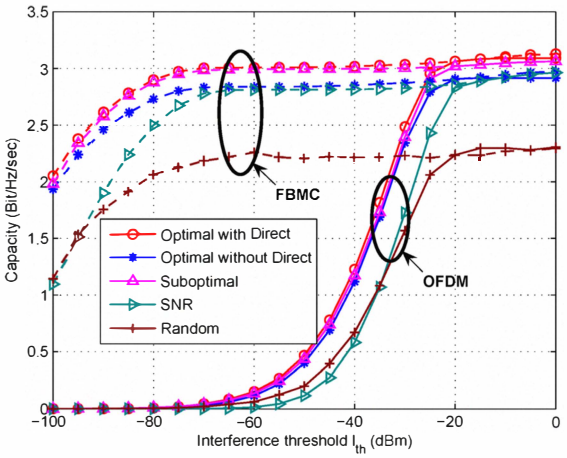

Fig. 1. Achieved capacity vs the interference threshold with $P_S = P_{R_m} = 0$. dBm. OFDM based system is plotted by the solid lines while the dashed ones represent the FBMC based systems.

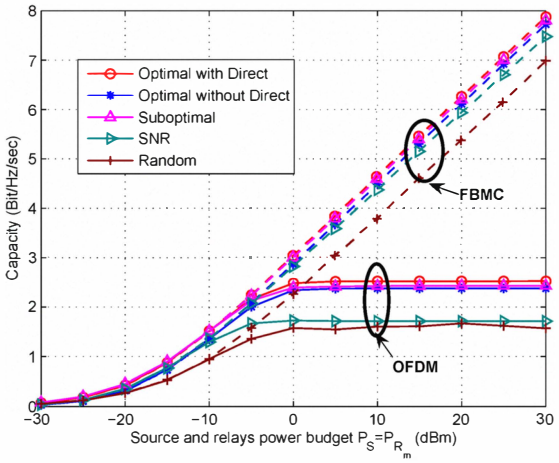

Fig. 2. Achieved capacity vs available power budget with $P_S = P_{R_m}$ when $I_{th} = -30$ dBm. OFDM based system is plotted by the solid lines while the dashed ones represent the FBMC based systems.

physical layers. For the OFDM case, It can be noticed that the capacity is increased by considering the relayed transmission with ability of using the direct link in some subcarriers. Additionally, as the interference threshold increases, the achieved capacity of the CR is also increases. This is can be justified by the increase of the CR system ability to use higher transmission powers on the subcarriers. In addition to that, one can notice the close performance of the *suboptimal* algorithm to that of the *optimal* algorithm and the superiority of the proposed schemes over the *SNR* and *random* algorithms. Furthermore, the gap between the *optimal* algorithm and the *SNR* algorithm is decreased as the interference threshold increases. This is because of the non-cognitive like behavior of the CR system in this region. Regarding the performance of OFDM and FBMC systems, two different performance regions can be identified as follows: (i) when $I_{th} \leq -30$ dBm: the capacity of the FBMC based CR systems is more that of the OFDM based ones. This is because of the small sidelobes of the FBMC systems in adition to the loss of the spectrum efficiency in OFDM due to the use of the CP. Therefore, the interference constraint generally has small effect on the performance of the FBMC based systems which is not the case in OFDM ones, (ii) when $I_{th} > -30$ dBm: both of the system has almost the same performance when operating with high interference thresholds or low power budgets. This is can be justified by noting that the systems in this region operate in noncognitive-like environment. Similarly, in Fig. 2, the region when $P_S = P_{R_m} \leq -5$ dBm represents the noncognitive-like environment; where the available power budget is not able to introduce high interference. When the power constraints increase more than this value, FBMC system has significantly improves the CR capacity since FBMC based systems can use more transmission power which increase the total system capacity.

VI. Conclusions

In this paper, we have considered the resource allocation problem in multiple relay DF OFDM and FBMC based CR system. To maximize the achieved capacity while maintain the interference introduced to the primary system below a pre-specified threshold, the network resources are optimized jointly using the dual decomposition technique. A greedy suboptimal algorithm is presented to reduce the computational complexity of the dual decomposition scheme. The suboptimal algorithm achieves a near optimal performance with much less complexity. Moreover, the proposed scheme outperforms the SNR and Random based algorithms. Additionally, the capacities achieved by OFDM and FBMC based systems is compared to prove the efficiency of using FBMC in the CR systems. The multiple hops scenario and the consideration of several interference constraints are possible future developments of this work.

Acknowledgments

This work was partially supported by COST Action IC0902, the European project ACROPOLIS-NoE (ICT-2009.1.1) and the National project Sofocles with code TEC 2010-21100.

References

[1] J. Jia, J. Zhang, and Q. Zhang, "Cooperative relay for cognitive radio networks," in *IEEE INFOCOM 2009*, apr. 2009, pp. 2304 –2312.

[2] L. Li, X. Zhou, H. Xu, G. Li, D. Wang, and A. Soong, "Simplified relay selection and power allocation in cooperative cognitive radio systems," *IEEE Transactions on Wireless Communications*, vol. 10, no. 1, pp. 33 –36, 2011.

[3] G. Zhao, C. Yang, G. Li, D. Li, and A. Soong, "Power and channel allocation for cooperative relay in cognitive radio networks," *IEEE Journal of Selected Topics in Signal Processing*, vol. 5, no. 1, pp. 151 –159, 2011.

[4] T. Weiss and J. Hillenbrand, "Mutual interference in OFDM-based spectrum pooling systems," in *Vehicular Technology Conference (VTC'04-Spring)*, vol. 4, May 2004.

[5] A. Skrzypczak, P. Siohan, and J. Javaudin, "Power spectral density and cubic metric for the OFDM/OQAM modulation," in *IEEE ISSPIT*, Vancouver-Canada, August 2006.

[6] G. Bansal, M. J. Hossain, and V. K. Bhargava, "Optimal and suboptimal power allocation schemes for OFDM-based cognitive radio systems," *IEEE Transactions on Wireless Communications*, vol. 7, no. 11, pp. 4710–4718, November 2008.

[7] W. Yu and R. Lui, "Dual methods for nonconvex spectrum optimization of multicarrier systems," *IEEE Transactions on Communications*, vol. 54, no. 7, pp. 1310 –1322, 2006.

[8] H. W. Kuhn, "The hungarian method for the assignment problem," in *50 Years of Integer Programming 1958-2008*. Springer Berlin Heidelberg, 2010, pp. 29–47.

[9] S. Boyd and L. Vandenberghe, *Convex optimization*. Cambridge, U.K.: Cambridge Univ. Press, 2004.

Relay Selection and Resource Allocation for Two-Way DF-AF Cognitive Radio Networks

Ahmad Alsharoa, *Member, IEEE*, Faouzi Bader, *Senior Member, IEEE*, and Mohamed-Slim Alouini, *Fellow, IEEE*

***Abstract*—In this letter, the problem of relay selection and optimal resource allocation for two-way relaying cognitive radio networks using half duplex amplify-and-forward and decode-and-forward protocols is investigated. The primary and secondary users are assumed to access the spectrum simultaneously, in a way that the interference introduced to the primary users should be below a certain tolerated limit. Dual decomposition and subgradient methods are used to find the optimal power allocation. A suboptimal approach based on a genetic algorithm is also presented. Simulation results show that the proposed suboptimal algorithm offers a performance close to the optimal performance with a considerable complexity saving.**

***Index Terms*—Cognitive radio networks, two-way relaying, genetic algorithm.**

I. Introduction

COGNITIVE Radio (CR) has recently attracted enormous attention by researchers in wireless communication [1]. It is considered as a promising solution towards a more efficient usage of the radio spectrum. The idea of CR spectrum sharing is to allow unlicensed users known also as Secondary Users (SUs) to utilize the spectrum band allocated to licensed users known also as Primary Users (PUs) at the same time. In order to protect the PUs, the interference due to the SUs should be kept under a certain interference level.

Exchanging different signals between two terminals in one-way relaying requires four time slot to accomplish the transmission. In order to improve the spectral efficiency, there has been recently a great deal of interest in two-way relaying transmission. The transmission process in this relaying technique takes place in two time slots. In the first slot, the terminals transmit their signals simultaneously to the relay. Subsequently, in the second slot, the relay broadcasts its signal to the terminals [2]. For instance, the authors in [3] proposed a useful framework to solve the optimal power allocation problem for a two-way relaying network. Their work shows that two-way relaying provides an improvement of spectral efficiency compared with one-way relaying transmission. Furthermore, the relay selection and power allocation problems for Amplify-and-Forward (AF) protocol in cooperative one-way and two-way relaying CR have been investigated in [4] and [5], respectively. However, to the best knowledge of the authors and contrary to the case of the AF protocol, the relay selection problem in two-way relaying CR networks using Decode-and-Forward (DF) protocol has not been discussed so far. In this letter, a best relay selection scheme for two-way half duplex relaying CR assuming channel reciprocity is considered. In the AF protocol, the relay broadcasts the amplified copy of the received signal to the terminals, i.e., the noise gets amplified too. On the other hand, in the DF protocol, the relay regenerates clean signals from the received signal and transmits the re-encoded message to the terminals. More specifically, the main contributions for our new proposed scheme can be summarized as follows: 1- Formulate a new relay selection scheme in two-way relaying CR system which selects between the AF and DF protocols depending on the higher Sum Rate (SR) achieved by a Secondary Network (SN) without affecting the Quality of Service (QoS) of a Primary Network (PN). For that reason, additional interference constraints are considered in the optimization problem for both time slots. 2- Derivation of the optimal terminals power and relay power that maximize the cognitive SR of the system. 3- Using dual decomposition and subgradient methods for both AF and DF protocols in order to solve the SR maximization problem and select the best relay with the best protocol. 4- Design a practical low complexity suboptimal approach based on Genetic Algorithm (GA) to solve the formulated optimization problem [6], and compare it with the optimal and Exhaustive Search (ES) solutions. Due to space limitations some of the details are given in a comparison technical report available online [7].

The results provided in Section V show that in our two-way relaying scheme and at high Signal-to-Noise-Ratio (SNR), the DF protocol becomes a bottleneck in the first phase, so higher SR can be achieved using the AF protocol. On the other hand, for low SNR, the relay with the DF protocol achieves higher SR.

II. System Model

In this section, the best relay selection scheme for CR two-way relaying is investigated. The SN is constituted of a cognitive Mobile User (MU), a Cognitive Base station (CB), and M Relay Stations (RSs). It is assumed that there is no direct link between the cognitive terminals and the single relay principle is applied to select the best relay. During the first time slot, the CB transmits its signal to RSs with power denoted P_{CB}. Concurrently, the secondary MU transmits its signal to RSs with power denoted P_S. This causes two interferences to the PU. In the second time slot, the selected RS broadcast its signal. This phase also causes interference to the PU from the active RS.

Manuscript received March 19, 2013. The associate editor coordinating the review of this letter and approving it for publication was I.-M. Kim.

A. Alsharoa and M.-S. Alouini are with the Computer, Electrical, and Mathematical Science of Engineering (CEMSE) Division, King Abdullah University of Science and Technology (KAUST), Thuwal, Makkah Province, Kingdom of Saudi Arabia (e-mail: {ahmad.sharoa, slim.alouini}@kaust.edu.sa).

F. Bader is with the Centre Tecnologic de Telecommunication de Catalunya (CTTC), Parc Mediterrani de la Tecnologia, Av. Carl Friedrich Gauss 7, 08860, Castelldefels-Barcelona, Spain (e-mail: faouzi.bader@cttc.es).

Digital Object Identifier 10.1109/WCL.2013.051513.130211

We assume that all the channel gains are perfectly known at the communication nodes. All channel gains for the network can be adopted by assuming channel reciprocity and classical channel estimation approaches [8]. The interference between the PN and SN is studied in Section III. Also, we assume that the PN and SN access the spectrum at the same time. Furthermore, the selection strategy between the AF and the DF protocols is applied in order to achieve the maximum SR of the SN without affecting the QoS of the PU measured by I_{th}. Finally, without loss of generality, all the noise variances are assumed to be equal to σ_n^2.

III. Problem Formulation

R_{AF} and R_{DF} denote the achievable secondary SR for the AF protocol, and the achievable secondary SR for the DF protocol, respectively. Let us define $f_1 = |h_m^{(CB-R)}|^2, f_2 = |h_m^{(S-R)}|^2, f_3 = |h^{(S-P)}|^2, f_4 = |h^{(CB-P)}|^2$, and $f_5 = |h_m^{(R-P)}|^2$ as the complex channel gain between the CB and RS m, MU and RS m, MU and PU, CB and PU, and RS m and PU, respectively.

The Optimization Problem1 (OP1) for a single relay selection can be formulated as

$$\text{(OP1):} \quad m^* = \underset{m\in\{1:M\}}{\operatorname{argmax}} \quad \max_{R} \quad \rho R_{DF} + (1-\rho)R_{AF}, \tag{1}$$

$$\text{s.t} \quad 0 \le P_S \le \bar{P}_S, \tag{2}$$

$$0 \le P_{CB} \le \bar{P}_{CB}, \tag{3}$$

$$0 \le P_{R,m} \le \bar{P}_R, \quad \forall m = 1, ..., M, \tag{4}$$

- interference constraint in the first time slot

$$\left[f_3 P_S + f_4 P_{CB}\right] \le I_{th}, \tag{5}$$

- interference constraint in the second time slot

$$f_5 P_{R,m} \le I_{th}, \quad \forall m = 1, ..., M, \tag{6}$$

where $\bar{P}_S, \bar{P}_{CB}$, and $\bar{P}_R$, are the peak transmit power of the secondary MU, CB, and *m*-th RS, respectively. In (1), ρ is a constant equal to either zero for the AF protocol or one for the DF protocol. Let x_1 and x_2 are the symbols transmitted by the MU and CB respectively. It is assumed that $\mathbb{E}(|x_1|^2) = \mathbb{E}(|x_2|^2) = 1$, where $\mathbb{E}(\cdot)$ denotes the expectation operator. In the first time slot, the received signal at the *m*-th relay is given by

$$r_m = \sqrt{P_S} h_m^{(S-R)} x_1 + \sqrt{P_{CB}} h_m^{(CB-R)} x_2 + z_m, \tag{7}$$

where z_m is the additive Gaussian noise at the *m*-th relay.

In order to simplify the formulated OP1, we solve it time slot per time slot. During the second phase, the power allocation at the *m*-th relay depends essentially on two constraints: the peak power constraint (4) and the interference constraint (6). For this reason, the optimal relay power can be expressed as

$$P_{R,m}^* = \min\left(\bar{P}_R, \frac{I_{th}}{f_5}\right), \quad \forall m = 1, ..., M. \tag{8}$$

The optimization problem during the first phase is therefore given by

$$\text{(OP2):} \quad m^* = \underset{m\in\{1:M\}}{\operatorname{argmax}} \quad \max_{R} \quad \rho R_{DF} + (1-\rho)R_{AF}, \tag{9}$$

$$\text{s.t} \quad (2), (3), (5) \tag{10}$$

We can decompose the OP2 outlined above into parallel subproblems using single relay principle, i.e., each independently solvable for a different relay and can be solved by applying the dual decomposition method [9]. Then, we select the relay that offers maximum SR. Therefore, the dual subproblem associated with OP2 can be written as

$$\min_{\boldsymbol{\lambda}\ge 0} \quad g(\boldsymbol{\lambda}), \tag{11}$$

where $\boldsymbol{\lambda}$ is a Lagrangian vector contains all Lagrangian multipliers. The dual function $g(\boldsymbol{\lambda})$ is defined as follows

$$g(\boldsymbol{\lambda}) = \max_{P_S\ge 0, P_{CB}\ge 0} \quad \mathcal{L}(\boldsymbol{\lambda}, P_S, P_{CB}). \tag{12}$$

A. Amplify-and-Forward Protocol

In this protocol, the relay amplifies the received signal by w_m and broadcasts it to the terminals. The relay power of the *m*-th relay node can be expressed as

$$P_{R,m} = \mathbb{E}(|w_m r_m|^2) = (P_S f_2 + P_{CB} f_1 + \sigma_n^2)|w_m|^2. \tag{13}$$

By using the perfect knowledge of the channel gains and channel reciprocity, the terminals can remove the self interference by eliminating their own signals. Thus, the SNR at MU and CB are given by (for details see [7])

$$\begin{aligned} \gamma_{m,S} &= \frac{P_{CB} P_{R,m}^* f_2 f_1}{\sigma_n^2 (P_{R,m}^* f_1 + P_S f_2 + P_{CB} f_1 + \sigma_n^2)}, \\ \gamma_{m,CB} &= \frac{P_S P_{R,m}^* f_2 f_1}{\sigma_n^2 (P_{R,m}^* f_2 + P_S f_2 + P_{CB} f_1 + \sigma_n^2)}. \end{aligned} \tag{14}$$

The achieved SR for AF protocol can be written as

$$R_{AF} = \frac{1}{2}\log_2(1+\gamma_{m,S}) + \frac{1}{2}\log_2(1+\gamma_{m,CB}). \tag{15}$$

Due to the non-convexity of the formula (15) for the AF protocol, a convex approximation when the system operates at high SNR region is presented as [5]

$$R_{AF} = \frac{1}{2}\log_2(\gamma_{m,S}\cdot\gamma_{m,CB}). \tag{16}$$

When $\rho = 0$ and due the fact that the logarithmic function is a monotonically increasing function of its arguments, the Lagrangian of OP2 can be written as

$$\begin{aligned} \mathcal{L}_{\text{AF}} =& \gamma_{m,S}.\gamma_{m,CB} - \lambda_S(P_S - \bar{P}_S) - \lambda_{CB}(P_{CB} - \bar{P}_{CB}) \\ & - \lambda_1(f_3 P_S + f_4 P_{CB} - I_{th}), \end{aligned} \tag{17}$$

where λ_S, λ_{CB}, and λ_1 represent the Lagrangian multipliers related to the peak power at the MU, peak power at the CB, and interference constraint in the first time slot, respectively. By applying the Karush-Kuhn-Tucker (KKT) optimality conditions [9], direct calculation yields [7]

$$P_S^* = \sqrt{\left(\frac{\sigma_n^4 A}{\sigma_n^4 f_2^2 + (\lambda_S + \lambda_1 f_3) P_{CB} P_{R,m}^{*^2} f_1^2 f_2^2}\right)^+}, \tag{18}$$

$$P_{CB}^* = \sqrt{\left(\frac{\sigma_n^4 B}{\sigma_n^4 f_1^2 + (\lambda_{CB} + \lambda_1 f_4) P_S P_{R,m}^{*^2} f_1^2 f_2^2}\right)^+}, \tag{19}$$

where $A = P_{R,m}^{*^2} f_2 f_1 + P_{R,m}^*(f_2\sigma_n^2 + f_1\sigma_n^2) + P_{CB}^2 f_1^2 + P_{CB}(2f_1\sigma_n^2) + P_{R,m}^* P_{CB}(f_2 f_1 + f_1^2) + \sigma_n^4$, $B = P_{R,m}^{*^2} f_2 f_1 + P_{R,m}^*(f_2\sigma_n^2 + f_1\sigma_n^2) + P_S^2 f_2^2 + P_S(2f_2\sigma_n^2) + P_{R,m}^* P_S(f_2 f_1 + f_2^2) + \sigma_n^4$, and $(x)^+$ denotes the maximum between x and zero.

B. Decode-and-Forward Protocol

Prior works in the literature have studied the sum rate for two-way relaying with the DF protocol [3], [10]. The max SR of the DF protocol can be expressed as

$$R_{DF} = \frac{1}{2}\min\Big[\min\{R_1, R_3\} + \min\{R_2, R_4\}, R_5\Big], \quad (20)$$

where $R_1 = \log_2\Big(1+\frac{P_S f_2}{\sigma_n^2}\Big)$ and $R_2 = \log_2\Big(1+\frac{P_{CB} f_1}{\sigma_n^2}\Big)$denote the rate from the MU and the CB to the relay in the first time slot, respectively. While $R_3 = \log_2\Big(1+\frac{P_R f_1}{\sigma_n^2}\Big)$ and $R_4 = \log_2\Big(1+\frac{P_R f_2}{\sigma_n^2}\Big)$denote the rate from the relay to the MU and to the CB in the second time slot, respectively. In (20), $R_5 = \log_2\Big(1+\frac{P_{CB} f_1 + P_S f_2}{\sigma_n^2}\Big)$ denotes the max SR can be achieved in both time slots.

It is assumed that the relay node decodes the high SNR signal (Down-Link (DL) signal) first, then decodes the other signal (Up-Link (UL) signal) after subtracting the decoded signal. For this reason additional Lagrangian multipliers are considered for UL and DL. When $\rho = 1$, the Lagrangian of OP2 can be written as (21) at the top of the next page. where λ_u and λ_d are the dual variables associated with the UL and DL rate constraints, respectively. Letting $\alpha = 2.\ln 2$ and applying the KKT optimality conditions, we obtain after simplification [7]

$$P_{CB}^* = \left(\frac{(1-\lambda_d)}{\alpha(\lambda_1 f_4 + \lambda_{CB})} - \frac{P_S f_2 + \sigma_n^2}{f_1}\right)^+, \quad (22)$$

$$P_S^* = \left(\frac{\frac{(\lambda_d-\lambda_u) f_2 f_1 (1-\lambda_d)}{\alpha(\lambda_1 f_4+\lambda_{CB})} - \frac{\sigma_n^2(1-\lambda_d)(\lambda_1 f_3+\lambda_S) f_1}{\lambda_1 f_4+\lambda_{CB}} - f_2}{\frac{(1-\lambda_d) f_2 f_1 (\lambda_1 f_3+\lambda_S)}{(\lambda_1 f_4+\lambda_{CB})} + (\lambda_d-\lambda_u) f_2^2 - (1-\lambda_u) f_2}\right)^+. \quad (23)$$

C. Dual Problem Solution

The dual problem of OP2 can be solved by using the subgradient method [11]. Therefore, to obtain the solution, we can start with any initial values for the different Lagrangian multipliers and evaluate the optimal powers. We then update the Lagrangian multipliers at the next iteration as

$$\lambda_S^{t+1} = \lambda_S^t - \delta(t)\Big[\bar{P}_S - P_S^*\Big], \quad (24)$$

$$\lambda_{CB}^{t+1} = \lambda_{CB}^t - \delta(t)\Big[\bar{P}_{CB} - P_{CB}^*\Big], \quad (25)$$

$$\lambda_1^{t+1} = \lambda_1^t - \delta(t)\Big[I_{th} - \Big(f_3 P_S^* + f_4 P_{CB}^*\Big)\Big], \quad (26)$$

$$\lambda_u^{t+1} = \lambda_u^t - \delta(t)\Big[\frac{1}{2}\log_2\Big(1+\frac{P_{R,m}^* f_1}{\sigma_n^2}\Big) - \frac{1}{2}\log_2\Big(1+\frac{P_S^* f_2}{\sigma_n^2}\Big)\Big], \quad (27)$$

$$\lambda_d^{t+1} = \lambda_d^t - \delta(t)\Big[\frac{1}{2}\log_2\Big(1+\frac{P_{R,m}^* f_2}{\sigma_n^2}\Big) + \frac{1}{2}\log_2\Big(1+\frac{P_S^* f_2}{\sigma_n^2}\Big) - \frac{1}{2}\log_2\Big(1+\frac{P_S^* f_2 + P_{CB}^* f_1}{\sigma_n^2}\Big)\Big], \quad (28)$$

where $\delta(t)$ is the step size updated according to the non-summable diminishing step lengths policy [11]. Using the subgradient method, the updated values of the optimal powers and the Lagrangian multipliers are repeated until convergence. The implementation procedures to solve the OP2 is described in details in the comparison technical report [7, Algorithm 1].

IV. Suboptimal Algorithm

The optimal solution for our non linear OP2 sometimes is difficult to solve due to its high computational complexity. Therefore, in order to solve the problem efficiently, we propose a low complexity suboptimal approach in discrete domain to find a suboptimal solution. In the first phase, we need to find the optimal power allocation over the terminals (i.e., P_S and P_{CB}) in order to maximize the SR of SN without interfering with the PU. In this section, we propose a heuristic GA with discrete number of power levels from zero to the peak power budget. In fact, each terminal can transmit its signals using one of the power levels between 0 and peak power budget, i.e., $\Big(P_S \in \Big\{0, \frac{\bar{P}_S}{N-1}, \frac{2\bar{P}_S}{N-1}, ..., \frac{(N-2)\bar{P}_S}{N-1}, \bar{P}_S\Big\}\Big)$, and $\Big(P_{CB} \in \Big\{0, \frac{\bar{P}_{CB}}{N-1}, \frac{2\bar{P}_{CB}}{N-1}, ..., \frac{(N-2)\bar{P}_{CB}}{N-1}, \bar{P}_{CB}\Big\}\Big)$ where N is the number of quantization levels. In this way, the transmitters have more flexibility to allocate their powers in the case where continuous power distribution is not available. The GA tries to find the optimal binary string that maximizes the SR expressed in (9). At the beginning, we generate randomly N binary strings each concatenating two binary words corresponding to P_S and P_{CB} to produce an initial population set S of N elements and each with $2K$ bits, where $K = \lceil \log_2(N) \rceil$ where $\lceil x \rceil$ denotes the smallest integer not less than x. The first K bits represent the equivalent binary string for P_S and the last K bits represent the equivalent binary string for P_{CB}. Initially, the GA computes the SR of all elements in S using (9). Then, it maintains the best β strings $\in S$ to the next population that verifies the interference constraint (5), and from them generates $N-\beta$ new strings by applying crossovers technique to form a new population S. This procedure is repeated until reaching convergence (i.e., SR remains constant for several iterations) or until reaching the maximum generation number I. Details of the proposed GA are given in [7, Algorithm 2].

The formulated OP2 can be, of course, solved via an ES algorithm by investigating all possible combinations of the transmitters power and select the best combinations that satisfied the interference constraint. This algorithm requires $M\sum_{i=0}^{2}\binom{2}{i}(N-1)^i = O(MN^2)$ operations [12]. However, our proposed GA requires MNI operations to reach a suboptimal solution. The last step in our proposed algorithm is selecting between the AF and DF protocols depending on the higher achieved SR. Hence, our proposed algorithm is able to reach a suboptimal solution with a considerable complexity saving. In addition to that, selected simulation results in Section V show that by increasing N, our proposed GA achieves almost the same performance as the optimal solution.

V. Simulation Results and Concluded Remarks

In this section, some selected simulation results are performed to show the benefits of our system. We assume a single cell subject to a small scale Rayleigh fading, consisting of one PU and a SN constituted by one CB, one secondary MU, and $M = 4$ relays. The variance σ_n^2 is assumed to be equal to 10^{-4}. We also assume that the transmit peak power constraint of MU, CB, and each RS are equal to P_{bar}. The crossover point is chosen randomly between 1 and $2K$ for each binary string with $\beta = 0.5N$ and we run the GA at most 10 times.

$$\mathcal{L}_{\text{DF}} = (1-\lambda_u-1+\lambda_d)\tfrac{1}{2}\log_2(1+\tfrac{P_S f_2}{\sigma_n^2})(1-\lambda_d)\tfrac{1}{2}\log_2(1+\tfrac{P_{CB}f_1+P_S f_2}{\sigma_n^2}) - \lambda_S(P_S-\bar{P}_S) - \lambda_{CB}(P_{CB}-\bar{P}_{CB}) \\ -\lambda_1(f_3 P_S + f_4 P_{CB} - I_{th}). \tag{21}$$

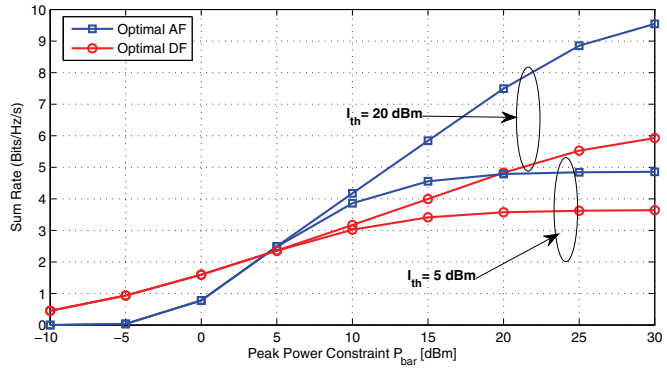

Fig. 1. . Achieved SR for the AF and DF protocols versus P_{bar}.

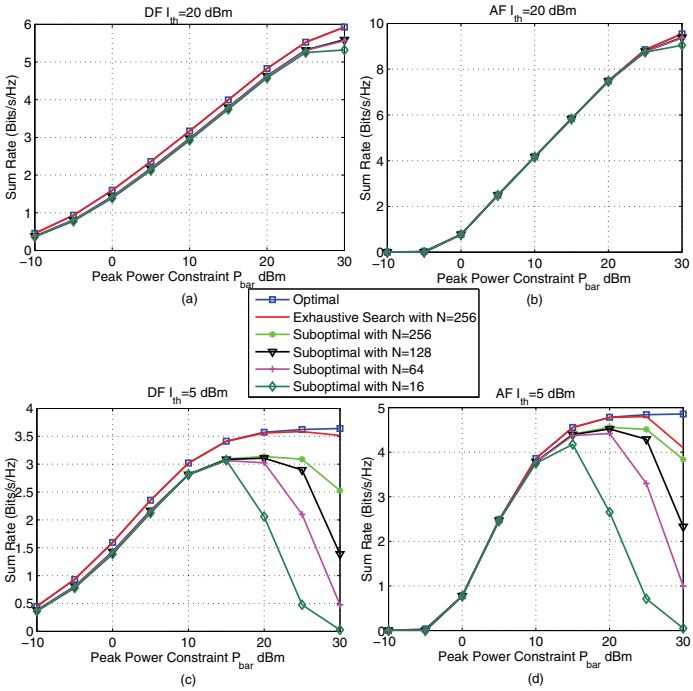

Fig. 2. . The achieved SR of the GA, the ES, and the optimal solutions with different I_{th} versus P_{bar}, for (a,c) DF protocol, (b,d) AF protocol.

The advantage of relay selection is depicted in Fig.1. The selection strategy can switch between the AF and DF protocols according to the better performance. In general, the results suggest the usage of the AF protocol for high SNR region and suggest the usage of the DF protocol for low SNR region. This can be justified by noticing that the SR value of the DF protocol becomes a bottleneck for the first phase in the high SNR regime. Furthermore, additional comparison between the performance of the one-way and two-way relaying CR networks is illustrated in the comparison technical report [7, Fig.3].

Fig.2 shows a comparison between the performance of the proposed GA with the optimal and ES solutions. We plot the achieved secondary SR versus P_{bar} for different values of $I_{th} = \{20, 5\}$ dBm and different relaying protocols. We can notice that, in the low P_{bar} region, the proposed GA, the optimal solution, and the ES have almost the same SR, while in the high P_{bar} region, a gap between these methods is observed. This gap is increasing with higher P_{bar} values. This is justified by the fact that starting from a certain value of P_{bar} the GA can not supply the selected relay with the full power budget. In fact, with high values of P_{bar}, the constraint (5) can be affected. For this reason, we introduce the discretization set to get more degrees of freedom by increasing N and as such enhance the SR. Indeed, thanks to the GA random evolution process, it provides more chance to find a close combination to ES combination. For instance, Fig.2(a) and Fig.2(b) plot the secondary SR for $I_{th} = 20$ dBm for DF protocol and AF protocol, respectively. It is shown that the GA achieves almost the same SR reached by the optimal solution. While when I_{th} is reduced, we notice a degradation of the GA performance at large values of P_{bar} as shown in Fig.2(c) and Fig.2(d). However, it can be shown that when $N \to \infty$, the proposed GA achieves the performance of the optimal solution. The same interpretation is applied where the achieved secondary SR is plotted versus the interference threshold for both relaying protocols [7, Fig.5].

REFERENCES

[1] S. Haykin, "Cognitive radio: brain-empowered wireless communications," *IEEE J. Sel. Areas Commun.*, vol. 23, no. 2, pp. 201–220, Feb. 2005.

[2] B. Rankov and A. Wittneben, "Spectral efficient protocols for half-duplex fading relay channels," *IEEE J. Sel. Areas Commun.*, vol. 25, no. 2, pp. 379–389, 2007.

[3] K. Jitvanichphaibool, R. Zhang, and Y.-C. Liang, "Optimal resource allocation for two-way relay-assisted OFDMA," *IEEE Trans. Veh. Technol.*, vol. 58, no. 7, pp. 3311–3321, Sep. 2009.

[4] L. Li, X. Zhou, H. Xu, G. Li, D. Wang, and A. Soong, "Simplified relay selection and power allocation in cooperative cognitive radio systems," *IEEE Trans. Wireless Commun.*, vol. 10, no. 1, pp. 33–36, Jan. 2011.

[5] P. Ubaidulla and S. Aissa, "Optimal relay selection and power allocation for cognitive two-way relaying networks," *IEEE Wireless Commun. Lett.*, vol. 1, no.3, pp. 225–228, Jun. 2012.

[6] R. L. Haupt and S. E. Haupt, *Practical Genetic Algorithms*, 2nd ed. John Wiley and Sons, Inc., 2004.

[7] A. Alsharoa, F. Bader, and M.-S. Alouini, "Relay selection and resource allocation for two way DF-AF cognitive radio networks," tech. rep., King Abdullah Univeristy of Science and Technology (KAUST), Mar. 2013. Available: http://arxiv.org/abs/1303.3489.

[8] R. Zhang, S. Cui, and Y.-C. Liang, "On ergodic sum capacity of fading cognitive multiple-access channel," in *Proc. 2008 Allerton Conference on Communication, Control, and Computing*.

[9] S. Boyd and L. Vandenberghe, *Convex Optimization*. Cambridge University Press, 2004.

[10] S. J. Kim, P. Mitran, and V. Tarokh, "Performance bounds for bidirectional coded cooperation protocols," *IEEE Trans. Inf. Theory*, vol. 54, pp. 5235–5241, Nov. 2008.

[11] S. Boyd and A. Mutapcic, "Stochastic subgradient methods," notes for EE364, Stanford University, Winter 2006-07.

[12] K. H. Rosen, *Discrete Mathematics and its Applications*, 6th ed. McGraw-Hill, 2007.

3.2 Coexistence capabilities

The growing economic and social impact of mobile telecommunication devices, together with the evolution of protocols and interoperability requirements among different standards for voice and data, have driving worldwide research towards the development of new waveforms with better coexistence capabilities in heterogeneous communication networks, and the implementation of fully-integrated multi-standards future (5G) transceivers. In this context I participated in the development and the coordination of the European project EMPhATIC[7] project, and also in the French National project PROFIL[8] where I conducted complementary researches to the EMPhAtiC project for the development of PMR communication systems. Both projects focuses on heterogeneous networks in general, and on systems coexistence in particular. The most important focus is the prospective evolution of PMR/PPDR system to provide a high data-rate service by utilizing fragments of a PMR frequency band partly occupied by narrow band legacy PMR signals with 10, 12.5, 25, 50, and/or 100 kHz channelization primary waveforms.
Part of my researches in these projects focused into the analysis of the use of flexible multi-carrier structures enabling coexistence and migration to future generation broadband professional radio communication. Main achieved coexistence capabilities and performance by using different waveforms in the PMR context are presented in the hereafter Subsection 3.2.1.

Extended analysis have been also conducted during my actual involvement in the ACCENT5[9] National french project, and over the PhD supervision of Mr. Quentin BODINIER (see details in Subsection 1.3.3.1, page 17). The ACCENT5 project targets innovative technological approaches for a smooth integration of Device-to-Device (D2D) communications in future (5G) wireless networks. Details on my main achieved results on the time-frequency misalignment effects of the D2D pair on the incumbent network, and the modeling of the interference in heterogeneous environment are presented in Subsection 3.2.2.

3.2.1 In Professional mobile communication context

Nowadays, Professional Mobile Radio (PMR) and Public Protection and Disaster Relief services (PPDR) are fundamentally used for low-rate data transmission like voice communications. This is due to the limited throughput resulting from the small frequency bands used by these systems. Recently, there is a trend to upgrade the PMR systems to support high-rate applications and broadband services. As described in [54], the possible deployment and introduction of broadband systems in PMR bands (within the current frequency allocation) is facing important challenges as several technical constraints must be overtaken, mainly those related to coexistence with the actually existing narrow band PMR commercial devices (primary systems). The primary goal is to examine the coexistence between PMR narrow-band systems with new broadband services. As a first step, different waveform strategies have been studied. These waveforms are multi-carrier waveforms. Multi-carrier transmission is the predominant technique used in current wireless communication systems (e.g. WLAN, WiMAX, DVB-T, LTE, etc.) and consists in splitting up a wide band signal at a high symbol rate into several lower rate signals, each one occupying a narrower band. Because of the various trade-off between time and frequency localization, each waveform has a particular interest for a given scenario. The aim of the conducted analysis is to give a synthesis view for the choice of the waveform adapted to the broadband PMR scenario.

The poor spectral containment of the CP-OFDM waveform, if applied in the considered coexistence scenario, imposes generous guard bands towards legacy channels due to very high adjacent sub-channel power rejection level. This is directly related to the intrinsic high spectrum side-lobes of the used CP-OFDM scheme, which creates interference to neighboring frequencies. Furthermore, the future broadband system has to support non-contiguous spectrum allocations, as reminded in the introduction. That is the reason to study and design new waveforms having in mind this particular coexistence constraints and thus very high spectral containment criterion. For detailed description of the methodology, please refer to [55] and [56]. A quite large part of the interference analysis for different waveforms (FBMC, GFDM and FMT schemes) and the respective performances have already been performed and presented in [56], and [C83, C80, C77] all depicted at the end of this Subsection 3.2.1. Many multi-carrier physical layers waveforms (PHY) are considered and analyzed for the coexistence analysis:

[7] Enhanced Multi-carrier Techniques for Professional Ad-hoc and Cell Based Communications- EMPhATIC, with code: ICT-318362 (see more details in Subsection 1.5.3, page 23).

[8] Broadband Professional Mobile Radio Based on Filter Band Multi-carrier Modulation project, funded by the French National Research Agency with code: ANR-13-INFR-0007-03 (see more details in Subsection 1.5.2, page 23).

[9] Advanced Waveforms, MAC Design and Dynamic Radio Resource Allocation for D2D in 5G Wireless Networks funded by the French National Research Agency with code: ANR- 14-CE28-0026-02 (see more details in Subsection 1.5.2, page 22).

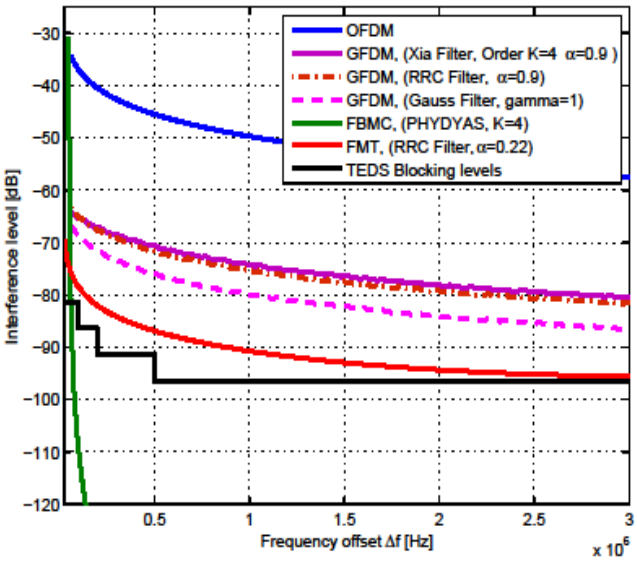

Figure 3.17: Effective interference powers [in dBc] of 1.4 MHz band of different multi-c waveforms versus 25KHz TEDS reception mask.

- CP-OFDM,
- GFDM: using different filter for the modulation (i.e. RRC filter, Gauss filter and Xia filter) [57],
- FBMC: PHYDYAS's project prototype filter with an overlapping factor K=4 [58, 59],
- FMT waveform as defined in [56].

Considering the adjacent sub-channel power rejection level criterion, it is obvious that only one candidate successfully achieves the required level of rejection. FBMC waveform is the only one that is able to reach the desired levels of spectral rejections close to the useful bandwidth. As a result, FBMC waveform will allow reduced frequency guard band between narrow band and broadband systems in the coexistence scenario. This seems to be the best candidate at least from a theoretical point of view.
Nevertheless, those results are digitally computed performances with ideal tools. One should take care that the real broadband radio communication system will of course use analog components and more specifically HPA (High Power Amplifier). Thus, achieving such rejections will be mitigated by RF non linearities. As a consequence, the gains and theoretical performances shown within the FBMC scheme will be less important and the difference with FMT will be reduced.
As far as GFDM waveforms are concerned, their own performances seem to be far from the desired ones, but FMT performances are finally relatively close to the requirements. One could imagine on one hand to improve a bit more the FMT pulse shaping filtering template by replacing ideal RRC filter by one more optimized, and on the other hand relaxing a bit the arbitrary constraint of the limited temporal support, or replacing FIR implementation by IIR implementation to decrease latency constraints. This would help reaching some supplementary dBc of rejection in order to be closer to the desired requirements.
To conclude, GFDM, FMT, FBMC waveforms have been studied in order to investigate our problematic. Each of those waveforms has its own advantages, benefits or drawbacks. Optimizations and improvements are still possible for each solution, but the general tendency is given in the comparison figure here over about rejection criterion.
More extended and deep results can be found in the technical deliverable [56], where OFDM (using time windowing, and carriers cancellation) and GFDM (with different filters as: Xia with order K=1,4 and roll-off=0.25,0.8 and Gaussian filter, and carriers cancellation techniques) waveforms have been compared using bandwidths 1.4 MHz, 2 MHz, and 5MHz.

Through the investigation of the impact of the time synchronization errors on the performance of the downlink of OFDM and FBMC based multi-cellular networks, it is shown that the timing errors between BSs in the OFDM case cause a severe degradation in system performance. This result is explained by the of orthogonality between all system subcarriers. In contrast to the OFDM system, the FBMC waveform is demonstrated to be less sensitive to timing errors between the different cells, due to the better frequency localization of the prototype filter [C80] (the first paper depicted in this Subsection 3.2).

The primary approach chosen in the European project EMPhAtiC is to reach the needed spectral agility is to utilize highly flexible, variable filter bank based waveform generation and detection methods. The idea is to develop a platform able to process simultaneously alternative filter bank based waveforms, with highly adjustable characteristics, and also able to do the channelization for the legacy signals following the SDR (software defined radio) model, e.g., in case of a multimode base station. One strong candidate is the fast convolution based variable filter bank processing approach of [60, 61] , the structure of which is illustrated in Figs. 2. and 3 in [C77] (the last paper depicted in this Subsection 3.2), depict an example of the subchannel frequency responses for a multimode filter bank which is able to accommodate simultaneously single carrier, FBMC/OQAM, and FMT waveforms. Such variable filter bank structures provide also additional flexibility in adapting to the transmission channel's time- and frequency-selectivity features, as it is possible to use different subchannel bandwidths or prototype filters for each individual user's signal. The proposed filter bank processing approach is particularly important for the base station transmitters and receivers, in which case there is a need to process simultaneously different FB-MC waveforms and legacy signals. Such scheme has proven its potential and capabilities for coexisting in heterogeneous communication environments (5G context evolution).

As a conclusion, from Fig. 3.17 and results depicted in [C83], and in [56], FMT scheme has several benefits in terms of implementation: the classical CP-OFDM digital processing chain is conserved, only adding the FMT filtering block after IFFT computation (Tx side), or before FFT computation (Rx side), with limited added complexity. As a consequence, the 3GPP LTE upper layer (MAC) could be kept identical: same number of resources (RE) and same pilot ratio (RS), more generally speaking, 3GPP LTE physical fields remain unchanged. This constitutes the main advantage of the FMT scheme: relatively good spectral performances in combination with 3GPP LTE upper layer compatibility. On the other hand, we are not able to benefit from enhanced data throughput due to CP removal for example. This is why FMT scheme could be considered as a first step towards broadband for PMR introduction.
From a spectral performances point of view (rejection performances close to the useful bandwidth), is it clear that FBMC waveform is the best choice (compared to FMT scheme). The spectral containment of FBMC scheme over performs the FMT one. Moreover, data throughput is significantly increased due to CP removal. Those great advantages are unfortunately balanced by the fact that the PHY layer frame structure has to be redefined in a very different manner compared to classical CP-OFDM (especially regarding RS structure). FBMC scheme, more promising, could be seen as a second step towards broadband for PMR introduction, implying more standardization efforts, and consequently, increasing the time-to-market.

To resume, all the publications (See Subsection 2.1.1, pp. 30-41) related with this research orientation are: Journals: [J18, J20, J26], Conferences: [C77, C80, C83, C87, C94].

Following are the corresponding depicted papers:

1. [C80]- Faouzi Bader, Musbah Shaat, and Yahia Medjahdi, "New Opportunities for Spectrum Coexistence Using Advanced Multi-carrier Scheme", at workshop on Cognitive Radio at Military Communications and Information Systems Conference MCC'2013 (Invited paper). Saint Malo, France, October 2013.

2. [C83]- Yahia Medjahdi, Didier le Ruyet, Faouzi Bader, and Laurent Martinod, "Integrating LTE Broadband System in PMR Band: OFDM vs. FBMC Coexistence Capabilities and Performances", in the Proc. of the 11th International Symposium on Wireless Communication Systems (ISWCS'2014). Barcelona, Spain. August 2014.

3. [C77]- Markku Renfors, Faouzi Bader, Leonardo Baltar, Didier Le Ruyet, Daniel Roviras, Philippe Mege, Martin Haardt, "On the Use of Filter Bank Based Multi-carrier Modulation for Professional Mobile Radio", at the IEEE Vehicular Technology Conference (VTC-Spring'2013), 2-5 June 2013. Dresden, Germany.

New Opportunities for Spectrum Coexistence Using Advanced Multicarrier Scheme

Faouzi Bader*, Musbah Shaat and Yahia Medjahdi**

*SUPELEC, Rennes-France
Avenue de la Boulaie CS 47601. F-35576 Cesson-Sévigné Cedex. Rennes-France.
Emails: faouzi.bader@supelec.fr , and musbah.shaat@iugaza.edu.ps
**Conservatoire National des Arts et Métiers-CNAM, Paris, 75003, France.
Email: yahia.medjahdi@cnam.fr

(**Invited paper**)

***Abstract*— This paper presents an analysis of capabilities of advanced filter bank based multicarrier schemes such as the FBMC (named also OFDM/OQAM), or the IOTA scheme in the context of spectrum sharing (Cognitive Radio). The throughput of orthogonal frequency division multiplexing (OFDM) and the filter bank multicarrier schemes are compared to reveal the efficiency of using FBMC in the cognitive radio systems. Different problems have been analysed; the spectrum and power allocation problem, the resource allocation in decode and forward multi-relay cognitive network, and finally the impact of the time synchronization errors on the performance of the downlink of OFDM and FBMC based multi-cellular networks. Simulation results contribute in recommending the use of advanced multicarrier filter bank (FBMC) physical layer in future cognitive radio systems.**

I. Introduction

Orthogonal frequency division multiplexing (OFDM) is the most common multicarrier (MC) technique and the most predominant technique used in nowadays wireless communication systems (e.g. WLAN, WiMAX, DVB-T, LTE, etc.). It is also considered by the IEEE 802.22 standard [1] TV based cognitive system that develops an unlicensed wireless regional area network (WRAN) to exploit the unused TV bands.

Using OFDM scheme, consists in splitting up a wide band signal at a high symbol rate into several lower rate signals, each one occupying a narrower band. Consequently, the system performance improves as subcarriers experience flat fading channels. The interference between subcarriers is reduced by maintaining the orthogonality between the different subcarriers. In spite of this, there are several factors that limit achieved capacity in OFDM systems. OFDM utilizes the transmission of the cyclic prefix (CP) to compact the effect of the multiple path propagation which reduces the overall spectral efficiency. In addition to the CP insertion, the large sidelobes of the OFDM frequency response cause high interference to the adjacent unsynchronized sub-carriers, this drawback is considered as the major shortcoming of the OFDM system specially in the spectrum sharing (Cognitive Radio-CR) context where the large sidelobes means more interference to the primary system.

Many techniques have been developed to solve the large sidelobes problem [2] [3]. Instead of using a rectangular pulse to shape the OFDM symbol, a window with soft transition among successive symbols can be used. The raised cosine (RC) windowing is one of the well known techniques to reduce the OFDM sidelobes [2]. One of the drawback of this technique is that it introduces a small reduction on sidelobes close to the mainlobe. It is shown in [2] that the high sidelobe suppression using RC windowing requires a prohibitive length of the cosine tail (overhead). The windowing at the receiver side is another type of techniques that can be used and it requires a suffix samples in addition to the CP which further reduces the bandwidth efficiency. Remark that windowing reduces delay spread tolerance too [2]. These problems are addressed with advanced MC waveforms based on filter bank (FBMC) approach by using a well designed shaping filters which produces a well localized subchannel in both time and frequency domain. Accordingly, FBMC (also named Offset-QAM/OFDM) scheme [9] [10] based on the recent successfully completed EC-funded ICT-PHYDYAS [1] project, made significant progresses in establishing filter bank based MC as a mature technology for spectrum sharing and CR consideration for the development of future wireless communication systems. FBMC has more spectral containment and provide more efficient use of the radio resources where no CP is needed [5] [6]. The spectra of OFDM and FBMC subcarriers are plotted in Fig 1. The OFDM signal has larger sidelobes than the FBMC one. The first sidelobe in OFDM is 13 dB below the mainlobe. In FBMC, the first sidelobe is 40 dB below the mainlobe and the filter attenuation exceeds 60 dB for the frequency range above two subchannel spacings.

This paper focuses on the potential use of advanced MC filter bank based (main emphasis is on PHYDYAS's filter bank prototype presented in [10]) systems for spectrum coexistence and cognitive radio for future generation of wireless communications. A comparative performance analysis with conventional OFDM scheme is presented. The paper addresses both the non-relayed and Decode and Forward (DF)-relayed transmission scenarios. Additionally, the problem of timing

[1] PHYDYAS-Physical Layer for Dynamic Spectrum Access and Cognitive Radio [4].

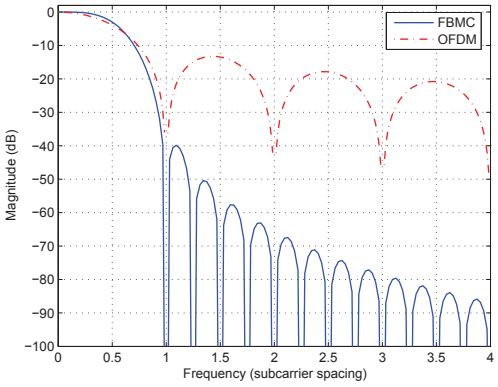

Fig. 1. Frequency response of OFDM and FBMC filters

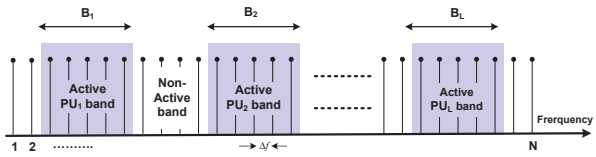

Fig. 2. Frequency distribution of the active and non-active primary bands.

misalignment between neighboring cells is addressed.

The rest of this paper is organized as follows: Section II describes the different scenarios that are considered in this paper. Additionally, the performance of the CR system using both the OFDM and the FBMC schemes is compared under the different scenarios. Section III, concludes the papers.

II. OFDM VERSUS FBMC PERFORMANCE ANALYSIS IN DIFFERENT SCENARIOS

In the sequel, a description of the different analyzed scenarios is provided including the main definitions related to each context/scenario.

A. Spectrum and power allocation in spectrum sharing scenario

Here, the downlink scenario is considered. The system sharing spectrum coexists with the primary users (PUs) radio in the same geographical location. The cognitive base station (CBS) transmits to its secondary users (SUs) and causes interference to the PUs. Moreover, the PUs base station interferes with the SUs. The CR system's frequency spectrum is divided into N subcarriers each having a Δf bandwidth. The side by side frequency distribution of the PUs and SUs is assumed as shown in Fig. 2. The frequency bands B_1, B_2,$\cdots$,B_L have been occupied by the PUs (active PU bands) while the other bands represent the non-active PU bands. It is assumed that the CR system can use the non-active and active PU bands provided that the total interference introduced to the l^{th} PU band does not exceed the value I_{th}^{l} which is the maximum interference power that can be tolerated by PU_l.

The interference introduced by the i^{th} subcarrier to l^{th} PU, $I_i^l\left(d_i,P_i\right)$, is the integration of the power spectral density (PSD), $\Phi_i\left(f\right)$, of the i^{th} subcarrier across the l^{th} PU band, B_l, and can be expressed as [7]

$$I_i^l\left(d_i,P_i\right)=\int_{di-B_l/2}^{di+B_l/2}\left|g_i^l\right|^2 P_i\Phi_i\left(f\right)\,df\triangleq P_i\,\Omega_i^l \tag{1}$$

where P_i is the total transmit power emitted by the i^{th} subcarrier and d_i is the spectral distance between the i^{th} subcarrier and the l^{th} PU band. g_i^l denotes the channel gain between the CBS and the l^{th} PU on the subcarrier i. Ω_i^l denotes the interference factor of the i^{th} subcarrier to the l^{th} PU band.

The interference power introduced by the l^{th} PU signal into the band of the i^{th} subcarrier is [2]

$$J_i^l\left(d_i,P_{PU_l}\right)=\int_{di-\Delta f/2}^{di+\Delta f/2}\left|y_i^l\right|^2\psi_l\left(e^{j\omega}\right)\,d\omega \tag{2}$$

where $\psi_l\left(e^{j\omega}\right)$ is the power spectral density (PSD) of the PU_l signal and y_i^l is the channel gain between the i^{th} subcarrier and l^{th} PU signal. The PSD expression, $\Phi_i\left(f\right)$, depends on the used MC technique.

The OFDM PSD is expressed as follows

$$\Phi_{OFDM}\left(f\right)=\frac{\sigma_x^2}{T}\sum_k\left|G_T\left(f-\frac{k}{N}\right)\right|^2 \tag{3}$$

where $G_T\left(f\right)$ is the Fourier transform of the pulse shape $g_T\left(n\right)$, $T=C+N$ is the length of the OFDM symbol in number of samples where C is the length of CP in number of samples and N is the IDFT size, σ_x^2 is the variance of the zero mean (symmetrical constellation) and uncorrelated input symbols and $\{k\}$ is the set of subcarrier indices. The pulse shape $g_T\left(n\right)$ can be chosen as

$$g_T\left(n\right)=\begin{cases}1 & n=0,1,\cdots,T-1\\ 0 & \text{otherwise}\end{cases} \tag{4}$$

and hence its Fourier transform is

$$\left|G_T\left(f\right)\right|^2=T+2\sum_{r=1}^{T-1}\left(T-r\right)\cos\left(2\pi fr\right) \tag{5}$$

Additionally, the PSD of the FBMC can be expressed by [10]

$$\Phi_{FBMC}=\frac{\sigma_r^2}{\tau_\circ}\sum_k\left|H\left(f-\frac{k}{N}\right)\right|^2 \tag{6}$$

where $H\left(f\right)$ is the frequency response of the prototype filter with coefficients $h\left[n\right]$ with $n=0,\cdots,W-1$, where $W=KN$, and K is the length of each polyphase components (overlapping factor) while N is the number of the subcarriers. Additionally, $\{k\}$ is the set of subcarrier indices, $\sigma_r^2=\frac{\sigma_x^2}{2}$ is the FBMC symbol variance, and τ_o is FBMC symbol duration. Assuming that the prototype coefficients have even symmetry around the $\left(\frac{KN}{2}\right)^{th}$ coefficient, and the first coefficient is zero we get

$$\left|H\left(f\right)\right|=h\left[W/2\right]+2\sum_{r=1}^{\frac{W}{2}-1}h\left[\left(W/2\right)-r\right]\cos\left(2\pi fr\right). \tag{7}$$

To make a parallel between OFDM and FBMC, we place ourselves in the situation where both systems transmit the same quantity of information. This is the case if they have the same number of subcarriers N together with duration of τ_o samples for FBMC real data and $T = 2\tau_o$ for the complex QAM ones [11]. Note that the objective here is to maximize the downlink capacity of the network under both total power and interference introduced to the primary users (PUs) constraints[2]. The performance of using FBMC instead of OFDM systems is depicted in Fig.3. The optimal solution is obtained by using the interior point method while the PI-solution is obtained by applying the low complexity two step algorithm described in details in [12]. Zhang-algorithm refers to the algorithm proposed in [13]. For FBMC system, the prototype coefficients are assumed to be equal to PHYDYAS coefficients with overlapping factor $K = 4$ [9] [10] and the OFDM system is assumed to have a CP of 6.67%. An MC system of three cognitive users with $N = 32$ subcarriers is assumed, also that each subcarrier can be used for transmission to at most one user at any given time and is assigned to the user who has the best channel gain for that subcarrier. The value of T_s, Δ_f and P_T are assumed to be 4μ second, 0.3125 MHz and 1 watt respectively. AWGN of variance 10^-6 is assumed. Without loss of generality, the interference induced by PU's to the SU's band is assumed to be negligible. The channel gains are outcomes of independent, identically distributed (i.i.d) Rayleigh distributed random variables (rv's) with mean equal to "1" and assumed to be perfectly known at the CBS. Two interference constraints belonging to two active PU bands , i.e. $L = 2$, is assumed. Each active PU band is assumed to have six subcarriers where $\mid N1 \mid = \mid N2 \mid = 16$. All the results have been averaged over 1000 iterations.

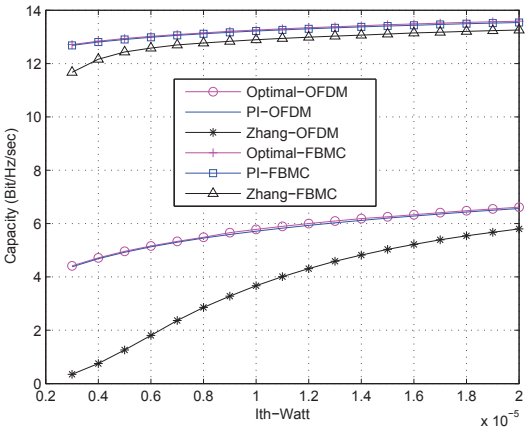

Fig. 3. : Achieved CR vs allowed interference threshold (low) for OFDM and FBMC based CR systems - Two active bands .

It can be noticed that Zhang algorithm has a limited performance with low interference constraints because the algorithm turns off the subcarriers that have a noise level more than the initial waterfilling level and never uses these subcarriers again even if the new waterfilling level exceeds its noise level. Moreover, the algorithm deactivates some subcarriers, i.e. transmit zero power, in order to ensure that the interference introduced to PU bands is below the pre-specified thresholds. The lower the interference constraints, the more the deactivated subcarriers which justifies the limited performance of this algorithm in low interference constraints. Note that achieved capacity of FBMC system is higher than that of OFDM based one because the sidelobes in FBMC PSD is smaller than that in OFDM which introduces less interference to the PUs. Moreover, the inserted CP in OFDM based CR systems reduces the total capacity of the system. It can be noticed also that the interference condition introduces limited restriction on the capacity of FBMC system based systems which is not the case when OFDM scheme is used. Results illustrated in Fig. 3 proves the efficiency of using FBMC in spectrum sharing CR context.

[2]see the optimisation problem formulation in equation (6) of reference [12].

B. DF in multi-relay spectrum sharing scenario

In this context, a cooperative CR system coexist in the same geographical area with the primary system. The CR system uses the vacant spectrum left by the primary system and should not introduce severe interference to it. The relays are assumed to operate in half-duplex mode with DF-protocol, thus receiving and transmitting in two different time slots. In the first time slot, the source transmits to the different relays while in the second time slot the relays decode the message, re-encode it and then forward it to the destination. The j^{th} subcarrier in the source should be paired with only one subcarrier k in the destination which may not be the same as j to form the (j,k) pair that should be assigned to only one relay m. The maximum total transmission powers that can be used in the source and the different relays are P_S and P_{R_m} respectively. The transmission rate of the j^{th} subcarrier in the source coupled with the k^{th} subcarrier in the destination and assigned to the m^{th} relay, $Rate_{m,(j,k)}$, can be evaluated as follows

$$Rate_{m,(j,k)} = \frac{1}{2}\min\left\{\begin{array}{l}\log_2\left(1+\frac{P^j_{SR_m}H^j_{SR_m}}{\sigma^2_{j,m}}\right)\\ \log_2\left(1+\frac{P^k_{R_mD}H^k_{R_mD}}{\sigma^2_{k,m}}\right)\end{array}\right. \quad (8)$$

where $P^j_{SR_m}(P^k_{R_mD})$ is the power transmitted over the $j^{th}(k^{th})$ subcarrier in the Source to$R_m(R_m$to Destination) link. R_m means the m^{th} relay. Moreover, $H^j_{SR_m}(H^k_{R_mD})$ is the square of the $j^{th}(k^{th})$ subcarrier fading gain over Source to$R_m(R_m$to Destination) link. $\sigma^2_{j,m(k,m)} = \sigma^2_{AWGN_{j,m(k,m)}} + J_{j(k)}$, where $\sigma^2_{AWGN_{j,m(k,m)}}$ is the variance of the additive white Gaussian noise (AWGN) on the Source to$R_m(R_m$to Destination) link, and $J_{j(k)}$ is the interference introduced by the PU signal into the $j^{th}(k^{th})$ subcarrier which is evaluated using (2) and can be modeled as AWGN (see in reference (6) in [14]). Without loss of generality, the noise variance is assumed to be constant for all subcarriers. If

the source transmits to the destination over the direct link, the transmission rate of the j^{th} subcarrier is given by

$$R_{Direct}(j) = \frac{1}{2}\log_2\left(1 + \frac{P_S^j H_{SD}^j}{\sigma_{j,D}^2}\right). \quad (9)$$

The main objective here is to maximize the CR system throughput by determining the subcarriers that will be used for the direct transmission and those which will be used for relayed transmission and optimize the subcarrier pairing and relays assignment for the subcarriers used for relayed transmission. The available power budgets in the source and the different relays should be distributed among the subcarriers so that the instantaneous interference introduced to the primary system is below the maximum limit. Therefore, the optimization problem can be following equations (5) and (6) in [14]. The optimal scheme adopts the dual decomposition technique and in order to reduce the computational complexity of the optimal scheme, a greedy suboptimal algorithm is developed in section IV of [14].

The simulations are performed under the assumption of having a multicarrier system of N = 64 subcarriers with M = 5 relays. The values of Ts, Δf, and σ^2 are assumed to be 4μ seconds, 0.3125 MHz and 10.6 respectively. The channel gains are outcomes of independent Rayleigh distributed random variables with mean equal to 1. All the results have been averaged over 1000 iterations. In the simulations, optimal with direct and suboptimal algorithms apply the dual decomposition technique presented in [14]. To maximize the achieved capacity while maintain the interference introduced to the primary system below a pre-specified threshold, the network resources are optimized jointly using the dual decomposition technique, and a greedy suboptimal algorithm is developed to reduce the computational complexity of the dual decomposition scheme. Details on above mentioned algorithms are out of the scope of this paper and can be found in [14]. Fig 4 shows the

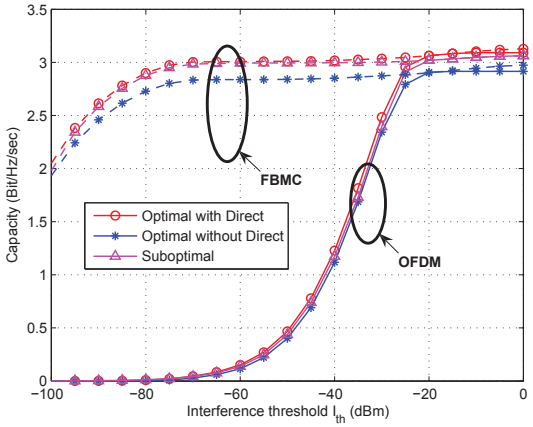

Fig. 4. : Achieved capacity vs. interference threshold with P_s=PR_m when PI_{th} = -30 dBm. OFDM system is plotted in solid lines, FBMC is plotted in dashed lines.

achieved capacity of the different algorithms vs. the interference threshold using OFDM and FBMC physical layers. For the OFDM case, It can be noticed that the capacity is increased by considering the relayed transmission with ability of using the direct link in some subcarriers. Additionally, as the interference threshold increases, the achieved capacity of the CR is also increases. This can be justified by the increase of the CR system ability to use higher transmission powers on the subcarriers. In addition to that, one can notice the close performance of the suboptimal algorithm to that of the optimal algorithm. This is because of the non-cognitive like behavior of the CR system in this region. Regarding the performance of OFDM and FBMC systems, two different performance regions can be identified as follows: (i) when I_{th} $\leq$30 dBm: the capacity of the FBMC based CR systems is more that of the OFDM based ones. This is because of the small sidelobes of the FBMC systems in adition to the loss of the spectrum efficiency in OFDM due to the use of the CP. Therefore, the interference constraint generally has small effect on the performance of the FBMC based systems which is not the case in OFDM ones, (ii) when I_{th} $\geq$30 dBm: both of the system has almost the same performance when operating with high interference thresholds or low power budgets. This can be justified by noting that the systems in this region operate in non cognitive-like environment. Similarly, in Fig. 5, the region

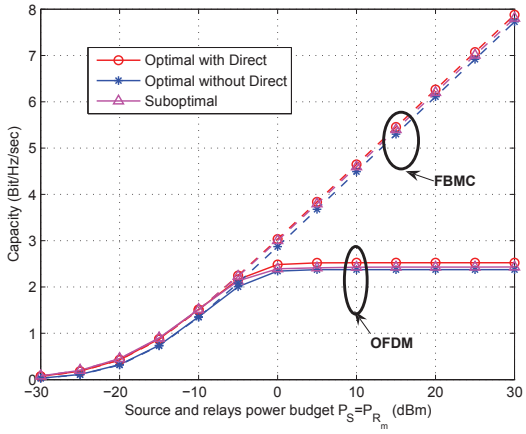

Fig. 5. : Achieved capacity vs. interference threshold with P_s=PR_m = 0 dBm. OFDM is plotted in solid lines, and FBMC is plotted in dashed lines.

when $P_S = P_{Rm}$ $\leq$-5 dBm represents the noncognitive-like environment; where the available power budget is not able to introduce high interference. When the power constraints increase more than this value, FBMC system has significantly improves the CR capacity since FBMC based systems can use more transmission power which increase the total system capacity.

C. Asynchronous multi-Cellular networks scenario

This subsection is devoted to describing the system model of the downlink of OFDM and FBMC based multi-cellular networks. The target of this study is to consider the case

the case where primary and secondary users have different physical layers standards and working in multi-cell scenario. The reference mobile user is located at (u, v). The reference base station is assumed to be situated at the origin $(u_0, v_0) = (0, 0)$. In this analysis, we consider two tiers of the neighboring cells that are surrounding the reference mobile user. Let the k-th base station be located at (u_k, v_k), then, the distance between the reference mobile user and the k-th base station is given by

$$d_k = \sqrt{(u_k - u)^2 + (v_k - v)^2} \tag{10}$$

Concerning the frequency reuse scheme, the subcarriers are allocated according to the most common subcarrier assignment scheme, namely, the subcarrier block assignment scheme [16]. In this scheme it is assumed that δ adjacent subcarriers to each block are free and serve as guard bands between the different blocks. All signals propagate through different multipath channels using a similar propagation model, where the impulse response of the multipath channel between the k-th base station and the reference mobile user is given by

$$h_k(t) = \sum_{i=0}^{L-1} h_{k,i}\delta(t - \tau_{k,i}) \tag{11}$$

Because of the timing misalignment between the neighboring cells and the reference one, the signals arriving from the cells in the vicinity will appear non-orthogonal to the desired signal. This non-orthogonality will generate interference and will degrade the SINR.

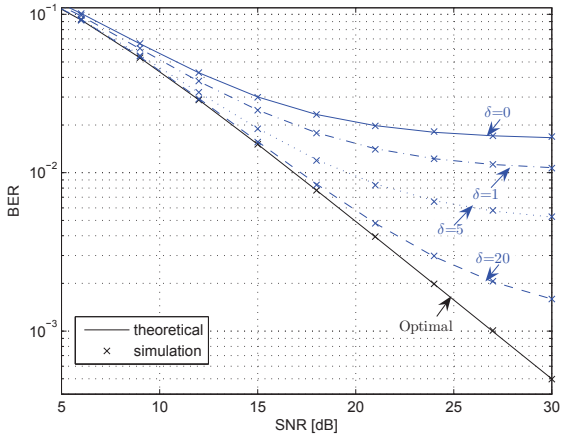

Fig. 6. : OFDM average BER vs. SNR for different guard band size δ=0,1,2 with $\tau \in$ [0,T]

The impact of the guard-band length δ on the system performance could be also observed. Fig.6 shows the OFDM average BER against the SNR for different guard band values δ =0, 1, 5 and 20 subcarriers. The timing offset τ is assumed to be a uniform RV defined on [0,T]. Comparing the different curves, one can see that the performance improves with increasing δ. However, there is still a remaining gap with respect to the optimal case even with a guard-band of δ= 20 subcarriers. In contrast to the OFDM case, the FBMC waveforms present, in Fig.7, an excellent performance and provide the same BER values as for the optimal case with a guard-band of a single subcarrier δ =1 in the case of PHYDYAS and 2 subcarriers δ = 2 for the IOTA case.

The BERs of PHYDYAS and IOTA (Isotropic Orthogonal Transform Algorithm) citeSiohan2006 filter based systems have also been evaluated in different timing offset scenarii : (a). $\tau \in$ [0,T/7] (b). $\tau \in$ [0,T/4] and (c). $\tau \in$ [0,T]. Through the results shown in Fig.7, it can be observed that the FBMC waveforms are not sensitive to the timing offset interval length because the significant interference (with a power level higher than 30 dB) is roughly invariant with respect to the timing offset value.

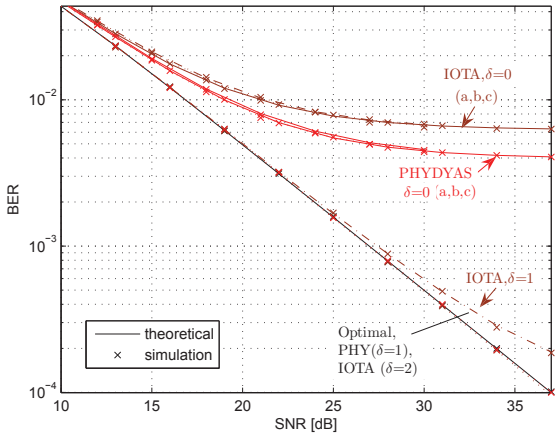

Fig. 7. : FBMC average BER vs. SNR for different guard band size δ=0,1,2 with (a). $\tau \in$[0,T/7] (b). $\tau \in$[0,T/4] (c). $\tau \in$[0,T]

The impact of timing synchronization errors on the BER performance of the downlink of OFDM and FBMC based multi-cellular networks has been investigated. Through this evaluation, we have shown that in OFDM case, timing errors between BSs cause a severe degradation in system performance. This result is explained by the loss of orthogonality between all system subcarriers. In contrast to the OFDM system, the FBMC waveforms are demonstrated to be less sensitive to timing errors between the different cells, due to the better frequency localization of the prototype filter.

New application of advanced filter based multicarrier schemes in the context of future broadband Professional Mobile Radio (PMR) communications -in particular the evolution of the Public Protection & Disaster Relief (PPDR)- is under development within the recently started EMPhAtiC[3] EC-funded project [17]. The target here is to provide broadband data services in coexistence with narrowband legacy services

[3]Enhanced Multicarrier Technicques for Professional Ad-hoc and Cell Based Communication.

of the TETRA family. The core idea is a multi-mode radio platform, based on variable filter-bank processing, which is able to perform modulation/detection functions simultaneously for different signal formats with adjustable center frequencies, bandwidths and subchannel spacings [18].

III. Conclusions

In this paper, we provided some performance comparisons between the usage of OFDM and filter based MC schemes as the IOTA and the developed within the PHYDYAS project (FBMC). Different spectrum sharing scenarios have been considered and analysed. In the context of spectrum and power allocation, obtained results prove that the FBMC based CR systems have more capacity than OFDM based ones, mainly under very low interference conditions which introduces limited restriction on the capacity of FBMC system based systems which is not the case when OFDM scheme is used. In the context of resource allocation problem in multiple relay DF with direct link, FBMC system has significantly improve the CR capacity since it can use more transmission power which increases the total system capacity.

To maximize the achieved capacity while maintaining the capacities achieved, FBMC scheme proved its high capacity in such scenarios compared with the OFDM. Through the investigation of the impact of the time synchronization errors on the performance of the downlink of OFDM and FBMC based multi-cellular networks, it is shown that the timing errors between BSs in the OFDM case cause a severe degradation in system performance. This result is explained by the loss of orthogonality between all system subcarriers. In contrast to the OFDM system, the FBMC waveform is demonstrated to be less sensitive to timing errors between the different cells, due to the better frequency localization of the prototype filter. As a general output from this paper, obtained results in the spectrum sharing (CR) context contribute in recommending the use of advanced multicarrier filter bank (FBMC) physical layer in future cognitive radio systems.

References

[1] Stevenson, C. Chouinard, G.; Zhongding Lei; Wendong Hu; Shellhammer, S.J.; Caldwell, W. "IEEE 802.22: The first Cognitive Radio Wireless Regional Area network standard," *IEEE Communications Magazine*, Volume: 47 , Issue: 1, pp. 130 - 138. January 2009

[2] T. Weiss, J. Hillenbrand, A. Krohn, and F.K. Jondral,"Mutual Interference in OFDM-based Spectrum Pooling Systems," in 59^{th} *Vehicular Technology Conference*, (VTC'2004), May 2004, vol. 4, pp. 1873 to 1877.

[3] R. Xu and M. Chen, "A Precoding Scheme for DFT-based OFDM to Suppress Sidelobes," *IEEE Communications Letters*, vol. 13, no. 10, pp.776 to 778, 2009.

[4] FP7-ICT PHYDYAS - Physical Layer for Dynamic Spectrum Access and Cognitive Radio. http://www.ict-phydyas.org

[5] H. Zhang, D. Le Ruyet, and M. Terré, "Spectral Efficiency Comparison between OFDM/OQAM and OFDM Based CR Networks," *Wireless Commun. and Mobile Computing Wiley*, vol. 9, pp. 1487 to 1501, Nov. 2009.

[6] B. Farhang-Boroujeny, "OFDM Versus Filter Bank Multicarrier," in *IEEE Signal Processing Magazine*, pp.92 to 112, May 2011.

[7] T. Weiss, J. Hill enbrand, A. Krohn, and F. K. Jondral, "Mutual Interference in OFDM-based Spectrum Pooling Systems," in Proceedings of the 59^th *IEEE Vehicular Technology Conference* (VTC'04), vol. 59, Milan, Italy, May 2004.

[8] B. Farhang-Boroujeny, "Filter Bank Spectrum Sensing for Cognitive Radios," in *IEEE Transactions on Signal Processing*, vol. 56, no. 5, pp. 1801 to 1811, 2008.

[9] M. G. Bellanger, "Specification and Design of a Prototype Filter for Filter Bank Based Multicarrier Transmission," in *Proc. IEEE Int. Conf. Acoustics, Speech, and Signal Processing*, pp. 2417 to 2420, Salt Lake City, USA, May 2001.

[10] M. G. Bellanger, "Phydyas : Analytical Expressions for the Reference Prototype filter," *Tech. report*, pp. 1-4, Feb. 2009, CNAM, Paris.

[11] Skrzypczak, A and Siohan, P and Javaudin, J.P, "Power Spectral Density and Cubic Metric for the OFDM/OQAM Modulation," in Proc. of the *IEEE Symposium on Signal Processing and Information Technology* (ISSPIT'2006). Vancouver-Canada. August 2006.

[12] M. Shaat and F. Bader, "A Two-Step Resource Allocation Algorithm in Multicarrier Based Cognitive Radio Systems," in Proc. *IEEE Wireless Communications and Networking Conference* (IEEE WCNC'2010). pp.1-6. Sydney, Australia. April 2010.

[13] Y. Zhang, "Resource allocation for OFDM-based cognitive radio systems", Ph.D. dissertation, University of British Columbia, Vancouver, Canada, December 2008.

[14] M. Shaat and F. Bader, "Joint Resource Optimization in Decode and Forward Multi-Relay Cognitive Network With Direct Link," in the Proc. *the IEEE Wireless Communications and Networking Conference* (IEEE WCNC'2012). Paris, France. April 2012.

[15] G. Stuber, S. Almalfouh and D. Sale, "Iterference analysis of TV-band whitespace," in the Proc. *the Proceedings of the IEEE*, vol. 97, nº4, pp.741-754. April 2009.

[16] Y. Medjahdi, M. Terré, D. Le Ruyet, and D. Roviras, and A. Dziri, "Performance Analysis in the Downlink of Asynchronous OFDM/FBMC Based Multi-Cellular Networks," *IEEE Transactions on Wireless Communications*, Vol. 10, Nº. 8, August 2011.

[17] European Funded research project on "Enhanced Multicarrier Technicques for Professional Ad-hoc and Cell Based Communication" ICT-EMPhAtiC wih code:318362),$http : //www.ict - emphatic.eu$ (visited 25 June 2013)

[18] M. Renfors, F. Bader, L. Baltar, D. Le Ruyet, D. Roviras, P. Mege, M. Haardt, "On the Use of Filter Bank Based Multicarrier Modulation for Professional Mobile Radio," at Proc. of the *IEEE Vehicular Technology Conference* (VTC-Spring'2013), Dresden, Germany. June 2013.

Integrating LTE Broadband System in PMR Band: OFDM vs. FBMC Coexistence Capabilities and Performances

Yahia Medjahdi[1], Didier le Ruyet[2], Faouzi Bader[3], and Laurent Martinod[4]
[1]ICTEAM, Université Catholique de Louvain. Place du Levant, 2, 1348 Louvain-la-Neuve, Belgium
Email: yahia.medjahdi@uclouvain.be
[2]CNAM, Paris, France. Email: didier.le_ruyet@cnam.fr
[3]SUPELEC, Rennes, France. Email: faouzi.bader@supelec.fr
[4]CASSIDIAN Systems, Elancourt, France. Email: laurent.martinod@cassidian.com

***Abstract*—This paper focuses on the use of Long Term Evolution (LTE) broadband system in coexistence with currently deployed Professional Mobile Radio (PMR) communication systems. The coexistence capabilities are analyzed using of an LTE like based system with Orthogonal Frequency Division Multiplexing (OFDM) and Filter Bank MultiCarrier (FBMC) physical layers. Obtained results show that, in order to achieve the LTE-PMR coexistence, we need to filter the synthesized OFDM signal. This filtering is made to protect the PMR (TETRA, TETRAPOL, TETRA TEDS standards, etc.) systems by reducing the sidelobes levels due the use of modulated OFDM scheme. On the other hand, the FBMC signal fits perfectly the LTE-TEDS harmful interference protection requirements starting from the minimum frequency offset allowed by the TEDS standard mask. This can be explained by the fact that a good frequency localization is achieved by the prototype filter used in the FBMC scheme.**

I. Introduction

Nowadays, PMR and Public Protection and Disaster Relief services (PPDR) are fundamentally used for low-rate data transmission like voice communications. This is due to the limited throughput resulting from the small bandwidths used by these systems [1]. Recently, there is a trend to upgrade the PMR systems to support high-rate applications and broadband services. To upgrade the PMR/PPDR networks (TETRA[1]1, TETRAPOL, TETRA Enhanced Data Services-TEDS, etc.) [1][2] towards supporting broadband data communications services, new capacity is required and can be achieved with two complementary ways; i) by obtaining new bandwidths for PMR/PPDR data services, and ii) by fitting a novel broadband data service within the scarcity (which is the European case) of available spectrum devoted to PMR systems (depending on customers, reserved bands are located in: 380-400 MHz, 410-430 MHz, or 450-470 MHz). To satisfy the growing demands, both directions actually have to be followed. One of the major issues is being able to introduce new broadband data services within the current frequency allocation, in coexistence and cohabitation with the currently deployed and active PMR/PPDR systems. Having in mind the widely expected dominance of 3GPP LTE systems, it is natural to consider the LTE system as a reference basis in the PMR/PPDR system development due to its high data rate, modularity, and adoption by world wide mobile companies. Broadband systems such as LTE rise as one of the most attractive candidates that can achieve very high data rates.

Multicarrier transmission is the predominant technique used in nowadays wireless communication systems (e.g. WLAN, WiMAX, DVB-T, LTE, etc.) where a wide band signal at a high symbol rate is split into several lower rate signals, each one occupying a narrower band. Consequently, the system performance improves as subcarriers experience flat fading channels and are by construction orthogonal to one another thus minimizing the threat of interference.

However, the possible deployment of broadband systems in PMR bands is still facing important challenges as several technical constraints must be overtaken, mainly those related to coexistence with the currently existing narrowband PMR commercial devices (primary systems). The primary objective of this paper is to examine the coexistence between PMR narrowband systems with LTE-based Broadband system. At the waveform level, the main issue is the poor spectral containment of the OFDM subcarriers, leading to high side-lobes of the modulated OFDM spectrum. These high side-lobes create interference to adjacent systems frequencies and are thus problematic in the coexistence scenario to be addressed. However, the filter bank multicarrier system (FBMC) does not require any CP extension and can overcome the spectral leakage problem by minimizing the sidelobes of each subcarrier and therefore lead to high efficiency [4], [5], [6]. Additionally, a high flexibility is needed to utilize effectively the variable spectral gaps between different narrowband PMR users.

In this paper, we analyze the interference effect caused by a deployed multicarrier broadband (LTE-like) system in the PMR channel. Two different multicarrier techniques are used: OFDM and FBMC schemes, and their direct impact and effect on the system coexistence performances are analyzed.

In the following, first in Section II we describe the coexistence scenario and PMR system requirement defined in the ETSI TETRA standard. In Section III, some key parameters

[1]TETRA: Terrestrial Trunked Radio

978-1-4799-5863-4/14/$31.00

related with the LTE system and used for the context analysis are defined. Section IV, encompass the interference performance analysis in PMR channel using a 1.4MHz,3MHz, and 5MHz LTE bands. The analysis includes achieved coexistence using OFDM and FBMC schemes.

II. Coexistence scenario and PMR system requirements

We analyze in this paper the possibility to deploy an LTE broadband system in a 5MHz PMR channel (located in the 400MHz band). As stated in the introduction, the broadband system should respect the constraints imposed by the already existing and operational PMR communication devices. The PMR system considered for the analysis is an ETSI TEDS standard [1] which is currently widely used by public safety organisms both privates and governmental, and by around two millions of business users over the world. Figure 1, illustrates the considered coexistence scenario in a 5MHz PMR band, where an LTE-like system is used. Note that different PMR equipments using TETRA1 and TETRA2 standards are currently deployed in the 5MHz bandwidth. Depicted systems in Figure 1 are two TEDS of 25kHz bandwidth each. The main goal (as it can be shown in Figure 1) is to deploy an LTE-like broadband system in the spectrum holes of the PMR bands by strictly accomplishing the PMR standards interference blocking recommendations. This can be achieved by respecting the reception masks of the currently active PMR systems. Here, Δf_1 and Δf_2 refer to the frequency distances between the nearest adjacent interferer channels and the nominal carrier frequencies of the existing active users in the band.

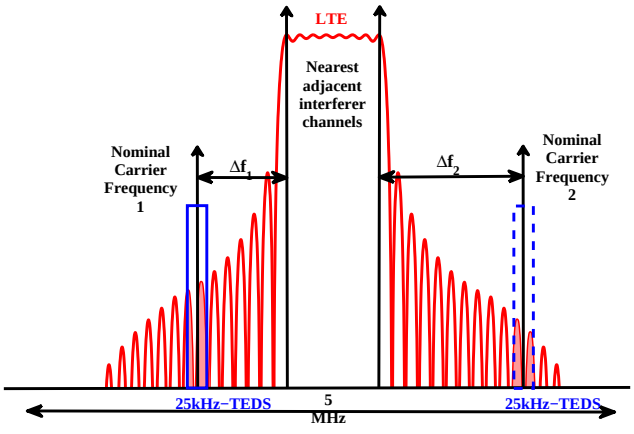

Fig. 1. LTE broadband in coexistence with narrowband PMR systems

In order to ensure the PMR/LTE cohabitation, the out-of-band radiation of the deployed LTE system should not exceed the levels defined by the reception mask of the TEDS standard. The TEDS reception mask can be computed based on the blocking levels presenting the interfering signal powers as function of frequency offsets between the nominal carrier frequency of the TEDS system and the nearest adjacent interfering channel. In this work, we focus on the 25 kHz-TEDS case, however, the extension to other PMR standards is straightforward.

Based on the blocking levels given in Table I, we can compute the TEDS reception mask corresponding to 4, 16, and 64 QAM constellations. A slight difference can be observed between the obtained masks. Accordingly, only the 4-QAM case will be considered in the sequel of this paper.

TABLE I
Blocking levels of the 25 kHz-TEDS receiver defined in [1]

offset from nominal Rx freq.	level of interfering signal
50 kHz to 100 kHz	-40 dBm
100 kHz to 200 kHz	-35 dBm
200 kHz to 500 kHz	-30 dBm
$>$ 500 kHz	-25 dBm

TABLE II
25 kHz-TEDS reception mask

offset from nominal Rx freq.	4-QAM	16-QAM	64-QAM
50 kHz to 100 kHz	-81.4 dBm	-81.4 dBm	-82.6 dBm
100 kHz to 200 kHz	-86.4 dBm	-86.4 dBm	-87.6 dBm
200 kHz to 500 kHz	-91.4 dBm	-91.4 dBm	-92.6 dBm
$>$ 500 kHz	-96.4 dBm	-96.4 dBm	-97.6 dBm

III. LTE-based broadband systems

In this paper, we consider the LTE system with different transmission bandwidths where main parameters summarized in Table III [12],

TABLE III
LTE PHY layer main parameters [3]

Transmission bandwidth	1.4 MHz	3 MHz	5 MHz
Subcarrier spacing	15 kHz	15 kHz	15 kHz
FFT size	128	256	512
Useful subcarriers(with DC)	73	181	301
Effective bandwidth	1.08 MHz	2.7 MHz	4.5 MHz

Furthermore, two multicarrier physical layers (PHY) are considered and analyzed for the coexistence analysis: i) the cyclic prefixed orthogonal frequency division multiplexing (CP-OFDM) using the rectangular pulse shape, ii) and the filterbank multicarrier technique (FBMC) using the prototype filter proposed in the European funded project "Physical Layer for Dynamic Access and Cognitive Radio-PHYDYAS" [7].

The interference analysis is based on the power spectral density (PSD) model which is commonly used in the scientific literature [9], [10]. This evaluation is based on the PSD method, and it is measured based on the spectral distance calculation of the out-of band radiation value between a designed carrier and its spectral distance from the primary

band. According to [10], the resulting interference power in a given bandwidth $[f_1, f_2]$ is defined by,

$$I = \int_{f_1}^{f_2} \Phi(f) df \tag{1}$$

where $\Phi(f)$ is the PSD which depends on the considered multicarrier technique. In case of CP-OFDM PHY systems, the normalized PSD has been computed as in [10] and is given by

$$\Phi_{\mathrm{OFDM}}(f) = T_{\mathrm{OFDM}} \left(\frac{sin(\pi f T_{\mathrm{OFDM}})}{\pi f T_{\mathrm{OFDM}}} \right)^2 \tag{2}$$

where $T_{\mathrm{OFDM}} = T + \Delta$, with T the useful symbol duration, and Δ the CP duration.
Concerning the FBMC system, the PSD of the PHYDYAS's project waveform is expressed as follows [11],

$$\Phi_{\mathrm{PHYDYAS}}(f) = (G(f))^2 \tag{3}$$

Here, $G(f)$ is the square root of the PHYDYAS filter frequency response which is given by,

$$G(f) = \sum_{k=-(K-1)}^{k=(K-1)} G_k \frac{\sin\left(\pi \left(f - \frac{k}{NK}\right) NK\right)}{NK \sin\left(\pi \left(f - \frac{k}{NK}\right)\right)} \tag{4}$$

where, K is the overlapping factor of the prototype filter and the coefficients G_k depend on the overlapping factor K. For example, when $K = 4$, we have $G_1 = 0.971960$, $G_2 = \sqrt{2}/2$, and $G_3 = 0.235147$ [11]. Figure 2 depicts the PSDs of

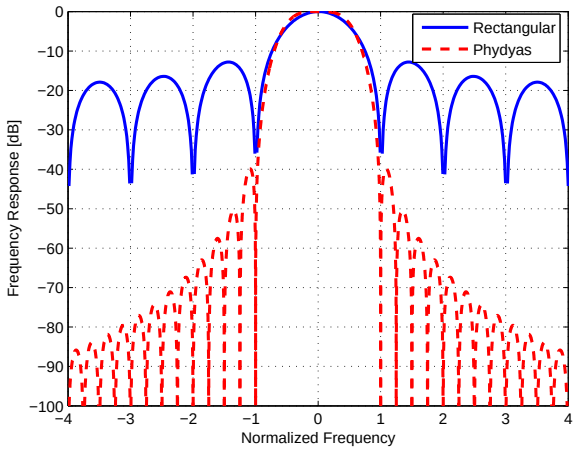

Fig. 2. OFDM (refereed as "rectangular") and FBMC (refereed as "Phydyas") Power Spectral Densities

single modulated subcarrier of both systems: the CP-OFDM (refereed as rectangular) and the FBMC (refereed as Phydyas). Comparing the two PSDs, it can be seen that the PHYDYAS scheme offers better frequency localization compared to the OFDM scheme using the rectangular pulse shape in the time domain. It is clear that the high frequency localization of the PHYDYAS filter prototype offers a much higher spectrum contention allowing higher capabilities for spectrum sharing and coexistence.

IV. Interference analysis

In what follows, the effective interference power caused by LTE systems is computed in a bandwidth of 25 kHz with respect to the different frequency offsets Δf given in Table II. It is worth noticing that the LTE transmit power, in the three cases, is fixed at 0 dBm. Furthermore, both the PMR base station and the LTE one are assumed to be adjacently situated (i.e. the PMR transmitter and the LTE one are at equal distances from the PMR-receiver).

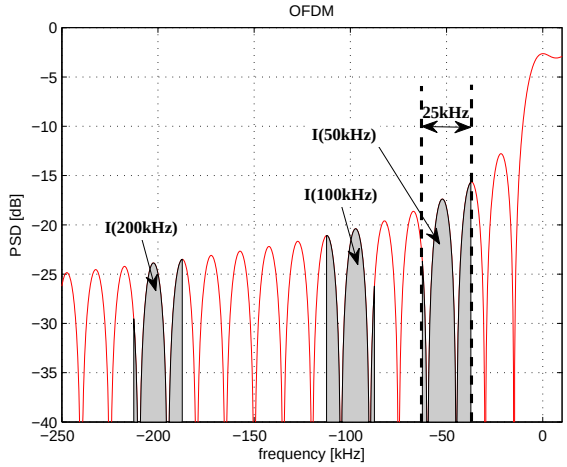

Fig. 3. : Effective interference levels of 1.4 MHz-LTE (73 active subcarriers) in 25 kHz-TEDS band, OFDM case

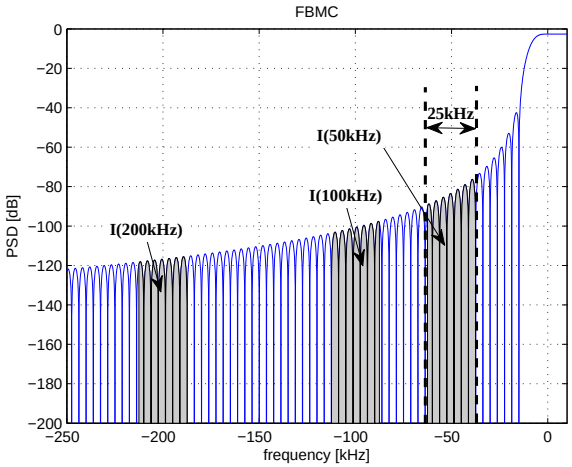

Fig. 4. : Effective interference levels of 1.4 MHz-LTE (73 active subcarriers) in 25 kHz-TEDS band, FBMC case

Figure 3 and 4 show an example of this interference when we have a 1.4 MHz-LTE system using OFDM and FBMC techniques, respectively. The gray-colored areas correspond

to the effective interference powers occurring in the 25 kHz-TEDS band for the frequency offsets Δf =50 kHz, 100 kHz and 200 kHz. Figure 5 depicts the variation of the effective interference levels [in dBm] generated by OFDM-based LTE system with respect to the frequency offset Δf.

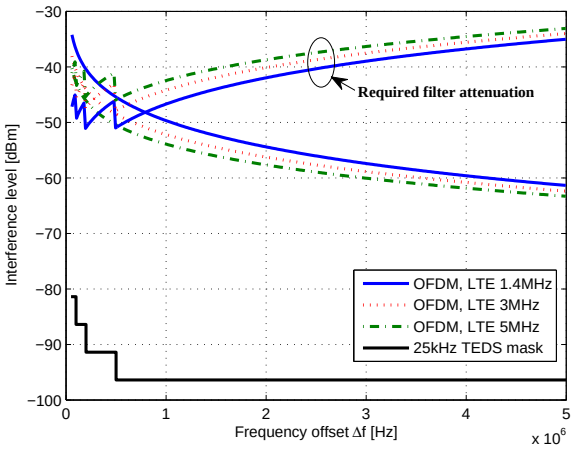

Fig. 5. OFDM based LTE effective interference powers [dBm] versus 25 kHz TEDS reception mask

Comparing the obtained interference levels (Figure 5) to the TEDS reception mask (black solid curve), we can see that the OFDM-based LTE system strongly violates the blocking levels required by the TEDS primary system. It can be also observed that the interference level of a 1.4 MHz-LTE system is much higher than in a 3 MHz and 5 MHz bandwidths.

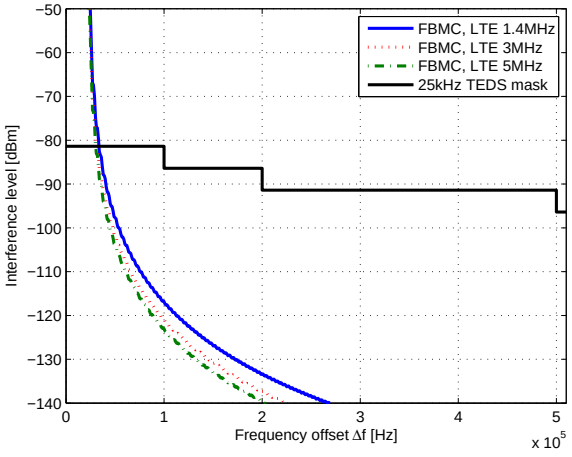

Fig. 6. FBMC based LTE effective interference powers [dBm] versus 25 kHz TEDS reception mask

This can be explained by the fact that the per-subcarrier transmit power level (the total transmit power P_{tot} is divided by the number of active subcarriers) is higher in the 1.4 MHz-LTE ($P_{\text{tot}}/72$) compared to those for the 3 MHz-LTE ($P_{\text{tot}}/180$) and 5 MHz-LTE ($P_{\text{tot}}/300$).

Consequently to ensure a possible coexistence between both systems, two options could be envisaged:

1) The 25 kHz-TEDS should be separated by very large guard bands.
2) If available bandwidth is very limited, we can reduce the number of active subcarriers or the transmit power in order to further reduce sidelobes.

However, both possibilities are detrimental and will affect the system spectral efficiency. In order to overcome this problem, filtering the synthesized OFDM signal could consist a practical solution allowing the TEDS-LTE coexistence.

As depicted in Figure 5, the required filter attenuation for each system can be seen as the difference between the effective LTE interference levels and the TEDS mask ones. In other words, the filtered LTE signal should fit perfectly with TEDS mask requirements.

Looking at the required attenuation curves depicted in Figure 5, we can see that the attenuation requested at the frequency offset $\Delta f = 0.5MHz$ is the most restrictive attenuation. These rejections are: 51 dB, 48 dB, and 45 dB for the 1.4, 3, and 5MHz LTE bands respectively. Therefore, the filter design will mainly depend on three parameters: the attenuation at $\Delta f = 0.5$ MHz, the signal bandwidth and the guard band separating PMR and LTE systems. We have designed various FIR equiriple lowpass filters allowing the PMR/LTE cohabitation. In Table IV, the orders of the required filters normalized by the system FFT size (i.e. the number of samples per OFDM block without CP) are summarized for the three considered LTE bandwidths. It is worth pointing out that the sampling frequency used in the filter design is 15.36MHz which is a common multiple of the sampling frequencies of the three considered LTE systems. The $\Delta f = 50kHz$ example can be seen as the design case. However, the other ones could also be interesting when strong constraints are imposed on the maximum latency tolerated by the system.

It is worth to underline that the filtering approach presents two drawbacks:

- the rejection performances depend on the shape of the filter used. A filter with a high number of coefficients brings better precisions, rejection, and nice spectrum windowing. However, the high number of samples necessary for obtaining such a result at the filtering output induces additional time delays. A possible optimization can be achieved by making a trade-off between the rejection performances and the latency introduced by the filter.
- Reducing the OFDM spectrum sidelobes will destroy the orthogonality between subcarriers. This loss of orthogonality is interpreted by the appearance of Inter-carrier interferences (ICI) by causing a degradation on the system performances.

Similarly, the effective interference powers of FBMC-based LTE systems is shown in Figure 6. In contrast to the OFDM case, achieved interference levels are very low compared to the 25 kHz-TEDS reception mask. Furthermore, the coexistence

TABLE IV
FILTER ORDER/SYSTEM FFT SIZE

Δf	1.4MHz LTE	3MHz LTE	5MHz LTE
50 kHz	0.8623	0.8301	0.7979
100 kHz	0.3965	0.3818	0.3672
200 kHz	0.1904	0.1836	0.1768
500 kHz	0.0742	0.0713	0.0693

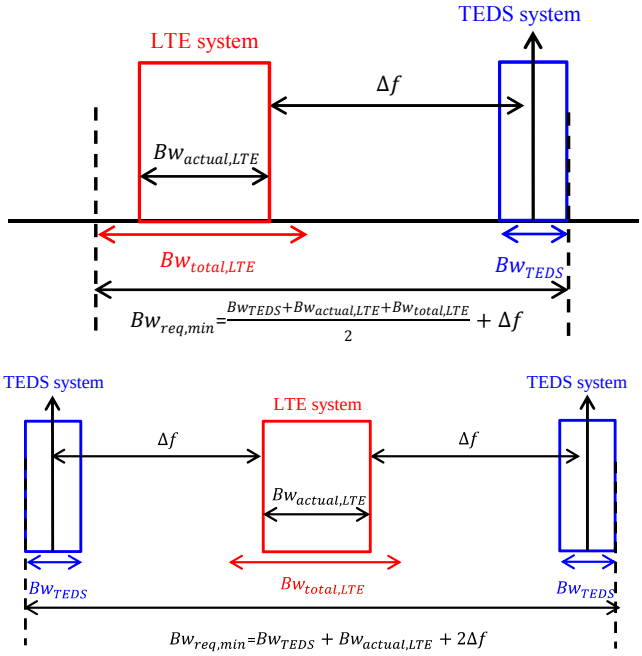

Fig. 7. Two coexistence configurations c.1 and c.2

of FBMC-LTE with a 25 kHz-TEDS is possible starting from the minimum frequency offset allowed by the TEDS reception mask (i.e at Δf=50 kHz). Therefore, increasing the number of FBMC-LTE active subcarriers can be considered which provides a higher spectral efficiency.

V. COEXISTENCE ANALYSIS IN SOME SPECIFIC CONFIGURATIONS

We examine in this section the feasibility of the coexistence between the 25 kHz-TEDS and the LTE-based broadband systems in 5 MHz PMR bandwidth. Two configurations are depicted in Figure 7.

The minimum bandwidth required in configurations (c.1) and (c.2) can be computed respectively by

$$B_{\text{req,min1}} = \frac{B_{\text{TEDS}} + B_{\text{effective,LTE}} + B_{\text{total,LTE}}}{2} + \Delta f_{\min} \quad (5)$$

$$B_{\text{req,min2}} = B_{\text{TEDS}} + B_{\text{effective,LTE}} + 2\Delta f_{\min} \quad (6)$$

where, B_{TEDS} is the TEDS bandwidth which is in our case 25 kHz, $B_{\text{effective,LTE}}$ is the sum of the bandwidth of the useful subcarriers used by the LTE system (see Table III), and $B_{\text{total,LTE}}$ is the total bandwidth of the LTE system (see Table III). $\Delta f_{\min}$ means the minimum spectral distance that should separate the TEDS nominal frequency from the nearest LTE active subcarrier.

Looking at the OFDM results shown in Figure 8, we can see that the OFDM-5MHz-LTE and the 25 kHz TEDS coexistence is not possible (i.e the minimum required bandwidth exceeds the 5 MHz available for PMR) in the case of minimum latency (when $\Delta f = 0.5MHz$). It is worth noticing that the case of OFDM with maximum latency (when $\Delta f = 50kHz$) is equivalent to FBMC one. As expected, the FBMC-LTE is able to cohabit with the 25 KHz-TEDS starting from the minimum spectral distance allowed by this latter that is 50 kHz. Since the required bandwidth $B_{\text{req,min}}$ is always below the 5 MHz available for PMR, it can be observed that the FBMC-TEDS coexistence is possible for figure 7 cases. Furthermore, since $B_{\text{req,min}}$ does not exceed 1.5 MHz, we can consider the insertion of additional FBMC-LTE systems (2× 1.4 MHz-LTE).

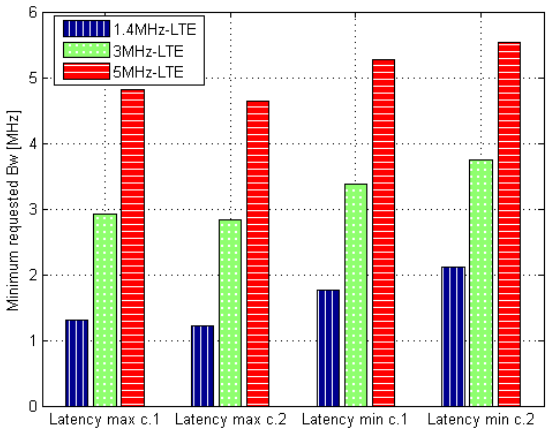

Fig. 8. Minimum required bandwidth (configurations c.1 and c.2) for OFDM case with maximum and minimum latency $\Delta f = 0.05, 0.5$ MHz

VI. CONCLUSION

In this paper, the coexistence between PMR narrowband systems with LTE-like broadband using different bandwidth has been examined. Based on the PSDs waveforms of OFDM and FBMC, we analyzed the interference effect caused by the deployed multicarrier broadband system in the PMR channel active systems. Obtained results show that, in order to make the LTE-TEDS coexistence possible, we need to filter the synthesized OFDM signal. This filtering is made to protect the TEDS systems by reducing the sidelobes levels of the modulated OFDM spectrum. We have also shown that better rejection performances require filters with long impulse responses, thus inducing additional delays. On the other hand, the FBMC signal fits perfectly the PMR-TEDS harmful interference protection requirements. Moreover, this cohabitation is

possible starting from the minimum frequency offset allowed by the TEDS reception mask. This can be explained by the fact that a good frequency localization is achieved by the prototype filter used by the FBMC (PHYDYAS scheme). Therefore, FBMC-broadband (LTE-like) system could be considered as a potential candidate to be deployed in the PMR band offering very high data rates to the next generation of PMR/PPDR systems. Future works will focus on optimization of the filter length giving the best rejection performances. Furthermore, the performance of LTE systems will be investigated since degradations are expected due to the loss of orthogonality between subcarriers induced by the sidelobes reduction.

VII. Acknowledgements

The authors acknowledge the financial support by the European Union FP7-ICT project EMPhAtiC under grant agreement no.318362, and the French ANR project PROFIL with grant agreement code: ANR-13-INFR-0007-03.

References

[1] ETSI TS 100 392-2, *Terrestrial Trunked Radio (TETRA)*; Voice plus Data (V+D); Part 2: Air Interface (AI), Oct. 2011

[2] ETSI TR 102 580 V1.1.1 *Terrestrial Trunked Radio (TETRA)*;Release 2; Designer's Guide; TETRA High-Speed Data (HSD); TETRA Enhanced Data Service (TEDS) (2007-10).

[3] 3GPP TR 25.814, *Physical layer aspects for evolved Universal Terrestrial Radio Access (UTRA)*

[4] B. Farhang-Boroujeny, "Filter Bank Spectrum Sensing for Cognitive Radios," in *IEEE Transactions on Signal Processing*, vol. 56, no. 5, pp. 1801-1811, 2008.

[5] Y. Medjahdi, M. Terré, D. Le Ruyet, and D. Roviras, "Interference tables: a useful model for interference analysis in asynchronous multicarrier transmission," *EURASIP Journal on Advances in Signal Processing*, vol. 2014.

[6] Y. Medjahdi, M. Terré, D. Le Ruyet, D. Roviras, and A. Dziri, "Performance analysis in the downlink of asynchronous ofdm/fbmc based multi-cellular networks," *IEEE Trans. on Wireless Commun.*, vol. 10, no. 8, pp. 2630–2639, Aug. 2011.

[7] M. G. Bellanger, "Specification and design of a prototype filter for filter bank based multicarrier transmission," in *Proc. IEEE Int. Conf. Acoustics, Speech, and Signal Processing*, pp. 2417-2420, Salt Lake City, USA, May 2001.

[8] H-P. A. Ketterling, *Introduction to Digital Professional Mobile Radio*, Artech House, Boston, 2004.

[9] H. Zhang, D. Le Ruyet, and M. Terré, "Spectral Efficiency Comparison between OFDM/OQAM and OFDM based CR Networks," *Wireless Commun. and Mobile Computing Wiley*, vol. 9, pp. 1487–1501, Nov. 2009.

[10] T. Weiss, J. Hillenbrand, A. Krohn, and F.K. Jondral, "Mutual Interference in OFDM-based Spectrum Pooling Systems," in *Vehicular Technology Conference, IEEE 59th*, May 2004, vol. 4, pp. 1873–1877.

[11] M. G. Bellanger, "Phydyas : Analytical expressions for the reference prototype filter," *Tech. report*, pp. 1-4, Feb. 2009, CNAM, Paris.

[12] Evolved Universal Terrestrial Radio Access (E-UTRA), *LTE physical layer: General description*,

On the Use of Filter Bank Based Multicarrier Modulation for Professional Mobile Radio

Markku Renfors[1], Faouzi Bader[2], Leonardo Baltar[3], Didier Le Ruyet[4],
Daniel Roviras[4], Philippe Mege[5], Martin Haardt[6], Tobias Hidalgo Stitz[7]
[1]Dept. of Electronics and Communications Engineering, Tampere University of Technology, Finland, markku.renfors@tut.fi
[2]CTTC, Castelldefels-Barcelona, Spain
[3]Circuit Theory and Signal Processing, Technische Universität München, Germany
[4]Electronics and Communications Laboratory, CNAM, Paris, France
[5]Cassidian, Elancourt, France
[6]Communications Research Laboratory, Ilmenau University of Technology, Ilmenau, Germany
[7]Magister Solutions Ltd, Tampere, Finland

***Abstract*—Our main emphasis is on the use of enhanced OFDM and filter bank based multicarrier (FB-MC) waveforms for utilizing effectively the available fragmented spectrum in heterogeneous radio environments. Special attention is on the broadband-narrowband coexistence scenario of the Professional Mobile Radio (PMR) evolution. The target here is to provide broadband data services in coexistence with narrowband legacy services of the TETRA family. The core idea is a multi-mode radio platform, based on variable filter bank processing, which is able to perform modulation/detection functions simultaneously for different signal formats with adjustable center frequencies, bandwidths and subchannel spacings.**

I. Introduction

Public Safety organizations are using radio communication systems for the day to day operational needs, for exceptional events, and for disaster recovery conditions. These usages are collectively called PPDR (Public Protection and Disaster Relief), which corresponds to the Professional Mobile Radio (PMR) services for Public Safety organizations [1] [2]. Today they use dedicated radio communications systems (APCO25 in North America; TETRA, TETRAPOL and TEDS in Europe and in a large part of the world) primarily for voice communications and also for low-rate data transmissions. This is due to the technological limitations of currently deployed PMR/PPDR systems, which only use a small radio channel bandwidth and have thus limited throughput.

There are various important services that need essentially higher data throughput and cannot be supported by the current networks. The new required capacity can be achieved in two complementary ways: by obtaining new frequency bands for PPDR data services and by fitting a novel broadband data service within the scarcely available spectrum devoted to PMR systems. To satisfy the growing demands, actually both directions have to be followed. The EU FP7 ICT project EMPhAtiC (http://www.ict-emphatic.eu) will focus on the latter approach, which can be seen as the technically more challenging path. One of the major issues is being able to introduce new broadband data services within the current frequency allocation at the 450 MHz frequency band, in coexistence/cohabitation with the current PMR/PPDR systems.

It is natural to consider the highly spectrally efficient 3GPP LTE system as a reference basis in the PMR/PPDR system development due to its modularity and wide adoption in the civil world. However, there is a clear need to go beyond LTE, especially improving the spectral characteristics and striving to maximize the spectral efficiency, while maintaining most of the functionalities intact, especially at the higher layers.

The considered coexistence scenario, aiming at the deployment of a broadband data service in a band already occupied by narrowband PMR channels, is illustrated in Fig. 1. Here high flexibility and spectral agility, in combination with efficient fragmented spectrum use are necessary requirements for the broadband system. To reach good spectral efficiency and minimize interferences between the different services, well-contained spectrum, providing improved adjacent channel protection, is critical. This is a general issue when considering challenging spectrum access scenarios, like cognitive radio and opportunistic dynamic spectrum use.

Various enhancements to the CP-OFDM multicarrier scheme have been proposed in the literature and are under active investigations. In particular, we are witnessing an expansion of technical publications that encourage and support the use of the filter bank modulation schemes as a solution for the drawbacks and limitations of the conventional CP-OFDM scheme, which are critical for the chosen PMR/PPDR concept [3] [4]. The main limitation is the poor spectral containment of the OFDM signal, which would necessitate relatively wide guard bands around the active groups of subcarriers to isolate the new broadband service and legacy narrowband services from each other. Using filter bank schemes, it is also possible to reduce the overhead in data transmission rate due to the cyclic prefix (CP).

Multicarrier signals present a high peak-to-average power ratio (PAPR) which, combined with the nonlinearity of transmitter power amplifiers, produce undesired signal distortion and spectral regrowth. PAPR reduction and mitigation of the nonlinearity effects are important aspects in all multicarrier systems, but since the focus of this paper is on spectral containment, we concentrate here on the reduction of OFDM spectrum sidelobes.

In the following, first in Section II we discuss techniques for sidelobe suppression in OFDM, introduce the filter bank

978-1-4673-6337-2/13/$31.00 ©2013 IEEE

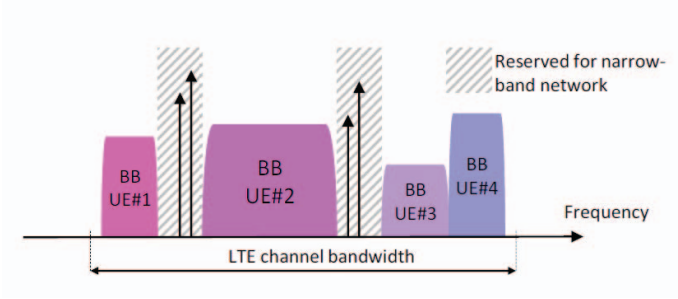

Fig. 1. Proposed future PMR broadband service in cohabitation with current systems.

multicarrier schemes and a fast convolution based flexible multimode filter bank structure. Section II also includes a comparison of the spectral characteristics of an enhanced OFDM scheme and FBMC/OQAM in a non-contiguous LTE like scenario. In Section III channel equalization and synchronization aspects in FBMC/OQAM are briefly discussed, together with important higher-layer aspects. Conclusions are drawn in Section IV.

II. Multicarrier Waveforms for Fragmented Spectrum Use

At the waveform level, the European project EMPhAtiC [5] focuses on heterogeneous networks in general. The most important example is the prospective evolution of PMR/PPDR to provide a high data-rate service by utilizing fragments of a PMR frequency band partly occupied by narrowband legacy PMR signals with 10, 12.5, 25, 50, and/or 100 kHz channelization. Here it is crucial to exploit the available frequency gaps efficiently while keeping the interferences in both directions at acceptable levels. Similar radio environments are encountered also in cognitive radio applications, however, with much higher variability of the primary waveforms. In cell-based PMR networks, all mobile stations are under the control of a base station. The PMR ad-hoc scenario resembles the cognitive radio case in the sense that different stations are not necessarily well-synchronized and the interferences in the environment are more difficult to handle.

OFDM solves the fundamental channel equalization problem in wideband wireless communications in an elegant and robust way, and it provides efficient means for channel aware scheduling of the transmission resources to different users in an optimal way. Due to the flat-fading channel characteristics, CP-OFDM is also an excellent basis for different multi-antenna (MIMO) techniques which are able to enhance the performance at link and system levels [6]. However, as mentioned above, OFDM has also a number of limitations, which have motivated research on various enhancements as well as on alternative waveforms.

A. Sidelobe Suppression in CP-OFDM

A very flexible way of approaching for facilitating the broadband narrowband coexistence can be named non-contiguous multicarrier modulation, as a generalization of non-contiguous OFDM scheme [7]. Here the idea is that the spectrum of the transmitted waveform can be controlled by activating only those subcarriers which are available and have been allocated for transmission, and modulating zero-symbols on the others. The approach is the same as the basic idea of OFDMA, but now the target is to be able to tolerate asynchronous waveforms in the unused frequency slots. Using basic OFDM in this way, the spectrum leakage would necessitate considerable guardbands between the active subcarriers and occupied frequency channels, and would thus lead to low spectrum efficiency.

OFDM systems maintain orthogonality between spectral components which are synchronized in time and frequency to satisfy the quasi-stationarity conditions. However, the spectral containment of the OFDM waveform is far from ideal, and the attenuation of a basic OFDM receiver for non-synchronized spectral components (interferences, adjacent channels) is limited. A straightforward approach to solve these issues is baseband filtering of the generated waveform on the transmitter side and digital channelization filtering before the FFT on the receiver side [8]. However, sharp filtering, with narrow transition band, increases the computational complexity significantly. More importantly, there is an increasing demand for spectrum agile waveform processing, in which case the post-/pre-filtering solutions would have high structural and computational complexity.

In addition to post- or pre-filtering, a number of techniques have been presented in the literature for reducing the spectral leakage in CP-OFDM based systems. One possibility is to use a tapered time-domain window for OFDM symbols [9], instead of rectangular windowing. Especially, the raised cosine window in combination with extended CP has been widely considered. For effective spectrum leakage suppression, the CP has to be significantly extended to accommodate a higher roll-off of the RC-window, leading to reduced spectrum efficiency. Raised-cosine windowing can be used also on the receiver side for better rejection of interference leakage from the unused spectral slots, with similar trade offs. In [10], it is proposed to use the windowing in edge subcarriers only to improve spectrum efficiency. Other approaches include subcarrier weighting [11], cancellation carrier method [7] [12], and precoding [13].

B. Filter Bank Multicarrier

Another approach for spectrally agile waveforms and signal processing is filter bank based multicarrier modulation (FB-MC) [4] [14] [15] [16]. Here the idea is to use spectrally well-contained synthesis and analysis filter banks in the transmultiplexer configuration, instead of the IFFT and FFT, respectively. The most common approach is to use modulated uniform polyphase filter banks based on a prototype filter design, which determines the spectral containment characteristics of the system. FB-MC is able to reduce the sidelobes to a level which depends in practice only on the spectral leakage (spectral regrowth) resulting from the transmitter power amplifier nonlinearities.

The two basic alternatives are filtered multitone modulation (FMT) [17] [18] and FBMC/OQAM (or OFDM/OQAM) [3] [4]. In FMT, the adjacent subchannels are isolated by designing them to have non-overlapping transition bands, and for each subcarrier basic subcarrier modulation, like QAM with Nyquist pulse shaping, can be used. The principle of FMT is just

frequency division multiplexing / multiple access. It relies on specific uniform multirate filter bank structures, typically based on IFFT/FFT transforms complemented by polyphase filtering structures. To reach high spectral efficiency, narrow transition bands should be used, leading to increased implementation complexity of the filter bank.

In typical FBMC/OQAM designs, each subchannel overlaps with the adjacent ones, but not with the more distant ones, and orthogonality of subcarriers is achieved by using offset-QAM modulation of subcarriers, in a specific fashion [3]. Due to the absence of cyclic prefix and reduced guardbands in frequency domain, FBMC/OQAM has the potential of reaching higher spectral efficiency than CP-OFDM. Within the FP7 PHYDYAS project [19] a significant advantage of FBMC/OQAM over CP-OFDM with the same number of subchannels per frequency band has been convincingly demonstrated [20]. However, the main benefits of FB-MC modulation formats can be found in scenarios benefiting from dynamic and non-contiguous (i.e., fragmented) spectrum allocation [21] [22]. The main drawback is higher computational complexity. In terms of real multiplication rate, the complexity of FBMC/OQAM is typically 3 to 5 times that of OFDM with the same transform size [23].

The primary approach chosen in EMPhAtiC to reach the needed spectral agility is to utilize highly flexible, variable filter bank based waveform generation and detection methods. The idea is to develop a platform able to process simultaneously alternative filter bank based waveforms, with highly adjustable characteristics, and also able to do the channelization for the legacy signals following the SDR (software defined radio) model, e.g., in case of a multimode basestation. One strong candidate is the fast convolution based variable filter bank processing approach of [24], the structure of which is illustrated in Fig. 2. Fig. 3 shows an example of the subchannel frequency responses for a multimode filter bank which is able to accommodate simultaneously single carrier, FBMC/OQAM, and FMT waveforms.

To the best of our knowledge, there exists no other multimode variable waveform processing structure with similar efficiency and flexibility. However, also the more traditional polyphase filter bank and tree-structured filter bank configurations are considered as alternative solutions.

Such variable filter bank structures provide also additional flexibility in adapting to the transmission channel's time- and frequency-selectivity features, as it is possible to use different subchannel bandwidths or prototype filters for each individual user's signal. The proposed filter bank processing approach is particularly important for the basestation transmitters and receivers, in which case there is a need to process simultaneously different FB-MC waveforms and legacy signals. On the terminal side and in the ad-hoc context, a down-scaled version of the filter bank can be used, supporting a limited set of waveforms with reduced complexity.

C. Example of Non-Contiguous Multicarrier

In summary, FB-MC and enhanced OFDM schemes are alternative approaches for developing flexible spectrum agile waveforms with improved spectral containment, which is particularly important in fragmented spectrum use. In this subsection we show examples of the spectral characteristics of non-contiguous multicarrier based on (i) raised-cosine windows and (ii) FBMC/OQAM, using plain CP-OFDM as a reference. We choose a parametrization based on 5 MHz LTE. Then the FFT size is $M = 512$ and 300 active subcarriers are used, along with (almost) symmetric guardbands and zero DC subcarrier. The 300 active subcarriers are scheduled in resource blocks of 12 subcarriers (180 kHz), i.e., there are 25 resource blocks. We consider the non-contiguous scenario of Fig. 4 which includes two gaps reserved for narrowband legacy transmissions. These gaps are of widths 1 resource block (12 subcarriers), and 2 resource blocks (24 subcarriers). Further, it is assumed that the LTE variant with extended CP of 128 samples is used as the basis. In the raised-cosine windowing case, these intervals are divided into a CP of 36 samples (as in the normal 5 MHz LTE mode) and smooth raise cosine-shaped transition period of 92 samples.

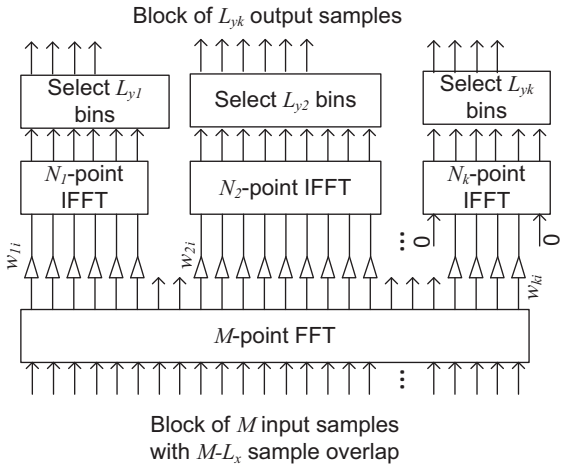

Fig. 2. Fast convolution based flexible analysis filter bank.

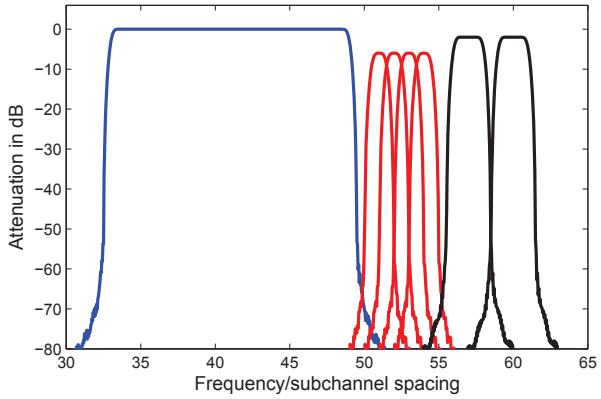

Fig. 3. Example of multiplexing different waveforms: Single-carrier signal with bandwidth of 512 bins and 6 % roll-off, FBMC/OQAM multiplex of 4 subchannels with 16 bin spacing and 100 % roll-off, FMT multiplex of 2 subchannels with 32 bin spacing and 33 % roll-off.

In the FBMC case, the PHYDYAS prototype filter designs [19] are used with overlapping factors $K = 3$ and $K = 4$, meaning that the prototype filter orders are $3M$ and $4M$, respectively.

Fig. 4 shows the overall spectra for the four cases, as well as the detailed spectra of the two gaps. To clarify the

figure, here just the envelope of the power spectrum is visible, not the stopband ripples. It can be seen that FBMC results in much lower spectrum leakage to the spectral gaps in this non-contiguous multicarrier case than plain CP-OFDM or OFDM with raised-cosine windowing. With the used parameters, raised-cosine windowing results in about 31 dB or 50 dB attenuation, with respect to the passband level, for 1 or 2 resource block gaps, respectively, when considering a 30 kHz (2 subcarriers) bandwidth in the center of the gap. The corresponding values with plain OFDM are 15 dB and 18 dB, respectively.

III. Multicarrier System Development for PMR

A. Channel equalization and Synchronization Aspects

Both FMT and FBMC/OQAM systems can be designed to have similar number of subcarriers as an OFDM system, in which case the channel can usually be considered as flat-fading at subcarrier level, and one-tap complex subcarrier-wise equalizers are sufficient. However, there is also the possibility of increase the subcarrier spacing, e.g., in order to relax the ICI effects with high mobility, in which case multi-tap equalizers are needed [16]. A convenient approach for realizing multitap subcarrier equalizers is based on frequency sampling [25]. This method can be adapted to the multi-mode receiver architecture in an effective way by modifying the weights in Figure 2.

The special OQAM-type signal structure has to be taken into account when designing the pilot structures for channel estimation and synchronization [26], and it introduces also difficulties in adapting certain multiantenna schemes to the FBMC/OQAM context.

The broadband PMR system should be able to support a wide range of link distances and thus relatively long channel delay spreads. This requirement is also emphasized by the propagation characteristics at the used relatively low frequency band. Also relaxed synchronization and power control requirements for mobile terminals are important targets. These aspects are in favor of using FB-MC waveforms which is able to support frequency division multiplexing of asynchronous transmissions with high spectral efficiency.

Regarding asynchronous FDMA channelization, including cell-based uplink and ad-hoc scenarios, the baseline approach is to use a narrow guard band (usually one subchannel) between different non-synchronized frequency channels. Then the filter bank based transmission modes allow fully asynchronous operation regarding timing offsets between transmissions and relatively coarse mutual frequency synchronization is sufficient. This allows the transmission of short data packets without initial synchronization, and maintaining the synchronization of idle stations is not critical. Also the latency due to initial synchronization can be minimized. The required timing and frequency offset compensation algorithms will be integrated with the variable filter bank structure. However, in case of continuous transmission in cell-based systems, there are good reasons for establishing synchronism between the uplink signals. These reasons include reduced signal processing complexity and minimization of the overheads in TDD and TDMA operation modes due to time-domain guard intervals between transmission bursts, which have to be able to absorb the timing uncertainties. The overall synchronization process for

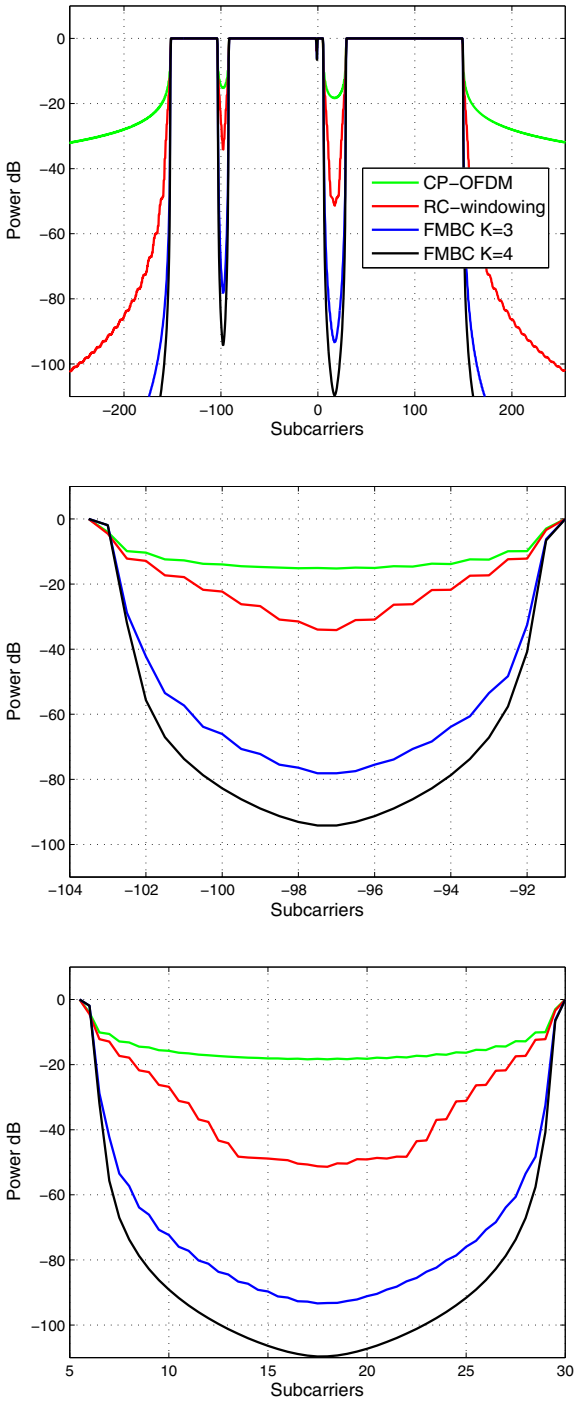

Fig. 4. Examples of the power spectra of non-contiguous multicarrier waveforms. (a) Overall spectra. (b) The gap of 12 subcarriers, (c) The gap of 24 subcarriers. Only the envelope of the spectra are shown, not the stopband ripples.

continuous transmission will be developed utilizing feedback information about synchronization offsets from basestations to mobiles.

B. Higher Layers and Demonstrator Development

In addition to the waveform and basic signal processing aspects of the physical layer, EMPhAtiC will also develop effective multi-antenna techniques for the FB-MC transmission schemes, and address relay and ad-hoc networking, radio resource management and cross-layer aspects as well as spectrum sensing methods utilizing the flexible multichannel architecture. The developed broadband PMR scheme and its coexistence with narrowband PMR services is planned to be highlighted through a demonstrator development.

IV. Concluding Remarks

We have discussed non-contiguous multicarrier schemes for heterogeneous radio environments aimed at effective use of fragmented spectrum for broadband data communications. The Professional Mobile Radio evolution, along with general cognitive radio development are important applications for these techniques. We have seen that while sidelobe suppression techniques for CP-OFDM are able to significantly reduce the spectrum leakage to the frequency slots of non-active subcarriers, the FBMC/OQAM approach has superior characteristics in this respect.

The main challenge, and the main topic for future studies is to include the effects of the power amplifier nonlinearity into consideration. In this context, methods for reducing the peak-to-average power ratio (PAPR) of the modulated waveform and power amplifier linearization techniques are central issues.

The multimode filter bank structure of Fig. 2 gives the opportunity to use single-carrier waveforms with the same spectral characteristics and reduced PAPR. This is especially the case on the terminal transmitter side. Unfortunately, it is not easy use fragmented spectrum by a single-carrier waveform. However, in the uplink case the user data rates are often lower than in the cellular downlink, and there are less demands for non-contiguous transmission by a mobile station.

Acknowledgment

The authors acknowledge the financial support by the European Union FP7-ICT project EMPhAtiC (http://www.ict-emphatic.eu) under grant agreement no. 318362.

References

[1] K. Balachandran, K. Budka, T. Chu, T. Doumi, and J. Kang, "Mobile responder communication networks for public safety," *IEEE Communications Magazine*, vol. 44, pp. 56–64, Jan. 2006.

[2] "Mobile broadband in a mission critical environment - as seen from a TETRA perspective," Feb. 2011, White Paper, Tetra Association.

[3] P. Siohan, C. Siclet, and N. Lacaille, "Analysis and design of OFDM-OQAM systems based on filterbank theory," *IEEE Trans. Signal Processing*, vol. 50, no. 5, pp. 1170–1183, May 2002.

[4] B. Farhang-Boroujeny and R. Kempter, "Multicarrier communication techniques for spectrum sensing and communication in cognitive radios," *IEEE Communications Magazine, Special Issue on Cognitive Radios for Dynamic Spectrum Access*, vol. 46, no. 4, pp. 80–85, April 2008.

[5] FP7-ICT Project EMPhAtiC - Enhanced Multicarrier Techniques for Professional Ad-Hoc and Cell-Based Communications. http://www.ict-emphatic.eu.

[6] E. Dahlman, S. Parkvall, and J. Sköld, *4G LTE / LTE-Advanced for Mobile Broadband*. Academic Press, 2011.

[7] Z. Yuan and A. Wyglinski, "On sidelobe suppression for multicarrier-based transmission in dynamic spectrum access networks," *IEEE Trans. Veh. Technol.*, vol. 59, no. 4, pp. 1998 – 2006, apr 2010.

[8] M. Faulkner, "The effect of filtering on the performance of OFDM systems," *IEEE Trans. Veh. Technol.*, vol. 49, no. 9, pp. 1877–1884, sep 2000.

[9] T. A. Weiss, J. Hillenbrand, A. Krohn, and F. K. Jondral, "Mutual interference in OFDM-based spectrum pooling systems," in *Proc. IEEE Veh. Technol. Conf. Spring*, Dallas, TX, USA, may 2004, pp. 1872–1877.

[10] A. Sahin and H. Arslan, "Edge windowing for OFDM based systems," *IEEE Commun. Lett.*, vol. 15, no. 11, pp. 1208–1211, nov 2011.

[11] I. Cosovic, S. Brandes, and M. Schnell, "Subcarrier weighting: a method for sidelobe suppression in OFDM systems," *IEEE Commun. Lett.*, vol. 10, no. 6, pp. 444–446, jun 2006.

[12] S. Brandes, I. Cosovic, and M. Schnell, "Sidelobe suppression in OFDM systems by insertion of cancellation carriers," in *Proc. IEEE Veh. Technol. Conf. Fall*, Los Angeles, CA, USA, sep 2005, pp. 152–156.

[13] H.-M. Chen, W.-C. Chen, and C.-D. Chung, "Spectrally precoded OFDM and OFDMA with cyclic prefix and unconstrained guard ratios," *IEEE Trans. Wireless Commun.*, vol. 10, no. 5, pp. 1416 – 1427, may 2011.

[14] R. Chang, "High-speed multichannel data transmission with bandlimited orthogonal signals," *Bell Sys. Tech. J.*, vol. 45, pp. 1775–1796, Dec. 1966.

[15] B. Saltzberg, "Performance of an efficient parallel data transmission system," *IEEE Trans. Commun. Technol.*, vol. 15, no. 6, pp. 805–811, dec 1967.

[16] B. Hirosaki, "An orthogonally multiplexed qam system using the discrete fourier transform," *IEEE Transactions on Communications*, vol. 29, no. 7, pp. pp. 982 – 989, Jul 1981.

[17] R. Vallet and K. H. Taieb, "Fraction spaced multi-carrier modulation," *Wireless Pers. Commun., Kluwer*, vol. 2, pp. 97–103, 1995.

[18] G. Cherubini, E. Eleftheriou, and S. Olcer, "Filtered multitone modulation for vdsl," *Proc. of IEEE Global Telecommunications Conference*, pp. 1139–1144, 1999.

[19] FP7-ICT Project PHYDYAS - Physical Layer for Dynamic Spectrum Access and Cognitive Radio. http://www.ict-phydyas.org.

[20] V. Ringset, H. Rustad, F. Schaich, J. Vandermot, and M. Najar, "Performance of a filterbank multicarrier (FBMC) physical layer in the WiMAX context," *Proc. Future Network and Mobile Summit 2010, Florence, Italy*, June 2010.

[21] M. Shaat and F. Bader, "Computationally efficient power allocation algorithm in multicarrier-based cognitive radio networks: OFDM and FBMC systems," *EURASIP J. Advances Signal Processing*, vol. 2010, pp. 1–13, 2010.

[22] H. Zhang, D. LeRuyet, D. Roviras, Y. Medjahdi, and H. Sun, "Spectral efficiency comparison of OFDM/FBMC for uplink cognitive radio networks," *EURASIP J. Advances Signal Processing*, vol. 2010, pp. 1–14, 2010.

[23] L. Baltar, F. Schaich, M. Renfors, and J. A. Nossek, "Computational complexity analysis of advanced physical layers based on multicarrier modulation," in *Proc. Future Network and Mobile Summit (FutureNetw)*, Warsaw, Poland, Jun. 15–17 2011, pp. 1–8.

[24] M. Renfors and f. harris, "Highly adjustable multirate digital filters based on fast convolution," *Proc. European Conference on Circuit Theory and Design, ECCTD 2011, Linköping, Sweden*, Aug. 2011.

[25] T. Ihalainen, A. Ikhlef, J. Louveaux, and M. Renfors, "Channel equalization for multi-antenna FBMC/OQAM receivers," *IEEE Trans. Veh. Technol.*, vol. 60, no. 5, pp. 2070–2085, May 2011.

[26] C. Lélé, J.-P. Javaudin, R. Legouable, A. Skrzypczak, , and P. Siohan, "Channel estimation methods for preamble-based ofdm/oqam modulation," *European Transactions on Telecommunications*, vol. 19, pp. 741–750, Sept. 2008.

3.2.2 In Device-to-Device communications context

As extension to previous works on systems coexistence in the PMR communication band, I focused my interests in the D2D communications scenario. The result of this interest is the preparation and the acceptance by the French National research agency (ANR) of the project ACCENT5, and the PHC ULYSSES[10] project between CentraleSupélec (France) and Trinity College of Dublin (Ireland) accepted by the "Campus France"[11] and the Irish Research Council [12] agencies respectively. Also the supervision of the PhD thesis (in progress) of Mr. Quentin BODINIER, and obtained results have been determinant for the development of coexistence issues in the D2D communication environment.

The target here is to demonstrate the feasibility and compare the efficiency of enhanced OFDM and different filter bank based multi-carrier waveforms in the D2D IMT advanced evolution (5G) context. Therefore, for coexistence purposes, the conducted studies focused on advanced filter based multi-carrier (FBMC) waveforms for D2D communications allowing a much higher relaxation (above the cyclic prefix time duration) on the synchronization constraint at the eNB (evolved Node B). Note that the context scenario is the use of D2D communications in a legacy band controlled by an operator that already deployed an LTE network in the same band.

Studies on interference caused by time-frequency misalignment are restricted to the case where the misaligned user has the same waveform as the other systems in the network [62], and very limited works addressed the interference caused by a given waveform[13] onto OFDM. On the other hand, power-loading studies rely on interference models which do not take time-frequency misalignment into account [63, 64, 65]. Therefore, it is crucial to analyze the effects of time-frequency misalignment on the interference caused by D2D pairs onto cellular users.

As it's well known, numerous new waveforms with intrinsic filtering properties have emerged for the 5G context. Almost of these waveforms are relied on filter bank based modulation. Four recently proposed FBMC based waveforms, namely Filtered Multi-Tone [66], OFDM/OQAM [67], Lapped FBMC [68], and GFDM [57] have been used to analyze, in the coexistence context, the time-frequency misalignment effects of the D2D pair on the incumbent network. The interference injected by the D2D pair has been analyzed on the incumbent network for each waveform separately. This is allowing us to build interference tables to be used as inputs to the power loading solution and analyze the maximum rate achievable through each waveform. Different resource sizes in time and frequency has been used and the resulting rate calculated.
For the interference analysis, to assign the power to be distributed on the D2D pairs, it's important to know how much power leaks to the adjacent band depending on which waveform is utilized by the D2D users. The classical way to compute the leakage is to integrate the Power Spectral Density (PSD) of the interfering signal on the band that suffers from the interference. However, this model does not take into account the time window of the incumbent. This is of paramount importance as the incumbent only considers a time window with a specific width based on its own parameters. Besides, it has been shown in [1], that the PSD is not a suitable practice to evaluate the inter system interference for the scenario of interest. We therefore employed the instantaneous interference model proposed in [1] to compute the interference I_m^l injected to the $l-th$ subcarrier of the incumbent by the D2D signal x_m where only subcarrier m is utilized.

For our analysis, we consider an incumbent system following similar parameters to 3GPP LTE standard. The OFDM cellular user occupies 180 subcarriers, which corresponds to 15 LTE resource blocks (RB) along the frequency axis. Besides, it uses a number of CP samples $NCP = 12$ samples. The length of the transmission window in time varies from $N_f = 1$ to 100 OFDM symbols. In the center of the incumbent band, a free band B_f divided into M_f subcarriers of 15 kHz is unused. This band is utilized by the D2D pair. No guard band is considered in this study.
Fig. 4 in [C97] ([C97] is the first paper depicted at the end of this Subsection 3.2.2) shows the interference that is injected by an active subcarrier with unitary power on 20 neighboring OFDM subcarriers as a function of δ_t for different waveforms. Interference caused by the Lapped FBMC and the OFDM/OQAM is weakly affected by the timing offset. GFDM and FMT show slight variations with respect to δ_t. On the contrary, the figure for OFDM shows high variations along the δ_t axis.

[10] for more details on this project see Subsection 1.5.3, page 23.
[11] http://www.campusfrance.org/en
[12] http://www.research.ie/
[13] different from OFDM scheme.

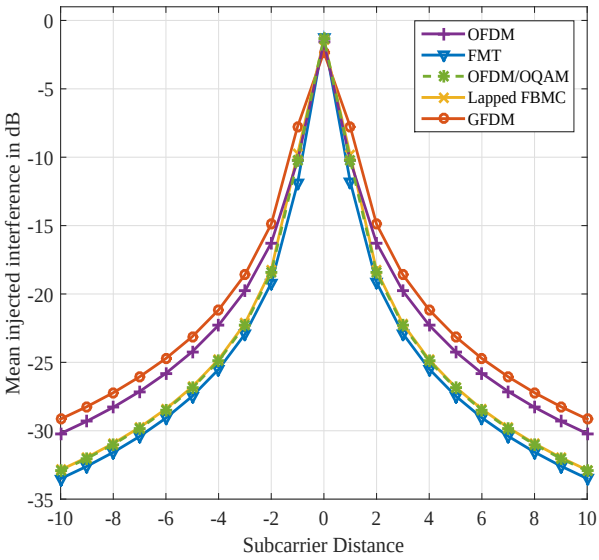

Figure 3.18: Mean Interference Table on OFDM receiver [C97].

Main observations are threefold:

1. It appears that OFDM is the only waveform that shows a significant difference between its mean and maximum injected interference on the OFDM based incumbent. Other waveforms show a difference of approximately about 0 to 1dB.

2. If mean interference is considered, GFDM causes the highest interference. However, if the maximum interference is considered, OFDM based D2D pair has the worst performance.

3. It's important to point out that values of interference injected by 5G waveforms are surprisingly high. For OFDM/OQAM for example, the PSD based model predicts an attenuation of 60 dB at subcarrier distance of 2 [1], whereas our interference tables show that the interference power seen by an OFDM receiver at subcarrier distance of 2 is 18.5 dB. This is due to the fact that the OFDM demodulator performs Fast Fourier Transform (FFT) on a time window that may be much shorter than the length of the symbol of the other waveform. Therefore the signal suffers from discontinuities that produce projections on the whole incumbent spectrum.

Obtained results bring insight into which waveform performs best for different time window lengths and interference constraint. It seems that for transmission windows shorter than 10 symbols, OFDM is the best choice, as it does not suffer from any transmission delay. Therefore, linearly pulse shaped waveforms can compete only when the transmission window starts getting wider than 10 OFDM symbols. It can be noticed that Lapped FBMC shows a promising performance. This is due to the fact that it has a very short delay about only one symbol, and injects interference comparable to that of OFDM/OQAM and FMT. FMT suffers from a large delay during transmission and seems not to be an appropriate candidate for low latency applications. However, OFDM/OQAM performance stays very close to the Lapped FBMC. Interestingly, the performance of OFDM starts to degrade for time windows of width larger than $N_f = 15$ regardless of the interference constraint. This is the result of the OFDM spectral efficiency loss due to the presence of a CP. Note that, even though GFDM seems to be a potential competitor to OFDM/OQAM and Lapped FBMC when the interference constraint is very relaxed, it cannot efficiently cope with stringent interference constraints. This is the consequence of its high interference leakage as it is shown in Figs. 3.18 and 3.19.
Through numerical results, we have shown that it is not worth synchronizing the D2D pair in time domain with respect to the incumbent network. Interference tables derived in this paper allowed us to analyze the maximum rate achievable by the D2D pair under different interference constraints. We also demonstrated that the communication window size has a direct impact on the efficacy of the waveform utilized by the D2D pair. For short D2D

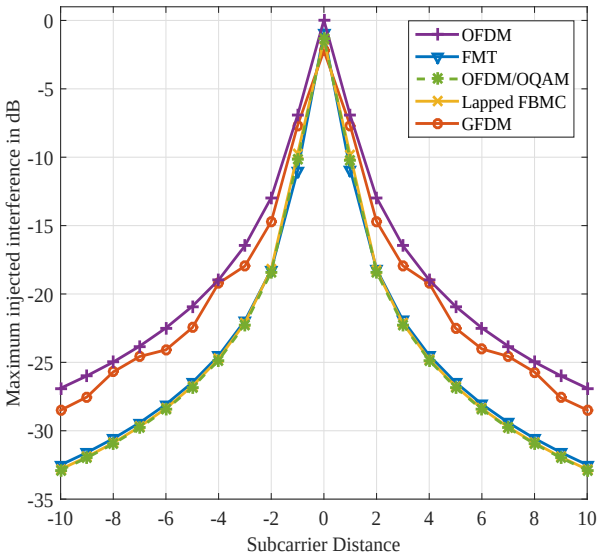

Figure 3.19: Maximum Interference Table on OFDM receiver [C97].

transmission windows, OFDM, GFDM and Lapped FBMC seem to be appropriate candidates. We also showed that under stringent interference constraints and wide transmission windows, OFDM/OQAM and Lapped FBMC are strong candidates.
More detailed and extended results on transmitted bits as a function of available OFDM time symbols in the transmission window, and also on transmitted bits by different waveforms over 12 subcarriers (1 RB) during one TTI in function of the interference threshold are presented in [C97] (this reference is the first publication depicted by the end of this Subsection 3.2.2).

From obtained results and observations in [C97], the main raised question is *"What are the Real Gains from Filter Banks and CP-OFDM systems coexistence?"*. Researches undertaken in [C100, C103], and [C105] focused on modeling the interference between OFDM/OQAM and CP-OFDM to give some answers to the previous question. The followed approach is the study of inter-user interference in scenarios where CP-OFDM and OFDM/OQAM users interfere with each other. It is shown in [C100] (this reference is the second publication depicted at the end of this Subsection 3.2.2) that the PSD based approach consists in modeling the interference at the input antenna of the interfered receiver, and totally omits the demodulation operations that are performed by the latter. The interference seen at the output of the demodulator of the interfered receiver is much higher than expected using the PSD based model. Moreover, the interference between the incumbent and secondary systems is symmetrical, which contradicts the results obtained with the PSD-based model.

We focused on rating the inter-user interference caused by the fact that different users transmit in an asynchronous manner with different waveforms. Therefore, we consider a simple scenario where an incumbent system $\mathcal{U}_1$ coexists with a secondary user $\mathcal{U}_2$ in the same band. Both systems use multi-carrier waveforms with the same subcarrier spacing ΔF, and each of them is assigned a set of subcarriers $\mathcal{L}_i$ $(i \in \{1, 2\})$. The incumbent $\mathcal{U}_1$ utilizes CP-OFDM, whereas two alternatives are studied for $\mathcal{U}_2$. The latter uses CP-OFDM in the case of a homogeneous scenario (referred to as *Hom*) and OFDM/OQAM in the case of a heterogeneous scenario (referred to as *Het*). The configurations studied in this context are summarized in Figs. 3.20 and 3.21[14].

First, the amount of interference suffered by $\mathcal{U}_1$ and $\mathcal{U}_2$ on each of their subcarriers is calculated using Monte-Carlo simulations for heterogeneous environment (See Section IV in [C100]). Second, we calculated the PSD-based model that consists in computing the leakage caused by users onto each other by integrating the PSD of the interfering signal on the band that suffers from the interference.

[14] where in Fig. 3.21, $\Phi_{\text{CP-OFDM}}$ (resp. Φ_{PHYDYAS}) is the PSD of the CP-OFDM signal (resp. of OFDM/OQAM with PHYDYAS filter in [58]).

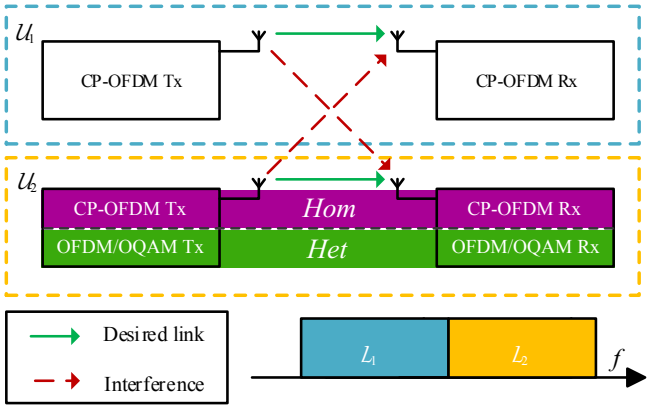

Figure 3.20: Graphical summary of the undertaken study: two users $\mathcal{U}_1$ and $\mathcal{U}_2$ transmit on adjacent bands $\mathcal{L}_1$ and $\mathcal{L}_2$ and interfere with each other. Channel is assumed perfect and no Gaussian noise is considered. $\mathcal{U}_2$ uses CP-OFDM in *Hom* scena

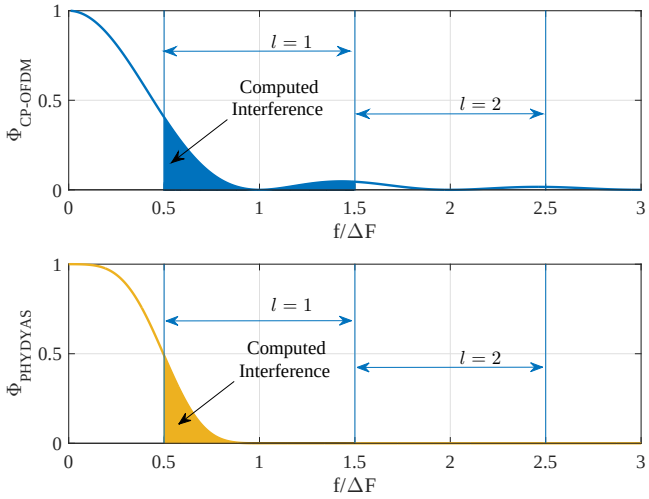

Figure 3.21: Modeling of injected interference with the PSD-based model for CP-OFDM (top) and OFDM/OQAM with PHYDYAS filter (bottom). The values of interference injected by subcarrier 0 on a subcarrier at a spectral distance of $l = 1$ correspond to the integration of the PSD from 0.5 ΔF to 1.5 ΔF.

As previously mentioned, the main drawback of the PSD-based model lies in the fact that it does not take into account the time window of the receiver. However, this is of paramount importance as the incumbent only considers a time window with a specific width based on its own parameters. In Fig. 3.22 a tremendous gap between the values of interference planned by the PSD-based model and the real ones. As a case in point, at $l = 2$, the PSD-based model plans that the value of the interference injected on the incumbent will be about 65 dB, whereas numerical simulations show that the actual interference value is 18.5 dB. Moreover, for $l = 20$,the PSD-based model predicts that the injected interference will be insignificant, whereas the numerical simulations show that it is still at a non-negligible level of 40 dB. This proves that in the Het scenario, the PSD-based model completely fails to give a good approximation of the interference injected by an OFDM/OQAM secondary user onto an incumbent CP-OFDM system.
The normalized Error Vector Magnitude (EVM) obtained for both users is plotted in Fig. 3.23. Here, the main observations are threefold:

- The PSD-based model approximates surprisingly well the interference seen by the secondary OFDM/OQAM user $\mathcal{U}_2$ in the *Het* scenario. This shows that the PSD-based model may still be suitable in some cases, especially when the time window of the receiver is longer than the interfering signal. However, the PSD-based model dramatically underestimates the interference seen by the incumbent receiver $\mathcal{U}_1$.
- The actual inter-user interference in the *Het* scenario is symmetrical. As a case in point, the obtained EVM

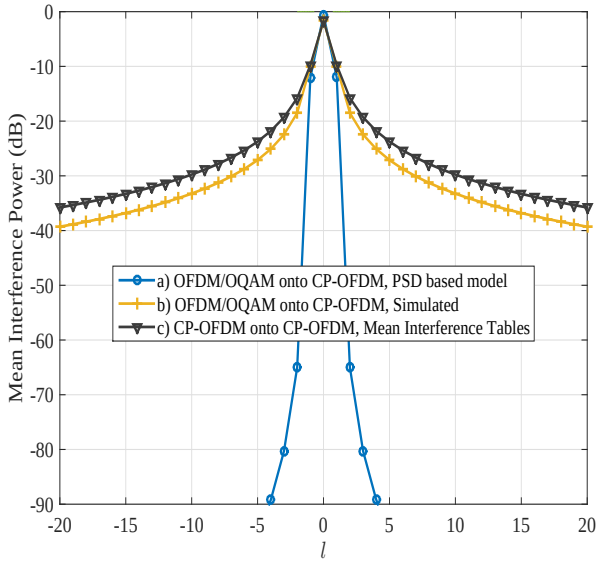

Figure 3.22: Comparison between interference values obtained with (a) OFDM/OQAM onto CP-OFDM with PSD-based model, (b) OFDM/OQAM onto CP-OFDM through numerical simulation, and (c) CP-OFDM onto CP-OFDM with mean interference tables [1].

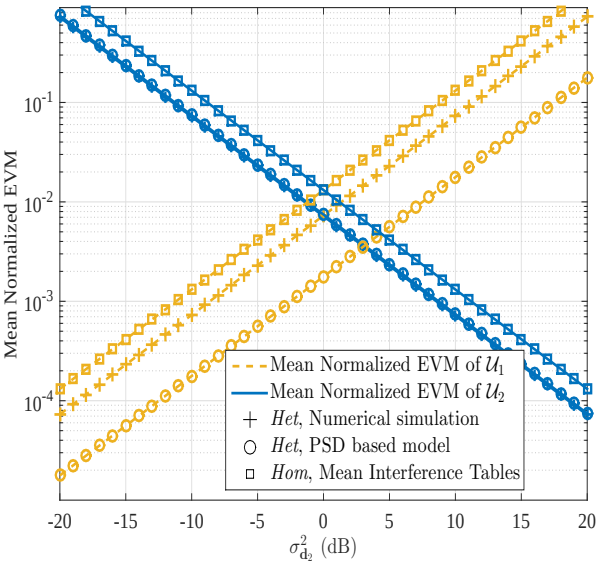

Figure 3.23: Mean Normalized EVM of users $\mathcal{U}_1$ and $\mathcal{U}_2$ in the scenarios *Het* and *Hom*

values for both users are equal when their transmission power is equal. This contradicts the PSD-based model, which predicts that the incumbent CP-OFDM $\mathcal{U}_1$ will be more protected than the secondary OFDM/OQAM $\mathcal{U}_2$: according to the PSD-based model, the normalized EVM values of both users are equal when $\sigma_{\mathbf{d}_2^2} = 3$ dB.

- Both $\mathcal{U}_1$ and $\mathcal{U}_2$ experience lower EVM in the *Het* scenario than in the *Hom* scenario.

More extended analysis and results can be found in the ICT'2016 paper [C100] depicted at the end of this Subsection 3.2.2.

As a general conclusion, it has been shown that the widely used PSD-based model is highly flawed and fails to give a good approximation of the interference seen by each user in heterogeneous scenarios. Indeed, presented numerical results showed that when the secondary system utilizes OFDM/OQAM, the actual values of interference are higher than those planned by the PSD based model by more than 50 dB. Furthermore, contrary to the widely spread idea that CP-OFDM interferes more onto OFDM/OQAM users than the opposite, we revealed that heterogeneous interference is symmetrical and that users interfere equally onto each other. Though it was shown that both users experience a slight improvement when the secondary user uses OFDM/OQAM modulation, the gain was shown to be much more limited than what was expected with the PSD-based model.

Results with exact mathematical close forms of the cross-interference between OFDM/OQAM and CP-OFDM systems due to their coexistence are provided in [C103, C105], where a copy of this last is depicted at the end of this Subsection 3.2.2. A Journal paper that gathers a deep analysis on the cross-interference with both numerical and the mathematical (theoretical) close form using generalized multi-Carrier waveform model based on linear and circular filter banks has been submitted to the IEEE Transactions on Communications Journal.

To resume, all the publications (See Subsection 2.1.1, pp. 30-41) related with the cited researches in this Subsection 3.2.2 are: Journals: one IEEE Transactions on Communications Journal submitted, Conferences: [C96, C97, C100, C103, C105, C106], the PhD thesis of Mr. Quentin BODINIER in progress, and the Master:

- Quentin Bodinier from Supélec. Master degree topic on: "Contributions to PHY and MAC layers for GFDM in the Context of Cognitive Radio", in collaboration with Trinity College in Dublin (Ireland). Supervisors: Dr. Christophe Moy and Faouzi Bader (Supélec), Dr. Hamed Ahmadi and Prof. Luiz DaSilva (Trinity College Dublin, Ireland). Period: March 2013-Aug 2014.

Following are the corresponding depicted papers:

1. [C97]- Quentin Bodinier, Arman Farhang, Faouzi Bader, Hamed Ahmadi, Jacques Palicot, and Luiz A. DaSilva,"5G Waveforms for Overlay D2D Communications: Effects of Time-Frequency Misalignment", in Proc. of the IEEE International Communications Conference (IEEE ICC '2016). Kuala Lumpur, Malaysia. May 2016.

2. [C100]- Quentin Bodinier, Faouzi Bader, and Jacques Palicot, "Modeling Interference Between OFDM/OQAM and CP-OFDM: Limitations of the PSD-Based Model", in Proc. of the International Conference on Telecommunications (ICT'2016), Thessaloniki-Greece. May 2016.

3. [C105]- Quentin Bodinier, Faouzi Bader, and Jacques Palicot, "Coexistence in 5G: Analysis of Cross-Interference between OFDM/OQAM and Legacy Users", in Proc. of the IEEE Global Communications Conference (Globecom'2016). Washington DC, USA, December 2016.

5G Waveforms for Overlay D2D Communications: Effects of Time-Frequency Misalignment

Quentin Bodinier*, Arman Farhang†, Faouzi Bader*, Hamed Ahmadi‡, Jacques Palicot*, and Luiz A. DaSilva†
*SCEE/IETR - CentraleSupelec, Rennes, France,
†CONNECT - Trinity College Dublin, Ireland,
‡University College Dublin, Ireland.
Email : quentin.bodinier@supelec.fr

***Abstract*—This paper analyses a scenario where a Device-To-Device (D2D) pair coexists with an Orthogonal Frequency Division Multiplexing (OFDM) based incumbent network. D2D transmitter communicates in parts of spectrum left free by cellular users, while respecting a given spectral mask. The D2D pair is misaligned in time and frequency with the cellular users. Furthermore, the D2D pair utilizes alternative waveforms to OFDM proposed for 5G. In this study, we show that it is not worth synchronising the D2D pair in time with respect to the cellular users. Indeed, the interference injected into the incumbent network has small variations with respect to time misalignment. We provide interference tables that encompass both time and frequency misalignment. We use them to analyse the maximum rate achievable by the D2D pair when it uses different waveforms. Then, we present numerical results showing what waveform should be utilized by the D2D pair according to the time-frequency resources that are not used by the incumbent network. Our results show that the delay induced by linearly convolved waveforms make them hardly applicable to short time windows, but that they dominate OFDM for long transmissions, mainly in the case where cellular users are very sensitive to interference.**

I. Introduction

The advent of Device-To-Device (D2D) communication as a new application in 5^{th} Generation wireless networks (5G) raises a number of challenges. In particular, coexistence of D2D pairs with cellular users may affect the performance observed by the latter. To avoid that, a first standard for D2D communication has been proposed [1], requiring consequent interaction between the base station and the D2D pairs.

With increasing number of D2D links, perfect synchronization between those and the native cellular subscribers is infeasible. Therefore, it is important to consider schemes where D2D users are not perfectly synchronized both in time and frequency with respect to the cellular users. In that case, it is well known that Orthogonal Frequency Division Multiplexing (OFDM) suffers from very high multiple user interference when timing and frequency offsets go beyond certain values [2], [3]. As a consequence, the overall quality of transmission seen by cellular users may decrease dramatically.

To cope with that challenge, a number of solutions based on both power loading and waveform design have been proposed [4]–[14]. On one hand, to the best of our knowledge, studies of interference caused by time-frequency misalignment are restricted to the case where the misaligned user has the same waveform as the others [3], [15], and there is no work addressing the interference caused by a given waveform onto OFDM. On the other hand, power-loading studies rely on interference models which do not take time-frequency misalignment into account [4]–[7]. However, accurately estimating the caused interference is of high importance, as D2D users aim to maximise their data rate subject to constraints of total power and maximum injected interference.

Therefore, it is crucial to analyse the effects of time-frequency misaligment on the interference caused by D2D pairs onto cellular users. In this paper, we derive interference tables that can be used to find the optimal solution of the power loading problem for D2D users following the model of [6]. These results allow us to analyse the performance of a D2D pair as a function of the waveform they utilise.

As a matter of fact, the rate achievable by D2D users is highly dependent on their air interface. Indeed, utilization of appropriate waveforms can limit Out Of Band (OOB) emissions of D2D users and therefore allows them to allocate higher power to their active subcarriers. It is well known that OFDM suffers from large sidelobes in frequency due to its rectangular window in time [11], [16], [17]. To overcome this problem, numerous new waveforms with intrinsic filtering properties have emerged [7]–[14]. These waveforms all rely on Filter Bank Multi Carrier (FBMC) modulation. In this work, we focus on four recently proposed FBMC based waveforms, namely Filtered Multi-Tone (FMT), Offset Quadrature Amplitude Modulated-Orthogonal Frequency Division Multiplexing (OFDM/OQAM), Lapped FBMC and GFDM.

In FMT modulation [8], [9], the assumption is that there is no overlapping between adjacent subcariers. Therefore, FMT suffers from some bandwidth efficiency loss. To increase spectral efficiency, OFDM/OQAM [10], [11] allows for adjacent subcarriers to overlap. Differently from FMT, real symbols having Pulse Amplitude Modulation (PAM) are transmitted on each subcarrier. A $\frac{\pi}{2}$ phase difference is applied to adjacent subcarriers, which provides real-domain orthogonality. However, OFDM/OQAM requires doubling the symbol rate. To avoid that, Lapped FBMC modulation has been recently proposed by Bellanger et al. in [12]. In this scheme, the number of subcarriers is doubled instead of the number of time symbols.

A drawback common to all the aforementioned modulations

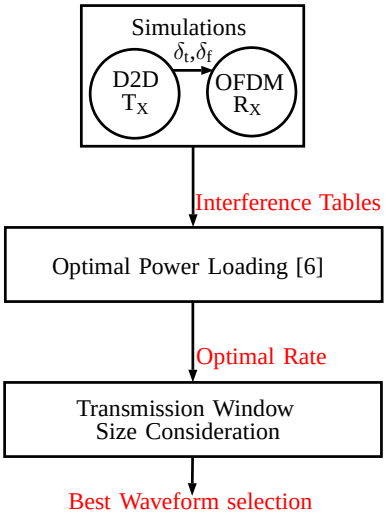

Fig. 1: Paper Synopsis

is the transient imposed by their transmit and receive filters. Generalized Frequency Division Multiplexing (GFDM) tackles this problem by application of cyclic pulse shaping [13]. However, this comes at the expense of higher OOB emissions, which is due do the discontinuities induced in the signal by truncation in time with a rectangular window [14].

In this paper, we analyse time-frequency misalignment effects of the D2D pair on the incumbent network. We evaluate the interference injected by the D2D pair on the incumbent network for each waveform separately. This allows us to build interference tables to be used as inputs to the power loading solution and analyse the maximum rate achievable through each waveform. We consider different resource sizes in time and frequency and calculate the resulting data rate. This analysis reveals the strength and weaknesses of different waveforms to be used by the D2D pair as a function of available time-frequency resources. Our approach is summarized in Fig. 1.

The remainder of this paper is organized as follows. In section II, the system model and the analysed waveforms are presented. Section III is dedicated to the interference analysis, whereas section IV presents the rate optimization problem and its solution. Section V presents simulation results. Finally, section VI concludes this paper.

II. Considered Scenario and Studied Waveforms

A. Considered scenario

In this study, we consider an OFDM based incumbent network with subcarrier spacing ΔF where a certain group of subcarriers is free and can be utilized by a D2D pair. It is assumed that the base station broadcasts information about its unused time-frequency resources. This information includes the number of free subcarriers M_{f} and the number of OFDM symbols during which the band will be free N_{f}. We define B_{i} as the band ocuppied by the cellular users, B_{f} the free band used by the D2D pair, and I_{th} as the interference threshold for B_{i}. It is assumed that the D2D pair can misalign its transmission frequency with respect to B_{f}. Besides, we assume that, even though the D2D transmission is

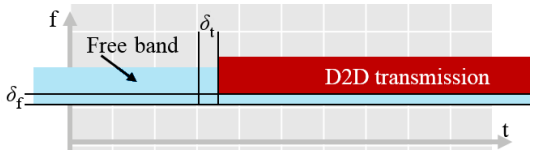

Fig. 2: Time-Frequency layout of the situation with time-frequency misplacement representation.

contained in the duration of the opportunity, time synchronism between D2D and cellular users at the symbol level may not be achieved. We denote δ_{t} and δ_{f} as the offsets in time and frequency. The scenario is presented in figure 2, where the grey grid represents the time-frequency resources of the incumbent network. These resources follow the 3GPP Long Term Evolution (LTE) standard.

B. Waveforms under consideration

To pave the way for the analysis conducted in Section III, we briefly explain the mathematical representation of the waveforms under study to be used by the D2D pair.

1) FMT: In this scheme, complex Quadrature Amplitude Modulation (QAM) symbols are linearly pulse shaped using the prototype filter $\mathbf{g} = [g[0] \dots g[KP-1]]^{\text{T}}$, where K is the overlapping factor and P is the number of samples per time symbol. M is the number of subcarriers, N the number of symbols in time, and $\mathbf{d}_m = [d_m[0] \dots d_m[N-1]]^{\text{T}}$ the vector of modulated symbols on the mth subcarrier. Finally, the FMT signal can be obtained as [9]

$$x_{\text{FMT}}[k] = \sum_{n=0}^{N-1}\sum_{m=0}^{M-1} d_m[n]g[k-nP]e^{j2\pi\frac{m}{M}k}, \quad \forall k = 0\dots(N+K-1)P-1. \tag{1}$$

2) OFDM/OQAM: In this modulation format, the signal can be derived in a similar way to FMT, where $P = M$, $\{d_m\}$ symbols are drawn from a PAM constellation, and a phase factor $\theta_m[n] = e^{j\frac{\pi}{2}\lfloor\frac{n+m}{2}\rfloor}$ is introduced where n and m the time-frequency indexes respectively. Besides, subsequent symbols are separated by $\frac{M}{2}$ samples in time, which implies doubling the symbol rate. Therefore, the transmit signal can be expressed as [18]

$$x_{\text{OQAM}}[k] = \sum_{n=0}^{N-1}\sum_{m=0}^{M-1}\left(d_m[n]\theta_m[n]g[k-n\frac{M}{2}] \times e^{j2\pi\frac{m}{M}(k-\frac{KM-1}{2})}\right), \quad \forall k = 0\dots(P+K-\frac{1}{2})M-1. \tag{2}$$

3) Lapped FBMC: This scheme is in essence similar to OFDM/OQAM systems. However, for this modulation the symbol rate is not doubled. As defined in [12], the emitted signal can be written as

$$x_{\text{Lapped}}[k] = \sum_{n=0}^{N-1}\sum_{m=0}^{M-1} d_m[n]g[k-nM]e^{j(k-\frac{1}{2}+\frac{M}{2})(m-\frac{1}{2})\frac{\pi}{M}}, \quad \forall k = 0\dots(P+1)M-1. \tag{3}$$

It is worth mentioning that the used filter is not tunable and is written as

$$g_{\text{Lapped}}[k] = -\sin\left[(k-\frac{1}{2})\frac{\pi}{2M}\right], \forall k = 0 \dots 2M-1. \quad (4)$$

4) GFDM: The data is packed in blocks of N_b symbols and a Cyclic Prefix (CP) is added to the beginning of each block. Every symbol is circularly convolved with a time shifted version of the same circular filter $\mathbf{g}$. Denoting as mod the modulo operation, the signal corresponding to one GFDM block is expressed as follows [14]

$$x_{\text{GFDM}}[k] = \sum_{n=0}^{N_\text{b}-1}\sum_{m=0}^{M-1} d_m[n] g\left[(k-nM) \text{mod}(N_\text{b}M)\right] e^{j2\pi k\frac{m}{M}}, \quad \forall k = 0 \dots MN_\text{b}-1. \quad (5)$$

III. Interference Analysis

To assign the optimal power distribution to the D2D subcarriers, it is vital to know how much power leaks to the adjacent band depending on which waveform is utilized by the D2D pair. The classical way to compute the leakage is to integrate the Power Spectral Density (PSD) of the interfering signal on the band that suffers from the interference. However, this model does not take into account the time window of the incumbent. This is of paramount importance as the incumbent only considers a time window with a specific width based on its own parameters. Besides, it has been shown in [19] that PSD is not a suitable measure to evaluate the inter-system interference for the scenario of interest to this paper. We therefore employ the instantaneous interference model proposed in [19] to compute the interference I_m^l injected to the lth subcarrier of the incumbent by the D2D signal x_m where only subcarrier m is utilized. This allows us to scrutinize the interference injected by each individual subcarrier to the incumbent network. Note that the same subcarrier spacing is used for both the D2D pair and the incumbent network. Therefore, we have

$$I_m^l = \int_{t=0}^{T} \left|\left(g_r^l * x_m\right)(t)\right|^2 dt, \quad (6)$$

where g_r^l is the receiver filter on subcarrier l and $*$ denotes the convolution operation. As the receiver suffering from interference is based on OFDM, in the discrete time domain, (6) becomes

$$I_m^l = \sum_{n=0}^{N-1} \frac{T_\text{s}}{M+N_\text{CP}} \sum_{k=n(M+N_\text{CP})+N_\text{CP}}^{(n+1)(M+N_\text{CP})} \left| x_m[k] e^{-j2\pi k\frac{l}{M}} \right|^2, \quad (7)$$

where N is the total number of OFDM symbols corresponding to the time span T, N_CP is the number of CP samples and M the number of samples per OFDM symbol of length T_s. According to the signal models presented in the former section, for any of the analysed waveforms, x_m can be written as

$$x_m[k] = a_m[k] e^{j2\pi k\frac{m}{M}}, \forall k = 0 \dots N(M+N_\text{CP})-1, \quad (8)$$

where a_m encompasses the modulated signal on subcarrier m. Therefore, putting (8) in (7) and taking into account timing and frequency offsets between the interferer and the receiver, we have

$$I_m^l(\delta_\text{t}, \delta_\text{f}) = \sum_{n=0}^{N-1} \left(\frac{T_\text{s}}{M+N_\text{CP}} \sum_{k=n(M+N_\text{CP})+N_\text{CP}}^{(n+1)(M+N_\text{CP})} \left| a_m[k] e^{j2\pi\left(k\frac{m-l+\delta_\text{f}}{M}+\frac{\delta_\text{t}}{M}\right)} \right|^2 \right). \quad (9)$$

Then, the mean interference seen at subcarrier l at the receiver of the incumbent can be written as

$$I_{m_\text{mean}}^l(\delta_\text{t}, \delta_\text{f}) = \frac{1}{N}\mathbb{E}_{d_m}(I_m^l(\delta_\text{t}, \delta_\text{f})), \quad (10)$$

where $\mathbb{E}_{d_m}$ represents the expectation with respect to the symbols transmitted on subcarrier m. We point out that when a larger number of subcarriers are utilized by the D2D pair, the total interference is equal to the sum of the interference caused by each subcarrier.

Finally, the total interference injected by the D2D transmission on the free band B_f to the incumbent band B_i is

$$I_{B_\text{i}}^{B_\text{f}} = \sum_{m\in B_\text{i},\ l\in B_\text{f}} \frac{P_m}{P_0} I_{m_\text{mean}}^l(\delta_\text{t}, \delta_\text{f}), \quad (11)$$

where P_m is the power assigned to the mth subcarrier and P_0 is a reference value of $1W$. This method can be used to compute the interference tables for the different analysed waveforms.

IV. D2D Pair Power Optimization

The interference tables that are derived in the previous section can be used as input to a power optimization block to maximize the rate of D2D users.

A. Power Optimization Problem

In the scenario of interest to this paper, the D2D transmitter has to optimize its power allocation to maximize its rate while satisfying the total power budget constraint, P_t, and maximum injected interference I_th to the incumbent band B_i. As shown in the previous section, interference injected onto cellular users depends on both the frequency and time misalignments of the D2D pair with respect to the incumbent network. However, it is assumed that the D2D pair is only aware of δ_t and δ_f ranges. $\delta_\text{t} \in \left[-0.5(\text{T}_\text{s}+\text{T}_\text{CP}), 0.5(\text{T}_\text{s}+\text{T}_\text{CP})\right)$ and $\delta_\text{f} \in \left[-\delta_{f_\text{max}}, \delta_{f_\text{max}}\right]$ where δ_{f_max} is the maximum misalignment in frequency.

In [19], the mean value of interference caused by δ_t is considered. However, a more stringent policy is required to fully protect the cellular users, as the interference caused by the D2D pair may take higher values than its mean. Therefore, we propose to perform the power allocation considering the maximum value for the injected interference. Hence, we define the maximum interference factor from a given subcarrier, m, to the incumbent band as

$$\Omega_m = \sum_{l\in B_\text{i}} \frac{\max\limits_{\delta_\text{f},\delta_\text{t}} I_{m_\text{mean}}^l(\delta_\text{t}, \delta_\text{f})}{P_0}. \quad (12)$$

TABLE I: Number of data symbols useful to D2D pairs

Waveform	Useful D2D Symbols
OFDM	N_{f}
FMT	$N_{\text{f}} - K + 1$
OFDM/OQAM	$\lfloor N_{\text{f}} \frac{M+N_{\text{CP}}}{M} - K + \frac{1}{2} \rfloor$
Lapped FBMC	$\lfloor N_{\text{f}} \frac{M+N_{\text{CP}}}{M} - 1 \rfloor$
GFDM	$N_b \lfloor \frac{N_{\text{f}}}{N_{\text{b}}} \frac{N_{\text{b}}(M+N_{\text{CP}})}{N_{\text{b}}M+N_{\text{CP}}} \rfloor$

On this basis, we define the following optimization problem for D2D pairs.

$$
\begin{aligned}
P1 : \max_{P_m} & \sum_{m=0}^{M_{\text{f}}-1} \log_2(1 + \frac{P_m^2}{\sigma^2_{\text{N+I}}}), \\
\text{s.t.} & \\
& \sum_{m \in B_{\text{f}}} P_m \Omega_m, \leq I_{\text{th}}, \\
& \sum_{m=0}^{M_{\text{f}}-1} P_m \leq P_{\text{t}}, \\
& P_m \geq 0, \forall m \in \{1 \dots M_{\text{f}}\}.
\end{aligned}
\tag{13}
$$

where $\sigma^2_{\text{N+I}}$ is the term accounting for both white noise and interference coming from cellular users.

After deriving the Karush-Kuhn-Tucker (KKT) conditions for the optimization in (13), the optical power allocation on subcarrier m is given by [6] as

$$
P_m^* = \max \left(0, \frac{1}{\alpha \Omega_m + \beta} - \sigma^2_{\text{N+I}} \right), \tag{14}
$$

α and β being the Lagrangian coefficients relative to (13).

B. Considering Transmission Window Duration

As a static interference constraint is assumed during the whole D2D transmission, we can simply compute the total number of bits transmitted as

$$
b = T_{\text{useful}} * \sum_{m=0}^{M_{\text{f}}-1} \log_2(1 + \frac{P_m^*}{\sigma^2_{\text{N+I}}}), \tag{15}
$$

where T_{useful} is the duration in which useful symbols can transmitted. This value depends on the utilized waveform. Indeed, for filter banks with linear pulse shaping like FMT and Lapped FBMC, the overlapping factor K introduces a delay of $K-1$ symbols in the time domain. For OFDM/OQAM, the delay imposed by the transmit and receive filters is $K - \frac{1}{2}$ symbols in time as symbols are separated by $\frac{T_s}{2}$. In contrast, OFDM and GFDM do not suffer from any delay. In fact, the block structure of GFDM brings some limitations, as the length of the whole block is fixed for any number of active symbols. Thus, the transmission window can only be fully utilized in time if its duration is a multiple of the GFDM block length. Table I presents the number of usable symbols for each waveform as a function of both D2D and incumbent parameters during a transmission window of length N_{f} symbols.

TABLE II: Proposed D2D Waveform Parameters

Waveform	Samples per symbol	CP samples	Filter	Overlapping factor.
OFDM	M	N_{CP}	Irrelevant	Irrelevant
FMT	$M + N_{\text{CP}}$	0	RRC, rolloff 0.2	6
OFDM/ OQAM	M	0	Phydias [18]	4
Lapped FBMC	M	0	Sine [12]	2
GFDM	M	N_{CP}	RRC, rolloff 0.2	5

V. Numerical Results

In this section, we present a broad set of numerical results analyzing the effects of time-frequency misalignment of the D2D pair and performance of the optimal power allocation scheme discussed in Section IV for different waveforms.

A. System Setup

We consider an incumbent system following similar parameters to 3GPP LTE standard. The OFDM cellular user occupies 180 subcarriers, which corresponds to 15 LTE resource blocks along the frequency axis. Besides, it uses $M = 180$ samples per symbol and $N_{\text{CP}} = 12$ samples. The length of the transmission window in time varies from $N_{\text{f}} = 1$ to 100 OFDM symbols. In the center of the incumbent band, a free band B_{f} divided into M_{f} subcarriers of 15 kHz is unused. This band is utilized by the D2D pair. No guard band is considered in this study. The parameters of each waveform under study for utilization by the D2D pair are listed in Table II. RRC refers to the Root Raised Cosine filter.

B. Computation of Interference Tables

In this subsection, we compute the interference caused by the D2D transmission according to (10). Fig. 3 illustrates the interference injected by one active subcarrier on the incumbent band as a function of δ_{t} when $\delta_{\text{f}} = 0$. We notice that OFDM based D2D transmission does not interfere at all if the timing offset is contained within the CP. However, when δ_{t} falls outside the CP, there is a big increase in the amount of interference to the incumbent band. On the other hand, the interference caused by other waveforms does not have a high variation with respect to δ_{t}. This result reveals that it may not be worth synchronising D2D transmission in time with the cellular users when different waveforms are utilised by the D2D pair.

Fig. 4 shows the interference that is injected by an active subcarrier with unitary power on 20 neighboring OFDM subcarriers as a function of δ_{t} for different waveforms. Interference caused by Lapped FBMC and OFDM/OQAM is weakly affected by the timing offset. GFDM and FMT show slight variations with respect to δ_{t}. On the contrary, the figure for OFDM shows high variations along the δ_{t} axis.

In addition, we evaluate the interference that is caused by the different waveforms. We present the mean and maximum interference with respect to δ_{t} in Figs. 5a and 5b.

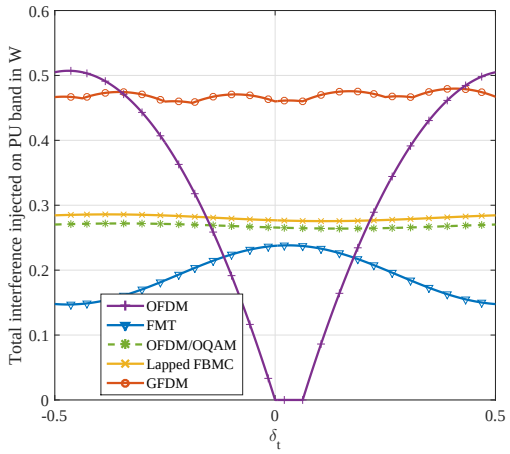

Fig. 3: Total injected interference on the incumbent band as a function of δ_t. Timing offset has limited impact on injected interference except in the case where D2D transmitters use OFDM.

Our observations are threefold: First, it appears that OFDM is the only waveform that shows a significant difference between its mean and maximum injected interference on the OFDM based incumbent. Other waveforms show a difference of approximately 0 to 1dB. Second, if mean interference is considered, GFDM causes the highest interference. However, if the maximum interference is considered, OFDM based D2D pair has the worst performance. Third, we point out that values of interference injected by 5G waveforms are surprisingly high. For OFDM/OQAM for example, the PSD based model predicts an attenuation of -60 dB at subcarrier distance of 2 [19], whereas our interference tables show that the interference power seen by an OFDM receiver at subcarrier distance of 2 is -18.5 dB. This is due to the fact that the OFDM demodulator performs Fast Fourier Transform (FFT) on a time window that may be much shorter than the length of the symbol of the other waveform. Therefore the signal suffers from discontinuities that produce projections on the whole incumbent spectrum.

Finally, we point out that interference tables are presented for $\delta_f = 0$. However, as δ_f only acts as a frequency shift in (10), when $\delta_f \neq 0$, the interference can be directly taken from interference tables by taking the corresponding subcarrier distance into account. As a case in point, if the subcarrier distance is -2 and $\delta_f = 1$, interference value corresponding to an actual subcarrier distance of -1 should be read from the table.

C. Transmission Performance

In this subsection, we consider the total amount of data that can be transmitted by the D2D pair during the transmission window as a measure to evaluate the performance of different waveforms. We use the interference tables derived in the previous subsection to calculate the total amount of data that can be transmitted during the transmission window based on the waveform that is utilised. We consider a transmission band consisting $M_f = 12$ free subcarriers, an interference constraint I_{th} of either 1 W or 1 mW, and variable number of

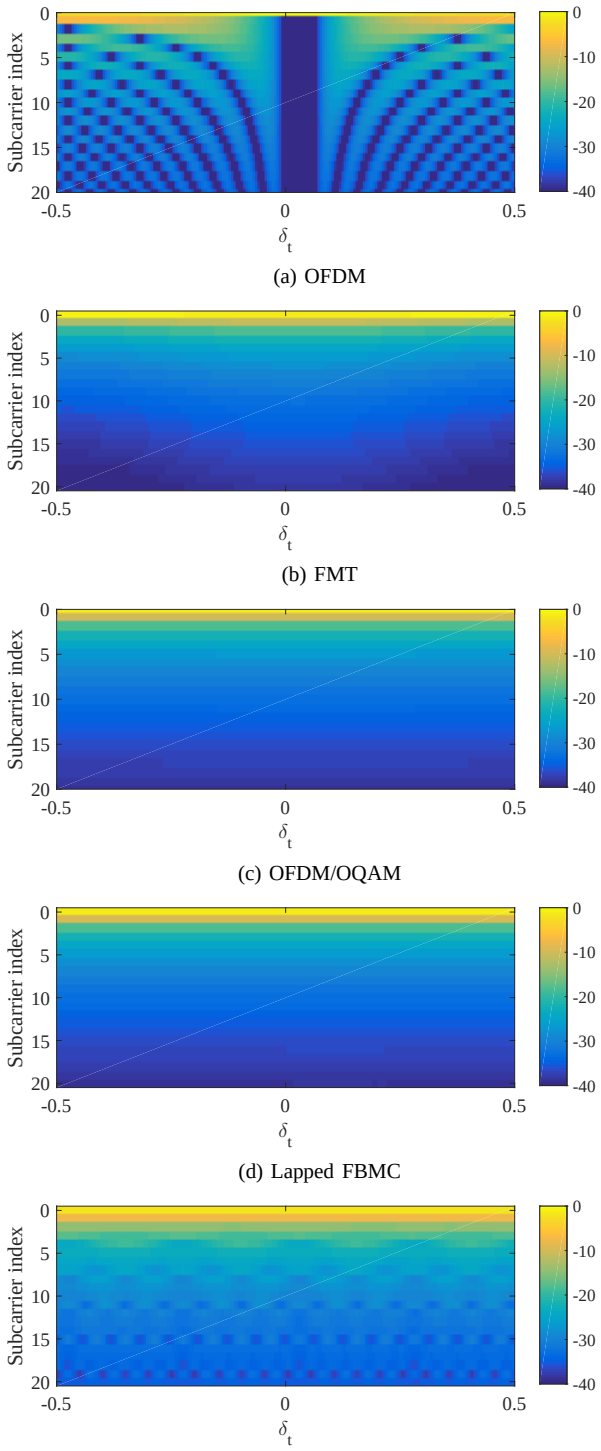

(a) OFDM

(b) FMT

(c) OFDM/OQAM

(d) Lapped FBMC

(e) GFDM

Fig. 4: Interference in dB caused by an active D2D at subcarrier 0 on 20 neighboring OFDM subcarriers of the incumbent in function of δ_t for different waveforms. Only OFDM shows a figure significantly varying along the δ_t axis. For the other studied waveforms, perfect time synchroization does not significantly reduce injected interference.

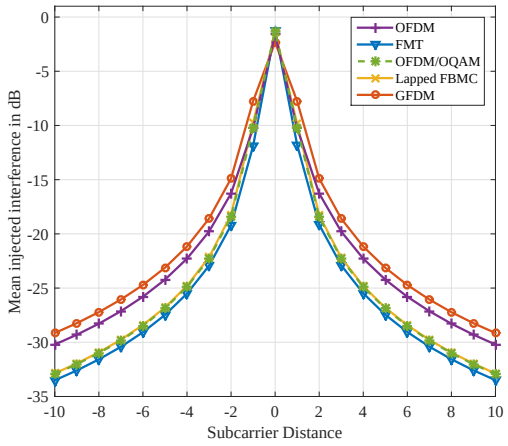

(a) Mean Interference Table on OFDM receiver

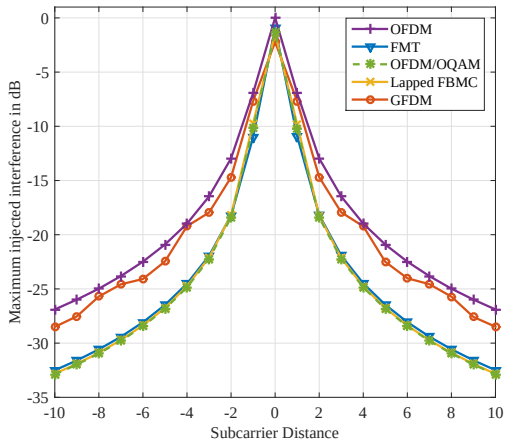

(b) Maximum Interference Table on OFDM receiver

Fig. 5: Maximum and Mean interference seen by a subcarrier of OFDM receiver as a function of its distance to an active 5G waveform subcarrier.

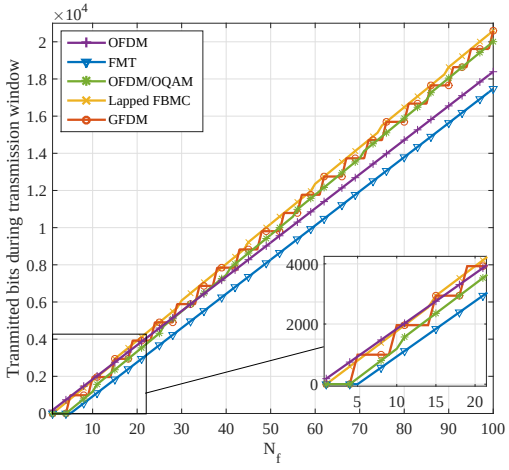

(a) $I_{\text{th}} = 1W$

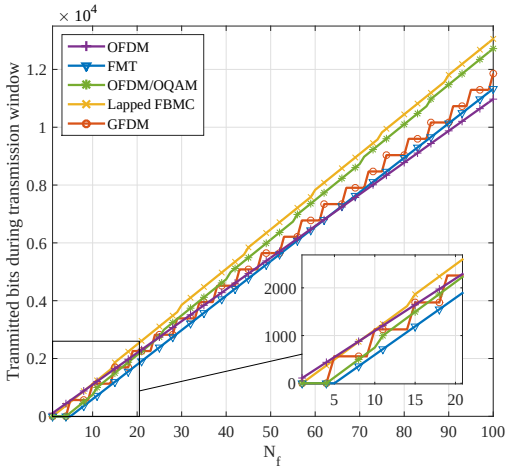

(b) $I_{\text{th}} = 1mW$

Fig. 6: Bits transmitted as a function of available OFDM time symbols in the transmission window

time symbols $N_{\text{f}} \in [1, 100]$. Besides, the maximum frequency misalignment is one subcarrier spacing (i.e. $\delta_{\text{f}_{\text{max}}} = 1$). Note that, $\sigma^2_{\text{N+I}}$ is assigned a low value of 10^{-6} to keep this paper focused on the interference injected by D2D pairs onto cellular users. The amount of data transmitted by the D2D pair as a function of N_{f} is obtained for two values of I_{th} in Fig. 6.

The presented results bring insight into which waveform performs best for different time window lengths and interference constraint. It seems that for transmission windows shorter than 10 symbols, OFDM is the best choice, as it does not suffer from any transmission delay. Therefore, linearly pulse shaped waveforms can compete only when the transmission window starts getting wider than 10 OFDM symbols. It can be noticed that Lapped FBMC shows a promising performance. This is due to the fact that it has a very short delay about only one symbol, and injects interference comparable to that of OFDM/OQAM and FMT. FMT suffers from a large delay during transmission and seems not to be an appropriate candidate for low latency applications. However, OFDM/OQAM performance stays very close to the Lapped FBMC. Interestingly, the performance of OFDM starts to degrade for time windows of width larger than $N_{\text{f}} = 15$ regardless of the interference constraint. This is the result of its spectral efficiency loss due to the presence of a CP. Note that, even though GFDM seems to be a potential competitor to OFDM/OQAM and Lapped FBMC when the interference constraint is very relaxed, it cannot efficiently cope with stringent interference constraints. This is the consequence of its high interference leakage as shown in Fig. 5.

Finally, we present results corresponding to a scenario where the time-frequency window is equal to 1 LTE Time Transmission Interval (TTI) and 12 subcarriers in frequency. This transmission window is indeed very short and hence waveforms with linear pulse shaping may suffer from the delay imposed by the transient of their transmit and receive filters. Fig. 7 depicts the performance of different waveforms as a function of the interference constraint. All the waveforms show a similar behaviour in which the number of transmitted bits saturate after a certain value of I_{th}. This corresponds to the

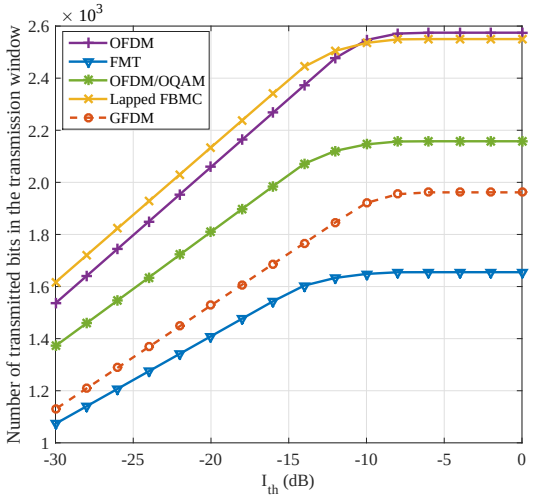

Fig. 7: Bits transmitted by different waveforms in 12 subcarriers during one TTI in function of the interference threshold.

point where the total power budget becomes the dominating factor to consider in (13). Furthermore, it can be seen once again that Lapped FBMC achieves the best performance as it offers a good trade-off between latency and interference. However, for $I_{\text{th}} \geq -10$ dB, OFDM achieves the best performance as the interference constraint is not restrictive anymore. It is worth mentioning that a specific number of symbols can be transmitted during a TTI corresponding to each waveform (see table I). In particular, GFDM performance is limited because it can only fit 10 symbols in the transmission window.

VI. Conclusion

In this study, we investigated a scenario where a D2D pair coexists with an OFDM based incumbent network. The D2D pair adopts an alternative 5G waveform to OFDM. Time-frequency misalignment of the D2D was taken into account to generate the interference tables from different waveforms to an OFDM receiver. This is in contrast to the usual analysis available in the literature, where the same waveform is considered for the source and the victim of interference. Through numerical results, we have shown that it is not worth synchronizing the D2D pair in time domain with respect to the incumbent network. Interference tables derived in this paper allowed us to analyse the maximum rate achievable by the D2D pair under different interference constraints. We have shown that the communication window size has a direct impact on the efficacy of the waveform utilized by the D2D pair. For short D2D transmission windows, OFDM, GFDM and Lapped FBMC seem to be appropriate candidates. We also showed that under stringent interference constraints and wide transmission windows, OFDM/OQAM and Lapped FBMC are strong candidates.

Acknowledgment

This work is an outcome of the mobility programm PHC Ulysses N34151SA funded by the French Ministry of Foreign Affairs and the Irish Research Council, and was partially funded through French National Research Agency (ANR) project ACCENT5 with grant agreement code: ANR-14-CE28-0026-02.

References

[1] 3GPP TR36.843, "Study on LTE device to device proximity services; Radio aspects (Release 12)," Tech. Rep., 2014.

[2] M. Morelli, C.-C. J. Kuo, and M.-O. Pun, "Synchronization Techniques for Orthogonal Frequency Division Multiple Access (OFDMA): A Tutorial Review," *Proceedings of the IEEE*, vol. 95, no. 7, pp. 1394–1427, Jul. 2007.

[3] B. Aziz, I. Fijalkow, and M. Ariaudo, "Intercarrier interference in uplink OFDMA systems with carrier frequency offset," *21st Annual IEEE International Symposium on Personal, Indoor and Mobile Radio Communications*, pp. 746–751, Sep. 2010.

[4] M. El-absi, M. Shaat *et al.*, "Power Loading and Spectral Efficiency Comparison of MIMO OFDM / FBMC for Interference Alignment Based Cognitive Radio Systems," in *ISWCS*, 2014, pp. 480–485.

[5] Y. Ma, Y. Xu, and D. Zhang, "Power allocation for orthogonal frequency division multiplexing-based cognitive radio systems with and without integral bit rate consideration," *IET Communications*, vol. 5, no. 5, p. 575, 2011.

[6] M. Shaat and F. Bader, "Low complexity power loading scheme in cognitive radio networks: FBMC capability," in *IEEE International Symposium on Personal, Indoor and Mobile Radio Communications*, 2009, pp. 2597–2602.

[7] G. Bansal, J. Hossain, and V. K. Bhargava, "Adaptive Power Loading for OFDM-Based Cognitive Radio Systems," in *IEEE International Conference on Communications*, 2007, pp. 5137–5142.

[8] A. M. Tonello, "Performance limits for filtered multitone modulation in fading channels," *IEEE Transactions on Wireless Communications*, vol. 4, no. 5, pp. 2121–2135, 2005.

[9] M. Renfors, J. Yli-Kaakinen *et al.*, "ICT-Emphatic, D2.1 : FB-MC and Enhanced OFDM Schemes," 2013.

[10] P. Siohan, C. Siclet, and N. Lacaille, "Analysis and design of OFDM/OQAM systems based on filterbank theory," *IEEE Transactions on Signal Processing*, vol. 50, no. 5, pp. 1170–1183, 2002.

[11] B. Farhang-Boroujeny, "OFDM versus filter bank multicarrier," *Signal Processing Magazine, IEEE*, no. MAY 2011, pp. 92–112, 2011.

[12] M. Bellanger, D. Mattera, and M. Tanda, "A Filter Bank Multicarrier Scheme Running at Symbol Rate for FutureWireless Systems," in *Wireless Telecommunications Symposium*, no. April, 2015.

[13] G. Fettweis, M. Krondorf, and S. Bittner, "GFDM-generalized frequency division multiplexing," in *IEEE Vehicular Technology Conference Sping*, 2009, pp. 1–4.

[14] N. Michailow, M. Matthe *et al.*, "Generalized Frequency Division Multiplexing for 5th Generation Cellular Networks," *IEEE Transactions on Communications*, vol. 62, no. 9, pp. 3045–3061, 2014.

[15] A. Aminjavaheri, A. Farhang *et al.*, "Impact of Timing and Frequency Offsets on Multicarrier Waveform Candidates for 5G," 2015. http://arxiv.org/abs/1505.00800

[16] L. G. Baltar, D. S. Waldhauser, and J. A. Nossek, "Out-Of-Band Radiation in Multicarrier Systems: A Comparison," in *Multi-Carrier Spread Spectrum 2007*. Springer Netherlands, 2007, vol. 1, pp. 107–116.

[17] H. Mahmoud, T. Yucek, and H. Arslan, "OFDM for cognitive radio: merits and challenges," *IEEE Wireless Communications*, vol. 16, no. April, pp. 6–15, 2009.

[18] A. Viholainen, M. Bellanger, and M. Huchard, "Prototype Filter and Structure Optimization," Phydias Project Consortium, Tech. Rep., 2009.

[19] Y. Medjahdi, M. Terré *et al.*, "Performance analysis in the downlink of asynchronous OFDM/FBMC based multi-cellular networks," *IEEE Transactions on Wireless Communications*, vol. 10, no. 8, pp. 2630–2639, 2011.

Modeling Interference Between OFDM/OQAM and CP-OFDM: Limitations of the PSD-Based Model

Quentin Bodinier, Faouzi Bader, and Jacques Palicot
SCEE/IETR - CentraleSupélec, Rennes, France,
Email : {firstname.lastname}@supelec.fr

***Abstract*—To answer the challenges put out by the next generation of wireless networks (5G), important research efforts have been undertaken during the last few years to find new waveforms that are better spectrally localized and less sensitive to asynchronism effects than the widely deployed Cyclic Prefix Orthogonal Frequency Division Multiplexing (CP-OFDM). One of the most studied schemes is OFDM-Offset Quadrature Amplitude Modulation (OFDM/OQAM) based on the PHYDYAS filter pulse. In the recent literature, spectrum coexistence between OFDM/OQAM and CP-OFDM is commonly studied based on the Power Spectral Density (PSD) model. In this paper, we show that this approach is flawed and we show that the actual interference injected by OFDM/OQAM systems onto CP-OFDM is much higher than what is classically expected with the PSD based model in the literature. We show that though using OFDM/OQAM in secondary systems is still advantageous, it brings limited gain in the context of coexistence with incumbent CP-OFDM systems.**

I. Introduction

The advent of the 5th Generation of wireless communication systems (5G) is envisioned to bring flexibility to cellular networks. New services as Device-To-Device (D2D) or Machine-To-Machine (M2M) communications are expected to be massively deployed in the near future. Such new communication devices have to coexist with incumbent legacy systems in the cell, i.e. Long-Term-Evolution Advanced (LTE-A) users. In such heterogeneous environments, perfect synchronization between the different types of systems is not feasible. This loss of synchronization will cause harmful interference between active users, which will in turn degrade the overall system performance.

This hurdle can be overcome through the design of new waveforms that are robust against asynchronism, and well localized in both time and frequency domains. As a matter of fact, it is now widely accepted that the Cyclic Prefix-Orthogonal Frequency Division Multiplexing (CP-OFDM) used in LTE-A is not adapted for flexible sharing and coexistence in fragmented spectrum for heterogeneous networks [1], [2]. Indeed, as soon as the orthogonality between CP-OFDM users is destroyed, for example because of the coexistence between unsynchronized incumbent and secondary systems, their performance shrinks dramatically [3]. This is mainly due to the fact that CP-OFDM systems filter symbols with a time-rectangular window, which causes poor frequency localization [4]–[6] and high asynchronism sensitivity in the multi-user context [6]–[9].

OFDM with Offset Quadrature Amplitude Modulation (OFDM/OQAM) [10], is one of the main new waveform schemes explored by the research community. Indeed, it overcomes the cited CP-OFDM limitations and enables both higher flexibility and reduction of interference leakage for multi-standard systems coexistence [4]–[6]. The coexistence between OFDM/OQAM based D2D pairs and CP-OFDM LTE users has been widely studied in [11], [12].

To the best of the authors knowledge, in all studies on coexistence between OFDM/OQAM secondary users [13]–[15] and CP-OFDM incumbent ones, the interference caused by the different types of users onto each other is quantified with the Power Spectral Density (PSD)-based model originally proposed in [16]. Yet, the authors pointed out in [12] that values of interference obtained by means of Monte-Carlo simulations were much higher than those obtained with the PSD-based model. In [17], Medjahdi *et. al.* designed a more precise interference model named ”instantaneous interference” that takes into account the demodulation operations and the time asynchronism between users. Nevertheless, the aforementioned study only analyzed the multiuser interference in cases where all users are using the same waveform, either CP-OFDM or OFDM/OQAM. No such analysis has been applied to heterogeneous scenarios where CP-OFDM and OFDM/OQAM system are deployed in the same geographical area and coexist in the same cell.

The approach of this paper is therefore to study inter-user interference in scenarios where CP-OFDM and OFDM/OQAM users interfere with each other. It is shown that the PSD based approach consists in modeling the interference at the input antenna of the interfered receiver, and totally omits the demodulation operations that are performed by the latter. We show that the actual interference seen at the output of the demodulator of the interfered receiver is much higher than expected using the PSD based model. Moreover, we show that interference between the incumbent and secondary systems is symmetrical, which contradicts the results obtained with the PSD-based model. Finally, the presented study nuances results classically shown in the literature, and diminishes the benefits expected from using OFDM/OQAM for coexistence with CP-OFDM incumbent systems.

The remainder of this paper is organized as follows: Section II presents the system model. In Section III, a short

This work was partially funded through French National Research Agency (ANR) project ACCENT5 with grant agreement code: ANR-14-CE28-0026-02.

978-1-5090-1990-8/16/$31.00 ©2016 IEEE

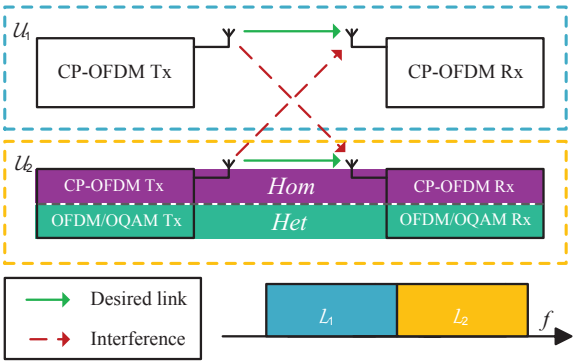

Fig. 1: Summary of the study led in the paper : two users $\mathcal{U}_1$ and $\mathcal{U}_2$ transmit on adjacent bands $\mathcal{L}_1$ and $\mathcal{L}_2$ and interfere with each other. Channel is assumed perfect and no Gaussian noise is considered. $\mathcal{U}_2$ uses CP-OFDM in *Hom* scenario and OFDM/OQAM in *Het* scenario.

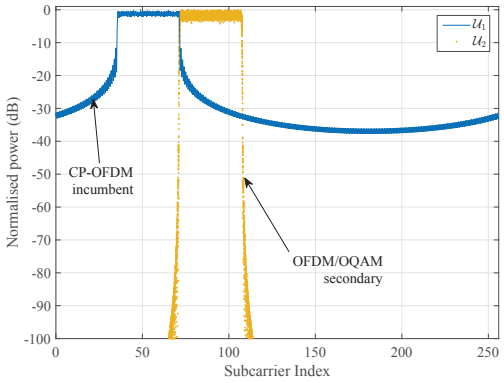

Fig. 2: Spectral representation of the *Het* scenario. CP-OFDM $\mathcal{U}_1$ and OFDM/OQAM $\mathcal{U}_2$ use directly adjacent bands $\mathcal{L}_1$ and $\mathcal{L}_2$ with same number of subcarriers.

overview on CP-OFDM and OFDM/OQAM systems is given. In Section IV, the different models used to rate heterogeneous interference between OFDM/OQAM and CP-OFDM are presented. In Section V, numerical results are presented and concluding remarks are provided in Section VI.

Notations: Throughout this paper, scalars are noted x, vectors are bold-faced as $\mathbf{x}$, k represents the discrete time sample index, n indexes symbols and m indexes subcarriers. $\mathcal{R}\{.\}$ is the real part operator and $E_\alpha\{.\}$ is the mathematical expectation with respect to the random variable α.

II. System Model

In this paper, we focus on rating the inter-user interference caused by the fact that different users transmit in an asynchronous manner with different waveforms. Therefore, we consider a simple scenario where an incumbent system $\mathcal{U}_1$ coexists with a secondary user $\mathcal{U}_2$ in the same band. Both systems use multicarrier waveforms with the same subcarrier spacing ΔF, and each of them is assigned a set of subcarriers $\mathcal{L}_i$. The incumbent $\mathcal{U}_1$ utilizes CP-OFDM, whereas two alternatives are studied for $\mathcal{U}_2$. The latter uses CP-OFDM in the case of a homogeneous scenario (referred to as *Hom*) and OFDM/OQAM in the case of a heterogeneous scenario (referred to as *Het*). The configurations studied in this paper are summarized in Fig. 1. To focus the study on interference coming from the coexistence between these two systems, all channels are assumed perfect, and no Gaussian noise is considered. Considering an infinite transmission on M subcarriers, the sequences of symbols estimated at the receiver of $\mathcal{U}_1$ and $\mathcal{U}_2$ are modeled by

$$\hat{\mathbf{d}}_{1,m}[n] = \mathbf{d}_{1,m}[n] + \boldsymbol{\eta}_m^{2\to1}[n], \quad (1)$$

$$\hat{\mathbf{d}}_{2,m}[n] = \mathbf{d}_{2,m}[n] + \boldsymbol{\eta}_m^{1\to2}[n], \quad (2)$$

$$\forall n \in \mathbb{N},\ \forall m = 0 \dots M-1$$

where $\mathbf{d}_{i,m}[n]$ is the n-th symbol transmitted on the m-th subcarrier by user $\mathcal{U}_i$, and $\boldsymbol{\eta}_m^{j\to i}[n]$ represents the interference injected by the user $\mathcal{U}_j$ onto the n-th time slot and m-th subcarrier of user $\mathcal{U}_i$.

In both analyzed scenarios, incumbent $\mathcal{U}_1$ and secondary $\mathcal{U}_2$ experience a loss of synchronization in time domain. Besides, the time duration between two subsequent CP-OFDM symbols transmitted by the incumbent system $\mathcal{U}_1$ is $T_\text{s} + T_\text{CP}$, where T_s is the time-symbol and T_CP accounts for the duration of the CP. It is assumed that the transmission of $\mathcal{U}_2$ starts with a delay τ with respect to the transmission of $\mathcal{U}_1$. τ is taken as a random variable uniformly distributed in the interval $[-\frac{T_\text{s}+T_\text{CP}}{2}\ \frac{T_\text{s}+T_\text{CP}}{2}[$. Therefore, the interference injected by the users onto each other is a function of the symbols they transmit and of the value of τ. The mean interference power seen by each user on their m-th subcarrier is expressed as

$$I_m^{1\to2} = E_{\mathbf{d}_1,\tau}\{|\boldsymbol{\eta}_m^{1\to2}[n]|^2\}, \quad (3)$$

$$I_m^{2\to1} = E_{\mathbf{d}_2,\tau}\{|\boldsymbol{\eta}_m^{2\to1}[n]|^2\}, \quad (4)$$

and the total interference injected by each user onto the other is

$$I^{1\to2} = \sum_{m\in\mathcal{L}_2} I_m^{1\to2} \quad (5)$$

$$I^{2\to1} = \sum_{m\in\mathcal{L}_1} I_m^{2\to1} \quad (6)$$

In the following, the structures of the CP-OFDM and OFDM/OQAM signals are briefly presented.

III. CP-OFDM and OFDM/OQAM PHY Characteristics

A. CP-OFDM

We consider a CP-OFDM system composed of M subcarriers out of which M_a are active. We define M vectors $\mathbf{d}_m$ such that $\mathbf{d}_m$ is constituted of complex Quadrature Amplitude Modulation (QAM) symbols if subcarrier m is active. Else, $\mathbf{d}_m[n] = 0, \forall n \in \mathbb{N}$. N_CP being the length of the CP, the n-th OFDM symbol is expressed as

$$\mathbf{x}_n[k] = \sum_{m=0}^{M-1} \mathbf{d}_m[n] e^{j2\pi \frac{m}{M} k}, \quad n(M+N_{CP}) - N_{CP} \leq k \leq n(M+N_{CP}) + M - 1, \tag{7}$$

and the total signal is expressed as $\mathbf{x}[k] = \sum_n \mathbf{x}_n[k]$.

To highlight the effects of inter-user interference only, we consider that the channel is perfect and that the CP-OFDM signal is polluted by an additive interfering signal $\mathbf{y}$. In that case, the n-th CP-OFDM estimated symbol is

$$\hat{\mathbf{d}}_m[n] = \mathbf{d}_m[n] + \underbrace{\sum_{k=n(M+N_{CP})}^{n(M+N_{CP})+M-1} \mathbf{y}[k] e^{j2\pi \frac{k}{M} m}}_{\boldsymbol{\eta}_m[n]}, \quad 0 \leq m \leq M-1 \tag{8}$$

where $\boldsymbol{\eta}_m[n]$ represent the total amount of interference that affects the estimated signal $\hat{\mathbf{d}}_m[n]$ as defined in (1) or (2).

B. OFDM/OQAM

The OFDM/OQAM system is composed of M subcarriers out of which M_a are active, where M vectors $\mathbf{d}_m$ contain real Pulse Amplitude Modulation (PAM) symbols if subcarrier m is active and $\mathbf{d}_m[n] = 0, \forall n \in \mathbb{N}$ otherwise. A phase factor $\boldsymbol{\theta}_n[m] = e^{j\frac{\pi}{2}\lfloor \frac{n+m}{2} \rfloor}$ is further added to the symbols $\mathbf{d}_m[n]$. OFDM/OQAM is a based on a uniform polyphase filter bank structure with a prototype filter $\mathbf{g}$ of length $L_{\mathbf{g}} = KM$, where K is called the overlapping factor, which is shifted to cover the whole of the system bandwidth. Subsequent symbols are separated by $\frac{M}{2}$ samples and are filtered through time-frequency shifted versions of $\mathbf{g}$. Therefore, each subcarrier is filtered by a filter $\mathbf{f}_m$ defined as :

$$\mathbf{f}_m[k] = \mathbf{g}[k] e^{j2\pi \frac{m}{M}(k - \frac{KM-1}{2})}, 0 \leq k \leq KM-1 \tag{9}$$

and the n-th modulated OFDM/OQAM symbol is written as

$$\mathbf{x}_n[k] = \sum_{m=0}^{M-1} \mathbf{d}_n[m] \boldsymbol{\theta}_n[m] \mathbf{g}[k - n\frac{M}{2}] \times e^{j2\pi \frac{m}{M}(k - \frac{KM-1}{2})}, \quad (n-K)\frac{M}{2} \leq k \leq (n+K)\frac{M}{2} - 1 \tag{10}$$

In this study, $\mathbf{g}$ is taken as the PHYDYAS filter with overlapping factor $K = 4$ [18]. The frequency response of g is expressed as

$$G(f) = \sum_{k=-(K-1)}^{K-1} G_{|k|} \frac{\sin(\pi(f - \frac{k}{KM})KM)}{KM\pi(f - \frac{k}{KM})}, \tag{11}$$

where $G_0 = 1$, $G_1 = 0.971960$, $G_2 = 1/\sqrt{2}$, and $G_3 = 0.235147$ (see [18] for more details on OFDM/OQAM modulation).

At the receiver, each subcarrier is filtered through the matched filter $\tilde{\mathbf{f}}_m$ and the real part of the signal is taken to remove purely imaginary intrinsic interference [4] generated by the prototype filter $\mathbf{g}$. Therefore, the estimated signal at the m-th subcarrier of the n-th symbol can be expressed as (13).

Based on the signal models defined in this section, we will hereafter discuss the modeling of the interference that the primary and secondary systems $\mathcal{U}_1$ and $\mathcal{U}_2$ inject onto each other.

IV. Modeling Heterogeneous Interference

A. Mean Interference

The amount of interference suffered by $\mathcal{U}_1$ and $\mathcal{U}_2$ on each of their subcarriers can be estimated from (3),(4). In the *Hom* scenario, both $\boldsymbol{\eta}^{1\to2}$ and $\boldsymbol{\eta}^{2\to1}$ are obtained by replacing $\mathbf{y}$ in (8) with $\mathbf{x}_n[k]$ expression of (7). Then, $I^{1\to2}$ and $I^{2\to1}$ are obtained by substituting (8) in (5) and (6) respectively. These derivations lead to the following expressions of the interference caused by $\mathcal{U}_1$ (resp. $\mathcal{U}_2$) onto $\mathcal{U}_2$ (resp. $\mathcal{U}_1$):

$$I_{Hom}^{1\to2} = \sigma_{\mathbf{d}_1^2} \sum_{m\in\mathcal{L}_2, q\in\mathcal{L}_1} I_{Hom}^{1\to2}(q-m), \tag{13}$$

$$I_{Hom}^{2\to1} = \sigma_{\mathbf{d}_2^2} \sum_{m\in\mathcal{L}_1, q\in\mathcal{L}_2} I_{Hom}^{2\to1}(q-m), \tag{14}$$

where $\sigma_{\mathbf{d}_i^2}$ is the variance of $\mathbf{d}_i$. Besides, $\forall l$, $I_{Hom}^{1\to2}(l)$ (resp. $I_{Hom}^{2\to1}(l)$) represents the interference injected by the signal on the q-th subcarrier of $\mathcal{U}_1$ (resp. $\mathcal{U}_2$) onto the m-th subcarrier m of (resp. $\mathcal{U}_1$) where $l = q - m$ is called the spectral distance. In *Hom* scenario, $\forall l, I_{Hom}^{1\to2}(l) = I_{Hom}^{2\to1}(l)$, and Mejdahdi *et. al.* have derived in [17] a closed-form of the interference $I_{Hom}^{1\to2}(l)$ and tabulated its values in so-called "Mean Interference Tables".

In *Het* scenario, the expression of $\boldsymbol{\eta}^{1\to2}$ (resp. $\boldsymbol{\eta}^{2\to1}$) is obtained by replacing $\mathbf{y}$ in (8) (resp. (13)) with the expression of $\mathbf{x}_n[k]$ in (10) (resp. (7)). Then, values of $I^{1\to2}$ (resp. $I^{2\to1}$) are finally rated by substituting the resulting expression in (5) (resp. (6)). After several derivation steps, we get, as in the *Hom* scenario,

$$I_{Het}^{1\to2} = \sigma_{\mathbf{d}_1^2} \sum_{m\in\mathcal{L}_2, q\in\mathcal{L}_1} I_{Het}^{1\to2}(q-m), \tag{15}$$

$$I_{Het}^{2\to1} = \sigma_{\mathbf{d}_2^2} \sum_{m\in\mathcal{L}_1, q\in\mathcal{L}_2} I_{Het}^{2\to1}(q-m). \tag{16}$$

Getting mathematical closed-forms of $I_{Het}^{1\to2}(l)$ and $I_{Het}^{2\to1}(l)$ is challenging, which is why, for sake of simplicity, most studies of mutual interference in heterogeneous scenarios are based on the PSD-based model [13]–[16].

B. PSD-based Interference Modeling

The PSD-based model consists in computing the leakage caused by users onto each other by integrating the PSD of the interfering signal on the band that suffers from the interference. Therefore, in the *Het* scenario, according to the PSD-based model, (15) and (16) are obtained by computing

$$I_{Het}^{1\to2}(l) = \int_{l-1/2\Delta F}^{l+1/2\Delta F} \Phi_{\text{CP-OFDM}}(f) df, \tag{17}$$

$$I_{Het}^{2\to1}(l) = \int_{l-1/2\Delta F}^{l+1/2\Delta F} \Phi_{\text{PHYDIAS}}(f) df, \tag{18}$$

$$\hat{\mathbf{d}}_n[m] = \mathbf{d}_n[m] + \underbrace{\mathcal{R}\left\{ \sum_{k=(n-K)\frac{M}{2}}^{(n+K)\frac{M}{2}} \mathbf{y}[k] \sum_{\nu=-2K+1}^{2K-1} (-1)^{m(\nu-n)} \times e^{-j2\pi \frac{m}{M}(k-\frac{KM-1}{2})} \mathbf{g}\left[k+(\nu-n)\frac{M}{2}\right] \right\}}_{\boldsymbol{\eta}_m[n]} \quad (12)$$

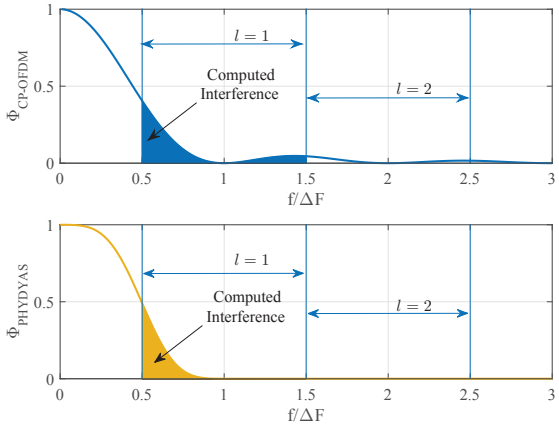

Fig. 3: Modeling of injected interference with the PSD-based model for CP-OFDM (top) and OFDM/OQAM with PHYDYAS filter (bottom). The values of interference injected by subcarrier 0 on a subcarrier at a spectral distance of $l = 1$ correspond to the integration of the PSD from $0.5\ \Delta F$ to $1.5\ \Delta F$.

where $\Phi_{\text{CP-OFDM}}$ (resp. Φ_{PHYDIAS}) is the PSD of the CP-OFDM signal (resp. of OFDM/OQAM with PHYDIAS filter). A graphical view of (17) and (18) is presented in Fig. 3. It can be seen than values of interference rated with the PSD-based model are not symmetrical. As a matter of fact, because the side-lobes of $\Phi_{\text{CP-OFDM}}$ are much higher than those of Φ_{PHYDIAS}, the PSD-based model will give $I_{Het}^{1\to2} \gg I_{Het}^{2\to1}$. Therefore, according to the PSD-based model, the CP-OFDM incumbent $\mathcal{U}_1$ interferes more onto the OFDM/OQAM secondary $\mathcal{U}_2$ than the opposite.

Besides, because the PSD-based model only rates the power of injected interference, it is challenging to map the obtained values of interference to higher level metrics, e.g. Bit Error Rate (BER). The only possibility offered by the PSD-based model is to approximate the statistics of heterogeneous interference as a white Gaussian noise the variance of which is given by (18), i.e

$$\boldsymbol{\eta}_m^{2\to1} \sim \mathcal{N}(0, \sum_{q\in\mathcal{L}_\infty} I_{Het}^{2\to1}(q-m)). \quad (19)$$

Then, classical expressions of transmission performance under white Gaussian noise in [19] can be applied.

C. Discussing the suitability of the PSD-based model

The main pitfall of the PSD-based model lies in the fact that it does not take into account the time window of the receiver.

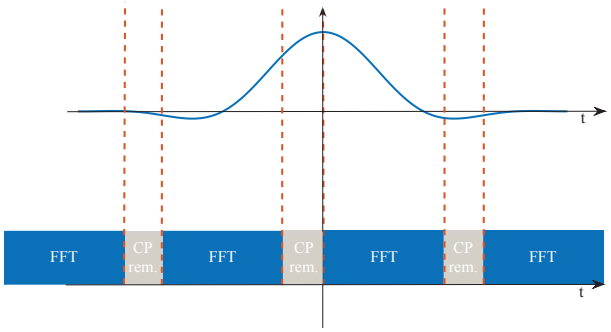

Fig. 4: Demodulation operations at the CP-OFDM receiver with an interfering OFDM/OQAM signal. The well-shaped PHYDYAS filter is cut in small non-contiguous parts on which FFT operations are performed.

However, this is of paramount importance as the incumbent only considers a time window with a specific width based on its own parameters. To illustrate this, Fig. 4 shows the demodulation operations that are performed by the CP-OFDM incumbent with an interfering secondary OFDM/OQAM signal. Though the PHYDYAS filter is well spectrally localized, it has a length of $L_{\text{PHYDYAS}} = KM$ samples. However, the CP-OFDM receiver window is of length $L_{\text{CP-OFDM}} = M$ samples. Therefore, as plotted in Fig. 4, the CP-OFDM incumbent demodulator performs Fast Fourier Transform (FFT) on a time window which is much shorter than the length of the prototype filter of OFDM/OQAM. In turn, the signal suffers from discontinuities that produce projections on the whole incumbent spectrum.

Moreover, Fig. 3 shows that the PSD based model consists in multiplying the interfering signal by a rectangular window in the frequency domain. In the time domain, this corresponds to filtering the interfering signal through an infinite sinc filter. Therefore, the PSD-based model does not reflect the actual demodulation operations that are processed at the CP-OFDM receiver that suffers from interference.

Besides, Fig. 4 shows that the prototype filter of OFDM/OQAM spans multiple time windows of the CP-OFDM incumbent receiver. Then, one OFDM/OQAM symbol interferes on several subsequent CP-OFDM symbols. This shows that the elements of $\boldsymbol{\eta}^{2\to1}$ cannot be considered independent. Therefore, though Gaussian, the heterogeneous interference between the two users in *Het* scenario is not white, but colored.

V. Numerical Results

In this section, we present several numerical results comparing values obtained with the PSD-based model and by

numerical simulations. Besides, both scenarios *Het* and *Hom* are studied to rate the advantages of using OFDM/OQAM in the secondary system.

A. System Setup

We consider an incumbent system $\mathcal{U}_1$ with 3GPP LTE standard parameters with $M_a = 36$ active subcarriers, which corresponds to 3 LTE resource blocks along the frequency axis, $M = 256$ samples per symbol and $N_{\text{CP}} = 18$ CP samples. The secondary user $\mathcal{U}_2$ also uses 3 LTE resource blocks along the frequency axis. No guard band is considered between the two users, and they are directly adjacent in the spectrum. More specifically, the sets of subcarriers occupied by the two users are defined as $\mathcal{L}_1 = [37 \dots 72]$ and $\mathcal{L}_2 = [73 \dots 108]$. Both users use the same subcarrier spacing $\Delta F = 15$ kHz. In *Hom* scenario, CP-OFDM based $\mathcal{U}_2$ uses the same parameters as $\mathcal{U}_1$. In the *Het* scenario, OFDM/OQAM based $\mathcal{U}_2$ uses $M = 256$ samples per symbol and the PHYDIAS filter with overlapping factor $K = 4$. In *Het* scenario, the performance of users is evaluated though empirical estimation of (5) and (6) based on Monte-Carlo simulation and compared with the values expected with the PSD-based model. CP-OFDM systems transmit complex symbols drawn from a 64-Quadrature Amplitude Modulation (QAM) constellation. To ensure fairness, OFDM/OQAM systems transmit twice as much real symbols drawn from a 8-Pulse Amplitude Modulation (PAM), which corresponds to a 64 QAM after reconstruction of a complex constellation. Moreover, $\mathcal{U}_2$ starts transmitting with a delay $\tau \in [-\frac{M+N_{\text{CP}}}{2} \ \frac{M+N_{\text{CP}}}{2}[$. Finally, numerical simulations are led on 10^5 symbols, each carrying 6 bits. Therefore, the BER curves drawn from numerical simulation are based on a transmission of $6 \times M_a \times 10^5 = 1.92 \times 10^7$ bits.

B. Interference Analysis

First, we aim to rate the interference caused by $\mathcal{U}_2$ on the incumbent $\mathcal{U}_1$. Fig. 5 presents the values of $I^{2\to1}(l)$ in dB for spectral distance $l \in [-20\ 20]$. For the *Het* scenario, i.e. when $\mathcal{U}_2$ uses OFDM/OQAM, we present values obtained with both the PSD-based model and through numerical simulations. We can observe in Fig. 5 a tremendous gap between the values of interference planned by the PSD-based model and the real ones. As a case in point, at $l = 2$, the PSD-based model plans that the value of the interference injected on the incumbent will be about -65 dB, whereas numerical simulations show that the actual interference value is -18.5 dB. Moreover, for $l = 20$, the PSD-based model predicts that the injected interference will be insignificant, whereas the numerical simulations show that it is still at a non-negligible level of -40 dB. This proves that in the *Het* scenario, the PSD-based model completely fails to give a good approximation of the interference injected by an OFDM/OQAM secondary user onto an incumbent CP-OFDM system.

Besides, the mean interference tables from [17] are plotted to rate the interference injected by $\mathcal{U}_2$ onto $\mathcal{U}_1$ for the *Hom* scenario, when both systems are using CP-OFDM. It shows

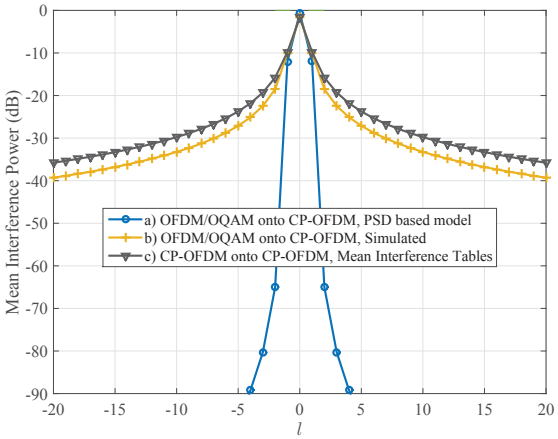

Fig. 5: Comparison between interference values obtained with (a) OFDM/OQAM onto CP-OFDM with PSD-based model, (b) OFDM/OQAM onto CP-OFDM through numerical simulation, and (c) CP-OFDM onto CP-OFDM with mean interference tables [17].

that the interference injected onto $\mathcal{U}_1$ can be reduced by approximately 5 dB if $\mathcal{U}_2$ uses OFDM/OQAM. Though much less than what was expected with the PSD-based model, this gain is still high enough to be noticed.

Having rated the power of injected interference, we focus now on the statistics of the latter in the *Het* scenario. To do so, we scrutinize the distribution of $\boldsymbol{\eta}_{72}^{2\to1}$, which corresponds to the interference injected by the OFDM/OQAM based $\mathcal{U}_2$ onto the closest subcarrier of $\mathcal{U}_1$. We show the Probability Distribution Function (PDF) of this interference signal in Fig. 6a. We can notice that it is well approximated by a Gaussian function of variance $I_{72,Het}^{2\to1}$. However, the covariance matrix of the studied interference, plotted in Fig. 6b is band-diagonal. This reveals a dependency between subsequent samples of the interference signal $\boldsymbol{\eta}_{72}^{2\to1}$. These two figures therefore corroborate the remarks we highlighted in Section IV-C and confirm the fact that heterogeneous interference is colored.

C. Transmission Performance

We now focus on the transmission performance of both users. To do so, we set the power of the symbols transmitted by the incumbent system $\mathcal{U}_1$ as $\sigma^2_{\mathbf{d}_1} = 0$ dB and we sweep $\sigma^2_{\mathbf{d}_2}$ from -20 dB to 20 dB. Here, we focus on the effects of inter-user interference caused by the adjacent transmissions of the two users. Therefore, no channel and no noise is considered. The normalized Error Vector Magnitude (EVM) obtained for both users is plotted in Fig. 7. Here, our observations are three-fold: first, the PSD-based model approximates surprisingly well the interference seen by the secondary OFDM/OQAM user $\mathcal{U}_2$ in the *Het* scenario. This shows that the PSD-based model may still be suitable in some cases, especially when the time window of the receiver is longer than the interfering signal. However, the PSD-based model dramatically underestimates

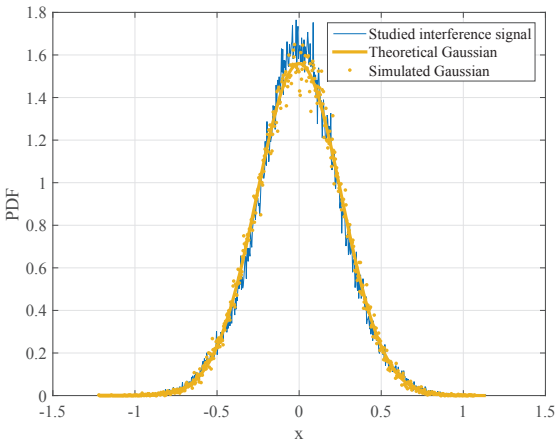

(a) Probability Distribution Function

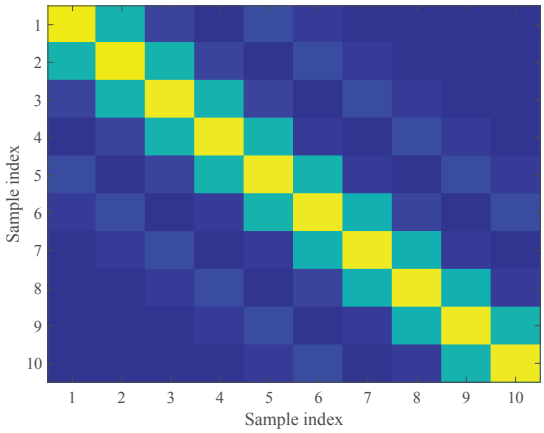

(b) Covariance matrix

Fig. 6: Statistics of interference signal caused by OFDM/OQAM onto CP-OFDM subcarrier 72. The different results show that it can be modeled by a colored Gaussian noise.

the interference seen by the incumbent receiver $\mathcal{U}_1$. Second, we point out that the actual inter-user interference in the *Het* scenario is symmetrical. As a case in point, the obtained EVM values for both users are equal when their transmission power is equal. This contradicts the PSD-based model, which predicts that the incumbent CP-OFDM $\mathcal{U}_1$ will be more protected than the secondary OFDM/OQAM $\mathcal{U}_2$: according to the PSD-based model, the normalized EVM values of both users are equal when $\sigma^2_{\mathbf{d}_2} = 3$ dB. Third, both $\mathcal{U}_1$ and $\mathcal{U}_2$ experience lower EVM in the *Het* scenario than in the *Hom* scenario.

Based on the above results, we analyze the BER for both users in Fig. 8. As said in Section IV-C, the interfering signal is approximated to a white Gaussian noise to compute the BER from the EVM for both the PSD-based model in the *Het* scenario and the instantaneous interference tables in the *Hom* scenario. This allows to compute BER thanks to the classical expressions of the BER of M-ary QAM constellations

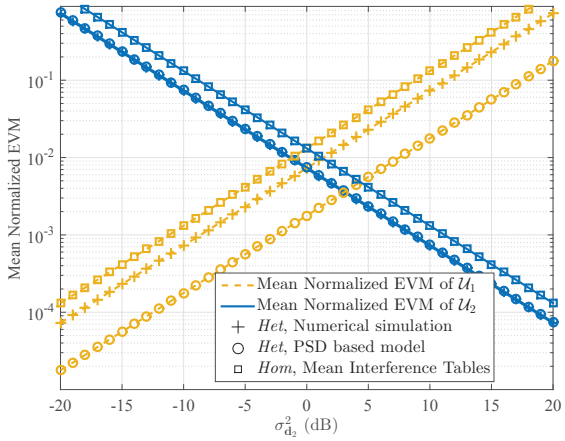

Fig. 7: Mean Normalized EVM of users $\mathcal{U}_1$ and $\mathcal{U}_2$ in the scenarios *Het* and *Hom*

[19]. As expected, the obtained BER performance confirms the EVM behaviour presented in Fig.7, and again, the PSD-based model is totally wrong for modeling the interference seen by the incumbent $\mathcal{U}_1$ in the *Het* scenario. Nevertheless, it gives a satisfying approximation of the BER of OFDM/OQAM based $\mathcal{U}_2$, especially for values of BER higher than 10^{-3}. However, when the BER of OFDM/OQAM based $\mathcal{U}_2$ becomes low (for $\sigma^2_{\mathbf{d}_2} > 10$ dB), the PSD-based model understimates it. This is due to the fact that the interference was approximated as a white gaussian signal whereas it has been shown that it is colored in Fig. 6b. Finally, Fig. 8 shows that the benefits of using OFDM/OQAM are not as high as what was expected with the PSD-based model. Yet, it shows that using OFDM/OQAM for the secondary $\mathcal{U}_2$ does still bring some advantage. For example, when both users have the same transmission power, the BER of each user in the *Het* scenario is equal to half what they experience in the *Hom* scenario.

Presented results show that, in scenarios where an incumbent CP-OFDM system coexists with an asynchronous user $\mathcal{U}_2$, it is still advantageous to both users that $\mathcal{U}_2$ uses OFDM/OQAM, though benefits are much less important than those planned with the PSD-based model in [14], [15]. To conclude this study, we focus on the BER of the incumbent $\mathcal{U}_1$ in both *Het* and *Hom* scenarios with a deterministic value of τ. Fig.9 highlights three different and interesting results: first, in the *Het* scenario, τ has no impact. This is mainly due to the fact that OFDM/OQAM and CP-OFDM systems are inherently asynchronous, as they do not have the same time spacing between subsequent symbols (see Fig.4). Second, in the *Hom* scenario, if the timing offset can be contained in the CP duration, the performance of incumbent $\mathcal{U}_1$ is not degraded at all. This is a well known result concerning Multi-User Interference in CP-OFDM systems. Third, as soon as τ grows higher than the CP duration, it is worth using OFDM/OQAM instead of CP-OFDM at the secondary system $\mathcal{U}_2$ to protect $\mathcal{U}_1$.

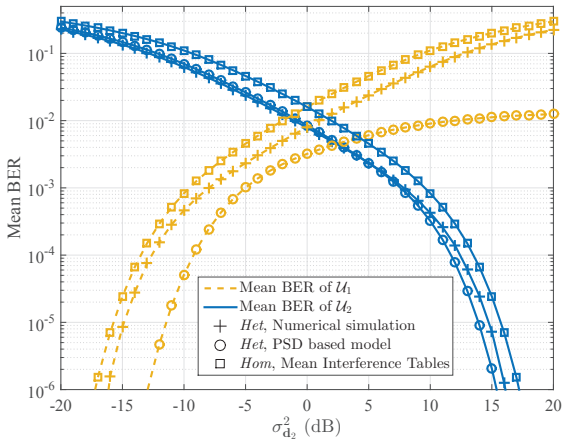

Fig. 8: Mean BER of users $\mathcal{U}_1$ and $\mathcal{U}_2$ in the scenarios *Het* and *Hom*

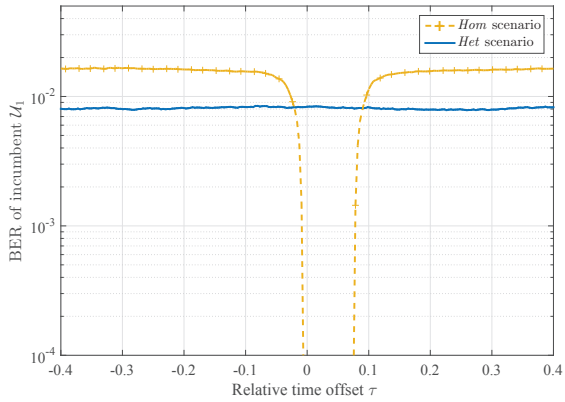

Fig. 9: Empirical BER of $\mathcal{U}_1$ versus the timing offset τ between $\mathcal{U}_2$ and $\mathcal{U}_1$, for *Het* and *Hom* scenarios.

VI. Conclusion

In this paper, we analyzed a scenario in which the coexistence between a legacy CP-OFDM incumbent system and an asynchronous secondary user produces inter-user interference. We analyzed the performance of users in the cases where the secondary user utilizes CP-OFDM or OFDM/OQAM waveform.

We showed that the widely used PSD-based model is highly flawed and fails to give a good approximation of the interference seen by each user in heterogeneous scenarios. Indeed, presented numerical results showed that when the secondary system utilizes OFDM/OQAM, the actual values of interference are higher than those planned by the PSD based model by more than 50 dB. Furthermore, contrary to the widely spread idea that CP-OFDM interferes more onto OFDM/OQAM users than the opposite, we revealed that heterogeneous interference is symmetrical and that users interfere equally onto each other.

Though it was shown that both users experience a slight improvement when the secondary user uses OFDM/OQAM modulation, the gain was shown to be much more limited than what was expected with the PSD-based model.

To conclude, we showed in this paper that models existing in the literature to rate interference in heterogeneous networks are not satisfying. Future work will therefore focus on deriving analytical closed-forms of heterogeneous interference that can be used to extensively investigate such scenarios.

References

[1] E. Lähetkangas and H. Lin, "Deliverable D2.1 - Requirement analysis and design approaches for 5G air interface," p. 72, 2013.

[2] G. Wunder *et al.*, "5GNOW: non-orthogonal, asynchronous waveforms for future mobile applications," *IEEE Communications Magazine*, vol. 52, no. February, pp. 97–105, 2014.

[3] Y. Medjahdi *et al.*, "Performance analysis in the downlink of asynchronous OFDM/FBMC based multi-cellular networks," *IEEE Transactions on Wireless Communications*, vol. 10, no. 8, pp. 2630–2639, 2011.

[4] B. Farhang-Boroujeny, "OFDM versus filter bank multicarrier," *Signal Processing Magazine, IEEE*, no. MAY 2011, pp. 92–112, 2011.

[5] L. G. Baltar, D. S. Waldhauser, and J. A. Nossek, "Out-Of-Band Radiation in Multicarrier Systems: A Comparison," in *Multi-Carrier Spread Spectrum 2007*. Springer Netherlands, 2007, vol. 1, pp. 107–116.

[6] H. Mahmoud, T. Yucek, and H. Arslan, "OFDM for cognitive radio: merits and challenges," *IEEE Wireless Communications*, vol. 16, no. April, pp. 6–15, 2009.

[7] K. Raghunath and a. Chockalingam, "SC-FDMA versus OFDMA: Sensitivity to large carrier frequency and timing offsets on the uplink," *GLOBECOM - IEEE Global Telecommunications Conference*, 2009.

[8] A. Aminjavaheri *et al.*, "Impact of timing and frequency offsets on multicarrier waveform candidates for 5g," in *Signal Processing and Signal Processing Education Workshop (SP/SPE), 2015 IEEE*, Aug 2015, pp. 178–183.

[9] M. Speth *et al.*, "Optimum receiver design for wireless broad-band systems using OFDM. I," *IEEE Transactions on Communications*, vol. 47, no. 11, pp. 1668–1677, 1999.

[10] M. Bellanger, "FBMC physical layer: a primer," pp. 1–31, 2010.

[11] H. Xing and M. Renfors, "Investigation of filter bank based device-to-device communication integrated into OFDMA cellular system," in *ISWCS*, 2014, pp. 513–518.

[12] Q. Bodinier *et al.*, "5G Waveforms for Overlay D2D Communications: Effects of Time-Frequency Misalignment," in *IEEE International Conference on Communications (ICC)*, Kuala Lumpur, 2016 (Accepted).

[13] R. Xu and M. Chen, "Spectral leakage suppression of DFT based OFDM via adjacent subcarriers correlative coding," in *Proccedings of IEEE Global Telecommunications Conference (GLOBECOM '08) December 2008.*, 2018, pp. 3029–3033.

[14] M. Shaat and F. Bader, "Computationally efficient power allocation algorithm in multicarrier-based cognitive radio networks: Ofdm and fbmc systems," *EURASIP Journal on Advances in Signal Processing*, vol. 2010, p. 5, 2010.

[15] A. Skrzypczak, J. Palicot, and P. Siohan, "OFDM/OQAM modulation for efficient dynamic spectrum access," *International Journal of Communication Networks and Distributed Systems*, vol. 8, no. 3-4, pp. 247–266, 2012.

[16] A. K. T. Weiss, J. Hillenbrand and F. K. Jondral, "Mutual Interference in OFDM-Basedased Spectrum Pooling Systems,," in *Proceedings of the 59th IEEE Vehicular Technology Conference (VTC '04). Milan, Italy.*, vol. 59, 2004.

[17] Y. Medjahdi *et al.*, "Interference tables: a useful model for interference analysis in asynchronous multicarrier transmission," *EURASIP Journal on Advances in Signal Processing*, vol. 2014, no. 54, pp. 1–17, 2014.

[18] M. Bellanger, "Specification and design of a prototype filter for filter bank based multicarrier transmission," in *2001 IEEE International Conference on Acoustics, Speech, and Signal Processing. Proceedings*, vol. 4, 2001, pp. 2417–2420.

[19] J. G. Proakis, "Optimum Receivers for the Additive White Gaussian Noise Channel," in *Digital Communications*, internatio ed., McGraw-Hill, Ed., 2001, pp. 231–332.

Coexistence in 5G: Analysis of Cross-Interference between OFDM/OQAM and Legacy Users

Quentin Bodinier, Faouzi Bader, and Jacques Palicot
SCEE/IETR - CentraleSupélec, Rennes, France,
Email : {firstname.lastname}@supelec.fr

***Abstract*—To optimize the use of the spectrum, it is expected that the next generation of wireless networks (5G) will enable coexistence of newly introduced services with legacy cellular networks. These new services, like Device-To-Device (D2D) communication, should require limited synchronization with the legacy cell to limit the amount of signaling overhead in the network. However, it is known that Cyclic Prefix-Orthogonal Frequency Division Multiplexing (CP-OFDM) used in Long Term Evolution-Advanced (LTE-A) is not fit for asynchronous environments. This has motivated the search for a new waveform, able to enhance coexistence with CP-OFDM. Namely, it has been widely suggested that new devices could use OFDM/Offset-Quadrature Amplitude Modulation (OFDM/OQAM) to reduce the interference they inject to legacy cellular users. However, values of interference are usually measured at the input antenna of the receiver, based on the PSD of the interfering signal. We showed in previous works that this measurement is not representative of the actual interference that is seen after the demodulation operations. Building on this finding, we provide in this paper the first exact closed forms of cross-interference between OFDM/OQAM and CP-OFDM users. Our results prove that using OFDM/OQAM only marginally reduces interference to legacy users, in contradiction with many results in the literature.**

I. Introduction

The advent of the 5th Generation of wireless communication systems (5G) is envisioned to bring flexibility to cellular networks. New services as Device-To-Device (D2D) or Machine-To-Machine (M2M) communications are expected to be massively deployed in the near future. Such new communication devices have to coexist with incumbent legacy systems in the cell, i.e. Long-Term-Evolution Advanced (LTE-A) users. In such heterogeneous environments, perfect synchronization between the different types of systems is not feasible. This loss of synchronization will cause harmful interference between active users, which will in turn degrade the overall system performance. This hurdle can be overcome through the design of new waveforms that are robust against asynchronism, and well localized in frequency. As a matter of fact, as soon as the orthogonality between CP-OFDM users is destroyed, for example because of the coexistence of unsynchronized incumbent and secondary systems, their performance shrinks dramatically [1]. This is mainly due to the fact that CP-OFDM systems filter symbols with a time-rectangular window, which causes poor frequency localization [2]–[4] and high asynchronism sensitivity in the multi-user context [4]–[6].

OFDM with Offset Quadrature Amplitude Modulation (OFDM/OQAM) [2], [7], is one of the main new waveform schemes explored by the research community. Indeed, it overcomes the cited CP-OFDM limitations and enables both higher flexibility and reduction of interference leakage for multistandard systems coexistence [2], [7]. The main selling point of OFDM/OQAM lies in its improved spectral containment that is obtained through the filtering of each subcarrier with a highly selective prototype filter. In this paper, we will study the case of OFDM/OQAM systems using the PHYDYAS filter [7]. Thanks to the enhanced spectral localization of the latter, OFDM/OQAM boasts hardly measurable out-of-band (OOB) emissions, as its Power Spectral Density (PSD) rapidly decreases below the ambient noise level.

Building on this, a number of papers, for example [8]–[10], have suggested to use OFDM/OQAM to coexist efficiently with CP-OFDM based networks. All the studies on that matter use the PSD-based model, originally proposed in [11], to rate the cross-interference between the OFDM/OQAM and CP-OFDM systems. This model consists in integrating the PSD of the interfering signal on each subcarrier of the user that suffers from interference. Because of the advantageous PSD properties of OFDM/OQAM, studies using the PSD-based model predicted that using this waveform instead of CP-OFDM for coexistence with LTE-A users would be highly beneficial.

However, the expected gains were not confirmed through simulations [12], [13]. Moreover, in [13], we explained in a qualitative manner why the PSD-based model was not fit to properly estimate the cross-interference that is seen after the demodulation operations at both the receivers of OFDM/OQAM and CP-OFDM systems. Furthermore, we showed through numerical simulations that the gains expected by following the PSD-based model were highly overestimated. However, a thorough mathematical analysis of the post-demodulation cross-interference arising between coexisting OFDM/OQAM and CP-OFDM systems is still lacking. This paper aims at resolving this issue by providing mathematical closed forms of cross-interference injected by OFDM/OQAM onto CP-OFDM and vice-versa. The provided closed-forms prove that OFDM/OQAM fails to protect incumbent legacy CP-OFDM users.

The remainder of this paper is organized as follows: Section II presents the system model and a short overview on CP-OFDM and OFDM/OQAM waveforms. In Section III, the analysis of cross-interference is led. In Section IV, the validity of the derived closed forms is asserted by comparison with

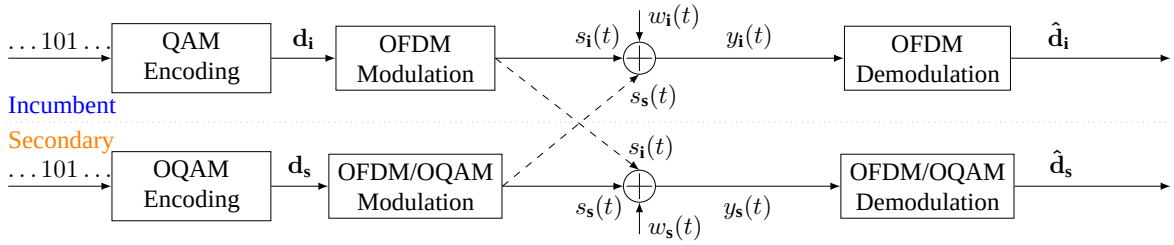

Fig. 1: Considered system model. Interference signals are marked with dashed arrows.

numerical simulations, and conclusions are given in Section V.

Notations: scalars are noted x,vectors are bold-faced as $\mathbf{x}$, and ensembles are represented by a calligraphy letter $\mathcal{X}$. n is the discrete symbol index, m indexes subcarriers and t is the continuous time. $*$ is the convolution operation, x^* is the complex conjugate of x, $E_\alpha\{\}$ is the mathematical expectation with regards to the random variable α and $\mathcal{R}\{x\}$ is the real part of x.

II. Background and System Model

A. Analyzed Coexistence Scenario

We consider a coexistence scenario where an incumbent CP-OFDM based system and an OFDM/OQAM secondary system share the same spectral band. The incumbent is assigned a set of active subcarriers $\mathcal{M}_\mathbf{i}$ and the secondary a set $\mathcal{M}_\mathbf{s}$. We assume that both systems use the same subcarrier spacing ΔF and time-symbol $T = \frac{1}{\Delta \mathrm{F}}$. To focus on cross-interference between users, we consider a transmission on an additive white gaussian noise (AWGN) channel and do not take into account any pathloss or shadowing effect. The corresponding system model is represented in Fig. 1 and an example of subcarriers distribution is given in Fig. 2.

Note that, strictly speaking, each interfering signal arrives at the receiver it interferes on with a certain delay. For example, naming $\delta_{\mathrm{t,s}}$ the propagation delay between the secondary transmitter and the incumbent receiver, the interfering signal received at the incumbent is not $s_\mathbf{s}(t)$ but $s_\mathbf{s}(t-\delta_{\mathrm{t,s}})$. However, we showed through simulation in [12] that this propagation delay has only little impact on the interference between OFDM/OQAM and CP-OFDM users. Without loss of generality, we will therefore neglect the propagation delays in our analysis.

Now that the system model is laid out, we present in the following Section a short background on CP-OFDM and OFDM/OQAM signal models.

B. CP-OFDM Incumbent System

We consider a CP-OFDM incumbent system with M subcarriers, time-symbol T and a CP duration of T_{CP}. As previously mentioned, it has a set of active subcarriers $\mathcal{M}_\mathbf{i}$. The CP-OFDM time-domain signal transmitted on each active subcarrier $m_\mathbf{i} \in \mathcal{M}_\mathbf{i}$ is expressed as

$$s_{m_\mathbf{i}}(t) = \sum_{n_\mathbf{i}\in\mathbb{Z}} \mathbf{d}_{m_\mathbf{i}}[n_\mathbf{i}] f_{\mathrm{T},\mathbf{i}}\left(t - n_\mathbf{i}(T+T_{\mathrm{CP}})\right) e^{j2\pi m_\mathbf{i}\frac{t-n_\mathbf{i}T_{\mathrm{CP}}}{T}}, \tag{1}$$

with $\mathbf{d}_{m_\mathbf{i}}$ the data vector of quadrature amplitude modulated (QAM) symbols transmitted on subcarrier $m_\mathbf{i}$ and $f_{\mathrm{T},\mathbf{i}}$ the CP-OFDM transmit filter defined as:

$$f_{\mathrm{T},\mathbf{i}}(t) = \begin{cases} \frac{1}{\sqrt{T}}, & t \in [-T_{\mathrm{CP}}, T] \\ 0, & \text{elsewhere.} \end{cases} \tag{2}$$

The total transmitted signal is expressed as

$$s_\mathbf{i}(t) = \sum_{m_\mathbf{i}\in\mathcal{M}_\mathbf{i}} s_{m_\mathbf{i}}(t), \forall t \in \mathbb{R}. \tag{3}$$

In this study, we consider an AWGN interference channel. Therefore, the signal at the input antenna of the CP-OFDM incumbent receiver is expressed as

$$y_\mathbf{i}(t) = s_\mathbf{i}(t) + s_\mathbf{s}(t) + w_\mathbf{i}(t), \forall t \in \mathbb{R} \tag{4}$$

where $s_\mathbf{s}(t)$ is the interfering OFDM/OQAM secondary signal whose expression will be detailed in the next section and $w_\mathbf{i}(t)$ is the AWGN seen at the incumbent receiver.

Assuming perfect synchronization between the CP-OFDM transmitter and receiver, the $n_\mathbf{i}$-th demodulated symbol on the $m_\mathbf{i}$-th subcarrier of the CP-OFDM receiver is expressed, $\forall n_\mathbf{i} \in \mathbb{Z}$, as

$$\hat{\mathbf{d}}_{m_\mathbf{i}}[n_\mathbf{i}] = \mathbf{d}_{m_\mathbf{i}}[n_\mathbf{i}] + \sum_{m_\mathbf{s}\in\mathcal{M}_\mathbf{s}} \eta_{m_\mathbf{s}\to m_\mathbf{i}}[n_\mathbf{i}] + \mathbf{w}_\mathbf{i}[n_\mathbf{i}], \tag{5}$$

where $\mathbf{w}_\mathbf{i}$ is the filtered white gaussian noise component expressed as

$$\mathbf{w}_\mathbf{i}[n_\mathbf{i}] = \int_{-\infty}^{\infty} f_{\mathrm{R},\mathbf{i}}(t - n_\mathbf{i}(T+T_{\mathrm{CP}})) e^{-j2\pi m_\mathbf{i}\frac{t-n_\mathbf{i}T_{\mathrm{CP}}}{T}} w_\mathbf{i}(t)dt, \forall n_\mathbf{i} \in \mathbb{Z} \tag{6}$$

and $\eta_{m_\mathbf{s}\to m_\mathbf{i}}$ is the interference injected by the $m_\mathbf{s}$-th subcarrier of the secondary onto the $m_\mathbf{i}$-th subcarrier of the incumbent, which is expressed $\forall n_\mathbf{i} \in \mathbb{Z}$ as

$$\eta_{m_\mathbf{s}\to m_\mathbf{i}}[n_\mathbf{i}] = \int_{-\infty}^{\infty} f_{\mathrm{R},\mathbf{i}}(t - n_\mathbf{i}(T+T_{\mathrm{CP}})) e^{-j2\pi m_\mathbf{i}\frac{t-n_\mathbf{i}T_{\mathrm{CP}}}{T}} s_{m_\mathbf{s}}(t)dt. \tag{7}$$

In (6) and (7), $f_{\mathrm{R},\mathbf{i}}$ is the receive filter of the incumbent and is expressed as

$$f_{\mathrm{R},\mathbf{i}}(t) = \begin{cases} \frac{1}{\sqrt{T}}, & t \in [0, T] \\ 0, & \text{elsewhere.} \end{cases} \tag{8}$$

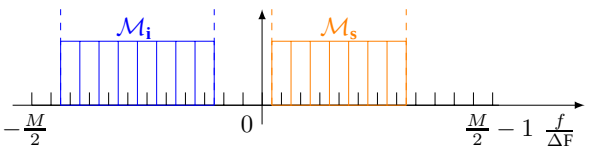

Fig. 2: Spectral representation of the considered scenario. The incumbent and secondary systems coexist in the same spectral band, and each one is assigned a different subset of subcarriers.

C. Secondary OFDM/OQAM System

We consider an OFDM/OQAM secondary system with M subcarriers and time-symbol T, and name $\mathcal{M}_\mathbf{s}$ its set of active subcarriers. The time-domain signal transmitted on each active subcarrier $m_\mathbf{s} \in \mathcal{M}_\mathbf{s}$ of the secondary OFDM/OQAM system is expressed as [14]

$$s_{m_\mathbf{s}}(t) = \sum_{n_\mathbf{s}\in\mathbb{Z}} (-1)^{m_\mathbf{s} n_\mathbf{s}} \mathbf{d}_{m_\mathbf{s}}[n_\mathbf{s}] \theta_{m_\mathbf{s}}[n_\mathbf{s}] f_{\mathrm{T},\mathbf{s}}\left(t - n_\mathbf{s}\frac{T}{2}\right) e^{j2\pi m_\mathbf{s}\frac{t}{T}} \tag{9}$$

where $\mathbf{d}_{m_\mathbf{s}}$ is the data vector of pulse amplitude modulated (PAM) real symbols and $\theta_{m_\mathbf{s}}[n_\mathbf{s}]$ is a phase factor added to the symbols and defined as [14]

$$\theta_{m_\mathbf{s}}[n_\mathbf{s}] = e^{j\frac{\pi}{2}\lfloor\frac{n_\mathbf{s}+m_\mathbf{s}}{2}\rfloor}. \tag{10}$$

Besides, $f_{\mathrm{T},\mathbf{s}}$ is the transmit filter of the secondary system expressed as

$$f_{\mathrm{T},\mathbf{s}}(t) = \begin{cases} g(t) & t \in [-\frac{KT}{2}, \frac{KT}{2}] \\ 0, & \text{elsewhere} \end{cases} \tag{11}$$

where K is called the overlapping factor, and g is the used prototype filter. In the remainder of this study, we take g as the PHYDYAS prototype filter with overlapping factor $K = 4$, [15], defined as

$$g(t) = \sum_{k=-K+1}^{K-1} \frac{G_{|k|}}{K} e^{j2\pi\frac{kt}{KT}}, t \in [-\frac{KT}{2}, \frac{KT}{2}], \tag{12}$$

with $G_0 = 1$, $G_1 = 0.971960$, $G_2 = \frac{1}{\sqrt{2}}$, $G_3 = 0.235147$. Note that g is a real and symmetric filter, such that $g^*(-t) = g(t), \forall t \in \mathbb{R}$.

The signal received at the input antenna of the OFDM/OQAM receiver is expressed in a similar manner as in (4) and is given by

$$y_\mathbf{s}(t) = s_\mathbf{s}(t) + s_\mathbf{i}(t) + w_\mathbf{s}(t), \forall t \in \mathbb{R} \tag{13}$$

At the OFDM/OQAM receiver, the received signal is passed through the receive filter $f_{\mathrm{R},\mathbf{i}}$ expressed as

$$f_{\mathrm{R},\mathbf{s}}(t) = \begin{cases} g^*(-t) = g(t) & t \in [-\frac{KT}{2}, \frac{KT}{2}] \\ 0, & \text{elsewhere.} \end{cases} \tag{14}$$

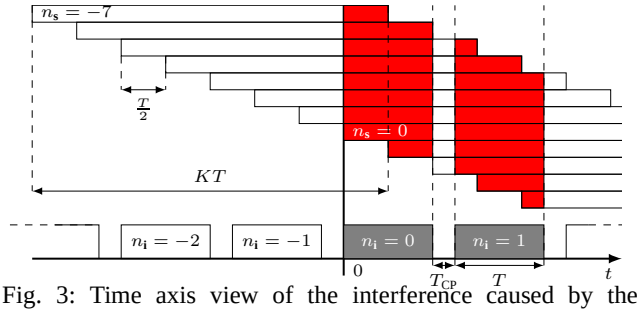

Fig. 3: Time axis view of the interference caused by the OFDM/OQAM transmission on CP-OFDM receiving windows $n_\mathbf{i} = 0$ and $n_\mathbf{i} = 1$. Both CP-OFDM symbols suffer the same amount of cross-interference.

Then, the real part of the filtered signal is taken to remove purely imaginary intrinsic interference [14]. Therefore, the $n_\mathbf{s}$-th demodulated symbol on the $m_\mathbf{s}$-th subcarrier of the OFDM/OQAM secondary receiver is expressed as

$$\hat{\mathbf{d}}_{m_\mathbf{s}}[n_\mathbf{s}] = \mathbf{d}_{m_\mathbf{s}}[n_\mathbf{s}] + \sum_{m_\mathbf{i}\in\mathcal{M}_\mathbf{i}} \eta_{m_\mathbf{i}\to m_\mathbf{s}}[n_\mathbf{s}] + \mathbf{w}_\mathbf{s}[n_\mathbf{s}], \tag{15}$$

with

$$\mathbf{w}_\mathbf{s}[n_\mathbf{s}] = \int_{-\infty}^{\infty} \mathcal{R}\{f_{\mathrm{R},\mathbf{s}}(t - n_\mathbf{s}\frac{T}{2}) e^{-j2\pi m_\mathbf{s}\frac{t}{T}} (-1)^{m_\mathbf{s} n_\mathbf{s}} w_\mathbf{s}(t)\} dt \tag{16}$$

$$\eta_{m_\mathbf{i}\to m_\mathbf{s}}[n_\mathbf{s}] = \int_{-\infty}^{\infty} \mathcal{R}\{f_{\mathrm{R},\mathbf{s}}(t - n_\mathbf{s}\frac{T}{2}) \times e^{-j2\pi m_\mathbf{s}\frac{t}{T}} (-1)^{m_\mathbf{s} n_\mathbf{s}} s_{m_\mathbf{i}}(t)\} dt. \tag{17}$$

III. Cross-Interference Analysis

A. Cross-Interference at the Incumbent CP-OFDM Receiver

Here, we derive the closed-form of interference seen at the incumbent CP-OFDM receiver as expressed in (7). Substituting the expression of $f_{\mathrm{T},\mathbf{s}}$ given by (11) in (9), and then putting both the resulting form of (9) and the expression of the incumbent receive filter $f_{\mathrm{R},\mathbf{i}}$ given by (8) in (7), we obtain the expression (18) of $\eta_{m_\mathbf{s}\to m_\mathbf{i}}[n_\mathbf{i}]$. In the following, we focus on the mean interference power caused by subcarrier $m_\mathbf{s}$ of the OFDM/OQAM secondary onto subcarrier $m_\mathbf{i}$ of the CP-OFDM incumbent, which we define as

$$\mathbf{I}_{m_\mathbf{s}\to m_\mathbf{i}}[n_\mathbf{i}] = E_{\mathbf{d}_\mathbf{s}}\{|\eta_{m_\mathbf{s}\to m_\mathbf{i}}[n_\mathbf{i}]|^2\} \tag{19}$$

$$= \frac{\sigma^2_{\mathbf{d}_\mathbf{s}}}{T} \sum_{n_\mathbf{s}\in\mathbb{Z}} \left| \int_{n_\mathbf{i}(T+T_{\mathrm{CP}})}^{n_\mathbf{i}(T+T_{\mathrm{CP}})+T} g\left(t - n_\mathbf{s}\frac{T}{2}\right) \times e^{j2\pi(m_\mathbf{s}-m_\mathbf{i})\frac{t}{T}} dt \right|^2, \tag{20}$$

$$\eta_{m_\mathbf{s}\to m_\mathbf{i}}[n_\mathbf{i}] = \frac{1}{\sqrt{T}} \sum_{n_\mathbf{s}\in\mathbb{Z}} (-1)^{m_\mathbf{s} n_\mathbf{s}} \mathbf{d}_{m_\mathbf{s}}[n_\mathbf{s}] \theta_{m_\mathbf{s}}[n_\mathbf{s}] \int_{n_\mathbf{i}(T+T_{\mathrm{CP}})}^{n_\mathbf{i}(T+T_{\mathrm{CP}})+T} g\left(t - n_\mathbf{s}\frac{T}{2}\right) e^{j2\pi(m_\mathbf{s}-m_\mathbf{i})\frac{t}{T}} dt, \forall n_\mathbf{i} \in \mathbb{Z}. \tag{18}$$

with $\sigma^2_{\mathbf{d_s}}$ the variance of the symbols modulated by the secondary OFDM/OQAM system. Note that this last expression is obtained by considering that the symbols $\mathbf{d_s}$ are independent and identically distributed (i.i.d.). Besides, note that the sum in (20) can be reduced to the values of $n_\mathbf{s}$ such that $g(t-n_\mathbf{s}\frac{T}{2})$ is not null everywhere on the reception window corresponding to the $n_\mathbf{i}$-th symbol of the receiver. This is shown in Fig. 3, where we also point out that the value of $n_\mathbf{i}$ does not affect the mean interference power seen at the receiver. Note also that only the difference $m_\mathbf{s}-m_\mathbf{i}$ plays a role in (20). Naming $l=m_\mathbf{s}-m_\mathbf{i}$ the spectral distance in terms of subcarriers, we therefore have $\mathbf{I}_{m_\mathbf{s}\to m_\mathbf{i}}[n_\mathbf{i}] = I_{\mathbf{s}\to\mathbf{i}}(l), \forall n_\mathbf{i}\in\mathbb{Z}$.

After operating the change of variable $t \mapsto t - n_\mathbf{i}(T+T_{\text{CP}})$ in (20), we obtain, $\forall n_\mathbf{i}\in\mathbb{Z}$,

$$\mathbf{I}_{m_\mathbf{s}\to m_\mathbf{i}}[n_\mathbf{i}] = \overbrace{\frac{\sigma^2_{\mathbf{d_s}}}{T}\sum_{\tau=-KT+\frac{T}{2}}^{\frac{T}{2}}\underbrace{\left|\int_0^T g(t-\tau)e^{j2\pi\frac{lt}{T}}dt\right|^2}_{I_{\mathbf{s}\to\mathbf{i}}(l,\tau)}}^{I_{\mathbf{s}\to\mathbf{i}(l)}} \quad (21)$$

By including in (21) the expression of g given in (12), we obtain, $\forall l\in\mathbb{Z}$,

$$I_{\mathbf{s}\to\mathbf{i}}(l,\tau) = \frac{1}{K^2}\left|\sum_{k=-K+1}^{K-1} G_{|k|}\int_0^T e^{j2\pi(\frac{k(t+\tau)}{KT}+\frac{lt}{T})}dt\right|^2 \quad (22)$$

$$= \frac{T}{K^2}\left|\sum_{k=-K+1}^{K-1} G_{|k|}e^{j\pi\frac{k}{K}\tau}\text{sinc}(\pi(\frac{k}{K}+l))\right|^2, \quad (23)$$

and the interference power injected by an OFDM/OQAM subcarrier to a CP-OFDM subcarrier at spectral distance l is finally given by

$$I_{\mathbf{s}\to\mathbf{i}}(l) = \frac{\sigma^2_{\mathbf{d_s}}}{K^2}\sum_{\tau=-KT+\frac{T}{2}}^{\frac{T}{2}}\left|\sum_{k=-K+1}^{K-1} G_{|k|}e^{j\pi\frac{k}{K}\tau} \times \text{sinc}(\pi(\frac{k}{K}+l))\right|^2 \quad (24)$$

B. Cross-Interference at the Secondary OFDM/OQAM Receiver

We now focus on the cross-interference that is injected by the CP-OFDM incumbent transmitter onto the OFDM/OQAM receiver, as expressed in (17). Substituting the expression of the CP-OFDM transmit filter (2) into (1), and then the resulting form of (1) and the expression of $f_{\text{R,s}}$ given by (14) into (17), we obtain the expression of (25), which is very close to (18), the only differences being the real part operator and some phase factors due to the OFDM/OQAM demodulation. In a similar way as (19), we define the mean interference power injected by subcarrier $m_\mathbf{i}$ of the incumbent onto the $m_\mathbf{s}$-th subcarrier of the secondary as

$$\mathbf{I}_{m_\mathbf{i}\to m_\mathbf{s}}[n_\mathbf{s}] = E_{\mathbf{d_i}}\{|\eta_{m_\mathbf{i}\to m_\mathbf{s}}[n_\mathbf{s}]|^2\} \quad (26)$$

$$= \frac{\sigma^2_{\mathbf{d_i}}}{2T}\sum_{n_\mathbf{i}\in\mathbb{Z}}\left|\int_{n_\mathbf{i}(T+T_{\text{CP}})-T_{\text{CP}}}^{n_\mathbf{i}(T+T_{\text{CP}})+T} g\left(t-n_\mathbf{s}\frac{T}{2}\right) \times e^{j2\pi(m_\mathbf{i}-m_\mathbf{s})\frac{t}{T}}dt\right|^2, \quad (27)$$

with $\sigma^2_{\mathbf{d_i}}$ the variance of the symbols $\mathbf{d_i}$. Note that the factor $\frac{1}{2}$ comes from the fact that only the real part of the signal is taken at the OFDM/OQAM receiver. The obtained expression is similar to (19) and the different observations made in the previous section still hold true here. Therefore, following developments similar to (19)-(24), the power of interference injected by a CP-OFDM subcarrier to an OFDM/OQAM subcarrier at spectral distance l is expressed as (28).

Note that, if both systems transmit with the same energy per symbol E_s, $\frac{\sigma^2_{\mathbf{d_i}}}{2} = \sigma^2_{\mathbf{d_s}} = \frac{E_s}{2}$ because each OQAM symbol transmits half the energy of a QAM symbol. Therefore, in the case where $T_{\text{CP}}=0$, which corresponds to a situation where the incumbent system does not use any CP, $I_{\mathbf{i}\to\mathbf{s}}(l) = I_{\mathbf{s}\to\mathbf{i}}(l), \forall l\in\mathbb{Z}$ and the incumbent and secondary systems interfere equally onto each other.

From both (28) and (24), it can be noticed that the rectangular time window of the CP-OFDM system incurs a sum of sine-cardinal in frequency, which slowly decrease and will therefore cause high interference to both systems, despite the well shaped prototype filter used by the OFDM/OQAM system.

C. Taking into Account Frequency Misalignments

The closed-forms we derived in the previous section were obtained in the case where the secondary and the incumbent systems agree on the exact same frequency basis. Therefore, the spectral distance l between each subcarrier of the secondary and each subcarrier of the incumbent is an integer, i.e. $l\in\mathbb{Z}$. This is correct if the local oscillators (LO) of all users are perfectly synchronized. However, in a real setup, this is not the case. Indeed, LOs of mobile terminals have a typical accuracy of ± 1 ppm with respect to their nominal frequency [16]. At a carrier frequency of 2 GHz, this can yield a misalignment between users of around 10^4 Hz, which can become significant as it is close to the LTE subcarrier width of 15 kHz.

Here, we consider that the transmitter and receiver in each system achieve perfect frequency synchronization. However,

$$\eta_{m_\mathbf{i}\to m_\mathbf{s}}[n_\mathbf{s}] = \frac{1}{\sqrt{T}}\sum_{n_\mathbf{i}\in\mathbb{Z}}\mathcal{R}\left\{\mathbf{d}_{m_\mathbf{i}}[n_\mathbf{i}]e^{-j2\pi m_\mathbf{i}\frac{n_\mathbf{i}T_{\text{CP}}}{T}}(-1)^{m_\mathbf{s}n_\mathbf{s}}\int_{n_\mathbf{i}(T+T_{\text{CP}})-T_{\text{CP}}}^{n_\mathbf{i}(T+T_{\text{CP}})+T_{\text{CP}}} g\left(t-n_\mathbf{s}\frac{T}{2}\right)e^{j2\pi(m_\mathbf{i}-m_\mathbf{s})\frac{t}{T}}dt\right\}, \forall n_\mathbf{s}\in\mathbb{Z} \quad (25)$$

$$I_{\mathbf{i}\to\mathbf{s}}(l) = \frac{\sigma^2_{\mathbf{d_i}}}{2K^2}(1+\frac{T_{\text{CP}}}{T})\sum_{\tau=-KT+\frac{T}{2}}^{\frac{T}{2}}\left|\sum_{k=-K+1}^{K-1} G_{|k|}e^{j\pi\frac{k}{K}\tau(1+\frac{T_{\text{CP}}}{T})}\text{sinc}\left(\pi\left(1+\frac{T_{\text{CP}}}{T}\right)\left(\frac{k}{K}+l\right)\right)\right|^2 \quad (28)$$

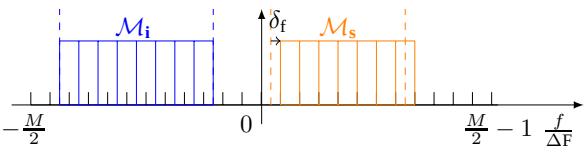

Fig. 4: Spectral representation of the considered scenario with frequency misalignment δ_f between coexisting systems.

the incumbent and secondary systems are not supposed to cooperate, and it is very likely that they will not be perfectly aligned in frequency. This means that, taking the incumbent system as a reference, the $m_\mathbf{s}$-th subcarrier of the secondary will not be modulated at base-band frequency $m_\mathbf{s}\Delta\mathrm{F}$ but at base-band frequency $(m_\mathbf{s}+\delta_\mathrm{f})\Delta\mathrm{F}$, where $\delta_\mathrm{f} \in]-0.5,\ 0.5]$ and is the frequency misalignment value between the secondary and incumbent systems. In other words, Fig. 2 is transformed into Fig. 4 where we see that the secondary transmission is misaligned with the band it should actually transmit in.

This simply leads to rewriting (4) and (13) as

$$y_\mathbf{i}(t) = s_\mathbf{i}(t) + s_\mathbf{s}(t)e^{j2\pi\delta_\mathrm{f}t} + w_\mathbf{i}(t), \tag{29}$$

$$y_\mathbf{s}(t) = s_\mathbf{s}(t) + s_\mathbf{i}(t)e^{-j2\pi\delta_\mathrm{f}t} + w_\mathbf{s}(t). \tag{30}$$

Then, the analysis is led exactly as (7) - (28). Redefining l as $l = m_\mathbf{s} + \delta_\mathrm{f} - m_\mathbf{i}$, mathematical derivation yield the exact same expression as (24) and (28). Therefore, the closed forms we derived are also applicable in the presence of frequency misalignment between the incumbent and secondary systems i.e. $\forall l \in \mathbb{R}$.

IV. Numerical Results

In Fig. 5, we represent the values of $I_{\mathbf{s}\to\mathbf{i}}(l)$ and $I_{\mathbf{i}\to\mathbf{s}}(l)$ according to the expressions of (28) and (24) for $T_\mathrm{CP} = \frac{T}{8}$. We observe that both systems interfere almost equally onto each other. Note that, if we had set $T_\mathrm{CP} = 0$, the two curves would perfectly overlap.

In Fig. 6, the derived theoretical expressions are compared to results obtained through Monte-Carlo simulations. We represent the interference power seen at each subcarrier of index l when the interferer transmits at subcarrier of index 0. Parameters are set as follows: both the CP-OFDM incumbent and the OFDM/OQAM secondary systems have $M = 512$ subcarriers. Both systems transmit symbols with unitary energy $\sigma^2_{\mathbf{d_i}} = 2\sigma^2_{\mathbf{d_s}} = E_s = 1$. Besides, we consider a CP of relative duration $T_\mathrm{CP} = \frac{T}{8}$ and $\delta_\mathrm{f} = 0$. Figures show that the expressions (24) and (28) perfectly match the simulation results.

Moreover, we show the results predicted by the PSD-based model used for example in [8]–[10]. It is worth noticing that the PSD-based model gives a good approximation of the interference injected by the CP-OFDM incumbent onto the OFDM/OQAM secondary. However, it completely fails in estimating the interference injected by the OFDM/OQAM secondary onto the CP-OFDM incumbent. As pointed out in [13], this is due to the fact that the PSD-based model does not take into account the rectangular receive window of

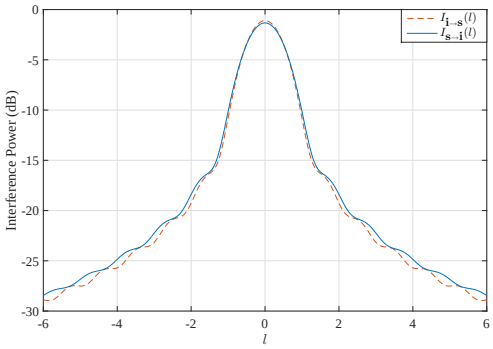

Fig. 5: Values of cross interference injected at spectral distance l, according to (28) and (24).

the CP-OFDM receiver. Because the receive window of the OFDM/OQAM receiver is larger than the transmit filter of the CP-OFDM, the PSD appears to be a good measure of $I_{\mathbf{i}\to\mathbf{s}}$. On the contrary, as shown in Fig. 3, the CP-OFDM receive window truncates each OFDM/OQAM symbol and the good PSD properties of the latter are lost in the process.

Finally, we compare the values of cross-interference in the considered scenario with those observed in a homogeneous scenario where both users would use CP-OFDM. To do so, in Fig. 7, we compare the expressions of (24) and (28) with the interference tables derived by Medjahdi et. al. in [1] in the case where both the secondary and the incumbent users use CP-OFDM. Note that the interference observed by the incumbent and secondary users when they both use CP-OFDM is, at maximum, only 3 dB higher to that observed when the secondary uses OFDM/OQAM. In real-world transmission, when the hardware impairments and the high power amplifier non-linearities come into play, this 3 dB gap will fade out and the benefits of using OFDM/OQAM for coexistence with CP-OFDM systems are likely to disappear.

V. Conclusion

In this paper, we were able to develop exact closed forms of the cross-interference between coexisting OFDM/OQAM and CP-OFDM systems. As OFDM/OQAM is seen as a potential contender for certain 5G applications, the analysis led in this paper can be useful to dimension networks in scenarios where secondary 5G devices coexist with incumbent legacy users. Besides, the led analysis can be generalized in the case where the secondary system would use other waveforms studied for 5G, such as filtered OFDM (f-OFDM) or Universal Filtered OFDM (UF-OFDM). Indeed, our analysis showed that the cross-interference is mainly caused by the rectangular window of the incumbent system. In other words, results presented in this paper show that coexistence with legacy CP-OFDM systems cannot be drastically improved by designing enhanced waveforms only, but that it is necessary to modify the CP-OFDM receiver itself.

Hence, the derived closed forms show that the PSD-based model, widely used in the literature, is not fit to study coexistence scenarios, as it does not take into account the

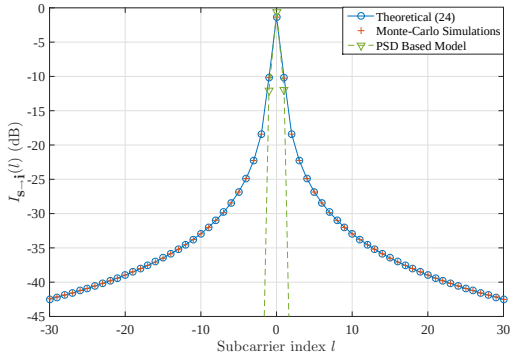

(a) Cross-interference seen at the Incumbent CP-OFDM receiver

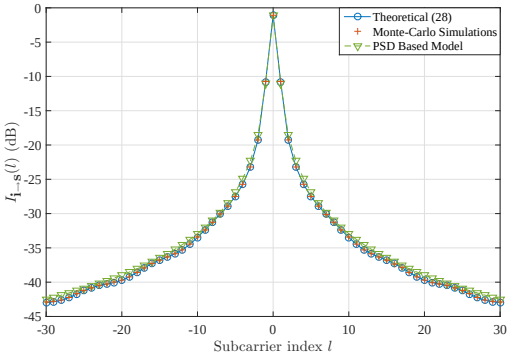

(b) Cross-interference seen at the Secondary OFDM/OQAM receiver

Fig. 6: Cross-interference values for $\delta_f = 0$.

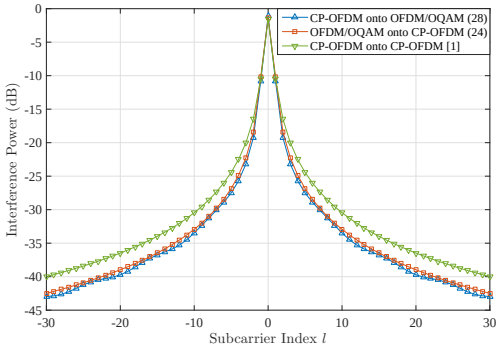

Fig. 7: Comparison of cross-interference values in the case where the secondary uses CP-OFDM or OFDM/OQAM.

receive operations of the terminal that suffers from interference. This observation has a wide array of consequences: indeed, it shows that all the studies which rely on OOB emissions or PSD to rate cross-interference between users are inherently flawed, especially in the context of coexistence between two systems with different waveforms. However, a large number of studies recently released on that matter rely on these two measurements to rate the performance of various waveforms.

Moreover, standards like LTE-A usually define spectral masks that systems should respect to coexist smoothly. However, as these masks are based on PSD measurements as well, our results show that they are not adapted to the management and dimensioning of 5G systems. Therefore, the results we derived in a particular scenario in this paper have broader applications and consequences. Especially, it is utterly important to rethink the models used to ensure coexistence between different physical layers. Future work will therefore focus on this particular aspect.

Acknowledgement

This work was partially funded through French National Research Agency (ANR) project ACCENT5 with grant agreement code: ANR-14-CE28-0026-02.

References

[1] Y. Medjahdi *et al.*, "Performance analysis in the downlink of asynchronous OFDM/FBMC based multi-cellular networks," *IEEE Trans. Wireless Commun.*, vol. 10, no. 8, pp. 2630–2639, 2011.

[2] B. Farhang-Boroujeny, "OFDM versus filter bank multicarrier," *IEEE Signal Process. Mag.*, no. May 2011, pp. 92–112, 2011.

[3] L. G. Baltar *et al.*, "Out-Of-Band Radiation in Multicarrier Systems: A Comparison," in *Multi-Carrier Spread Spectrum 2007*. Springer Netherlands, 2007, vol. 1, pp. 107–116.

[4] H. Mahmoud *et al.*, "OFDM for cognitive radio: merits and challenges," *IEEE Wireless Commun. Mag.*, vol. 16, no. April, pp. 6–15, 2009.

[5] K. Raghunath and a. Chockalingam, "SC-FDMA versus OFDMA: Sensitivity to large carrier frequency and timing offsets on the uplink," in *GLOBECOM - IEEE Global Telecommunications Conference*, 2009.

[6] A. Aminjavaheri *et al.*, "Impact of timing and frequency offsets on multicarrier waveform candidates for 5G," in *IEEE Signal Processing and Signal Processing Education Workshop (SP/SPE)*, Aug 2015, pp. 178–183.

[7] M. Bellanger, "FBMC physical layer: a primer," Project PHYDYAS, Tech. Rep., January 2010.

[8] M. Shaat and F. Bader, "Computationally efficient power allocation algorithm in multicarrier-based cognitive radio networks: OFDM and FBMC systems," *EURASIP Journal on Advances in Signal Processing*, vol. 2010, p. 5, 2010.

[9] A. Skrzypczak *et al.*, "OFDM/OQAM modulation for efficient dynamic spectrum access," *International Journal of Communication Networks and Distributed Systems*, vol. 8, no. 3-4, pp. 247–266, 2012.

[10] T. Ihalainen *et al.*, "On spectrally efficient multiplexing in cognitive radio systems," in *Wireless Pervasive Computing, 2008. ISWPC 2008. 3rd International Symposium on*, May 2008, pp. 675–679.

[11] A. K. T. Weiss, J. Hillenbrand and F. K. Jondral, "Mutual Interference in OFDM-Basedased Spectrum Pooling Systems,," in *Proceedings of the 59th IEEE Vehicular Technology Conference (VTC '04). Milan, Italy.*, vol. 59, 2004.

[12] Q. Bodinier *et al.*, "5G Waveforms for Overlay D2D Communications: Effects of Time-Frequency Misalignment," in *IEEE International Conference on Communications (ICC)*, Kuala Lumpur, 2016.

[13] ——, "Modeling Interference Between OFDM / OQAM and CP-OFDM : Limitations of the PSD-Based Model," in *International Conference on Telecommunications (ICT)*, Thessaloniki, 2016.

[14] M. Caus *et al.*, "Capacity Analysis of WCC-FBMC/OQAM Systems," in *ICASSP, IEEE International Conference on Acoustics, Speech and Signal Processing - Proceedings*, Shanghai, 2016.

[15] M. Bellanger, "Specification and design of a prototype filter for filter bank based multicarrier transmission," in *2001 IEEE International Conference on Acoustics, Speech, and Signal Processing. Proceedings*, vol. 4, 2001, pp. 2417–2420.

[16] D. R. I. Brown and A. G. Kelin, "Synchronization Concepts," in *Coordinated Multi-Point in Mobile Communications: From Theory to Practice*, P. Marsch and G. P. Fettweis, Eds. Cambridge Univeristy Press, 2011, ch. 8.1, pp. 161–170.

3.3 Signal processing for OFDM and beyond OFDM

This Subsection includes research lines carried out on the OFDM scheme, on advanced multi-carrier schemes (named beyond OFDM) in general, and on OFDM/OQAM (FBMC) in particular. From one hand, my preliminary research works using OFDM scheme started from my PhD studies period at UPM (1998-2002) where although the investigated scheme was the MC-CDMA (SS-OFDM), the OFDM scheme was always indirectly there in all my research analysis (See references cited in Subsection 1.1, in page 15). Works strictly dealing with signal processing for OFDM have been undertaken since my advice (2005-2009) of Mr. Ismael Gutierrez Gonzalez PhD thesis on "Adaptive Communications for Next Generation Broadband Wireless Access Systems" (see related publications and details in page 19).

From an other hand, although my researches related with OFDM/OQAM (FBMC) signal started during my involvement in the European funded PHYDYAS project in 2008, where my main focuses were on: pilot pattern design for channel estimation in SISO and MIMO cases (see references [C58, J9, 69, 70]), and on interference alignment with MIMO in CR environment (see references [C82, C85, C86, C87], and [J19]), my involvement in the ANR French project PROFIL allowed me to undertake from 2014 a research focus on signal processing using blind equalization techniques on OQAM/OFDM signal. In fact the blind equalization use in OFDM/OQAM is one of the interesting research aspects not addressed neither in the PHYDYAS project nor in the project EMPhATIC. One can do the simple exercise of typing at the IEEE Xplore[15] digital library the key words "OFDM blind", and do the same for "OFDM/OQAM blind". The result is overwhelming[16] (see the result at footnote[16]) and in favor of OFDM scheme. This is saying a lot on the available research potential for combining blind equalization and channel estimation techniques with OFDM/OQAM scheme. My researches undertaken in this field were in collaboration with Dr. Vincent Savaux, and Dr. Malek Naoues, postdocs (see Subsection 1.3.2 in page 17 for more details) under the ANR French project PROFIL.

First work in this context dealt with an adaptation of the constant norm algorithm (CNA) class for frequency blind equalization in OFDM modulation as a first step toward its extension to the OFDM/OQAM scheme. Overviews and comparative studies of data-aided channel estimation methods for OFDM systems are provided in [71, 72, 73]. Once estimated, the channel can be directly inverted with a one-tap per carrier equalization. However, the use of the CP and pilot symbols may drastically reduce the useful data rate. Therefore, the pilot density reduction or the CP length shortening is recommended for higher data rate transmissions. Such capabilities can be reached, in particular by means of blind equalization.

First works dealing with blind equalization have been undertaken by Sato [74] in 1975, but one of the most used algorithms is the constant modulus algorithm (CMA) proposed by Godard [75] in 1980, a nice overview on blind equalization using CMA is presented by Johnson et al. in [76]. The CMA converges independently of the phase, but this feature leads to a misadjustment in the detected symbols, which needs to be corrected.
The multi-modulus algorithm (MMA) presented in [77] (originally called modified CMA) has been proposed to solve the phase ambiguity issue by employing the CMA on both the real and imaginary parts of the received symbols. More recently, MMA-based methods have been derived in order to improve the performance of CMA for high-order constellations [78, 79]. In particular, the β-MMA method such as proposed in [80] has proven to outperform both CMA and MMA.
In CP-OFDM systems, the blind equalization is generally carried out for two purposes; i) performing a channel shortening, when the delay spread is longer than the CP duration. In that case, a deconvolution filter is used as time-domain equalizer (TEQ). The equalizer coefficients can then be updated by using some features of the OFDM signal. A solution consists of minimizing the difference between the last samples of the OFDM symbol and the corresponding samples in the CP, as presented in [81], ii) performing a simple frequency per-carrier equalization. In [82], the simple decision directed algorithm is used, in which the considered cost function compares the received signal and the detected data after a decoding stage. The authors in [83] have proposed an algorithm based on the maximum likelihood (ML) criterion. Although this blind equalizer shows good performance, it is particularly complex, especially if numerous subcarriers and high order constellations are considered.

The CNA for frequency blind equalization was originally designed in single-carrier systems [84, 85], the convergence analysis of CNA during our investigations has been carried out for an adaptation to OFDM. It results that

[15] http://ieeexplore.ieee.org/Xplore/home.jsp
[16] Displaying result is: 1361 for OFDM, 18 for OFDM/OQAM, and 7 for FBMC. [Accessed]: 20/08/2016.

a phase adaptation of the equalizer coefficient has to be undertaken to ensure a convergence toward the expected value, leading to the proposed phase adaptation procedure (PAP). Furthermore, a sub-optimal initialization strategy (see Section 5 in [J23] on "Correcting CNA Phase Mismatch Phenomena in Frequency Blind Equalization for OFDM Systems", depicted at the end of this Subsection 3.3) has been also proposed, which allows to improve the convergence speed of the algorithm. Simulations show that the proposed CNA with PAP outperforms the constant modulus algorithm (CMA) for both the convergence speed and the steady-state performance. Furthermore, a gain in number of iterations of up to 50% is achieved when the proposed sub-optimal initialization is used compared with a fixed initialization value.
Note that from achieved results the adapted CNA family has proved to be very relevant when a square constellation as 16-QAM is used, but has only been implemented in single carrier systems [84, 85]. It has been shown from our obtained results that the CNA with $p = \infty$ ($p - norm$) the constant square algorithm (CQA) is not able to recover the phase. Due to the features of CQA, this phase mismatch induces a convergence of the equalizer coefficients $F_{m,n}$ (see footnote[17]) toward erroneous values, which limits the performance of this algorithm in OFDM. In order to overcome this problem, a procedure for the phase adaptation of the coefficients $F_{m,n}$ called (PAP) has been proposed and it has been shown that CNA-6 and CQA with PAP outperform the CMA as well as the β-MMA. In fact, it has been demonstrated that CNA has a higher convergence speed and achieves a lower MSE than CMA for a 16-QAM constellation. Furthermore, the capability of CNA with proposed PAP to track the channel variations has been also demonstrated. Finally, thanks to the proposed initialization strategy, an increase of the convergence speed is achieved. All the details of this work is available in [J23] depicted at the end of this Subsection 3.3.

An extension of the work on correcting the CNA phase mismatch in frequency blind equalization for OFDM to OFDM/OQAM has been undertaken in [C91, C92, C99, C104] and partially in [J24], where different aspects has been investigated. In our work in [C91], a suboptimal initialization strategy allowing to drastically reduce the transient state of the blind iterative process is presented for OFDM/OQAM scheme. The issue of initialization for blind equalizer in FBMC has been dealt with in [86], where the authors presented a thorough convergence study, and proposed to set the initialized coefficients to a weak value. However, such an initialization is not optimal with regard to the convergence speed toward the steady-state. As a matter of fact, it is possible to take advantage of the OFDM/OQAM feature to assess a sub-optimal initialization coefficient for each subcarrier as presented in our work in [C91]. The main drawback of the one-tap blind equalizer for FBMC is the possible convergence of the update algorithm toward local minima, which induces a delay in the convergence process. In order to avoid it, the authors in [86] proposed to set the initialized coefficient $F_{m,0}$[17] to a value near to zero. However, this solution does not ensure a fast convergence toward the steady state of the update algorithm. It has been proved that optimal solutions cannot be achieved in the complex field, but sub-optimal real values can be derived, and such a sub-optimal initialization strategy allows to improve the convergence speed of the equalizer. Numerical results have shown that thousands of iterations are gained by using the proposed initialization strategy in [C91] compared with the initialized coefficient $F_{m,0} \ll 1$.

As a continuity to our works in [C91] and in [C99, C104], an OFDM/OQAM blind equalization technique using CNA approach is presented in [J24][18] (see the reference in Subsection 2.1.1, page 30). In [J24], the CNA is designed to fit the complex square constellations with high order. As a consequence, the received signal is reshaped in order to change the real OQAM symbols into complex ones. Although it increases the intrinsic interferences of the OFDM/OQAM signal, it is proved by analysis and through simulations that the CNA with proposed reshaped signal achieves better mean square error (MSE) performance than CMA applied to the received OFDM/OQAM signal. Performance analysis of CNA-6 Adapted to OFDM/OQAM has been developed, and the reshape of complex symbols as described in Fig. 3.24 has opened new perspectives for blind equalization in filter bank-based modulations, as specific cost functions (not limited to the real field) can now be used and investigated.
The CNA, which can be seen as a generalized CMA, has been developed. To be effective, the CNA requires a signal using a complex constellation. Therefore, it has been proposed to reshape the “real” received OQAM symbols to obtain “complex” 16-QAM symbols. The performance of the proposed method has been analyzed, and it has been proved that, despite the increase of the interference level due to the reshape, the CNA applied to the new signal achieves better performance than the CMA applied to the OFDM/OQAM signal.

Furthermore, the principle of changing the shape of the received signal opens new perspectives for the blind

[17] $F_{m,n}$ is the initialized coefficient, where $\{m, n\}$ indexes means frequency and time directions respectively
[18] a copy of this paper is available at the end of this Subsection

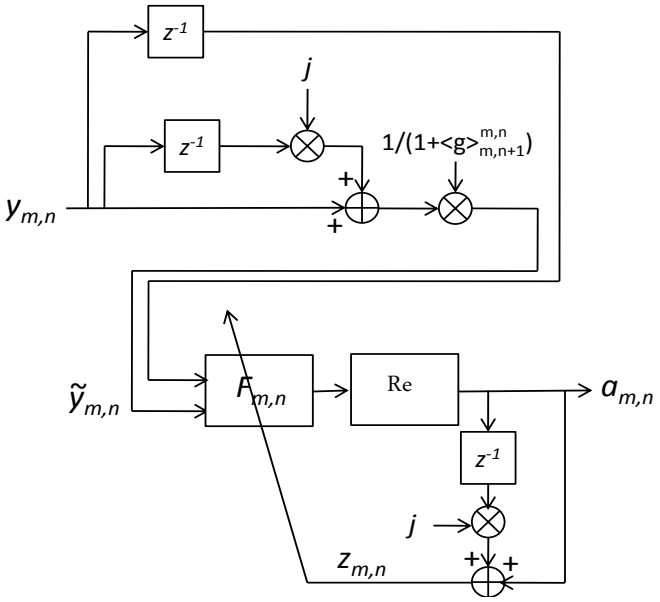

Figure 3.24: Proposed blind equalizer using CNA, adapted to OFDM/OQAM system in [J24].

equalization in the FBMC-based modulations, as specific cost functions (not limited to the real field) can now be investigated. In addition, a sub-optimal initialization strategy, in the sense of the mean square error, has been presented. Numerical results revealed that the CNA and the proposed initialization method allows to reduce by 2000 the number of iterations of the blind equalizer. Moreover, the performances of CMA and CNA-6 have been studied in conditions where the receiver is not well-synchronized with the transmitter and the channel is time-varying. Results have shown that this degrades the performance.
In order to overcome these deterioration, a relevant solution consists of using preamble, from which the synchronization and accurate initialization can be obtained.

All the publications (See Subsection 2.1.1, pp. 30-42) related with the above mentioned research work on signal processing for blind equalization in CP-OFDM and OFDM/OQAM are: Journals: [J24, J23, J20], Conferences [C104, C101, C99, C92, C91], Other: [O1].

Following are the corresponding depicted papers:

1. [J23]- Vincent Savaux, Faouzi Bader, and Jacques Palicot, "Correcting CNA Phase Mismatch Phenomena in Frequency Blind Equalization for OFDM Systems", Elsevier Signal Processing Journal, vol. 127, pp. 227–238, doi: 10.1016/j.sigpro.2016.02.024, October 2016.

2. [C101]- Vincent Savaux, Yves Louet, and Faouzi Bader, "Low-Complexity Approximations for LMMSE Channel Estimation in OFDM/OQAM", in Proc. of the International Conference on Telecommunications (ICT'2016), Thessaloniki-Greece. May 2016.

3. [J24]- Vincent Savaux, Faouzi Bader, and Jacques Palicot, "OFDM/OQAM Blind Equalization Using CNA Approach", IEEE Transactions on Signal Processing, vol. 64, issue 9, pp.2324-2333, doi: 10.1109/TSP.2016.2519000, May 2016.

Signal Processing 127 (2016) 227–238

Contents lists available at ScienceDirect

Signal Processing

journal homepage: www.elsevier.com/locate/sigpro

Correcting CNA phase mismatch phenomena in frequency blind equalization for OFDM systems

Vincent Savaux [a,*], Faouzi Bader [a], Jacques Palicot [a]

[a] SCEE team/IETR, CentraleSupélec, Rennes, France

ARTICLE INFO

Article history:
Received 23 July 2015
Received in revised form
17 February 2016
Accepted 26 February 2016
Available online 15 March 2016

Keywords:
Blind equalization
Constant norm algorithm
OFDM

ABSTRACT

This paper presents an adaptation of the constant norm algorithm (CNA) class for frequency blind equalization in orthogonal frequency division multiplexing (OFDM) modulation. Originally designed in single-carrier systems, the convergence analysis of CNA is investigated in OFDM. It results that a phase adaptation of the equalizer coefficient has to be undertaken to ensure a convergence toward the expected value, leading to the proposed phase adaptation procedure (PAP). Furthermore, a sub-optimal initialization strategy is proposed, which allows to improve the convergence speed of the algorithm. Simulations show that the proposed CNA with PAP outperforms the constant modulus algorithm (CMA) for both the convergence speed and the steady-state performance. Furthermore, a gain in number of iterations of up to 50% is achieved when the proposed sub-optimal initialization is used compared with a fixed initialization value.

1. Introduction

The robustness of orthogonal frequency division multiplexing with cyclic prefix (CP-OFDM) against multipath channels has made it a very popular modulation scheme that has been adopted in a large number of communication standards. The use of a CP longer than the delay spread of the channel allows us to suppress the inter-symbols interference and recover the orthogonality between subcarriers at the receiver. Furthermore, the remaining channel distortions can be easily estimated by using pilot symbols that are multiplexed in the data stream. Overviews and comparative studies of data-aided channel estimation methods for OFDM systems are provided in [1–3]. Once estimated, the channel can be directly inverted with a one-tap per carrier equalization. However, the use of the CP and pilot symbols may drastically reduce the useful data rate. Therefore, the pilot density reduction or the CP length shortening is recommended for higher data rate transmissions. Such capabilities can be reached, in particular by means of blind equalization.

First works dealing with blind equalization have been undertaken by Sato [4] in 1975, but one of the most used algorithms is the constant modulus algorithm (CMA) proposed by Godard [5] in 1980 (and independently in [6] in 1983), and an overview on blind equalization using CMA is presented by Johnson et al. [7]. The CMA converges independently of the phase, but this feature leads to a misadjustment in the detected symbols, which needs to be corrected. The multimodulus algorithm (MMA) presented in [8] (originally called modified CMA [9,10]) has been proposed to solve the phase ambiguity issue by employing the CMA on both the real and imaginary parts of the received symbols. More recently, MMA-based methods have been derived in order to improve the performance of CMA for high-order constellations [11,12]. In particular, the β-MMA method such as proposed in [13,14] has proven to outperform both CMA and MMA.

In CP-OFDM systems, the blind equalization is generally carried out for two purposes:

(i) Performing a channel shortening, when the delay spread is longer than the CP duration. In that case, a deconvolution filter is used as time-domain equalizer (TEQ). The equalizer coefficients can then be updated by using some features of the OFDM signal. A solution consists of minimizing the difference between the last samples of the OFDM symbol and the corresponding samples in the CP, as presented in [15]. In [16], the authors propose to use a mean square criterion on the "artificial" null symbols between subcarriers. Another method in [17] aims to maximize the signal to interference plus noise ratio (SINR).

(ii) Performing a simple frequency per-carrier equalization. In [18], the simple decision directed algorithm is used, in which the considered cost function compares the received signal and the detected data after a decoding stage. The authors in [19] have proposed an algorithm based on the maximum

* Corresponding author.
E-mail addresses: vincent.savaux@centralesupelec.fr (V. Savaux), Faouzi.Bader@supelec.fr (F. Bader), jacques.palicot@centralesupelec.fr (J. Palicot).

http://dx.doi.org/10.1016/j.sigpro.2016.02.024
0165-1684/

likelihood (ML) criterion. Although this blind equalizer shows good performance, it is particularly complex, especially if numerous subcarriers and high order constellations are considered.

Alternatively, both channel shortening and frequency equalization can be performed by the per-tone equalization method which has been originally proposed in [20], and transposed to blind receivers in [21,22]. In this paper, we rather focus on per-carrier frequency equalization. This task is performed by using the constant norm algorithm (CNA) proposed in [23,24]. This method can be seen as a generalization of the CMA, in which the modulus is substituted by a norm on the complex plane. In this way, a specific norm fits a particular constellation which allows us to reduce the noise of the algorithm. The CNA has been presented for single-carriers systems in [24], and to the best of the authors' knowledge, it has not been used in multicarrier systems. It is worth noting that the special case of the infinity norm has been independently proposed in [24–27], and has been originally called *square contour algorithm* (SQA). One of the main goals of this paper is to extend the CNA to the OFDM context by including specific adaptations. As a matter of fact, the phase mismatch between the channel and the equalizer coefficient has to be taken into account to ensure that the update algorithm converges toward the expected value. Thus, we propose to add a phase adaptation procedure (PAP) to the CNA in order to cancel the phase mismatch phenomenon. Furthermore, a quasi-optimal initialization strategy for each of the equalizer's coefficients is proposed.

The remaining of the paper is organized as follows: Section 2 presents the system model and the used equalization algorithms. The convergence behavior of CNA is analyzed in Section 3, and the proposed phase adaptation procedure is presented in Section 4. Then, a sub-optimal initialization value is provided in Section 5. Simulations will show achieved performances of the CNA with its adaptations to OFDM in Section 6, and we draw our conclusions in Section 7.

2. Background

2.1. System model

The transmission of OFDM symbols over a multipath channel is considered with a perfect time and frequency synchronization. It is assumed that the cyclic prefix (CP) duration is longer than the maximum delay spread of the channel. Therefore, after the fast Fourier transform (FFT) of size M and the CP removal, the nth received OFDM signal is expressed as

$$\mathbf{Y}_n = \mathbf{H}_n\mathbf{X}_n + \mathbf{W}_n, \tag{1}$$

where $\mathbf{X}_n$ and $\mathbf{Y}_n$ are the $M \times 1$ vectors containing the transmitted and received complex symbols $Y_{m,n}$ and $X_{m,n}$ respectively, and the m subscript is pointing out the subcarrier index. The vector $\mathbf{W}_n$ is composed of M independent zero-mean Gaussian noise samples whose variance is σ^2, and $\mathbf{H}_n$ is the $M \times M$ diagonal matrix of the channel with entries

$$H_{m,n} = H_m = \sum_{l=0}^{L-1} h_l e^{-2j\pi\frac{m\tau_l}{M}}, \tag{2}$$

on the diagonal. The removal of the subscript n in (2) means that the channel is assumed to be static throughout the paper. The constant L in (2) is the number of paths of the channel, h_l is the path gain, and τ_l is the corresponding delay. More details related to the derivation of (1) and (2) are provided in Chapter 1 of [28].

2.2. Blind equalization: problem formulation

The equalization aims at recovering the transmitted data $\mathbf{X}_n$ from the received signal $\mathbf{Y}_n$. The equalization in OFDM systems can be undertaken on each subcarrier independently of each other by the following expression:

$$Z_{m,n} = F_{m,n}Y_{m,n} = F_{m,n}(H_{m,n}X_{m,n} + W_{m,n}), \tag{3}$$

where $F_{m,n}$ is the equalizer coefficient on the mth subcarrier. In this paper, the coefficients $F_{m,n}$ are blindly adapted by solving the following optimization problem:

$$F_m^{opt} = \min_{F_m}(E\{J(Z_m)\}), \tag{4}$$

where $E\{\cdot\}$ is the mathematical expectation, and J is a given cost function that will be determined afterward. The minimization problem in (4) can be carried out by employing the classical stochastic gradient algorithm as

$$F_{m,n+1} = F_{m,n} - \mu\frac{\partial J(Z_{m,n})}{\partial Z_{m,n}}, \tag{5}$$

where μ is the appropriate step-size parameter. Since the cost function J may be phase-blind, the demodulation stage in (1) and the convergence process in (5) may lead to a phase error $\phi_{m,n}$. As a consequence, a phase recovery and tracking algorithm must be added to the equalizer in order to track both the phase and the modulus of the transmitted symbols [5,29,10], such as depicted in Fig. 1, and expressed as

$$\phi_{m,n+1} = \phi_{m,n} - \mu_\phi f(\tilde{Z}_{m,n}), \tag{6}$$

where μ_ϕ is the step size parameter for the phase tracking algorithm, and f is a given function. The simple decision directed has been used in [5] for the phase tracking, but this method is limited when the variation speed of the phase is to high. Some more recent techniques have been proposed in the literature in order to overcome this problem, such as in [30,31]. However, it has been aforementioned that the symbols $Y_{m,n}$ are received with perfect synchronization, and the channel is supposed to be static. Therefore, the phase tracking is out of the scope of this paper, and we focus on the way to perform (5) in the following.

2.3. Constant norm algorithm

As a general rule, the cost function J in (5) compares the output of the equalizer $Z_{m,n}$ with a constant value. One of the most frequently used cost function is the CMA presented by Godard [5]. CMA is particularly adapted for constant modulus constellations as phase shift keying (PSK), but also works for square constellation as QAM. A generalization of this function called CNA has been proposed in [24]. The authors have shown that CNA fits better QAM constellations than CMA, as a particular norm can be adapted for each modulation. As presented in [24], the cost function of CNA can be written as

$$J(Z_m) = \frac{1}{ab}\,\big|\,|Z_m|^a - R\big|^b, \tag{7}$$

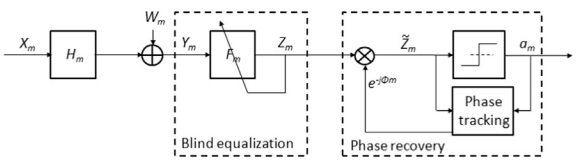

Fig. 1. Blind equalization and phase recovering process on each subcarrier m at the OFDM receiver.

where $\|\cdot\|$ is a norm defined on $\mathbb{C}$, R is a real positive constant that depends on the constellation type, and a and b are two parameters that give two degrees of freedom to the algorithm. However, the most frequently used values are $a = b = 2$[1] and will be considered throughout the present paper. It has been demonstrated in [5,24] that the optimal value $\alpha_m = |F_m H_m| = 1$ should be reached if

$$R = \frac{E\{\| X_m \|^{2a}\}}{E\{\| X_m \|^{a}\}}. \tag{8}$$

We can consider (8) as the most general expression of R, which is valid for any norm, and whose derivation is provided by (9)–(14) in [24]. In the rest of the paper, we consider the p-norm family, which is expressed for any complex z on the plane $\mathbb{C}$ as

$$\| z \|_p = \sqrt[p]{|\mathrm{Re}\{z\}|^p + |\mathrm{Im}\{z\}|^p}. \tag{9}$$

The CMA is obtained by considering $p=2$, i.e. the "usual norm". In that case, the update algorithm in (5) can be rewritten as follows:

$$F_{m,n+1} = F_{m,n} - \mu(|Z_{m,n}|^2 - R)Z_{m,n}Y^*_{m,n}. \tag{10}$$

Thus, CMA is a particular case of the more general CNA family. In [24], the cases $p=6$ and $p = \infty$ have also been studied as they are relevant for QAM constellations (especially 16-QAM). Since we focus our developed analysis on the square 16-QAM constellation, we will consider these two norms in the rest of the paper.[2] Note that the update algorithms related to CNA-6 and CNA $-\infty$ are

$$F_{m,n+1} = F_{m,n} - \mu(\| Z_{m,n} \|_6^2 - R) \times \frac{\mathrm{Re}\{Z_{m,n}\}^5 + j\,\mathrm{Im}\{Z_{m,n}\}^5}{\| Z_{m,n} \|_6^4} Y^*_{m,n}, \tag{11}$$

and

$$F_{m,n+1} = F_{m,n} - \mu(\| Z_{m,n} \|_\infty^2 - R) f(Z_{m,n}) Y^*_{m,n}, \tag{12}$$

where the infinite norm is $\| Z_{m,n} \|_\infty = \max(|\mathrm{Re}\{Z_{m,n}\}|, |\mathrm{Im}\{Z_{m,n}\}|)$ and f is a function defined as

$$f(Z_{m,n}) = \begin{cases} \mathrm{Re}\{Z_{m,n}\}, & \text{if } |\mathrm{Re}\{Z_{m,n}\}| > |\mathrm{Im}\{Z_{m,n}\}| \\ j\,\mathrm{Im}\{Z_{m,n}\}, & \text{otherwise} \end{cases}. \tag{13}$$

As it was highlighted in [23,24], the infinite norm does not belong to the p-norm family, and the derivation of (12) requires specific developments. Besides, the unit ball of the infinite norm is a square of side 2, therefore the authors of [23,24] named the update algorithm in (12) Constant sQuare Algorithm (CQA). It is worth noting that the output of the equalizer is constrained by the unit ball of the utilized norm. For instance, the equalized symbols $Z_{m,n}$ are on a circle when CNA-2 (CMA) is used, whereas they are on a square if CQA is chosen.[3] Fig. 2 depicts the unit balls of the modulus and the infinite norms compared with the symbols of a 16-QAM. Since the steady-state performance of the algorithm depends on the mean distance $E\{l\}$ between the constellation symbols and the unit ball (see Section 2 in [23] for more details), it can be easily shown that $E\{l_\infty\} < E\{l_2\}$. In fact, if it is supposed that the circle in Fig. 2 has a radius of 1, then we obtain:

$$E\{l_\infty\} = \frac{4 \times 1 + 12 \times 0}{16} = 0.25$$

$$E\{l_2\} = \frac{8 \times 0.0541 + 4 \times 0.5286 + 4 \times 0.4142}{16} = 0.2627,$$

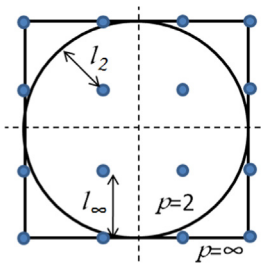

Fig. 2. Distance between the unit balls corresponding to CMA (circle) and CNA $-\infty$ (square), and the symbols of the 16-QAM constellation.

where 0.0541, 0.5286, and 0.4142 correspond to the distances between the points $\{\pm\frac{1}{3} \pm j, \pm 1 \pm \frac{1}{3}j\}$, $\{\pm\frac{1}{3} \pm \frac{1}{3}j\}$, and $\{\pm 1 \pm j\}$ respectively, and the unit circle. Thus, the performance of the CNA $-\infty$ should be better than that of CMA using a 16-QAM constellation. This will be further explained and shown through simulations in Section 6.

As previously mentioned, the CNA has been proposed for single carrier systems where the blind equalization is a blind deconvolution [24]. To the best of the authors' knowledge, this concept has not been adapted and used in OFDM systems, which is the main purpose of this paper.

3. Convergence analysis of CNA in OFDM

One of the advantages of the CMA is its phase-independence nature as demonstrated in [5,7]. This can be straightforwardly shown by substituting $Z_{m,n} = F_{m,n}Y_{m,n}$ into (10), which yields the following expression:

$$F_{m,n+1} = F_{m,n}(1 - \mu(|Z_{m,n}|^2 - R)|Y_{m,n}|^2). \tag{14}$$

It can be noticed that $(1 - \mu(|Z_{m,n}|^2 - R)|Y_{m,n}|^2)$ (14) is real. It results that the phase of $F_{m,n}$ is that used at the initialization $F_{m,n=0}$. Geometrically, the CMA can be interpreted as a projection of the received symbols $Y_{m,n}$ on a given circle as shown in Fig. 2. As a consequence, the direction of $F_{m,n}$ is not a limiting parameter for the convergence of CMA.

It has been stated in [23,24] that the CNA is able to recover the phase in single carrier systems. However, this is obtained to the cost of an additive delay in the convergence process compared with CMA. Such a result is valid for a blind deconvolution in single carrier systems but might be reconsidered in the present OFDM context where the equalization is performed by a single coefficient per carrier as in (11) and (12). In particular, it can be noticed for CQA that

$$E\{\arg(F_{m,n+1})\} = E\{\arg(F_{m,n})\} = E\{\arg(F_{m,n=0})\}. \tag{15}$$

The difference between the result in (14) and (15) is that CMA converges in the same direction as $F_{m,n=0}$ in a deterministic way (it is a projection), whereas CQA converges "in average" in the direction of $F_{m,n=0}$. The equality in (15) is proved in Appendix A. The unit ball of CMA is a circle, so the phase of $F_{m,n}$ does affect its modulus when the steady-state is reached. On the other hand the unit ball of CQA is a square, therefore the convergence of $F_{m,n}$ in the direction of the side or the corner of the square shall not lead to the same results, reflecting that the convergence of CQA depends on the phase of $F_{m,n=0}$ as shown in (15).

Besides the previous geometrical considerations, it is possible to mathematically show that the result $|F_m^{opt} H_m| = \alpha_m = 1$, which is verified for any $F_{m,0}$ value using CMA, is not ensured anymore for CQA. To achieve this, the optimization problem in (4) is solved by

[1] It has been stated in [5] that it is very difficult to ensure the convergence of the algorithm for a and b values higher than 2.

[2] More generally, it has been shown by the authors of [24] that for any constellation corresponds a specific norm.

[3] The equalities $\| Z_{m,n} \|^2 - R = 0$ and $\| Z_{m,n} \|_\infty^2 - R = 0$ are achieved in (10) and (12) if the steady state is reached, and correspond to the equations of the circle and the square on the complex plane, respectively.

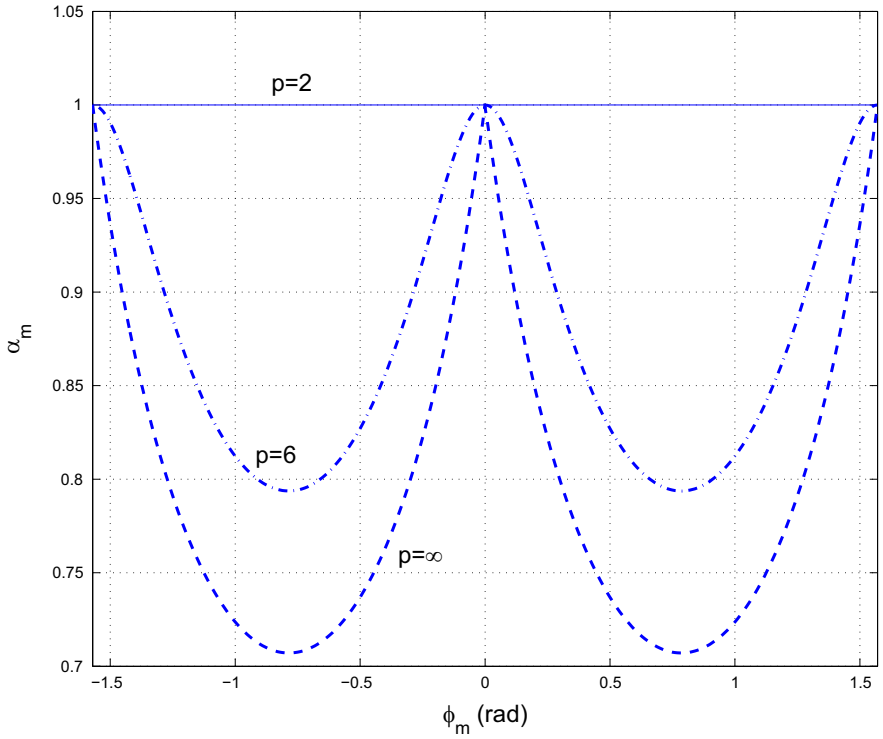

Fig. 3. Achieved α_m in (17) versus phase mismatch ϕ_m for $p=2$, $p=6$, and $p=\infty$.

assuming (i) a noiseless transmission, (ii) the optimal value F_m^{opt} is reached with a phase mismatch ϕ_m with the channel such as $F_m^{opt}H_m = \alpha_m^{opt}e^{j\phi_m}$ (i.e. ϕ_m is the angle between F_m and H_m) and (iii) R is defined as in (8). For sake of simplicity, further developments are carried out considering that $a = b = 2$. The optimal value α_m^{opt} is obtained by solving the following expression:

$$\left.\frac{\partial E\{J(Z_m)\}}{\partial \alpha_m}\right|_{\alpha_m=\alpha_m^{opt}} = 0. \tag{16}$$

The optimization problem is rewritten by substituting (7) into (16) leading to

$$\begin{aligned}\left.\frac{\partial E\left\{\frac{1}{4}\,\|Z_m\|^2 - R\|^2\right\}}{\partial \alpha_m}\right|_{\alpha_m=\alpha_m^{opt}} &= 0 \Leftrightarrow E\{\alpha_m^3 \,\|\, e^{j\phi_m}X_m\,\|^2\}\\ &= E\{\alpha_m R \,\|\, e^{j\phi_m}X_m\,\|\} \Leftrightarrow \alpha_m\\ &= \left(\frac{R\cdot E\{\|\, e^{j\phi_m}X_m\,\|^2\}}{E\{\|\, e^{j\phi_m}X_m\,\|^4\}}\right)^{\frac{1}{2}}.\end{aligned} \tag{17}$$

Fig. 3 depicts achieved α_m versus ϕ_m from $-\frac{\pi}{2}$ to $\frac{\pi}{2}$ for $p=2$, $p=6$, and $p=\infty$. The used constellation is a 4-QAM. Fig. 3 confirms that CMA (i.e. CNA with $p=2$) converges to the optimal value $\alpha_m = 1$ whatever the phase ϕ_m is. However, it can be observed that the phase mismatch ($\phi_m \neq 0$) for $p=6$ and $p=\infty$ will conduct to a non-optimal value $\alpha_m \neq 1$. In particular, it can be observed for $p=\infty$ that at $\phi_m = \pm\frac{\pi}{4}$ we have $\alpha_m = 1/\sqrt{2}$, which corresponds to the length of half the diagonal of a square of side 2. The phase mismatch $\phi_{m,n}$ has no incidence if $p=2$ since the unit ball is a circle, but induces an increase of $1/\alpha_m$ if $p > 2$. Fig. 4 illustrates this phenomenon for CQA (for which the unit ball is a square) using $\arg(F_{m,n=0}) = 0$, and $\phi_m < 0$. Thus, $|F_{m,n}|$ converges to $\frac{\alpha_m}{|H_{m,n}|}$ with $\alpha_m \leq 1$.

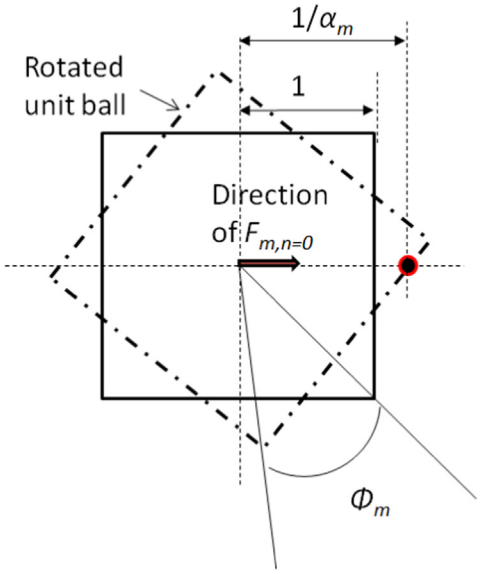

Fig. 4. Geometrical interpretation of the effect of the phase rotation ϕ_m on α_m, using $p=\infty$.

It has been proved in (15) that CQA converges in the same direction as $F_{m,n=0}$, whereas the phase mismatch between $F_{m,n}$ and $H_{m,n}$ leads to an erroneous $F_{m,n}$ value. Therefore, the convergence of $F_{m,n}$ to non-optimal values such as $\alpha_m \leq 1$ seems to be an inherent property of CQA in OFDM, whereas as aforementioned, the sole effect of the phase mismatch in single carrier systems as in [24] seems to be a delay in the convergence process, in comparison with CMA. In order to overcome this problem, the coefficients $F_{m,n}$ should be chosen with a phase mismatch $\phi_m = 0$. A solution allowing to achieve this result is proposed in Section 4.

4. CNA in OFDM with phase adaptation procedure

4.1. Basic principle of the phase adaptation procedure

In this section, we propose a procedure for the phase adaptation of the coefficients $F_{m,n}$ allowing to obtain $\phi_m = 0$, and therefore $\alpha_m = 1$. Although the problem of convergence due to the phase mismatch has been shown for the particular case $p = \infty$, the proposed algorithm remains valid whatever the degree p of CNA is. In fact, simulation results in Section 6 show that CNA-6 is able to cancel the phase mismatch in OFDM (with an increase of the convergence delay), whereas the phase mismatch is persistent for CQA. As a consequence, a method that adapts the phase of $F_{m,n}$ according to that of $H_{m,n}$ should be mandatory for CQA, while it shall reduce the convergence time of CNA when $p \neq \infty$. Since the phase adaptation can be used for any p value, we adopt the general formulation "CNA" throughout the section.

The basic idea behind the proposed phase adaptation procedure (PAP)[4] is to re-inject, at a given iteration, the result of the phase recovery $\phi_{m,n}$ in the equalizer coefficient value $F_{m,n}$ instead of the equalized symbol $Z_{m,n}$. This can be viewed as a reset of the equalizer coefficient by replacing $F_{m,n}$ by $F_{m,n}e^{j\phi_{m,n}}$. It must be emphasized that this phase adaptation is relevant only when $\phi_{m,n}$ has converged. This issue is discussed afterward. The steps of the proposed PAP are summarized as follows, and illustrated in Fig. 5.

- If $\phi_{m,n}$ has converged, then
  (a) $F_{m,n} \leftarrow F_{m,n}e^{j\phi_{m,n}}$;
  (b) $\phi_{m,n} \leftarrow 0$;
- else, the iterative blind equalization continues as usual.

4.2. Decision rule for performing the PAP

We propose three decision rules for the implementation of the PAP:

1. Decision rule 1 (DR1): An iteration number n_{PAP} is a priori fixed such as if $n = n_{PAP}$, then the PAP is performed. This rule is very simple to implement, but either the PAP is carried out too early and the convergence of $\phi_{m,n}$ is not certainly achieved, or the phase is adapted too late which could affect the convergence speed of the blind equalizer. In order to ensure an optimal value of n_{PAP}, the convergence behavior of $\phi_{m,n}$ should be a priori known, but this is not available in practice. However, this solution can be used as a point of comparison for other methods.
2. Decision rule 2 (DR2): This rule consists of comparing a threshold γ_ϕ with the mean square error (MSE) defined by

$$MSE_{phi,n} = \frac{1}{M}\sum_{m=0}^{M-1} |\phi_{m,n} - \phi_{m,n-1}|^2. \tag{18}$$

   The decision rule using $MSE_{phi,n}$ is defined as follows: the threshold $\gamma_\phi > 0$ is set such as if $MSE_{phi,n} < \gamma_\phi$, then the PAP is performed.
3. Decision rule 3 (DR3): Instead of using the MSE in (18), the decision is made independently on each subcarrier $m \in \{0, 1, .., M-1\}$ by using a "local" error

$$\Delta_{m,n}^{phi} = |\phi_{m,n} - \phi_{m,n-1}|^2. \tag{19}$$

   Therefore, the PAP is carried out on the mth subcarrier if $\Delta_{m,n}^{phi} < \gamma_\phi$. It must be noticed that the threshold γ_ϕ is the same for DR2 and DR3 as DR2 is only the averaged version of DR3.

[4] Note that we have called the proposed method "phase adaptation procedure" in order to avoid any confusion with the phase tracking algorithm given in (6).

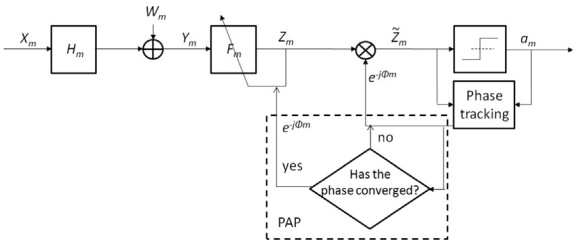

Fig. 5. Receiver structure with blind equalization, phase recovering, and phase adaptation procedure (PAP).

Compared with DR2, DR3 takes into account the different convergence speeds of the phases $\phi_{m,n}$, but the variance of the processes $\Delta_{m,n}^{phi}$ is also larger than that of $MSE_{phi,n}$, which could induce erroneous decisions.

The choice of a convenient value of γ_ϕ is discussed hereafter. The optimal value γ_ϕ^{opt} can be expressed when the phase $\phi_{m,n}$ has converged by the following expression:

$$\gamma_\phi^{opt} = E\{|\phi_{m,n} - \phi_{m,n-1}|^2 = \mu_\phi^2 E\{\mathrm{Im}\{\tilde{Z}_{m,n}(\tilde{Z}_{m,n} - a_{m,n})^*\}^2\}. \tag{20}$$

As previously mentioned, the optimal value γ_ϕ^{opt} remains the same for both DR2 and DR3, since the average in (18) is only an approximation of the expectation in (20). Due to the convergence behavior of CQA described in Fig. 4, it would be very difficult to obtain an exact expression of γ_ϕ^{opt} in (20). However, thanks to some approximations, a minimum value of γ_ϕ can be derived. To achieve this, we rewrite $\tilde{Z}_{m,n} = Z_{m,n}e^{-j\phi_{m,n}}$ and we obtain the following expression:

$$\begin{aligned}\tilde{Z}_{m,n} &= \underbrace{F_{m,n}e^{-j\phi_{m,n}}H_{m,n}X_{m,n}}_{a_{m,n}+\epsilon_{m,n}} + F_{m,n}e^{-j\phi_{m,n}}W_{m,n} \\ &= a_{m,n} + \underbrace{\epsilon_{m,n} + F_{m,n}W_{m,n}}_{\tilde{W}_{m,n}},\end{aligned} \tag{21}$$

where $\epsilon_{m,n}$ is the error between the equalized symbol and the closest constellation element, and $\tilde{W}_{m,n}$ is equivalent to a noise sample with zero-mean and with variance $\tilde{\sigma}^2$. Due to the presence of $\epsilon_{m,n}$ and $F_{m,n}$ in the expression of $\tilde{\sigma}^2$, it can be assumed that $\tilde{\sigma}^2 \geq \sigma^2$. Therefore, a straightforward development by substituting (21) into (20) yields (more details are in A.1)

$$\gamma_\phi = \mu_\phi^2 E\{\mathrm{Im}\{\tilde{Z}_{m,n}\tilde{W}_{m,n}^*\}^2\} \geq \mu_\phi^2\sigma^2 E\{\mathrm{Re}\{a_{m,n}\}^2 + \mathrm{Im}\{a_{m,n}\}^2\}, \tag{22}$$

where $E\{\mathrm{Re}\{a_{m,n}\}^2 + \mathrm{Im}\{a_{m,n}\}^2\} = 2$ in the case of a 4-QAM, and equal to 10 if a 16-QAM is used. Thus, (22) shows that the chosen value of γ_ϕ depends on the noise level and the constellation size.

5. Sub-optimal initialization strategy

When the blind equalization is carried out with a deconvolution filter in time domain for single carrier systems as in [24], the initialized equalizer consists of a vector composed of zeros except for a unique coefficient that is set to one. In the same ways for OFDM modulations, the initialization strategy consists of setting a unique value $F_{m,n=0}$ for all $0 \leq m \leq M-1$, e.g. $F_{m,n=0} = 1$. However, such an initialization is not optimal with regard to the convergence speed toward the steady-state.

Actually, it is possible to take advantage of the OFDM feature to assess a (sub-)optimal initialization coefficient $F_{m,n=0}^{opt}$ for each subcarrier. For sake of clarity, it is assumed that $n=0$ in the

hereafter expressions. The optimal initialization value in the sense of the mean square error criterion can be calculated by minimizing the following cost function:

$$J_m^{ini} = E\{|F_{m,0}Y_{m,0} - X_{m,0}|^2\}. \tag{23}$$

After some straightforward mathematical developments, solving $\frac{\partial J_m^{ini}}{\partial F_{m,0}} = 0$ (i.e. finding the MMSE) leads to

$$F_{m,0}^{opt} = \frac{H_{m,0}^* E\{|X_{m,0}|^2\}}{E\{|Y_{m,0}|^2\}}. \tag{24}$$

One should notice that the equality $E\{|Y_{m,0}|^2\} = |H_{m,0}|^2 E\{|X_{m,0}|^2\}$ holds in noise-free conditions, and hence (24) reduces to $F_{m,0}^{opt} = \frac{1}{H_{m,0}}$. However, it must be emphasized that the value of $H_{m,0}$ is unknown, and the evaluation of $E\{|Y_{m,0}|^2\}$ in (24) requires the prior knowledge of the noise variance, when this is not supposed to be null. Therefore, the optimal initialization coefficient in (24) cannot be assessed in practice. However, a sub-optimal value $F_{m,0}^{s-opt}$ can be derived from (24) by constraining $F_{m,0}^{s-opt} \propto \frac{1}{|H_{m,0}|}$ instead of $F_{m,0}^{opt} = \frac{1}{H_{m,0}}$ when the noise level tends to zero. This feature can be achieved by defining

$$F_{m,0}^{s-opt} = \sqrt{\frac{E\{|X_{m,0}|^2\}}{|Y_{m,0}|^2 + \kappa}}, \tag{25}$$

where κ is a real-valued positive constant that avoids the divergence of $F_{m,0}^{s-opt}$ when $Y_{m,0}$ is very close to zero. In practice, it is chosen such that $\kappa \ll 1$. The sub-optimal nature of $F_{m,0}^{s-opt}$ is proved hereafter. The mean error between the square moduli of the invert of $F_{m,0}^{s-opt}$ and $H_{m,0}$ is defined as

$$\epsilon_F = E\left\{\frac{1}{|F_{m,0}^{s-opt}|^2} - |H_{m,0}|^2\right\}. \tag{26}$$

It must be reminded that the noise samples $W_{m,0}$ are zero-mean, have a variance $\sigma^2 = E\{|W_{m,0}|^2\}$, and are uncorrelated with $H_{m,0}$ and $X_{m,0}$ samples. Therefore, the ϵ_F value in (26) can be simplified as

$$\begin{aligned}\epsilon_F &= E\left\{\frac{|Y_{m,0}|^2 + \kappa}{E\{|X_{m,0}|^2\}} - |H_{m,0}|^2\right\} \\ &= E\left\{\frac{|H_{m,0}X_{m,0}|^2 + |W_{m,0}|^2 + (H_{m,0}X_{m,0})W_{m,0}^*}{E\{|X_{m,0}|^2\}}\right. \\ &\quad \left. + \frac{(H_{m,0}X_{m,0})^* W_{m,0} + \kappa}{E\{|X_{m,0}|^2\}} - |H_{m,0}|^2\right\} = \frac{\sigma^2 + \kappa}{E\{|X_{m,0}|^2\}}.\end{aligned} \tag{27}$$

It can be noticed in (27) that we asymptotically obtain

$$\epsilon_F = \frac{\kappa}{E\{|X_{m,0}|^2\}} \ll 1 \tag{28}$$

when σ^2 tends to 0 (i.e. when the signal-to-noise ratio tends to infinity). Therefore, the initialization strategy proposed in (25) is sub-optimal, which should improve the convergence speed compared with $F_{m,0=0} = 1$. This behavior will be numerically verified in the hereafter Section 6.

6. Simulations results

6.1. Simulations setup

The numerical results presented in this section use the following parameters. The OFDM signal is composed of $M = 128$ subcarriers and CP duration is 10% of the OFDM symbol time length. Whatever the chosen algorithm is, the equalizer coefficients are initialized at $F_{m,n} = 1$, and the step-size parameter for the phase is set to $\mu_\phi = 0.1$. Simulations are carried out with a 16-QAM modulation since the used CQA is especially designed to fit this modulation. Furthermore, a SNR of 30 dB is considered in order to compare the limit of the methods, independently of the added noise distortions. The Proakis' channel [32] (refereed as "Proakis 1") whose path coefficients are given by the vector $[0.04, -0.05, 0.07, -0.21, -0.5, 0.72, 0.36, 0, 0.21, 0.03, 0.07]$ is used for simulations. The length of the channel is 86% that of the CP, which guarantees a transmission without intersymbol interference.

The blind equalization algorithms have been compared with the data-aided least square (LS) channel estimation method. In that case, the channel is estimated thanks to a preamble composed of M pilot tones. The power of the preamble has been set equal to the signal. The LS channel estimate is given by

$$H_{m,n}^{LS} = \frac{Y_{m,n}}{X_{m,n}} = H_{m,n} + \frac{W_{m,n}}{X_{m,n}}, \tag{29}$$

where $X_{m,n}$ in (29) is a pilot, whose value is known from the receiver. The channel is then inverted by using the zero forcing equalizer (ZF), whose coefficients are $F_{m,n} = \frac{1}{H_{m,n}^{LS}}$. More details relative to channel estimation is provided in [28]. Furthermore, CMA and CNA are compared with the blind β-MMA equalizer, the update algorithm of which is detailed in (17) in [13].

The analyzed methods (CMA, CNA, β-MMA, and LS) are compared by using the following MSE:

$$MSE = \frac{1}{M}\sum_{m=0}^{M-1}(|\tilde{Z}_{m,n}| - |X_{m,n}|)^2. \tag{30}$$

This measure allows us to compare performed algorithms in terms of their converge speeds as well as their steady-state performances. It has been stated in [5] that the optimal step-size parameter should be chosen as $\mu = (30E\{|X_{m,n}|^2\})^{-1}$. However, three blind algorithms (CMA, CNA-6, and CQA) are compared in this paper, and each of them has a different behavior (in terms of convergence speed and/or of steady state performance) for a given μ value. As a consequence, it should be more relevant to adjust the step-size parameter of each of the methods in order to obtain same convergence speed (and then compare the steady state MSE values), or on the other hand, to compare the convergence speed given the same steady-state performance. In the following, all the plotted results have been obtained after an average over 100 realizations.

6.2. Numerical results

Fig. 6 compares the steady-state performance of CMA, CNA-6 and CQA when carried out without PAP, and β-MMA. To be fair, the compared algorithms start with the same convergence speed, therefore the step-size parameter μ has been specifically set for each of them. It can be seen that the CQA achieves an MSE steady-state performance equal to -9.5 dB whereas the CMA reaches -17.5 dB. This result is consistent with the analysis undertaken in Section 3. Furthermore, algorithm behaviors in Fig. 6 show that CMA converges faster than CNA-6, but the latter has a lower steady-state than CMA (and has a weaker MSE for $n \geq 4000$ iterations). This proves that CNA-6, unlike CQA, does not require any phase adaptation to converge toward the optimum, but the phase recovering delays the convergence. Furthermore, it can be observed that the β-MMA achieves the lowest steady-state MSE, but to the cost of a longer delay of convergence. This result is consistent with those that are shown in [13].

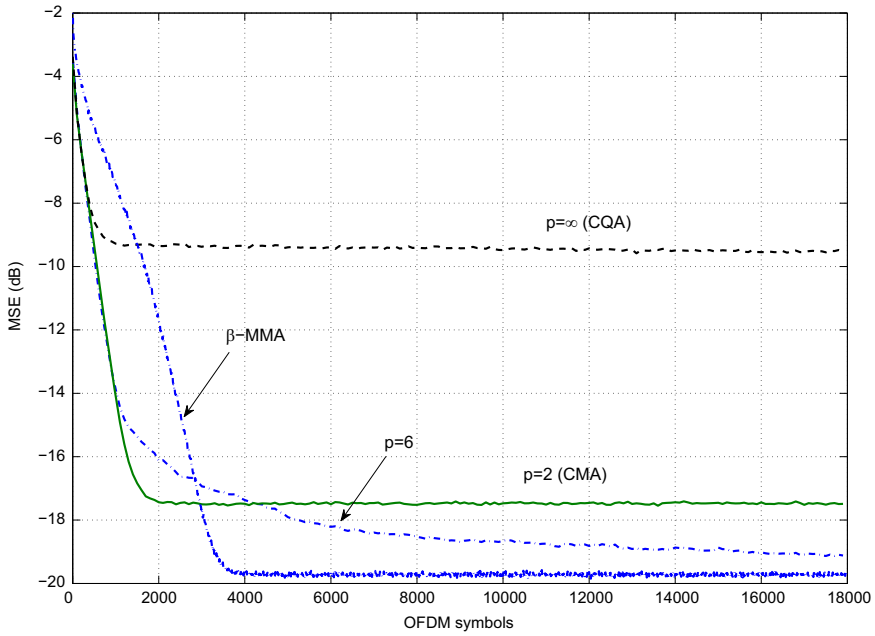

Fig. 6. CMA, CNA-6, β-MMA, and CQA performances versus OFDM symbols numbers on Proakis 1 channel, without PAP.

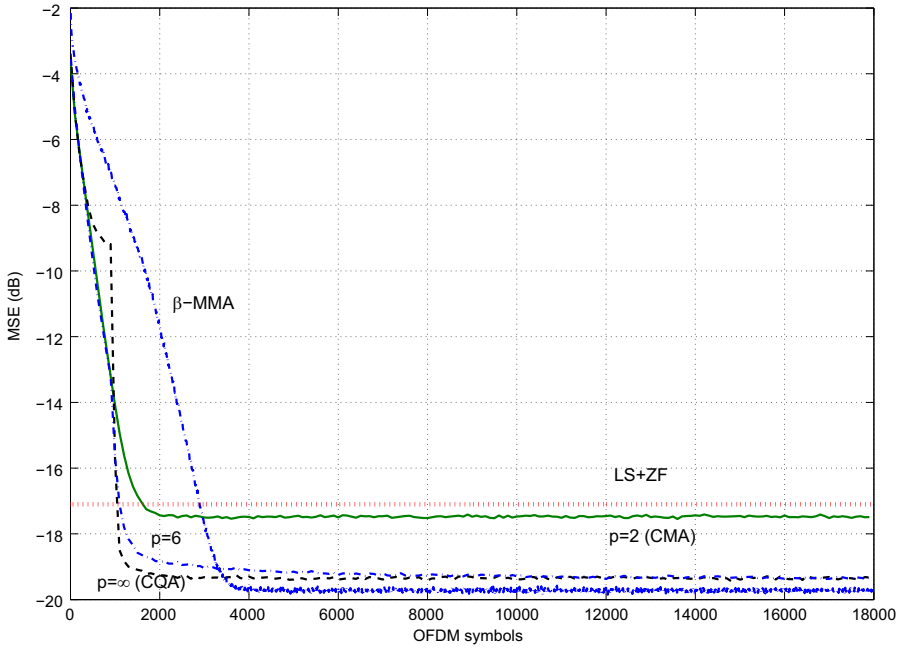

Fig. 7. CMA, CNA-6, β-MMA, and CQA performances versus OFDM symbol numbers on Proakis 1 channel, with PAP using DR1. Comparison with data-aided LS+ZF equalization.

The same parameters as in Fig. 6 are used to compare the MSE performance of CMA, β-MMA, CNA-6 and CQA with proposed PAP using DR1 with $n_{PAP} = 1000$ (this value has been *a posteriori* set using results from Fig. 9) in Fig. 7. Furthermore, the achieved MSE of LS estimation in (29) with ZF equalization is plotted as well. It can be observed that CNA-6 and CQA have the same steady-state performance at -19.5 dB, and CQA has a slightly higher convergence speed than CNA-6. Furthermore, Fig. 7 shows that CNA-6 and CQA achieve higher convergence rate and lower MSE than CMA. It proves that the PAP proposed in Section 4 allows the CQA to be adapted in OFDM systems to achieve similar performances as those observed for single carrier systems in [24,23]. Moreover, although CNA-6 has the same steady-state performance with or without phase adaptation, we draw from Fig. 7 that the PAP increases the convergence speed of the algorithm. The comparison with the pilot-aided LS+ZF method reveals that several hundreds of iterations are required by the blind algorithm to reach the same MSE as LS+ZF, since the latter achieves its steady-state from the first OFDM symbol. However, this drawback is compensated by the fact that a MSE gain of 2.5 is achieved by CNA-6 and CQA in comparison with the data-aided method. Furthermore, the gain of β-MMA is about 0.5 dB compared with the CNA methods, but it requires 2000 more iteration than CNA to converge. Thus, the performance gain is low in comparison to the additional delay. In addition to the above, the blind methods allows to maximize the spectral efficiency of the signal, since no pilots are used.

Unlike previous figures, Fig. 8 shows the convergence speed of CMA, β-MMA, CNA-6 and CQA with PAP using DR1 ($n_{PAP} = 1000$)

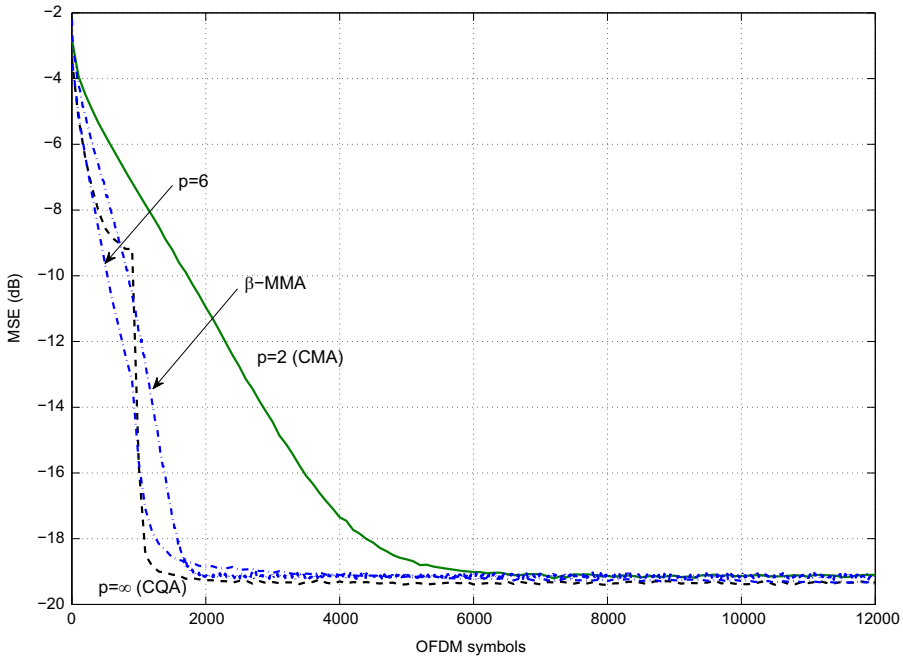

Fig. 8. Convergence speed of CMA, CNA-6, β-MMA, and CQA with PAP using DR1 for a given steady-state performance.

for the same steady state MSE set to ≈ -19.5 dB. Therefore, the step-size parameters μ of CMA and β-MMA have been chosen to obtain this steady-state performance. It can be seen that β-MMA, CNA-6 and CQA converges faster than CMA (e.g. CQA reaches its steady-state at $n=2000$ whereas that of CMA is reached at $n=7000$). We conclude from Figs. 7 and 8 that, for a fixed convergence rate, CNA with PAP achieves a lower MSE than CMA, and for a fixed steady-state performance, CNA with PAP converges faster than CMA. It is worth noting that these results are consistent with those observed in [24,23] and prove that CNA-6 and CQA are more efficient than CMA when a 16-QAM is used. Furthermore, we conclude from Fig. 8 that, for a desired steady-state performance, β-MMA, CNA-6 and CQA are equivalent methods. As a consequence, CNA-6 and CQA are potential alternatives to β-MMA.

Fig. 9 shows the performance comparison of CQA using the PAP with DR1 for $n_{PAP} = 250$, 1000, and 4000. The CMA is plotted as reference. It can be observed that DR1 with $n_{PAP}=1000$ and 4000 have the same steady-state performance, but as expected, $n_{PAP}=1000$ converges faster than $n_{PAP}=4000$. Furthermore, Fig. 9 shows that the case DR1 with $n_{PAP}=250$ converges faster than DR1 with $n_{PAP}=1000$ but achieves higher MSE than the latter. This is due to the fact that the phase updating algorithm in (6) has

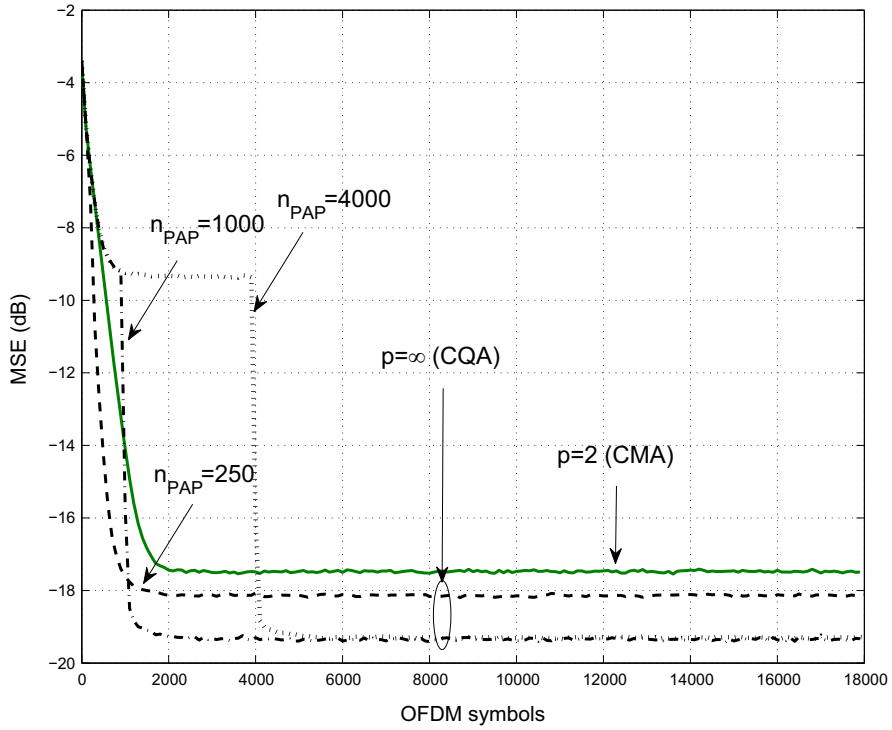

Fig. 9. MSE performance comparison of CQA with PAP using DR1 for $n_{PAP} = 250$, 1000, and 4000.

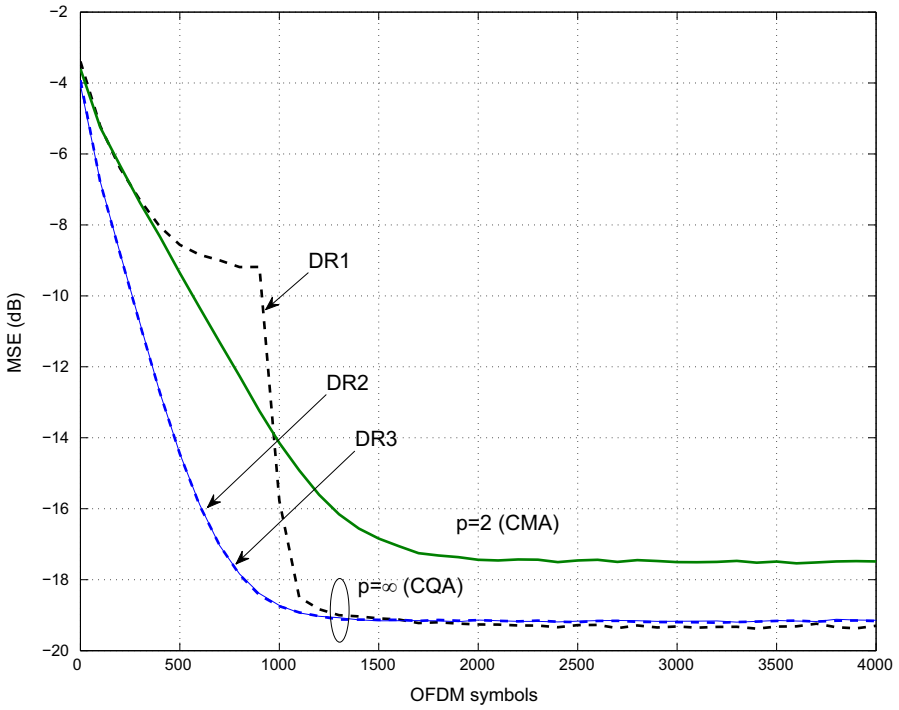

Fig. 10. MSE performance comparison of CQA with PAP using DR1 ($n_{PAP}=1000$), DR2, and DR3.

converged at $n_{PAP}=250$ only for a set of subcarriers (leading to a fast convergence rate), but not for the others, which induces a higher steady-state performance than the case $n_{PAP}=1000$. It results that a relevant value of n_{PAP} cannot be a priori chosen, which limits the implementation of DR1.

Achieved MSEs of CQA using DR1 (with $n_{PAP}=1000$), DR2, and DR3 are compared in Fig. 10. For both DR2 and DR3, the threshold γ_ϕ has been set to 0.004, based on the recommendation made in Section 4. It can be seen that DR2 and DR3 have a higher convergence speed than DR1 and CMA (a gain of 500 iterations can be observed at MSE $=-14$ dB, namely a gain of 50%), and reach almost the same steady-state performance than DR1. As a consequence, we conclude that both decision rules for the PAP can be used as a solution for the implementation of CNA in OFDM. Furthermore, it must be noticed that DR2 and DR3 have exactly the same trajectories, whereas the decision rules are different. This

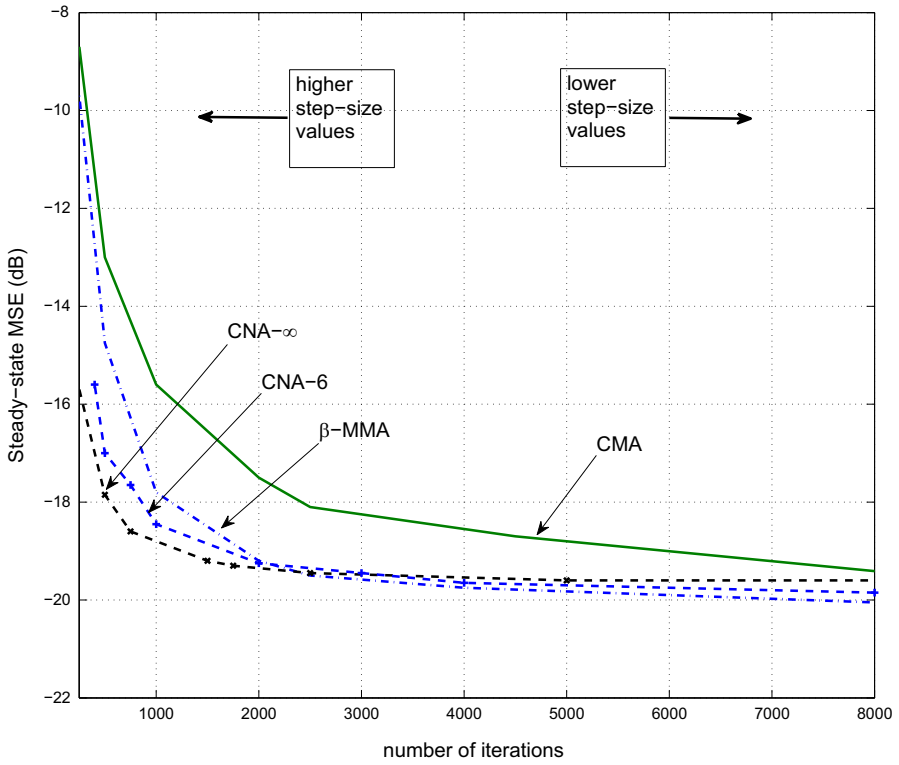

Fig. 11. Steady-state MSE performance versus iterations required to achieve the steady-state.

result is quite surprising, but can be explained by the fact that the MSE in (30) is averaged over 100 realizations, and for $M=128$. Therefore, it could be highlighted from Fig. 10 that DR2 and DR3 have the same performance "in average".

In order to provide a fair comparison of the performance of the different algorithms, Fig. 11 depicts the steady-state MSE performance versus iterations required to achieve the steady-state. The curves in Fig. 11 have been obtained from a set of traces corresponding to different step-size parameters values. Thus, the achieved performances in the left side of the plot correspond to high μ values (i.e. high convergence speed but low precision), whereas those on the right side of Fig. 11 correspond to lower μ values (i.e. low convergence speed but high precision). Note that both CNA-6 and CNA $-\infty$ are performed with PAP using DR2. It can be observed that in the "higher convergence speed" range (i.e. in the left side of the figure), both CNA-6 and CNA $-\infty$ outperforms β-MMA in terms of steady-state MSE. It is worth mentioning that a gain of up to 6 dB is achieved by CNA $-\infty$ compared with β-MMA where 250 iterations are required to reach the steady-state. On the other hand, β-MMA achieves a gain less than 1 dB in the "lower convergence speed" range compared with CNA-6 and CNA $-\infty$. These results reveal that CNA $-\infty$ using PAP allows us to obtain a blind equalizer combining a good convergence speed with low steady-state MSE performance.

Other simulations have been performed to analyze the behavior of CNA with PAP using DR2 when the channel changes. To be done, the same parameters as before are considered, but the coefficients of the channel are multiplied by a coefficient equal to $0.9e^{j\frac{\pi}{4}}$ at the 4000th OFDM symbol, which changes both modulus and phase. Fig. 12 shows achieved MSE performance using the CMA, CNA-6 and CQA. A peak appears in the trajectories of CNA for $p=2$, $p=6$, and $p=\infty$ at the 4000th OFDM symbol, and about 800 iterations are required by the algorithms to converge again. It can be seen that the achieved steady-state performance after the channel variation is the same as before the 4000th iteration. This result shows the capability of CNA with PAP to track the channel variations in terms of both phase and modulus.

The convergence speed of CMA and CNA-6 using the proposed sub-optimal initialization value $F_{m,n}^{s-opt}$ given in (25) is compared with the case $F_{m,n=0}=1$ in Fig. 13. It can be observed that CMA with $F_{m,n}^{s-opt}$ experiences a gain of 1000 iterations (or equivalently 1000 OFDM symbols) to reach its steady-state. Moreover, at $MSE=-16$ dB, a gain of 500 iterations is achieved by CNA-6 with $F_{m,n}^{s-opt}$ compared with $F_{m,n=0}=1$. This result validates the use of the proposed sub-optimal initialization strategy proposed Section 5 to improve the convergence speed of the CNA in OFDM systems.

6.3. Discussion

The previous results showed that the proposed correction of the phase mismatch allows us to adapt the CNA-6 and CQA techniques in OFDM. Moreover, these methods are able to achieve better performance in terms of MSE and convergence speed than the β-MMA [13] for high step-size parameter values. Another advantage of the CNA lies in the fact that it can be adapted to square and non-square constellations since norms can be specifically designed for all kinds of constellations. On the contrary, β-MMA is a simple method which shows good performance in the case of square constellations. Other series of simulations revealed that a blind equalizer achieves at least as good performance as pilot-aided methods. However, simulations have been undertaken in a static propagation channel. As a consequence, these blind receivers could be relevant in a broadcast context, where the channels are usually assumed to be static or quasi-static. In that scenario, a short preamble in comparison with the data sequence may not reduce that much the spectral efficiency of the data aided signal. However, the use of a preamble could increase the PAPR of the transmitted signal, whereas the PAPR of the signal using a blind receiver is that of the OFDM, i.e. about 12 dB.

7. Conclusion

In this paper, we have proposed an adaptation of the CNA for frequency blind equalization in OFDM. The CNA family has proved to be very relevant when a square constellation as 16-QAM is used, but has only been implemented in single carrier systems [23,24]. It

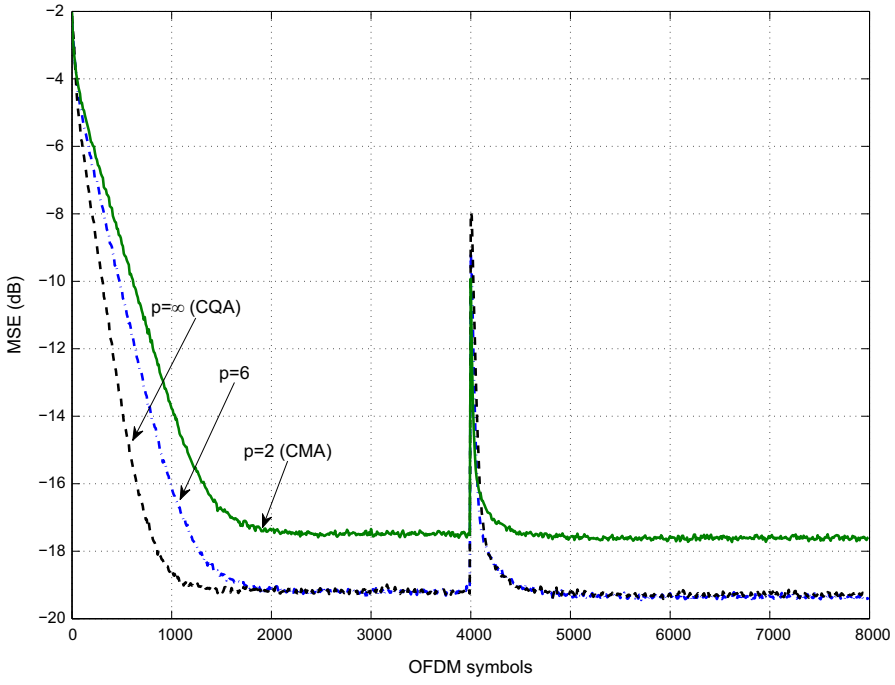

Fig. 12. Tracking performance of CMA, CNA-6, and CQA with PAP using DR2.

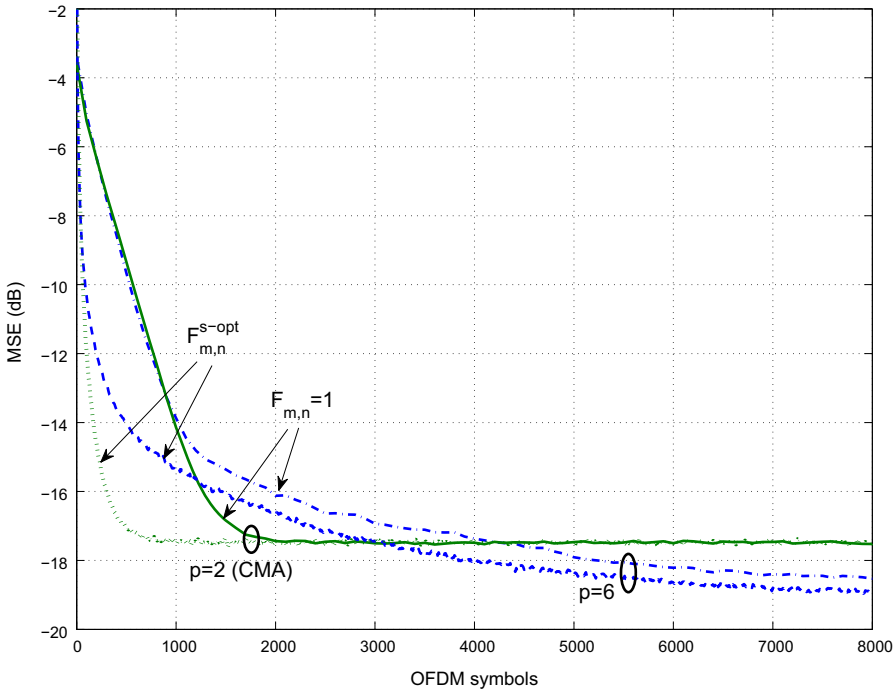

Fig. 13. MSE performance of CMA and CNA-6 with sub-optimal initialization strategy.

has been shown in (15) that the CNA with $p = \infty$ (CQA) is not able to recover the phase. Due to the features of CQA, this phase mismatch induces a convergence of the equalizer coefficients $F_{m,n}$ toward erroneous values, which limits the performance of this algorithm in OFDM. In order to overcome this problem, a procedure for the phase adaptation of the coefficients $F_{m,n}$ called (PAP) has been proposed in Section 4. Simulations have shown that CNA-6 and CQA with PAP outperforms the CMA, and achieves as well as β-MMA. In fact, it has been demonstrated that CNA has a higher convergence speed and achieves a lower MSE than CMA for a 16-QAM constellation. Furthermore, the capability of CNA with proposed PAP to track the channel variations has been highlighted. Finally, thanks to the proposed initialization strategy, an increase of the convergence speed is achieved.

Acknowledgment

This work is supported by the project PROFIL (Evolution of the wideband PROfessional Mobile Radio based on the FILter Bank MultiCarrier modulation) funded by the French National Research Agency with grant agreement code ANR-13-INFR-0007-03 and ICT EC-funded project Newcom# with code FP7-IC-318306.

Appendix A. Proof of (15)

In this appendix, we prove that the equalizer coefficients $F_{m,n+1}$ of CQA in (15) converge in average in the same direction as $F_{m,n=0}$. For sake of simplicity, a 4-QAM is considered hereafter. For any $n \in \mathbb{N}$ we rewrite $E\{\arg(F_{m,n+1})\}$ in (A.1) by substituting (12) into (15). It is assumed that $P(|\mathrm{Re}\{Z_{m,n}\}| > |\mathrm{Im}\{Z_{m,n}\}|) = P(|\mathrm{Im}\{Z_{m,n}\}| > |\mathrm{Re}\{Z_{m,n}\}|) = \frac{1}{2}$. Then, we can express $E\{\arg(A_R)\}$ as in (A.2). Since $P(Y^*_{m,n} = \pm 1 \pm j) = \frac{1}{4}$, we obtain (A.3):

$$\begin{aligned} E\{\arg(F_{m,n+1})\} &= P(|\mathrm{Re}\{Z_{m,n}\}| > |\mathrm{Im}\{Z_{m,n}\}|) \\ &\quad \times E\left\{\arg(\underbrace{F_{m,n} - \mu(|\mathrm{Re}\{Z_{m,n}\}|^2 - R)\,\mathrm{Re}\{Z_{m,n}\}Y^*_{m,n}}_{A_R})\right\} \\ &\quad + P(|\mathrm{Im}\{Z_{m,n}\}| > |\mathrm{Re}\{Z_{m,n}\}|) \\ &\quad \times E\left\{\arg(\underbrace{F_{m,n} - \mu(|\mathrm{Im}\{Z_{m,n}\}|^2 - R)\,\mathrm{Im}\{Z_{m,n}\}Y^*_{m,n}}_{A_I})\right\}. \end{aligned} \tag{A.1}$$

$$\begin{aligned} E\{\arg(A_R)\} &= P(Y^*_{m,n} = 1 + j) \\ &\quad E\Big\{\arg\Big(F_{m,n} - \mu(|\mathrm{Re}\{Z_{m,n}\}|^2 - R)\,\mathrm{Re}\{Z_{m,n}\}H_{m,n}(1 + j)\Big)\Big\} \\ &\quad + P(Y^*_{m,n} = 1 - j) \\ &\quad E\Big\{\arg\Big(F_{m,n} - \mu(|\mathrm{Re}\{Z_{m,n}\}|^2 - R)\,\mathrm{Re}\{Z_{m,n}\}H_{m,n}(1 - j)\Big)\Big\} \\ &\quad + P(Y^*_{m,n} = -1 + j) \\ &\quad E\Big\{\arg\Big(F_{m,n} - \mu(|\mathrm{Re}\{Z_{m,n}\}|^2 - R)\,\mathrm{Re}\{Z_{m,n}\} \\ &\quad H_{m,n}(-1 + j)\Big)\Big\} + P(Y^*_{m,n} = -1 - j) \\ &\quad E\Big\{\arg\Big(F_{m,n} - \mu(|\mathrm{Re}\{Z_{m,n}\}|^2 - R)\,\mathrm{Re}\{Z_{m,n}\} \\ &\quad H_{m,n}(-1 - j)\Big)\Big\}. \end{aligned} \tag{A.2}$$

$$\begin{aligned} E\{\arg(A_R)\} &= \tfrac{1}{4}E\Big\{\arg\Big(F_{m,n} - \mu(|\mathrm{Re}\{Z_{m,n}\}|^2 - R)\,\mathrm{Re}\{Z_{m,n}\}H_{m,n}(1 + j)\Big) \\ &\quad + \arg\Big(F_{m,n} - \mu(|\mathrm{Re}\{Z_{m,n}\}|^2 - R)\,\mathrm{Re}\{Z_{m,n}\}H_{m,n}(1 - j)\Big) \\ &\quad + \arg\Big(F_{m,n} - \mu(|\mathrm{Re}\{Z_{m,n}\}|^2 - R)\,\mathrm{Re}\{Z_{m,n}\}H_{m,n}(-1 + j)\Big) \\ &\quad + \arg\Big(F_{m,n} - \mu(|\mathrm{Re}\{Z_{m,n}\}|^2 - R)\,\mathrm{Re}\{Z_{m,n}\}H_{m,n}(-1 - j)\Big)\Big\} \end{aligned} \tag{A.3}$$

It is straightforward to show that for any $(z_1, z_2) \in \mathbb{C}^2$, we have

$$\arg\left(z_1 + z_2 e^{j\frac{\pi}{4}}\right) + \arg\left(z_1 + z_2 e^{j\frac{3\pi}{4}}\right) + \arg\left(z_1 + z_2 e^{-j\frac{\pi}{4}}\right) + \arg\left(z_1 + z_2 e^{-j\frac{3\pi}{4}}\right) = 4\arg(z_1). \tag{A.4}$$

Then, by substituting the result in (A.4) into (A.3), we obtain that $E\{\arg(A_R)\} = \arg(F_{m,n})$. The same development can be carried out with $E\{\arg(A_I)\}$ leading to the equality $E\{\arg(F_{m,n+1})\} = E\{\arg(F_{m,n})\}$ in (A.1). As this result is valid for any $n \in \mathbb{N}$, a simple mathematical induction yields

$$E\{\arg(F_{m,n+1})\} = E\{\arg(F_{m,n=0})\}. \tag{A.5}$$

A.1. Proof of (22)

The substitution of (21) into (20) yields

$$\begin{aligned}\gamma_\phi &= \mu_\phi^2 E\{\mathrm{Im}\{\tilde{Z}_{m,n}\tilde{W}_{m,n}^*\}^2\} = \mu_\phi^2 E\{\mathrm{Im}\{a_{m,n}\tilde{W}_{m,n}^* + |\tilde{W}_{m,n}|^2\}^2\} \\ &= \mu_\phi^2 E\left\{\left(\mathrm{Im}\{a_{m,n}\}\,\mathrm{Re}\{\tilde{W}_{m,n}^*\} + \mathrm{Re}\{a_{m,n}\}\,\mathrm{Im}\{\tilde{W}_{m,n}^*\}\right)^2\right\}.\end{aligned} \tag{A.6}$$

The expectation of the cross-factors obtained from the development of the third line in (A.6) are equal to zero since both $a_{m,n}$ and $\tilde{W}_{m,n}$ are variables with zero mean. Hence, using $\tilde{\sigma}^2 \geq \sigma^2$ leads to the following:

$$\begin{aligned}\gamma_\phi &= \mu_\phi^2 E\{\mathrm{Im}\{a_{m,n}\}^2\,\mathrm{Re}\{\tilde{W}_{m,n}^*\}^2 + \mathrm{Re}\{a_{m,n}\}^2\,\mathrm{Im}\{\tilde{W}_{m,n}^*\}^2\} \\ &\geq \mu_\phi^2 \tilde{\sigma}^2 E\{\mathrm{Re}\{a_{m,n}\}^2 + \mathrm{Im}\{a_{m,n}\}^2\} \\ &\geq \mu_\phi^2 \sigma^2 E\{\mathrm{Re}\{a_{m,n}\}^2 + \mathrm{Im}\{a_{m,n}\}^2\}.\end{aligned} \tag{A.7}$$

Note that the covariance of $\mathrm{Im}\{a_{m,n}\}^2$ and $\mathrm{Re}\{\tilde{W}_{m,n}^*\}^2$ has been omitted in the second line of (A.7), which justify the use of the inequality.

References

[1] M. Morelli, U. Mengali, A comparison of pilot-aided channel estimation methods for OFDM systems, IEEE Trans. Signal Process. 49 (12) (2001) 3065–3073.

[2] M.K. Ozdemir, H. Arslan, Channel estimation for wireless OFDM systems, IEEE Commun. Surv. Tutor. 9 (2) (2007) 18–48.

[3] Y. Liu, Z. Tan, H. Hu, L.J. Cimini, G.Y. Li, Channel estimation for OFDM, IEEE Commun. Surv. Tutor. 16 (4) (2014) 1891–1908.

[4] Y. Sato, A method of self-recovering equalization for multilevel amplitude-modulation systems, IEEE Trans. Commun. 23 (6) (1975) 679–682.

[5] D.N. Godard, Self-recovering equalization and carrier tracking in two-dimensional data communication systems, IEEE Trans. Commun. 28 (11) (1980) 1867–1875.

[6] J. Treichler, B. Agee, A new approach to multipath correction of constant modulus signals, IEEE Trans. Acoust. Speech Signal Process. 31 (2) (1983) 459–472.

[7] R. Johnson, Jr., P. Schniter, T. Endres, J. Behm, D. Brown, R. Casas, Blind equalization using the constant modulus criterion: a review, Proc. IEEE 86 (10) (1998) 1927–1950.

[8] J. Yang, J.-J. Werner, Dumont, G.A. The multimodulus blind equalization and its generalized algorithms, IEEE Trans. Sel. Areas Commun. 20 (5) (2002) 997–1015.

[9] K. Wesolowski, Analysis and properties of the modified constant modulus algorithm for blind equalization, Eur. Trans. Telecommun. 3 (1992) 225–230.

[10] K.N. Oh, Y.O. Chin, Modified constant modulus algorithm: blind equalization and carrier phase recovery algorithm, in: ICC'95, vol. 1, Seattle, WA, 1995, pp. 498–502.

[11] S. Abrar, A.K. Nandi, Blind equalization of square-QAM signals: a multi-modulus approach, IEEE Trans. Commun. 58 (6) (2010) 1674–1685.

[12] J. Mendes Filho, M.D. Miranda, M.T.M. Silva, A regional multimodulus algorithm for blind equalization of QAM signals: introduction and steady-state analysis, Signal Process. 92 (11) (2012) 2643–2656.

[13] S. Abrar, A.K. Nandi, Adaptive solution for blind equalization and carrier-phase recovery of square-QAM, IEEE Signal Process. Lett. 17 (9) (2010) 791–794.

[14] A.W. Azim, S. Abrar, A. Zerguine, A.K. Nandi, Steady-state performance of multimodulus blind equalizers, Signal Process. 108 (2015) (2015) 509–520.

[15] T.C. Hewavithana, D.M. Brookes, Blind adaptive channel equalization for OFDM using the cyclic prefix data, in: GLOBECOM'04, vol. 4, 2004, pp. 2376–2380.

[16] M. de Courville, P. Duhamel, P. Madec, J. Palicot, Blind equalization of OFDM systems based on the minimization of a quadratic criterion, in: ICC'96, vol. 3, Dallas, TX, 1996, pp. 1318–1322.

[17] H. Zamiri-Jafarian, H. Khoshbin, S. Pasupathy, Time-domain equalizer for OFDM systems based on SINR maximization, IEEE Trans. Commun. 53 (6) (2005) 924–929.

[18] M. Luise, R. Reggiannini, G. Vitetta, Blind equalization/detection for OFDM signals over frequency-selective channels, IEEE Trans. Sel. Areas Commun. 16 (8) (1998) 1568–1578.

[19] T. Al-Naffouri, A. Dahman, M. Sohail, W. Xu, B. Hassibi, Low-complexity blind equalization for OFDM systems with general constellations, IEEE Trans. Signal Process. 60 (12) (2012) 6395–6407.

[20] K. Van Acker, G. Leus, M. Moonen, O. Van de Viel, T. Pollet, Per tone equalization for DMT-based systems, IEEE Trans. Commun. 49 (1) (2001) 109–119.

[21] R.K. Martin, Blind, adaptive equalization for multicarrier receivers (Ph.D. thesis), Cornell University, Ithaca, NY, 2004.

[22] B.H.B. Naeeni, H. Amindavar, H. Bakhshi, Blind per tone equalization of multilevel signals using support vector machines for OFDM in wireless communication, Int. J. Electron. Commun. 64 (2) (2010) 186–190.

[23] A. Goupil, J. Palicot, Constant norm algorithms class, in: Proceedings of EUSIPCO'02, Toulouse, France, 2002.

[24] A. Goupil, J. Palicot, New algorithms for blind equalization: the constant norm algorithm family, IEEE Trans. Signal Process. 55 (4) (2007) 1436–1444.

[25] T. Thaiupathump, New algorithms for blind equalization and blind source separation/phase recovery (Ph.D. thesis), University of Pennsylvania, Philadelphia, PA, January 2002.

[26] T. Thaiupathump, L. He, S.A. Kassam, Square contour algorithm for blind equalization of QAM signals, Signal Process. 86 (11) (2006) 3357–3370.

[27] N. Benvenuto, G. Cherubini, Algorithms for Communications Systems and their Applications, Wiley, Chichester, England, 2002.

[28] V. Savaux, Contribution to multipath channel estimation in OFDM context (Ph. D. thesis), Supélec, Rennes, France, November 2013.

[29] G. Picchi, G. Prati, blind equalization and carrier recovery using a "stop-and-go" decision-directed algorithm, IEEE Trans. Commun. 35 (9) (1987) 877–887.

[30] A. Belouchrani, W. Ren, Blind carrier phase tracking with guaranteed global convergence, IEEE Trans. Signal Process. 45 (7) (1997) 1889–1894.

[31] Y. Ha, W. Chung, Non-data-aided phase noise suppression scheme for CO-OFDM systems, IEEE Photon. Technol. Lett. 25 (17) (2013) 1703–1706.

[32] J.G. Proakis, Communication through band-limited channels, in: Digital Communications, Mc Graw-Hill, New York, 1995, pp. 583–635 (Chapter 10).

CMA-Based Blind Equalization and Phase Recovery in OFDM/OQAM Systems

*Vincent Savaux, **Faouzi Bader, and **Jacques Palicot
**SCEE/IETR - CentraleSupélec, Rennes.
Avenue de la Boulaie, 35576 Cesson - Sévigné Cedex, France.
Emails: faouzi.bader@supelec.fr, and jacques.palicot@centralesupelec.fr

***Abstract*—This paper deals with a constant modulus algorithm-(CMA) based blind equalization method for orthogonal frequency division multiplexing/offset quadrature amplitude modulation (OFDM/OQAM) scheme. The authors propose to combine the CMA with a *low-pass* filter in order to increase the convergence speed of the equalizer, and to avoid the detection of the received symbols with phase mismatch. Simulations results show that the convergence speed is largely increased, and the proposed method achieves bit error rate (BER) performance very close to that of the perfect channel estimation and equalization.**

***Index Terms*—Blind equalization, OFDM/OQAM, CMA, Impulse Noise Cancellation.**

I. Introduction

The blind equalization is an interesting solution for the channel inversion (or deconvolution) since it guarantees the signal a maximum spectral efficiency. Indeed, these techniques do not use pilots, the blind equalizer only takes advantage of a few signal features to perform the channel inversion. In [1], B. Farhang-Boroujeny has adapted the blind equalization using the constant modulus algorithm (CMA) proposed by D. N. Godard in [2] to the cosine modulated filter bank (CMFB) modulation. In [3] the authors proposed to use the second order moment of the received signal, while the CMA is used in [1].

In filter bank multicarrier (FBMC), and in particular in orthgonal frequency division multiplexing/offset quadrature amplitude modulation (OFDM/OQAM), only few papers deals with blind equalization. Due the convergence delay of the blind methods and the uncertainty on the phase of the recovered symbols, the blind channel equalization remains a pending challenge not much studied by the scientific community, in particular in FBMC.

In this paper we propose a constant modulus algorithm-based (CMA) blind equalizer for OFDM/OQAM systems. As in [1], we consider a one-tap per carrier equalization, since it is particularly adapted to the multicarrier systems. As mentioned in [4], this type of technique may lead to local solutions and implies that the symbols are detected with a phase shift of 0 or π. The proposed method consists of filtering the equalizer response in order to smooth the channel frequency response. The principle of the proposed technique is simple, since it is similar to a low-pass filter as used in channel estimation [5]. The addition of a differential phase coding allows to suppress any uncertainty on the phase of the recovered symbols. Furthermore, the proposed techniques largely increases the convergence speed of the CMA. The idea behind CMA applied in OFDM/OQAM is to iteratively update the algorithm by comparing the real part of the output of the equalizer with a given real constant that depends on the constellation size. However, it is worth noting that CMA is equivalent to Sato's algorithm [6], and the constant norm algorithm (CNA) [7], due to the use of real transmitted OQAM symbols. Therefore, this limits the choice of the cost function to those that are adapted to real constellation, whereas numerous cost functions adapted to different complex constellations have been proposed in the scientific literature [7]–[9].

The rest of the paper is organized as follows: Section II presents the system model and the CMA, and we propose our equalizer with IN cancellation in Section III. Simulations shows the performance of the method in terms of mean square error (MSE) and BER in Section IV, and we draw conclusions in Section V.

II. System Model

We consider the transmission of OFDM/OQAM symbols over a frequency selective channel, with perfect time and frequency synchronization. At the frequency-time position (m,n), the output of the analysis filter bank (AFB) is written as

$$y_{m,n} = H_{m,n}x_{m,n} + \underbrace{j\sum_{(p,q)\in\Omega} H_{p,q}x_{p,q} < g >_{p,q}^{m,n}}_{I_{m,n}} + w_{m,n}, \tag{1}$$

where $x_{m,n}$ is the real symbol transmitted at frequency-time position (m,n), $H_{m,n}$ is the complex channel frequency response (CFR). A detailed description of the synthesis filter bank (SFB) and the AFB is available in [10]. $w_{m,n}$ and $I_{m,n}$ are the complex additive white Gaussian noise (AWGN) and the interference terms whose variances are σ^2 and σ_I^2 respectively. The term $j < g >_{p,q}^{m,n}$ is called the intrinsic

*CentraleSupélec is the former institution of Vincent Savaux, actually with b<>com research institute. E-mail: vincent.savaux@b-com.com. This work is supported by the project PROFIL (Evolution of the wideband PROfessional Mobile Radio based on the FILter Bank MultiCarrier modulation) funded by the French national research agency (ANR) with grant agreement code: ANR-13-INFR-0007-03.

978-1-5090-1990-8/16/$31.00 ©2016 IEEE

interference due to the prototype filter $g_{m,n}(t)$ that is given by

$$g_{m,n}[i] = g(i - n\frac{M}{2}) e^{\frac{2j\pi m}{M}(i - \frac{L_f - 1}{2})} e^{j\phi_{m,n}}, \quad (2)$$

where the phase term is $\phi_{m,n} = (\pi/2)(m+n) + mn\pi$ as defined in [10]. It should be noted that the real symbols $x_{m,n}$ are transmitted with a period $\frac{M}{2}$ twice shorter than that of OFDM signal where symbols are complex. The used filter has a length $L_f = KM$, where K is the overlapping factor and M is the total number of carriers. Thus, even in absence of the multipath channel, there will be some intercarrier and intersymbol purely imaginary interferences. In fact, $g_{m,n}$ is orthogonal in the real field, which allows to perfectly recover the real OQAM symbols. However, it can be seen in (1) that the CFR $H_{p,q}$ induces some distortions from the time-frequency positions (p,q) that belongs to the set Ω[1] and have to be estimated and corrected.

In this paper, the signal is blindly equalized, by using the simple one-tap per-carrier CMA equalizer. To summarize, the aim of the CMA is to tends toward the optimal equalizer coefficient $F_{m,n}^{opt}$ thanks to the update algorithm, which can be written as

$$F_{m,n+1} = F_{m,n} - \mu y_{m,n}^* sign(a_{m,n})(|a_{m,n}| - \gamma). \quad (3)$$

where $F_{m,n}$ is the equalizer coefficient, and $a_{m,n} = \Re\mathrm{e}(F_{m,n} y_{m,n})$, μ is the step-size parameter, and γ is a real-valued constant which is defined as $\gamma = \frac{E\{|x|^4\}}{E\{|x|^2\}}$ (see [2] for more details). The CMA has a low complexity, but it suffers from two drawbacks: i) it requires a long convergence time, and ii) it is phase blind, i.e. the real equalized symbols $a_{m,n}$ can be detected with a phase equal to 0 or π. In the following, we propose a simple method that reduces the delay of convergence of CMA, and avoids the phase incertainty.

III. CMA Blind Equalization with Impulse Noise Cancellation

It has been shown in [1], [4] that the CMA applied to the real OQAM symbols converges toward the optimal coefficient value $|F_{m,n}^{opt}|$ with a phase shift equal to 0 or π. The solution that consists of using a differential phase coding as in [1] do not ensure a low bit error rate (BER) value when a large number of received symbols are detected with an opposite phase. In this section, we propose to consider the issue of convergence toward $F_{m,n}^{opt}$ or $-F_{m,n}^{opt}$ from an original point of view, which is described just below.

A. Equalization with Impulsive Noise Cancellation

Fig. 1 shows the real part of a frequency response of the invert of the equalizer coefficients $1/F_{m,n}^{opt}$ (using CMA) compared with the exact channel frequency response $H_{m,n}$, knowing that $|F_{m,n}^{opt} H_{m,n}| = 1$. It can be seen that the frequency positions m=11, 29, and 92 correspond to the opposite minima $-F_{m,n}^{opt}$.

[1] Ω is the set of positions p,q that surround the position m,n

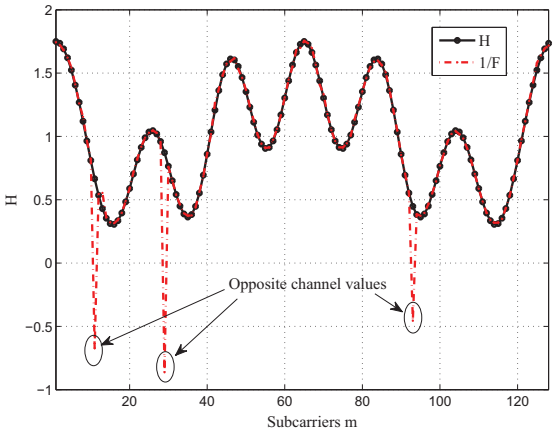

Fig. 1: Real part of H and $1/F$ showing opposite equalizer coefficient values.

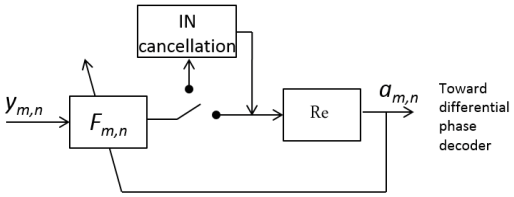

Fig. 2: Proposed equalizer structure with impulse noise cancellation.

The optimal solutions with opposite phase depicted in Fig. 1 can be seen as an impulsive noise (IN) in the channel frequency response, which can be filtered in a simple way as described in [11]. The IN cancellation can be seen as a low-pass filtering, but performed in the time domain. This technique is also usually used in channel estimation techniques in order to filter the noise or to perform an interpolation [5]. In the considered blind equalization context, the IN cancellation should be seen as a smoothing stage applied to the equalizer coefficients $F_{m,n}$, and allows full blind equalization as it does not require any pilot for the phase estimation. The proposed equalizer regularly switch to the IN cancellation block as depicted in Fig. 2.

The steps into the "IN cancellation" block in Fig. 2 are described as follows:

1) $\forall m \in 0, M-1$, the channel frequency response (CFR) samples are obtained by $\hat{H}_{m,n} = 1/F_{m,n}$, and stored in the vector $\hat{\mathbf{H}}_n$ of size $M \times 1$.
2) The estimated channel impulse response (CIR) is achieved by applying an IFFT: $\hat{\mathbf{h}}_n = IFFT(\hat{\mathbf{H}}_n)$.
3) The CIR is multiplied by a rectangular window Π defined by

$$\Pi_m = \begin{cases} 1, & \text{if } m \leq L_\Pi \\ 0, & \text{else} \end{cases}, \quad (4)$$

such as $\bar{\mathbf{h}}_n = \hat{\mathbf{h}}_n \Pi$, where the length of Π denoted by L_Π must be at least equal to channel length L.

4) The filtered CFR is obtained by the FFT as $\bar{\mathbf{H}}_n = FFT(\bar{\mathbf{h}}_n)$ and then the equalizer coefficients by $F_{m,n} = 1/\bar{H}_{m,n}$.

Note that in practice, the L value is unknown, so L_Π is chosen in order to overestimate the length of the channel. The advantages of the IN cancellation process are multiple: in addition to suppress the opposite solutions that are seen as an impulsive noise, it also avoids the possible convergence of the coefficients toward local minima[2]. Therefore, it offers the possibility of initialization strategies different from the one proposed in [1]. Moreover, as observed in [5] for the channel estimation, the IN cancellation mitigates the noise and the interferences level. In an OFDM/OQAM context in which the interference term may be not negligible, this smoothing stage may appear to be very convenient.

Also, it is worth highlighting that the proposed IN cancellation process using scheme in Fig. 2 may lead to two solutions: i) all the M coefficients $F_{m,n}$ converge toward their optimal solutions without phase shift $F^{opt}_{m,n}$, ii) all the coefficients $F_{m,n}$ are equal to the opposite expected solutions $-F^{opt}_{m,n}$.

That is the main difference with the CMA in (3) where each coefficient $F_{m,n}$ may converge to the optimal value or its opposite. In our solution, if all the coefficients $F_{m,n}$ converge to their opposite optimal solution, the differential phase decoding stage leads to a single error[3] which could be easily suppressed by means of a channel code. If no IN cancellation is performed as in [1], a large number of phases may be erroneous because they are detected with a difference equal to π. In the latter case, the differential phase encoding becomes inefficient and therefore the channel coding as well. In the hereafter section, we will focus on the way of applying the proposed IN cancellation stage in Fig. 2.

B. How to apply the IN Cancellation?

There are three possible ways to perform the IN cancellation stage, which are hereafter explained:

- The IN cancellation is used only one time during the convergence process. It could be a convenient solution if only few $F_{m,n}$ coefficients are detected with an opposite phase (see the example in Fig. 1). However, if a large number of phases are detected with a shift equal to π, a single IN cancellation stage is not sufficient to suppress the appearance of the impulse noise and this solution is similar to the CMA approach. Furthermore, this option raises the issue of the choice of the appropriate starting point to proceed the smoothing stage.
- The IN cancellation is employed at each iteration. Here, the update algorithm (3) does not have any sense since it is fed by a coefficient $F_{m,n}$ that is not the one obtained at the previous iteration. In other words, this solution is not anymore a blind equalization, and should lead to unsuitable coefficients $F_{m,n}$.
- The operation is performed with a reasonable regularity regarding to the convergence speed of the update algorithm (3). Thus, the process either performs the IN cancellation as long as optimal solutions with opposite phases remain, or performs a noise cancellation due to the nature of the filter. This solution seems to be the way to carry out the proposed CMA with IN cancellation in Fig. 2.

In order to formalize these three solutions, we define N_i the time delay between two consecutive smoothing operations. Thus, the first solution corresponds to $N_i = +\infty$, the second one to $N_i = 1$ and the third one to a value of N_i conveniently chosen. It is worth noticing that simulations revealed that the first two solutions lead to unsatisfactory results. As a consequence, we only focus on the third solution in the next section.

IV. Simulations Results

In this section, we present simulations results which show the performance of the proposed blind equalizer. Since we are comparing obtained results with the CMA in (3), we will use the same parameters as described in [1] where the CMA is used in FBMC. We consider a constant multipath channel whose CIR is $\mathbf{h} = [1, -0.2, 0.3, 0.2, 0.1, 0.2, 0.35, -0.2]$. The real part of the corresponding CFR is displayed in Fig. 1. The results are presented for a 4-QAM constellation, i.e. for binary OQAM symbols. As a consequence, note that $\gamma = 1$. Each OFDM/OQAM symbol is composed of $M = 128$ carriers. Two initialisation values are tested: a constant initialization $F_{m,0} = 0.01$ for any $m = 0, 1, .., M-1$ such as proposed in [1], and the sub-optimal initialization strategy $F^{s-opt}_{m,0} = \sqrt{\frac{E\{x_{m,0}\}^2}{|y_{m,0}|^2}}$ such as proposed in [12]. In both cases, the step-size parameters is set at $\mu = 0.015$. In the following, the performance of the data-aided interference approximation method (IAM) is also plotted for reference. A detailed description of the IAM is provided in [10]. The performance of the different blind equalizers is assessed by using the mean square error MSE defined as

$$\text{MSE} = E\{(|a_{m,n}| - |x_{m,n}|)^2\}. \quad (5)$$

In Fig. 3, the CMA is compared with the proposed CMA using IN cancellation (denoted by INC in the figures) for $N_i = 1$ and $N_i = +\infty$, where it is performed at the 200th and at the 2000th iterations. The results are obtained for SNR=30 dB, and $F_{m,0} = 0.01$. Moreover, achieved MSE values with IAM pilot aided pattern is plotted as a reference.

It can be observed that CMA achieves better performance than CMA with IN cancellation when it is performed with $N_i = 1$ and has a similar MSE than CMA using IN cancellation where $N_i = +\infty$. Having $N_i = 1$, the MSE has a "chaotic" behavior, but has a lower bound around -14 dB, whereas the CMA achieves a MSE lower than -17 dB. These observations

[2] In fact, local minima can also be seen as peaks in the estimated CFR

[3] If all the phases are detected with an error equal to π, the difference of phase between to consecutive symbols is the same as if the phase error is 0, excepted for the first symbol.

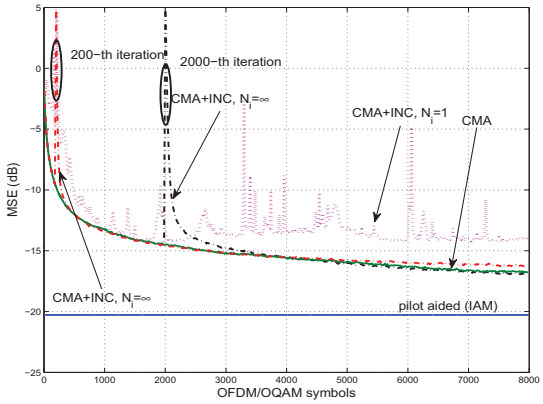

Fig. 3: MSE of CMA and CMA with impulse noise cancellation (INC) versus OFDM/OQAM symbols for $N_i = 1$ and $N_i = +\infty$, SNR=30 dB.

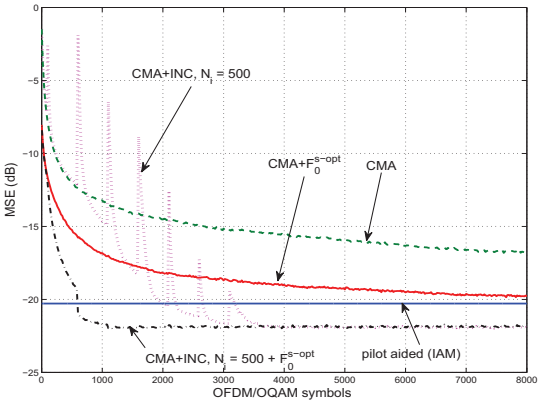

Fig. 4: MSE of the CMA using IN cancellation versus iterations compared with CMA, $N_i = 500$, SNR=30 dB.

confirm that the gradient update in (3) does not make sense in the case $N_i = 1$. For $N_i = +\infty$, one can observe that once the smoothing stage has been performed (at the 200th or 2000th iteration), the trajectories of CMA using IN cancellation are the same as those with CMA. The peaks that appear at iterations 200 and 2000 can be interpreted as a reset of the equalizer coefficient due to the IN cancellation stage, and this indicates that the option $N_i = 1$ is not suitable when too much coefficients $F_{m,n}$ converge to their opposite solutions. More generally, results presented in Fig. 3 show that the IN cancellation with $N_i = 1$ and $N_i = +\infty$ does not improve CMA as proposed in [1]. These results are consistent with the a priori remarks we made in Section III-B. Note that none of the presented methods is able to reach the performance of the pilot-aided estimation using IAM. This is mainly due to the facts that: i) IAM is an accurate channel estimation method, and ii) CMA is known to be a simple method, but achieves weak performance. In Fig. 4 we compare the MSE performance of the proposed CMA in Fig. 2 for a regular IN mitigation stage performed every $N_i = 500$ iterations. Furthermore, the initialization $F_{m,0}^{s-opt}$ is compared with the constant $F_{m,0} = 0.01$ value.

It can be observed that CMA with sub-optimal initialization achieves a gain of 2000 iteration at MSE=-15 dB compared with the "classical" CMA such as proposed in [1]. Fig. 4 also highlights that the CMA using IN cancellation with $N_i = 500$ reaches its lower bound equal to MSE=-22 dB at the 3500-th iteration, and when $F_{m,n}^{s-opt}$ is used, this MSE floor is reached at the 1000-th iteration. These results show the capability of the proposed CMA-based equalizer with convenient N_i value to have a high convergence speed compared with CMA. Furthermore, it must be noticed that this advantage is accompanied with a good performance, as a MSE gain of 6 dB is achieved by the proposed method compared to the CMA at the 4000-th iteration. Also, it can be seen that CMA with IN cancellation achieves a gain of 2 dB of MSE compared with the pilot-aided method.

For proposed CMA approach with IN cancellation, one can notice that peaks appear at the iterations corresponding to the application of IN cancellation stages. This is due to the fact that the IN cancellations gradually suppress the peaks in the equalizer coefficients. Although the proposed equalizer in Fig. 2 with the initialization in $F_{m,0}^{s-opt}$ has a remarkable convergence speed, it can be observed that the initialization $F_{m,0}^{s-opt}$ alone with the CMA allows to get a satisfactory fast convergence as well, such as shown in [12]. However, the MSE defined in (5) does not take into account the phase shift of 0 or π. In fact it does not affect the absolute values of the expected equalizer coefficients $|F_{m,opt}|$ but plays a key role in the BER performance, as it is shown afterward. Fig. 5 depicts the MSE-floor values of CMA, and CMA using IN cancellation with sub-optimal initialization value, and IAM, when the steady-state is reached, versus SNRs. Once again, it can be concluded from Fig. 5 that the blind equalizers achieve better performance than the data aided method (at least for the same channel as in [1]) for SNR values $<$24 dB using CMA and $<$40 dB using CMA with IN cancellation ($N_i = 500$). Furthermore, the latter has lower MSE values than the "usual" CMA for SNR$>$10 dB. This result reflects the fact that the IN cancellation stage is also able to smooth the noise of the channel frequency response (step 3) in the algorithm presented in Section III.

Fig. 6 shows the BER performance of the proposed blind equalizer versus the SNR, and also that of CMA approach using both the constant initialization and $F_{m,0}^{s-opt}$. The BER is obtained by using a differential phase coding and a convolutional coding with code rate 1/2 and a Viterbi decoder. The BER is calculated at the 4000th iteration, by averaging the results on 10^7 random transmitted bits. The data aided estimation and equalization using IAM is also depicted, and the equalizer using perfect CSI is plotted as a reference.

It can be clearly observed that the proposed technique

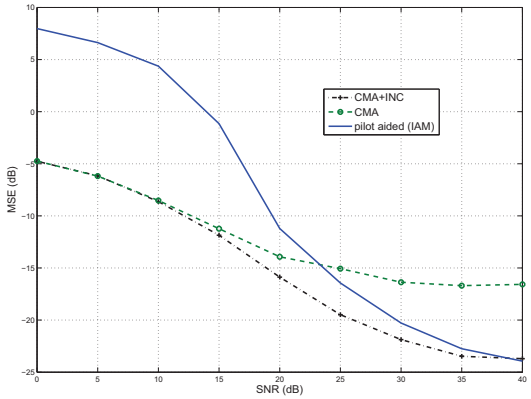

Fig. 5: MSE performance versus SNR. Comparison between CMA, CMA using IN cancellation (ICN) with sub-optimal initialization value, and pilot-aided method (IAM).

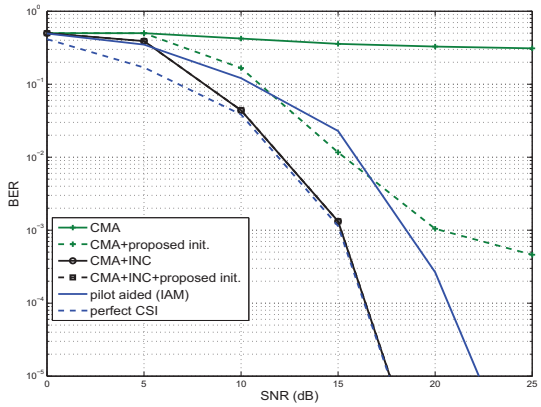

Fig. 6: BER versus SNR of the proposed equalizer compared to [1].

outperforms the blind equalizer using CMA proposed in [1]. This reflects the fact that a large number of coefficients $F_{m,n}$ converge toward their opposite optimal values. Consequently, when CMA is used alone, a large number of symbols are detected with a phase shift equal to π. In that case, the differential phase decoder and the Viterbi decoder are unable to recover the expected correct binary symbols. With the proposed blind equalizer, this problem is solved since all the symbols are detected with the correct phase thanks to both the differential and Viterbi decoders. Moreover, it should be noticed that a SNR gain of 3 dB is achieved by the CMA with IN cancellation compared with the pilot aided estimation and equalization, which is consistent with the MSE result. Furthermore, the CMA with IN cancellation losses less than 0.2 dB compared with the equalizer with perfect CSI. This is an important result since it shows that blind equalization (once the steady-state is reached) is able in our context to outperform data-aided techniques, in terms of both BER performance and spectral efficiency. Fig. 6 also reveals that the use of the sub-optimal initialization has almost no influence on the BER performance. However, it has been shown that largely improves the convergence speed of the equalizer. From the performance analyzed in both Figs. 4 and 6, we conclude that the combination of the proposed method with the initialization $F_{m,0}^{s-opt}$ leads to i) a fast equalizer, ii) a low MSE floor value, and iii) a high BER performance, compared with CMA alone, and with IAM. Furthermore, the proposed with IN cancellation allows to achieve a full blind equalizer and phase recovery, since no pilot is used.

V. Conclusion

In this paper, we presented a simple blind equalization technique for OFDM/OQAM systems. The principle is to combine the CMA and a low-pass filtering in order to increase the convergence speed of the blind equalizer, and to avoid the convergence of the coefficients toward wrong phase values. Simulations revealed that the proposed method achieves performance close to the perfect channel estimation and equalization. Further work will deal with the extension of proposed method to larger constellation sizes.

References

[1] B. Farhang-Boroujeny, "Multicarrier Modulation With Blind Detection Capability Using Cosine Modulated Filter Banks," *IEEE Transactions on Communications*, vol. 51, no. 12, pp. 2057 – 2070, December 2003.

[2] D. N. Godard, "Self-Recovering Equalization and Carrier Tracking in Two-Dimensional Data Communication Systems," *IEEE Transactions on Communications*, vol. com-28, no. 11, pp. 1867 – 1875, November 1980.

[3] H. Bölcskei, P. Duhamel, and R. Hleiss, "A Subspace-Based Approach to Blind Channel Identification in Pulse Shaping OFDM/OQAM Systems," *IEEE Transactions on Signal Processing*, vol. 49, no. 7, pp. 1594 – 1598, July 2001.

[4] L. Lin and B. Farhang-Boroujeny, "Convergence analysis of blind equalizer in a cosine modulated filter bank-based multicarrier communication system," in *proc. of SPAWC'03*, Roma, Italy, June 2003, pp. 368 – 372.

[5] J. Schoukens, R. Pintelon, and H. V. Hamme, "The Interpolated Fast Fourier Transform: A Comparative Study," *IEEE Transactions on Instrumentation and Measurement*, vol. 41, no. 2, pp. 226 – 232, April 1992.

[6] Y. Sato, "A Method of Self-Recovering Equalization for Multilevel Amplitude-Modulation Systems," *IEEE Transactions on Communications*, vol. 23, no. 6, pp. 679 – 682, June 1975.

[7] A. Goupil and J. Palicot, "New Algorithms for Blind Equalization: The Constant Norm Algorithm Family," *IEEE Transactions on Signal Processing*, vol. 55, no. 4, pp. 1436 – 1444, April 2007.

[8] K. N. Oh and Y. O. Chin, "Modified constant modulus algorithm: blind equalization and carrier phase recovery algorithm," in *proc. of ICC'95*, vol. 1, Seattle, WA, June 1995, pp. 498 – 502.

[9] S. Barbarossa, "Blind Equalization Using Cost Function Matched to the Signal Constellation," in *proc. of ACSSC'97*, vol. 1, Pacific Grove, CA, USA, November 1997, pp. 550 – 554.

[10] E. Kofidis, D. Katselis, A.Rontogiannis, and S. Theodoridis, "Preamble-based channel estimation in OFDM/OQAM systems: A review," *Signal Processing, Elsevier*, vol. 93, pp. 2038 – 2054, January 2013.

[11] S. V. Vaseghi, *Advanced Digital Signal Processing and Noise Reduction*. John Wiley & Sons, 2000, ch. 12, pp. 355 – 377.

[12] V. Savaux and F. Bader, "Sub-Optimal Initialization for Blind Equalization with Fast Convergence in OFDM/OQAM Modulation," in *proc. of EuCNC'15*, Paris, France, June - July 2015.

OFDM/OQAM Blind Equalization Using CNA Approach

Vincent Savaux, *Associate Member, IEEE*, Faouzi Bader, *Senior Member, IEEE*, and Jacques Palicot

***Abstract*—This paper deals with blind equalization based on the constant norm algorithm (CNA) in orthogonal frequency division multiplexing/offset quadrature amplitude modulation (OFDM/OQAM). The CNA is designed to fit the complex square constellations with high order. As a consequence, the received signal is reshaped in order to change the real OQAM symbols into complex ones. Although it increases the intrinsic interferences of the OFDM/OQAM signal, it is proved by analysis and through simulations that the CNA with proposed reshaped signal achieves better mean square error (MSE) performance than CMA applied to the received OFDM/OQAM signal. Furthermore, a suboptimal initialization strategy is proposed, which ensures a high convergence speed. The behavior of the proposed blind equalization method is analyzed under synchronization mismatch as well as in time-varying propagation environment.**

***Index Terms*—Blind equalization, OFDM/OQAM, iterative methods, CMA, CNA, impulse noise cancellation.**

I. Introduction

FILTER BANK MULTICARRIER (FBMC), and in particular the orthogonal frequency division multiplexing/Offset quadrature amplitude modulation (OFDM/OQAM) is a good alternative to the OFDM for systems coexistence and spectrum sharing as it achieves better spectral containment [1], [2]. Furthermore, it provides higher useful bit rate as it does not require any cyclic prefix addition. However, the good properties of OFDM/OQAM are due to subcarrier functions that are only orthogonal in the real field. As a consequence, the presence of imaginary intrinsic interference and the complex channel frequency response lead to develop some equalization methods specific to OFDM/OQAM.

As in any modulation scheme, the channel estimation and equalization techniques in OFDM/OQAM can be classified into two main categories:

i) the data-aided methods, in which pilots are multiplexed in the data stream and the signal is equalized using the estimated channel (see [3]–[6] for data aided estimation methods). The usual zero forcing (ZF) and minimum mean square error (MMSE) equalizer are presented in a FBMC context in [7], and the authors of [8] propose to split the phase and the modulus equalization. In [9], the topic of channel equalization has been extended to FBMC modulation scheme in multiple antennas systems.
ii) the blind techniques, which use only few features of the signal to invert the channel (see [10]–[12]).

Although data-aided methods are simple to implement and widely employed, they may reduce the spectral efficiency of the transmitted signal. On the other hand, blind techniques have not been so deeply studied in OFDM/OQAM context, and the topic remains a pending challenge.

In [10], the cyclostationarity induced by the use of the OFDM/OQAM pulse shape is exploited in order to perform a second order blind equalization. However, this technique has a high complexity, and very long data records have to be stored to obtain good estimates of the second-order statistics of the signal. The more "classical" constant modulus algorithm (CMA) has been adapted to FBMC (cosine modulated filter bank) in [11], and its convergence behavior has been analyzed in [12]. The idea behind CMA applied in OFDM/OQAM is to iteratively update the algorithm by comparing the real part of the output of the equalizer with a given real constant that depends on the constellation size. However, it is worth noting that CMA is equivalent to Sato's algorithm [13], the multimodulus algorithm (MMA) [14], and the constant norm algorithm (CNA) [15], due to the use of real transmitted OQAM symbols. Therefore, this limits the choice of the cost function to those that are adapted to real constellation, whereas numerous cost functions adapted to different complex constellations have been proposed in the scientific literature [15]–[17].

In this paper, it is proposed to reshape the received signal by summing two consecutive symbols such that, from the equalizer point of view, the received symbols are complex. This provides an additional degree of freedom regarding the choice of the cost function of the update algorithm. As a consequence, we take advantage of these reshaped complex symbols to carry out a blind equalization using the CNA proposed in [15], which has proven to be particularly adapted to square constellations. This algorithm can be seen as a generalization of the CMA, where the modulus is substituted by a norm which is determined as a function of the considered constellation. The performance of the proposed CNA adapted to OFDM/OQAM is analyzed, and

Manuscript received June 24, 2015; revised November 18, 2015 and January 06, 2016; accepted January 06, 2016. Date of publication January 18, 2016; date of current version March 30, 2016. The associate editor coordinating the review of this manuscript and approving it for publication was Dr. Yue Rong. This work is supported by the project PROFIL (Evolution of the Wideband Professional Mobile Radio Based on the Filter Bank MultiCarrier Modulation) funded by the French national research agency with grant agreement code: ANR-13-INFR-0007-03, and ICT EC-funded project Newcom# with code: FP7-IC-318306.

The authors are with the Signal, Communication & Embedded Electronics (SCEE) team/IETR, CentraleSupélec, Rennes, France (e-mail: vincent.savaux@b-com.com; jacques.palicot@centralesupelec.fr; faouzi.bader@supelec.fr).

Color versions of one or more of the figures in this paper are available online at http://ieeexplore.ieee.org.

Digital Object Identifier 10.1109/TSP.2016.2519000

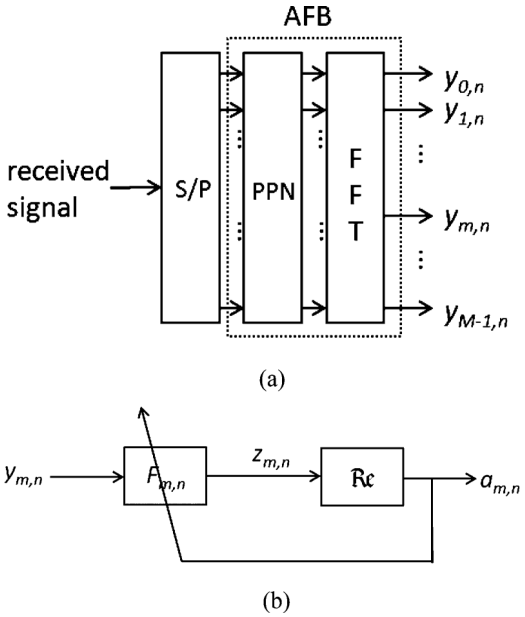

Fig. 1. Blind OFDM/OQAM receiver structure with (a) AFB, and (b) blind equalizer.

it is proved that the CNA achieves better performance than the CMA.

The rest of the paper is organized as follows: the blind OFDM/OQAM receiver structure is presented in Section II. The proposed CNA using a reshaped received signal is developed in Section III. Section IV provides simulations results that show the performance of the proposed blind equalization techniques. Finally, we draw our conclusions in Section V.

II. Blind OFDM/OQAM Receiver

The blind OFDM/OQAM receiver is presented in Fig. 1. The demodulator consists of a serial to parallel converter (denoted by S/P), and an analysis filter bank (AFB). The latter is composed of i) the polyphase network (PPN) that contains a set of digital filters, and ii) the fast Fourier transform (FFT) of size M (M is also the number of subcarriers).

In the following expression, the receiver is considered to be perfectly synchronized with the transmitter in both time and frequency domains, and the channel delay is assumed to be short compared to the length of the used prototype filter, in such a way that the output of the AFB described in Fig. 1-(a) can be written as

$$y_{m,n} = H_{m,n}x_{m,n} + \underbrace{j\sum_{(p,q)\in\Omega} H_{p,q}x_{p,q}\langle g\rangle_{m,n}^{p,q}}_{I_{m,n}} + w_{m,n}, \quad (1)$$

where the subscripts "m,n" denote the frequency-time position. $H_{m,n}$ is the channel frequency response (CFR), $w_{m,n}$ is the complex Gaussian noise sample with circular covariance matrix $\mathbf{R}_w$. Note that for convenience, this matrix is commonly approximated by $\sigma^2\mathbf{I}$, where σ^2 is the noise level, and $\mathbf{I}$ is the identity matrix. $x_{m,n}$ is the real OQAM symbol that is carried by the prototype filter g which is given by

$$g_{m,n}[i] = g\Big(i - n\frac{M}{2}\Big)e^{\frac{2j\pi m}{M}(i-\frac{L_f-1}{2})}e^{j\phi_{m,n}}, \quad (2)$$

where the phase term is $\phi_{m,n} = (\pi/2)(m+n) + mn\pi$ as defined in [18]. It should be noted that the real symbols $x_{m,n}$ are transmitted with a period $\frac{M}{2}$ twice shorter than that of OFDM signal where symbols are complex. Therefore, the data rate in OFDM/OQAM is the same as in OFDM. The specificity of the OFDM/OQAM modulation scheme lies in the presence of interferences denoted by $I_{m,n}$ in (1), which is due to the used prototype filter g. The term $j\langle g\rangle_{m,n}^{p,q}$ in (1) is called "intrinsic interference" (according to the definition in [6]), and is defined as the scalar product

$$\sum_i g_{m,n}[i]g^*_{p,q}[i]dt = \begin{cases} 1, & \text{if } (p,q)=(m,n) \\ j\langle g\rangle_{p,q}^{m,n}, & \text{else} \end{cases}. \quad (3)$$

In this paper, the Bellanger's filter is employed, but other filters with self interference effect could be used. This filter is also known as "PHYDYAS filter", and its frequency response can be expressed as (see [19] for details)

$$G[f] = \sum_{k=-(K-1)}^{K-1} G_k \frac{\sin\left(\pi\left(f-\frac{k}{L_f}\right)L_f\right)}{L_f\pi\left(f-\frac{k}{L_f}\right)}, \quad (4)$$

where $G_0 = 1$, $G_1 = 0.971960$, $G_2 = 1/\sqrt{2}$, and $G_3 = 0.235147$ according to [19], and $G_k = G_{-k}$. L_f is the length of the filter defined as $L_f = KM$, where K is called overlapping factor. As mentioned in [6]-(13), the weights $\langle g\rangle_{m,n}^{p,q}$ of any well-chosen prototype filter have a symmetrical property as

$$\begin{matrix} (-1)^p a & -b & (-1)^p a \\ -(-1)^p c & 1 & (-1)^p c \\ (-1)^p a & b & (-1)^p a \end{matrix}, \quad (5)$$

where the weight 1 corresponds to the position (m,n), and where a, b, and c values depend on M and K. Note that, due to (5), the noise component $w_{m,n}$ cannot be white. However, the assumption of "whiteness" of the noise in OFDM/OQAM has proven to be accurate, such as in [20].

The pulse shape g allows the OFDM/OQAM signal to have a good spectral containment, but it is orthogonal only in the real field. Thus, the interference term $I_{m,n}$ is purely imaginary if $H_{m,n} = 1$, and therefore the real OQAM symbols can be recovered by $\hat{x}_{m,n} = \Re\mathfrak{e}\{y_{m,n}\}$. However, the presence of the channel gain $H_{m,n} \in \mathbb{C}$ induces complex interferences from all the symbols at positions $(p,q) \in \Omega$, where Ω is the set of frequency-time positions that surround (m,n). As a consequence, the distortion due to the channel must be canceled in order to recover the real orthogonality between subcarriers and symbols.

It is worth noting that in practice, the received signal $y_{m,n}$ in (1) is also distorted by some residual channel frequency offset (CFO) and time synchronization mismatch [21]–[23]. In this paper, it is assumed that the misalignment between the carrier frequencies generated at the transmitter and the receiver can be neglected in comparison with the subcarrier distance. However, the time synchronization mismatch induces a phase rotation after the demodulation stage, in such a way that the received signal should be rewritten $y_{m,n}e^{-2j\pi\frac{\tau_k m}{M}}$ where τ_k is the time shift.

In this paper, the signal is blindly equalized, which maximize its spectral efficiency since no pilot is used. Some techniques

have been proposed in the literature for both single-carrier as in [16], [24], [25] and [15] and in multicarrier systems as OFDM/OQAM [10]–[12]. The basic idea behind the blind equalization is to iteratively update the equalizer coefficient $F_{m,n}$ by using only few features of the signal. In the OFDM/OQAM modulation scheme, this iterative process is carried out on each subcarrier $m \in [\![0, M-1]\!]$, as described in Fig. 1-(b). The corresponding output of the equalizer can be expressed as

$$a_{m,n} = \mathfrak{Re}(F_{m,n} y_{m,n}). \tag{6}$$

The optimal coefficient $F_{m,n}^{\text{opt}}$ can be obtained on each subcarrier by solving the optimization problem defined as

$$F_{m,n}^{\text{opt}} = \min_{F_{m,n}} J(a_{m,n}), \tag{7}$$

where J is a given cost function that needs to be defined. In the rest of the paper, the minimization step in (7) is achieved by means of the usual stochastic gradient method as in [11], [24] and [15], and which can be expressed as

$$F_{m,n+1} = F_{m,n} - \mu \phi(a_{m,n}), \tag{8}$$

where μ is the step-size parameter of the update algorithm, and

$$\phi(a_{m,n}) = \frac{\partial J(a_{m,n})}{\partial F_{m,n}^*}. \tag{9}$$

It should be noticed that $a_{m,n} = \mathfrak{Re}(F_{m,n} y_{m,n})$ is not an holomorphic function. Therefore, the Wirtinger's derivation [26] is used in (9) instead of the usual complex derivation. It has been demonstrated in [11] that the constant modulus algorithm (CMA) proposed by Godard in [24] is suitable to OFDM/OQAM. Furthermore, note that for the same reason, the modified CMA (MCMA) in [16] (also called multimodulus algorithm (MMA) in [14]) is exactly the same as CMA in the OFDM/OQAM modulation scheme. The cost function of CMA is written as

$$J(a_{m,n}) = E\{(|a_{m,n}|^2 - \gamma)^2\}, \tag{10}$$

where γ is a real-valued constant that is defined hereafter[1]. The update algorithm can be rewritten by substituting (10) into (8) as

$$F_{m,n+1} = F_{m,n} - 2\mu(|a_{m,n}|^2 - \gamma)\frac{\partial |a_{m,n}|^2}{\partial F_{m,n}^*}. \tag{11}$$

The modulus $|a_{m,n}|^2$ can be rewritten as

$$\begin{aligned} |a_{m,n}|^2 &= \frac{1}{4}(F_{m,n} y_{m,n} + (F_{m,n} y_{m,n})^*)^2 \\ &= \frac{1}{4}(F_{m,n} y_{m,n})^2 + \frac{1}{4}((F_{m,n} y_{m,n})^*)^2 \\ &\quad + \frac{1}{2} F_{m,n} y_{m,n} (F_{m,n} y_{m,n})^*. \end{aligned} \tag{12}$$

Furthermore, the Wirtinger's derivative leads to $\frac{\partial z}{\partial z^*} = \frac{\partial z^*}{\partial z} = 0$ for any $z \in \mathbb{C}$ (see Theorem 2.5 in [26]), then the substitution of (12) into (11) yields

$$F_{m,n+1} = F_{m,n} - 2\mu y_{m,n}^* a_{m,n}(|a_{m,n}|^2 - \gamma). \tag{13}$$

[1]Note that the CMA can be written in a normalized manner, by factorizing by γ.

As indicated in [24], the optimal value of the constant γ must be chosen as

$$\gamma = \frac{E\{|x|^4\}}{E\{|x|^2\}}. \tag{14}$$

In the following, we propose two alternatives to CMA for blind equalization in OFDM/OQAM. Based on the results obtained for single-carrier modulation scheme in [15], we adapt the CNA to OFDM/OQAM systems in hereafter Section III.

III. Adapting the CNA in OFDM/OQAM

The basic idea behind the CNA is to use a k-norm, $k > 2$, instead of the modulus in the cost function of the equalizer (10). It has been proved in [15] that CNA achieves better performance than CMA for square constellations as 16-QAM, since CMA is adapted for constant modulus constellations. Furthermore, it has been shown in [15] that for each square constellation corresponds a given k-norm that maximizes the performance of the equalizer. However, the transmitted symbols in (1) are real, therefore the use of CNA in OFDM/OQAM requires some adaptations. Principally, the received signal in (1) must be redesigned and the symbols combined in order to highlight complex transmitted symbols. Since CNA is suitable for high order constellations, we consider throughout this section that the real OQAM symbols $x_{m,n}$ are randomly chosen among the set $\{-3, -1, 1, 3\}$, which corresponds to the real part of 16-QAM. The aims of this section are twofold: i) presenting the reshaping of the input signal $y_{m,n}$ in (1) in order to highlight complex-valued symbols $\tilde{x}_{m,n}$, and ii) proving that carrying out the CNA using the reshaped inputs $\tilde{x}_{m,n}$ lieds to better performance than using CMA with real inputs $x_{m,n}$.

A. Rewriting the Received Signal With Complex Input Symbols

Since the transmitted symbols $x_{m,n}$ are real, the first step before applying the CNA consists of converting the received symbols into complex data. To achieve this, the following procedure is carried out:

1) Build $y_{m,n}^c$ defined as the sum of two consecutive received symbols $y_{m,n}$ and $y_{m,n+1}$ as

$$\begin{aligned} y_{m,n}^c &= j y_{m,n} + y_{m,n+1} \\ &= H_{m,n} j x_{m,n} + H_{m,n+1} x_{m,n+1} \\ &\quad + j I_{m,n} + I_{m,n+1} + j w_{m,n} + w_{m,n+1}. \end{aligned} \tag{15}$$

Note that $H_{m,n} = H_{m,n+1}$ in (15), which leads to further developments.

2) $y_{m,n}^c$ can be rewritten by substituting (1) into (15) as

$$\begin{aligned} y_{m,n}^c = {} & H_{m,n}\left(j x_{m,n}\left(1 + \langle g \rangle_{m,n+1}^{m,n}\right)\right. \\ & \left. + x_{m,n+1}\left(1 - \langle g \rangle_{m,n}^{m,n+1}\right)\right) \\ & \underbrace{- \sum_{\substack{(p,q)\in\Omega \\ q \neq n+1}} H_{p,q} x_{p,q} \langle g \rangle_{m,n}^{p,q}}_{\tilde{I}_{m,n}} + \underbrace{j \sum_{\substack{(p,q)\in\Omega \\ q \neq n}} H_{p,q} x_{p,q} \langle g \rangle_{m,n+1}^{p,q}}_{\tilde{I}_{m,n+1}} \\ & + j w_{m,n} + w_{m,n+1}. \end{aligned} \tag{16}$$

It must be emphasized that (16) holds since the channel is assumed to be static. The effect of channel variations on

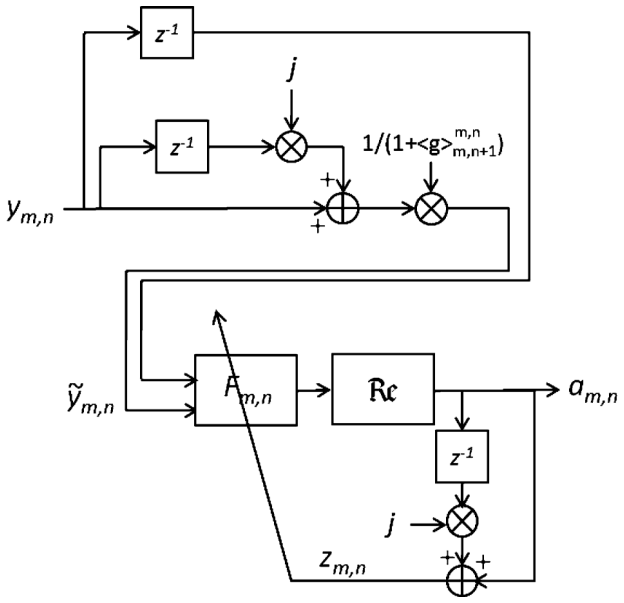

Fig. 2. Proposed blind equalizer using CNA, adapted to OFDM/OQAM system.

the accuracy of (16) will be investigated in Section IV. The symmetry property of weights $\langle g \rangle_{m,n}^{p,q}$ given in (5) yields $\langle g \rangle_{m,n+1}^{m,n} = -\langle g \rangle_{m,n}^{m,n+1}$, and therefore we can define $\tilde{y}_{m,n}$ from $y_{m,n}^{c}$ in (16) as

$$\begin{aligned}\tilde{y}_{m,n} &= \frac{y_{m,n}^{c}}{1+\langle g \rangle_{m,n+1}^{m,n}} \\ &= H_{m,n}\underbrace{(jx_{m,n}+x_{m,n+1})}_{\tilde{x}_{m,n}} \\ &\quad \times \underbrace{\frac{-\tilde{I}_{m,n}+\tilde{I}_{m,n+1}}{1+\langle g \rangle_{m,n+1}^{m,n}}}_{\tilde{I}_{m,n}^{r}} + \underbrace{\frac{jw_{m,n}+w_{m,n+1}}{1+\langle g \rangle_{m,n+1}^{m,n}}}_{\tilde{w}_{m,n}}, \end{aligned} \quad (17)$$

where $\tilde{x}_{m,n}$ is a 16-QAM symbol.

It is worth noticing that the redesigned received signal in (17) is exactly equivalent to the transmission of complex 16-QAM symbols $\tilde{x}_{m,n}$ over the channel $H_{m,n}$, with additive interference $\tilde{I}_{m,n}^{r}$ and non-white Gaussian noise $\tilde{w}_{m,n}$. Therefore, the CNA can now be employed as blind equalizer whose input $z_{m,n}$ is defined as

$$z_{m,n} = ja_{m,n} + a_{m,n+1}, \quad (18)$$

where $a_{m,n}$ and $a_{m,n+1}$ are the outputs of the equalizer given by (6). The specific update algorithm for $F_{m,n}$ is described in the hereafter Section III.B. The overall principle of the blind equalizer using CNA adapted to OFDM/OQAM is depicted in Fig. 2.

B. Deriving CNA in OFDM/OQAM

The cost function of the CNA can be formulated in a general expression as

$$J(z_{m,n}) = \frac{1}{ab}|\|z_{m,n}\|^{a} - \gamma|^{b}, \quad (19)$$

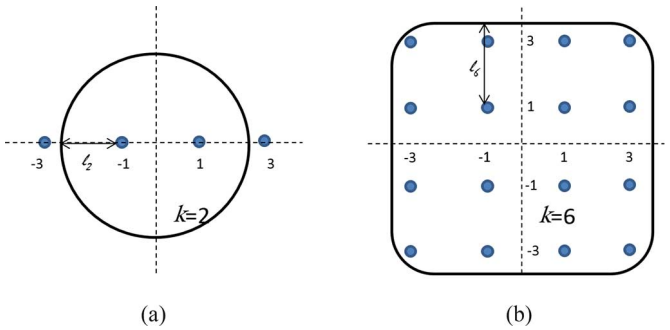

(a) (b)

Fig. 3. Balls of (a) CNA-2 (CMA) in (10) compared with $\{-3,-1,1,3\}$, and (b) CNA-6 in (22) compared 16-QAM.

where $\|\cdot\|$ is a norm defined on $\mathbb{C}$, and a and b are two parameters that give two degrees of freedom to the algorithm. In the following, it will be assumed that[2] $a = b = 2$. Since $x_{m,n}$ is taken from a 16-QAM constellation, the real positive constant γ should be rewritten as

$$\gamma = \frac{E\{\|x_{m,n}\|^4\}}{E\{\|x_{m,n}\|^2\}} = 13.2. \quad (20)$$

The k-norm family $\|\cdot\|$ considered in this paper can be formulated for any complex z on the plane $\mathbb{C}$ as

$$\|z\|_k = \sqrt[k]{|\mathrm{Re}\{z\}|^k + |\mathrm{Im}\{z\}|^k}. \quad (21)$$

Note that the CNA reduces to the CMA when $k = 2$. It has been demonstrated in [15] that the case $k = 6$ (denoted by CNA-6) is very suitable for 16-QAM constellation. According to this result, we hereafter employ the CNA-6 whose update algorithm can be adapted to OFDM/OQAM using (17) as

$$\begin{aligned}F_{m,n+1} = F_{m,n} - \mu\left(\|z_{m,n}\|_6^2 - \gamma\right) \\ \times \frac{\mathfrak{Re}\{z_{m,n}\}^5 + j\mathfrak{Im}\{z_{m,n}\}^5}{\|z_{m,n}\|_6^4}\tilde{y}_{m,n}^{*}. \end{aligned} \quad (22)$$

The steady-state performance of any constant norm-based equalizers can be characterized by the average distance $E\{l\}$ between the constellation symbols and the ball defined in (10) and (19) (see details [27]). Fig. 3 shows the balls of the modulus and the 6-norm compared with the 16-QAM in 3-(b), and with the corresponding real OQAM symbols $\{-3,-1,1,3\}$ in 3-(a). It can be deduced from Fig. 3 that $E\{l_6\} = 1.0586 > E\{l_2\} = 1$. The developments leading to this results are provided in Appendix A. As a consequence, the performance of the CNA-6 using the proposed reshaped symbols $\tilde{y}_{m,n}$ in (17) should be lower than that of CMA using $y_{m,n}$ in (1). However, the distance $E\{l\}$ does not take into account the interferences, and therefore a deeper analysis must be undertaken in order to show the influence of the interferences on the performance of the CMA and CNA-6.

[2]This choice is motivated, once again, by the difficulty of setting a proper step-size μ value when a and b increase.

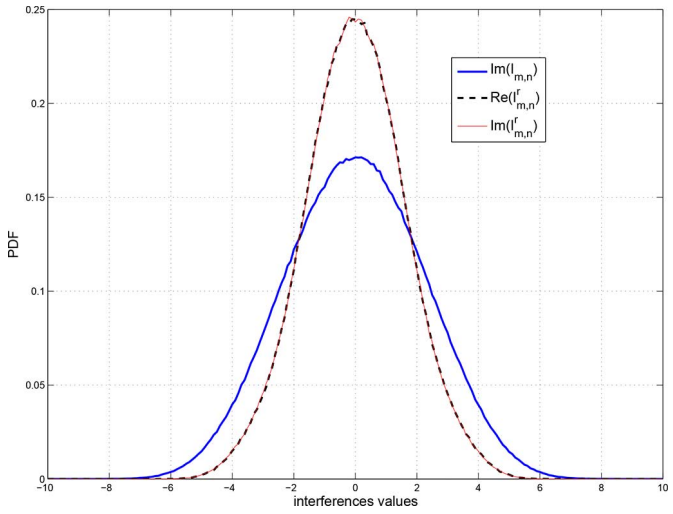

Fig. 4. Distributions of the interferences $I_{m,n}$ in (1) and $\tilde{I}^r_{m,n}$ in (17).

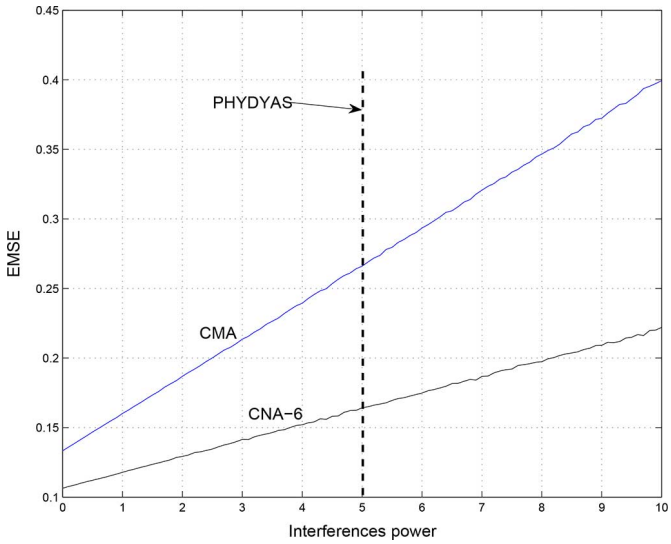

Fig. 5. EMSE versus interference power, comparison between CMA and CNA-6.

C. Performance Analysis of CNA-6 Adapted to OFDM/OQAM

The proposed development leading to $\tilde{y}_{m,n}$ in (17) induces some changes on the noise variance and on the energy of the interferences. Thus, the variance $\tilde{\sigma}^2$ of the noise $\tilde{w}_{m,n}$ can be expressed as

$$\tilde{\sigma}^2 = E\{|\tilde{w}_{m,n}|^2\} = \frac{2\sigma^2}{\left|1 + \langle g \rangle^{m,n}_{m,n+1}\right|^2}. \tag{23}$$

It should be emphasized that $\tilde{\sigma}^2$ in (23) depends on the chosen filter g, and thus, the noise level could be either higher or lower than the original noise variance σ^2. In the considered case of PHYDYAS's filter, the noise variance is reduced as $\tilde{\sigma}^2 = 0.8172\sigma^2$.

Fig. 4 depicts the probability density functions (PDFs) of the interferences $\Im\mathrm{m}\,(I_{m,n})$, $\Re\mathrm{e}\,(\tilde{I}^r_{m,n})$, and $\Im\mathrm{m}\,(\tilde{I}^r_{m,n})$ in (1) and (17), respectively. These have been obtained thanks to an histogram over 10000 simulation runs. One can observe that $\Im\mathrm{m}\,(I_{m,n})$ is purely real (by definition) with a variance $\sigma^2_I = 5$, whereas $\tilde{I}^r_{m,n}$ is complex with a variance $\sigma^2_{\tilde{I}} = 5.387$. Knowing that $x_{m,n} \in \{-3,-1,1,3\}$ whereas $\tilde{x}_{m,n}$ are 16-QAM symbols, we can conclude that the signal to interference ratios related to the CMA and the CNA-6 are such that

$$\frac{E\{|x_{m,n}|^2\}}{\sigma^2_I} < \frac{E\{|\tilde{x}_{m,n}|^2\}}{\sigma^2_{\tilde{I}}}. \tag{24}$$

We can deduce from (24) that the signal used for the CNA-6 should be less sensitive to interference than that used for the CMA, even if $\sigma^2_{\tilde{I}} > \sigma^2_I$.

In addition to (24), the performances of the equalizers can be compared in terms of excess mean square error (EMSE), which assesses the noise of the equalizer in the steady-state. From [15], the EMSEs of CMA and CNA-6 denoted by Γ_{CMA} and Γ_{CNA6} can be approximated as in (25) and (26), shown at the bottom of the page, where a_{op} and z_{op} are the perfectly equalized symbols (i.e., when $F^{\mathrm{opt}}_m H_m = 1$ is assumed) in (6) and (18), respectively, and P_y and $P_{\tilde{y}}$ are the powers of the corresponding input signals $y_{m,n}$ and $\tilde{y}_{m,n}$, respectively.

It is worth noting that Γ_{CMA} in (25) and Γ_{CNA6} in (26) are linear functions of P_y and $P_{\tilde{y}}$ respectively. Since these inputs powers are functions of the interferences, it is possible to compare the achieved Γ_{CMA} and Γ_{CNA6} values in function of the interference power, as depicted in Fig. 5. The step-size μ value has been arbitrarily set equal to 4.10^{-4} (in practice, the step-size parameter of CMA is larger than CNA's, as described in Section IV). Note that different μ values would only lead to a change in the slope of the curves. It can be observed that $\Gamma_{\mathrm{CNA6}} < \Gamma_{\mathrm{CMA}}$ for any interference power value. It reflects the fact that the CNA-6 with the proposed solution described in Fig. 2 achieved better performance than CMA using the real OQAM symbols as in [11]. This theoretical performance results will be confirmed through simulations in Section IV.

Beyond the application of the blind equalizer using CNA-6 in OFDM/OQAM, the reshape of complex symbols as described in Fig. 2 opens new perspectives for blind equalization in filter bank-based modulations, as specific cost functions (not limited to the real field) can now be used and investigated.

$$\Gamma_{\mathrm{CMA}} \approx \mu P_y \frac{E\{|a_{op}|^6 - 2\gamma|a_{op}|^4 + \gamma^2|a_{op}|^2\}}{E\{4|a_{op}|^2\} - 2\gamma}, \tag{25}$$

$$\Gamma_{\mathrm{CNA6}} \approx \mu P_{\tilde{y}} \frac{E\left\{\left(\|z_{op}\|^2_6 - \gamma\right)^2 \left(\Re\mathrm{e}\,(z_{op})^{10} + \Im\mathrm{m}\,(z_{op})^{10}\right)/\|z_{op}\|^8_6\right\}}{E\left\{\left[(4\gamma - 2\|z_{op}\|^2_6)\left(\Re\mathrm{e}\,(z_{op})^{10} + \Im\mathrm{m}\,(z_{op})^{10}\right) + 5\|z_{op}\|^6_6\left(\|z_{op}\|^2_6 - \gamma\right)\left(\Re\mathrm{e}\,(z_{op})^4 + \Im\mathrm{m}\,(z_{op})^4\right)\right]/\|z_{op}\|^{10}_6\right\}}, \tag{26}$$

D. Proposed Initialization Strategy

Since the proposed blind equalizer avoids the convergence of the coefficients $F_{m,n}$ toward local minima, it is not mandatory to choose a very low initialization value $F_{m,0}$ as proposed in [11], [12]. This solution may especially appear not adapted for channels with deep fading as the optimal coefficients $|F_{m,n}^{\text{opt}}|$ have high values, which should lead to a long convergence time. It has been demonstrated in [28] that a sub-optimal initialization value (in the mean square error sense) can be assessed in order to take into account the channel value for each frequency position m. To achieve this, the coefficients can be defined for $n = 0$ and for any $m \in \{0, 1, \ldots, M-1\}$ as

$$F_{m,0}^{s-\text{opt}} = \sqrt{\frac{E\left\{x_{m,0}^2\right\}}{|y_{m,0}|^2 + \alpha}}, \tag{27}$$

where α is a real constant that avoids the divergence of $F_{m,0}$ when $y_{m,0}$ is very close to zero. In practice, α is chosen such that $\alpha \ll 1$.

The sub-optimal nature of the initialization $F_{m,0}^{s-\text{opt}}$ is shown hereafter, and compared with the solution $|F_{m,0}| \ll 1$ proposed in [11], [12]. The mean error between the square moduli of the inverse of $F_{m,0}^{s-\text{opt}}$ and $H_{m,0}$ is defined as

$$\epsilon_F = E\left\{\frac{1}{\left|F_{m,0}^{s-\text{opt}}\right|^2} - |H_{m,0}|^2\right\}. \tag{28}$$

Note that the noise samples $w_{m,0}$ have a variance σ^2, and are uncorrelated with $x_{m,0}$, $H_{m,0}$, and $I_{m,0}$. Therefore, the mean error ϵ_F in (28) can be rewritten by substituting (1) into (27) and (28) as

$$\begin{aligned}
\epsilon_F &= E\left\{\frac{|y_{m,0}|^2 + \alpha}{E\left\{x_{m,0}^2\right\}} - |H_{m,0}|^2\right\} \\
&= E\left\{\frac{|x_{m,0}H_{m,0} + I_{m,0} + w_{m,0}|^2 + \alpha}{E\left\{x_{m,0}^2\right\}} - |H_{m,0}|^2\right\} \\
&= \frac{\overbrace{E\{2\mathfrak{Re}\left(x_{m,0}H_{m,0}I_{m,0}^*\right)\}}^{\sigma_{HI}^2} + \sigma^2 + \alpha}{E\left\{x_{m,0}^2\right\}} \\
&= \frac{\sigma^2 + \alpha}{E\left\{x_{m,0}^2\right\}},
\end{aligned} \tag{29}$$

since $\mathfrak{Re}\left(x_{m,0}\right) = x_{m,0}$ is a real zero-mean variable, which is independent of $H_{m,0}$ and $I_{m,0}$. Thus, a qualitative comparison with the solution $|F_{m,0}| \ll 1$ can be made. In fact, it should be noticed that $\epsilon_F \gg 1$ if $|F_{m,0}| \ll 1$ is substituted in (28) instead of $F_{m,0}^{s-\text{opt}}$, whereas the error ϵ_F using the proposed initialization in (29) is inversely proportional to the symbol power to noise power ratio. Therefore, we conclude that the sub-optimal $F_{m,0}^{s-\text{opt}}$ solution in (27) should achieve better performance than $|F_{m,0}| \ll 1$. This behavior will be numerically verified in Section IV. Furthermore, the computation of $F_{m,0}^{s-\text{opt}}$ in (27) requires one multiplication for $|y_{m,0}|^2$, one addition, and one division. The value of $E\{x_{m,0}^2\}$ only depends on the constellation size, and therefore it can be computed off-line.

IV. Simulations Results

In this section, simulations results show the performance of the different blind equalization methods proposed in this paper.

A. Simulations Parameters

Since we compare the solution proposed in Section III with the CMA in [11] and [12], the same simulation parameters described in [11] are considered. The path gains of the constant multipath channel are $\mathbf{h} = [1, -0.2, 0.3, 0.2, 0.1, 0.2, 0.35, -0.2]$, and the phase of the channel is uniformly chosen in $[-\frac{\pi}{2}, \frac{\pi}{2}]$. Each transmitted OFDM/OQAM symbol is composed of $M = 128$ subcarriers of 15 kHz width. The system operates at a carrier frequency of 400 MHz. According to [11] the constant initialization is set equal to $F_{m,0} = 0.01$ for any $m \in \{0, 1, \ldots, M-1\}$. In order to avoid the divergence of the algorithm when the proposed initialization $F_{m,0}^{s-\text{opt}}$ is used, we take $\alpha = 0.01$. Furthermore, a 16-QAM constellation is used, i.e., OQAM symbols are randomly chosen among $\{-3, -1, 1, 3\}$, and the CMA in (13) is carried out with $p = 2$ and $\mu = 0.0033$. This configuration is also used to test the equalizer using the CNA-6 in OFDM/OQAM.

The performance of the different blind equalizers is assessed by using the mean square error MSE defined as

$$\text{MSE} = E\{(|a_{m,n}| - |x_{m,n}|)^2\}. \tag{30}$$

The achieved MSEs of the blind equalizers are also compared with that of the data-aided estimation using interference approximation method (IAM) proposed in [4]. The preamble of IAM is designed as follows: for any pilot $x_{m,n} = \pm\mathcal{P}$, then the symbols at positions $n-1$ and $n+1$ are zero, and $x_{m-1,n} = -x_{m+1,n}$. Therefore the transmultiplexer gain described in (5) yields a received pilot with an energy larger than $|\mathcal{P}|^2$. This property makes IAM one of the most robust channel estimator in OFDM/OQAM, and we denote by $\hat{H}_{m,n}^{\text{IAM}}$ the estimated channel coefficients. The channel is then inverted with the zero-forcing (ZF) equalizer such as $F_{m,n}^{\text{IAM}} = 1/\hat{H}_{m,n}^{\text{IAM}}$. Note that the energy of the pilot is the same as the transmitted symbols, i.e., $|\mathcal{P}|^2 = 5$. It must be emphasized that the results presented for the estimator using IAM are only indicative. In fact, a fair comparison would induce to test different channel estimation methods (IAM-R [6], MMSE [20]), pilot energy, or equalizers [8]. A more exhaustive comparison with pilot-aided methods is out of the scope of this paper, but numerous estimation and equalization techniques can be found [6], [8], [20].

B. Performance of CNA-6 in OFDM/OQAM

First series of simulations have been performed to analyze the performance of blind equalization using CNA-6 in OFDM/OQAM. Fig. 6 shows the trajectories of the CMA and the CNA-6 versus the OFDM/OQAM symbols, for a signal-to-noise ratio (SNR) of 30 dB. Two initialization values $F_{m,0} = 0.01$ and $F_{m,0}^{s-\text{opt}}$ have been tested. Furthermore, the achieved MSE of IAM is given as reference. It can be seen that the steady-state performance of CNA-6 has 1 dB gain compared

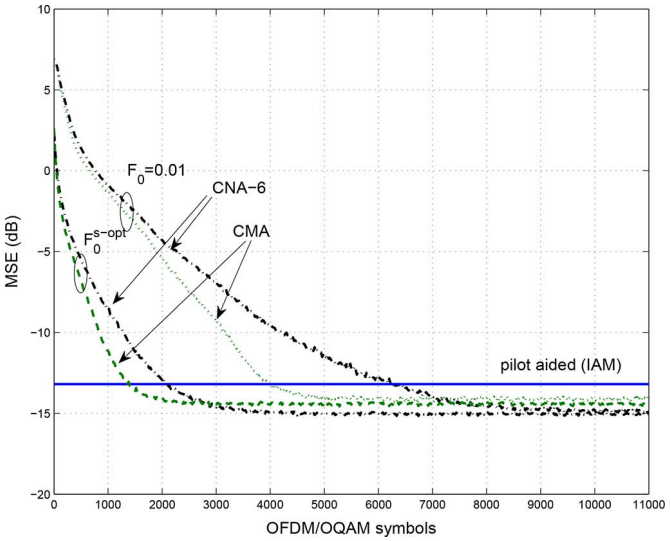

Fig. 6. MSE performance versus OFDM/OQAM symbols. Comparison between CNA-6, CNA-2 (CMA) using $F_{m,0} = 0.01$ and $F_{m,0}^{s-\mathrm{opt}}$, and pilot-aided method (IAM).

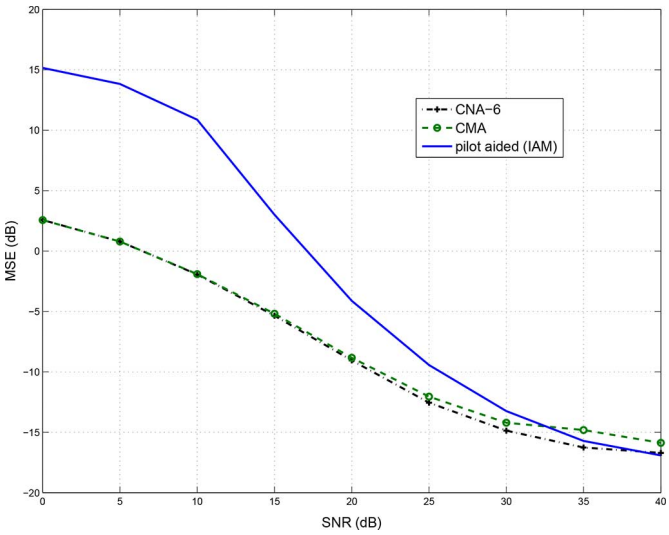

Fig. 7. MSE performance versus SNR. Comparison between CNA-6, CNA-2 (CMA) at the 3000-th iteration, and pilot-aided method.

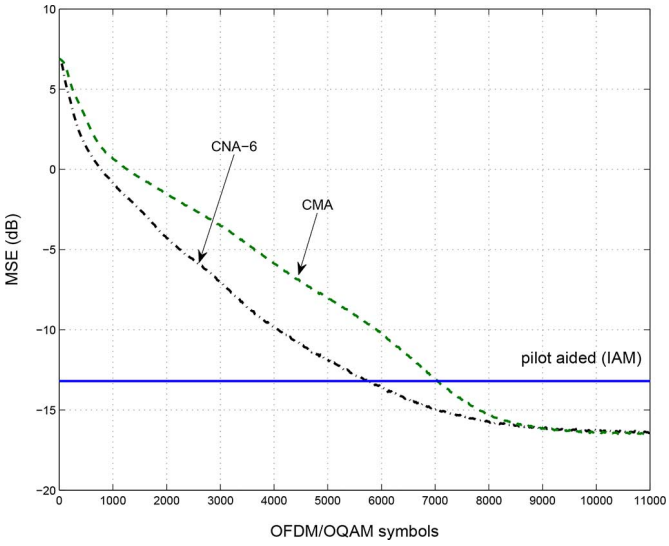

Fig. 8. MSE performance versus OFDM/OQAM symbols. Comparison between CNA-6, CNA-2 (CMA), and pilot-aided method.

with the MSE floor using CMA. This result is consistent with the analysis undertaken in Section III.C. However, the CNA-6 using $F_{m,0} = 0.01$ requires at least 1000 OFDM/OQAM symbols more than CMA to achieve a given MSE value. This loss is reduced by half when the algorithms are initialized with $F_{m,0}^{s-\mathrm{opt}}$. This delay in the convergence is due to the intrinsic phase adjustment when using CNA-6. The basic idea behind this phenomenon can be described by using the balls of the equalizers in Fig. 3. In fact, it can be observed in Fig. 3-(a) that CMA is phase-independent since the balls of CMA is a circle. However, the optimal equalizer coefficient value depends on the phase of $F_{m,n}$ (see Fig. 3-(b)), therefore the phase adjustment slows down the convergence of CNA-6. This phenomenon has been described in detail in [15]. It is also worth noticing that the use of the sub-optimal $F_{m,0}^{s-\mathrm{opt}}$ value allows the algorithm to gain 2000 iterations compared with $F_{m,0} = 0.01$ for both CMA and CNA-6. Finally, Fig. 6 highlights that a gain of 1 dB and 2 dB is achieved by CMA and CNA-6 respectively compared with IAM. This shows the capability of the blind equalization to outperform data-aided techniques.

Fig. 7 depicts the MSE-floor values of CMA, CNA-6, and IAM when the steady-state is reached (at the 3000-th iteration) versus SNR. It can be observed that the blind equalizers achieved an MSE gain (up to 12 dB at SNR $= 5$ dB) compared with IAM for SNR values <30 dB. This reflects the fact that the updated coefficients $F_{m,n}$ in (13) or (22) are less disturbed in noisy conditions than the ZF coefficient $F_{m,n}^{\mathrm{IAM}}$ using IAM. However, it is worth noticing that these results are obtained after 3000 iterations, whereas no convergence delay is required for data-aided methods (see Fig. 6 for instance). Furthermore, the MSE value of the IAM also depends on the pilot energy $|\mathcal{P}|^2$. Otherwise, it can be also observed that CNA-6 achieves better performance than CMA for SNR > 20 dB.

Fig. 8 presents the results of simulations undertaken to compare the convergence speed of CMA and CNA-6 for a given steady-state performance. Thus, the μ values have been tuned so that the MSE floor values of both equalizers reach the same value at -16.5 dB. It can be observed that CNA-6 converges faster than CMA, e.g., a gain of 1200 iterations is achieved using CNA-6 at MSE $= -13.5$ dB (which corresponds to the MSE of estimation using IAM) compared with CMA. We conclude from Figs. 6 and 8 that, for a given convergence rate (i.e., for the same μ value) the CNA-6 achieves lower MSE than CMA, and for a given steady-state the CNA-6 converges faster than CMA.

As indicated in Section II, the blind receiver may suffer from synchronization mismatch. The effect of such a time synchronization mismatch on the performance of CMA and CNA-6 is depicted in Fig. 9. The time shift between the transmitter and the receiver is given as a percentage of the prototype filter length L_f. The performance of the system using IAM is shown as well, but it is only indicative. It can be observed that time synchronization mismatches of 1%, 3%, and 5% induce MSE losses

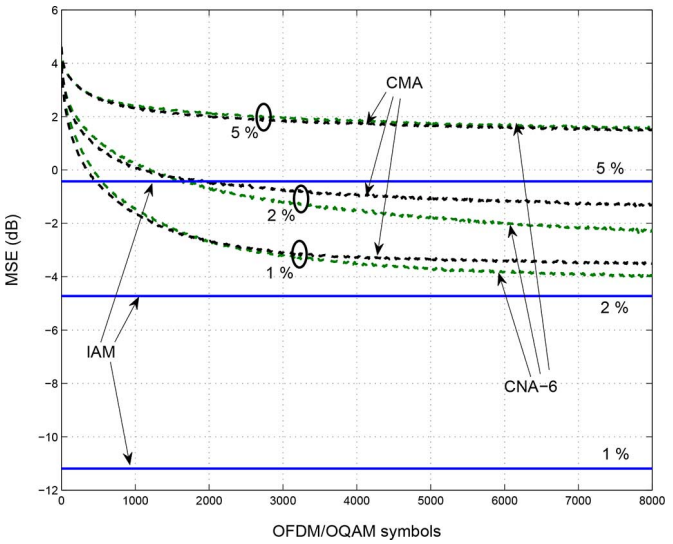

Fig. 9. MSE performance of CNA-6, CNA-2 (CMA), and pilot-aided method versus OFDM/OQAM symbols in presence of time synchronization mismatch. The synchronization mismatch is given as a percentage of $L_f = \{1\%, 2\%, 5\%\}$.

of 11, 13, and 16.5 dB, respectively, compared with the results given in Fig. 6. Such a MSE loss is due to the interferences induced by the synchronization mismatch. Furthermore, additional simulations revealed that a time shift larger than 5% leads to instability, i.e., the blind equalizer diverges. These results show that both CMA and CNA-6 require a very accurate synchronization process in order to work at their best performance.

Fig. 10 shows the MSE performance of CNA-6, CNA-2 (CMA) versus OFDM/OQAM symbols for three receiver speeds: (a) 1 km/h, (b) 3 km/h, and (c) 10 km/h. Two different initialization strategies have been considered: i) using $F_{m,0}^{s-\mathrm{opt}}$, and ii) using a preamble such that $F_{m,0} = 1/\hat{H}_{m,n}^{\mathrm{IAM}}$ (referred to "pilot init." on the figures). It can be observed that the equalizers performances tend to the MSE level whatever the initialization is (for 1 km/h, this limit is outside the OFDM/OQAM symbols range). However, the MSE starts at 4 dB where $F_{m,0}^{s-\mathrm{opt}}$ is used, whereas it starts at -8.5 dB when $F_{m,0} = 1/\hat{H}_{m,n}^{\mathrm{IAM}}$ is used. Thus, it can be noted that the CMA and CNA-6 equalizer using $F_{m,0} = 1/\hat{H}_{m,n}^{\mathrm{IAM}}$ outperforms those using $F_{m,0}^{s-\mathrm{opt}}$ from 0 to 5000 iterations and from 0 to 2500 iteration for 3 km/h and 10 km/h respectively. Furthermore, it can be also noted in (a) and (b) that CMA achieves 0.5 MSE gain compared with CNA-6 where the steady state is reached the steady-state. This is mainly due to the approximation in (16), which does not hold anymore when time selectivity of the channel increases.

C. Discussion

The practical use of blind equalizers such as CMA and CNA-6 is discussed in this section. We deduce from Figs. 6 and 8 that, even if the use of $F_{m,0}^{s-\mathrm{opt}}$ and CNA-6 reduces the convergence delay, blind equalizers still require more than 1000 OFDM/OQAM symbols to converge. As a consequence, the use of these methods requires is limited by the length of the signal packets. Thus, broadcast applications could be a possible context to operate blind receivers. Note that the reuse of the received symbols as input of the equalizers seems to be a good solution to further reduce the convergence delay [29].

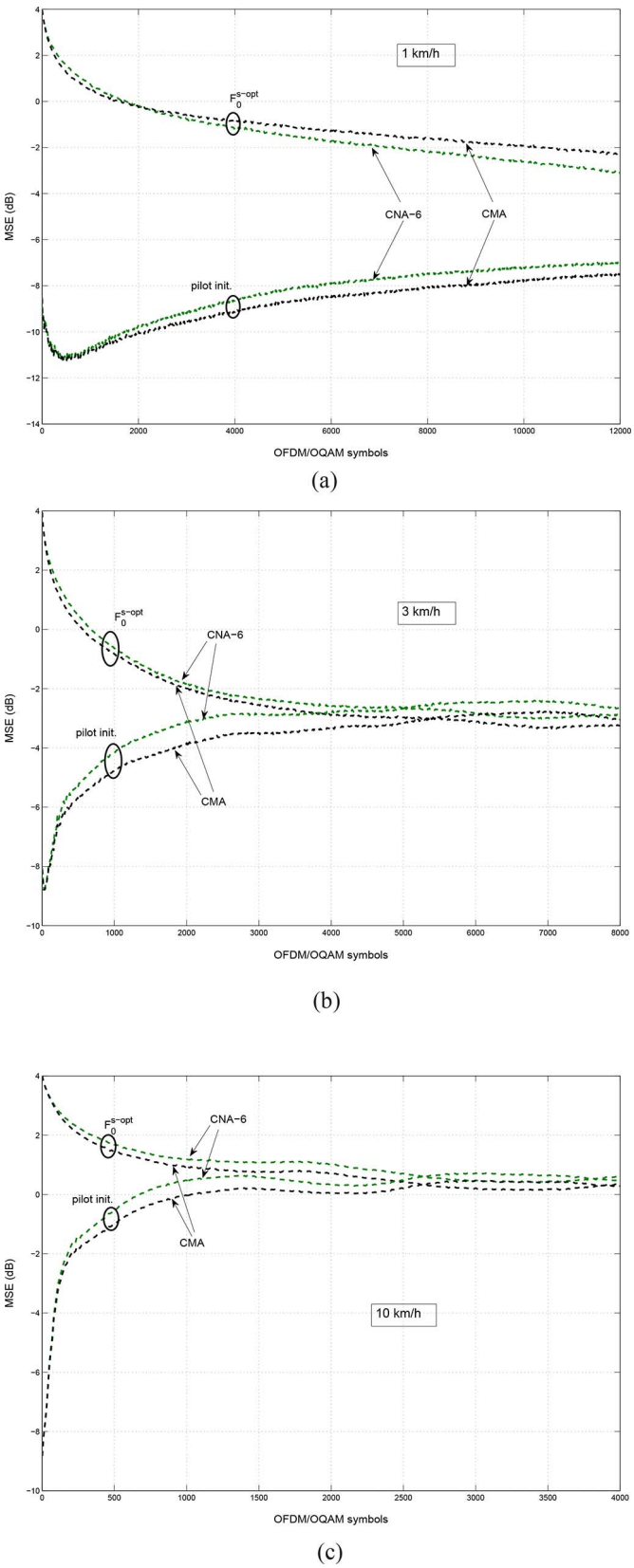

Fig. 10. MSE performance of CNA-6, CNA-2 (CMA) versus OFDM/OQAM symbols using the initialization $F_{m,0}^{s-\mathrm{opt}}$ compared with the initialization using a preamble, for three receiver speeds: (a) 1 km/h, (b) 3 km/h, and (c) 10 km/h.

It has been shown in Fig. 9 that the blind equalizers are very sensitive to time synchronization mismatch. Therefore, an accurate synchronization process is required. A usual solution is to undertake this task thanks to a preamble [22]. Furthermore, this preamble could be used for channel estimation. Fig. 10 revealed that an initialization of the blind equalizers thanks to an accurate estimate of the channel allows to hold lower MSE values much more longer than when using $F_{m,0}^{s-\mathrm{opt}}$ in slowly time-varying environments. Thus, instead of using full-blind equalizers as in Figs. 6 and 8, one can deduce from Figs. 9 and 10 that the use of regular preamble (e.g., at the beginning of each frame) could tackle the issue of synchronization mismatch, as well as allowing blind equalizers to operate in weakly time-selective channels.

V. Conclusion

In this paper, we have presented an adaptation of the CNA blind equalizer for OFDM/OQAM modulation. In Section III, the CNA, which can be seen as a generalized CMA, has been developed. To be effective, the CNA requires a signal using a complex constellation. Therefore, it has been proposed to reshape the "real" received OQAM symbols to obtain "complex" 16-QAM symbols. The performance of the proposed method has been analyzed, and it has been proved that, despite the increase of the interference level due to the reshape, the CNA applied to the new signal achieves better performance than the CMA applied to the OFDM/OQAM signal. Furthermore, the principle of changing the shape of the received signal opens new perspectives for the blind equalization in the FBMC-based modulations, as specific cost functions (not limited to the real field) can now be investigated. In addition, a sub-optimal initialization strategy, in the sense of the mean square error, has been presented. Numerical results revealed that the CNA and the proposed initialization method allows to reduce by 2000 the number of iterations of the blind equalizer. Moreover, the performances of CMA and CNA-6 have been studied in conditions where the receiver is not well-synchronized with the transmitter and the channel is time-varying. Results have shown that this degrades the performance. In order to overcome these deteriorations, a relevant solution consists of using preamble, from which the synchronization and accurate initialization can be obtained.

Appendix

A. Obtaining the Average Distances $E\{l_6\}$ and $E\{l_2\}$

The ball corresponding to the CMA is generated by $|a_{m,n}|^2-\gamma=0$, i.e., it is a circle of radius $\sqrt{\gamma}=\sqrt{8.2}$. Since $\mathbb{P}(x_{m,n}=\pm1)=\mathbb{P}(x_{m,n}=\pm3)=0.5$, the average distance $E\{l_2\}$ can be expressed as

$$\begin{aligned}E\{l_2\}&=\mathbb{P}(x_{m,n}=\pm1)(\sqrt{\gamma}-1)+\mathbb{P}(x_{m,n}=\pm3)(3-\sqrt{\gamma})\\&=1\end{aligned}\tag{31}$$

The ball corresponding to the CNA-6 is defined by $\|z_{m,n}\|_6^2-\gamma=0$, and it is depicted in Fig. 3-(b). The radius of this ball along the X axis is $\sqrt{\gamma}=\sqrt{13.2}$, while its radius along the axis $y=x$ is given by $\frac{\sqrt{2\gamma}}{2^{1/6}}$. Since $\mathbb{P}(x_{m,n}=\pm1\pm j)=\mathbb{P}(x_{m,n}=\pm3\pm3j)=\mathbb{P}(x_{m,n}=\pm1\pm3j)=\mathbb{P}(x_{m,n}=\pm3\pm j)=0.25$, the average distance $E\{l_6\}$ can be expressed as

$$\begin{aligned}E\{l_6\}&=\mathbb{P}(x_{m,n}=\pm1\pm j)(\sqrt{\gamma}-1)\\&\quad+\mathbb{P}(x_{m,n}=\pm3\pm3j)\left(\sqrt{18}-\frac{\sqrt{2\gamma}}{2^{1/6}}\right)\\&\quad+\mathbb{P}(x_{m,n}=\pm1\pm3j)(\sqrt{\gamma}-3)\\&\quad+\mathbb{P}(x_{m,n}=\pm3\pm j)(\sqrt{\gamma}-3)\\&=1.0586\end{aligned}\tag{32}$$

References

[1] B. L. Floch, M. Alard, and C. Berrou, "Coded orthogonal frequency division multiplex," *Proc. IEEE*, vol. 83, no. 6, pp. 982–996, Jun. 1995.

[2] B. Farhang-Boroujeny, "OFDM versus filter bank multicarrier," *IEEE Signal Process. Mag.*, vol. 28, no. 3, pp. 92–112, May 2011.

[3] J.-P. Javaudin, D. Lacroix, and A. Rouxel, "Pilot-aided channel estimation for OFDM/OQAM," in *Proc. VTC'03 Spring*, Jeju, Korea, Apr. 2003, vol. 3, pp. 1581–1585.

[4] C. Lélé, J.-P. Javaudin, R. Legouable, A. Skrzypczak, and P. Siohan, "Channel estimation methods for preamble-based OFDM/OQAM modulations," *Eur. Trans. Telecommun.*, vol. 19, no. 7, pp. 741–750, Nov. 2008.

[5] D. Katselis, E. Kofidis, A. Rontogiannis, and S. Theodoris, "Preamble-based channel estimation for CP-OFDM and OFDM/OQAM systems: A comparative study," *IEEE Trans. Signal Process.*, vol. 58, no. 5, pp. 2911–2916, Feb. 2010.

[6] E. Kofidis, D. Katselis, A. Rontogiannis, and S. Theodoridis, "Preamble-based channel estimation in OFDM/OQAM systems: A review," *Signal Process., Elsevier*, vol. 93, pp. 2038–2054, Jan. 2013.

[7] G. Lin, L. Lundheim, and N. Holte, "On efficient equalization for OFDM/OQAM systems," in *Proc. InOWo'05*, Hamburg, Germany, Aug. 31–Sep. 1, 2005, pp. 1–5.

[8] T. Ihalainen, T. H. Stitz, M. Rinne, and M. Renfors, "Channel equalization in filter bank based multicarrier modulation for wireless communications," *EURASIP J. Adv. Signal Process.*, vol. 2007, pp. 1–18, Aug. 2007.

[9] T. Ihalainen, A. Ikhlef, J. Louveaux, and M. Renfors, "Channel equalization for multi-antenna FBMC/OQAM receivers," *IEEE Trans. Veh. Technol.*, vol. 60, no. 5, pp. 2070–2085, Apr. 2011.

[10] H. Bölcskei, P. Duhamel, and R. Hleiss, "A subspace-based approach to blind channel identification in pulse shaping OFDM/OQAM systems," *IEEE Trans. Signal Process.*, vol. 49, no. 7, pp. 1594–1598, Jul. 2001.

[11] B. Farhang-Boroujeny, "Multicarrier modulation with blind detection capability using cosine modulated filter banks," *IEEE Trans. Commun.*, vol. 51, no. 12, pp. 2057–2070, Dec. 2003.

[12] L. Lin and B. Farhang-Boroujeny, "Convergence analysis of blind equalizer in a cosine modulated filter bank-based multicarrier communication system," in *Proc. SPAWC'03*, Roma, Italy, Jun. 2003, pp. 368–372.

[13] Y. Sato, "A method of self-recovering equalization for multilevel amplitude-modulation systems," *IEEE Trans. Commun.*, vol. 23, no. 6, pp. 679–682, Jun. 1975.

[14] J. Yang, J.-J. Werner, and G. A. Dumont, "The multimodulus blind equalization and its generalized algorithms," *IEEE Trans. Sel. Areas Commun.*, vol. 20, no. 5, pp. 997–1015, Jun. 2002.

[15] A. Goupil and J. Palicot, "New algorithms for blind equalization: The constant norm algorithm family," *IEEE Trans. Signal Process.*, vol. 55, no. 4, pp. 1436–1444, Apr. 2007.

[16] K. N. Oh and Y. O. Chin, "Modified constant modulus algorithm: Blind equalization and carrier phase recovery algorithm," in *Proc. ICC'95*, Seattle, WA, USA, Jun. 1995, vol. 1, pp. 498–502.

[17] S. Barbarossa, "Blind equalization using cost function matched to the signal constellation," in *Proc. ACSSC'97*, Pacific Grove, CA, USA, Nov. 1997, vol. 1, pp. 550–554.

[18] P. Siohan, C. Siclet, and N. Lacaille, "Analysis and design of OFDM/OQAM systems based on filterbank theory," *IEEE Trans. Signal Process.*, vol. 50, no. 05, pp. 1170–1183, May 2002.

[19] M. Bellanger, "Specification and design of a prototype filter for filter bank based multicarrier transmission," in *Proc. ICASSP'01*, Salt Lake City, UT, USA, May 2001, vol. 4, pp. 2417–2420.

[20] V. Savaux, F. Bader, and Y. Louët, "A joint MMSE channel and noise variance estimation for OFDM/OQAM modulation," *IEEE Trans. Commun.*, vol. 63, no. 11, pp. 4254–4266, Nov. 2015.
[21] Y. Medjahdi, M. Terre, D. Le Ruyet, D. Roviras, and A. Dziri, "The impact of timing synchronization errors on the performance of OFDM/FBMC systems," in *Proc. ICC'11*, Kyoto, Japan, Jun. 2011, pp. 1–5.
[22] N. Cassiau, D. Kténas, and J.-B. Doré, "Time and frequency synchronization for CoMP with FBMC," in *Proc. ISWCS'13*, Ilmenau, Germany, Aug. 2013, pp. 1–5.
[23] Y. Zeng and M. W. Chia, "Joint time-frequency synchronization and channel estimation for FBMC," in *Proc. PIMRC'14*, Washington, DC, USA, Sep. 2014, pp. 1–5.
[24] D. N. Godard, "Self-recovering equalization and carrier tracking in two-dimensional data communication systems," *IEEE Trans. Commun.*, vol. Com-28, no. 11, pp. 1867–1875, Nov. 1980.
[25] R. Johnson, Jr, P. Schniter, T. Endres, J. Behm, D. Brown, and R. Casas, "Blind equalization using the constant modulus criterion: A review," *Proc. IEEE*, vol. 86, no. 10, pp. 1927–1950, Oct. 1998.
[26] P. Bouboulis, "Wirtinger's calculus in general Hilbert spaces," May 2010, pp. 1–27, arXiv:1005.5170v1.
[27] A. Goupil and J. Palicot, "Constant norm algorithms class," presented at the EUSIPCO, Toulouse, France, Sep. 2002.
[28] V. Savaux and F. Bader, "Sub-optimal initialization for blind equalization with fast convergence in OFDM/OQAM modulation," presented at the EuCNC'15, Paris, France, Jun.–Jul. 2015.
[29] V. Savaux, M. Naoues, F. Bader, and J. Palicot, "Ultra-fast blind equalization for OFDM: Principle and steps towards implementation," in *Proc. ISWCS'15*, Brussels, Belgium, Aug. 2015, pp. 1–5.

Vincent Savaux (AM'15) received the engineer degree from the High School of Engineering, ECAM Rennes, the M.Sc. degree from the University of Rennes 1, France, in 2010, and the Ph.D. degree in telecommunications from École Supérieure d'Electricité Supélec, in 2013. Since January 2014, he has been a Postdoctoral Researcher with the Signal, Communication, and Embedded Electronics (SCEE) Research Group at CentraleSupélec, Campus de Rennes, France. His research activities include channel estimation, equalization for multicarrier modulations as OFDM and OFDM/OQAM, spectrum sensing. He received the Exemplary Reviewer 2014 appreciation from IEEE WIRELESS COMMUNICATIONS LETTERS and IEEE COMMUNICATIONS LETTERS.

Faouzi Bader (SM'07) received the Ph.D. degree (with Honours) in telecommunications from Universidad Politécnica de Madrid (UPM), Madrid, Spain, in 2002. He joined the Centre Technologic de Telecomunicacions de Catalunya (CTTC), Barcelona, Spain, as Associate Researcher, in 2002, and was nominated in 2006 as a Senior Research Associate at same institution. Since June 2013, he has worked as an Associate Professor at École Supérieur d'Electricité-SUPELEC in Rennes, France. His research activities mainly focus on IMT-Advanced systems, system design, advanced multicarrier waveforms (OFDM(A), (non-)uniform multimode filter based multicarrier schemes), and frequency allocation techniques in relay cognitive environment. He has been involved in several European projects from the 5th–7th EC research frameworks, and from 2012 to 2013 he was nominated the General Coordinator and Manager of the EC funded research project ICT EMPhAtiC project, Enhanced Multicarrier Techniques for Professional Ad-Hoc and Cell-Based Communications. He has published over 120 papers in peer-reviewed journals and international conferences, more than 13 book chapters, and 3 books. He served as Technical Program Committee member in major IEEE ComSoc and VTS conferences, and as the General Chair of the 11th edition of the ISWCS'2014 conference, and the Cochair of the ISWCS 2015 edition.

Jacques Palicot received, in 1983, his Ph.D. degree in signal processing from the University of Rennes. Since 1988, he has been involved in studies about equalization techniques applied to digital transmissions and analog TV systems. Since 1991 he has been involved mainly in studies concerning the digital communications area and automatic measurements techniques. He has taken an active part in various international bodies EBU, CCIR, URSI, and within RACE, ACTS and IST European projects. He has published various scientific articles notably on equalization techniques, echo cancellation, hierarchical modulations and Software Radio techniques. He is author or co-author of more than 300 publications with more than 50 in prestigious journals, two books and 22 patents. He is currently involved in adaptive Signal Processing, digital communications, Software Radio, Cognitive radio and Green Radio. From November 2001 to September 2003 he had a temporary position with INRIA/IRISA in Rennes. He serves as Associate Editor for EURASIP JASP since 2008. He also served as lead guest editor for several Special Issues on Software Radio, Cognitive Radio and Green Radio. He was Co General Chairman of ISCIT 2011, Co General Chairman of Next-GWiN 2014, Technical Program Chairman of CROWNCOM 2009, Technical Program Chairman of GREENCOM 2013 and Technical Program Chairman of CRN Symposium of ICC 2014. Since October 2003 he is with CentraleSupélec in Rennes where he leads the Signal Communications and Embedded Electronics (SCEE) research team.

Others research aspects related with signal processing for OFDM and OFDM/OQAM signal is that related with the development of techniques for peak to average power ratio (PAPR) reduction. These works have been undertaken through the advice of the PhD thesis of Mr. Lamarana DIALLO (2012-2016), and that of Ms. Marwa CHAFII[19] (2013-2016).

One of the aspects investigated is that related with the the tones reservation (TR), that is one of the most popular approach that allows to carry the addition of a signal for PAPR reduction with neither degradation of the bit error rate (BER), nor an increase of the out-of-band (OOB) pollution [87]. As TR approach uses reserved tones, there is no need for additional processing at the receiver to process the data information. This last is what makes the tone reservation a widely used and implemented approach already used in commercial standards such as the digital video broadcasting-terrestrial (DVBT2) system. Note that a large number of research works exist with a specific focus on how to compute the adding signal by using the TR principle. In [87, 88], the authors proposed to use a quadratic constrained quadratic program (QCQP) and a second order cone program (SOCP) respectively to set the appropriate values on the reserved tones (carriers) for the PAPR mitigation. However, the computational complexity of these approaches is very high and not affordable for real time systems. To reduce the computation complexity, various methods have been proposed as: the active-set method in [89], the selective mapping of partial tones reservation approach (SMOPT) in [90], and a modified version of the clipping method in [91, 92], all with the purpose of peak cancellation using TR principle. It is worth to mention that the best technique that provides the most appropriate compromise between PAPR reduction and computational complexity is the TR method that uses the gradient project (GP) algorithm to compute the adding signal by maximizing the signal to clipping ratio, in other words this is equivalent to minimize the clipping noise as indicated in [93].

Based on developed work in Lamarana's DIALLO dissertation, a new TR method using the gradient project (TR-GP) algorithm has been proposed. The main idea behind this approach is to modify the classical TR structure by exploiting the decomposition of the useful OFDM symbol as the combinations of two multi-carrier symbols, where each one contains a number of subcarriers two times less than the original OFDM symbol. This proposed approach is named, modified tones reservation (MTR), and consists in minimizing the partials clipping noise effect with respect to the different resulted signals of the useful OFDM symbol after the decomposition process. Therefore, the proposed MTR technique allows us to relax some constraints relative to the classical TR approach without degrading the orthogonality between reserved tones, the BER, and the OOB that can harmful the possible adjacent systems in the band.

Proposed MTR approach consists in modifying the classical TR structure by exploiting the decomposition of the useful OFDM symbol as a mixture of two times shorter multi-carrier symbols by containing each two times less carriers. Thus, by decomposing jointly the $J_{[\mathbf{x}_n]}(.)$ as a sum of a partial clipping noise signals with respect to the decomposed parts of the useful OFDM symbol, the MTR proposed approach consists in jointly minimizing the partial clipping noise over the decomposed structures of the OFDM signal by using the gradient project algorithm (MTR-GP) subject to the predefined TR positions.

The OFDM symbol $x(t)$ of duration T_u can be expressed as follows by

$$x(t) = \sqrt{\frac{1}{M}} \sum_{m=0}^{M-1} X_m e^{j2\pi mFt} \ , \ 0 \leq t \leq T_u \tag{3.21}$$

where M is the total number of carriers, $F = \frac{1}{T_u}$ is the inter-carrier spacing and X_m the symbol carried out by the $m-th$ carrier at instant T_u. After oversampling the signal by a factor L, x_l with $\{l = 0, \ldots, LM-1\}$ will denote the discrete time samples at the instant lT_e of $x(t)$ where $T_e = \frac{T_u}{LM}$ is the time sampling. We denote the vector containing the time samples of $x(t)$ after the oversampling operation by $\mathbf{x} = [x_0, \ldots, x_{LM-1}]$. This vector can be efficiently computed by using an inverse discrete Fourier transform (IDFT)[20] and can be expressed by the following matrix

$$\mathbf{x} = F_{ML}\breve{\mathbf{X}}, \tag{3.22}$$

where F_{LM} is the $LM \times LM$ normalized IDFT square matrix scaled by $\sqrt{L}$ with the $k-th$ vector column expressed

[19] See more details on L. DIALLO's and M. CHAFII's PhDs in Subsection 1.3.3.2, page 18

[20] In this paper, we use the zero-inserting scheme to calculate $\mathbf{x}$, i.e., the IFFT operation is applied to the extended vector $\breve{\mathbf{X}} = [X_0, \ldots, X_{\frac{M}{2}-1}, \underbrace{0, \ldots, 0}_{(L-1)M \text{ Zeros}}, X_{\frac{M}{2}}, \ldots, X_{M-1}]$

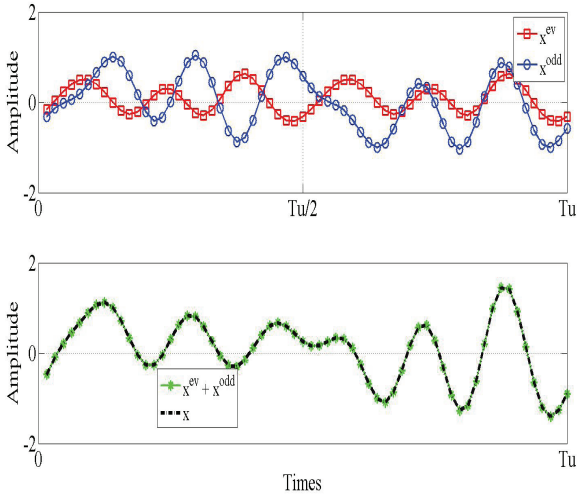

Figure 3.25: Time domain signals comparison. In the Upper figure the two signals x^{ev} and x^{odd} are drawn. In the bottom Figure the summation $x^{ev} + x^{odd}$ is drawn and compared with the original signal x.

as following

$$\begin{aligned} \mathbf{F}_{ML}^{k} &= \frac{1}{\sqrt{M}}\left[1, e^{j2\pi\frac{1.k}{LM-1}}, \ldots, e^{j2\pi\frac{(LM-1)k}{LM-1}}\right]^T \\ & k = 0, \ldots, LM-1 \end{aligned} \tag{3.23}$$

The main idea is to decompose the multi-carrier (MC) signal and to represent it as the summation of two others MC signals, one being symmetrical and the second one anti-symmetrical. These two signals are each the result of the concatenation of other two MC signals with half duration each (i.e. comprising half number of carriers). Let consider the OFDM symbol $x(t)$ in (3.21), and two MC signals of same duration T_u, $x^{ev}(t)$ and $x^{odd}(t)$ obtained by replacing the values of X_m in (3.21) with $\mathbf{X}^{ev} = [X_0^{ev}, 0, X_2^{ev}, 0, \ldots, X_{M-2}^{ev}, 0]$ and $\mathbf{X}^{odd} = [0, X_1^{odd}, 0, X_3^{odd}, 0, \ldots, 0, X_{M-1}^{odd}]$ respectively such that (see fig. 3.25)

$$\begin{aligned} x^{ev}(t) &= \sqrt{\frac{1}{M}} \sum_{m=0}^{M-1} X_m^{ev}\, e^{j2\pi mFt},\ 0 \le t \le T_u \\ x^{odd}(t) &= \sqrt{\frac{1}{M}} \sum_{m=0}^{M-1} X_m^{odd}\, e^{j2\pi mFt},\ 0 \le t \le T_u \end{aligned} \tag{3.24}$$

In others words $x^{ev}(t)$ corresponds to the signal modulated on the even subcarriers whereas $x^{odd}(t)$ is the result of those modulated n the odd subcarriers. It can be easily noticed that $x(t) = x^{ev}(t) + x^{odd}(t)$, where $x^{ev}(t)$ and $x^{odd}(t)$ are symmetrical and anti-symmetrical respectively with respect to $\frac{T_u}{2}$. This means that for each $t \in \left[0, \frac{T_u}{2}\right]$, $x^{ev}(t) = x^{ev}(t + \frac{T_u}{2})$ and $x^{odd}(t) = -x^{odd}(t + \frac{T_u}{2})$. Now let's decompose again both signals $x^{ev}(t)$ and $x^{odd}(t)$ such that they result as the concatenation of two new signals with half number of subcarriers with the following expressions

$$\begin{aligned} x^{(ev,1)}(t) &= \sqrt{\frac{2}{M}} \sum_{m=0}^{\frac{M}{2}-1} X_m^{(ev,1)} e^{j2\pi m\ F_0 t} g_0(t) \\ x^{(ev,2)}(t) &= \sqrt{\frac{2}{M}} \sum_{m=0}^{\frac{M}{2}-1} X_m^{(ev,2)} e^{j2\pi m\ F_0 t} g_0(t - T_0) \end{aligned} \tag{3.25}$$

$$
\begin{aligned}
x^{(odd,1)}(t) &= \sqrt{\frac{2}{M}} \sum_{m=0}^{\frac{M}{2}-1} X_m^{(odd,1)} e^{j2\pi(m\ F_0+F)t} g_0(t) \\
x^{(odd,2)}(t) &= \sqrt{\frac{2}{M}} \sum_{m=0}^{\frac{M}{2}-1} X_m^{(odd,2)} e^{j2\pi(m\ F_0+F)t} g_0(t-T_0)
\end{aligned}
\tag{3.26}
$$

where $T_0 = \frac{T_u}{2}$, $F_0 = \frac{1}{T_0} = 2F$, and g_0 a rectangular window of duration T_0. Note that in (3.25), $X_m^{(ev,1)} = X_m^{(ev,2)} = \frac{X_{2m}^{ev}}{\sqrt{2}}$, however, in (3.26), $X_m^{(odd,1)} = X_m^{(odd,2)} = \frac{X_{2m+1}^{odd}}{\sqrt{2}}$. Thus, from (3.25) and (3.26) the time discrete signal $\mathbf{x}$ in (3.22) can be reconstructed as the following

$$
\begin{aligned}
\mathbf{x} \;=\; & \left[\overbrace{x_0^{(ev,1)}, \ldots, x_{\frac{M}{2}-1}^{(ev,1)}}^{\mathbf{x}^{(ev,1)}}, \overbrace{x_0^{(ev,2)}, \ldots, x_{\frac{M}{2}-1}^{(ev,2)}}^{\mathbf{x}^{(ev,2)}(=\mathbf{x}^{(ev,1)})} \right] \\
& + \left[\underbrace{x_0^{(odd,1)}, \ldots, x_{\frac{M}{2}-1}^{(odd,1)}}_{\mathbf{x}^{(odd,1)}}, \underbrace{x_0^{(odd,2)}, \ldots, x_{\frac{M}{2}-1}^{(odd,2)}}_{\mathbf{x}^{(odd,2)}(=-\mathbf{x}^{(odd,1)})} \right]
\end{aligned}
\tag{3.27}
$$

Using an MTR approach based on the first decomposition (1-MTR-GP) according to the useful OFDM symbol decomposition, the clipping noise $J(.)$ (cost function in TR-GP method) is also decomposed as a sum of the partial clipping noise $J_1(.)$ and $J_2(.)$.

Going more deeply into the decomposition approach of the OFDM signal, a second decomposition on the x(t) symbol has been proceeded. For this purpose, the symbols derived from the first decomposition are decomposed similarly as in Annexe A in [C102][21]. Through this double decomposition, the x of e.g., of M=64 subcarriers, can be expressed as a mixture of 16 multi-carrier symbols each with a duration of $\frac{Tu}{4}$ and $M2 = \frac{M}{2}$ carriers (useful and reserved). Conjointly to this double decomposition, the cost function $J(.)$ is also decomposed as a sum of 4 partial clipping noise $J_{1,1}(.)$, $J_{1,2}(.)$, $J_{2,1}(.)$, and $J_{2,2}(.)$. Fig. 3.28 gives an illustration of the partial clipping noise derived from the decomposition of the clipping noise depicted in Fig. 3.26. Details using the MTR approach based on the double decomposition (2-MTR-GP) are presented in Subsections A and B in [C102].

Simulations performed with a 16-QAM modulated OFDM system that has $M = 256$ carriers wherein $M_R = 12$ carriers are reserved for PAPR reduction. The signal is oversampled by a factor of four ($L = 4$). The set of reserved tones is $\mathcal{R} = [123, 124, \ldots, 133, 134]$. Obtained CCDF before and after the PAPR reduction using the TR-GP method, the 1-MTR-GP and 2-MTRGP methods after $N_{max} = 10$ (number of performed iterations by the GP algorithm) featuring different normalized thresholds of $\rho = 5$dB and 6dB, show that the proposed approaches outperform the classical TR-GP method in terms of PAPR reduction. In fact, with $\rho = 6$ dB ($\rho = 5$ dB respect.) and $N_{max} = 10$, the achieved PAPR at a clip rate 10^4 of the CCDF for the TR-GP, 1-MTR-GP, and 2-MTR-GP are 10.9 dB, 10.4 dB, and 9.9 dB (10.9 dB, 10.45 dB, and 10.12 dB respect.) respectively. Thus, the MTR solutions allow us to improve the PAPR reduction about approximately 1dB. Besides, it can be also noticed that the deeper is the decomposition process of the OFDM signal $x(t)$, better is the PAPR reduction performance achieved of the MTR-GP method.

Given the good results obtained thanks to this operated modification on the classical TR method on the symbol of interest [C93], the method was extended iteratively to new orders of decomposition to define news structures of insertion for the PAPR correcting signal. There was thus obtained the 2-MTR-GP, and extended it to 3-MTR-GP, 4-MTR-GP, and finally 5-MTR-GP (a journal paper including a synthesis analysis from 1-MTR-GP to 5-MTR-GP is under preparation for its submission to the IEEE Transactions on Communications). Concerning the 2-MTR-GP

[21] A copy of this paper titled: "Modified Tone Reservation for PAPR Reduction in OFDM Systems", by Marwa Chaffi, Mamadou Lamarana Diallo, Jacques Palicot, and Faouzi Bader, is depicted at the end of this Subsection.

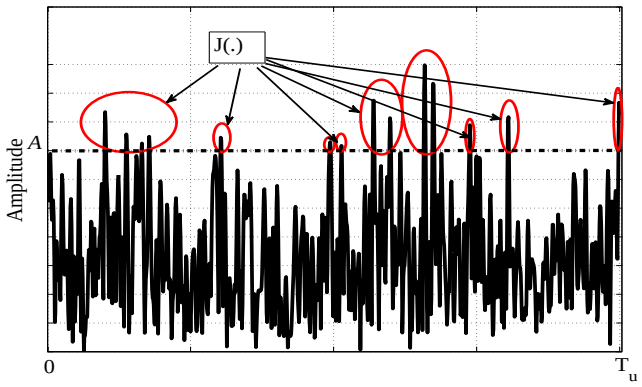

Figure 3.26: Illustration of the cost function in TR-GP method.

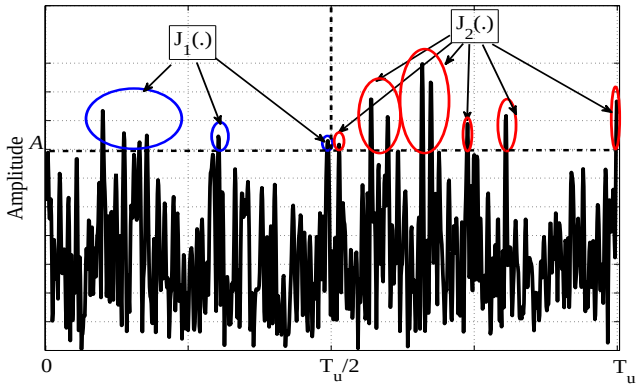

Figure 3.27: Illustration of the clipping partial noise $J_1(.)$ and $J_2(.)$.

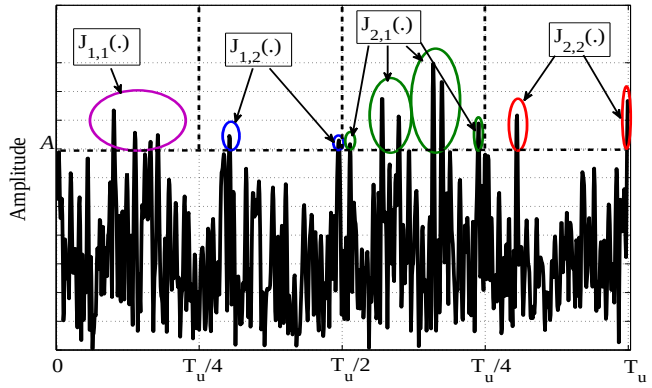

Figure 3.28: Illustration of the clipping partial noise $J_{1,1}(.)$, $J_{1,2}(.)$, $J_{2,1}(.)$ and $J_{2,2}(.)$.

the different steps of this method is detailed in [C102][22] (a double-decomposition of the symbol for defining the inserted structure and the decomposition of the cost function structures associated with this double decomposition). As for method 1-MTR-GP, the 2-MTR-GP does not require the knowledge of the symbols from the double decomposition but only the matrix generation of the components of the PAPR correction signal.
We then showed that the construction of this matrix can be made with the knowledge from of the 1-MTR-GP structure basis. From this work, a recursive algorithm for the generation of the matrix of the PAPR correcting signal the k-MTR-GP decomposition methods has been proposed for all $k \geq 2$.
It has been also shown that for the same complexity, the MTR method has allowed a considerable improvement with the TR-GP method in reducing the value of the PAPR. For the 5-MTR-GP method, we have found that it can provide a significant gain in the PAPR reduction with a slight increase of the average power. Note that, the choice of the reserved carriers (TR technique) has also an impact on the PAPR performances [J22, C95, C98].

Different clipping techniques have been also developed in [C89, J22], the adaptive clipping is one of the main developed approach. It has been demonstrated that unlike clipping at predefined threshold, the developed adaptive clipping method is carried out in two stages. The first stage consist in calculating the adapted clipped threshold in function of the targeted PAPR at the output of each data symbol. Second stage, consist in clipping this symbol via a hard clipping function. From the previously cited works, it has been shown that unlike the classical clipping method (clipping with a predefined threshold), the adaptive clipping method allows an enhancement of the BER and to reduce the pollution of the adjacent channels [94] for the same level of PAPR reduction.

All the publications (See Subsection 2.1.1, pp. 30-42) related with the above mentioned signal processing developments for PAPR reduction are: Journals: [J22], Conferences: [C89, C93, C95, C98, C102], and the participation to the French ANR project ACCENT5 in the technical deliverable D2.1 in [95], and the PhD thesis of Mr. Lamarana DIALLO (2012-2016).

The research work undertaken in M. CHAFII's PhD thesis, focused on the PAPR issue but has a different angle of analysis than the previous work where main target is the design of new techniques and approximations for reducing the PAPR effect. These approximations of the distribution of PAPR of OFDM present in previous work and in the scientific literature, do not explicitly come out the dependence of the PAPR of the modulation waveform. Therefore, the main target was to check whether this dependence is true or not. A general approximation distribution of PAPR that explicitly reveals this dependence was derived in [J25][23]. Thus, instead of using PAPR reduction techniques [96, 97, 98, 99], one can change the PAPR performance by changing the characteristics of the waveform, which gives new insights regarding PAPR reduction. In this work, we show analytically that having a temporal support strictly less than the symbol period is a necessary condition on alternative waveforms with better PAPR than OFDM.

For this study, a multi-carrier system with generalized waveform GWMC (generalized waveforms for multicarrier systems) has been considered. The GWMC transmitted signal is expressed as

$$X(t) \quad = \quad \sum_{n \in Z} \sum_{m=0}^{M-1} C_{m,n} \underbrace{g_m(t - nT)}_{g_{m,n}(t)}, \tag{3.28}$$

where M denotes the number of carriers, $C_{m,n}$ stands for the complex input symbol, time index n, modulated by carrier index m, and T is the GWMC symbol period. The modulation transform and the pulse shaping filter are jointly modeled by a family of functions denoted by $(g_m)_{m \in [\![0, M-1]\!]}$. Note that the model in (3.28) includes the single carrier case. We define the PAPR of the GWMC signal as follows

[22] A copy of this paper titled: "Modified Tone Reservation for PAPR Reduction in OFDM Systems", by Marwa Chaffi, Mamadou Lamarana Diallo, Jacques Palicot, and Faouzi Bader, is depicted at the end of this Subsection.
[23] This Journal paper titled: "A Necessary Condition for Waveforms with Better PAPR than OFDM", by Marwa Chafii, Jacques Palicot, Rémi Gribonval, and Faouzi Bader, is depicted at the end of this Subsection.

$$\begin{aligned} \text{PAPR} &= \frac{\max_{t\in[0,T]} |X(t)|^2}{P_{mean}}, \\ P_{mean} &= \lim_{t_0\to+\infty} \frac{1}{2t_0} \int_{-t_0}^{t_0} E(|X(t)|^2)\, dt. \end{aligned}$$

$E(.)$ is the expectation operator. The mean power P_{mean} is defined over an infinite integration time, because our scenario assumes an infinite transmission time, but the observation is limited to a single GWMC symbol. Note that the PAPR reduction problem can be formulated as the following constrained optimization problem.

$$\begin{aligned} \underset{(g_m)_{m\in[\![0,M-1]\!]}}{\text{maximize}} \quad & \int_0^T \ln(1 - \mathrm{e}^{\frac{-\gamma \sum_{m=0}^{M-1} \|g_m\|^2}{T \sum_{n\in Z} \sum_{m=0}^{M-1} |g_{m,n}(t)|^2}})\, dt, \\ \text{subject to} \quad & A := \min_{m,t} \sum_{n\in Z} |g_{m,n}(t)|^2 > 0. \end{aligned} \tag{3.29}$$

The quantity that we want to maximize in the PAPR optimization problem is equivalent to minimizing the approximation of the complementary cumulative distribution function (CCDF) of the PAPR, subject to the constraint expressed in (3.29). The CCDF is the probability that the PAPR exceeds a defined value γ, i.e. $\Pr(\text{PAPR} \geq \gamma)$.

The condition (3.29), roughly means that the translated versions of every carrier g_m are overlapping in time, and the waveform g_m does not vanish within the symbol period T. If there exists at least an index $m_0 \in [\![0, M-1]\!]$ such that g_{m_0} vanishes in a time interval in the symbol period T and its support is of length at most T, then the family of functions $(g_m)_{m\in[\![0,M-1]\!]}$ does not satisfy the constraint (3.29). In this case, we can also say that g_{m_0} has a temporal support strictly smaller than the symbol period T.

A particular consequence is that g_{m_0} is likely to have a larger frequency support and then a worse frequency localization. This is due to the fact that time frequency localization measure is limited by the Heisenberg uncertainty principle [24].

In order to formulate the PAPR optimization problem, we have first derived in [11] an approximation of the CCDF of the PAPR for the GWMC systems. Based on the Lyapunov central limit theorem (CLT), we showed that the distribution of the signal is approximately Gaussian, and then we derived the approximate distribution of the PAPR by considering a simplifying assumption related to the independence of the samples. To apply the Lyapunov CLT, Lyapunov conditions should be verified. For this purpose, we assumed that the modulation functions satisfy the conditions in (3.29) and $B := \max_{m,t} \sum_{n\in Z} |g_m(t - nT)| < +\infty$, where the second condition is always satisfied for all the functions belonging to L_I^∞ space. In practice, all the waveforms should be bounded and have a finite support, therefore they necessarily belong to L_I^∞, that is why this condition does not appear in the PAPR optimization problem.

It is important to highlight that the assumption of independence of the samples is not always verified in practice, which makes the derived distribution only an approximation. Simulation results showed that for a large number of carriers, the curve based on the theoretical approximation fits the empirical one. For more details about why we need (3.29) to satisfy Lyapunov conditions and how we derive the CCDF approximation based on Lyapunov CLT, the reader can refer to the the work in [11].

An extended theoretical analysis of the PAPR optimization problem can be found in Section III and main obtained results by simulations in Section IV of [J25]. Several families of modulation functions (the modulation transform and the pulse shaping filter) that does not vanish in the symbol period have been investigated and a comparison in terms of PAPR performance between each considered multi-carrier system and the conventional OFDM is presented. Among the analyzed waveforms we have the Walsh-Hadamard-MC (WH-MC) scheme, the weighted cyclic prefix-OFDM (WCP-OFDM) as a variant of the OFDM scheme which gives a weighted version of the cyclic prefix-OFDM by using non-rectangular pulse shapes. The prototype filter out-of-band energy (OBE) defined in

[24] Or sometimes the Heisenberg-Gabor theorem, it states that a function cannot be both time-limited and band-limited (a function and its Fourier transform cannot both have bounded domain). Then, one cannot simultaneously sharply localize a signal in both the time domain and the frequency domain. More details can be found in [100]

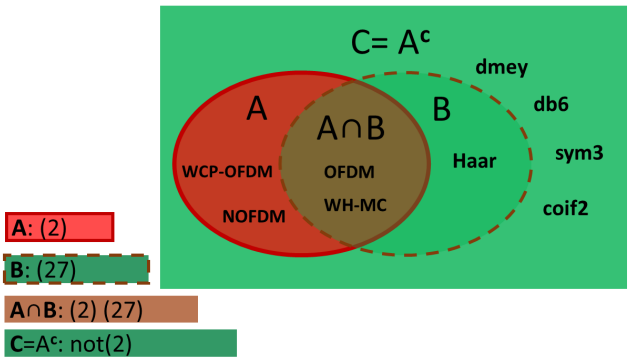

Figure 3.29: Taxonomy of multi-carrier waveforms regarding the PAPR performance, condition (2) here correspond to (3.29) in this manuscript, and (27) is the Lebesgue measure expression of the interval $\mathcal{A}^+$ defined in [J25].

[101] is used in WCP-OFDM, this waveform is also known as orthogonal wavelet division multiplexing (OWDM) [102]. Several wavelets can be used to modulate the input symbols, such as Daubechies, Coiflets, and Symlets. In this work we were interested on the Haar wavelet, which belongs to the family of Daubechies wavelets. The PAPR of other examples of multi-carrier systems from the literature have been also be discussed as the NOFDM, the FBMC, the IOTA FBMC systems based on IOTA, or SRRC filters for example, as well as the universal-filtered multi-carrier (UFMC) systems [103] that have a worse PAPR than the OFDM signal since they do not satisfy the necessary condition stated in (3.29).

Fig. 3.29 summarizes the conclusions of this study. The rectangle represents the set of all GWMC waveforms $\in L_I^\infty$. The optimization problem analyzed in this work is for the waveforms belonging to the set A, which means satisfying (3.29). Systems in $A \cap B$ (including OFDM, WH-MC) have the best possible PAPR performance *among all systems in* A. Any system with better PAPR performance than OFDM must be in C. There are indeed systems (Daubechies 6, Symlet 3, Coiflet 2) in C with better PAPR performance than OFDM. Some are even in B (Haar wavelets), but not in A.
To summarize, It can be concluded that it exists an infinite number of GWMC systems that are optimal in terms of PAPR performance, and conventional OFDM based on the Fourier transform and the rectangular filter belongs to this family. In addition, we have deduced that the PAPR performance of GWMC systems cannot be better than OFDM system without reducing the temporal support of the modulation functions compared to the symbol period. It is worth mentioning that, by limiting the support of the individual carriers, we are moving more and more from a multi-carrier system to a single carrier system. Some examples to illustrate our theoretical results have been provided: WH-MC has a PAPR performance equal to that of OFDM, which is optimal among systems which satisfy condition (3.29), the WCP-OFDM's waveform is not constant over time and thus it is worse than conventional OFDM in terms of PAPR performance. By not satisfying constraint (3.29), it is possible to achieve a better PAPR performance, as it has been shown for the Haar wavelets. Moreover, the work in [J25] also provides a theoretical explanation about why several advanced multi-carrier systems such as NOFDM, FBMC, UFMC, do not achieve a better PAPR than OFDM.
All the publications related with the above mentioned research on the dependence of the PAPR of the modulation waveform are: Journals: [J25, 11], Conferences: [C102, 12, C98, 13, 16, 17], and the PhD thesis of Ms. Marwa CHAFII (2013-2016).

Following are the corresponding depicted papers:

1. [C102]- Mamadou Lamarana Diallo, Marwa Chafii, Jacques Palicot, and Faouzi Bader,"Modified Tone Reservation for PAPR Reduction in OFDM Systems", in Proc. of th European Signal Processing Conference (EUSIPCO'2016), Budapest, Hungary. September 2016.

2. [J25]- Marwa Chafii, Jacques Palicot, Rémi Gribonval, and Faouzi Bader, "A Necessary Condition for Waveforms with Better PAPR than OFDM", IEEE Transactions on Communications, vol. 64, issue: 8, pp. 3395-3405, doi 10.1109/TCOMM.2016.2584068, August 2016.

Modified Tone Reservation for PAPR Reduction in OFDM Systems

Mamadou Lamarana Diallo, Marwa Chafii, Jacques Palicot and Faouzi Bader
CentraleSupélec/IETR/SCEE
Avenue de la boulaie-CS 47601-35576 Cesson Sévigné, Rennes, France
Email: {mamadou-lamarana.diallo,marwa.chafii,jacques.palicot,Faouzi.bader}@supelec.fr

***Abstract*—One of the main drawbacks of orthogonal frequency division multiplex modulation is its high peak-to-average power ratio (PAPR) which can induce poor power efficiency at high power amplifier. Tone reservation (TR) is the most popular PAPR mitigation technique that uses a set of reserved tones to design peak cancelling signal for PAPR reduction. Finding an effective peak cancelling for PAPR reduction in the time domain by using only a small number of reserved tones, is not straightforward. Therefore, we are led to a trade-off between computational complexity and PAPR reduction. The TR method based on the gradient projection algorithm gives the best compromise. In this paper, we propose to modify the classical TR structure. The new proposed method achieves an improvement up to $1.2\,dB$ in terms of PAPR performance without increasing the complexity. The effectiveness of this solution is confirmed through theoretical analysis and simulation results.**

***Index Terms*—OFDM, PAPR, Tone Reservation, CCDF**

I. Introduction

Orthogonal frequency division multiplex (OFDM) modulation, although being used in standards such as IEEE 802.16, IEEE 802.11a/g., HIPERLAN/2, and digital video broadcasting terrestrial (DVB-T2) [1], suffers from high peak-to-average power ratio (PAPR). A signal with high PAPR requires a linear high power amplifier (HPA), which is inefficient in terms of power consumption. To overcome this downside, a larger number of PAPR mitigation techniques have been proposed in the scientific community [2]. Tone reservation (TR) [3] is the most popular adding signal technique for PAPR reduction without bit error rate (BER) distortion and out-of-Band pollution. In fact, the TR approach consists in using a set of reserved tones in order to design the peak cancelling signal. As TR works on reserved tones, no additional signal processing is required at the receiver to extract the data information. Due to these reasons, TR is quite popular for practical implementations and therefore, it was adopted for commercial standards such as (DVB-T2).

There are several studies in the literature about finding the suitable peak cancelling subject to TR constraint [3], [4], [5], [6], [7]. In [3] and [4] the authors propose to use a quadratic constrained quadratic program (QCQP) and a second order cone program (SOCP) respectively, to set the appropriate values on the reserved tones for PAPR mitigation. However, these approaches increase drastically the mean power of the signal and their complexity is very high, which make them not adequate for real time systems. To lower the computation complexity, various methods have been proposed to design the peak cancelling signal subject to TR principle, such as the active-set method [5], one tone-one peak (OPTOP) method [6], and transformation of clipping method as TR method [8]. Actually, the best technique that provides the best compromise between PAPR reduction and computational complexity is the TR method that uses the gradient project algorithm to compute the adding signal by maximizing the signal to clipping ratio, which is equivalent to minimizing the clipping noise [7]. In this paper, a new TR method using the gradient project algorithm is proposed. The main idea of this approach is to modify the classical TR structure by exploiting the decomposition of the useful OFDM symbol as a mixture of two times shorter multicarrier symbols, each containing two times less carriers. Thus, by decomposing conjointly the clipping noise with respect to the decomposition of the useful OFDM symbol, this new approach named modified tone reservation (MTR) consists in minimizing these partial clipping noise subject to the TR constraint with respect to the different components of the useful OFDM symbol after the decomposition.

The remainder of this paper is organized as follows: Section II, briefly reviews the TR principle. Section III describes the MTR principle. The simulation results are presented in Section IV, while in Section V a conclusion is drawn.

II. Overview of TR Techniques

A. Notations and Definitions

Throughout this paper, an OFDM symbol $x(t)$ of duration T_u is used and expressed as follows

$$x(t) = \sqrt{\frac{1}{M}} \sum_{m=0}^{M-1} X_m e^{j2\pi mFt}\ ,\ 0 \leq t \leq T_u. \tag{1}$$

Where M is the total number of carriers, $F = \frac{1}{T_u}$ is the inter-carrier spacing and X_m the symbol carried out by the $m-th$ carrier during T_u. After oversampling the signal by a factor L, x_l, $\{l = 0, \ldots, LM-1\}$ are the discrete time domain samples at the instant lT_e where $T_e = \frac{T_u}{LM}$.
We denote $\mathbf{x} = [x_0, \ldots, x_{LM-1}]$ the vector of the samples of $x(t)$ after the oversampling operation. This vector can be efficiently computed by using an inverse fast Fourier transform (IFFT), and it can be expressed as follows

$$\mathbf{x} = \mathbb{F}_M \breve{\mathbf{X}}. \tag{2}$$

Where $\mathbb{F}_M$ is the normalized IFFT matrix scaled by $\sqrt{L}$ and $\breve{\mathbf{X}}$ is the vector obtained by zero-padding on $\mathbf{X}$. Let $\mathcal{R} = [m_1, \ldots, m_{M_R}] \subset [0, \ldots, M-1]$ be a set of M_R reserved tones. Then, $\mathbb{F}_{M,\mathcal{R}}$ denotes a sub-matrix of $\mathbb{F}_M$ indexed by the column vectors that belong to $\mathcal{R}$. The matrix $\mathbb{F}_{M,\mathcal{R}}$ has LM rows and M_R columns and is used in [7] for the computation of the suitable frequencies data carried by the reserved tones for PAPR reduction.

Hereafter, $\mathbb{F}_K$ represents, more generally, the normalized IFFT matrix of size LK scaled by $\sqrt{L}$ and $\mathbb{F}_{K,\mathcal{X}}$ a sub-matrix of $\mathbb{F}_K$ containing only the column that belong to $\mathcal{X}$.

B. Overview of TR based approaches for PAPR mitigation

The main idea of the TR approach is to use a set of M_R reserved tones (named $\mathcal{R}$) to design the peak cancelling signal. TR approach prevents then BER degradation and out-of-band emissions [7]. In fact, let $\mathbf{c}$ be the peak cancelling addressed to reduce the PAPR of the useful symbol $\mathbf{x}$. Therefore, under the TR constraint $\mathbf{x}+\mathbf{c}$ satisfies the following equation

$$\frac{1}{L}(\mathbf{F}^{\text{Col}}_{M,m})^H(\mathbf{x}+\mathbf{c}) = X_m + C_m = \begin{cases} X_m & \text{if } m \notin \mathcal{R} \\ C_m & \text{if } m \in \mathcal{R} \end{cases}, \quad (3)$$

where $\mathbf{F}^{\text{Col}}_{M,m}$ is the m-*th* column of the matrix $\mathbb{F}$. The scaling by $\frac{1}{L}$ is due to $(\mathbb{F}_M)^H\mathbb{F}_M = L\mathbb{I}$ with $\mathbb{I}$ is the identity matrix. From the (3), it can be remarked that $\mathbf{c} = \mathbb{F}_{M,\mathcal{R}}\mathbf{C}$. Then the TR method rely on finding the suitable frequency vector $\mathbf{C}$. For this purpose, several studies have been proposed in the literature, in order to find the effective peak cancelling signal $\mathbf{c}$ for PAPR reduction [3], [4], [5], [7], [8]. All these approaches are focused on the way of the effective $\mathbf{c}$ can be computed. For instance, in [7] the authors have formulated the computation of $\mathbf{c}$ as a Quadratically Constrained Quadratic Program (QCQP). This approach allows to achieve a good performance in terms of PAPR reduction. Nevertheless, this approach requires high numerical complexity. For real time systems, the best technique that provides the best compromise between PAPR reduction and computational complexity is the TR-Gradient Project (TR-GP) [7] which consists in minimizing the clipping noise by adding a peak cancelling signal subject to TR constraint [3]. This algorithm has been suggested for PAPR reduction in the DVB-T2 standard [1].

Let $\mathbf{x}+\mathbf{c}$ be the transmitted symbol after PAPR reduction. The clipping noise of this symbol is defined in [7] as follows:

$$J(.) = \|\mathbf{x}+\mathbf{c} - f(\mathbf{x}+\mathbf{c}, A)\|_2^2. \quad (4)$$

Where A is a clipping magnitude and $f(.,.)$ a hard clipping function. Fig. 1 gives an illustration of $J(.)$ that we want to minimize by adding a peak cancelling signal.

The TR-GP method, proposed in [7], relies on finding the peak cancelling signal $\mathbf{c}$ by minimizing $J(\mathbf{c})$ via the gradient project algorithm [9] subject to TR constraint, i.e,

$$\min_{\mathbf{C}} \quad \left(\|\mathbf{x}+\mathbb{F}_{M,\mathcal{R}}\mathbf{C} - f(\mathbf{x}+\mathbb{F}_{M,\mathcal{R}}\mathbf{C})\|_2^2\right) \quad (5)$$

Starting with the initial condition of $\mathbf{x}^{(0)} = \mathbf{x}$, it has been shown in [7] that the TR-GP method reduce iteratively the PAPR as follows,

$$\mathbf{x}^{(i+1)} = \mathbf{x}^{(i)} - \mu \sum_{|x_l^{(i)}|>A} \alpha_l^{(i)}\mathbf{P}_l, \quad (6)$$

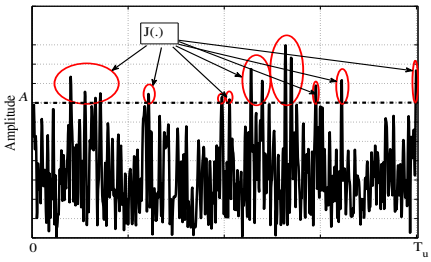

Fig. 1. Illustration of the cost function in TR-GP method.

where $\mathbf{P}_l$ is the l-th line of matrix $\mathbb{P} = \mathbb{F}_R(\mathbb{F}_R)^H$ and $\alpha_l^{(i)} = (x_l^{(i)} - Ae^{j\arg(x_l^{(i)})})$. Note that the matrix $\mathbb{P}$ can be pre-calculated and stored, the numerical complexity of the TR-GP is then $\mathcal{O}(ML)$.

III. Modified Tone Reservation Principle and Problem Formulation

The MTR approach consists in modifying the classical TR structure by using the decomposition of the useful OFDM symbol as a mixture of 4 multi-carriers (after first decomposition) signal or 16 multi-carriers signal (after the double decomposition), see Annexe III-A and Subsection III-B. Thus, by decomposing conjointly $J(.)$ as a sum of a partial clipping noise with respect to the decomposed parts of the useful OFDM symbol, the MTR approach propose to minimize conjointly these partial clipping noise by using the gradient project algorithm (MTR-GP) subject to prevent BER from degrading.

A. The MTR approach based on the first decomposition

Let $\mathbf{x}^1$, $\mathbf{x}^2$, $\mathbf{x}^3$ and $\mathbf{x}^4$ be the multi-carriers symbols derived from the decomposition of $\mathbf{x}$, see Appendix A. Assuming that $\mathbf{x}$ satisfies the TR constraint, i.e, all reserved tones are set to zero, it can be easily verified that (use (21) and (24))

$$\begin{aligned}
\frac{1}{L}(\mathbf{F}^{\text{Col}}_{M_1,m})^H\mathbf{x}^1 = X^1_m &= \begin{cases} X^1_m & \text{Si } m \notin \mathcal{K}^{(0)} \\ 0 & \text{if } m \in \mathcal{K}^{(0)} \end{cases} \\
\frac{1}{L}(\mathbf{F}^{\text{Col}}_{M_1,m})^H\mathbf{x}^3 = X^3_m &= \begin{cases} X^3_m & \text{Si } m \notin \mathcal{K}^{(0)} \\ 0 & \text{if } m \in \mathcal{K}^{(0)} \end{cases} \\
\frac{1}{L}(\mathbf{F}^{\text{Col}}_{M_1,m})^H(\mathbb{D}_{M_1})^H\mathbf{x}^2 = X^2_m &= \begin{cases} X^2_m & \text{Si } m \notin \mathcal{K}^{(1)} \\ 0 & \text{if } m \in \mathcal{K}^{(1)} \end{cases} \\
\frac{1}{L}(\mathbf{F}^{\text{Col}}_{M_1,m})^H(\mathbb{D}_{M_1})^H\mathbf{x}^4 = X^4_m &= \begin{cases} X^4_m & \text{Si } m \notin \mathcal{K}^{(1)} \\ 0 & \text{if } m \in \mathcal{K}^{(1)} \end{cases}
\end{aligned}, \quad (7)$$

where $\mathcal{K}^{(0)} = \frac{\mathcal{R}^{(0)}}{2}$, $\mathcal{K}^{(1)} = \frac{\mathcal{R}^{(1)}-1}{2}$ and $\mathbf{F}^{\text{Col}}_{M_1,m}$ is the m-*th* row of the matrix $\mathbb{F}_{M_1}$ which is a normalized IFFT matrix of size M_1L. The construction of such a matrix is given in Section II-A.

According to the useful OFDM symbol decomposition, the clipping noise $J(.)$ (cost function in TR-GP method) is also decomposed as a sum of the partial clipping noise $J_1(.)$ and $J_2(.)$.

$$\begin{aligned}
J_1(.) &= \|(\mathbf{x}^1+\mathbf{x}^2) - f(\mathbf{x}^1+\mathbf{x}^2, A)\|_2^2 \\
J_2(.) &= \|(\mathbf{x}^3+\mathbf{x}^4) - f(\mathbf{x}^3+\mathbf{x}^4, A)\|_2^2
\end{aligned} \quad (8)$$

Fig. 2 gives an illustration of the partial clipping noise derived from the decomposition of the clipping noise represented in the Fig. 1.

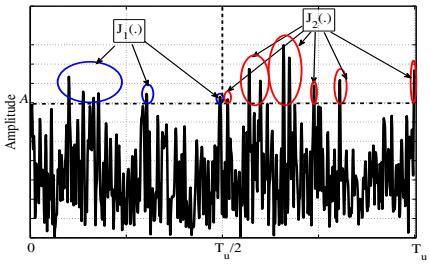

Fig. 2. Illustration of the clipping partial noise $J_1(.)$ and $J_2(.)$.

By using the reserved tones of the symbols derived from the decomposition of the useful symbol $\mathbf{x}$, see (7), the MTR approach consists in finding the signal $\mathbf{c}^1$ and $\mathbf{c}^2$ ($\mathbf{c}^3$ and $\mathbf{c}^4$ respect.) by minimizing $J_1(\mathbf{c}^1+\mathbf{c}^2)$ ($J_2(\mathbf{c}^3+\mathbf{c}^4)$ respect.). The objective is to construct the peak cancelling signal for PAPR reduction $\mathbf{c}$ using $\mathbf{c}^1$, $\mathbf{c}^2$, $\mathbf{c}^3$ and $\mathbf{c}^4$ derived from its decomposition, i.e

$$\mathbf{c} = [\mathbf{c}^1 \bullet \mathbf{c}^3] + [\mathbf{c}^2 \bullet \mathbf{c}^4]. \tag{9}$$

Where $\bullet$ stands for the vectors concatenation operator.

In other words, the MTR-GP method consists in solving the following optimization problems

$$\begin{aligned}\min_{\mathbf{C}^1,\mathbf{C}^2} \quad & (\|\mathbf{x}^1+\mathbf{x}^2+\mathbb{F}_{M_1,\mathcal{K}^{(0)}}\mathbf{C}^1+\tilde{\mathbb{F}}_{M_1,\mathcal{K}^{(1)}}\mathbf{C}^2 \\ & -f(\mathbf{x}^1+\mathbf{x}^2+\underbrace{\mathbb{F}_{M_1,\mathcal{K}^{(0)}}\mathbf{C}^1}_{\mathbf{c}^1}+\underbrace{\tilde{\mathbb{F}}_{M_1,\mathcal{K}^{(1)}}\mathbf{C}^2}_{\mathbf{c}^4},A)\|_2^2),\end{aligned} \tag{10}$$

and,

$$\begin{aligned}\min_{\mathbf{C}^3,\mathbf{C}^4} \quad & (\|\mathbf{x}^1+\mathbf{x}^2+\mathbb{F}_{M_1,\mathcal{K}^{(0)}}\mathbf{C}^3+\tilde{\mathbb{F}}_{M_1,\mathcal{K}^{(1)}}\mathbf{C}^4 \\ & -f(\mathbf{x}^1+\mathbf{x}^2+\underbrace{\mathbb{F}_{M_1,\mathcal{K}^{(0)}}\mathbf{C}^3}_{\mathbf{c}^3}+\underbrace{\tilde{\mathbb{F}}_{M_1,\mathcal{K}^{(1)}}\mathbf{C}^4}_{\mathbf{c}^4},A)\|_2^2).\end{aligned} \tag{11}$$

Let $\mathbb{A}$ be a matrix of dimension $(LM, 2M_R)$ defined by (12) and $\bar{\mathbf{C}} = \left[\mathbf{C}^1 \bullet \mathbf{C}^2 \bullet \mathbf{C}^3 \bullet \mathbf{C}^4\right]$.

$$\mathbb{A} = \begin{bmatrix} \mathbb{F}_{M_1,\mathcal{K}^{(0)}} & \mathbf{0}_{LM_1,K_0} & \tilde{\mathbb{F}}^1_{M_1,\mathcal{K}^{(1)}} & \mathbf{0}_{LM_1,K_1} \\ \mathbf{0}_{LM_1,K_0} & \mathbb{F}_{M_1,\mathcal{K}^{(0)}} & \mathbf{0}_{LM_1,K_1} & \tilde{\mathbb{F}}^2_{M_1,\mathcal{K}^{(1)}} \end{bmatrix} \tag{12}$$

where $\mathbf{0}_{t,z}$ represents a null matrix of size (t,z), K_0 and K_1 denote the number of even and odd tones in $\mathcal{R}$ respectively.

The optimization problems (10) and (11) can be conjointly formulated as follows, thanks to the matrix $\mathbb{A}$

$$\min_{\check{\mathbf{C}}} \left(\|\mathbf{x}+\mathbb{A}\check{\mathbf{C}}-f(\mathbf{x}+\mathbb{A}\bar{\mathbf{C}})\|_2^2\right) \tag{13}$$

It may be noticed that $\mathbf{x}^1$, $\mathbf{x}^2$, $\mathbf{x}^3$ and $\mathbf{x}^4$ are not used in the computation of the peak cancelling signal $\mathbf{c} = \mathbb{A}\bar{\mathbf{C}}$, see (13). The decomposition of the OFDM symbol presented in the Annex allows us only to modify the classical TR structure.

It is important to highlight that $\mathbf{C}^1 \neq \mathbf{C}^3$ and $\mathbf{C}^2 \neq -\mathbf{C}^4$ (the cost functions $J_1(.)$ and $J_2(.)$ are a priori different). Therefore, the peak cancelling signal $\mathbf{c}$ will interfere with the useful carriers of the symbol $\mathbf{x}$. To prevent BER degradation,

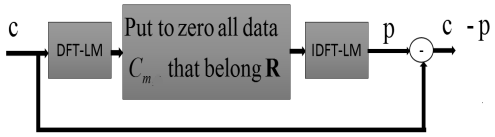

Fig. 3. Digital Frequency Domain Filtering scheme.

a digital frequency domain filtering described in Fig. 3 are proposed.

Let $\mathbf{c}^{ev} = [\mathbf{c}^1 \bullet \mathbf{c}^3]$ and $\mathbf{c}^{odd} = [\mathbf{c}^2 \bullet \mathbf{c}^4]$, from Fig. 3, it can be shown that $C_m^{ev} = \mathbf{F}^{\text{Col}}_{M,m}(\mathbf{c}^{ev})$ and $C_m^{od} = \mathbf{F}^{\text{Col}}_{M,m}(\mathbf{c}^{od})$ satisfy (14) and (15) respectively.

$$C_m^{ev} = \begin{cases} \underbrace{\frac{\mathbf{F}^H_{M_1,p}\mathbb{D}^H_{M_1}\mathbb{F}_{M_1,\mathcal{K}^{(0)}}}{L\sqrt{2}}(\mathbf{C}^1-\mathbf{C}^3)}_{\neq 0} & \text{if } m \in \mathcal{R}^{(1)} \\ C^1_{\frac{m}{2}} + C^3_{\frac{m}{2}} & \text{if } m \in \mathcal{R}^{(0)} (\frac{m}{2} \in \mathcal{K}^{(0)}) \\ 0 & \text{if } m \notin \mathcal{R} \end{cases} \tag{14}$$

$$C_m^{od} = \begin{cases} \underbrace{\frac{\mathbf{F}^H_{M_1,p}\mathbb{D}^H_{M_1}\mathbb{F}_{M_1,\mathcal{K}^{(1)}}}{L\sqrt{2}}(\mathbf{C}^2-\mathbf{C}^4)}_{\neq 0} & \text{if } m \in \mathcal{R}^{(0)} \\ C^2_{\frac{m-1}{2}} + C^4_{\frac{m-1}{2}} & \text{if } m \in \mathcal{R}^{(1)} (\frac{m-1}{2} \in \mathcal{K}^{(1)}) \\ 0 & \text{if } m \notin \mathcal{R} \end{cases} \tag{15}$$

From (14) and (15), it can be observed that $\mathbf{c}^1 \neq \mathbf{c}^3$ and $\mathbf{c}^2 \neq \mathbf{c}^4$ despite the filtering stage. This property represents the new degree of freedom in the optimization problem that will allows us to outperform the classical TR-GP method in terms of PAPR reduction. In fact, subject to $\mathbf{c}^1 = \mathbf{c}^3$ and $\mathbf{c}^2 = \mathbf{c}^4$, i.e, $\mathbf{C}^1 = \mathbf{C}^3$ and $\mathbf{C}^2 = \mathbf{C}^4$, it can be shown through a change of variable that (13) can be formulated as the classical TR-GP method defined by (5). Due to the digital frequency domain filtering stage which requires an FFT and IFFT operation, the MTR-GP method is more complex than the classical TR-GP method. Then, to reduce the computational complexity of the MTR-GP method, we propose to include the frequency domain filtering process directly in the optimization problem. In fact, from the proposed digital frequency domain filtering (see Fig. 3) the signal $\mathbf{p}$ can be computed as follows

$$\mathbf{p} = \frac{1}{L}\left(\mathbb{F}_{M,\mathcal{R}^c}(\mathbb{F}_{M,\mathcal{R}^c})^H\mathbb{A}\right)\check{\mathbf{C}}. \tag{16}$$

Where $\mathcal{R}^c$ is the complementary of $\mathcal{R}$ including the carriers due to the zero padding operation. Therefore, to prevent BER degradation, the optimization problem (13) and the filtering stage can be simultaneously formulated through the following optimization problem

$$\min_{\check{\mathbf{C}}} \left(\|\mathbf{x}+\tilde{\mathbb{A}}\check{\mathbf{C}}-f(\mathbf{x}+\tilde{\mathbb{A}}\check{\mathbf{C}})\|_2^2\right), \tag{17}$$

where $\tilde{\mathbb{A}} = \mathbb{A} - \frac{1}{L}\left(\mathbb{F}_{M,\mathcal{R}^c}\mathbb{F}^H_{M,\mathcal{R}^c}\mathbb{A}\right)$.

As in [7], (17) can be solved thanks to (6) by replacing $\mathbb{P}$ by $\tilde{\mathbb{A}}\tilde{\mathbb{A}}^H$. These two methods have the same computational complexity because $\tilde{\mathbb{A}}\tilde{\mathbb{A}}^H$ can be pre-calculated, and stored. This method will be called as 1-MTR-GP and in following subsection we will briefly extend the MTR principle by iterating the OFDM symbol decomposition.

B. MTR based on the double decomposition: 2-MTR-GP

Going more deeply into the decomposition of the OFDM signal, we proceed, similarly as Appendix A, a second decomposition of the symbol $x(t)$. For this purpose, the symbols

derived from the first decomposition are decomposed similarly as in Annexe A. Through this double decomposition, $\mathbf{x}$ can be expressed as a mixture of 16 multi-carrier symbols with a duration of $\frac{T_u}{4}$ and $M_2 = \frac{M}{4}$ carriers (useful and reserved). Conjointly to this double decomposition, the cost function $J(.)$ is also decomposed as a sum of 4 partial clipping noise $J_{1,1}(.)$, $J_{1,2}(.)$, $J_{2,1}(.)$ and $J_{2,2}(.)$. Fig. 4 gives an illustration of the partial clipping noise derived from the decomposition of the clipping noise depicted in Fig. 1.

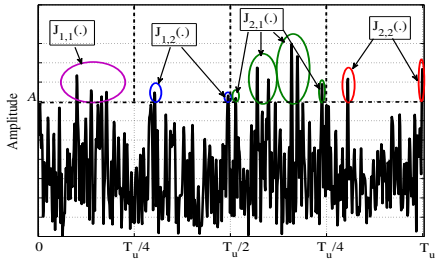

Fig. 4. Illustration of the double decomposition of $J_{[\mathbf{x}]}(.)$

As in Section III-A, the 2-MT-GP method consists in finding the substructures of the peak cancelling signal thanks to the reserved tones of the symbols derived from the double decomposition, by minimizing $J_{1,1}(.)$, $J_{1,2}(.)$, $J_{2,1}(.)$ and $J_{2,2}(.)$. Thus, similarly as in Section III-A, it can be shown that the 2-MTR-GP consists in finding the peak cancelling by solving the following optimisation problem

$$\min_{\breve{\mathbf{C}}_n} \left(\|\mathbf{x} + \mathbb{B}\breve{\mathbf{C}}_n - f(\mathbf{x} + \mathbb{B}\breve{\mathbf{C}}_n)\|_2^2 \right), \tag{18}$$

where $\bar{\mathbf{C}}$ is a frequency vector constructed similarly as in (13), and $\mathbb{B}$ is a matrix of dimension $LM \times 4M_R$ defined as follows

$$\mathbb{B} = \begin{bmatrix} \mathbb{B}^1 & \mathbf{0}_{M_1 L, K_0} & \mathbb{D}_{M_1 L}\mathbb{B}^2 & \mathbf{0}_{M_1 L, K_1} \\ \mathbf{0}_{M_1 L, K_0} & \mathbb{B}^1 & \mathbf{0}_{M_1 L, K_1} & -\mathbb{D}_{M_1 L}\mathbb{B}^2 \end{bmatrix}. \tag{19}$$

The matrix $\mathbb{B}^1$ and $\mathbb{B}^2$ are defined in Appendix B.

To avoid BER degradation, a similar process as in (III-A) can be undertaken. In other words, this is equivalent to solve the following problem

$$\min_{\breve{\mathbf{C}}} \left(\|\mathbf{x} + \tilde{\mathbb{B}}\breve{\mathbf{C}} - f(\mathbf{x} + \tilde{\mathbb{B}}\breve{\mathbf{C}})\|_2^2 \right), \tag{20}$$

where $\tilde{\mathbb{B}} = \mathbb{B} - \frac{1}{L}\left(\mathbb{F}_{M,\mathcal{R}^c} \mathbb{F}_{M,\mathcal{R}^c}^H \mathbb{B} \right)$. This problem can iteratively solved thanks to the gradient project algorithm as previously.

IV. Simulation results

Simulations are performed with a 16-QAM modulated OFDM system that has $M = 256$ carriers wherein $M_R = 12$ carriers are reserved for PAPR reduction. The signal is over-sampled by a factor of four ($L = 4$). The set of reserved tones is $\mathcal{R} = [123, 124, \ldots, 133, 134]$.

Fig. 6 and 5, depict the CCDF before and after PAPR reduction using the TR-GP method , 1-MTR-GP and 2-MTR-GP methods after $N_{\max} = 10$ (number of performed iterations by the GP algorithm) featuring different normalized thresholds $\rho = 5$dB and 6dB. The simulation results depicted in Fig. 6 show that the proposed approaches outperform the classical TR-GP method in terms of PAPR reduction. In fact, with

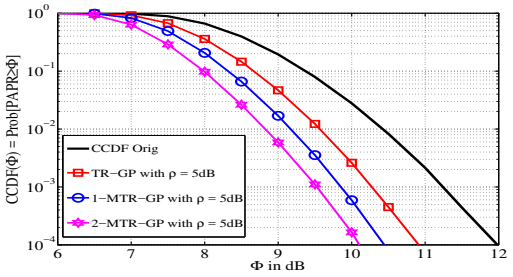

Fig. 5. Performance in term of PAPR reduction with $\rho = 5$dB.

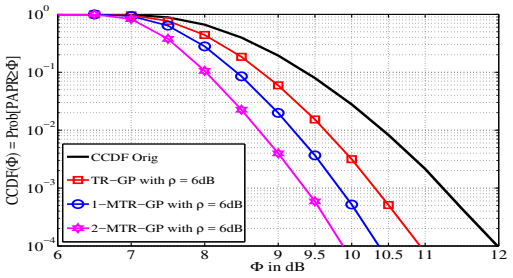

Fig. 6. Performance in term of PAPR reduction with $\rho = 6$dB.

$\rho = 6\,dB$ ($\rho = 5\,dB$ respect.) and $N_{max} = 10$, the achieved PAPR at a clip rate 10^{-4} of the CCDF for the TR-GP, 1-MTR-GP, and 2-MTR-GP are $10.9\,dB$, $10.4\,dB$, and $9.9\,dB$ ($10.9\,dB$, $10.45\,dB$, and $10.12\,dB$ respect.) respectively. Thus, the MTR scheme allow us to improve the PAPR reduction of approximately 1dB. Besides, it can be also noticed that the deeper is the decomposition process of the signal $x(t)$, the better is the PAPR reduction performance achieved of the MTR-GP method.

Fig. (7) evaluates the BER versus E_b/N_0 curves in AWGN channels, where E_b denotes the average bit energy and N_0 is the one-sided power spectral density of the noise component. From these simulation results, it is worth noting that both proposed MTR-GP methods and the classical TR approach prevent the BER degradation as it is noticed in Subsection III-A and III-B.

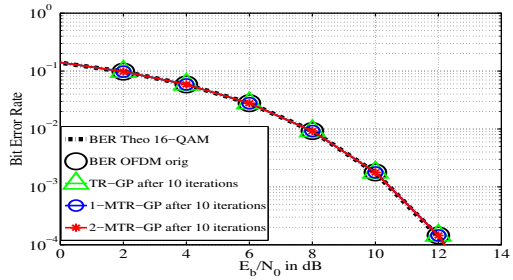

Fig. 7. BER performance of the signal before and after PAPR reduction.

V. Conclusion

In this paper, a new approach of designing the adding signal for PAPR mitigation by modifying the classical TR scheme is proposed. Using the gradient algorithm for the computation of the peak cancelling for PAPR mitigation, we have shown theoretically that it can be expected that our proposed solution outperforms the classical TR-GP method with the same computational complexity. Simulation results approved these theoretical analyses. Moreover, we have shown that going deeply in the decomposition process of the useful OFDM signal achieves better performance for the MTR-GP method. In our future works, the MTR will be analysed for higher decomposition levels.

Appendix A
OFDM symbol decomposition

In this section, we show that an OFDM symbol $x(t)$ can be seen as a mixture of 4 multi-carriers symbols.

Let $\mathbf{X}^1$, $\mathbf{X}^2$, $\mathbf{X}^3$ and $\mathbf{X}^4$ be the data vectors in frequency domain, of size $\frac{M}{2}$ defined as follows:

$$X^1_p = X^3_p = X_{2p} \text{ and } X^2_p = X^4_p = X_{2p+1}. \tag{21}$$

Note that $\mathbf{X}^1$ and $\mathbf{X}^3$ ($\mathbf{X}^2$ and $\mathbf{X}^4$ respect.) contain the data of $\mathbf{X}$ indexed by the even tones (odd tone respect.). Now, let $x^1(t)$, $x^2(t)$, $x^3(t)$ and $x^4(t)$ be the multi-carriers signals defined as

$$\begin{aligned}
x^1(t) &= \sqrt{\frac{1}{M_1}} \sum_{m=0}^{M_1-1} X^1_m e^{j2\pi m F_1 t}, 0 \le t \le T_1,\\
x^3(t) &= \sqrt{\frac{1}{M_1}} \sum_{m=0}^{M_1-1} X^3_m e^{j2\pi m F_1 t}, T_1 \le t \le 2T_1,\\
x^2(t) &= \sqrt{\frac{1}{M_1}} \sum_{m=0}^{M_1-1} X^2_m e^{j2\pi (m F_1+F) t}, 0 \le t \le T_1,\\
x^4(t) &= \sqrt{\frac{1}{M_1}} \sum_{m=0}^{M_1-1} X^4_m e^{j2\pi (m F_1+F) t}, T_1 \le t \le 2T_1.
\end{aligned} \tag{22}$$

with $T_1 = \frac{T_u}{2}$, $M_1 = \frac{M}{2}$ and $F_1 = 1/T_1$.

From 21 and 22 we have

$$x(t) = \begin{cases} x^1(t) + x^2(t), & \text{if } t \in \left]0, \frac{T_u}{2}\right] \\ x^3(t) + x^4(t), & \text{if } t \in \left[\frac{T_u}{2}, T_u\right[\end{cases}. \tag{23}$$

After oversampling using the same oversample rate, let $\mathbf{x}^1$, $\mathbf{x}^2$, $\mathbf{x}^3$ and $\mathbf{x}^4$ be the vectors of the samples of the symbols $x^1(t)$, $x^2(t)$, $x^3(t)$ and $x^4(t)$ respectively. Therefore, after some derivations, we obtain:

$$\begin{aligned}
\mathbf{x}^1 &= \mathbb{F}_{M_1} \check{\mathbf{X}}^1, \quad \text{and} \quad \mathbf{x}^3 = \mathbb{F}_{M_1} \check{\mathbf{X}}^3,\\
\mathbf{x}^2 &= \tilde{\mathbb{F}}_{M_1} \check{\mathbf{X}}^2, \quad \text{and} \quad \mathbf{x}^4 = -\tilde{\mathbb{F}}_{M_1} \check{\mathbf{X}}^4.
\end{aligned} \tag{24}$$

where $\mathbb{F}_{M_1}$ is the normalized IFFT matrix of size $(M_1 L)$, $\tilde{\mathbb{F}}_{M_1} = \mathbb{D}_{M_1} \mathbb{F}_{M_1}$, and $\mathbb{D}_{M_1}$ is a diagonal matrix whose the diagonal is the vector $\mathbf{d} = [1, e^{j2\pi \frac{1}{M_1 L}}, \ldots, e^{j2\pi \frac{M_1 L - 1}{M_1 L}}]$. For $i = 1, .., 4$, the vector $\check{\mathbf{X}}^{(i)}$ is a vector obtained thanks to the zero-padding operation.

Therefore, using (23) $\mathbf{x}$ can be expressed versus $\mathbf{x}^1$, $\mathbf{x}^2$, $\mathbf{x}^3$ and $\mathbf{x}^4$ as follows:

$$\mathbf{x} \quad = \quad [\mathbf{x}^1 \bullet \mathbf{x}^3] + [\mathbf{x}^2 \bullet \mathbf{x}^4]. \tag{25}$$

where $\bullet$ denotes the concatenation operation.

Appendix B
Construction of the MTR matrix

Let $\mathcal{K}^{(0),ev}$ and $\mathcal{K}^{(0),od}$ ($\mathcal{K}^{(1),ev}$ and $\mathcal{K}^{(1),od}$ respect.) be the subsets of $\mathcal{K}^{(0)}$ ($\mathcal{K}^{(1)}$ respect.) containing its even and odd tones (indices) respectively. From these subsets, let $\mathcal{P}^{(0)}$, $\mathcal{P}^{(1)}$, $\mathcal{Q}^{(0)}$, $\mathcal{Q}^{(1)}$ be the following subsets

$$\begin{aligned}
\mathcal{P}^{(0)} &= \frac{\mathcal{K}^{(0),ev}}{2}, \quad \text{and } \mathcal{P}^{(1)} = \frac{\mathcal{K}^{(0),od}}{2},\\
\mathcal{Q}^{(0)} &= \frac{\mathcal{K}^{(1),ev} - 1}{2}, \quad \text{and } \mathcal{Q}^{(1)} = \frac{\mathcal{K}^{(1),od} - 1}{2}.
\end{aligned} \tag{26}$$

The matrix $\mathbb{B}^1$ and $\mathbb{B}^2$ are then defined as follows

$$\mathbb{B}^1 = \begin{bmatrix} \mathbb{F}_{M_2,\mathcal{P}^{(0)}} & \mathbf{0}_{M_2 L, P_0} & \tilde{\mathbb{F}}^1_{M_2,\mathcal{P}^{(1)}} & \mathbf{0}_{M_2 L, P_1} \\ \mathbf{0}_{M_2 L, P_0} & \mathbb{F}_{M_2,\mathcal{P}^{(0)}} & \mathbf{0}_{M_2 L, P_1} & \tilde{\mathbb{F}}^2_{M_2,\mathcal{P}^{(1)}} \end{bmatrix}. \tag{27}$$

where $M_2 = \frac{M}{4}$, P_0 is the cardinal of $\mathcal{P}^{(0)}$ (i.e number of the even tones in $\mathcal{K}^{(0)}$) and P_1 is the cardinal of $\mathcal{P}^{(1)}$ (i.e number of the odd tones in $\mathcal{K}^{(0)}$).

$$\mathbb{B}^2 = \begin{bmatrix} \mathbb{F}_{M_2,\mathcal{Q}^{(0)}} & \mathbf{0}_{M_2 L, Q_0} & \tilde{\mathbb{F}}^1_{M_2,\mathcal{Q}^{(1)}} & \mathbf{0}_{M_2 L, Q_1} \\ \mathbf{0}_{M_2 L, Q_0} & \mathbb{F}_{M_2,\mathcal{Q}^{(0)}} & \mathbf{0}_{M_2 L, Q_1} & \tilde{\mathbb{F}}^2_{M_2,\mathcal{Q}^{(1)}} \end{bmatrix}. \tag{28}$$

where Q_0 is the cardinal of $\mathcal{Q}^{(0)}$ (i.e number of the even tones in $\mathcal{K}^{(1)}$) and Q_1 is the cardinal of $\mathcal{Q}^{(1)}$ (i.e number of the odd tones in $\mathcal{Q}^{(1)}$).

Acknowledgment

Part of this work is supported by the project ACCENT5 (Advanced Waveforms, MAC Design and Dynamic Radio Resource Allocation for D2D in 5G Wireless Networks) funded by the French national research agency with grant agreement code: ANR-14-CE28-0026-02.

References

[1] *DVB: Frame Structure Channel Coding and Modulation for a Scecond Generation Digital Terrestrial Television Broadcasting System DVB-T2*, TR, TR Std., Juin 2008.

[2] H. B. G. Wunder, R. Fischer and S. Litsyn, "The PAPR Problem in OFDM Transmission: New directions for a long-lasting problem," *IEEE Signal Processing Magazine*, pp. 130–140, October 2013.

[3] J. Tellado-Mourelo, "Peak to Average Power Reduction for Multicarrier Modulation," Ph.D. dissertation, Standford University, 1999.

[4] S. Zabre, J. Palicot, Y. Louet, and C. Lereau, "SOCP Approach for OFDM Peak-to-Average Power Ratio Reduction in the Signal Adding Context," in *Signal Processing and Information Technology, 2006 IEEE International Symposium on*, 2006, pp. 834–839.

[5] B. S. Krongold and D. Jones, "A new tone reservation method for complex-baseband par reduction in ofdm systems," in *Acoustics, Speech, and Signal Processing (ICASSP), 2002 IEEE International Conference on*, vol. 3, May 2002, pp. III–2321–III–2324.

[6] E. Bouquet, S. Haese, M. Drissi, C. Moullec, and K. Sayegrih, "An innovative and low complexity papr reduction technique for multicarrier systems," in *Wireless Technology, 2006. The 9th European Conference on*, Sept 2006, pp. 162–165.

[7] J. Tellado and J. Cioffi, "Efficient algorithms for reducing par in multicarrier systems," in *Information Theory, 1998. Proceedings. 1998 IEEE International Symposium on*, Aug 1998, pp. 191–.

[8] L. Wang and C. Tellambura, "Analysis of Clipping Noise and Tone-Reservation Algorithms for Peak Reduction in OFDM Systems," *Vehicular Technology, IEEE Transactions on*, vol. 57, no. 3, pp. 1675–1694, 2008.

[9] A. Hjorungnes and D. Gesbert, "Complex-valued matrix differentiation: Techniques and key results," *Signal Processing, IEEE Transactions on*, vol. 55, no. 6, pp. 2740–2746, June 2007.

A Necessary Condition for Waveforms with Better PAPR than OFDM

Marwa Chafii, *Member, IEEE,* Jacques Palicot, *Member, IEEE,* Rémi Gribonval, *Fellow, IEEE,* and Faouzi Bader, *Senior, IEEE*

***Abstract*—This paper establishes a necessary condition that must be satisfied by the modulation waveforms of any generalized waveforms for multicarrier (GWMC) system with better peak-to-average power ratio (PAPR) than conventional orthogonal frequency division multiplexing (OFDM). GWMC systems include in particular all classical multicarrier modulation systems. As a consequence, we show that OFDM has the best PAPR performance over all GWMC systems that do not satisfy this necessary condition. We also identify an infinite family of GWMC systems with the same PAPR performance as OFDM. To illustrate our results, we present simulations of the PAPR behaviour for different GWMC systems, including some with better PAPR performance than OFDM.**

***Index Terms*—Peak-to-Average Power Ratio (PAPR), Orthogonal Frequency Division Multiplexing (OFDM), Generalized Waveforms for Multi-Carrier (GWMC), Fourier Transforms.**

I. Introduction

THe peak-to-average power ratio (PAPR) [1], [2] is a random variable that measures the power variations of the multicarrier modulation signals. The fluctuations of a multicarrier signal envelope generate non-linear distortions when we introduce the signal into the high power amplifier (HPA), due to the non-linearity of the HPA response. To avoid these distortions, an input back-off is needed in order to amplify the signal in the linear area of the HPA. The larger the PAPR, the larger the input back-off introduced, and the smaller the HPA efficiency. The energy consumption of the power amplifier represents 60% of the total energy consumption in a base station [3]. Therefore, the signal amplitude variations should be reduced in order to reach a better HPA efficiency and minimize the power consumption.

As presented later in the state of the art, several multicarrier modulation systems based on different waveforms have been proposed in the literature as alternatives to conventional orthogonal frequency division multiplexing (OFDM) [4]. In addition to the PAPR, there are several relevant criteria for selecting or designing new waveforms for future multicarrier systems, which include, among others:

- Bit error rate to evaluate reliability of the transmission.
- Complexity to ensure feasibility of the system.
- Bandwidth efficiency to ensure a high transmission rate using the available resources.
- Latency to reduce the delay of the transmission.
- Data rate to meet the needs of high-speed applications.

In this paper, we focus on the PAPR criterion, and we investigate the behaviour of the PAPR regarding to the modulation waveforms. It has been proved that the PAPR depends on the waveform used in the modulation [5], [6]. Thus, instead of using PAPR reduction techniques [7]–[11], one can change the PAPR performance by changing the characteristics of the waveform, which gives new insights regarding PAPR reduction. In this work, we show analytically that *having a temporal support* [1] *strictly less than the symbol period is a necessary condition on alternative waveforms with better PAPR than OFDM* [2].

In fact, we prove that, if the previous necessary condition is not satisfied, i.e if the waveforms have a temporal support larger than or equal to the symbol period, then their PAPR performance cannot be better than that of conventional OFDM. In addition, we identify several multicarrier modulation systems with the same PAPR performance as OFDM. Fig. 9 provides an insight into the conclusions of this work.

A. Paper outline

Our main contributions are to prove that:

1) Among systems which waveforms have a temporal support larger than or equal to the symbol period:
   – The (distribution of the) PAPR is optimal only if the sum of the squared modulus of the individual (multicarrier) waveforms is constant over time. (See (4)).
   – An infinite number of GWMC systems are optimal in terms of PAPR performance.
   – OFDM is among this class of GWMC systems.
   – No better PAPR compared to OFDM is possible, without reducing the temporal support of the waveforms.
2) Signal sets may have better PAPR than OFDM, when the temporal support is limited (e.g. Haar wavelet).

M. Chafii, J. Palicot and Faouzi Bader are with the CentraleSupélec/IETR, 35576 Cesson-Sévigné, France (e-mail:{marwa.chafii, jacques.palicot,faouzi.bader} @supelec.fr).

R. Gribonval is with Inria Rennes-Bretagne Atlantique, 35042 Rennes Cedex, France (e-mail:remi.gribonval@inria.fr.

This work has received a French state support granted to the CominLabs excellence laboratory and managed by the National Research Agency in the "Investing for the Future" program under reference Nb. ANR-10-LABX-07-01. The authors would also like to thank the Region Bretagne, France, for its support of this work.

[1]The support of a function means here the interval outside which the function is equal to zero.

[2]The study here considers OFDM without guard interval, but the analysis is the same for OFDM with cyclic prefix, since the addition of a cyclic prefix does not give any additional information about the peak power.

This article has been accepted for publication in a future issue of this journal, but has not been fully edited. Content may change prior to final publication. Citation information: DOI 10.1109/TCOMM.2016.2584068, IEEE Transactions on Communications

B. State of the art

Several classes of multicarrier modulation systems can be defined [12], [13], based on several characteristics, including whether the modulation is based on the discrete Fourier transform or other transforms, and orthogonal or non-orthogonal schemes. A first distinction can be made:

- **Modulations based on the Fourier transform:** the modulation scheme can be based on the inverse fast Fourier transform (IFFT) at the transmitter side and the fast Fourier transform (FFT) at the receiver side. After the IFFT block, the signal is filtered with pulse shaping filters. Depending on the selected filter, the resulting signal is orthogonal or non-orthogonal. Hereafter, we provide some examples of such waveforms:
  - *OFDM* is a well known orthogonal scheme based on the Fourier transform and the rectangular filter.
  - *NOFDM*: non-orthogonal frequency division multiplexing [14] is a multicarrier modulation system that does not have any restriction about the distance between pulses in the time-frequency plane, and the design of the pulse shape, which leads to a better bandwidth efficiency, while the time frequency location and the shape of the pulses for conventional OFDM are strictly defined.
  - *OFDM/OQAM*:(offset quadrature amplitude modulation) [15]–[17] is a filter bank multicarrier (FBMC) [18] system that allows a flexible selection of the pulse shaping filters, such as the isotropic orthogonal transform algorithm (IOTA) [19], the extended Gaussian functions (EGF), the PHYDYAS filter [3], and the Hermite filters, in order to reduce side lobes without using guard bands in contrast to conventional OFDM. OFDM/OQAM does not use a cyclic prefix.
  - *GFDM*: generalized frequency division multiplexing [20], [21] is a non-orthogonal scheme which allows the use of well-localized filters to avoid out-of-band emissions. The modulation is performed block by block, where each GFDM data block consists of a certain number of carriers and symbols. A cyclic prefix can be added in the GFDM data block, along with tail biting in the pulse shape.

  For more details, a taxonomy of multicarrier modulation systems is proposed in [12]. For the different pulse shaping filters, the reader can refer to [13] that defines and gives the analytical expression and characteristics of the most popular prototype filters in the literature.
- **Modulations based on other transforms**: instead of performing the modulation based on the Fourier transform, other transforms can be used. These are examples reported in the literature:
  - *The Wavelet Transform* is widely used in wireless communication applications. These multicarrier modulation systems can be based on the discrete wavelet transform (DWT) [22] or the wavelet packet transform (WPT) [23].
  - *The Walsh-Hadamard Transform* can be used as a modulation basis for multicarrier modulation systems. In [24], the author introduces the Walsh-Hadamard transform for multicarrier modulation applications, and compares it with the Fourier transform in conventional OFDM. It has been also showed that multicarrier modulation systems based on the Walsh-Hadamard transform are more suitable for optical communications than OFDM at short distance transmission, in terms of computational complexity [25].
  - *The Discrete Cosine Transform (DCT)* has been proposed in the literature [26], [27] as a modulation basis for multicarrier systems. In [28], the multicarrier modulation scheme based on the DCT has been proved better than OFDM in terms of BER under certain channel conditions.

The remainder of this paper is structured as follows. In Section II, we define the generalized waveforms for multicarrier (GWMC) system considered in our derivations, and we formulate the PAPR reduction problem as an optimization problem. The solution of this problem is given in Section III with the whole proof behind. To support the theoretical results, we illustrate some examples of multicarrier modulation systems in Section IV. Finally, Section V concludes the paper and opens new perspectives of the work.

II. Problem Formulation

A. Notation: the GWMC model

The GWMC system is a generalization of classical multicarrier modulation systems based on a larger choice of modulation schemes. The GWMC transmitted signal is expressed as

$$X(t) \quad = \quad \sum_{n\in} \sum_{m=0}^{M-1} C_{m,n} \underbrace{g_m(t-nT)}_{g_{m,n}(t)}, \tag{1}$$

where M denotes the number of carriers, $C_{m,n}$ stands for the complex input symbol, time index n, modulated by carrier index m, and T is the GWMC symbol period. The modulation transform and the pulse shaping filter are jointly modeled by a family of functions denoted by $(g_m)_{m\in[\![0,M-1]\!]}$. Note that the model in (1) includes the single carrier case.

We define the PAPR of the GWMC signal as follows

$$\begin{aligned} \text{PAPR} &= \frac{\max_{t\in[0,T]} |X(t)|^2}{P_{mean}}, \\ P_{mean} &= \lim_{t_0\to+\infty} \frac{1}{2t_0} \int_{-t_0}^{t_0} E(|X(t)|^2)\, dt. \end{aligned}$$

$E(.)$ is the expectation operator. The mean power P_{mean} is defined over an infinite integration time, because our scenario assumes an infinite transmission time, but the observation is limited to a single GWMC symbol.

B. Main assumptions

The number of carriers is supposed to be $M \geq 8$. This is an assumption made for the validity of the central limit theorem. We assume that $(C_{m,n})_{(m\in[\![0,M-1]\!],\, n\in\mathbb{Z})}$ are independent and identically distributed, with zero mean and unit variance σ_C^2. Let $(g_m)_{m\in[\![0,M-1]\!]} \in L_I^\infty$, where L_I^∞ is the space of essentially bounded functions which vanish outside a finite interval I. Then we have

$$\forall m \in [\![0, M-1]\!] \quad \forall t \notin I \quad g_m(t) \quad = \quad 0.$$

[3]Physical Layer For Dynamic Spectrum Access And Cognitive Radio, more details on http://www.ict-phydyas.org/

This article has been accepted for publication in a future issue of this journal, but has not been fully edited. Content may change prior to final publication. Citation information: DOI 10.1109/TCOMM.2016.2584068, IEEE Transactions on Communications

C. Optimization problem associated to PAPR reduction

As we will soon recall in Section II-E, the PAPR reduction problem can be formulated as the following constrained optimization problem.

The PAPR Optimization Problem.

$$\underset{(g_m)_{m\in[\![0,M-1]\!]}}{\textit{maximize}} \quad \int_0^T \ln(1-\mathrm{e}^{\frac{-\gamma\sum_{m=0}^{M-1}\|g_m\|^2}{T\sum_{n\in\mathbb{Z}}\sum_{m=0}^{M-1}|g_{m,n}(t)|^2}})\,dt,$$
$$\textit{subject to} \quad A := \min_{m,t}\sum_{n\in Z}|g_{m,n}(t)|^2 > 0. \tag{2}$$

The quantity that we want to maximize in the PAPR optimization problem is equivalent to minimizing the approximation of the complementary cumulative distribution function (CCDF) of the PAPR, subject to the constraint expressed in (2). The CCDF is the probability that the PAPR exceeds a defined value γ, i.e. $\Pr(\text{PAPR} \geq \gamma)$.

D. The meaning of condition (2)

Roughly speaking, (2) means that the translated versions of every carrier g_m are overlapping in time, and the waveform g_m does not vanish within the symbol period T.

If there exists at least an index $m_0 \in [\![0, M-1]\!]$ such that g_{m_0} vanishes in a time interval in the symbol period T and its support is of length at most T, then the family of functions $(g_m)_{m\in[\![0,M-1]\!]}$ does not satisfy (2). In this case, we can also say that g_{m_0} has a temporal support strictly smaller than the symbol period T.

A particular consequence is that g_{m_0} is likely to have a larger frequency support and then a worse frequency localization. This is due to the fact that time frequency localization measure is limited by the Heisenberg uncertainty principle [4].

E. Origins of the optimization problem formulation

In order to formulate the PAPR optimization problem, we have first derived in [6] an approximation of the CCDF of the PAPR for the GWMC systems. Based on the Lyapunov central limit theorem (CLT), we showed that the distribution of the signal is approximately Gaussian, and then we derived the approximate distribution of the PAPR by considering a simplifying assumption related to the independence of the samples. To apply the Lyapunov CLT, Lyapunov conditions should be verified. For this purpose, we assumed that the modulation functions satisfy the conditions in (2) and $B := \max_{m,t}\sum_{n\in Z}|g_m(t-nT)| < +\infty$, where the second condition is always satisfied for all the functions belonging to L_I^∞ space. In practice, all the waveforms should be bounded and have a finite support, therefore they necessarily belong to L_I^∞, that is why this condition does not appear in the PAPR optimization problem.

It is important to highlight that the assumption of independence of the samples is not always verified in practice, which makes the derived distribution only an approximation. Simulation results showed that for a large number of carriers, the curve based on the theoretical approximation fits the empirical one. For more details about why we need (2) to satisfy Lyapunov conditions and how we derive the CCDF approximation based on Lyapunov CLT, the reader can refer to the authors work in [6].

[4]Or sometimes the Heisenberg-Gabor theorem, it states that a function cannot be both time-limited and band-limited (a function and its Fourier transform cannot both have bounded domain). Then, one cannot simultaneously sharply localize a signal in both the time domain and the frequency domain. More details can be found in [29].

III. Main Theoretical Results

In this section, the solution of the PAPR optimization problem is presented. The PAPR optimality of conventional OFDM is also proved and discussed. The early work in this context goes back to the study undertaken by A. Skrzypczak et al. for OFDM/OQAM and oversampled OFDM [30], where it has been shown analytically that the PAPR performance for the latest two multicarrier modulation systems based on different pulse shapes is not better than that of conventional OFDM with the rectangular pulse shape.

Based on simulation results, A. Kliks [31] has further noticed that, when simulating the CCDF of the PAPR for the generalized multicarrier (GMC) signal for different pulses, the lowest values are obtained for the rectangular pulse. In the analysis conducted in this paper, we consider the GWMC system, which is a generalization of classical multicarrier modulation systems and based on a larger choice of modulation schemes.

A. Overview of the main results

Let $H_0 \approx 0.63$ be the unique solution to the equation $1 - 2H_0 + 2H_0\mathrm{e}^{\frac{-1}{H_0}} = 0$ (see Appendix). For a given GWMC system $\{g_m\}$, we define the "critical" value of γ for this system as

$$\gamma_{\text{crit}}(\{g_m\}) \quad := \quad \sup_{t\in[0,T]} \frac{T\sum_{m=0}^{M-1}\sum_{n\in}|g_{m,n}(t)|^2}{H_0\sum_{m=0}^{M-1}\|g_m\|^2}. \tag{3}$$

Our main technical result is the following proposition, where the proof will be provided in Section III-C.

Property 1. *(*Sufficient condition for optimality*)*
Assume that $\gamma \geq 1/H_0$ and consider any GWMC system $\{g_m^*\}$ satisfying (2) *and*

$$\sum_{m=0}^{M-1}\sum_{n\in}|g_{m,n}^*(t)|^2 \qquad \textit{is constant over time.} \tag{4}$$

For this system $\gamma_{crit}(\{g_m^*\}) = 1/H_0$ has the minimum possible value.
At level γ, the CCDF of the PAPR of the system $\{g_m^*\}$ is lower (corresponding to a better PAPR) than that of any other system $\{g_m\}$ satisfying (2) *such that $\gamma \geq \gamma_{crit}(\{g_m\})$.*

In other words, the GWMC system $\{g_m^*\}$ has globally optimal PAPR performance at level γ among all GWMC systems satisfying (2) *and $\gamma \geq \gamma_{crit}(\{g_m\})$.*

The condition in (4) means that the statistical mean of the instantaneous power of the transmitted signal $E(|x(t)|^2)$ is constant over time.

Corollary 1. *(*Optimality of conventional OFDM*)*
Consider $\{g_m\}$ a GWMC system satisfying (2)*. For any $\gamma \geq$*

This article has been accepted for publication in a future issue of this journal, but has not been fully edited. Content may change prior to final publication. Citation information: DOI 10.1109/TCOMM.2016.2584068, IEEE Transactions on Communications

$\gamma_{crit}(\{g_m\})$, this system has PAPR performance at level γ no better than that of OFDM, the Walsh-Hadamard system, and of any other GWMC system satisfying (4).

These results will be illustrated in Sections IV-A and IV-B.

Hence, the logical contraposition of Corollary 1 gives the following Theorem.

Theorem. (Necessary condition for improving PAPR performance)
Consider a GWMC system $\{g_m\}$ and $\gamma \geq \gamma_{crit}(\{g_m\})$. If this GWMC system has better PAPR performance at level γ than OFDM, then $\{g_m\}$ necessarily violates condition (2).

As explained in Section II-D, the fact that GWMC violates condition (2) means that the temporal support of at least one modulation function must be strictly smaller than the symbol period. Thus, we are led to a trade-off between frequency localization of multicarrier waveforms and PAPR performance. This phenomenon will be illustrated in Section IV-C.

B. Discussion

The condition $\gamma \geq \gamma_{\text{crit}}(\{g_m\})$ satisfied by a GWMC system means that our results are valid for the values of γ greater than a threshold value $\gamma_{\text{crit}}(\{g_m\})$.

For any GWMC system satisfying (2) such that OFDM or Walsh-Hadamard multicarrier system, we have $\gamma_{\text{crit}} \approx 2$dB. For the weighted cyclic prefix-OFDM system discussed in Section IV-B, we have $\gamma_{\text{crit}} \approx \frac{1.2}{H_0} = 2.7$dB.

Our analysis does not cover the values of γ smaller than γ_{crit}. In practice, the PAPR of multicarrier modulation systems is greater than γ_{crit}. Thus, this interval does not represent an interval of interest.

C. Proof

Replacing the PAPR Optimization Problem with a Simpler Problem. In order to characterize the optima of the PAPR optimization problem, we first show that it can be rewritten in a simpler form. We start by noticing that the functions $(g_m)_{m\in[\![0,M-1]\!]}$ perform the same role and only the sum $\sum_{n\in\mathbb{Z}}\sum_{m=0}^{M-1}|g_{m,n}(t)|^2$ is involved in the maximized quantity, the maximization can thus be performed over only one non-negative function $G(t)$, such that

$$G(t) = \sum_{m=0}^{M-1}\sum_{n\in\mathbb{Z}}|g_{m,n}(t)|^2. \tag{5}$$

Note that (2) implies that $a := \inf_t G(t) > 0$. Similarly, $G \in L^\infty([0,T])$, L^∞ is the space of essentially bounded functions. Moreover,

$$\begin{aligned}\int_0^T G(\tau)d\tau &= \int_0^T \sum_{m=0}^{M-1}\sum_{n\in} |g_{m,n}(t)|^2\, dt \\ &= \sum_{m=0}^{M-1}\sum_{n\in}\int_{nT}^{nT+T}|g_m(t)|^2\, dt \\ &= \sum_{m=0}^{M-1}\int_{-\infty}^{+\infty}|g_m(t)|^2\, dt \\ &= \sum_{m=0}^{M-1}\|g_m\|^2. \end{aligned}\tag{6}$$

The optimization problem can thus be expressed as

$$\begin{aligned}\underset{G\in L^\infty([0,T])}{\text{maximize}} \quad & \beta(G) = \int_0^T \ln(1-\mathrm{e}^{\frac{-\gamma\int_0^T G(\tau)d\tau}{TG(t)}})\, dt. \\ \text{subject to} \quad & \exists\, a \text{ such that} \\ & G(t) \geq a > 0.\end{aligned}\tag{7}$$

Finally, the condition $\gamma \geq \gamma_{\text{crit}}(\{g_m\})$ is equivalent to

$$\sup_{t\in[0,T]} G(t) \leq \gamma H_0 \int_0^T G(\tau)d\tau.$$

Remark 1. *Denoting $H(t) := G(Tt)$, we have*

$$\begin{aligned}\beta(G) &= T\int_0^1 \ln(1-\mathrm{e}^{\frac{-\gamma\int_0^1 H(\tau)d\tau}{H(t)}})\, dt &(8)\\ &=: T\tilde{\beta}(H), &(9)\\ \text{and} \quad & H \geq a > 0. &(10)\end{aligned}$$

Maximizing β with respect to $G \in L^\infty([0,T])$ is then equivalent to maximizing $\tilde{\beta}$ with respect to $H \in L^\infty([0,1])$.

Moreover the expression of $\tilde{\beta}(H)$ does not change if we multiply the function $H(t)$ by a scalar: for all $\lambda \in \mathbb{R}^{*+}$, we have

$$\tilde{\beta}(\lambda H) = \tilde{\beta}(H). \tag{11}$$

It follows that if the problem in (7) *has an optimal solution, then there exists an infinite set of optimal solutions obtained by scaling the first solution.*

From Remark 1, we can search the maximizer of $\tilde{\beta}$ under the additional normalization constraint

$$\gamma\int_0^1 H(\tau)d\tau = 1. \tag{12}$$

If G is an optimum of problem (7), then $H(t) := \frac{TG(tT)}{\gamma\int_0^T G(\tau)d\tau}$ is an optimum of the following optimization problem

$$\begin{aligned}\underset{H\in L^\infty([0,1])}{\text{maximize}} \quad & \tilde{\beta}(H) := \int_0^1 \ln(1-\mathrm{e}^{\frac{-1}{H(t)}})\, dt. \\ \text{subject to} \quad & H \text{ satisfies (12) and } \exists\, a \text{ such that} \\ & H(t) \geq a > 0.\end{aligned}\tag{13}$$

Vice-versa, if H is an optimum of the above problem then $G(t) = H(t/T)$ is an optimum of problem (7). The rest of the study therefore focuses on characterizing the optima of problem (13).

Note that the condition $\gamma \geq \gamma_{\text{crit}}(\{g_m\})$ now read simply

$$\sup_{t\in[0,T]} H(t) \leq H_0.$$

Theoretical Analysis. We define the following convex subsets of L^∞:

- $\mathcal{F} := \left\{H : [0,1] \to \mathbb{R}^{*+} \text{ such that } \int_0^1 H(\tau)d\tau = \frac{1}{\gamma}\right\}$,
- $\mathcal{F}_a := \mathcal{F} \cap \{H : [0,1] \to \mathbb{R}^{*+} \text{ such that } H \geq a\}$,
- $\mathcal{F}_+ := \underset{a>0}{\cup}\mathcal{F}_a$.

We consider here the optimization problem in (13). To characterize its optima, we first recall the definition of its stationary points.

Definition 1. *We say that a function $H^* \in \mathcal{F}_a$ is a stationary point of $\tilde{\beta}$ defined in* (13) *if and only if: for any $\varphi \in L^\infty([0,1])$ such that*

$$\int_0^1 \varphi(t)\, dt = 0, \tag{14}$$

This article has been accepted for publication in a future issue of this journal, but has not been fully edited. Content may change prior to final publication. Citation information: DOI 10.1109/TCOMM.2016.2584068, IEEE Transactions on Communications

we have

$$\left.\frac{d\tilde{\beta}(H^*+\epsilon\varphi)}{d\epsilon}\right|_{\epsilon=0} = 0. \quad (15)$$

Notice that for all φ satisfying (14), the function $H = H^* + \epsilon\varphi$ satisfies (12). For a small enough ϵ, $H = H^* + \epsilon\varphi$ also satisfies (10).

The solution of the optimization problem is organized as follows

Lemma 1.
Let H_0 be the unique solution to the equation $1 - 2H_0 + 2H_0 e^{\frac{-1}{H_0}} = 0$. For any $\varphi \in L^\infty([0,1])$ which satisfies (14)*, we have: for any $H \in \mathcal{F}_+$,*

$$\text{If} \quad \sup_t H(t) \le H_0, \quad \text{then} \quad \left.\frac{d^2\tilde{\beta}(H^*+\epsilon\varphi)}{d\epsilon^2}\right|_{\epsilon=0} \le 0. \quad (16)$$

Lemma 2.
The constant function $H^* = \frac{1}{\gamma}$ is the unique stationary point of the optimization problem (13) *over the set $\mathcal{F}_+$.*

Corollary 2. *If $\gamma \ge \frac{1}{H_0}$ then the constant function $H^* = \frac{1}{\gamma}$ is a local maximum of problem* (13)*. Moreover, it is a* global *maximum of* (13) *among all H such that $\sup_t H(t) \le H_0$.*

Hereafter, the proofs are presented.

1) Proof of Lemma 1: Let H_0 be the unique solution to the equation $1 - 2H_0 + 2H_0 e^{\frac{-1}{H_0}} = 0$ (see Appendix), and $H \in \mathcal{F}_+$.

Since $H \in \mathcal{F}_+$ and φ is bounded, there is $\epsilon_0 > 0$ such that for any ϵ such that $|\epsilon| \le \epsilon_0$, the constraint in (10) holds. We now explicit the derivatives involved in (15). We have

$$\tilde{\beta}(H+\epsilon\varphi) = \int_0^1 \ln(1 - e^{\frac{-1}{H(t)+\epsilon\varphi(t)}})\, dt$$

$$\frac{d\tilde{\beta}(H+\epsilon\varphi)}{d\epsilon} = \int_0^1 \frac{\frac{-\varphi(t)}{(H(t)+\epsilon\varphi(t))^2} e^{\frac{-1}{(H(t)+\epsilon\varphi(t))}}}{1 - e^{\frac{-1}{(H(t)+\epsilon\varphi(t))}}} dt \quad (17)$$

$$\frac{d^2\tilde{\beta}(H+\epsilon\varphi)}{d\epsilon^2} = \int_0^1 \frac{d}{d\epsilon}\left(\frac{\frac{-\varphi(t)}{(H(t)+\epsilon\varphi(t))^2} e^{\frac{-1}{(H(t)+\epsilon\varphi(t))}}}{1 - e^{\frac{-1}{(H(t)+\epsilon\varphi(t))}}}\right) dt$$

$$= \int_0^1 \frac{\left(\frac{2\varphi^2}{(H-\epsilon\varphi)^3} + \frac{\varphi^2}{(H+\epsilon\varphi)^4}\right) e^{\frac{-1}{H+\epsilon\varphi}} (1 - e^{\frac{-1}{H+\epsilon\varphi}})}{(1 - e^{\frac{-1}{H+\epsilon\varphi}})^2} dt$$

$$+ \int_0^1 \frac{\left(\frac{\varphi}{(H+\epsilon\varphi)^2} e^{\frac{-1}{H+\epsilon\varphi}}\right)\left(\frac{-\varphi}{(H+\epsilon\varphi)^2} e^{\frac{-1}{H+\epsilon\varphi}}\right)}{(1 - e^{\frac{-1}{H+\epsilon\varphi}})^2} dt,$$

$$\left.\frac{d^2\tilde{\beta}(H+\epsilon\varphi)}{d\epsilon^2}\right|_{\epsilon=0} = -\int_0^1 \frac{\left(\frac{-2\varphi^2}{H^3} + \frac{\varphi^2}{H^4}\right) e^{\frac{-1}{H}} (1 - e^{\frac{-1}{H}})}{(1 - e^{\frac{-1}{H}})^2} dt$$

$$- \int_0^1 \frac{\frac{\varphi^2}{H^4} e^{\frac{-2}{H}}}{(1 - e^{\frac{-1}{H}})^2} dt.$$

$$\left.\frac{d^2\tilde{\beta}(H+\epsilon\varphi)}{d\epsilon^2}\right|_{\epsilon=0} = -\underbrace{\int_0^1 \frac{\frac{\varphi^2}{H^4} e^{\frac{-1}{H}}}{(1 - e^{\frac{-1}{H}})^2}}_{\ge 0} \underbrace{(1 - 2H + 2He^{\frac{-1}{H}})}_{s(H)} dt.$$

In Appendix, we show that $s(H) \ge 0$ whenever $H \le H_0$. We conclude that, if $\sup_t H(t) \le H_0$ then

$$\frac{d^2\tilde{\beta}(H^*+\epsilon\varphi)}{d\epsilon^2} \le 0. \quad (18)$$

2) Proof of Lemma 2: Consider $H^* \in \mathcal{F}_+$. Let $\varphi \in L^\infty([0,1])$ be such that (14) holds. We have from (17)

$$\left.\frac{d\tilde{\beta}(H+\epsilon\varphi)}{d\epsilon}\right|_{\epsilon=0} = \int_0^1 \frac{\frac{-\varphi(t)}{H^2(t)} e^{\frac{-1}{H(t)}}}{1 - e^{\frac{-1}{H(t)}}} dt.$$

Defining

$$\zeta(t) = \frac{e^{\frac{-1}{H^*(t)}}}{[1 - e^{\frac{-1}{H^*(t)}}] H^{*2}(t)}, \quad (19)$$

it follows that (15) is equivalent to,

$$\int_0^1 \varphi(t)\zeta(t)dt = 0. \quad (20)$$

At this stage, we can check that if $H^* = \frac{1}{\gamma}$ then $\zeta(t) = c_0$ does not depend on t, hence we have established that for any $\varphi(t)$ satisfying (14), we must have: $\int_0^1 \zeta(t)\varphi(t)dt = c_0 \int_0^1 \varphi(t)dt = 0$, i.e. (15) holds. This shows, as claimed, that $H^* = \frac{1}{\gamma}$ is a stationary point of (13) under the constraints in (10) and (12). We will now prove the converse.

We assume now that $H^* \in F_+$ is a stationary point of (13) with the constraints in (10) and (12). What we have just established is that (20) must hold for all φ that satisfies (14). ζ is then orthogonal to all the zero mean functions $\varphi \in L^\infty$. Thus, ζ is a constant c_0, i.e.

$$\frac{e^{\frac{-1}{H^*(t)}}}{[1 - e^{\frac{-1}{H^*(t)}}] H^{*2}(t)} = c_0. \quad (21)$$

Hence, $\exists\, c_0 \in \mathbb{R}$ such that $\forall t \in [0,1]$ $H^*(t)$ belongs to the set of solutions of the equation $J(H) = c_0$ with

$$J(H) = \frac{e^{\frac{-1}{H}}}{[1 - e^{\frac{-1}{H}}] H^2}. \quad (22)$$

To conclude that H^* itself be constant, we now analyse the variations of the function $J(H)$.

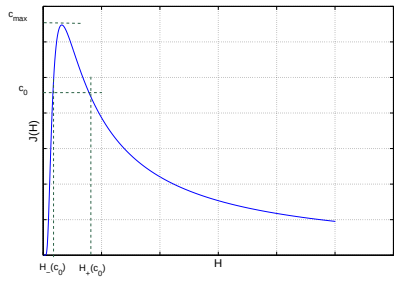

Figure 1: Curve of the function $J(H)$.

The simulation of $J(H)$ in Fig. 1, shows that for a certain value c_0, the line of equation $J(H) = c_0$ cuts the curve of the function J in a single point which coincides with the maximum value of J that we note $c_{\max}$, and two distinct points when c_0 is less than $c_{\max}$. When c_0 is greater than $c_{\max}$ the line does not cut the curve of J.

Thus, the set S_J of solutions for (21) is

$$S_J = \begin{cases} H_+(c_0), H_-(c_0) & \text{if} \quad 0 < c_0 \le c_{\max}, \\ \emptyset & \text{if} \quad c_0 > c_{\max}. \end{cases} \quad (23)$$

This article has been accepted for publication in a future issue of this journal, but has not been fully edited. Content may change prior to final publication. Citation information: DOI 10.1109/TCOMM.2016.2584068, IEEE Transactions on Communications

Table I: Solutions of (21) for different values of c_0.

c_0	$H_-(c_0)$	$H_+(c_0)$
0.64	0.720	00.72
0.62	0.510	00.83
0.60	0.450	00.90
0.50	0.360	01.34
0.40	0.300	01.90
0.30	0.250	02.76
0.20	0.210	04.46
0.10	0.170	09.48
0.05	0.145	19.50
0.02	0.091	49.49
0.01	0.085	99.49

Table II: Variations of H_+, H_- and $\frac{1}{H_+-H_-}$ as a function of c_0.

c_0	0	$c_{\max}$
H_+	$+\infty$ ↘	$H_{\max}$
H_-	0 ↗	$H_{\max}$
$\frac{1}{H_+-H_-}$	0 ↗	$+\infty$

Note that when $c_0 = c_{\max}$, we have $H_+(c_0) = H_-(c_0)$. $H_+(c_0)$ is the greatest solution, and $H_-(c_0)$ is the smallest one $(H_-(c_0) \leq H_+(c_0))$.

The following property summarizes what we have established so far

Property 2. *Let $H^* \in \mathcal{F}_+$ be a stationary point of $\tilde{\beta}$, under the constraints in* (10) *and* (12)*. There exists a constant $c_0 \in [0, c_{\max}]$, a set $\mathcal{A}_+$ and a set $\mathcal{A}_- = [0,1] \setminus \mathcal{A}_+$ such that*

$$H_{|\mathcal{A}_+} = H_+(c_0), \quad \textit{and} \quad H_{|\mathcal{A}_-} = H_-(c_0). \tag{24}$$

$H_{|\mathcal{A}_+}$ ($H_{|\mathcal{A}_-}$ respectively) is the restriction of the function H over the set $\mathcal{A}_+ \subset [0,1]$ ($\mathcal{A}_- \subset [0,1]$ respectively).

Corollary 3. *The Lebesgue measure of the interval $\mathcal{A}_+$ can be expressed as*

$$\tilde{L}_{\mathcal{A}_+(c_0)} = \frac{\frac{1}{\gamma} - H_-(c_0)}{H_+(c_0) - H_-(c_0)} \in [0,1]. \tag{25}$$

In fact, from (12) and Property 1, we have

$$\tilde{L}_{\mathcal{A}_+}(c_0) H_+(c_0) + (1 - \tilde{L}_{\mathcal{A}_+}) H_-(c_0) = \frac{1}{\gamma}, \tag{26}$$

$$\tilde{L}_{\mathcal{A}_+}(c_0)(H_+(c_0) - H_-(c_0)) = \frac{1}{\gamma} - H_-(c_0). \tag{27}$$

Property 3. *Let $H^* \in \mathcal{F}_+$ be a stationary point of $\tilde{\beta}$, under the constraints in* (10) *and* (12)*. Then, the value of c_0 solves the following optimization problem*

$$\begin{aligned} \underset{c_0}{\textit{maximize}} \quad & \tilde{\beta}(c_0) = \tilde{L}_{\mathcal{A}_+}(c_0) \ln(1 - \mathrm{e}^{-\frac{1}{H_+(c_0)}}) \\ & \qquad + (1 - \tilde{L}_{\mathcal{A}_+}(c_0)) \ln(1 - \mathrm{e}^{-\frac{1}{H_-(c_0)}}), \\ \textit{subject to} \quad & \tilde{L}_{\mathcal{A}_+}(c_0) \in [0,1]. \end{aligned}$$

Numerical Results: Table I shows for each value of c_0 the set of solutions S_J of (21). As we can see, $H_-(c_0)$ is an increasing function of c_0 and $H_+(c_0)$ is a decreasing function of c_0, we can resume these conclusions in Table II.

Now, we should study the variations of $\tilde{\beta}(c_0)$, which depend on the monotonicity of $\tilde{L}_{\mathcal{A}^+}$. We have $\frac{1}{\gamma} \geq H_-$ since $\tilde{L}_{\mathcal{A}^+}$ is positive, so we cannot decide directly on the monotonicity of $\tilde{L}_{\mathcal{A}^+}$, because it is the product of a positive decreasing function $c_0 \mapsto \frac{1}{\gamma} - H_-(c_0)$ and a positive increasing function $c_0 \mapsto \frac{1}{H_+(c_0) - H_-(c_0)}$. Therefore, we simulate the variations of $\tilde{L}_{\mathcal{A}^+}$ and $\tilde{\beta}(c_0)$ as depicted in Fig. 2 and Fig. 3.
To maximize $\tilde{\beta}$ we should minimize $\tilde{L}_{\mathcal{A}^+}$ under the constraint of $0 \leq \tilde{L}_{\mathcal{A}^+} \leq 1$. For $\tilde{L}_{\mathcal{A}^+} = 0$, we have $H_- = \frac{1}{\gamma}$ and $\tilde{\beta}^* = \ln(1 - \mathrm{e}^{-\gamma})$. Thus, H^* takes a single value H_- and $H^* = \frac{1}{\gamma}$. To conclude, for $H^* \in \mathcal{F}_+$ a stationary point of $\tilde{\beta}$ under the constraint in (12), we have $H^* = \frac{1}{\gamma}$. This concludes the proof of Lemma 2.

3) Proof of Corollary 2: The set $\mathcal{F}_+ \cap \{H : \sup_t H(t) \leq H_0\}$ is convex. We deduce from Lemma 1 that $\tilde{\beta}$ is a concave function on this convex set. Therefore, its local maximum is a global maximum over this set [32]. From Lemma 2, $H^* = \frac{1}{\gamma}$ is the unique stationary point of $\tilde{\beta}$ over $\mathcal{F}_+$, hence it is the global maximum of $\tilde{\beta}$ over $\mathcal{F}_+ \cap \{H : \sup_t H(t) \leq H_0\}$.

4) Proof of the main result: Property 1: Property 1 follows from Corollary 2 using two simple observations that we highlight:

- The Property (4) is equivalent to the condition $H(t) = H^*(t) = \frac{P}{\gamma T}$;
- The property $\gamma \geq \gamma_{\text{crit}}(\{g_m\})$ is equivalent to the condition $\sup_t H(t) \leq H_0$.

IV. Analysis by Simulations

In order to illustrate our theoretical results, we consider three different multicarrier modulation systems, which are based on different families of modulation functions, and we analysed the CCDF of their PAPR. A comparison in terms of PAPR performance, between each considered multicarrier system and the conventional OFDM is presented.

A. Walsh-Hadamard-MC (WH-MC)

Instead of using the IFFT for the modulation, we can use the inverse Walsh-Hadamard transform (IWHT). The family of the modulation functions is expressed as:

$$g_m[k] = W_q[k],$$

where W_q represent the Walsh functions (see Fig. 4) and are columns of Hadamard matrix of dimension $M = 2^Q$, which is defined by the following recursive formula:

$$H_w(2^1) = \begin{pmatrix} 1 & 1 \\ 1 & -1 \end{pmatrix}, \tag{28}$$

and for $2 \leq q \leq Q$:

$$H_w(2^q) = \begin{pmatrix} H_w(2^{q-1}) & H_w(2^{q-1}) \\ H_w(2^{q-1}) & -H_w(2^{q-1}) \end{pmatrix} = H_w(2) \otimes H_w(2^{q-1}),$$

This article has been accepted for publication in a future issue of this journal, but has not been fully edited. Content may change prior to final publication. Citation information: DOI 10.1109/TCOMM.2016.2584068, IEEE Transactions on Communications

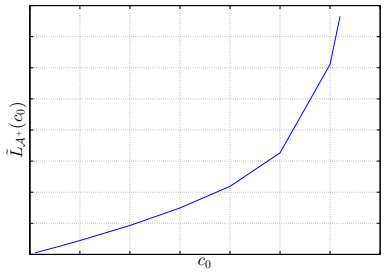

Figure 2: Curve of the function $\tilde{L}_{\mathcal{A}^+}(c_0)$.

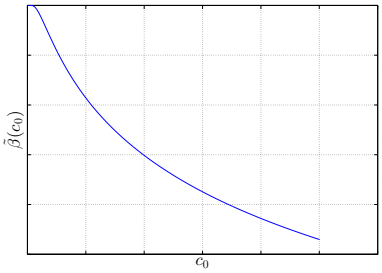

Figure 3: Curve of the function $\tilde{\beta}(c_0)$.

where $\otimes$ denotes the Kronecker product.

Note that the Hadamard matrix consists only of $+1$ and -1 entries, that is why the implementation has a simple structure featuring only additions and subtractions. In fact, IWHT can be implemented using the radix-2 algorithm, which means that there are only $M \log_2 M$ required complex additions [33].

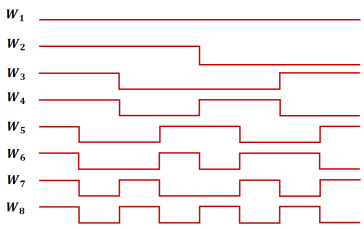

Figure 4: Walsh-Hadamard functions.

Fig. 4 depicts the shape of the Walsh functions for $Q = 3$. As we can notice, all the functions have the same modulus and this modulus is constant over time. From Corollary 1, WH-MC has the same PAPR performance as conventional OFDM.

Let us check this conclusion by simulation. To do so, we generate 10000 realizations of the WH-MC symbol using the quadrature phase-shift keying (QPSK) constellation, and $M = 64$ carriers. The CCDF of the PAPR of WH-MC and OFDM are compared in Fig. 5.

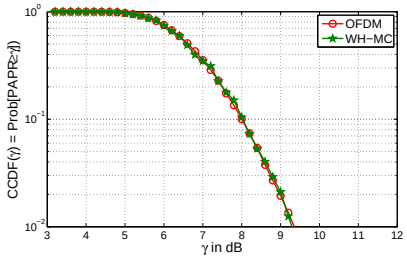

Figure 5: CCDF of the PAPR for conventional OFDM and WH-MC.

We can observe that OFDM and WH-MC have the same PAPR distribution function, hence the same PAPR performance. Indeed, this observation is consistent with the theoretical predictions undertaken in Corollary 1 .

B. WCP-OFDM

Weighted cyclic prefix-OFDM (WCP-OFDM) is another variant of OFDM, which gives a weighted version of the cyclic prefix-OFDM, by using non-rectangular pulse shapes. The prototype filter out-of-band energy (OBE) defined in [34] is used in WCP-OFDM. In this case, the family of modulation functions is expressed as $g_m[k] = g[k]e^{j2\pi \frac{m}{M}k}$ such that $g[k]$ is defined as [5]

$$g[k]\mathrm{e}^{j2\pi \frac{m}{M}k} = \begin{cases} \frac{1}{\sqrt{M'}} \cos(a + b\frac{2k+1}{2\Delta})\mathrm{e}^{j2\pi \frac{m}{M}[k]} \\ \text{if} \quad 0 \leq k \leq \Delta - 1, \\ \frac{1}{\sqrt{M'}}\mathrm{e}^{j2\pi \frac{m}{M}[k]} \\ \text{if} \quad \Delta \leq k \leq M' - 1, \\ \frac{1}{\sqrt{M'}} cos(a + b\frac{2(M-k)+1}{2\Delta})\mathrm{e}^{j2\pi \frac{m}{M}[k]} \\ \text{if} \quad M' \leq k \leq M - 1, \\ 0, \quad \text{else.} \end{cases}$$

with $g[k]$ is the OBE filter.

We can easily check that $g[k]$ satisfies the condition in (2). In addition, we notice that $\forall m \in [\![0, M-1]\!]$ the modulus $|g_m[k]|^2 = |g[k]\mathrm{e}^{j2\pi \frac{m}{M}k}|^2 = |g[k]|^2$ depends on time. From Corollary 1, the PAPR performance of WCP-OFDM has to be worse than conventional OFDM system.

To approve this conclusion, we simulate the CCDF of the PAPR by considering the OBE filter.

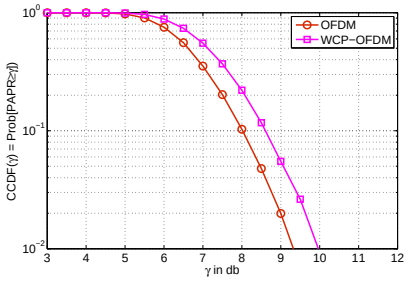

Figure 6: CCDF of the PAPR for conventional OFDM and WCP-OFDM.

Fig. 6 represents a comparison of the CCDF of the PAPR between conventional OFDM and WCP-OFDM. We can notice that the curve of WCP-OFDM is shifted to the right, compared

[5] $M = 80$, $M' = 4/5M$, $\Delta = M' - M$, $M_0 = \frac{M}{\Delta}$, $b = \frac{1}{\alpha + \beta M_0}$, $a = \frac{\pi}{4} - \frac{1}{2}b$, $\alpha = -0.1714430594740783$, $\beta = -0.5852184808129936$.

This article has been accepted for publication in a future issue of this journal, but has not been fully edited. Content may change prior to final publication. Citation information: DOI 10.1109/TCOMM.2016.2584068, IEEE Transactions on Communications

to OFDM. Thus, OFDM has a better PAPR performance than WCP-OFDM, which matches our theoretical results.

C. Wavelet-OFDM

Wavelet-OFDM, or also known as orthogonal wavelet division multiplexing (OWDM) [35], is a multicarrier system based on the wavelet transform. The principle of the wavelet transform is to decompose the signal in terms of small waves components called wavelets. The Wavelet-OFDM transmitted signal can be defined as:

$$X(t) = \sum_{n}\sum_{j=J_0}^{J-1}\sum_{k=0}^{2^j-1} w_{j,k}\psi_{j,k}(t-nT) + \sum_{n}\sum_{q=0}^{2^{J_0}-1} a_{J_0,q}\phi_{J_0,q}(t-nT).$$

- $J-1$: last scale considered, with $M=2^J$;
- J_0: first scale considered ($J_0 \leq j \leq J-1$);
- $w_{j,k}$: wavelet coefficients located at k-th position from scale j;
- $a_{J_0,q}$: approximation coefficients located at q-th position from the first scale J_0;
- $\psi_{j,k} = 2^{j/2}\psi(2^j t - kT)$: the wavelet orthonormal family, ψ is the mother wavelet function;
- $\phi_{J_0,q} = 2^{\frac{J_0}{2}}\phi(2^{J_0}t - qT)$: the scaling orthonormal family at the scale J_0, ϕ is the mother scaling function.

Note that the wavelet functions and the scaling functions have identical energy. For more details about the wavelet theory, the reader can refer to [36].

Several wavelets can be used to modulate the input symbols, such as Daubechies, Coiflets, and Symlets. We are interested here to the Haar wavelet, which belongs to the family of Daubechies wavelets. The Haar mother wavelet function $\psi_{\text{haar}}(t)$ is expressed as:

$$\text{with} \quad \psi_{\text{haar}}(t) = \begin{cases} \frac{1}{\sqrt{T}} & \text{if } 0 \leq t \leq \frac{T}{2}, \\ -\frac{1}{\sqrt{T}}, & \text{if } \frac{T}{2} \leq t \leq T, \\ 0, & \text{else.} \end{cases} \tag{29}$$

The scaling function $\phi_{\text{haar}}(t)$ can be described as:

$$\text{and} \quad \phi_{\text{haar}}(t) = \begin{cases} \frac{1}{\sqrt{T}} & \text{if } 0 \leq t \leq T, \\ 0, & \text{else.} \end{cases} \tag{30}$$

Fig. 7 describes Haar wavelet functions $\psi_{j,k}^{\text{haar}}$ for $J_0 = 0$ and $M = 8$. As we can notice, the temporal support of the contracted versions of the mother wavelet function ψ^{haar} are smaller than the symbol period T, therefore this family of functions does not satisfy the constraint in (2). From Property III-A, we can reach a better PAPR performance than using the Fourier transform. To check this claim by simulation, we consider the Haar wavelet transform, and we extract the detail and approximation coefficients at the maximal level 6 ($J_0 = 0$) for a number of carriers $M = 64$.

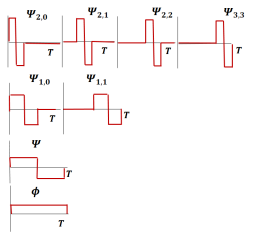

Figure 7: Haar wavelet function for different scales.

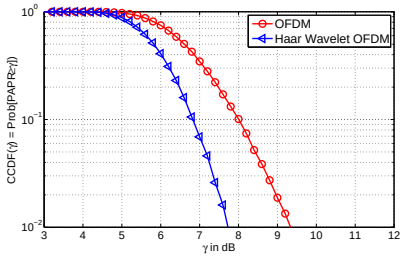

Figure 8: CCDF of the PAPR for conventional OFDM and Haar Wavelet based OFDM.

We can observe in Fig. 8 that the curve of the Haar Wavele-OFDM is shifted to the left, compared to OFDM. Thus, the Haar Wavelet-OFDM has a better PAPR performance than conventional OFDM.

Note here that, by changing the modulation waveform, the PAPR is reduced. As explained previously, without using the classical PAPR reduction methods, the PAPR can be reduced by selecting the appropriate waveform.

Complexity of implementation of Wavelet-OFDM: according to the Mallat Algorithm in [36], the wavelet modulation can be implemented based on the inverse discrete wavelet transform (IDWT). The IDWT consists of up-sampling by a factor of two and filtering the approximation coefficients $a_{j,k}$ (scaling coefficients) and the detail coefficients $w_{j,k}$ (wavelet coefficients) respectively by a low-pass filter g and a high-pass filter h associated to the wavelet used. Let L be the length of the filters h and g ($L=2$ in the case of the Haar wavelet). Let $M=2^J$ be the number of carriers which is equal to the number of the input coefficients. The wavelet modulation is calculated with a number of operations bounded by

$$\sum_{j=J_0+1}^{J} 2^j L \leq \sum_{j=1}^{J} 2^j L \tag{31}$$

$$= 2ML. \tag{32}$$

The complexity order in terms of the number of additions and multiplications is therefore $\mathcal{O}(ML)$. Knowing that the complexity order of the FFT or the IFFT is $\mathcal{O}(Mlog_2(M))$, the complexity increase order is about $\mathcal{O}(\frac{L}{log_2(M)})$, which is affordable since L is bounded, and the number of carriers M is usually large.

Other examples of multicarrier systems from the literature can also be discussed:

- The PAPR of NOFDM is evaluated by simulation for Hanning and Kaiser windows in [12]. The PAPR performance of NOFDM is shown experimentally to be worse than OFDM. Corollary 1 gives a theoretical explanation to these simulation results.

This article has been accepted for publication in a future issue of this journal, but has not been fully edited. Content may change prior to final publication. Citation information: DOI 10.1109/TCOMM.2016.2584068, IEEE Transactions on Communications

- According to the necessary condition theorem, we understand now why FBMC systems based on IOTA or SRRC filters for example as well as the universal-filtered multicarrier (UFMC) systems [37] do not have better PAPR than OFDM, since they do not satisfy the necessary condition stated in the theorem.

Fig. 9 summarizes the conclusions of this study. The rectangle represents the set of all GWMC waveforms $\in L_I^\infty$. The optimization problem analysed in this work is for the waveforms belonging to the set A, which means satisfying (2). Systems in $A \cap B$ (including OFDM, WH-MC) have the best possible PAPR performance *among all systems in* A. Any system with better PAPR performance than OFDM must be in C. There are indeed systems (Daubechies 6, Symlet 3, Coiflet 2) in C with better PAPR performance than OFDM. Some are even in B (Haar wavelets), but not in A.

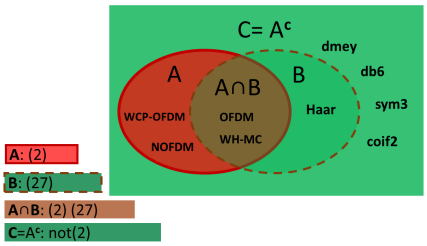

Figure 9: Taxonomy of multicarrier waveforms regarding the PAPR performance.

V. Conclusion

In this paper, we have investigated the GWMC system based on the family of modulation functions (the modulation transform and the pulse shaping filter) which does not vanish in the symbol period, and we have proved analytically that the PAPR, which depends on the modulation waveform, is optimal only if the sum of these waveforms over the number of carriers and the number of symbols is constant over time. We have concluded that there exists an infinite number of GWMC systems that are optimal in terms of PAPR performance, and conventional OFDM based on the Fourier transform and the rectangular filter belongs to this family. In addition, we have deduced that the PAPR performance of GWMC systems cannot be better than OFDM system without reducing the temporal support of the modulation functions compared to the symbol period. It is worth mentioning that, by limiting the support of the individual carriers, we are moving more and more from a multicarrier system to a single carrier system.

We have provided some examples to illustrate our theoretical results: WH-MC has a PAPR performance equal to that of OFDM, which is optimal among systems which satisfy condition (2), the WCP-OFDM's waveform is not constant over time and thus it is worse than conventional OFDM in terms of PAPR performance. By not satisfying constraint (2), it is possible to achieve a better PAPR performance, as has been shown for the Haar wavelets. Moreover, our work also provides a theoretical explanation about why several advanced multicarrier systems such as NOFDM, FBMC, UFMC, do not achieve a better PAPR than OFDM.

Table III: Study of the positivity of the function s.

H	0		H_0		$+\infty$
$s''(H)$			$+$		
$s'(H)$		-2		0	
$s(H)$		1		0	-1

Our future work will focus on designing a new waveform with low PAPR than OFDM, by acting on the number of intervals that vanish over time, and taking into consideration other constraints such as the bit error rate, the complexity and the spectral efficiency. If we would like to design a new waveform as a candidate for the next generation of mobile communication systems, it should not be selected from the excluded region A, because in this case, it will not improve the PAPR performance. Waveforms with reduced PAPR can be found in particular in the region B (as depicted in Fig. 9).

Appendix

We study the variations of the function $s(H) = 1 - 2H + 2He^{\frac{-1}{H}}$, we have

$$s'(H) = -2 + 2e^{\frac{-1}{H}} + \frac{2}{H}e^{\frac{-1}{H}}, \quad (33)$$

$$s''(H) = \frac{2}{H^2}e^{\frac{-1}{H}} + 2(-\frac{1}{H^2}e^{\frac{-1}{H}} + \frac{1}{H}\frac{1}{H^2}e^{\frac{-1}{H}}),$$
$$= \frac{2}{H^3}e^{\frac{-1}{H}} \geq 0. \quad (34)$$

As we can see in Table III, the function s is positive when $0 < H \leq H_0$. A numerical approximation gives $H_0 \approx 0.63$.

References

[1] H. Ochiai and H. Imai, "On the Distribution of the Peak-to-Average Power Ratio in OFDM Signals," *Communications, IEEE Transactions on*, vol. 49, no. 2, pp. 282–289, 2001.

[2] T. Jiang, M. Guizani, H.-H. Chen, W. Xiang, and Y. Wu, "Derivation of PAPR Distribution for OFDM Wireless Systems Based on Extreme Value Theory," *Wireless Communications, IEEE Transactions on*, vol. 7, no. 4, pp. 1298–1305, 2008.

[3] G. Auer, O. Blume, V. Giannini, I. Godor, M. Imran, Y. Jading, E. Katranaras, M. Olsson, D. Sabella, P. Skillermark *et al.*, "D2. 3: Energy Efficiency Analysis of the Reference Systems, Areas of Improvements and Target Breakdown," *EARTH*, 2010.

[4] R. V. Nee and R. Prasad, *OFDM for Wireless Multimedia Communications*. Inc.: Artech House, 2000.

[5] A. Skrzypczak, P. Siohan, and J.-P. Javaudin, "Analysis of the Peak-to-Average Power Ratio for OFDM/OQAM," in *Signal Processing Advances in Wireless Communications, 2006. SPAWC'06. IEEE 7th Workshop on*. IEEE, 2006, pp. 1–5.

[6] M. Chafii, J. Palicot, and R. Gribonval, "Closed-form Approximations of the Peak-to-Average Power Ratio Distribution for Multi-Carrier Modulation and their Applications," *EURASIP Journal on Advances in Signal Processing*, vol. 2014, no. 1, pp. 1–13, 2014.

[7] T. Jiang and G. Zhu, "Complement block coding for reduction in peak-to-average power ratio of ofdm signals," *Communications Magazine, IEEE*, vol. 43, no. 9, pp. S17–S22, 2005.

[8] M. Deumal, A. Behravan, and J. L. Pijoan, "On Cubic Metric Reduction in OFDM Systems by Tone Reservation," *Communications, IEEE Transactions on*, vol. 59, no. 6, pp. 1612–1620, 2011.

[9] C. Li, T. Jiang, Y. Zhou, and H. Li, "A Novel Constellation Reshaping Method for PAPR Reduction of OFDM Signals," *Signal Processing, IEEE Transactions on*, vol. 59, no. 6, pp. 2710–2719, 2011.

[10] T. Jiang and C. Li, "Simple Alternative Multisequences for PAPR Reduction without Side Information in SFBC MIMO-OFDM Systems," *Vehicular Technology, IEEE Transactions on*, vol. 61, no. 7, pp. 3311–3315, 2012.

[11] S. Y. Le Goff, B. K. Khoo, C. C. Tsimenidis, and B. S. Sharif, "A Novel Selected Mapping Technique for PAPR Reduction in OFDM Systems," *Communications, IEEE Transactions on*, vol. 56, no. 11, pp. 1775–1779, 2008.

[12] H. Bogucka, A. M. Wyglinski, S. Pagadarai, and A. Kliks, "Spectrally Agile Multicarrier Waveforms for Opportunistic Wireless Access," *Communications Magazine, IEEE*, vol. 49, no. 6, pp. 108–115, 2011.

[13] A. Sahin, I. Guvenc, and H. Arslan, "A Survey on Multicarrier Communications: Prototype Filters, Lattice Structures, and Implementation Aspects," *Communications Surveys & Tutorials, IEEE*, vol. 16, no. 3, pp. 1312–1338, 2012.

[14] W. Kozek and A. F. Molisch, "Nonorthogonal Pulseshapes for Multicarrier Communications in Doubly Dispersive Channels," *Selected Areas in Communications, IEEE Journal on*, vol. 16, no. 8, pp. 1579–1589, 1998.

[15] P. Siohan, C. Siclet, and N. Lacaille, "Analysis and Design of OFDM/OQAM Systems based on Filterbank Theory," *Signal Processing, IEEE Transactions on*, vol. 50, no. 5, pp. 1170–1183, 2002.

[16] L. Vangelista and N. Laurenti, "Efficient Implementations and Alternative Architectures for OFDM-OQAM Systems," *Communications, IEEE Transactions on*, vol. 49, no. 4, pp. 664–675, 2001.

[17] T. Jiang, C. Ni, D. Qu, and C. Wang, "Energy-efficient NC-OFDM/OQAM-based Cognitive Radio Networks," *Communications Magazine, IEEE*, vol. 52, no. 7, pp. 54–60, 2014.

[18] B. Farhang-Boroujeny, "OFDM versus Filter Bank Multicarrier," *Signal Processing Magazine, IEEE*, vol. 28, no. 3, pp. 92–112, 2011.

[19] B. Le Floch, M. Alard, and C. Berrou, "Coded Orthogonal Frequency Division Multiplex," *Proceedings of the IEEE*, vol. 83, no. 6, pp. 24–182, 1995.

[20] G. Fettweis, M. Krondorf, and S. Bittner, "Gfdm-generalized frequency division multiplexing," in *Vehicular Technology Conference, 2009. VTC Spring 2009. IEEE 69th*. IEEE, 2009, pp. 1–4.

[21] N. Michailow, I. Gaspar, S. Krone, M. Lentmaier, and G. Fettweis, "Generalized frequency division multiplexing: Analysis of an alternative multi-carrier technique for next generation cellular systems," in *Wireless Communication Systems (ISWCS), 2012 International Symposium on*. IEEE, 2012, pp. 171–175.

[22] R. Kanti and M. Rai, "Comparative Analysis of Different Wavelets in OWDM with OFDM for DVB-T," *International Journal of Advancements in Research & Technology*, vol. 2, no. 3, 2013.

[23] K. M. Wong, J. Wu, T. N. Davidson, Q. Jin, and P.-C. Ching, "Performance of Wavelet Packet-Division Multiplexing in Impulsive and Gaussian Noise," *Communications, IEEE Transactions on*, vol. 48, no. 7, pp. 1083–1086, 2000.

[24] A. Aboltins, "Comparison of Orthogonal Transforms for OFDM Communication System," *Electronics and Electrical Engineering Journal*, vol. 111, no. 5, pp. 77–80, 2011.

[25] M. Bernhard and J. Speidel, "Multicarrier Transmission using Hadamard Transform for Optical Communications," *ITG-Fachbericht-Photonische Netze*, 2013.

[26] P. Tan and N. C. Beaulieu, "A Comparison of DCT-based OFDM and DFT-based OFDM in Frequency Offset and Fading Channels," *Communications, IEEE Transactions on*, vol. 54, no. 11, pp. 2113–2125, 2006.

[27] G. D. Mandyam, "On the Discrete Cosine Transform and OFDM Systems," in *Acoustics, Speech, and Signal Processing, 2003. Proceedings.(ICASSP'03). 2003 IEEE International Conference on*, vol. 4. IEEE, 2003, pp. IV–544.

[28] A. Deshmukh and S. Bodhe, "Performance of DCT Based OFDM Communication System Working in 60 GHz Band," *International Journal of Engineering Science & Technology*, vol. 4, no. 1, 2012.

[29] N. De Bruijn, "Uncertainty Principles in Fourier Analysis," *Inequalities*, vol. 2, pp. 57–71, 1967.

[30] A. Skrzypczak, P. Siohan, and J.-P. Javaudin, "Peak-to-Average Power Ratio Issues for Pulse-Shaped Multicarrier Modulations," in *Advances on Processing for Multiple Carrier Schemes: OFDM & OFDMA*, F. Bader and N. Zorba, Eds. Nova Science Publishers, Inc., 2011, pp. 43–90.

[31] A. Kliks, "New Transmission and Reception Techniques of the Generalized Multicarrier Signals," Ph.D. dissertation, Poznan University of Technology, 2011.

[32] S. Boyd and L. Vandenberghe, *Convex Optimization*. Cambridge University Press, 2004.

[33] B. Evans *et al.*, "Hardware Structure for Walsh-Hadamard Transforms," *Electronics Letters*, vol. 34, no. 21, pp. 2005–2006, 1998.

[34] D. Roque, "Modulations Multiporteuses WCP-OFDM: évaluation des performances en environnement radiomobile," Ph.D. dissertation, Grenoble University, 2012.

[35] S. L. Linfoot, M. K. Ibrahim, and M. M. Al-Akaidi, "Orthogonal Wavelet Division Multiplex: An Alternative to OFDM," *Consumer Electronics, IEEE Transactions on*, vol. 53, no. 2, pp. 278–284, 2007.

[36] S. Mallat, *A Wavelet Tour of Signal Processing*. Academic press, 1999.

[37] F. Schaich and T. Wild, "Waveform Contenders for 5G-OFDM vs. FBMC vs. UFMC," in *Communications, Control and Signal Processing (ISCCSP), 2014 6th International Symposium on*. IEEE, 2014, pp. 457–460.

This article has been accepted for publication in a future issue of this journal, but has not been fully edited. Content may change prior to final publication. Citation information: DOI 10.1109/TCOMM.2016.2584068, IEEE Transactions on Communications

Marwa Chafii (M'13) is currently doing her PhD at the Communication and Electronic Embedded Systems (SCEE) research team of CentraleSupélec, Campus of Rennes-France. Her research interests include advanced waveforms for multi-carrier systems and the peak-to-average power ratio (PAPR) reduction problem. She received in 2013, her research master's degree in the field of advanced wireless communication systems (SAR) from CentraleSupélec at Paris-France, and her engineering diploma in telecommunications from Institut National des Postes et Télécommunications (INPT) in Morocco. Between 2014 and 2015, she has been visiting, for short scientific research missions, Poznan University of Technology (Poland), University of York (UK), and Yokohama National University (Japan).

Jacques Palicot received, in 1983, his PhD degree in Signal Processing from the University of Rennes. Since 1988, he has been involved in studies about equalization techniques applied to digital transmissions and analog TV systems. Since 1991 he has been involved mainly in studies concerning the digital communications area and automatic measurements techniques. He has taken an active part in various international bodies EBU, CCIR, URSI, and within RACE, ACTS and IST European projects. He has published various scientific articles notably on equalization techniques, echo cancellation, hierarchical modulations and Software Radio techniques. He is author or co-author of more than 300 publications with more than 50 in journals, two books and 22 patents. He is currently involved in adaptive Signal Processing, digital communications, Software Radio, Cognitive radio and Green Radio. From November 2001 to September 2003 he had a temporary position with INRIA/IRISA in Rennes. He serves as Associate Editor for EURASIP JASP since 2008. He also served as lead guest editor for several Special Issues on Software Radio, Cognitive Radio and Green Radio. He was Co General Chairman of ISCIT 2011, Co General Chairman of Next-GWiN 2014, Technical Program Chairman of CROWNCOM 2009, Technical Program Chairman of GREENCOM 2013 and Technical Program Chairman of CRN Symposium of ICC 2014. Since October 2003 he is with CentraleSupÃ©lec in Rennes where he leads the Signal Communications and Embedded Electronics (SCEE) research team.

Rémi Gribonval (M'02,SM'08,FM'14) is a Senior Researcher with Inria (Rennes, France), and the scientific leader of the PANAMA research group on sparse audio processing. A former student at École Normale Supérieure (Paris, France), he received the Ph. D. degree in applied mathematics from Université de Paris-IX Dauphine (Paris, France) in 1999, and his Habilitation à Diriger des Recherches in applied mathematics from Université de Rennes I (Rennes, France) in 2007. His research focuses on mathematical signal processing, machine learning, approximation theory and statistics, with an emphasis on sparse approximation, audio source separation and compressed sensing. He founded the series of international workshops SPARS on Signal Processing with Adaptive/Sparse Representations. In 2011, he was awarded the Blaise Pascal Award in Applied Mathematics and Scientific Engineering from the SMAI by the French National Academy of Sciences, and a starting investigator grant from the European Research Council.

Faouzi Bader (SM'07) received his PhD degree (with Honours) in Telecommunications in 2002 from Universidad Politécnica de Madrid (UPM), Madrid-Spain. He joined the Centre Technologic de Telecomunicacions de Catalunya (CTTC) in Barcelona-Spain as Associate researcher in 2002, and nominated in 2006 Senior Research Associate at same institution. Since June 2013, he is as Associate Professor at CentraleSupélec in Rennes- France. His research activities mainly focus on advanced multi-carrier waveforms (OFDM(A), (non-) uniform multimode filter based multicarrier schemes) and frequency allocation techniques in relay cognitive environment. He has been involved in several European projects from the 5th-7th EC research frameworks, and from 2012-2013 he was nominated general coordinator and manager of the EC funded research project ICT "EMPhAtiC" focusing on "Enhanced Multicarrier Techniques for Professional Ad-Hoc and Cell-Based Communications". He has published over 120 papers in peer-reviewed journals and international conferences, more than 13 book chapters, and published 3 books. He served as Technical Program Committee member in major IEEE ComSoc and VTS conferences, and as the general chair of the eleventh edition of the ISWCS'2014 conference, and the co-chair of the ISWCS 2015 edition. He is IEEE Senior Member from 2007.

Chapter 4

Future perspectives

From my point of view, the future perspectives should pass through two aspects, one purely academic, and a second focusing on the advance and the development of many of the research lines mentioned in Chapter 3. These two aspects are of course directly correlated and they are mutually influenced.
From my short research career between 2002 to nowadays (2016) the interest of the scientific community to future multi-carrier systems has tremendously increased. This can be just observed over the increased number of the scientific publications, research labs, and the European funded projects[1] where tremendous advances have been achieved in this field (e.g., FMT, FBMC, GFDM, UFMC, and F-OFDM, among many others variants) from 2007 the year of the starting funding of the EU PHYDYAS project. The actual 5G and IoT context has even boosted the involvement and the R&D dedication of the telecommunication operators and worldwide manufacturers like Alcatel-Lucent, Huawei, Ericsson, and many others, into the design of future flexible radio access technologies (RATs) using advanced multi-carrier schemes. Saying this, style big efforts have to be made to transfer to academia, and therefore, to undergraduate and postgraduate students the critical knowledge and background to be able to better understand these new communication schemes and to participate in a more active manner to their development. It's nowadays easy to found a plethora of detailed information in lectures and tutorials, free access software and platforms, based on the OFDM communication scheme and its basic standards. However, information or open testing platforms for academic purposes or research are very limited to not saying rares for the above mentioned multi-carrier schemes. Several factors are behind this lack of information, among them the natural cycle that has to undertake any industrial product from its successful development to its wide adoption by the mass consumers, for thus being after widely learned in the universities at undergraduate or postgraduate levels. Same experience has been observed in the past for the GSM, UMTS, WiFi, DVB-T and many other "standardized" communication systems. Another aspect no less important is related with the development of more didactic and simplistic ways of teaching many of the signal processing, filtering concepts required for the generation of these multi-carrier schemes not necessarily easy to assimilate by the students as those used for OFDM scheme.
The book of M. Bellanger in [104], and more recent ones as that of F. L. Luo and C. J. Zhang in [105], that of A. Osseiran et al., in [106], or that under edition in [B4], although their way of writing is more oriented to postgraduate and senior researchers or experts than undergraduate students, are a big support that foster and encourage the dissemination of advanced results and uses of the above flexible waveforms in different future communication environments. To what I'm concerned with this aspect my future efforts will be on the elaboration of undergraduate and/or Master courses focusing on two parts; one on the theoretical design, implementation, and concept of the previously mentioned waveforms and their possible applications, and the second part on more practical aspects as the development of software/hardware platform that serves for both teaching and the development of more advanced research aspects. To this last, some steps have been already undertaken under the French ANR PROFIL project.

Regarding the second aspect that concerns the main future research aspects from the actually listed in Chapter 3, I would name the following:

- Obtained results from cited researches in Subsections 3.2.1 and 3.2.2 have demonstrated the importance of the choice of the multi-carrier waveforms on the overall coexistence capabilities of different systems using different physical layers and communicating side by side in the same band. It has been also demonstrated that the PSD based approach consists in modeling the interference at the input antenna of the interfered

[1] from the FP7 European Union's Research and Innovation funding programme for 2007-2013, and the current Horizon 2020 programme.

receiver, and totally omits the demodulation operations that are performed by the latter. Thus, this model does not take into account the time window size of the incumbent system. Therefore, the interference seen at the output of the demodulator of the interfered receiver is much higher than expected using the PSD based model. Moreover, the interference between the incumbent and secondary systems is symmetrical, which contradicts the results obtained with the PSD-based model. Our analysis in [C103, C105] showed that the cross-interference is mainly caused by the rectangular window of the incumbent system. In other words, presented results show that coexistence with legacy CP-OFDM systems cannot be drastically improved by designing enhanced waveforms only, but that it is necessary to modify the CP-OFDM receiver itself. This results is a key result that may change the perception of the scientific community on the way of measuring the cross-interference between systems with different waveforms in heterogeneous communication environments. More deep signal processing researches have to be undertaken at the LTE and future LTE-Advanced receivers to enhance the coexistence capability, and therefore the interference with future deployed systems using a different waveform and coexisting in the same band.

- Besides researches on coexistence in D2D scenario, in the collaborations within the PHC ULYSSES project [C106], we considered a scenario whereby asynchronous D2D communication underlays an OFDMA macro-cell in the uplink. Motivated by the superior performance of new waveforms with increased spectral localization in the presence of frequency and time misalignment, we compared the system-level performance of a set-up for when D2D pairs use either OFDM or FBMC/OQAM. We first demonstrated that inter-D2D interference, resulting from misaligned communications, plays a significant role in clustered D2D topologies. We then demonstrated that the resource allocation procedure can be simplified when D2D pairs use FBMC/OQAM, since the high spectral localization of FBMC/OQAM results in negligible inter-D2D interference. Specifically, we identified that FBMC/OQAM is best suited to scenarios consisting of small, densely populated D2D clusters located near the encompassing cell's edge. Given recent developments in self-interference cancellation, in band full duplex (FD) [107, 108, 109] is attracting much interest for 5G due to promises of potentially doubled spectral efficiency. We are interested in investigating the system level implications of using FD. We can identify two main tracks for future researches incorporating FD into our current collaborative works:

  1. FD and new waveforms: is FD waveform dependent?
  2. FD and D2D: resource management and adaptive switching for FD capable D2D pairs. How the measured cross-interference generated for different 5G candidates waveforms can play a role in this context?

- Always on the continuity of researches on RA/RM, coexistence (PMR, D2D), and spectrum sharing, and following the actual evolution and the development of the 5G context, the IoT is also a fundamental aspect for future researchers. In relation with "barrier in terms of fragmented spectrum and massive IoT deployment", The expected massive increase of LPWA traffic applications and its densification may raise questions on the spectrum availability license/exempt needed for the IoT service reliability. Actually, licensed spectrum may become overloaded with traffic of higher ARPU (average Revenue per User) and IoT traffic may be moved to less costly spectrum for the operator: unlicensed spectrum. However, QoS is not guaranteed on such spectrum and it may be required to develop techniques to aggregate multiple unlicensed bands to mitigate possible saturation issues on a given band. Despite this theoretical limitation, many IoT devices are served by radio technologies that operate on unlicensed spectrum and that are designed for short-range connectivity with limited QoS and security requirements typically applicable for a home or indoor environment. Currently, there are two alternative connectivity tracks for the many IoT applications that depend on wide-area coverage:

  1. Cellular technologies: 3GPP technologies like GSM, WCDMA, LTE and future 5G. These WANs operate on licensed spectrum and historically have primarily targeted high-quality mobile voice and data services. Now, however, they are being rapidly evolved with new functionality and the new radio access technology narrow band IoT (NB-IoT) specifically tailored to form an attractive solution for emerging low power wide area (LPWA) applications.
  2. Unlicensed LPWA: new proprietary radio technologies, provided by, for example, Sigfox and LoRa, have been developed and designed solely for machine-type communication (MTC) applications addressing the ultra-low-end sensor segment, with very limited demands on throughput, reliability or QoS

  My future researchers will focus on driving the IoT with carrier aggregation (CA) which is a key concept in LTE-Advanced enabling the operators to allocate a higher bandwidth than the LTE to supply even higher

bandwidth than LTE, to support such connected devices. As its name suggests, carrier aggregation combines two or more carriers in order to offer a greater throughput. Capacity is essential for IoT, as hundreds of devices are in constant communication with the LTE-A network. One of the focuses will be to investigate the possible use of carrier aggregation for IoT, providing on one hand the possibility to combine low frequency carriers with high frequency ones, but at the cost of more complex and power consuming Hardware (HW). Another challenge is to provide tools for flexible waveforms, and spectrum use with optimized resource. Even when existing 3GPP end-to-end connectivity is not feasible, cellular technology can still provide key benefits when used as a bridging option, i.e. as an aggregation and routing solution. This capillary network approach allows end devices to utilize varying access solutions from either the short range or LPWA domain and access the cellular networks via a gateway device. Capillary networks enable the reuse of cellular functions and assets such as security, device management, billing and QoS without requiring each end device to be cellular enabled.

- The developed fast convergence method based on the sub-optimal initialization strategy value, in the sense of the mean square error, for OFDM/OQAM blind equalization with CNA opens new perspectives for the blind equalization in the FBMC-based modulations and its possible implementation in static or semi-static channel environments. The extension of the undertaken research work to the MIMO case using the OFDM/OQAM seems a natural evolution. Similar to the SISO blind equalization signal processing context, there is limited researches carried out for the MIMO OFDM/OQAM compared to OFDM signal . This extension would be the basis of the pilot decontamination in OFDM/OQAM based massive MIMO networks. Multiple research groups in recent years have studied a variety of implementation issues related to massive MIMO systems the only limiting factor of the network capacity in the single-cell scenario is the coherence time of the channel which needs to be much larger than the number of mobile users (MU) in order to facilitate accurate channel estimation and allow for data transmission. However, multi-cellular time-division duplex (TDD) networks suffer from a pilot contamination, this problem which was first reported by Jose et al., in [110]. Thus, the channel estimates at each BS will contain the channel information of the MUs positioned in the other cells as well as its own users. As a result, when the BS combines the received signal in order to decode the transmitted symbols of its MUs, it also combines the data symbols of the users of other cells which results in inter-cell interference. Recent solutions have been developed to mitigate the effect of the pilot contamination in [111, 112] using OFDM signal. The authors in [113] have proposed the blind equalization capability using cosine modulated multitone (CMT), and its extension to massive MIMO. The work in [C91] achieved blind equalization with fast convergence than that in [113] using OFDM/OQAM modulation. Thus the extension of its capability to massive MIMO context could bring interesting results for its implementation.

- While 5G networks has an established road-map towards technology validation, specifications and tests by industry, outstanding new scientific opportunities are blooming in the field of networking research, with the objective of bringing little explored technologies and system concepts closer to exploitation. Future innovative research actions are going (among others) towards novel use of the spectrum potential, de-risking technological building blocks at frequencies above 90 Ghz up to THz communications [114] backed by innovative usage scenarios [115], to develop radically new approaches for spectrum efficiency, and to reach Tbps in wireless communications. The beyond 90 GHz frequency bands provide unused, large bandwidths with specific characteristics (some of them similar and some others different to the ones below 90 GHz) such as high path loss (leading to short-range transmissions), high-data rates (multiple Gb/s), distance-dependent bandwidth (requiring advanced distance-aware signal processing algorithms) and higher spatial resolution due to the possibility of very large antenna arrays of limited size. Moreover, mostly LOS conditions (and directional antennas) are expected although NLOS transmissions in distances from 100 m to 200 m have been reported [116]. Additionally, synchronization is challenging both at the receiver and among transmitters when cooperating, due to very short symbol periods. Applications for both indoor and outdoor environments are envisioned such as in small cells and heterogeneous networks, kiosk downloading, terabits WLANs and cellular back-hauling [115]. From more than two decades, the MC scheme is the undisputed pattern (with OFDM as the leader) scheme in frequency bands up to 6 GHz. However, the special characteristics in above 90 GHz band and associated channels make single-carrier (SC) modulation schemes, as opposed to the popular MCM ones, potentially more appropriate for communication systems operating in such bands. This last opens new and serious questions regarding the automatic jumping to establish MC schemes as key modulation scheme for such communication environment.

- From all the above cited future research orientations, there is a key issue that should be not forgotten which is the "green aspect". Energy efficiency to optimize the capacity/efficiency of IoT networks by trading between perfect scheduled and fully decentralized systems by tuning and optimizing the feedback needs is one of the essential objectives. In the D2D context, since the energy is usually limited in mobile system, main focus will be on increasing power efficiency of D2D users and satisfying service rate requirements. Main target here is also to propose an energy-efficient scheduling scheme for D2D users, that jointly optimizes resource allocation and power control with interference limitations and required transmission rate constraints. The signaling schemes to cope with high numbers of D2D candidate is also one of the less developed aspect to be analyzed. The introduction of FD in the D2D context in particular and in Hetnet in general, will allow some advances on energy efficiency [117].

Bibliography

[1] Y. Medjahdi, M. Terre, D. L. Ruyet, D. Roviras, and A. Dziri, "Performance Analysis in the Downlink of Asynchronous OFDM/FBMC Based Multi-Cellular Networks," *IEEE Transactions on Wireless Communications*, vol. 10, pp. 2630 – 2639, August 2011.

[2] N. Yee, J. P. M. G. Linnartz, and G. Fetteweis, "Multi-Carrier CDMA in Indoor Wireless Radio Networks," in *in the Proc. of the IEEE Personal, Indoor and Mobile Radio Communications (PIMRC 93), pp. 109-113. Yokohama, Japan*, Sept 1993.

[3] K. Fazel, "Performance of CDMA/OFDM for Mobile Communication System," in *Proc. of the IEEE Personal, Indoor and Mobile Radio Communications (PIMRC 93), pp. 468-472, Yokohama, Japan*, Sept 1993.

[4] L. Vandendorpe, "Multitone Spread Spectrum Multiple Access Communications Systems in Multipath Rician Fading Channel," in *Proc. of the IEEE First Symposium of Communication and Vehicular Technology. pp 4.1-1-4.1.8, Benelux, Delf, the Netehrlands*, Oct 1993.

[5] S. H. Kim, K. Ha, and C. W. Lee, "A frame Synchronization Scheme for Uplink MC-CDMA Systems," in *Proc. of the IEEE Vehicular Technology Conference- (VTC99)*, September 1999.

[6] J. S. Lee and L. E. L. Miller, "CDMA Systems Engineering Hand Book," in *Artech House Publishers ed.*, 1998.

[7] T. M. Schmidl and D. C. Cox, "Low-Overhead, Low Complexity [Burst] Synchronization for OFDM," in *the IEEE International Conference on Communications (ICC'96)*, vol. 3, pp. 1301–1306, June 1996.

[8] T. M. Schmidl and D. C. Cox, "Robust Frequency and Timing Synchronisation for OFDM," *IEEE Transactions on Communications*, vol. 45, pp. 1613–1621, December 1997.

[9] Z. Wang and G. B. Giannakis, "Wireless MMulticarrier Communications Where Fourier Meets Shannon," *IEEE Signal Processing Magazine*, pp. .29–48, May 2000.

[10] S. Verdu, *Multiuser Detection*. Cambridge University Press, ISBN: 0-521-59373-5, 1998.

[11] M. Chafii, J. Palicot, and R. Gribonval, "Closed-form Approximations of the Peak-to-Average Power Ratio Distribution for Multi-Carrier Modulation and their Applications," *EURASIP Journal on Advances in Signal Processing*, vol. 2014, no. 1, pp. 1–13, 2014.

[12] M. Chafii, a. J. Palicot, R. Gribonval, and A. Burr, "Power Spectral Density Limitations of the Wavelet-OFDM System," in *in the Proc. of the European Signal Processing Conference (Eusipco'16)*, 2016.

[13] M. Chafii, Y. Harbi, A. Burr, and J. Palicot, "Wavelet-OFDM vs. OFDM : Performance Comparison," in *in Proc of the IEEE International Conference on Telecommunications (ICT'16)*, 2016.

[14] M. Chafii, J. Palicot, and R. Gribonval, "La modulation en ondelettes : une modulation alternative ible consommation d'energie," in *International Union of Radio Science (URSI'16), Rennes, France*, 2016.

[15] M. Chafii, J. Palicot, and R. Gribonval, "L'optimalit l'OFDM en termes de performance en PAPR," in *GRETSI' 2015*, 2015.

[16] M. Chafii, J. Palicot, and R. Gribonval, "Closed-Form Approximations of the PAPR Distribution for Multi-Carrier Modulation Systems," in *in Proc. of the European Signal Processing Conference (Eusipco'14)*, 2014.

[17] M. Chafii, J. Palicot, and R. Gribonval, "A PAPR upper bound of Generalized Waveforms for Multi-Carrier modulation systems," in *in Proc. of the 6th International Symposium on Communications, Control and Signal Processing (ISCCSP'14)*, 2014.

[18] J. Mitola, "Cognitive radio for flexible mobile multimedia communications," in *the Proc. of the IEEE International Workshop on Mobile Multimedia Communications, MoMuC'99.*, November 1999.

[19] "Spectrum Policy Task Force," tech. rep., Federal Communication Commission, November 2002.

[20] T. Weiss and F. K. Jondral, "Spectrum Pooling: An Innovative Strategy for the Enhancement of Spectrum Efficiency," *IEEE Communications Magazine*, vol. 42, pp. 8–14, March 2004.

[21] T. Weiss and J. Hillenbrand, "Mutual Interferencein OFDM-Based Sprectrum Pooling Systems," in *the Proc. of the IEEE Vehicular Technology Conference (IEEE VTC'04-Spring)*, vol. 4, May 2004.

[22] G. Bansal, M. J. Hossain, and V. K. Bhargava, "Optimal and Suboptimal Power Allocation Scheme for OFDM-Based Cognitive Radio Systems," *IEEE Transactions on Wireless Communications*, vol. 7, pp. 4710–4718, November 2008.

[23] P.Wang, M. Zhao, L. Xiao, S. Zhou, and J. Wang, "Power Allocation in OFDM-Based Cognitive Radio Systems," in *the Proc. of the IEEE Global Telecommunication Conference (GLOBECOM'07)*, pp. 4061 – 4065, November 2007.

[24] T. Qin and C. Leung, "Fair Adaptive Resource Allocation for Multiuser OFDM Cognitive Radio Systems," in *the Proc. of the Second International Conference on Communications and Networking in China (CHINACOM'07)*, August 2007.

[25] B. Farhang-Borounjeny and R. Kempter, "Multicarrier Communication Techniques for Spectrum Sensing and Communication in Cognitive Radios," *IEEE Communications Magazine (Special Issue on Cognititve Radios for Dynamic Spectrum Access)*, vol. 48, pp. 80–85, April 2008.

[26] J. Jang and K. Lee, "Transmit Power Adaptation for Multiuser OFDM Systems," *IEEE Journal on Selected Areas in Communications*, vol. 21, pp. 171–178, February 2003.

[27] S. Boy and L. Vandenberghe, *Convex Optimization*. Cambridge University Press, 2004.

[28] Y. Zhang and C. Leung, "An Efficient Power-Loading Scheme for OFDM-Based Cognitive Radio systems," *IEEE Transactions on Vehicular Technology*, vol. 59, pp. 1858 – 1864, May 2010.

[29] N. Papandreou and T. Antonakopoulos, "Bit and Power Allocation in Constrained Multicarrier Systems: Single-User Case," *EURASIP Journal on Advanced Signal Processing*, vol. 2008, p. 14 pages, 2008.

[30] Z. Hasan, G. Bansal, E. Hossain, and V. Bhargava, "Energy-Efficient Power Allocation in OFDM-Basedased Cognitive Radio Systems: A Risk-Return Model," *IEEE Transactions on Wireless Communications*, vol. 8, pp. 6078–6088, December 2008.

[31] M. Shaat and F. Bader, "Computationally Efficient Power Allocation Algorithm in Multicarrier Based Cognitive Radio Networks: OFDM and FBMC Systems," *EURASIP Journal on Advanced Signal Processing*, vol. 2010, no. ID 528378, 2010.

[32] F. Digham, "Joint Power and Channel Allocation for Cognitive Radios," in *Proc. of the IEEE Wireless Communications and Networking Conference, (WCNC08)*, pp. 882–887, April 2008.

[33] A. Attar, M. Nakhai, and A. Aghvami, "Cognitive Radio Game for secondary Spectrum Access Problem," *IEEE Transactions on Wireless Communications*, vol. 8, pp. 2121–2131, April 2009.

[34] L. Gao and S. Cui, "Efficient Subcarrier, Power, and Rate Allocation with Fairness Consideration for OFDMA Uplink," *IEEE Transactions in Wireless Commununications*, vol. 7, no. 5, pp. 1507–1511, 2008.

[35] S. M. Almalfouh and G. L. Stuber, "Interference-Aware Power Allocation in Cognitive Radio Networks with Imperfect Spectrum Sensing," in *Proc. of the IEEE International Conference on Communications (ICC'2010)*, pp. 1–6, May 2010.

[36] C. T. Qin, C. Leung, and Z. Shen:, "Resource Allocation in a Cognitive Radio System with Imperfect Channel State Estimation," *IEEE Journal of Electrical and Computer Engineering*, 2010.

[37] R. Zhang, "Optimal Power Control over Fading cognitive Radio Channel by Exploiting Primary User CSI," in *Proc. of the IEEE Global Telecommunications Conference, (IEEE GLOBECOM08)*, pp. 1– 5, December 2008.

[38] R. Zhang, S. Cui, and Y.-C. Liang, "On Ergodic Sum Capacity of Fading Cognitive Multiple-access and Broadcast Channels," *IEEE Transactions on Information Theory*, vol. 11, no. 55, p. 5161 5178, 2009.

[39] W. Wang, Q. Lu, and T. Peng, "An Uplink Resource Allocation Scheme for OFDMA-based Cognitive Radio Networks," *Int.ernational Journal on Communication Systems*, vol. 5, no. 22, pp. 603–623, 2009.

[40] K. Kim, Y. Han, and S.-L. Kim, "Joint Subcarrier and Power allocation in Uplink OFDMA Systems," *IEEE Communications Letters*, vol. 9, no. 6, pp. 526–528, 2005.

[41] O. Simeone, Y. Bar-Ness, and U. Spagnolini, "Stable Throughput of Cognitive Radios with and Without Relaying Capability," *IEEE Transactions on Communications*, vol. 55, no. 12, p. 2351 2360, 2007.

[42] S. Golrezaei-Khuzani and M. Nasiri-Kenari, "Orthogonal Frequency Division Multiple Access-based Cognitive Radio Networks with Relaying Capability," *IET Communications*, vol. 4, p. 395 409, March 2010.

[43] T. Luo, F. Lin, T. Jiang, M. Guizani, and W. Chen, "Multicarrier Modulation and Cooperative communication in Multihop Cognitive Radio Networks," *Transactions on Wireless Communications*, vol. 18, pp. 38–45, February 2011.

[44] J. Jia, J. Zhang, and Q. Zhang, "Cooperative Relay for Cognitive Radio Networks," in *IEEE INFOCOM*, pp. 2304–2312, April 2009.

[45] U. D. T. Nadkar, V. Thumar and S. Merchant, "Judicious Power Loading for a Cognitive Relay Scenario," in *International Symposium on Intelligent Signal Processing and Communication Systems (ISPACS2009)*, pp. 327–330, January 2009.

[46] T. Nadkar, V. Thumar, U. Desai, and S. Merchant, "Optimum Bit Loading for Cognitive Relaying," in *IEEE Wireless Communications and Networking Conference (WCNC10)*, pp. 1–6, April 2010.

[47] L. Li, X. Zhou, H. Xu, G. Y. Li, D. Wang, and A. Soong, "Simplified Relay Selection and Power Allocation in Cooperative Cognitive Radio Systems," *IEEE Transactions on Wireless Communications*, vol. 10, no. 1, pp. 33–36, 2011.

[48] G. Zhao, C. Yang, G. Li, D. Li, and A. Soong, "Power and Channel Allocation for Cooperative Relay in Cognitive Radio Networks," *IEEE Journal of Selected Topics in Signal Processing*, vol. 5, no. 1, pp. 151–159, 2011.

[49] K. Jitvanichphaibool, R. Zhang, and Y.-C. Liang, "Optimal Resource Allocation for Two-Way Relay-Assisted OFDMA," *IEEE Transactions on Vehicular Technology*, vol. 58, no. 7, pp. 3311 –3321, 2009.

[50] L. Li, X. Zhou, H. Xu, G. Li, D. Wang, and A. Soong, "Simplified Relay Selection and Power Allocation in Cooperative Cognitive Radio Systems," *IEEE Transactions in Wireless Commununications*, vol. 10, pp. 33–36, Jan 2011.

[51] P. Ubaidulla and S. Aissa, "Optimal Relay Selection and Power Allocation for Cognitive Two-Wayay Relaying Networks," *IEEE Wireless Communications Letters*, vol. 1, pp. 225 – 228, June 2012.

[52] R. L. Haupt and S. E. Haupt, eds., *Practical Genetic Algorithms*. 2nd ed. John Wiley and Sons, 2004.

[53] A. Alsharoa, F. Bader, and M.-S. Alouini, "Relay Selection and Resource Allocation for Two Way DF-AF Cognitive radio Networks," tech. rep., King Abdullah Univeristy of Science and Technology (KAUST). Available: http://arxiv.org/abs/1303.3489, March 2013.

[54] L. Martinod, J.-B. Dore, F. Bader, and V. Savaux, " L0.1: Broadband Professional Mobile Radio Based on Filter Bank Multicarrier modulation-Context and Typical Scenario. Available: http://www.anr-profil.com. [Accessed: 14- August- 2016]," tech. rep., 2014.

[55] L. Martinod and J.-B. Dore, " L1.1: Broadband Professional Mobile Radio Based on Filter Bank Multicarrier modulation-Coexistence studies specifications and metrics. Available: http://www.anr-profil.com. [Accessed: 14- August- 2016]," tech. rep., 2014.

[56] F. Bader, V. Savaux, A. Amri, J.-B. Dore, V. Berg, and L. Martinod, " L2.1: Broadband Professional Mobile Radio Based on Filter Bank Multicarrier modulation-Physical Layer Specifications. Available: http://www.anr-profil.com. [Accessed: 14- August- 2016]," tech. rep., 2014.

[57] N. Michailow, M. Matth. S. Gaspar, A. N. Caldevilla, L. L. Mendes, A. Festag, and G. Fettweis, "Generalized Frequency Division Multiplexing for 5th Generation Cellular Networks," *IEEE Transactions on Communications*, vol. 62, no. 9, pp. 3045 – 3061, 2014.

[58] M. G. Bellanger, "Specification and Design of a Prototype Filter for Filter Bank Based Multicarrier Transmission," in *in Proc. IEEE Int. Conf. Acoustics, Speech, and Signal Processing (ICASSP'2001)*, pp. 2417 – 2420, May 2001.

[59] "FP7-ICT Project PHYDYAS - Physical Layer for Dynamic Spectrum Access and Cognitive Radio. [Online] http://www.ict-phydyas.org.,"

[60] M. Renfors and F. Harris, "Highly Adjustable Multirate Digital filters Based on Fast Convolution," in *the Proc. European Conference on Circuit Theory and Design, ECCTD 2011*, August 2011.

[61] M. Renfors, J. Yli-Kaakinen, and F. J. Harris, "Analysis and Design of Efficient and Flexible Fast-Convolution Based Multirate Filter Banks," *Transactions on Signal Processing*, vol. 62, pp. 3768 – 3783, August 2014.

[62] A. Aminjavaheri, A. Farhang, A.-R. Reyhani, and B. Farhang-Boroujeny, "Impact of Timing and Frequency Offsets on Multicarrier Waveform Candidates for 5G," in *arXiv:1505.00800*, September 2015.

[63] G. Bansal, J. Hossain, and V. K. Bhargava, "Adaptive Power Loading for OFDM-Based Cognitive Radio Systems," in *Proc. of the IEEE International Conference on Communications (ICC'07). Glasgow, Scotland*, pp. 5137–5142, 2007.

[64] M. Shaat and F. Bader, "Low Complexity Power Loading scheme in Cognitive Radio Networks: FBMC Capability," in *Proc. of the IEEE International Symposium on Personal, Indoor and Mobile Radio Communications (PIMRC'09), Tokyo, Japan*, pp. 2597–2602, 2009.

[65] Y. Ma, Y. Xu, and D. Zhang, "Power Allocation for Orthogonal Frequency Division Multiplexing-Based Cognitive Radio Systems with and without Integral Bit Rate Consideration," *IET Communications*, vol. 5, pp. 575 – 586, March 2011.

[66] A. M. Tonello, "Performance Limits for Filtered Multitone Modulation in Fading Channels," *IEEE Transactions on Wireless Communications*, vol. 4, pp. 2121–2135, September 2005.

[67] B. Farhang-Boroujeny, "OFDM versus Filter Bank Multicarrier," *IEEE Signal Processing Magazine*, vol. 28, pp. 92 –112, May 2011.

[68] M. Bellanger, D. Mattera, and M. Tanda, "A Filter Bank Multicarrier Scheme Running at Symbol Rate for Future Wireless Systems," in *Wireless Telecommunications Symposium (WTS'15)*, April 2015.

[69] J. Louveaux, L. Baltar, D. Waldhauser, M. Renfors, M. Tanda, F. Bader, and E. Kofidis, "Deliverable D3.1: PHYDYAS-Equalization and demodulation in the receiver (single antenna), [Online]: http://www.ict-phydyas.org/. [Accessed: 20/08/2016] ," tech. rep., 2008.

[70] M. Najar, F. Bader, F. Rubio, E. Kofidis, M. Tanda, J. Louveaux, M. Renfors, and D. L. Ruyet, "Deliverable D4.1: PHYDYAS- MIMO Transmit and Receive Processing, [Online]: http://www.ict-phydyas.org/. [Accessed: 20/08/2016] ," tech. rep., 2008.

[71] M. Morelli and U. Mengali, "A Comparisaon of Pilot-Aided Channel Estimation Methods for OFDM Systems," *IEEE Transactions on Signal Processing*, vol. 49, pp. 3065–3073, December 2001.

[72] M. K. Ozdemir and H. Arslan, "Channel Estimation for Wireless OFDM Systems," *IEEE Communications Surveys and Tutorials*, vol. 9, pp. 18 – 48, Second Quarter 2007.

[73] Y. Liu, Z. Tan, H. Hu, L. J. Cimini, and G. Y. Li, "Channel Estimation for OFDM," *IEEE Communication Surveys and Tutorials*, vol. 16, pp. 1891–1908, Fourthquarter 2014.

[74] Y. Sato, "A Method of Self-Recovering Equalization for Multilevel Amplitude-Modulation Systems," *IEEE Transactions on Communications*, vol. 23, pp. 679– 682, June 1975.

[75] D. N. Godard, "Self-Recovering Equalization and Carrier Tracking in Two-Dimensional Data Communication Systems," *IEEE Transactions on Communications*, vol. 28, pp. 1867 – 1875, November 1980.

[76] R. Johnson, J. P. Schniter, T. Endres, J. Behm, D. Brown, and R. Casas, "Blind Equalization Using the Constant Modulus Criterion: A Review," *Proceedings of the IEEE*, vol. 86, pp. 1927 –1950, October 1998.

[77] J. Yang, J. J. Werner, and G. A. Dumont, "The Multimodulus Blind Equalization and its Generalized Algorithms," *IEEE Journal on Selected Areas in Communications*, vol. 20, pp. 997 –1015, June 2002.

[78] S. Abrar and A. K. Nandi, "Blind Equalization of Square-QAM Signals: A Multimodulus Approach," *IEEE Transactions in Wireless Commununications*, vol. 58, pp. 1674 – 1685, June 2010.

[79] J. M. Filho, M. D. Miranda., and M. T. M. Silva, "A Regional Multimodulus Algorithm for Blind Equalization of QAM Signals: Introduction and Steady-State Analysis," *Elsevier, Signal Processing*, vol. 92, no. 11, pp. 2643– 2656, 2012.

[80] A. W. Azim, S. Abrar, A. Zerguine, and A. K. Nandi, "Steady-State Performance of Multimodulus Blind Equalizers," *, Elsevier, Signal Processing*, vol. 108, no. 2015, pp. 509 –520, 2014.

[81] T. C. Hewavithana and D. M. Brookes, "Blind Adaptive Channel Equalization for OFDM Using the Cyclic Prefix Data," in *in Proc. of the IEEE Global Telecommunications Conference (GLOBECOM04). Dallas, Texas, USA*, pp. 2376 –2380., December 2004.

[82] M. Luise, R. Reggiannini, and G. Vitetta, "Blind Equalization/Detection for OFDM Signals over Frequency-Selective Channels," *IEEE Transactions on Selected Areas in Communications*, vol. 16, pp. 1568 –1578, October 1998.

[83] T. Al-Naffouri, A. Dahman, M. Sohail, W. Xu, and B. Hassibi, "Low-Complexity Blind Equalization for OFDM Systems With General Constellations," *IEEE Transactions on Signal Processing*, vol. 60, pp. 6395 – 6407, December 2012.

[84] A. Goupil and J. Palicot, "Constant Norm Algorithms Class," in *in Proc. of the 11th European Signal Processing Conference (EUSIPCO'02), Toulouse, France*, September 2002.

[85] A. Goupil and J. Palicot, "New Algorithms for Blind Equalization: The Constant Norm Algorithm Family," *IEEE Transactions on Signal Processing*, vol. 55, pp. 1436 –1444, April 2007.

[86] L. Lin and B. Farhang-Boroujeny, "Convergence Analysis of Blind Equalizer in a Cosine Modulated Filter Bank-Based Multi-carrier Communication System," in *in the proc. of the IEEE International workshop on Signal Processing advances in Wireless Communications (SPAWC'03). Rome, Italy*, pp. 368 –372, June 2003.

[87] J. Tellado-Mourelo, *Peak to Average Power Reduction for Multicarrier Modulation.* PhD thesis, Standford University, 1999.

[88] S. Zabre, J. Palicot, Y. Louet, and C. Lereau, "SOCP Approach for OFDM Peak-to-Average Power Ratio Reduction in the Signal Adding Context," in *in Proc. of the International Symposium on Signal Processing and Information Technology,*, pp. 834–839, 2006.

[89] B. S. Krongold and D. Jones, "A New Tone Reservation Method for Complex-Baseband par Reduction in OFDM Systems," in *in Proc. of the International Conference in Acoustics, Speech, and Signal Processing (ICASSP'02)*, vol. 3, pp. 2321–2324, May 2002.

[90] S. Yoo, S. Yoon, S. Y. Kim, and I. Song, "A Novel PAPR Reduction Scheme for OFDM Systems: Selective Mapping of Partial tones (SMPT)," *IEEE Transactions on Consumer Electronics*, vol. 52, no. 1, pp. 40–43, 2006.

[91] D. Guel and J. Palicot, "FFT/IFFT Pair Based Digital Filtering for the Transformation of Adding Signal PAPR Reduction Techniques in Tone Reservation Techniques," in *in the Proc. of the IEEE 5th Conference on Wireless and Mobile Communications (ICWMC 09)*, pp. 200–204, 2009.

[92] L. Wang and C. Tellambura, "Analysis of Clipping Noise and Tone-Reservation Algorithms for Peak Reduction in OFDM Systems," *IEEE Transactions on Vehicular Communications*, vol. 57, no. 3, pp. 1675–1694, 2008.

[93] J. Tellado and J. Cioffi, "Efficient Algorithms for Reducing PAPR in Multicarrier Systems," in *in Proc. of the IEEE International Symposium on Information Theory*, 1998.

[94] X. Li and L. J. Cimini., "Effects of Clipping and Filtering on the Performance of OFDM," *IEEE Communication Letter*, vol. 2, pp. 131–133, May 1998.

[95] "ACCENT5. Dliverable D2.1: Energy-Efficient Power Controls and Interference Mitigation (first issue). [Online]: http://accent5.fr. [Accessed: 20/08/2016]," tech. rep., 2016.

[96] T. Jiang and G. Zhu, "Complement Block Coding for Reduction in Peak-to-Average Power Ratio of OFDM Signals," *IEEE Communications Magazine*, vol. 43, pp. S17–S22, September 2005.

[97] M. Deumal, A. Behravan, and J. L. Pijoan, "On Cubic Metric Reduction in OFDM Systems by Tone Reservation," *IEEE Transactions on Communications*, vol. 59, pp. 1612–1620, April 2011.

[98] T. Jiang and C. Li, "Simple Alternative Multisequences for PAPR Reduction without Side Information in SFBC MIMO-OFDM Systems," *IEEE Transactions on Vehicular Communications*, vol. 61, pp. 3311–3315, June 2012.

[99] S. Y. L. Goff, B. K. Khoo, C. C. Tsimenidis, and B. S. Sharif, "A Novel Selected Mapping Technique for PAPR Reduction in OFDM Systems," *IEEE Transactions on Communications*, vol. 56, pp. 1775–1779, November 2008.

[100] N. D. Bruijn, *Uncertainty Principles in Fourier Analysis.* Technological University, Eindhoven, Netherlands, 1967. 57-71.

[101] D. Roque, *Modulations Multiporteuses WCP-OFDM: Evaluation des Performances en Environnement Radiomobile.* PhD thesis, Grenoble University, France, 2012.

[102] S. L. Linfoot, M. K. Ibrahim, and M. M. Al-Akaidi, "Orthogonal Wavelet Division Multiplex: An Alternative to OFDM," *IEEE Transactions on Consumer Electronics*, vol. 53, pp. 278–284, July 2007.

[103] F. Schaich and T. Wild, "Waveform Contenders for 5G-OFDM vs. FBMC vs. UFMC," in *in the Proc. of the IEEE 6th International Symposium on Communications, Control and Signal Processing (ISCCSP'14)*, pp. 457–460, 2014.

[104] M. Bellanger, *Digital Processing of Signals: Theory and Practice, 3rd edition.* Wiley, 2000.

[105] F.-L. Luo and C. J. Zhang, eds., *Signal Processing for 5G: Algorithms and Implementations.* Wiley-IEEE Press, October 2016.

[106] A. Osseiran, J. F. Monserrat, P. Marsch, M. Dohler, and T. Nakamura, eds., *5G Mobile and Wireless Communications Technology, 1st Edition.* Cambridge University Press, June 2016.

[107] S. Ali, A. Ghazanfari, N. Rajatheva, and M. Latva-aho, "Effect of Residual of Self-Interference in Performance of Full-Duplex D2D Communication," in *The 1st International Conference on 5G for Ubiquitous Connectivity (5GU'2014)*, November 2014.

[108] G. Zhang, K. Yang, P. Liu, and J. Wei, "Power Allocation for Full-Duplex Relaying-Based D2D Communication Underlaying Cellular Networks," *IEEE Transactions on Vehicular Technology*, vol. 64, pp. 4911–4916, October 2015.

[109] A. C. Cirik, K. Rikkinen, and M. Latva-aho, "Joint Subcarrier and Power Allocation for Sum-Rate Maximization in OFDM Full-Duplex Systems," in *in the Proc. of the IEEE 81st Vehicular Technology Conference (VTC Spring'15)*, pp. 1–5, May 2015.

[110] J. Jose, A. Ashikhmin, T. Marzetta, and S. Vishwanath, "Pilot Contamination Problem in Multi-cell TDD Systems," in *in the Proc. of the IEEE International Symposium on Information Theory, (ISIT'09)*, pp. 2184–2188, June 2009.

[111] H. Q. Ngo and E. Larsson, "EVD-based Channel Estimation in Multicell Multiuser MIMO Systems with Very Large Antenna Arrays," in *in the Proc. of the IEEE International Conference on Acoustics, Speech and Signal Processing (ICASSP'12)*, pp. 3249–3252, March 2012.

[112] H. Yin, D. Gesbert, M. Filippou, and Y. Liu, "A Coordinated Approach to Channel Estimation in Large-Scale Multiple-Antenna Systems," *IEEE Journal on Selected Areas in Communications*, vol. 31, pp. 264–273, February 2013.

[113] B. Farhang-Boroujeny, "Multicarrier Modulation with Blind Detection Capability Using Cosine Modulated Filter Banks," *IEEE Transactions on Communications*, vol. 51, no. 2, pp. 2057–2070, 2003.

[114] A. Moldovan, M. A. Ruder, I. F. Akyildiz, and W. H. Gerstacker, "LOS and NLOS Channel Modeling for Terahertz Wireless Communication with Scattered Rays," in *in the Proc. of the IEEE Global Communications Conference (Globecom 2014), Workshop - Mobile Communications in Higher Frequency Bands*, pp. 388–392, 2014.

[115] G. Fettweis, F. Guderian, and S. Krone, "Entering the Path Towards Terabit/s Wireless Links," in *in Proc. of the IEEE Design, Automation & Test in Europe Conference & Exhibition (DATE'11)*, May 2011.

[116] P. Wang, Y. Li, L. Song, and B. Vucetic, "Multi-Gigabit Millimeter Wave Wireless Communications for 5G: from Fixed Access to Cellular Networks," *IEEE Communications Magazine*, vol. 53, pp. 168–178, January 2015.

[117] T. Chen, G. Liu, Z. Ma, and P. Fan, "Energy-Efficient Resource Allocation in HetNets with Full Duplex and D2D Communications," in *in the Proc. of the 25th Wireless and Optical Communication Conference (WOCC'16)*, 2016.